Alan G. Davenport Wind Engineering Group

A STUDY OF WIND EFFECTS FOR

INDIAN RIVER INLET BRIDGE DELAWARE, USA

J.P.C. KING / J. GALSWORTHY / P.J. VICKERY / M. MIKITIUK / L. KONG

BLWT-SS31-2004 / February 2005

The Boundary Layer Wind Tunnel Laboratory
The University of Western Ontario, Faculty of Engineering Science
London, Ontario, Canada N6A 5B9; Tel: (519) 661-3338; Fax: (519) 661-3339
Internet: www.blwtl.uwo.ca; E-mail: info@blwtl.uwo.ca

TABLE OF CONTENTS

ACKNOWLEDGEMENTS **xi**

SUMMARY AND MAIN FINDINGS **xii**

DETAILS OF THE STUDY **1**

1 INTRODUCTION **2**
1.1 General 2
1.2 Scope of Report 2

2 THE MODELLING OF THE SITE AND THE WIND **7**
2.1 Introduction 7
2.2 Analysis of Surface Wind Data 7
2.3 Monte Carlo Simulation of Hurricane Winds 8
2.4 Design Wind Climate for Bridge Site 9

3 SECTION MODEL STUDY – BRIDGE DECK **31**
3.1 General 31
3.2 Dynamic Response Testing 31
3.2.1 General 31
3.2.2 Modeling of Wind 32
3.2.3 Dynamic Bridge Response 32
3.3 Static Response Testing – Bridge Deck 33

4 EQUIVALENT STATIC LOAD ANALYSIS FOR BRIDGE DECK **49**
4.1 General 49
4.2 Adaptation of Section Model Tests Results 49

5 SECTION MODEL STUDY – ARCH SECTION **57**
5.1 General 57
5.2 Static Testing – Arch Rib 57

6 STRUCTURAL LOADS ON ARCH RIB **67**
6.1 Approach for Loads Analysis 67
6.2 Equivalent Static Loads 67

7 FULL AEROELASTIC MODEL STUDY **76**
7.1 General 76
7.2 Dynamic Similarity 76
7.3 Description of Model Design 77
7.3.1 Arch 78
7.3.2 Deck 78
7.3.3 Tie-Beam (Construction Stage) 78
7.3.4 Connections and Bearings 79
7.3.5 Cables 79
7.3.6 Construction Equipment 79
7.3.7 Effect of Revision to Prototype Properties 79
7.4 Instrumentation 80
7.5 Wind Simulation 81
7.6 Wind Speed Measurements 82
7.7 Aeroelastic Model Test Procedure 82

7.8 Response of Completed Bridge and Construction Stage Configurations 83
7.8.1 General 83
7.8.2 Completed Bridge 83
7.8.3 Bridge Under Construction 85

REFERENCES **128**

APPENDIX A THE SECTION MODEL APPROACH FOR THE STUDY OF WIND ACTION ON LONG SPAN BRIDGES

APPENDIX B RESULTS OF DYNAMIC SECTION MODEL TESTS – BRIDGE DECK

APPENDIX C RESULTS OF STATIC SECTION MODEL TESTS – BRIDGE DECK

APPENDIX D FLUTTER INSTABILITY CRITERIA

APPENDIX E DYNAMIC WIND LOAD FORCES ON LONG SPAN BRIDGES USING EQUIVALENT STATIC LOADS

APPENDIX F RESULTS OF STATIC SECTION MODEL TESTS – ARCH SECTION

APPENDIX G DEVELOPMENT OF THE PEAK RESPONSE DUE TO ALONG-WIND LOADING OF THE ARCH RIB

APPENDIX H RESULTS OF FULL BRIDGE AEROELASTIC TESTS, COMPLETED BRIDGE

APPENDIX I RESULTS OF FULL BRIDGE AEROELASTIC TESTS, CONSTRUCTION STAGE – CANTILEVERED TIE-BEAM

APPENDIX J RESULTS OF FULL BRIDGE AEROELASTIC TESTS, CONSTRUCTION STAGE – CANTILEVERED ARCH

APPENDIX K RESULTS OF FULL BRIDGE AEROELASTIC TESTS, CONSTRUCTION STAGE – BRIDGE PRIOR TO DECK COMPLETION

LIST OF TABLES

TABLE I PREDICTED HOURLY-MEAN WIND SPEEDS AT VARIOUS HEIGHTS FOR WINDS OVER WATER XVII

TABLE II SUMMARY OF STATIC TEST RESULTS – BRIDGE DECK XVIII

TABLE III SUMMARY OF DYNAMIC TEST RESULTS XIX

TABLE IV SUMMARY OF RESULTS FROM STATIC TESTS ON INDIAN RIVER INLET BRIDGE ARCH XX

TABLE V MAGNITUDE OF PRESSURES FOR THE VARIOUS COMPONENTS OF THE EQUIVALENT STATIC LOAD DISTRIBUTIONS CORRESPONDING TO A 100-YEAR RETURN PERIOD MEAN HOURLY WIND SPEED AT ARCH CROWN = 110 MPH XXI

TABLE VI SUMMARY OF FULL BRIDGE AEROELASTIC MODEL TESTS, INDIAN RIVER INLET BRIDGE XXII

TABLE VII SUMMARY OF FULL BRIDGE AEROELASTIC MODEL TESTS, COMPLETED BRIDGE CONFIGURATION XXIII

TABLE 2.1 PREDICTED HOURLY-MEAN WIND SPEEDS AT VARIOUS HEIGHTS FOR WINDS BLOWING OVER WATER 10

TABLE 3.1 SECTION MODEL SCALING PARAMETERS 35

TABLE 3.2 FULL SCALE AND MODEL SCALE PROPERTIES FOR THE BASIC DECK SECTION 36

TABLE 3.3 RESULTS OF DYNAMIC SECTION MODEL TESTS 37

TABLE 3.4 STATIC FORCE COEFFICIENTS, SIDEWALK UPSTREAM, SMOOTH FLOW 38

TABLE 3.5 STATIC FORCE COEFFICIENTS, SIDEWALK UPSTREAM, TURBULENT FLOW 39

TABLE 3.6 STATIC FORCE COEFFICIENTS, SIDEWALK DOWNSTREAM, SMOOTH FLOW 40

TABLE 3.7 STATIC FORCE COEFFICIENTS, SIDEWALK DOWNSTREAM, TURBULENT FLOW 41

TABLE 4.1 SUMMARY OF PROTOTYPE PROPERTIES 51

TABLE 4.2 SUMMARY OF MODEL PROPERTIES 52

TABLE 4.3 SUMMARY OF WIND CHARACTERISTICS 53

TABLE 5.1 SUMMARY OF RESULTS FROM STATIC TESTS ON INDIAN RIVER INLET BRIDGE ARCH 59

TABLE 6.1 RESULTS FROM DETAILED ANALYSIS OF WIND-INDUCED RESPONSE OF THE ARCH RIB 68

TABLE 6.2 MAGNITUDE OF PRESSURES FOR THE VARIOUS COMPONENTS OF THE EQUIVALENT STATIC LOAD DISTRIBUTIONS CORRESPONDING TO A 100-YEAR RETURN PERIOD MEAN HOURLY WIND SPEED AT ARCH CROWN = 110 MPH 68

TABLE 6.3 VARIATION OF MEAN WIND SPEED AT ARCH HEIGHT ROUGHNESS LENGTH, Z_O WITH RETURN PERIOD 69

TABLE 7.1 AEROELASTIC SCALING PARAMETERS (FROUDE SCALED) 87

TABLE 7.2 PARAMETERS FOR DESIGN OF THE AEROELASTIC MODEL 88

TABLE 7.3 INSTRUMENTATION LOCATIONS, INDIAN RIVER INLET BRIDGE, COMPLETED BRIDGE 90

TABLE 7.4 SUMMARY OF FULL BRIDGE AEROELASTIC MODEL TESTS, INDIAN RIVER INLET BRIDGE 91

TABLE 7.5 SUMMARY OF FULL BRIDGE AEROELASTIC MODEL TESTS, COMPLETED BRIDGE CONFIGURATION 92

TABLE 7.6 SUMMARY OF FULL BRIDGE MODEL PROPERTIES, COMPLETED BRIDGE 93

TABLE 7.7 SUMMARY OF TURBULENCE INTENSITIES (IN TEST AND TARGET VALUES) 94

TABLE 7.8 PEAK RESPONSES AND PEAK FACTORS FOR SELECTED TESTS AND CHANNELS, COMPLETED BRIDGE 95

TABLE 7.9 PEAK RESPONSES AND PEAK FACTORS FOR SELECTED TESTS AND CHANNELS, CANTILEVERED TIE BEAM 96

TABLE 7.10 PEAK RESPONSES AND PEAK FACTORS FOR SELECTED TESTS AND CHANNELS, CANTILEVERED ARCH 97

TABLE 7.11 PEAK RESPONSES AND PEAK FACTORS FOR SELECTED TESTS AND CHANNELS, BRIDGE PRIOR TO FINAL DECK COMPLETION 98

LIST OF FIGURES

FIGURE I RELATIVE IMPORTANCE FACTORS FOR VARIOUS WIND DIRECTIONS AND MAXIMUM WIND SPEEDS WITH DIFFERENT RECURRENCE INTERVALS AT 83.5 M (274 FT) ABOVE WATER LEVEL FOR INDIAN RIVER INLET XXIV

FIGURE II PREDICTED EXTREME HOURLY-MEAN WIND SPEEDS FOR VARIOUS RETURN PERIODS FOR HURRICANE WINDS AT 10 M (33 FT), 16.8 M (DECK HEIGHT OF 55 FT), 83.5 M (ARCH LEVEL OF 274 FT) AND 500 M LEVEL (1640 FT) XXV

FIGURE III SKETCH SHOWING SIGN CONVENTION OF FORCES XXVII

FIGURE IV STATIC FORCE COEFFICIENTS – SIDEWALK UPSTREAM XXVIII

FIGURE V DYNAMIC TEST RESULT, TURBULENT FLOW AT 0° ANGLE OF ATTACK, SIDEWALK UPSTREAM WITH MODIFIED FREQUENCIES XXIX

FIGURE VI MODE SHAPES USED IN THE EQUIVALENT STATIC LOAD ANALYSIS – BRIDGE DECK XXX

FIGURE VII WIND LOAD COMPONENTS FOR THE BRIDGE DECK – COMPLETED BRIDGE CONFIGURATION XXXI

FIGURE VIII SKETCH SHOWING THE SIGN CONVENTION OF FORCES – ARCH SECTION XXXII

FIGURE IX DISTRIBUTION WITH HEIGHT OF THE VARIOUS COMPONENTS OF EQUIVALENT STATIC LOADS XXXIII

FIGURE X SPANWISE DISTRIBUTION OF THE MEAN AND QUASI-STEADY (TOP) AND SYMMETRIC AND ANTI- SYMMETRIC COMPONENTS (BOTTOM) OF THE EQUIVALENT STATIC LOADS XXXIV

FIGURE 1.1 PROTOTYPE DIMENSIONS – BRIDGE OUTLINE 4

FIGURE 1.2 PROTOTYPE DIMENSIONS – BRIDGE DECK CROSS SECTION 5

FIGURE 1.3 PROTOTYPE DIMENSIONS – ARCH SECTION 6

FIGURE 2.1 LOCATIONS OF THE INDIAN RIVER INLET BRIDGE AND PRIMARY WEATHER STATIONS 11

FIGURE 2.2 ANNUAL PROBABILITY DISTRIBUTION OF SURFACE HOURLY-MEAN WIND SPEED AND WIND DIRECTION – DOVER AFB, DELAWARE (1942-2003) 12

FIGURE 2.3 SEASONAL PROBABILITY DISTRIBUTION OF SURFACE HOURLY-MEAN WIND SPEED AND WIND DIRECTION – DOVER AFB, DELAWARE (1942-2003) 13

FIGURE 2.4 ANNUAL PROBABILITY DISTRIBUTION OF SURFACE HOURLY-MEAN WIND SPEED AND WIND DIRECTION – ATLANTIC CITY, NEW JERSEY (1958-1999) 14

FIGURE 2.5 SEASONAL PROBABILITY DISTRIBUTION OF SURFACE HOURLY-MEAN WIND SPEED AND WIND DIRECTION – ATLANTIC CITY, NEW JERSEY (1958-1999) 15

FIGURE 2.6 ANNUAL PROBABILITY DISTRIBUTION OF SURFACE HOURLY-MEAN WIND SPEED AND WIND DIRECTION – WALLOPS ISLAND, VIRGINIA (1966-1996) 16

FIGURE 2.7 SEASONAL PROBABILITY DISTRIBUTION OF SURFACE HOURLY-MEAN WIND SPEED AND WIND DIRECTION – WALLOPS ISLAND, VIRGINIA (1966-1996) 17

FIGURE 2.8 ANNUAL RELATIVE IMPORTANCE FACTORS FOR VARIOUS WIND DIRECTIONS AND MAXIMUM WIND SPEEDS WITH DIFFERENT RECURRENCE INTERVALS, DOVER AFB, DELAWARE (1942-2003) 18

FIGURE 2.9 SEASONAL RELATIVE IMPORTANCE FACTORS FOR VARIOUS WIND DIRECTIONS AND MAXIMUM WIND SPEEDS WITH DIFFERENT RECURRENCE INTERVALS, DOVER AFB, DELAWARE (1942-2003) 19

FIGURE 2.10 ANNUAL RELATIVE IMPORTANCE FACTORS FOR VARIOUS WIND DIRECTIONS AND MAXIMUM WIND SPEEDS WITH DIFFERENT RECURRENCE INTERVALS, ATLANTIC CITY, NEW JERSEY (1958-1999) 20

FIGURE 2.11 SEASONAL RELATIVE IMPORTANCE FACTORS FOR VARIOUS WIND DIRECTIONS AND MAXIMUM WIND SPEEDS WITH DIFFERENT RECURRENCE INTERVALS, ATLANTIC CITY, NEW JERSEY (1958-1999) 21

FIGURE 2.12 ANNUAL RELATIVE IMPORTANCE FACTORS FOR VARIOUS WIND DIRECTIONS AND MAXIMUM WIND SPEEDS WITH DIFFERENT RECURRENCE INTERVALS, WALLOPS ISLAND, VIRGINIA (1966-1996) 22

FIGURE 2.13 SEASONAL RELATIVE IMPORTANCE FACTORS FOR VARIOUS WIND DIRECTIONS AND MAXIMUM WIND SPEEDS WITH DIFFERENT RECURRENCE INTERVALS, WALLOPS ISLAND, VIRGINIA (1966-1996) 23

FIGURE 2.14 PREDICTED EXTREME HOURLY-MEAN SURFACE AND GRADIENT WIND SPEEDS FOR VARIOUS RETURN PERIODS AT DOVER AFB, ATLANTIC CITY AND WALLOPS ISLAND 24

FIGURE 2.15 TROPICAL STORMS PASSING WITHIN A 250 KM RADIUS OF INDIAN RIVER INLET BRIDGE FOR THE RECORD PERIOD 1886-2000 – ALL STORMS CASE 25

FIGURE 2.16 TROPICAL STORMS PASSING WITHIN A 250 KM RADIUS OF INDIAN RIVER INLET BRIDGE FOR THE RECORD PERIOD 1886-2000 – STORM SEQUENCES REACHING "HURRICANE" STAGE (V>33M/S) 26

FIGURE 2.17 TROPICAL STORMS PASSING WITHIN A 250 KM RADIUS OF INDIAN RIVER INLET BRIDGE FOR THE RECORD PERIOD 1886-2000 – STORM SEQUENCES REACHING "TROPICAL STORM" STAGE (V<33M/S) 27

FIGURE 2.18 ANNUAL PROBABILITY DISTRIBUTION OF HOURLY-MEAN WIND SPEED AND WIND DIRECTION AT 83.5 M (274 FT) ABOVE WATER LEVEL FOR INDIAN RIVER INLET OBTAINED FROM MONTE CARLO SIMULATION OVER 100,000 YEARS (37,150 STORMS) 28

FIGURE 2.19 RELATIVE IMPORTANCE FACTORS FOR VARIOUS WIND DIRECTIONS AND MAXIMUM WIND SPEEDS WITH DIFFERENT RECURRENCE INTERVALS AT 83.5 M (274 FT) ABOVE WATER LEVEL FOR INDIAN RIVER INLET 29

FIGURE 2.20 PREDICTED EXTREME HOURLY-MEAN WIND SPEEDS FOR VARIOUS RETURN PERIODS FOR HURRICANE WINDS AT 10 M (33 FT), 16.8 M (DECK HEIGHT OF 55 FT), 83.5 M (ARCH LEVEL OF 274 FT) AND 500 M LEVEL (1640 FT) 30

FIGURE 3.1 SECTION MODEL TEST SET-UP – BRIDGE DECK 42

FIGURE 3.2 CLOSE-UP VIEWS OF THE SECTION MODEL 43

FIGURE 3.3 MODEL DRAWINGS – DECK SECTION 44

FIGURE 3.4 TURBULENCE SPECTRA (FULL SCALE AND GRID-TURBULENCE) 45

FIGURE 3.5 SKETCH SHOWING SIGN CONVENTION OF FORCES 46

FIGURE 3.6 STATIC FORCE COEFFICIENTS – SIDEWALK UPSTREAM 47

FIGURE 3.7 STATIC FORCE COEFFICIENTS – SIDEWALK DOWNSTREAM 48

FIGURE 4.1 DYNAMIC TEST RESULT, TURBULENT FLOW AT 0° ANGLE OF ATTACK 54

FIGURE 4.2 MODE SHAPES USED IN THE ANALYSIS 55

FIGURE 4.2 MODE SHAPES USED IN THE ANALYSIS 55

FIGURE 4.3 WIND LOAD COMPONENTS FOR COMPLETED BRIDGE 56

FIGURE 5.1 SECTION MODEL TEST SET-UP – ARCH SECTION 60

FIGURE 5.2 CLOSE-UP VIEW OF THE ARCH SECTION MODEL 60

FIGURE 5.3 MODEL DRAWINGS – ARCH SECTION 61

FIGURE 5.4 TURBULENCE SPECTRA (FULL SCALE AND GRID-TURBULENCE) 62

FIGURE 5.5 SKETCH SHOWING SIGN CONVENTION OF FORCES, ARCH SECTION 63

FIGURE 5.6 STATIC FORCE COEFFICIENTS, ARCH SECTION 64

FIGURE 6.1 DEFINITIONS OF GEOMETRY AND COORDINATE SYSTEM 70

FIGURE 6.2 INFLUENCE FUNCTIONS FOR THE BENDING MOMENT RESPONSE AT THE DECK/ARCH INTERSECTION 71

FIGURE 6.3 INFLUENCE FUNCTIONS FOR THE BENDING MOMENT RESPONSE AT THE REDUCTION IN CROSS SECTION ON THE ARCH RIB 72

FIGURE 6.4 DISTRIBUTION WITH HEIGHT OF THE VARIOUS COMPONENTS OF EQUIVALENT STATIC LOADS 73

FIGURE 6.5 SPANWISE DISTRIBUTION OF THE MEAN AND QUASI-STEADY (TOP) AND SYMMETRIC AND ANTI- SYMMETRIC COMPONENTS (BOTTOM) OF THE EQUIVALENT STATIC LOADS 74

FIGURE 6.6 VARIATION OF EQUIVALENT STATIC LOAD COMPONENTS WITH RETURN PERIOD 75

FIGURE 7.1 THE FULL BRIDGE AEROELASTIC MODEL IN THE WIND TUNNEL 99

FIGURE 7.2 FULL BRIDGE AEROELASTIC MODEL - DETAILS OF MODEL AND INSTRUMENTATION, COMPLETED BRIDGE 102

FIGURE 7.3 FULL BRIDGE AEROELASTIC MODEL, CONSTRUCTION STAGE – CANTILEVERED TIE BEAM 104

FIGURE 7.4 FULL BRIDGE AEROELASTIC MODEL, CONSTRUCTION STAGE – CANTILEVERED ARCH 105

FIGURE 7.5 FULL BRIDGE AEROELASTIC MODEL, CONSTRUCTION STAGE – BRIDGE PRIOR TO DECK COMPLETION 106

FIGURE 7.6 THE FULL BRIDGE AEROELASTIC MODEL - HURRICANE EXPOSURE 107

FIGURE 7.7 THE FULL BRIDGE AEROELASTIC MODEL - OPEN COUNTRY EXPOSURE 109

FIGURE 7.8 DEFINITION OF LOCAL WIND AZIMUTH 111

FIGURE 7.9 THE 1:150 SCALE AEROELASTIC MODEL, COMPLETED BRIDGE 112

FIGURE 7.10 THE 1:150 SCALE AEROELASTIC MODEL, CONSTRUCTION STAGE, BRIDGE PRIOR TO DECK COMPLETION 117

FIGURE 7.11 BRIDGE SIGN CONVENTION AND INSTRUMENTATION LOCATIONS 120

FIGURE 7.12 WIND PROFILES USED IN THE FULL BRIDGE MODEL TESTS, OPEN COUNTRY AND SUBURBAN EXPOSURES 121

FIGURE 7.13 WIND SPECTRA AT DECK HEIGHT, HURRICANE EXPOSURE 122

FIGURE 7.14 WIND SPECTRA AT DECK HEIGHT, OPEN COUNTRY EXPOSURE 123

FIGURE 7.15 RATIO OF PROBABLE MAXIMUM SPEED AVERAGED OVER T SECONDS TO HOURLY MEAN SPEED 124

FIGURE 7.16 DEFINITION OF WIND SPEEDS FOR VARIOUS AVERAGING TIME 125

FIGURE 7.17 COHERENCE OF THE DECK LIFT DISPLACEMENTS AT THE TWO ¼ POINTS (B AND F) FOR THE FIRST VORTEX PEAK (DECK ASYMMETRIC LIFT MODE AT 7.5 HZ) AT 45 MPH DECK HEIGHT, SMOOTH FLOW 126

FIGURE 7.18 COHERENCE OF THE DECK TORSION AT THE TWO ¼ POINTS (B AND F) FOR THE SECOND VORTEX PEAK (DECK SYMMETRIC TORSION MODE AT 13.7 HZ) AT 80 MPH (DECK HEIGHT), SMOOTH FLOW.....127

ACKNOWLEDGEMENTS

The study of wind effects for the Indian River Inlet Bridge, Delaware, was initiated by Mr. Denney Pate of Figg Bridge Engineers. The assistance and continued co-operation and support of Messrs. Denney Pate, Tom Jenkins, Pat Hickox and Dwight Dempsey, all of Figg Bridge Engineers is acknowledged. The continued support of Ms. Linda Figg, President of Figg Engineering Group is greatly appreciated.

Acknowledgment is also made of the contributions by various members of the technical staff of the Laboratory, particularly: Messrs. Gerry Dafoe, Alex Shyluk and Chris Gavin who carried out the experimental phases of the study, Mr. Tomasz Kawa who made some of the illustrations for the report. The CAD models for the bridge deck and arch section models, as well as the full bridge aeroelastic model were made by Mr. Christopher Vandelaar of the University Machine Services. Mr. Vandelaar also took the lead in the direction of his team members in the fabrication of the section and full aeroelastic models.

SUMMARY AND MAIN FINDINGS

This report on the study of wind action on the Indian River Inlet Bridge, Delaware, provides information from the deck and arch section model tests as well as the full bridge aeroelastic model tests. The aim of this study was to provide:

1. Wind climate and wind speed information at the project site;
2. Basic aerodynamic information for the deck and arch designs;
3. Investigation of the overall stability of the deck section in high wind conditions;
4. Investigation of the deck section behavior with respect to vortex shedding induced oscillation in smooth wind;
5. Definition of the behavior of the deck section due to buffeting in turbulent wind;
6. Determination of the static force coefficients in both smooth and turbulent flows for the deck section;
7. Determination of the static force coefficients in both smooth and turbulent flows for the arch section, and their dependency on the Reynolds number;
8. Determination of the equivalent static wind loads for the deck and arch sections;
9. Determination of the response characteristics of the full bridge aeroelastic model to three dimensional turbulent wind over a full range of wind speeds for the completed bridge and three different construction stages;
10. Determination of the response characteristics of the full bridge aeroelastic model in winds with low turbulence conditions to confirm the potential for vortex shedding induced bridge response and flutter instability for the completed bridge and three different construction stages.

The deck section model was constructed at a geometric scale of 1:80 relative to full scale, while the arch section model was constructed at a scale of 1:40. Both the deck and arch section models were tested at the inlet to the high speed test section of the Boundary Layer Wind Tunnel II. The deck section model test was performed in two phases: i) on a static force balance in which the overall static forces and moment in vertical, lateral and torsional directions were measured at different angles of vertical wind inclination; and ii) with scaled dynamic structural properties of the prototype, to monitor the dynamic response. The arch section model was tested using the static force balance only. Both section models were tested in smooth flow and grid-generated turbulent wind representative of the natural wind conditions at the project site. The section model test methodology is presented in Appendix A.

The full bridge aeroelastic model was constructed at a geometric scale of 1:150 relative to the prototype. The model was tested on the turntable of the Low Speed Test Section of the Boundary Layer Wind Tunnel II in three dimensional turbulent wind conditions. The long upwind fetch within the wind tunnel allows extended modeling of upwind terrains, thus permits the simulation of wind conditions representative of those anticipated for the project site. Two upstream terrain conditions, a hurricane profile and an open country exposure, were used in the tests. The existing bridge (upwind of the proposed Indian River Inlet Bridge for a wind angle of 90°) was also constructed, in order to assess its effect on the proposed bridge. Five different wind angles (0°, 30°, 60°, 90° and 270° relative to the longitudinal axis of the bridge) were examined in the test. A 90° wind angle is defined as when the pedestrian walkway on the proposed bridge is upstream.

A design probability distribution of surface wind speed and direction was developed for the bridge site on the basis of full scale meteorological records from the weather stations in the area. In addition, a study was carried out to include Monte Carlo computer simulations of the tropical storms and to assess their impact on the climate of extreme winds. The methodology and the wind speed results from these analyses are given in Section 2 of this report.

The highlights and main findings of these studies are as follows:

Wind Climate

- A wind climate study was carried out for the Indian River Inlet Bridge. The design probability distribution of surface wind speed and direction was developed on the basis of full scale meteorological records from nearby weather stations, including stations at Atlantic City, NJ, Wallops Island, VA and Dover AFB in Delaware. Monte Carlo simulations of the tropical storms were carried out and their impact on extreme winds was analyzed.
- The directional characteristics associated with hurricane winds are shown in Figure i for various return periods. It can be seen that strong winds during hurricane events are equally likely to come from any wind direction with a slight preference to the northeast sector.
- Predictions of the hourly mean wind speed for winds over water at various heights, regardless of wind direction, are shown in Figure ii. The predicted hourly mean wind speeds at various heights for wind over water are also presented in Table i.

Static Test of Section Model – Bridge Deck

- The 1:80 scale section model was mounted on the BLWTL Bridge Section Model force balance which is capable of measuring the total forces on the section (X and Z body forces, as well as the torque). Tests were carried out in both smooth and grid-generated turbulent flow conditions for angles of mean vertical inclination between -12° to +12° in increments of 1°.
- The static test was performed for the completed bridge deck configuration for winds from the two primary wind directions normal to the longitudinal axis of the bridge.
- The static force coefficients at 0° angle of attack are listed in Table ii for both sidewalk upstream and downstream tests. The sign convention for the bridge deck forces is given in Figure iii and the static force coefficients for the test of sidewalk upstream is plotted in Figure iv. All static test results including tables and plots are also given in Section 3 and Appendix C.
- There are no significant differences observed between the smooth and turbulent flow test results for any of the coefficients at small angles of attack for either wind direction. The coefficients differ for the two flow conditions only at high negative angles of attack for the sidewalk upstream case.
- The coefficients show that there is a positive slope in the aerodynamic lift and torsional force coefficient curves for small angles of attack. This is indicative of good aerodynamic stability characteristics.

Dynamic Test of Section Model – Bridge Deck

Response to Extreme Wind in Smooth Flow Conditions:

- These tests were conducted to provide: a) lower bound estimates of the response to vortex shedding and b) estimates of the wind speeds associated with any possible flutter instability up to the design wind speed.
- The dynamic tests were performed in two stages. Initial properties of the bridge deck were used in the first stage with a torsional to vertical frequency ratio of 2.22. A second series of section model tests were carried out with a new torsional to vertical frequency ratio of 1.19, as a result of modifications to the structural design of the bridge.
- All dynamic section model tests were performed at relatively low damping with a nominal value of 0.5% of critical in both vertical and torsional directions. Another series of tests was performed with extremely low damping (0.1-0.2% of critical) in an attempt to ascertain whether vortex shedding induced response was present. All tests conducted in both stages were summarized in Table iii.

- The onset of a “Flutter Instability” was defined as when the character of the response changed from a random type motion to that of a regular, sinusoidal motion, involving either pure torsional or a coupled vertical-torsional vibration. This can be clearly identified through an examination of the “peak factor” which is defined as the ratio of the largest observed reading during the sample period to the Root Mean Square (RMS) of the sample. A random signal has peak factors in the 3-4 range, while a sinusoid has a peak factor of $\sqrt{2}$ or 1.41.
- The model was subjected to scaled mean wind speeds in smooth flow of up to 220 mph at deck height with no sign of torsional instability (flutter).
- No instance of vortex shedding induced oscillation of the bridge deck was observed through the range of wind speeds examined.

Response to Winds in Expected Site Turbulence Conditions:

- These tests were conducted to provide: a) estimates of the response to turbulent buffeting and b) permit the assessment of Equivalent Static Wind Loads on the bridge deck.
- Turbulence in the wind tunnel was generated by a grid placed upstream of the model. The mesh size and bar spacing were selected to give a reasonable representation of the natural wind at the frequency range of interest. The vertical I_w, and horizontal I_u turbulence intensities measured using this grid is about 4% and 5% respectively. Turbulence developed using the fixed grid technique is normally lacking sufficient energy in the low frequency - large scale range to match full scale, resulting in an overall lower turbulence intensity than that expected at the site. The energy in the high frequency end of the spectrum, however, is well modeled and is critical for the definition of resonant response and the overall behavior of the structure to turbulent wind.
- All section model tests reached the target maximum wind speeds.
- The response of the bridge deck was characterized by turbulent buffeting with no sign of torsional or vertical instability.
- A sample plot is given in Figure v for the test condition of 0° angle of attack, 0.5% damping and sidewalk upstream in turbulent flow.

Equivalent Static Loads – Bridge Deck

- Wind loads were estimated for the deck section of the complete bridge. The analysis is based upon the measured response of the section model in turbulent flow, with suitable corrections for discrepancies in the intensity and spectrum of turbulence, the damping and the mode shapes. The design loads were determined from estimates of the dynamic motion in the lowest symmetric and anti-symmetric modes as well as the mean load and is fully described in Appendix E. The distribution of each load component follows the computed mode shapes of the bridge shown in Figure vi.
- The equivalent static wind load plots resulting from this analysis at 0 degrees are presented in Figure vii. These wind loads are obtained for an assumed prototype damping of 0.5% of critical or a logarithmic decrement of 0.031 for all modes. A mean hourly wind speed of 91mph at deck height is used as a reference wind speed for the purposes of illustration and the equivalent static loads at this wind speed are reproduced in equation form as shown below. The equivalent static loads at other wind speeds can be estimated from the plots.

$$W_x(\eta)\ lb/ft = 177\alpha(\eta) \pm \gamma_{1x} 271\alpha_{1x}(\eta) \pm \gamma_{2x} 129\alpha_{2x}(\eta) \quad (1)$$

$$W_z(\eta)\ lb/ft = 551\alpha(\eta) \pm \gamma_{1z} 3520\alpha_{1z}(\eta) \pm \gamma_{2z} 4756\alpha_{2z}(\eta) \quad (2)$$

$$W_\theta(\eta)\ lb\cdot ft/ft = 7947\alpha(\eta) \pm \gamma_{1\theta} 56191\alpha_{1\theta}(\eta) \quad (3)$$

- In the equations, W_x (lb/ft), W_z (lb/ft) and W_θ (lb-ft/ft) are the desired wind loads per unit length resulting from the application of: $\overline{W}$ (lb/ft), the mean, distributed according to $\alpha(\eta)$ (normally with a constant value of 1), $\tilde{W}_1$ (lb/ft), the symmetric, according to $\alpha_1(\eta)$ and $\tilde{W}_2$ (lb-ft/ft), the asymmetric, according to $\alpha_2(\eta)$. These distribution functions vary according to the mode shapes presented in Figure vi with a maximum value of 1.0.
- To reflect the multitude of combinations with which the fluctuating loads can occur, the load combination factors γ_{1x}, γ_{2x} γ_{1z}, γ_{2z}, $\gamma_{1\theta}$, $\gamma_{2\theta}$ should be used in any combination of the modal terms whose values are taken as follows: γ=±1.0 if only one modal term is included; ±0.8 for two terms; ±0.7 for three terms and ±0.6 for four or more terms. This applies to all modal terms whether they are in X, Z and θ, singly or together.

Static Test of Section Model – Arch Section

- The 1:40 scale arch section model was mounted on the BLWTL Bridge Section Model force balance. The sign convention for the definition of the force coefficients is given in Figure viii.
- Tests were carried out in the same flow fields (smooth and turbulent) as the bridge deck. A similar range of Reynolds numbers was investigated. However, unlike the bridge deck results, a strong Reynolds number dependency in the results was observed.
- Therefore, another series of tests were conducted to investigate the extent of the Reynolds number dependency. The static aerodynamic coefficients from these tests are summarized in Table iv for both turbulent and smooth flow, along with the slopes of the coefficients. The full set of results is given in Section 5 and Appendix F.
- The slope of the vertical force coefficient curve provides an indication of dynamic stability for cross-wind motion or "galloping". Using Den Hartog's criteria, if $(C_x + \frac{\partial C_y}{\partial \alpha}) < 0$, there will be an aerodynamic force in the vertical direction, proportional to the velocity of the motion or a negative aerodynamic damping term, and a cross-wind instability would occur. This is not the case for the arch due to the large drag force and the near-zero slope in the vertical force coefficient. Therefore, "galloping" motions are not expected to occur within the range of wind speeds investigated.

Equivalent Static Loads – Arch Section

- Equivalent static loads were derived based on the overall bending moment at the base of the arch. The loads are presented as statically acting pressures with four components: (1) mean, (2) quasi-steady (slowly varying and hence similar in distribution to the mean), (3) symmetric and (4) anti-symmetric. The maximum magnitudes of the various components are given in Table v.
- The distributions with height of the components are given in Figure ix, while the distributions with distance along the deck from the arch – deck intersection are given in Figure x.
- The loads are combined as usual with the load combination factor, γ, when more than one load effect is combined. γ equals 1.0 when the load effect due to any one of P_Q, P_{sym} or $P_{antisym}$ is added to the mean load effect, 0.8 when any two are added and 0.7 when all three are added simultaneously.

Bridge Aeroelastic Model Tests

- The 1:150 scale bridge aeroelastic model faithfully reproduced the dynamic characteristics of the prototype bridge in an intermediate stage of the design process. However, the test results are expected to be appropriate for the final design. Four bridge configurations were tested, including

the completed bridge and three under construction stages of the cantilevered tie-beam, cantilevered arch and bridge prior to final deck completion.

- Two wind profiles, a hurricane exposure (Z_o=0.025ft) and an open country exposure (Z_o=0.1ft), were used to model the general terrain conditions upstream of the project. Tests were conducted for five different wind angles of 0°, 30°, 60°, 90° and 270°. The 90° wind denotes the pedestrian walkway upstream. In addition, tests were also conducted at 90° wind with the existing bridge upwind to assess its effect on the proposed Indian River Bridge.
- No flutter instability was observed in any of the tests performed for all bridge configurations up to a full scale wind speed of 139 mph (3-second gust of 199 mph) at deck height.
- No vortex shedding induced instability was observed in any of the tests performed for the completed bridge configuration with either the hurricane profile or the open country profile, except a small vortex peak at about 45 mph (3-second gust of 64 mph) in limited test conditions.
- In addition, no significant vortex shedding peaks were observed in any of the tests conducted in the hurricane and open country exposures for the three under construction stages. The various vortex shedding peaks observed are small and are not expected to manifest themselves in prototype conditions.
- The effect of the existing bridge upstream of the proposed Indian River Bridge, is small in both terrain conditions of hurricane and open country exposures.
- The response of the bridge in turbulent wind was characterised by turbulent buffeting, with dynamic responses generally proportional to the intensity of turbulence (i.e. larger responses were found in the tests under open country exposure conditions than those in the hurricane exposure).
- Tests performed for the aeroelastic model are summarized in Table vi for all bridge configurations. The test results for the completed bridge configuration are given in Table vii. All test results, including the detailed response plots, are given in Appendices H, I, J and K respectively for the four bridge configurations: a) the completed bridge, b) the cantilevered tie-beam, c) the cantilevered arch and d) the bridge prior to final deck completion.

TABLE i PREDICTED HOURLY-MEAN WIND SPEEDS AT VARIOUS HEIGHTS FOR WINDS OVER WATER

Return Period (Years)	Arch Height (274')			Deck Height (55')			Standard Anemometer Height (33')		
	m/s	mph	mph*	m/s	mph	mph*	m/s	mph	mph*
50	43.1	96	147	35.9	80	122	33.6	75	114
100	49.1	110	167	40.7	91	138	38.0	85	129
500	60.4	135	205	49.5	111	168	46.0	103	156
1000	63.8	143	217	52.1	117	177	48.4	108	165
5000	70.5	158	240	57.7	129	196	53.4	119	182
10000	72.6	162	247	58.8	132	200	54.5	122	185

Note: mph* - equivalent 3-second gust speed (mph)

TABLE ii SUMMARY OF STATIC TEST RESULTS – BRIDGE DECK

		Smooth Flow	Turbulent Flow
Sidewalk Upstream	Angle of Attack α	0°	0°
	X-Force C_X	0.072	0.075
	Z-Force C_Z	-0.258	-0.279
	Lift Slope $dC_Z/d\alpha$	8.34	7.57
	Torque C_m	0.010	0.005
	Torque Slope $dC_m/d\alpha$	1.91	1.87
Sidewalk Downstream	Angle of Attack α	0°	0°
	X-Force C_X	0.076	0.075
	Z-Force C_Z	-0.362	-0.396
	Lift Slope $dC_Z/d\alpha$	6.46	6.99
	Torque C_m	0.015	0.012
	Torque Slope $dC_m/d\alpha$	1.02	1.04

TABLE iii SUMMARY OF DYNAMIC TEST RESULTS

Indian River Inlet Bridge, Dynamic Section Model Test Result Summary from Two Different Stages, 0 Degree Angle of Attack

SECTION MODEL TESTING with initial frequencies, February 2004

					Prototype Properties				Vmax at deck height	Flutter instability	Vortex induced vibration
NO.	**Test**	**Flow**	**Damping**	**Walkway Location**	**Mass**	**MMI**	**fv**	**ft**	**mph**		
					Lb/ft	Lb-ft^2/ft	Hz	Hz			
1	EYT301	smooth	0.1% in lift & 0.26% in torsion	upstream	45619	3.42E+07	0.77	1.71	220	Not observed	Not observed
2	DYN101	smooth	0.5% in lift & torsion	upstream	45619	3.42E+07	0.77	1.71	202	Not observed	Not observed
3	EYT201	turbulent	0.1% in lift & 0.26% in torsion	upstream	45619	3.42E+07	0.77	1.71	219	Not observed	Not observed
4	DYT101	turbulent	0.5% in lift & torsion	upstream	45619	3.42E+07	0.77	1.71	218	Not observed	Not observed
5	EYN101	smooth	0.1% in lift & 0.26% in torsion	downstream	45619	3.42E+07	0.77	1.71	229	Not observed	Not observed
6	DYN301	smooth	0.5% in lift & torsion	downstream	45619	3.42E+07	0.77	1.71	219	Not observed	Not observed
7	EYT101	turbulent	0.1% in lift & 0.26% in torsion	downstream	45619	3.42E+07	0.77	1.71	226	Not observed	Not observed
8	DYT102	turbulent	0.5% in lift & torsion	downstream	45619	3.42E+07	0.77	1.71	218	Not observed	Not observed

SECTION MODEL TESTING with modified frequencies, June 2004

					Prototype Properties				Vmax at deck height	Flutter instability	Vortex induced vibration
NO.	**Test**	**Flow**	**Damping**	**Walkway Location**	**Mass**	**MMI**	**fv**	**ft**	**mph**		
					Lb/ft	Lb-ft^2/ft	Hz	Hz			
1	PWU101	smooth	0.13% in lift & 0.6% in torsion	upstream	45619	3.42E+07	0.73	0.87	231	Not observed	Not observed
2	PWD101	smooth	0.13% in lift & 0.6% in torsion	downstream	45619	3.42E+07	0.73	0.87	230	Not observed	Not observed
3	PWD201	turbulent	0.5% in lift & 0.6% in torsion	downstream	45619	3.42E+07	0.73	0.87	239	Not observed	Not observed
4	PWU201	turbulent	0.5% in lift & 0.6% in torsion	upstream	45619	3.42E+07	0.73	0.87	239	Not observed	Not observed

TABLE iv SUMMARY OF RESULTS FROM STATIC TESTS ON INDIAN RIVER INLET BRIDGE ARCH

	Recommended Value for Design	Slope
C_{Fx}	0.95	
C_{Fy}	0.45	~ 0
C_{Mz}	0.07	-0.21

TABLE v MAGNITUDE OF PRESSURES FOR THE VARIOUS COMPONENTS OF THE EQUIVALENT STATIC LOAD DISTRIBUTIONS CORRESPONDING TO A 100-YEAR RETURN PERIOD MEAN HOURLY WIND SPEED AT ARCH CROWN = 110 MPH

Component	Magnitude
Mean, P_{mean} *	30 psf
Quasi-Steady, P_Q	15 psf
Symmetric, P_{sym}	40 psf
Anti-Symmetric, $P_{antisym}$	8.5 psf

TABLE vi SUMMARY OF FULL BRIDGE AEROELASTIC MODEL TESTS, INDIAN RIVER INLET BRIDGE

Bridge Configuration	No. of Tests	Flow Conditions	Wind Directions	Existing Bridge and Construction Cranes
Completed Bridge	15	Smooth flow, low turbulent flow, hurricane exposure and open country exposure	0° (along deck), 30°, 60°, 90° (perpendicular to deck) and 270°	Existing bridge
Cantilevered Tie-Beam*	11	Smooth flow, hurricane exposure and open country exposure	0° (along deck), 30°, 60°, 90° (perpendicular to deck) and 270°	Existing bridge
Cantilevered Arch*	12	Smooth flow, hurricane exposure and open country exposure	0° (along deck), 30°, 60°, 90° (perpendicular to deck) and 270°	Existing bridge and one construction crane on arch
Bridge Prior to Deck Completion*	13	Smooth flow, hurricane exposure and open country exposure	0° (along deck), 30°, 60°, 90° (perpendicular to deck) and 270°	Existing bridge and two construction cranes on deck

***** Supporting towers were used at both sides of the bridge in the under-construction stages in the test to support the arch.

TABLE vii SUMMARY OF FULL BRIDGE AEROELASTIC MODEL TESTS, COMPLETED BRIDGE CONFIGURATION

Test File	Test No.	Flow condition	Existing bridge	Wind direction (Test angle)	V_{deck} (mph) Maximum wind speed at deck height	Vortex Peak Locations
IFA102	1	Bare tunnel floor (low turbulent flow)	No	Perpendicular to bridge (90°)	155	40 ~ 50 mph, 80 mph, 105 mph, 135 mph
ITA201	2	Hurricane profile	Yes	Perpendicular to bridge (90°)	142	40 ~ 50 mph
IFA201	3	Hurricane profile	No	Perpendicular to bridge (90°)	141	40 ~ 50 mph
IFB201	4	Hurricane profile	No	60° to the bridge	141	50 mph
IFC201	5	Hurricane profile	No	30° to the bridge	143	N/A
IFD201	6	Hurricane profile	No	Along the bridge (0°)	144	N/A
IFE201	7	Hurricane profile	No	Perpendicular to bridge (270°)	141	40 mph
IFA301	8	Open Country profile	Yes	Perpendicular to bridge (90°)	143	40 mph
IFA302	9	Open Country profile	No	Perpendicular to bridge (90°)	143	40 mph
IFB302	10	Open Country profile	No	60° to the bridge	141	N/A
IFC302	11	Open Country profile	No	30° to the bridge	146	N/A
IFD302	12	Open Country profile	No	Along the bridge (0°)	145	N/A
IFE302	13	Open Country profile	No	Perpendicular to bridge (270°)	144	40 mph
IFA303	14	Open Country Profile (higher arch damping)	No	Perpendicular to bridge (90°)	144	N/A
IFA402	15	Smooth Flow (bridge elevated)	No	Perpendicular to bridge (90°)	148	45 mph, 80 mph, 110 mph, 140 mph

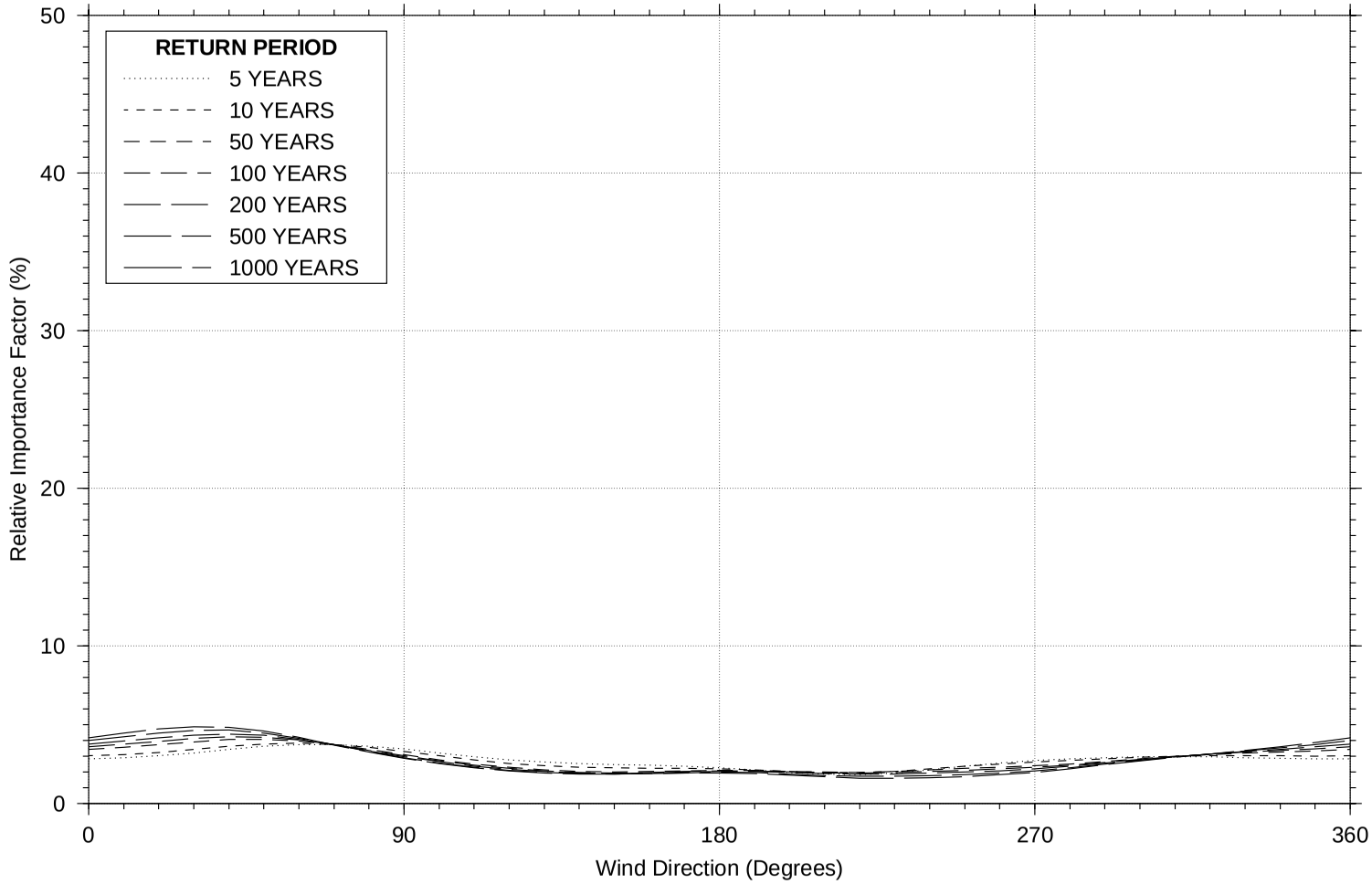

FIGURE i RELATIVE IMPORTANCE FACTORS FOR VARIOUS WIND DIRECTIONS AND MAXIMUM WIND SPEEDS WITH DIFFERENT RECURRENCE INTERVALS AT 83.5 m (274 ft) ABOVE WATER LEVEL FOR INDIAN RIVER INLET

FIGURE ii PREDICTED EXTREME HOURLY-MEAN WIND SPEEDS FOR VARIOUS RETURN PERIODS FOR HURRICANE WINDS AT 10 m (33 ft), 16.8 m (DECK HEIGHT OF 55 ft), 83.5 m (ARCH LEVEL OF 274 ft) AND 500 m LEVEL (1640 ft)

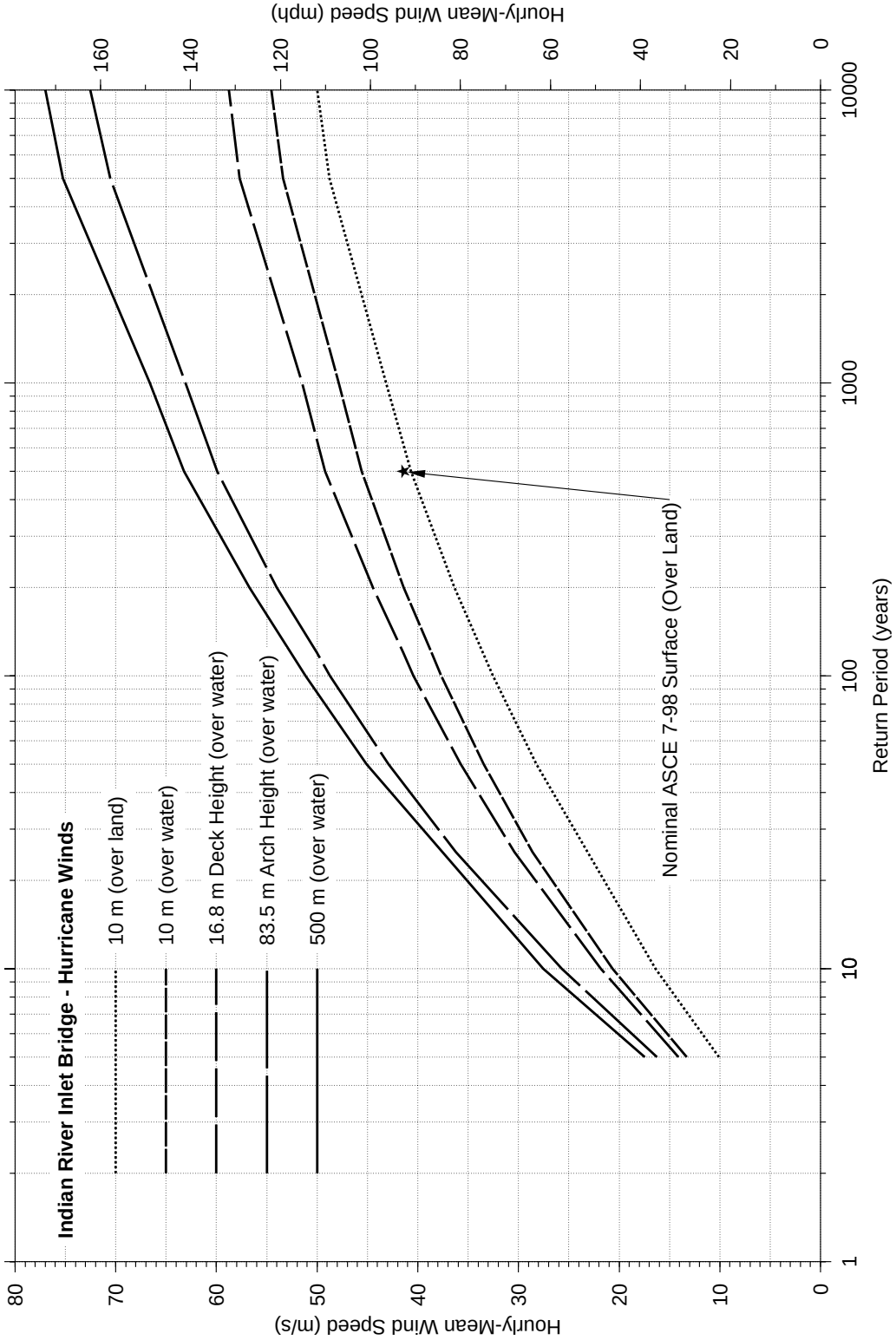
Indian River Inlet Bridge - Hurricane Winds
10 m (over land)
10 m (over water)
16.8 m Deck Height (over water)
83.5 m Arch Height (over water)
500 m (over water)
Nominal ASCE 7-98 Surface (Over Land)
Hourly-Mean Wind Speed (m/s)
Hourly-Mean Wind Speed (mph)
Return Period (years)
0
10
20
30
40
50
60
70
80
0
20
40
60
80
100
120
140
160
1
10
100
1000
10000

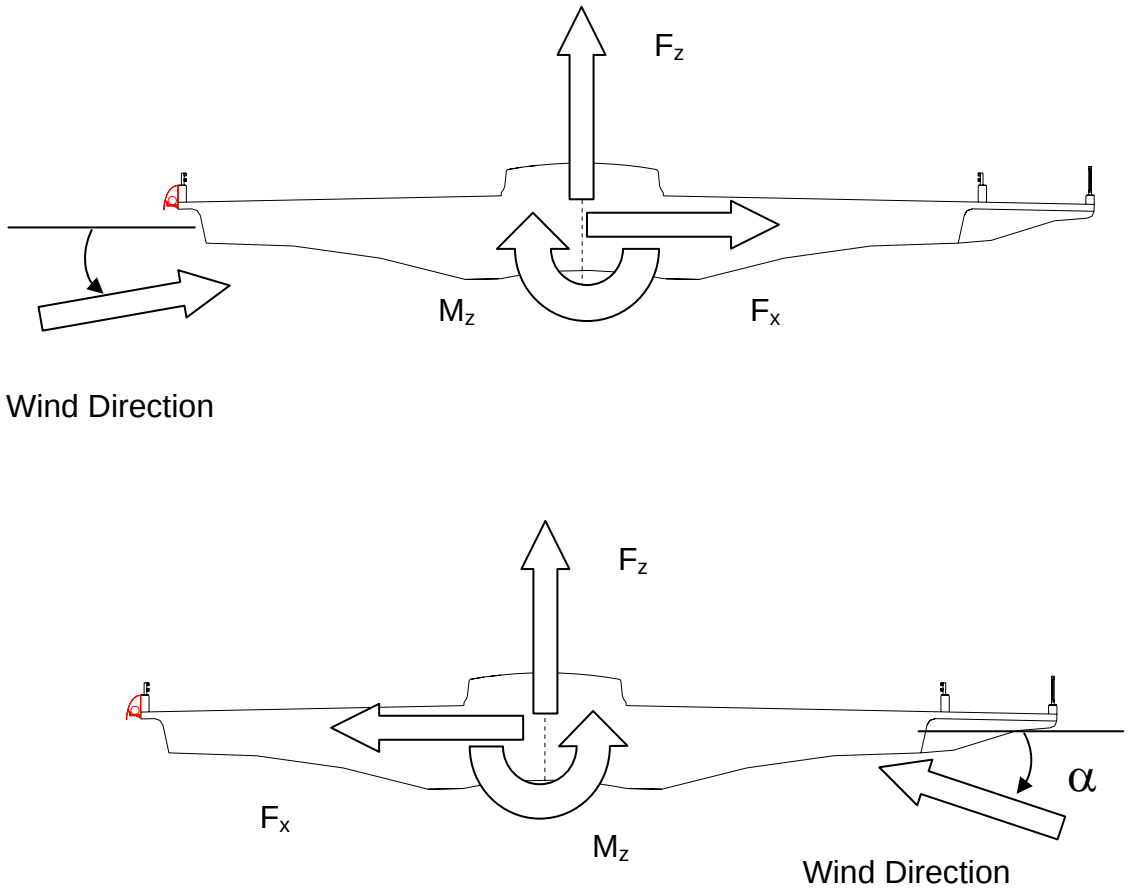

FIGURE iii SKETCH SHOWING SIGN CONVENTION OF FORCES

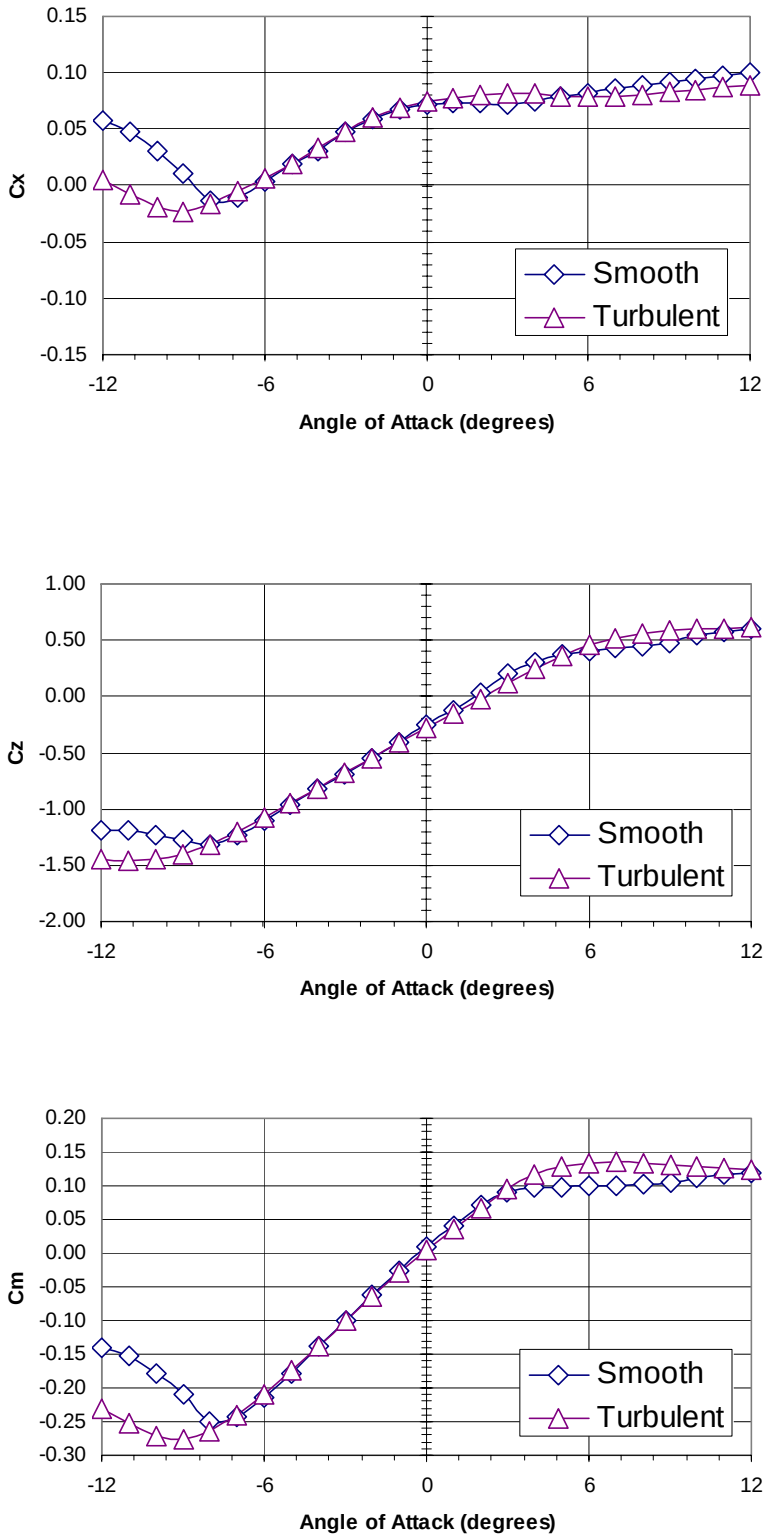

FIGURE iv STATIC FORCE COEFFICIENTS – SIDEWALK UPSTREAM

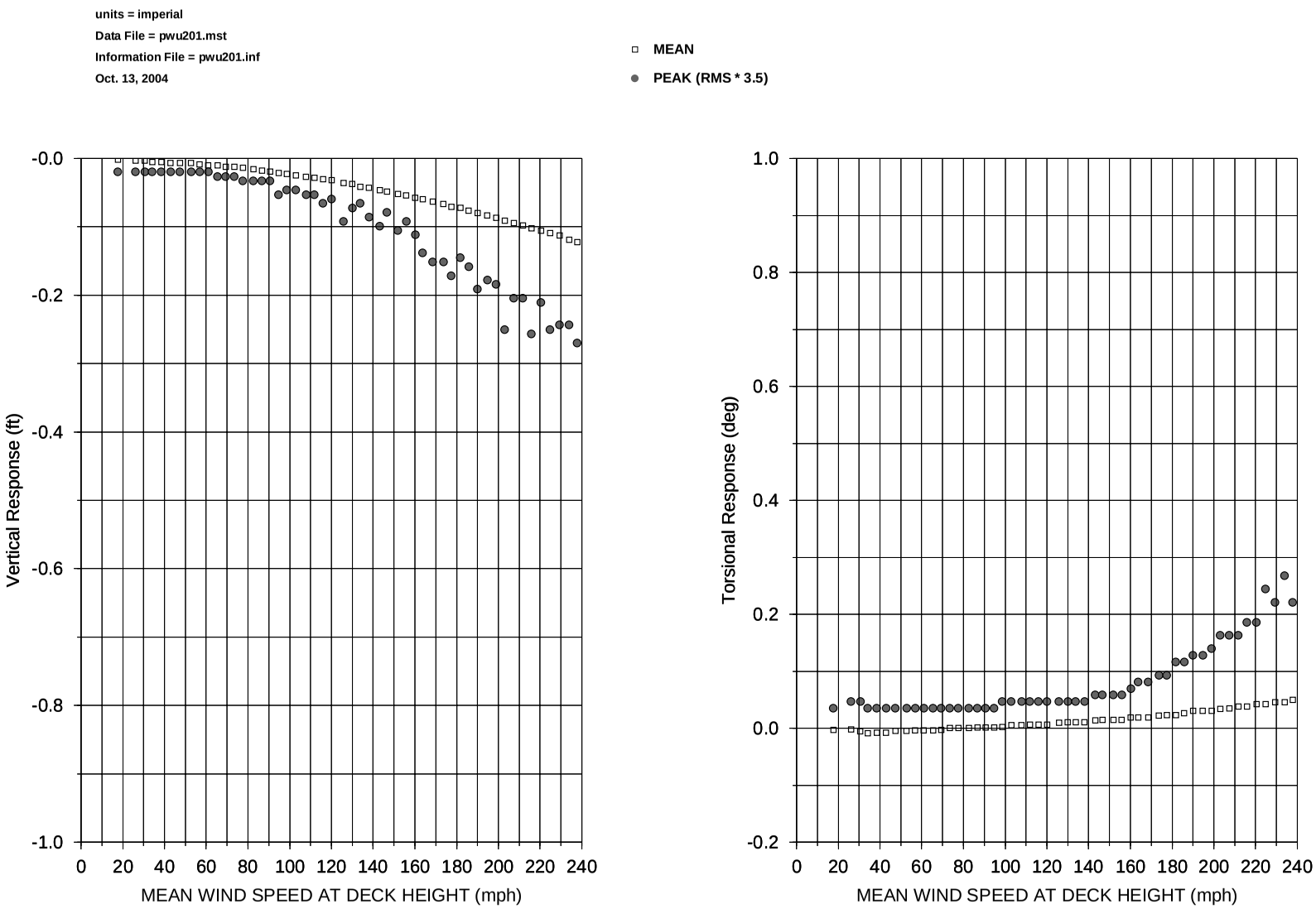

IRIB - Revised Properties, Sidewalk Upstream, Turb Flow, 0.5% Damping

FIGURE v DYNAMIC TEST RESULT, TURBULENT FLOW AT 0° ANGLE OF ATTACK, SIDEWALK UPSTREAM WITH MODIFIED FREQUENCIES

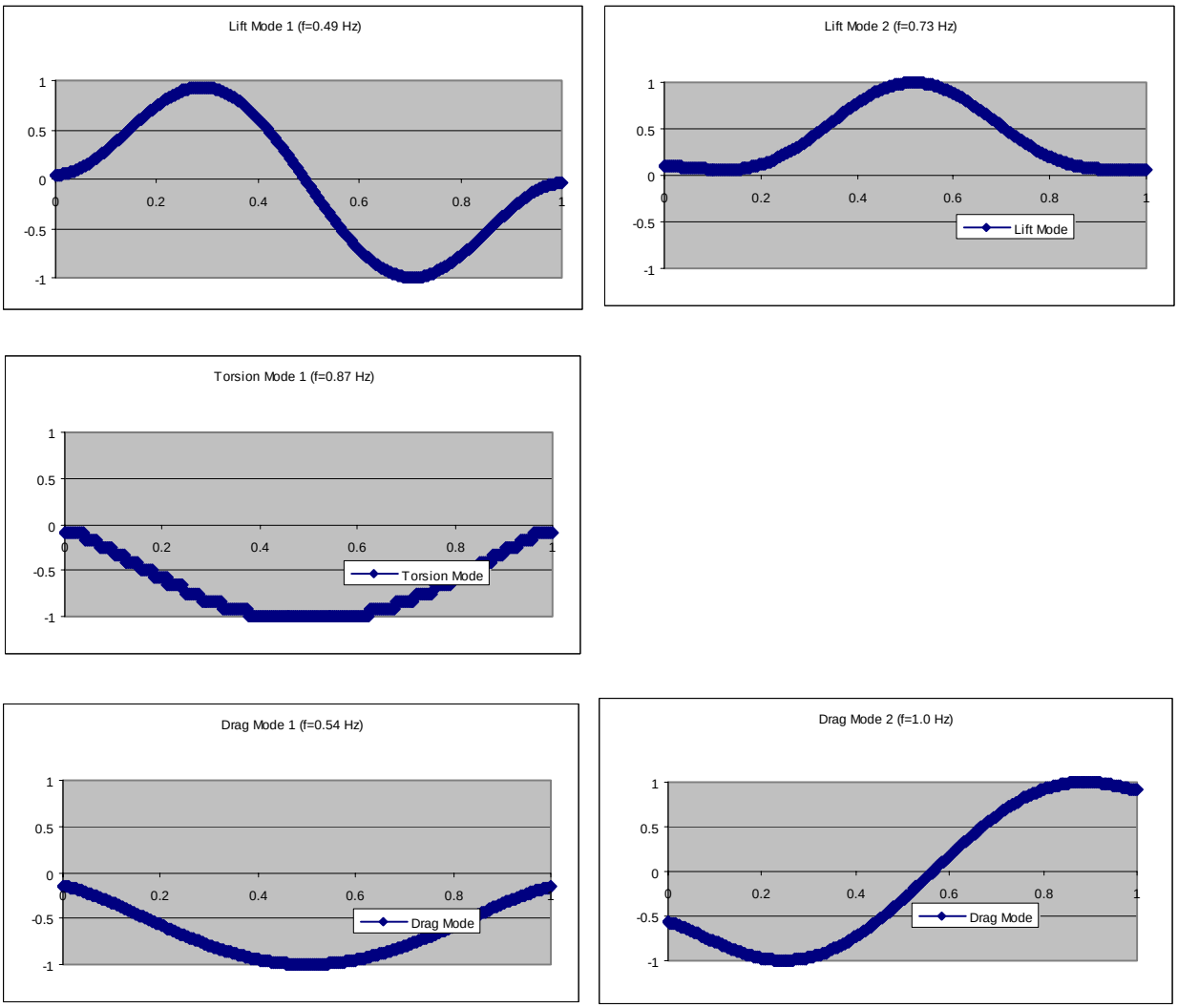

FIGURE vi MODE SHAPES USED IN THE EQUIVALENT STATIC LOAD ANALYSIS – BRIDGE DECK

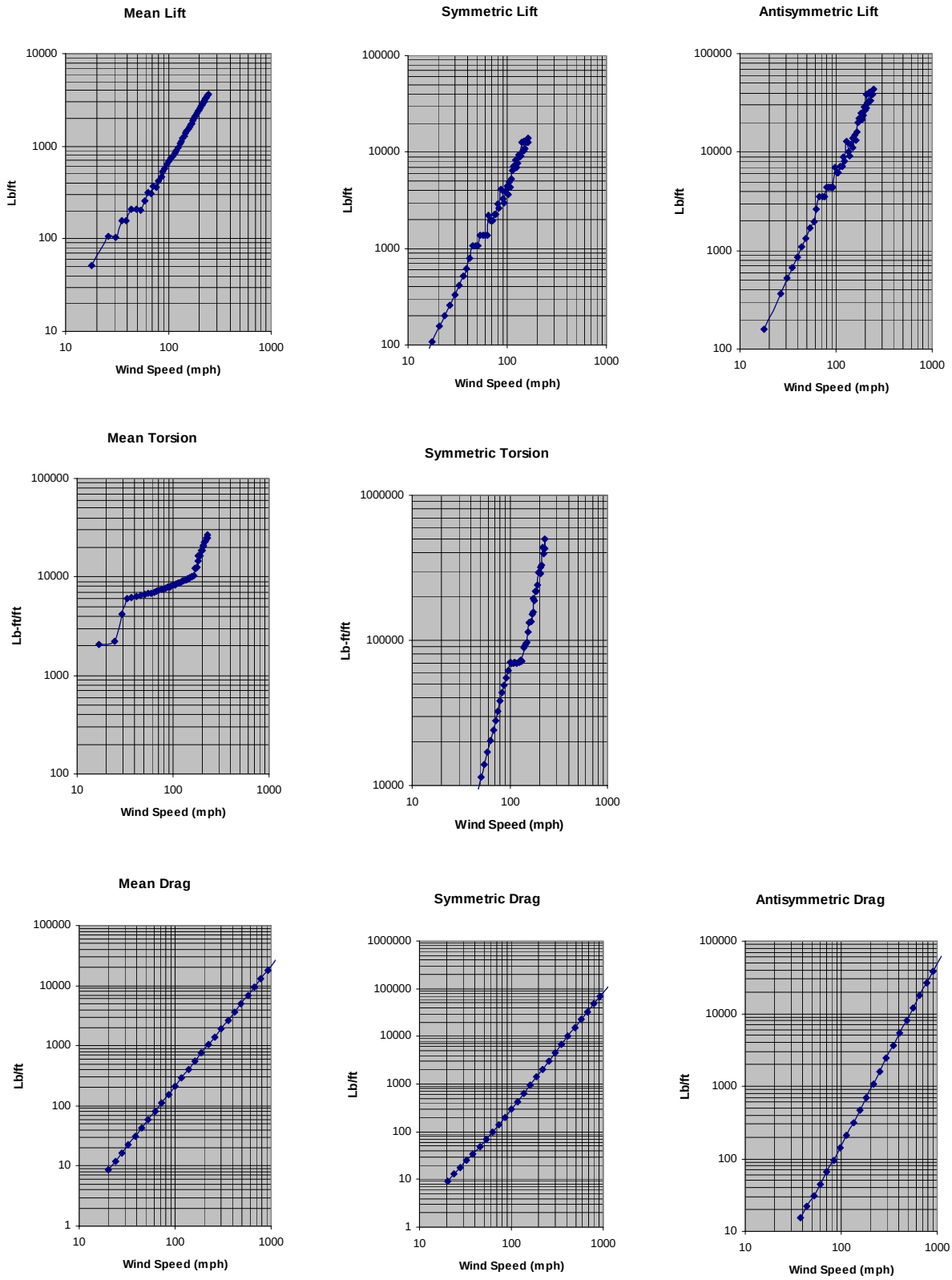

FIGURE vii WIND LOAD COMPONENTS FOR THE BRIDGE DECK – COMPLETED BRIDGE CONFIGURATION

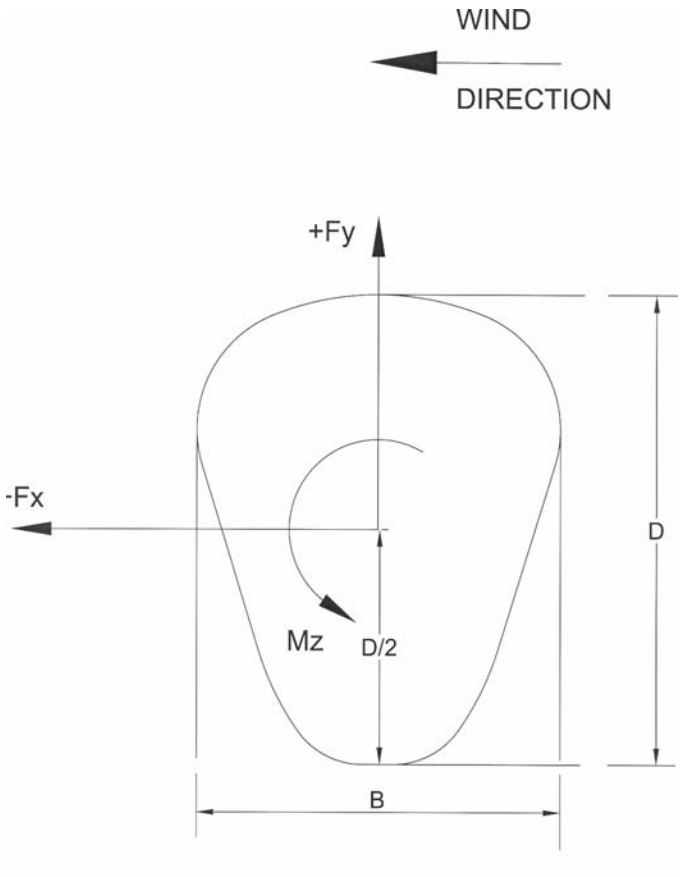

FIGURE viii SKETCH SHOWING THE SIGN CONVENTION OF FORCES – ARCH SECTION

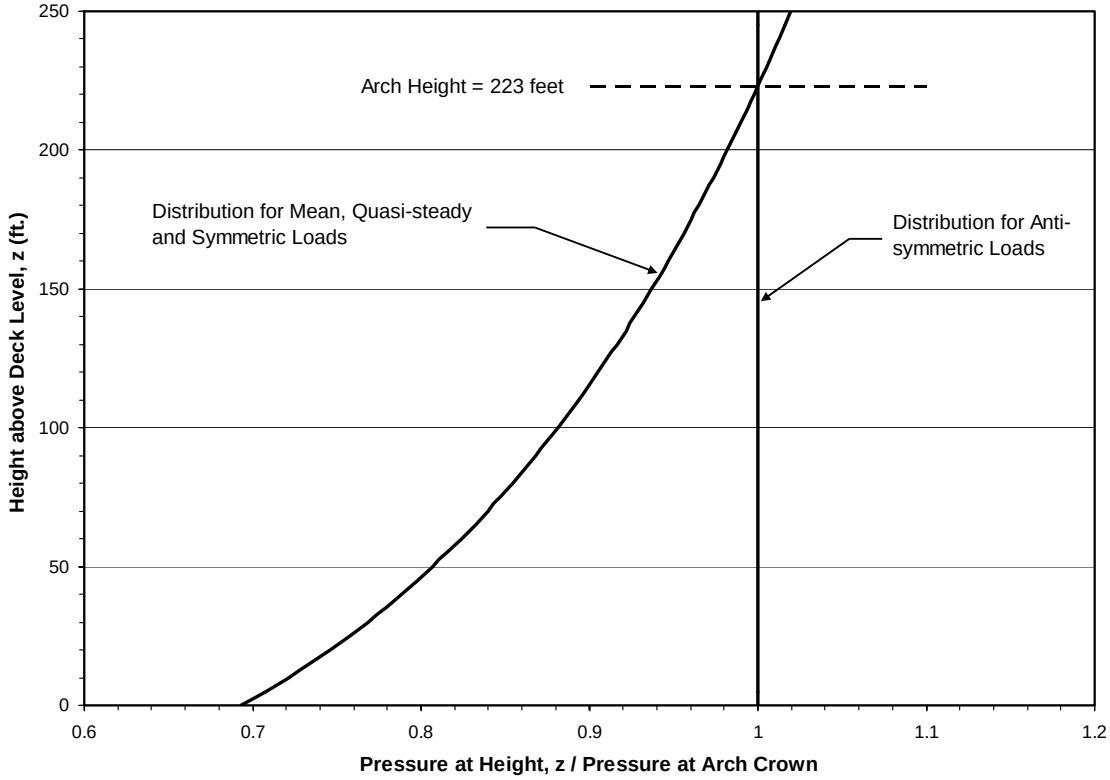

FIGURE ix DISTRIBUTION WITH HEIGHT OF THE VARIOUS COMPONENTS OF EQUIVALENT STATIC LOADS

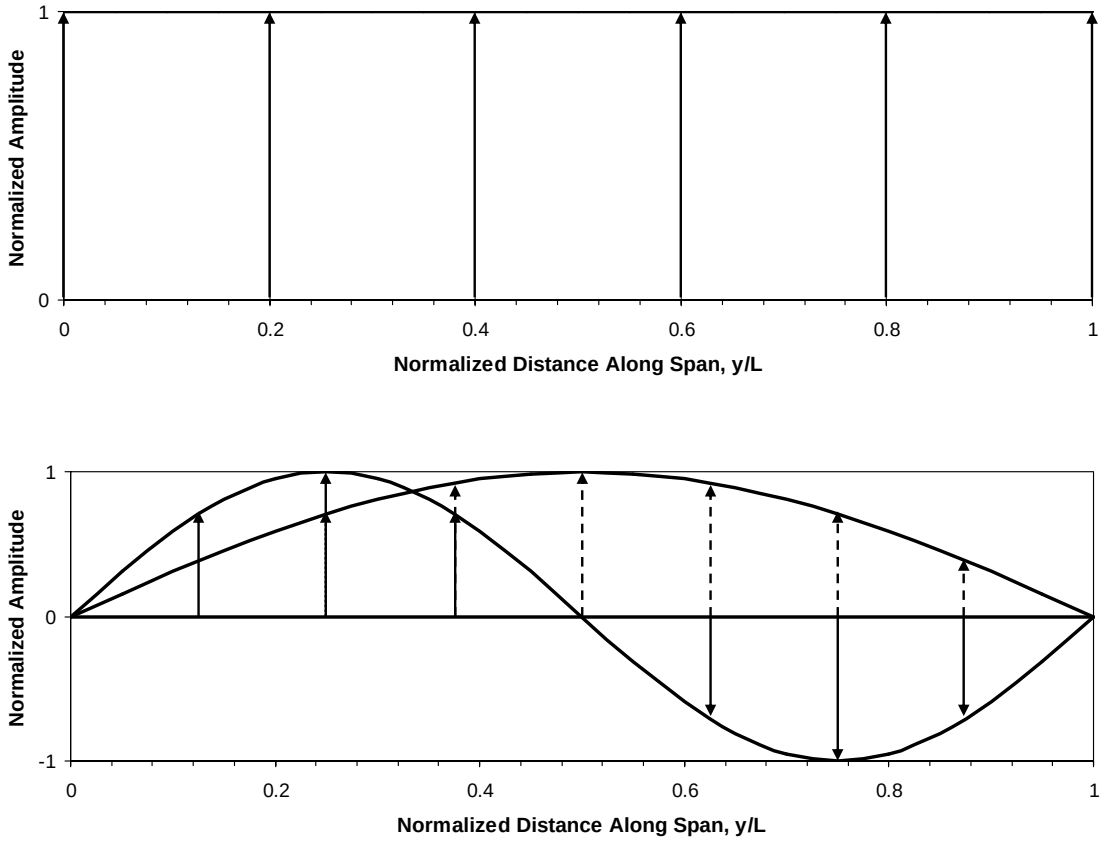

FIGURE x SPANWISE DISTRIBUTION OF THE MEAN AND QUASI-STEADY (TOP) AND SYMMETRIC AND ANTI- SYMMETRIC COMPONENTS (BOTTOM) OF THE EQUIVALENT STATIC LOADS

DETAILS OF THE STUDY

Project Name: The Indian River Inlet Bridge

Project Location: Indian River Inlet, Delaware.

Project Descriptions: The proposed Indian River Inlet bridge is a tied-arch bridge with a 1000 ft main span and two side spans of 150 ft. A 23 ft deep arch with a single plane of suspenders supports the 108'-6" wide deck. The deck sections are composed of precast concrete sections with traffic barrier, rounded nosing on one side and a cantilevered sidewalk on the other.

Test Dates:
Deck Section Model (Dynamic, initial frequencies) – February 2004
Deck Section Model (Static) – February 2004
Arch Section Model (Static) – February 2004
Deck Section Model (Dynamic, revised frequencies) – June 2004
Full Aeroelastic Model, completed bridge – May to June 2004
Full Aeroelastic Model, Construction Stages – September to November 2004

Preliminary Reporting:
Deck Section Model (Dynamic, initial frequencies) – March 2004
Deck Section Model (Static) – March 2004
Arch Section Model (Static) – March 2004
Deck Section Model (Dynamic, revised frequencies) – June 2004
Equivalent Static Loads for Bridge Arch – May 2004
Equivalent Static Loads for Bridge Deck – October 2004
Full Aeroelastic Model, completed bridge – May to June 2004
Full Aeroelastic Model, Construction Stages – September to November 2004

Report Scope: The report is organized as follows:

Section 1 – Introduction
Section 2 – The Modeling of the Wind
Section 3 - Section Model Study – Bridge Deck
Section 4 - Equivalent Static Load Analysis for Bridge Deck
Section 5 – Section Model Study – Arch Section
Section 6 – Structural Loads on Arch Rib
Section 7 – Full Aeroelastic Model Study

1 INTRODUCTION

1.1 General

This report describes the section model and full aeroelastic model studies of the proposed Indian River Inlet Bridge in Delaware. The proposed bridge is a tied arch with a 1000 ft main span and two side spans of 150 ft. A 23 ft deep arch with a single plane of suspenders supports the 108'-6" wide deck. The deck sections are composed of precast concrete sections with traffic barrier, rounded nosing on one side and a cantilevered sidewalk on the other.

Figure 1.1 shows the bridge and its overall dimensions. General outlines of the deck section and the supporting arch are shown in Figures 1.2 and 1.3 respectively.

A primary objective of the section model study for the deck section was to investigate the overall aeroelastic stability in high wind conditions and define the wind speeds associated with possible flutter instability and vortex shedding induced oscillation within the design criteria for wind. The investigation also served the purpose to define the dynamic response characteristics of the section to turbulent wind over a full range of wind speed and to provide information for the design of the overall structure against wind effects. The main purpose of the section model study for the arch section was to investigate the extent of the Reynolds number dependency in consideration of its curved surface. The bridge aeroelastic model was designed and constructed to determine the response characteristics of the bridge to three dimensional turbulent flow in simulated site wind conditions, over a full range of wind speeds. Four bridge configurations, including the completed bridge and three under construction stages, were studied in the aeroelastic model investigation.

Behavior of the 1:80 scale deck section model and the 1:40 scale arch section model were studied in the 3.4m wide by 2.5m high High-Speed Test Section in the Boundary Layer Wind Tunnel II (BLWTII) located at the Boundary Layer Wind Tunnel Laboratory, the University of Western Ontario. Section model tests were conducted at the inlet to the test section in both smooth flow and grid-generated turbulent flow conditions. The 1:150 scale bridge aeroelastic models were tested on the turntable in the Low Speed Test Section of BLWTII under two wind profiles, a hurricane profile corresponding to a roughness length of Z_o=0.025ft and a typical open country exposure corresponding to a roughness length of Z_o=0.1ft. An additional "smooth flow" test was carried out with the bridge model elevated above the boundary layer of the tunnel floor in order to identify any potential vortex shedding induced vibration and flutter instability.

1.2 Scope of Report

A wind climate study was carried out for the Indian River Inlet Bridge (see Section 2). The design probability distribution of surface wind speed and direction was developed on the basis of full scale meteorological records from nearby weather stations. Monte Carlo simulations of the tropical storms were also carried out to assess their impact on extreme winds expected to affect the Indian River Bridge.

A rigid section model for the basic deck cross section was designed and constructed at a scale of 1:80. The total length of the model was 7ft. The section model was ballasted to the appropriate scaled mass and mass moment of inertia of the prototype and mounted on a dynamic test rig. The stiffness of the model support system was adjusted to simulate the appropriate scaled frequencies of the prototype in lift and torsion. The model was tested in both smooth and turbulent flow conditions to measure the response of the deck section (see Section 3).

Information from the static and dynamic section model tests were used in combination with mode shapes and frequencies to predict the full scale equivalent static loads for the structure (see Section 4).

An arch section model was constructed at a scale of 1:40, which was tested with the static force balance. Tests were carried out in the same flow fields (smooth and turbulent) as the bridge deck. A similar range of Reynolds numbers was investigated. In addition, a second series of tests were conducted to investigate the extent of the Reynolds number dependency because of its curved surface (see Section 5).

The structural loads analysis for the arch structure follows the well established procedure for calculating the response of line-like structures to wind action. The details of this procedure are presented in Appendix G. Equivalent static loads were then derived based on the overall bending moment at the base of the arch (see Section 6).

Full aeroelastic models of the bridge were designed and constructed at a geometric scale of 1:150 relative to the prototype. Four bridge configurations, including the completed bridge and three under construction stages, were studied. The models were tested for representative site wind conditions (see Section 7). Two typical upstream terrain conditions, a hurricane exposure and an open country exposure, were used in the tests. Measurements of bridge responses were taken at five different wind angles of 0°, 30°, 60°, 90° and 270°. The 90° wind denotes the pedestrian walkway upstream. The wind characteristics generated in the wind tunnel are considered to be good representation of the wind conditions at the bridge site. In addition, tests were also conducted at 90° wind with the existing bridge upwind to assess its effect on the proposed Indian River Bridge. An additional “smooth flow” test was carried out with the bridge model elevated above the boundary layer of the tunnel floor in order to identify any potential vortex shedding induced vibration and flutter instability.

Presented in this report are results from:

- the results of the meteorological study;
- the static section model tests of the bridge deck (the static force coefficients);
- the dynamic section model tests of the bridge deck (response to vortex shedding and flutter instability in smooth flow, and buffeting responses in turbulent flow);
- the equivalent static loads of the bridge deck;
- the static section model tests of the arch section (the static force coefficients and their variations with Reynolds number);
- the equivalent static loads of the arch section;
- the bridge aeroelastic model tests for four bridge configurations, including the completed bridge and three under construction stages.

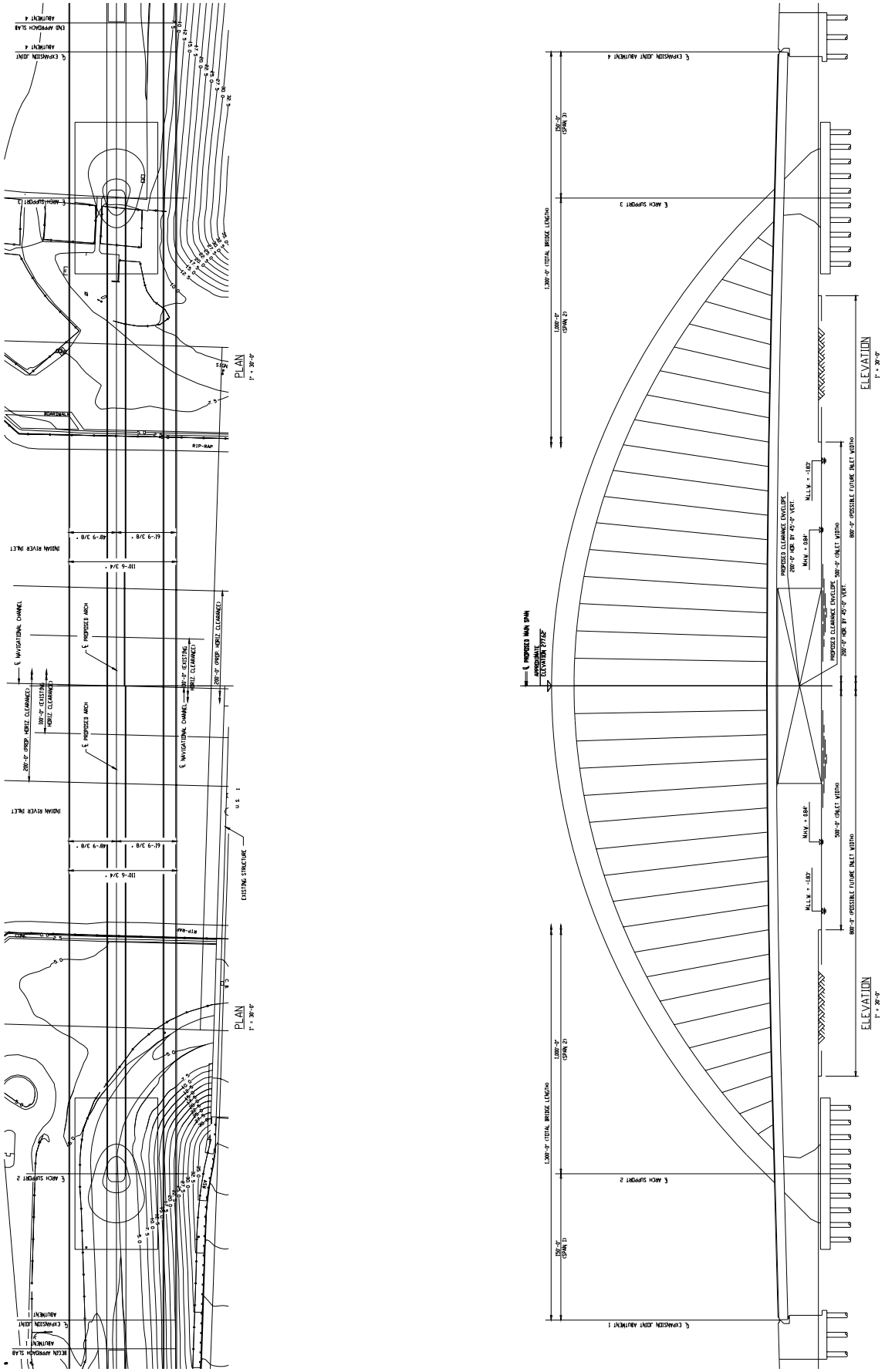

FIGURE 1.1 PROTOTYPE DIMENSIONS – BRIDGE OUTLINE

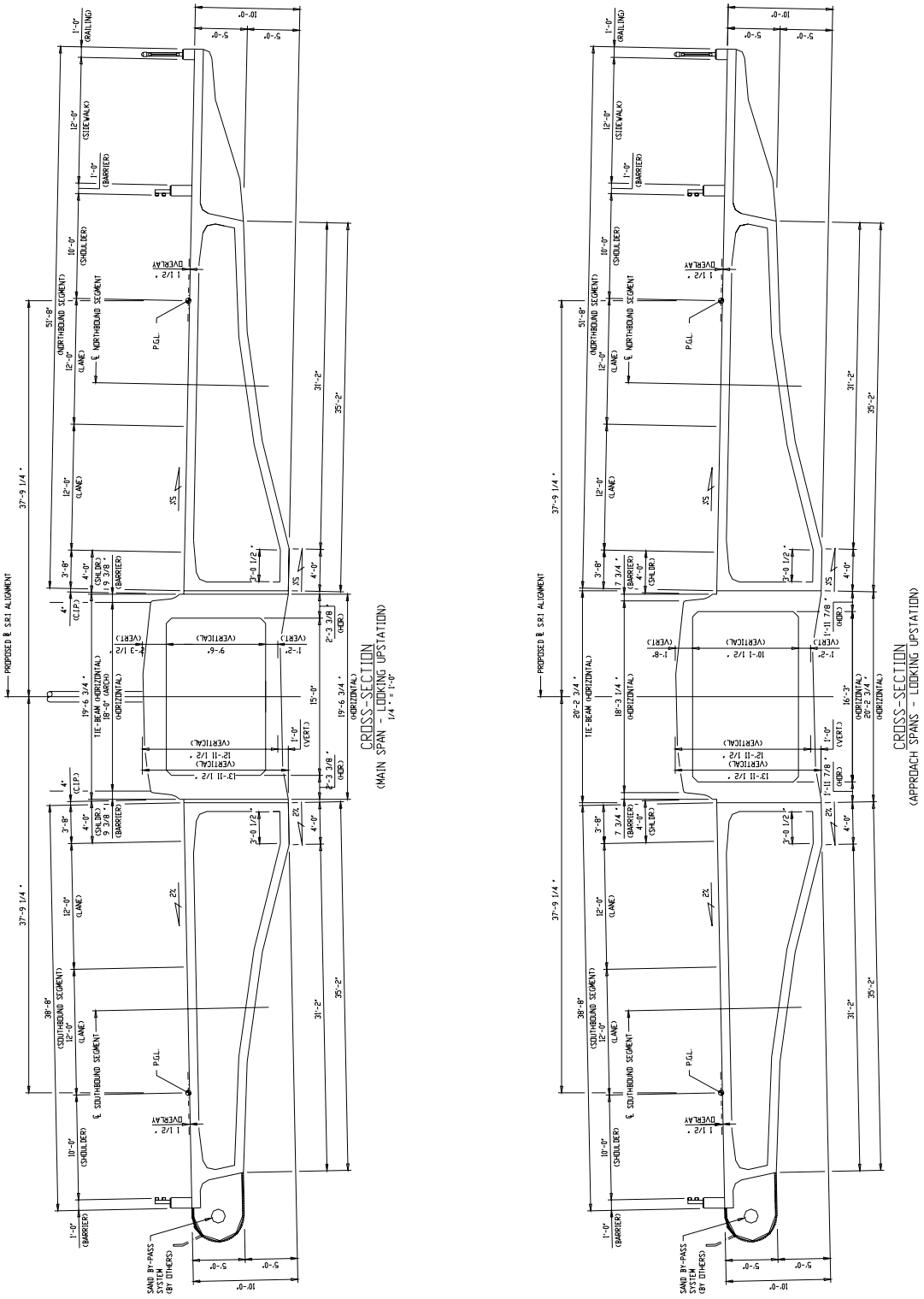

FIGURE 1.2 PROTOTYPE DIMENSIONS – BRIDGE DECK CROSS SECTION

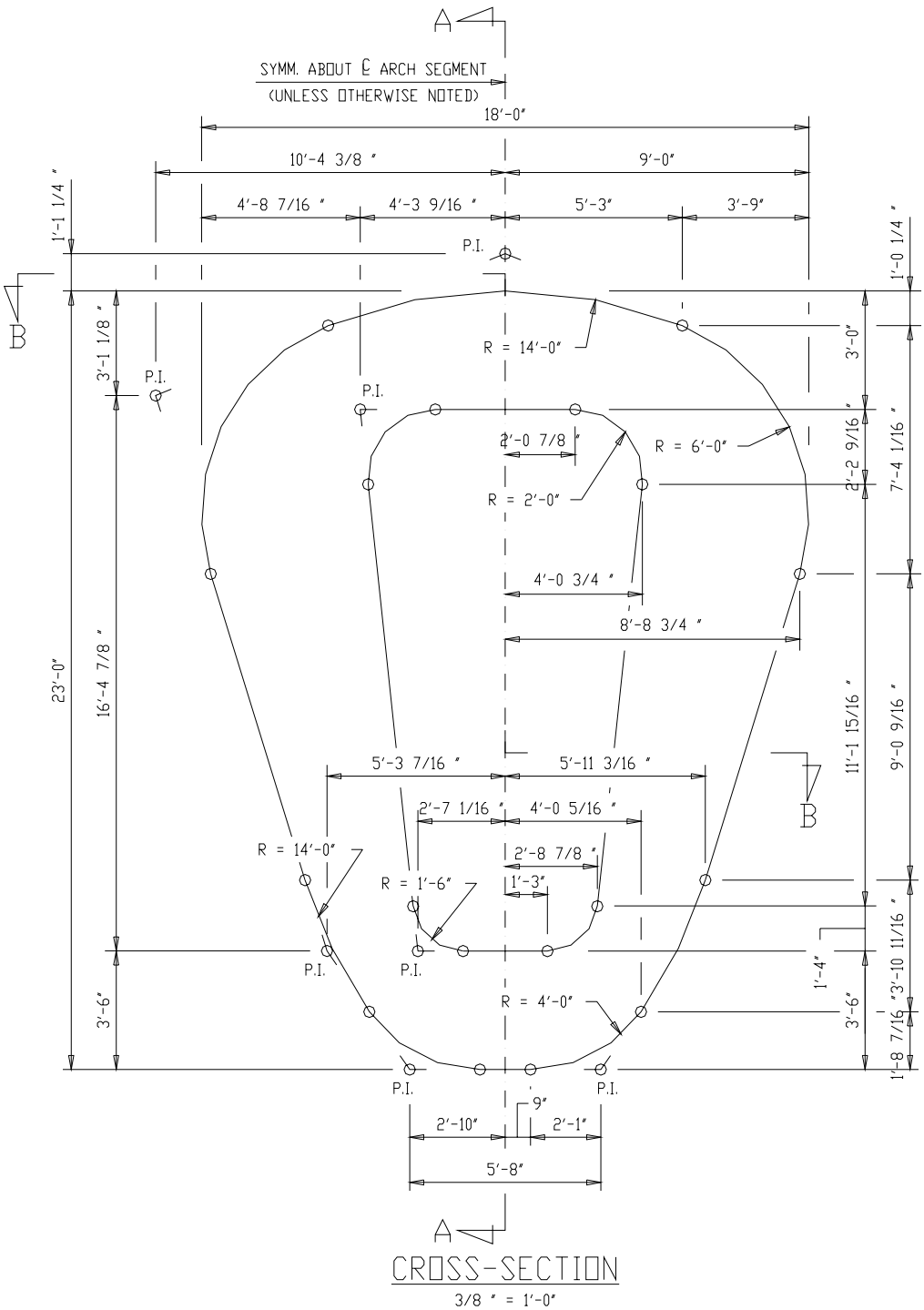

FIGURE 1.3 PROTOTYPE DIMENSIONS – ARCH SECTION

2 THE MODELLING OF THE SITE AND THE WIND

2.1 Introduction

This report presents the findings of a study carried out to evaluate the statistical wind climate for the Indian River Inlet Bridge. This is a companion study to the wind tunnel investigations in support of the design for the Bridge. Wind tunnel model studies provide information on wind forces and different measures of the bridge performance during wind events for which the speed and the direction of the approach wind are known. The wind climate provides a statistical prediction of the combinations of wind speed and wind direction which are expected at the bridge site. This information is then used to put the wind tunnel findings into context and to assess the risk of exceeding different levels of the bridge response during its design lifetime and beyond.

A statistical model of the wind climate can be determined from historical records of previously-observed wind speed and wind directions at particular weather stations. The locations of these weather stations should be such that the observed winds can be reliably related to those at the site of interest. Figure 2.1 shows the location of the bridge and the locations of the three principal nearby weather stations. These are weather stations at Atlantic City, NJ, Wallops Island, VA and Dover AFB in Delaware. Surface wind-speed observations are typically made at 10 m above local ground in open-country type exposures at these airports. These sites are usually free of the influence of the local terrain roughness and provide representative measures of wind speed and wind direction for the region.

The study also includes Monte Carlo computer simulations of tropical storms and assesses their impact on extreme winds expected to affect the Indian River Inlet Bridge in the future. The findings of the Monte Carlo simulations show that extreme winds in the Indian River Inlet area are expected to result due to hurricanes rather than extratropical storms. This diminishes the importance of historical records of surface wind data. Typical record lengths of such observations are not long enough to predict future hurricane events; hence the reliance on Monte Carlo simulations to assess hurricane risk. With the importance of surface data diminished, the detailed reconciliation of data at the Atlantic City, Wallops Island and Dover AFB anemometers becomes less important, except for commonly-occurring winds.

2.2 Analysis of Surface Wind Data

While the directional characteristics of surface data tend to be biased by local topographic differences, they are usually recorded much more frequently (8-24 readings per day) than upper-level measurements and hence offer better statistical estimates. An appropriate average conversion factor, relating mean surface and gradient wind speeds, can usually be estimated for sites with an open exposure (i.e. airports). The bases for such conversion factors are the power law (see Appendix A of Reference 1) and established values for the power law exponent and gradient height. Thus, the overall speed predictions arising from surface data are generally better than their directional characteristics.

Surface wind speed and wind direction data for Atlantic City, NJ, Wallops Island, VA and Dover AFB in Delaware were obtained as time histories of wind speed and direction. A location map for the various sites is shown in Figure 2.1. The time histories of wind speed and direction were processed to remove any data associated with known historical tropical storms in the area and then formed into monthly and annual frequency histograms of wind speed versus wind direction. The annual and seasonal frequency histograms were analyzed using the methodology outlined in Reference 1.

The main characteristics of the surface wind climate for Dover AFB are summarized in Figures 2.2 and 2.3. Figure 2.2 shows the shows the annual probability distribution of the mean hourly wind speed and wind direction at the surface (10m) level. The radial distance to a probability contour for a particular wind direction indicates the wind speed which is exceeded with that probability level within a sector of 22.5^{o}. The innermost contour indicates the directional variation of common wind speeds (exceeded an average of 1% of the time from each azimuth sector) and is comparable to a conventional wind rose. The shape of the outermost contour indicates the directional preferences of extreme winds. The data

presented in Figure 2.2 indicate a directional preference of strong winds at the airport site from the northwest quadrant with a secondary lobe from the east.

Seasonal probability distributions are presented in Figure 2.3 (Winter season is the combined months of December, January and February). Summer is the least windy period with maximum winds most likely in the spring and winter. The directional characteristics of the wind climate do not change significantly with season.

Similar plots for the Atlantic City and Wallops Island sites are shown in Figures 2.4 through 2.7. Both of these stations show a directional preference of strong winds from the northwest and northeast sectors.

The directional characteristics of the surface wind climates are further illustrated in Figure 2.8 through 2.13. These diagrams shows the relative contribution of particular azimuth sectors to the exceedance of wind speeds associated with different recurrence frequencies. Data here are presented for average occurrence rates ranging from once per week through once per 500 years. Extreme winds are predominant from the northeast and northwest sectors.

The overall strength of the wind climate can be ascertained from the prediction of the hourly mean wind speed expected for a given return period, regardless of wind direction. The hourly-mean wind speeds predicted for various return periods at these stations, at a 10 m reference height in open-country exposure, are summarized in Figure 2.14

Also shown in Figure 2.14 is the nominal ASCE 7-98 [2] surface (over land) hourly mean wind speed. It is important to note that the current approach of the ASCE 7-98 is to predict 500-year wind speed and to reduce this by the square-root of the load factor to arrive at the “basic” wind speed. The basic wind speed is no longer directly associated with a 50-year return period.

The parent surface wind climate models were extrapolated to gradient height using the ASCE 7-98 Exposure ‘D’ power-law relationship (i.e. a factor of 1.4). Predicted hourly-mean wind speeds for various return periods are shown in Figure 2.14 by the group of curves labelled as ‘Gradient’.

2.3 Monte Carlo Simulation of Hurricane Winds

Historical wind records at a particular weather station are insufficient to reliably predict extreme wind speeds which may be expected due to future hurricane passages. Typically weather data are available for station records of 20 to 40 years and are unlikely to capture a significant number of hurricane events during the recording life of the station. The approach used to overcome this difficulty is to determine the statistical parameters of tropical storms for the project area and to use a Monte Carlo simulation of hurricane events over a period of 100,000 years so that a statistically meaningful sample of extreme winds at the project site can be examined. The average annual occurrence rate of these storms in the Indian River Inlet area is approximately 0.37. That is, on average, the area experiences one storm every three years. Depending on the storm track and the translation velocity, the duration of each storm passage may be 1 to 2 days. The procedures followed in such Monte Carlo simulations at the BLWTL are described elsewhere (Refs. 1 and 3).

Figure 2.15 shows the tracks of all tropical storms which have passed within 250 km of Indian River Inlet within the 1886 to 2000 period. Tropical storms are labelled as hurricanes when the one-minute sustained wind speed at 10 m above the water surface exceeds 64 knots anywhere within the storm system. The portions of tropical storm tracks with a sustained one-minute wind speed in excess of 64 knots (i.e. hurricane strength) are shown in Figure 2.16. The portions of tropical storms tracks which have reached tropical-storm strength are shown in Figure 2.17. In the northern hemisphere, the maximum wind speeds within a hurricane storm cell are to the right of the track which traces the movement of the eye of the hurricane. From Figure 2.16 it is clear that the majority of past hurricanes have passed to the south and the east of the bridge site and the corresponding maximum winds would have been experienced over water. This is fortuitous.

2.4 Design Wind Climate for Bridge Site

In addition to selecting a full-scale wind speed which is unaffected by the local terrain, it is also important that this reference value can be related to wind speeds in the wind tunnel model simulation. This matching of model and full-scale reference speeds is essential in order to permit the transfer of wind-tunnel data to full scale. For this reason, two reference levels for the final design wind climate models were chosen to be the deck height (i.e. 55 feet or 16.8 m above water level) and the top of the bridge arch (i.e. 274 feet or 83.5 m above water level). The choice of these reference levels is consistent with state-of-the-art wind tunnel modelling techniques and properly relates model and full-scale values.

The variation of wind speed with height (from the surface upwards) has been modeled using a logarithmic profile law, which is valid in the lower ~100m of the boundary layer. The variation of the hourly-mean wind speed with height is given as:

$$U(z) = U_{10} \frac{\ln(z / z_o)}{\ln(10 / z_o)}$$

where *U(z)* is the hourly-mean wind speed at height *z*, U_{10} is the hourly-mean wind speed at a height of 10m above the surface and z_o is the aerodynamic surface roughness length, which is normally assigned a value of 0.03 m for smooth open terrain (typical of an airport).

The hurricane wind speeds are given for the case of the wind blowing over the water, and thus the surface roughness parameter, z_o varies with the mean wind speed. The variation of the roughness length with wind speed is modeled through the following:

$$z_o = 10.0 \times \exp(-0.4 / \sqrt{C_d})$$
$$C_d = (1.026 \times 0.05366 U_{10}) \times 10^3$$

Figure 2.18 shows the probability distribution of wind speeds and directions at the 274 ft (83.5 m) level for Indian River Inlet area obtained from the Monte Carlo simulation of hurricane passages over a simulation period of 100,000 years. The characteristics of these hurricanes, including the central pressure, the translational speed, the track angle and the distance to the maximum wind speed are described by their statistical properties, as determined from tropical storms passing within 250 km of the bridge site (see Figure 2.15).

Relative importance factors for the hurricane wind climate model are shown in Figure 2.19. Strong winds during hurricane events are equally likely to come from any wind direction with a slight preference to the northeast sector. This is consistent with the observation that the majority of hurricane tracks pass to the southeast of the site, thus locating Indian River Inlet on the 'weaker' side of the eye wall.

Predictions of the hourly-mean wind speed for winds blowing over water at various heights, regardless of wind direction, are shown in Figure 2.20. Predicted hourly-mean wind speeds at various heights above water for wind blowing over water are also presented in Table 2.1.

The prediction of extreme winds likely to be seen by the bridge does not rely on a reconciliation of the directional characteristics of the surface non-hurricane wind data. Extreme winds in the Indian River Inlet area are expected to result due to tropical rather than extratropical storms.

TABLE 2.1 PREDICTED HOURLY-MEAN WIND SPEEDS AT VARIOUS HEIGHTS FOR WINDS BLOWING OVER WATER

Return Period (Years)	Arch Height (274 ft)			Deck Height (55 ft)			Standard Anemometer Height (33 ft)		
	m/s	mph	mph*	m/s	mph	mph*	m/s	mph	mph*
50	43.1	96	147	35.9	80	122	33.6	75	114
100	49.1	110	167	40.7	91	138	38.0	85	129
500	60.4	135	205	49.5	111	168	46.0	103	156
1000	63.8	143	217	52.1	117	177	48.4	108	165
5000	70.5	158	240	57.7	129	196	53.4	119	182
10000	72.6	162	247	58.8	132	200	54.5	122	185

Note: mph* - equivalent 3-second gust speed (mph)

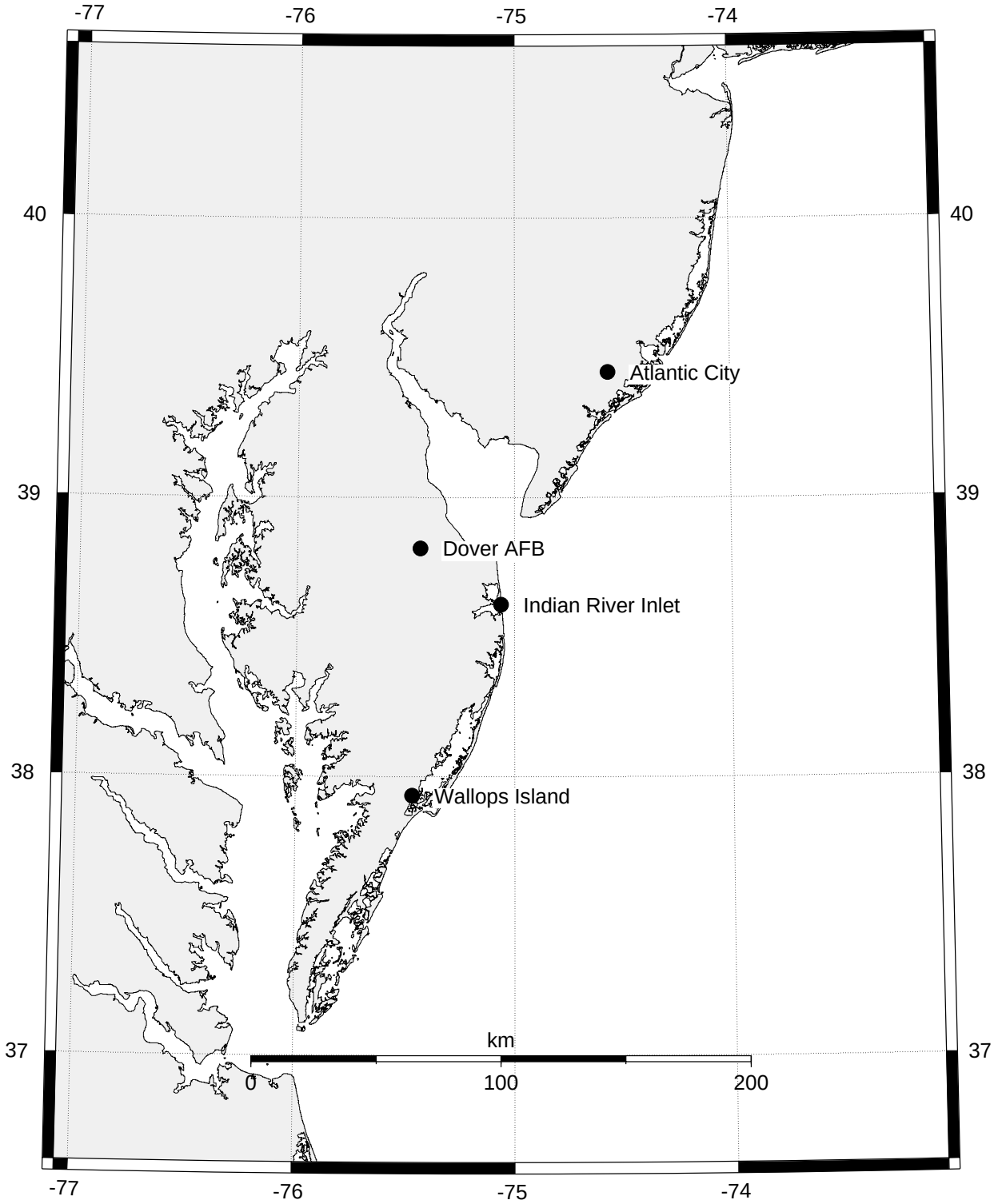

FIGURE 2.1 LOCATIONS OF THE INDIAN RIVER INLET BRIDGE AND PRIMARY WEATHER STATIONS

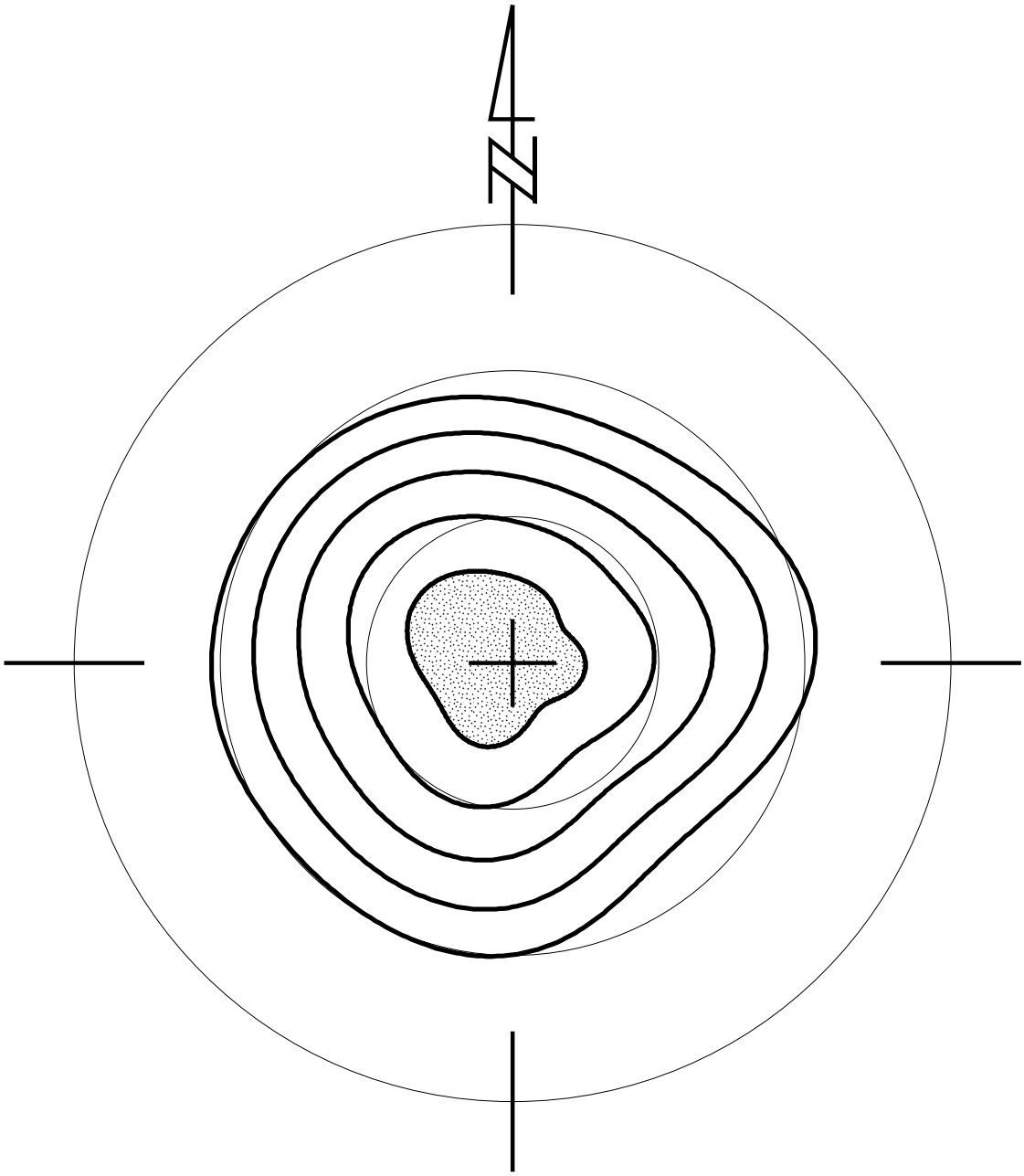

ANNUAL

Radial distances indicate wind speed in m/s

0 10 20

A point along the innermost contour represents the wind speed exceeded on average 1% of the time within a 22.5 degree sector centred on that direction. Other contours represent probability levels of 0.1%, 0.01%, 0.001% and 0.0001%, respectively.

Dover AFB - Surface

FIGURE 2.2 ANNUAL PROBABILITY DISTRIBUTION OF SURFACE HOURLY-MEAN WIND SPEED AND WIND DIRECTION – DOVER AFB, DELAWARE (1942-2003)

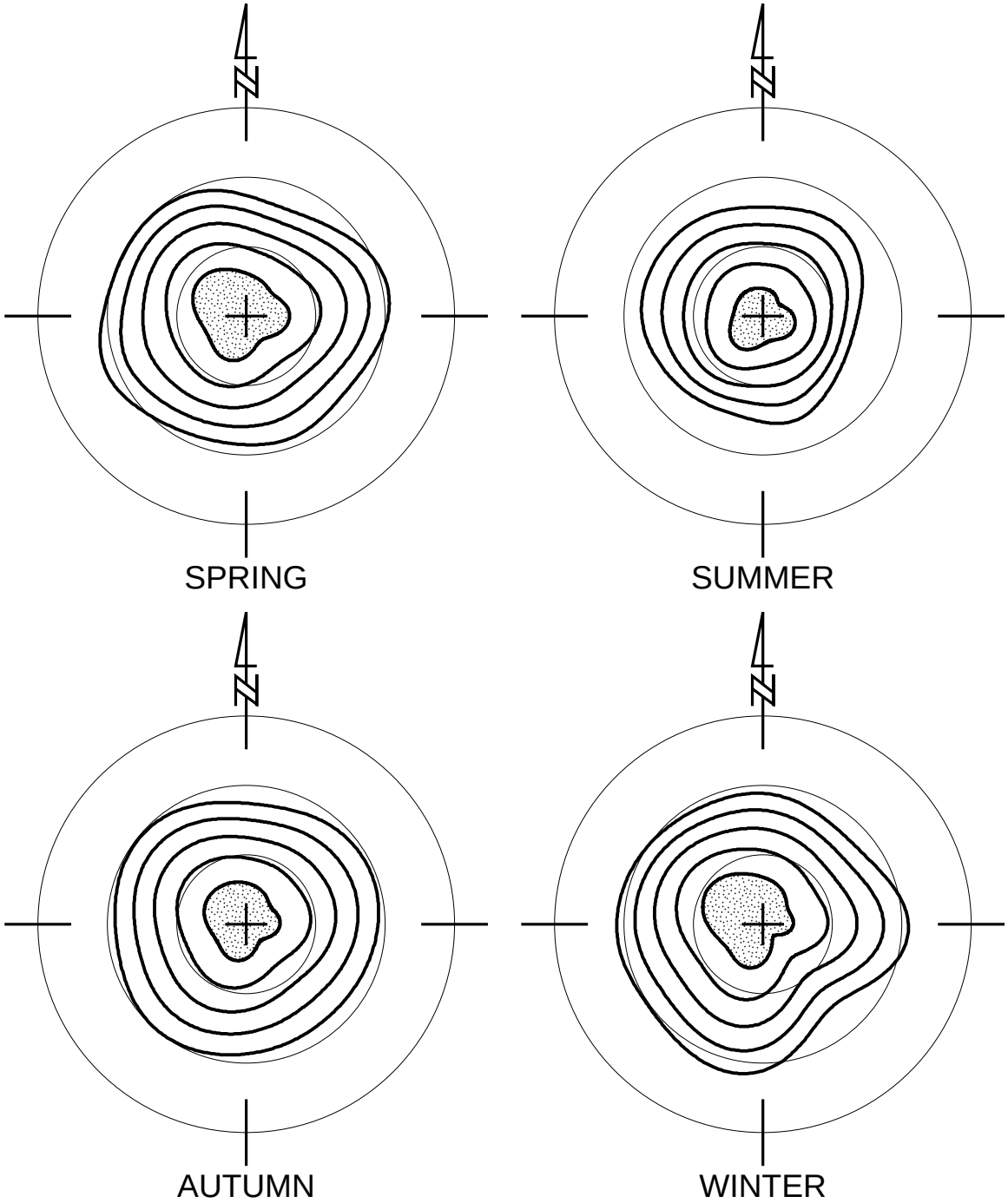

Radial distances indicate wind speed in m/s

0 10 20

A point along the innermost contour represents the wind speed exceeded on average 1% of the time within a 22.5 degree sector centred on that direction. Other contours represent probability levels of 0.1%, 0.01%, 0.001% and 0.0001%, respectively.

Dover AFB - Surface

FIGURE 2.3 SEASONAL PROBABILITY DISTRIBUTION OF SURFACE HOURLY-MEAN WIND SPEED AND WIND DIRECTION – DOVER AFB, DELAWARE (1942-2003)

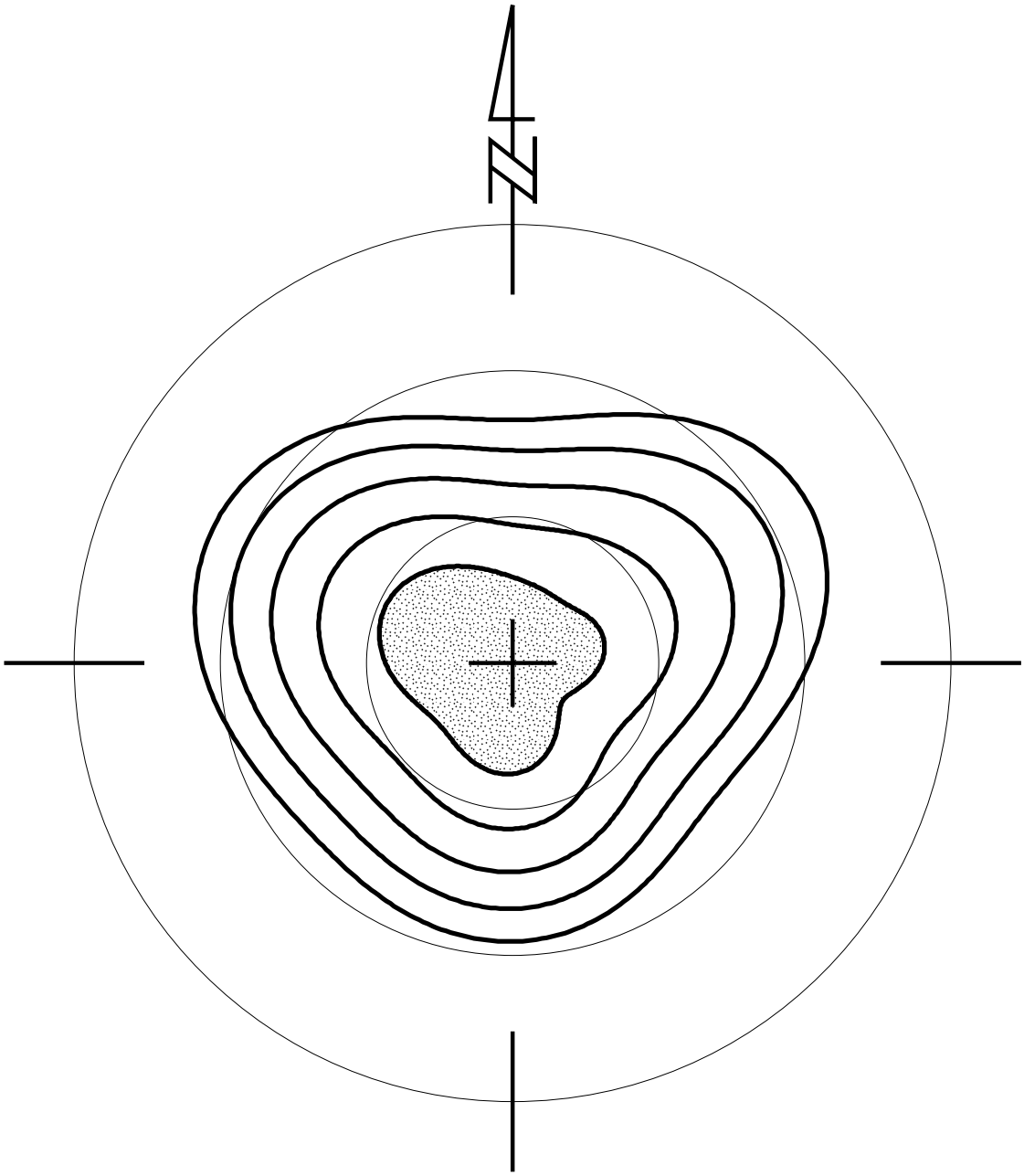

ANNUAL

Radial distances indicate wind speed in m/s

0 10 20

A point along the innermost contour represents the wind speed exceeded on average 1% of the time within a 22.5 degree sector centred on that direction. Other contours represent probability levels of 0.1%, 0.01%, 0.001% and 0.0001%, respectively.

Atlantic City - Surface

FIGURE 2.4 ANNUAL PROBABILITY DISTRIBUTION OF SURFACE HOURLY-MEAN WIND SPEED AND WIND DIRECTION – ATLANTIC CITY, NEW JERSEY (1958-1999)

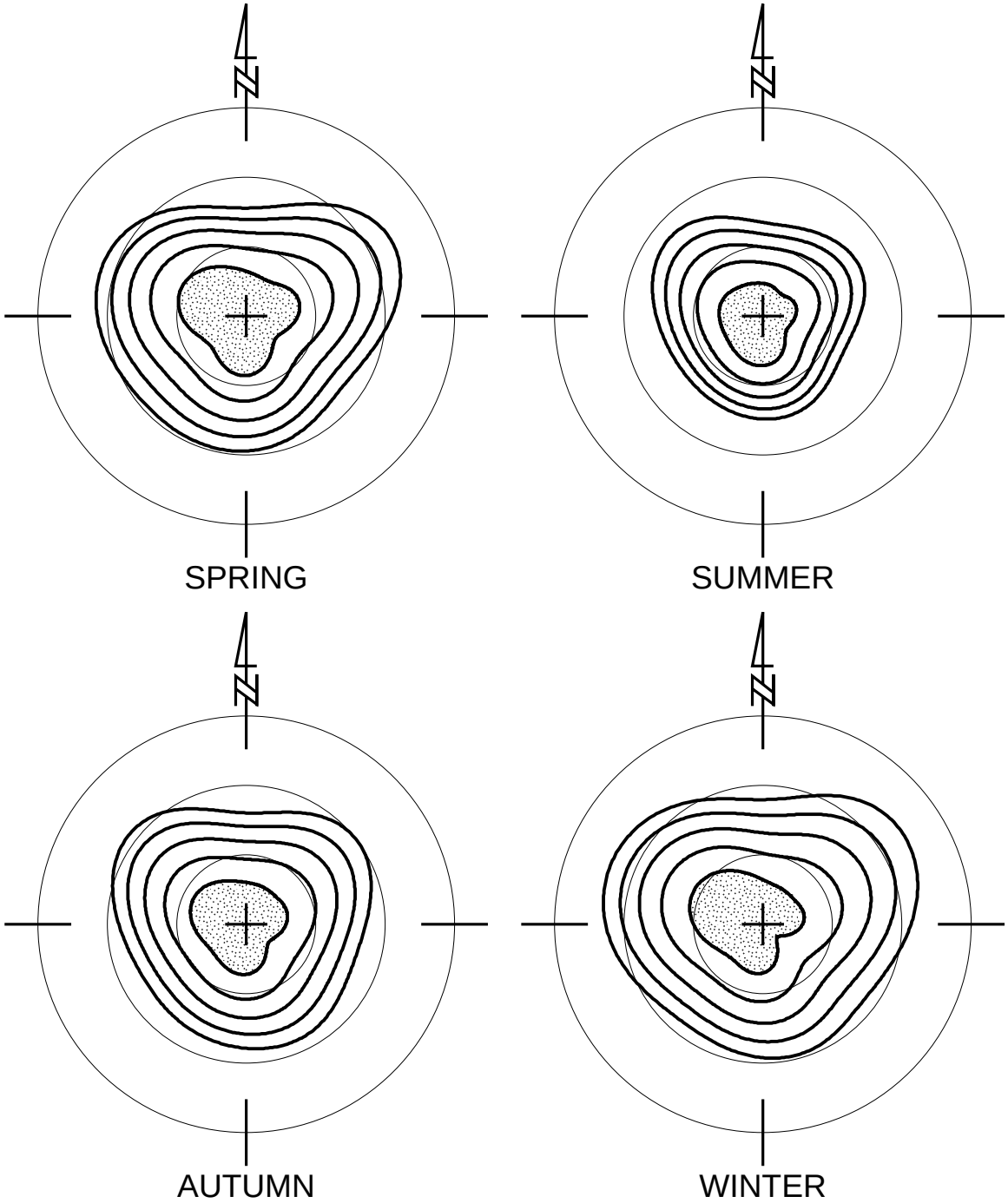

Radial distances indicate wind speed in m/s

0 10 20

A point along the innermost contour represents the wind speed exceeded on average 1% of the time within a 22.5 degree sector centred on that direction. Other contours represent probability levels of 0.1%, 0.01%, 0.001% and 0.0001%, respectively.

Atlantic City - Surface

FIGURE 2.5 SEASONAL PROBABILITY DISTRIBUTION OF SURFACE HOURLY-MEAN WIND SPEED AND WIND DIRECTION – ATLANTIC CITY, NEW JERSEY (1958-1999)

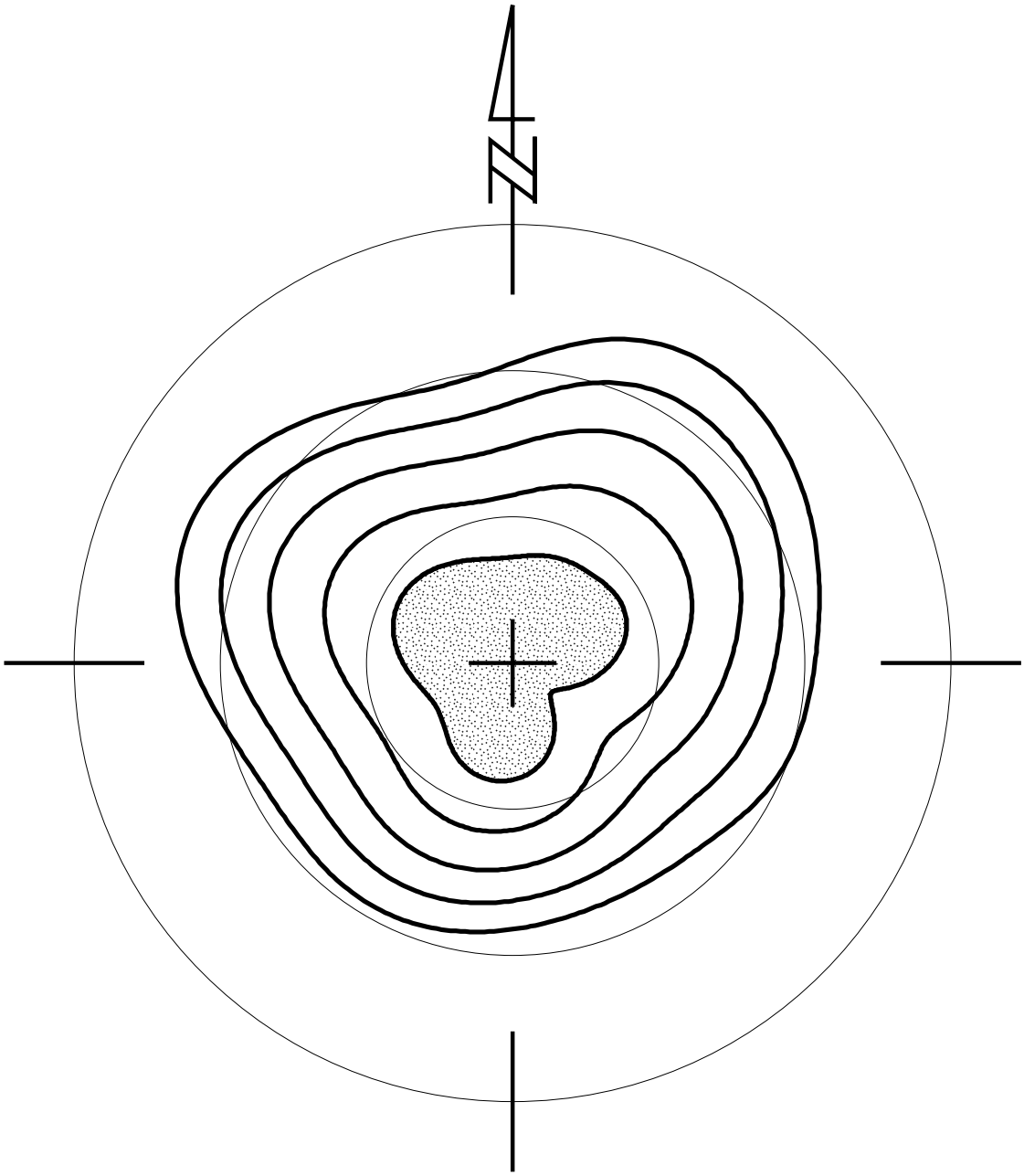

ANNUAL

Radial distances indicate wind speed in m/s

0 10 20

A point along the innermost contour represents the wind speed exceeded on average 1% of the time within a 22.5 degree sector centred on that direction. Other contours represent probability levels of 0.1%, 0.01%, 0.001% and 0.0001%, respectively.

Wallops Island - Surface

FIGURE 2.6 ANNUAL PROBABILITY DISTRIBUTION OF SURFACE HOURLY-MEAN WIND SPEED AND WIND DIRECTION – WALLOPS ISLAND, VIRGINIA (1966-1996)

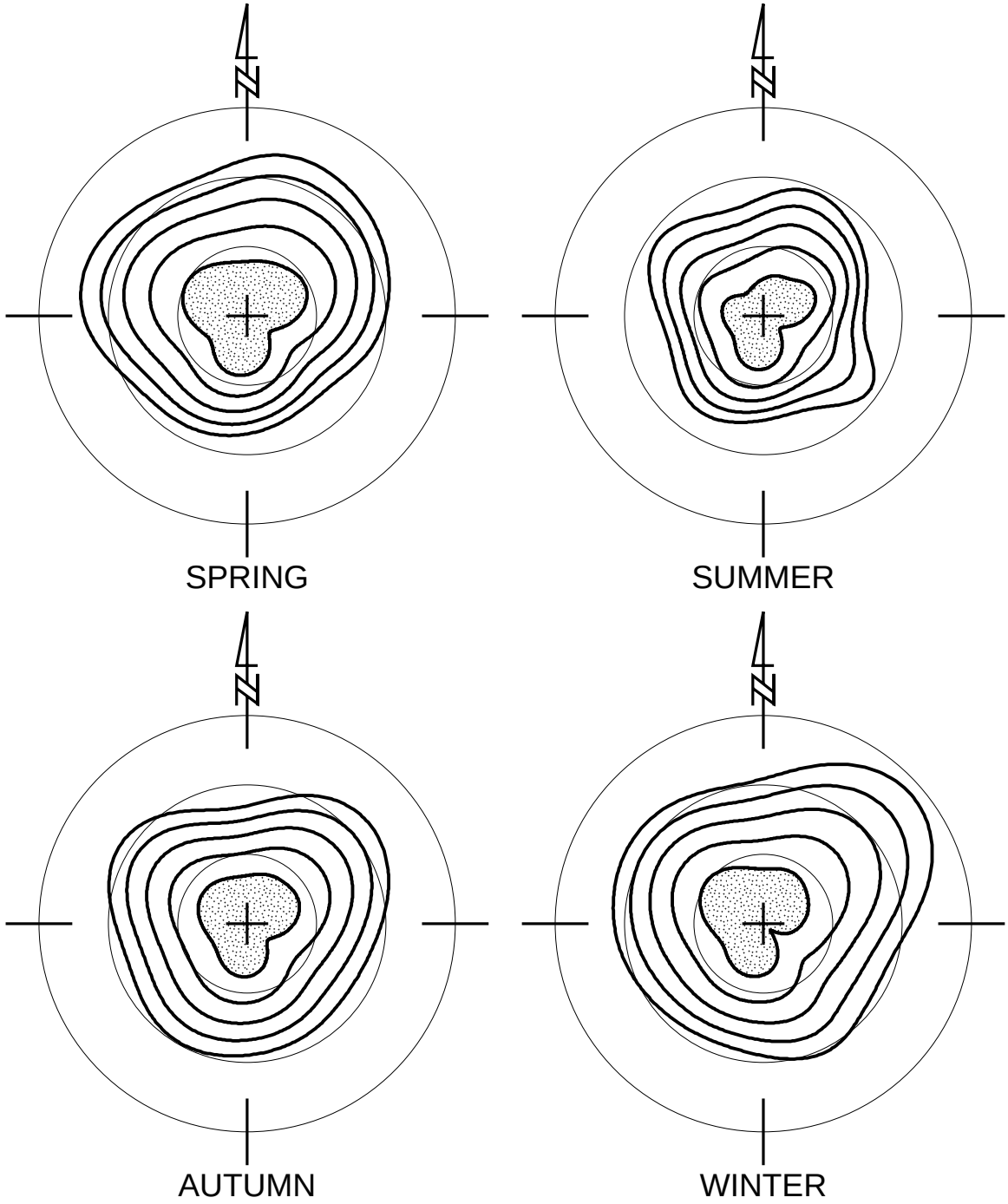

Radial distances indicate wind speed in m/s

0 10 20

A point along the innermost contour represents the wind speed exceeded on average 1% of the time within a 22.5 degree sector centred on that direction. Other contours represent probability levels of 0.1%, 0.01%, 0.001% and 0.0001%, respectively.

Wallops Island - Surface

FIGURE 2.7 SEASONAL PROBABILITY DISTRIBUTION OF SURFACE HOURLY-MEAN WIND SPEED AND WIND DIRECTION – WALLOPS ISLAND, VIRGINIA (1966-1996)

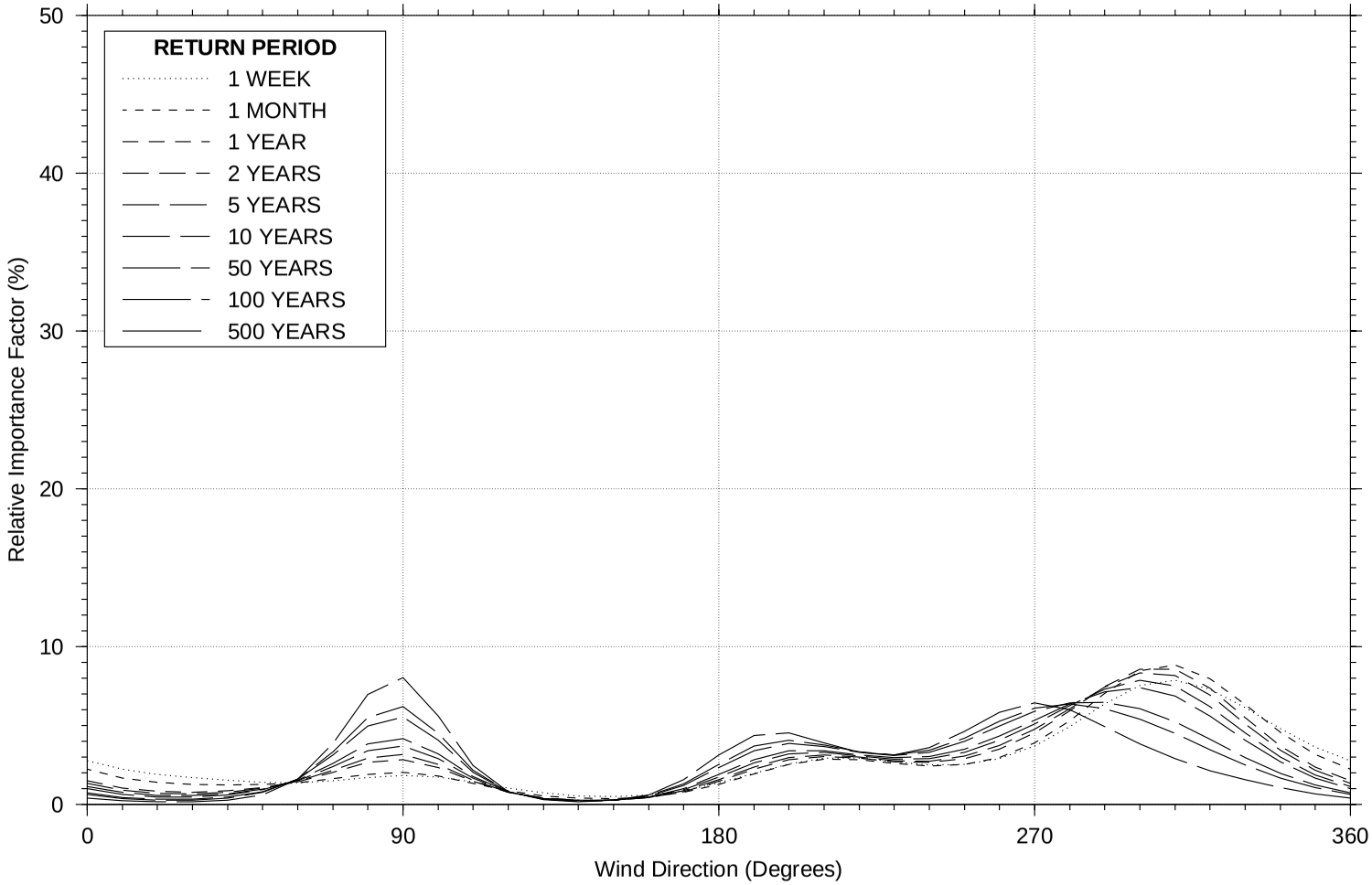

FIGURE 2.8 ANNUAL RELATIVE IMPORTANCE FACTORS FOR VARIOUS WIND DIRECTIONS AND MAXIMUM WIND SPEEDS WITH DIFFERENT RECURRENCE INTERVALS, DOVER AFB, DELAWARE (1942-

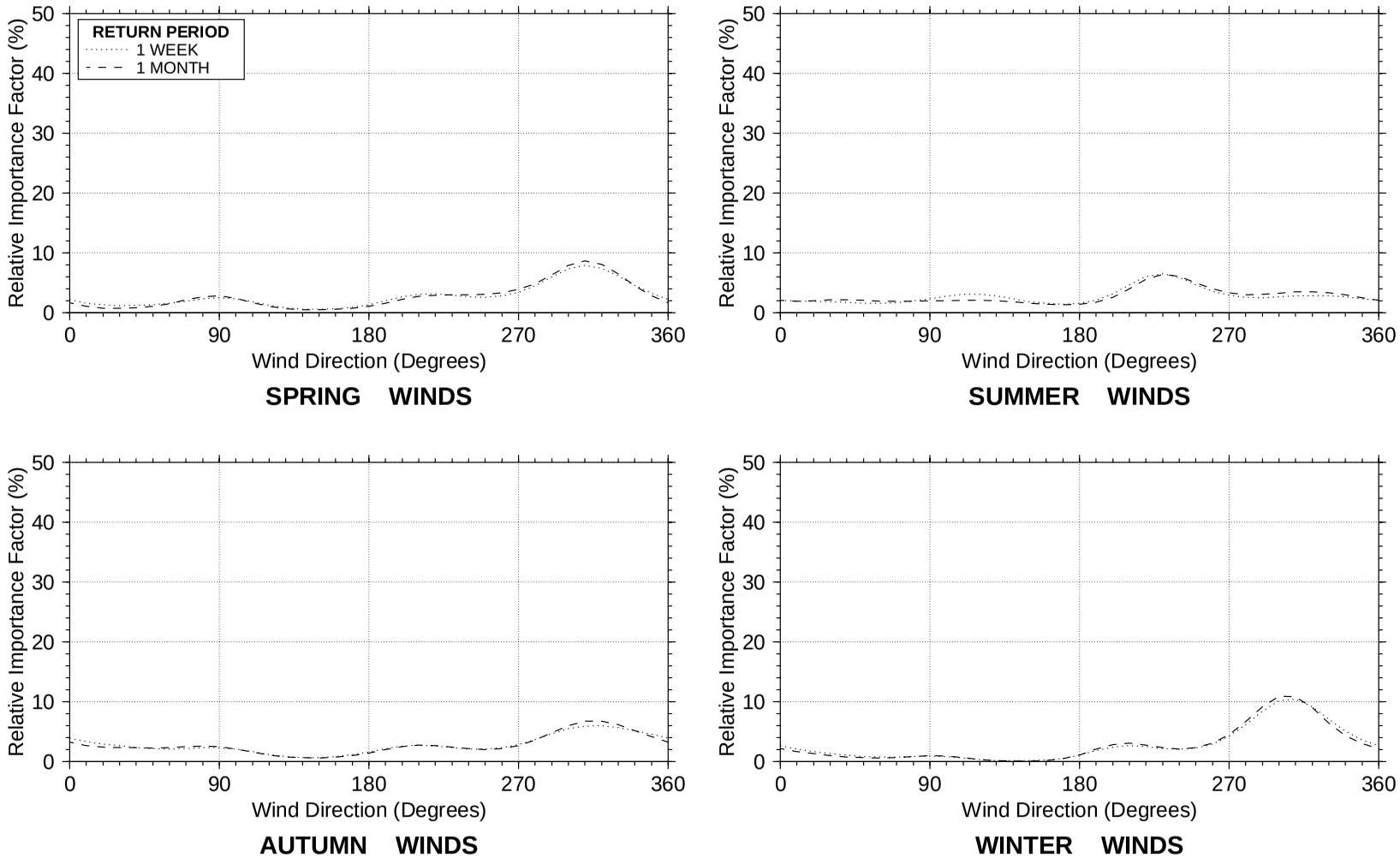

FIGURE 2.9 SEASONAL RELATIVE IMPORTANCE FACTORS FOR VARIOUS WIND DIRECTIONS AND MAXIMUM WIND SPEEDS WITH DIFFERENT RECURRENCE INTERVALS, DOVER AFB,

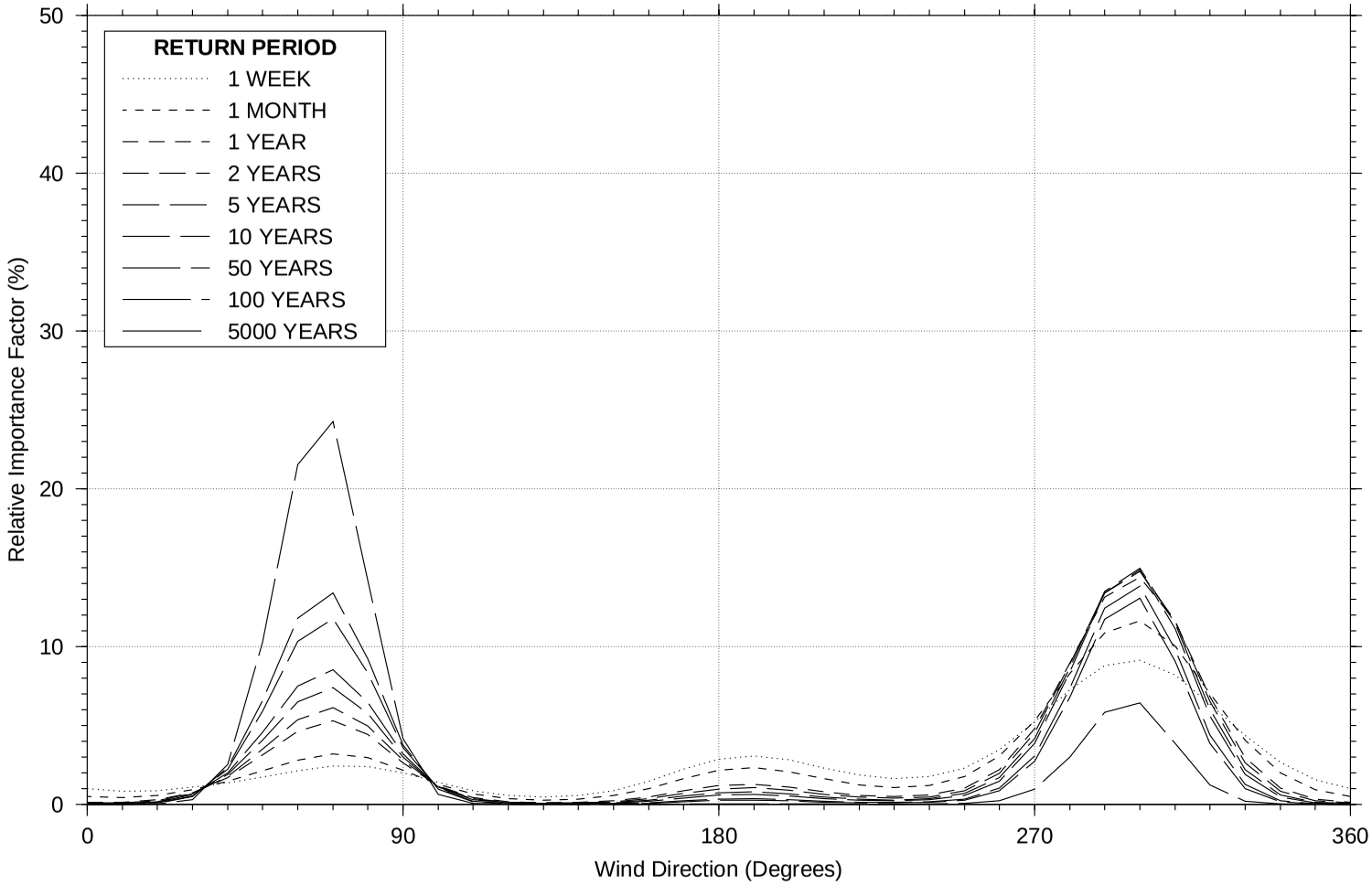

FIGURE 2.10 ANNUAL RELATIVE IMPORTANCE FACTORS FOR VARIOUS WIND DIRECTIONS AND MAXIMUM WIND SPEEDS WITH DIFFERENT RECURRENCE INTERVALS, ATLANTIC CITY, NEW JERSEY

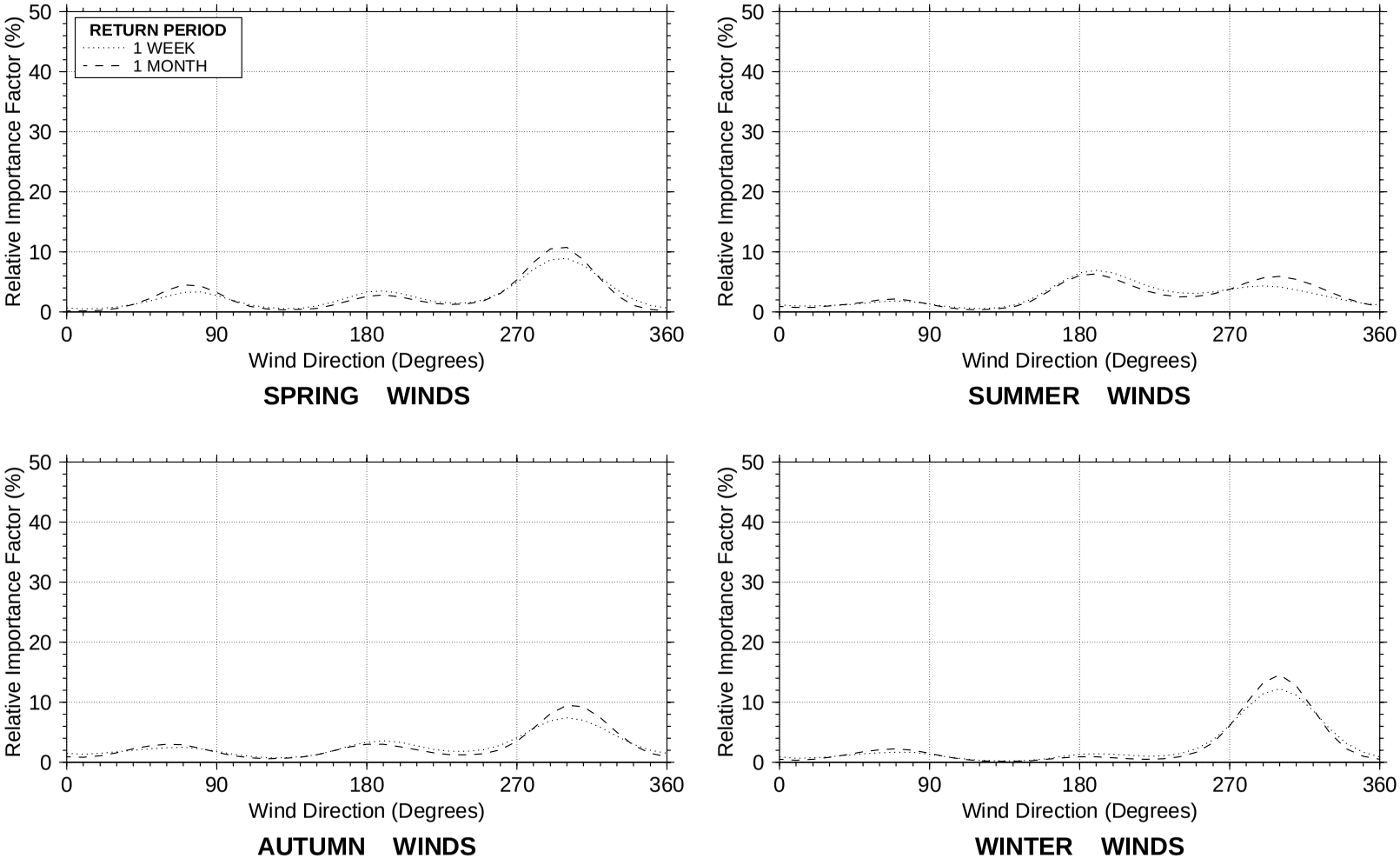

FIGURE 2.11 SEASONAL RELATIVE IMPORTANCE FACTORS FOR VARIOUS WIND DIRECTIONS AND MAXIMUM WIND SPEEDS WITH DIFFERENT RECURRENCE INTERVALS, ATLANTIC CITY, NEW

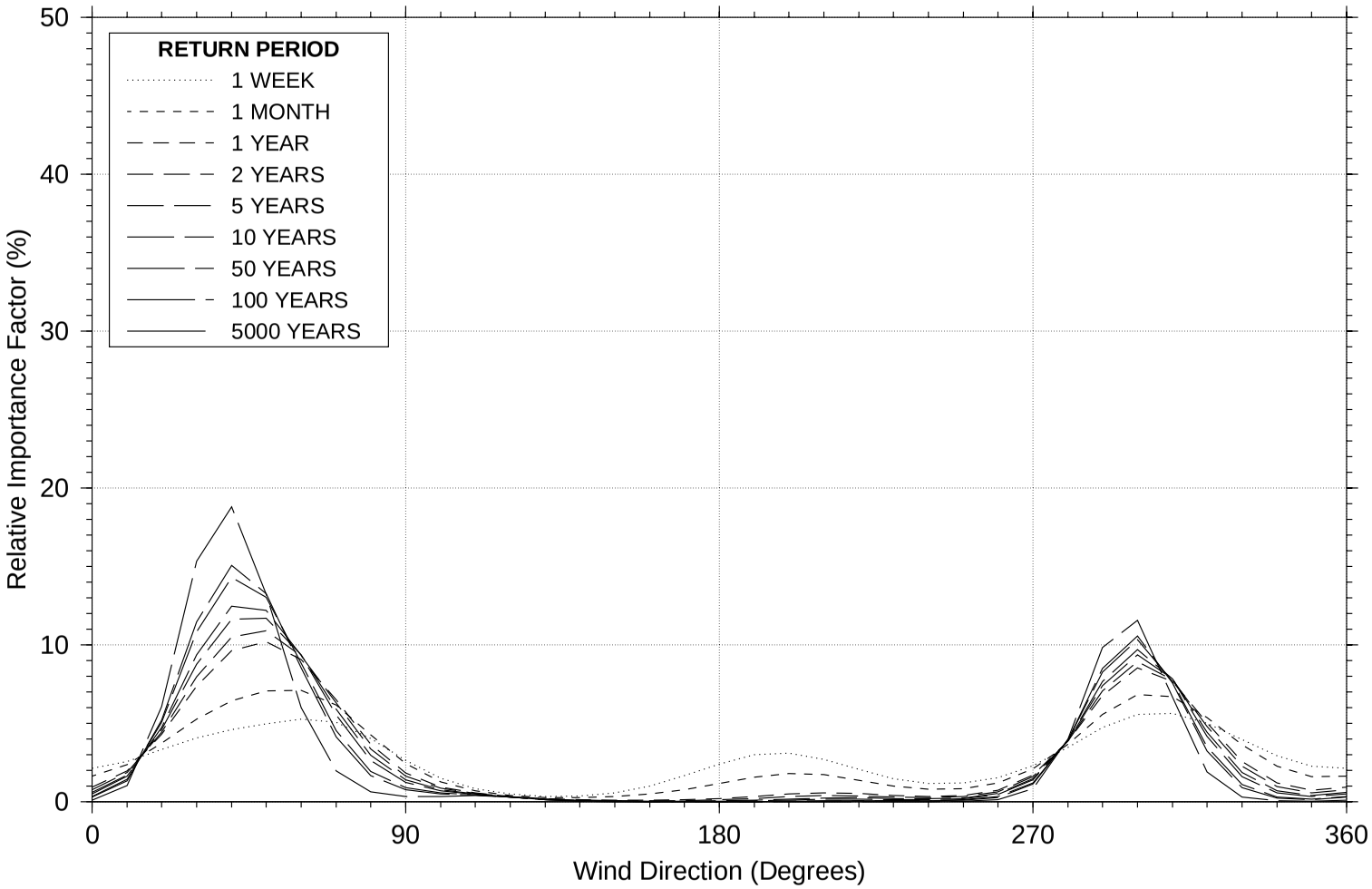

FIGURE 2.12 ANNUAL RELATIVE IMPORTANCE FACTORS FOR VARIOUS WIND DIRECTIONS AND MAXIMUM WIND SPEEDS WITH DIFFERENT RECURRENCE INTERVALS, WALLOPS ISLAND, VIRGINIA

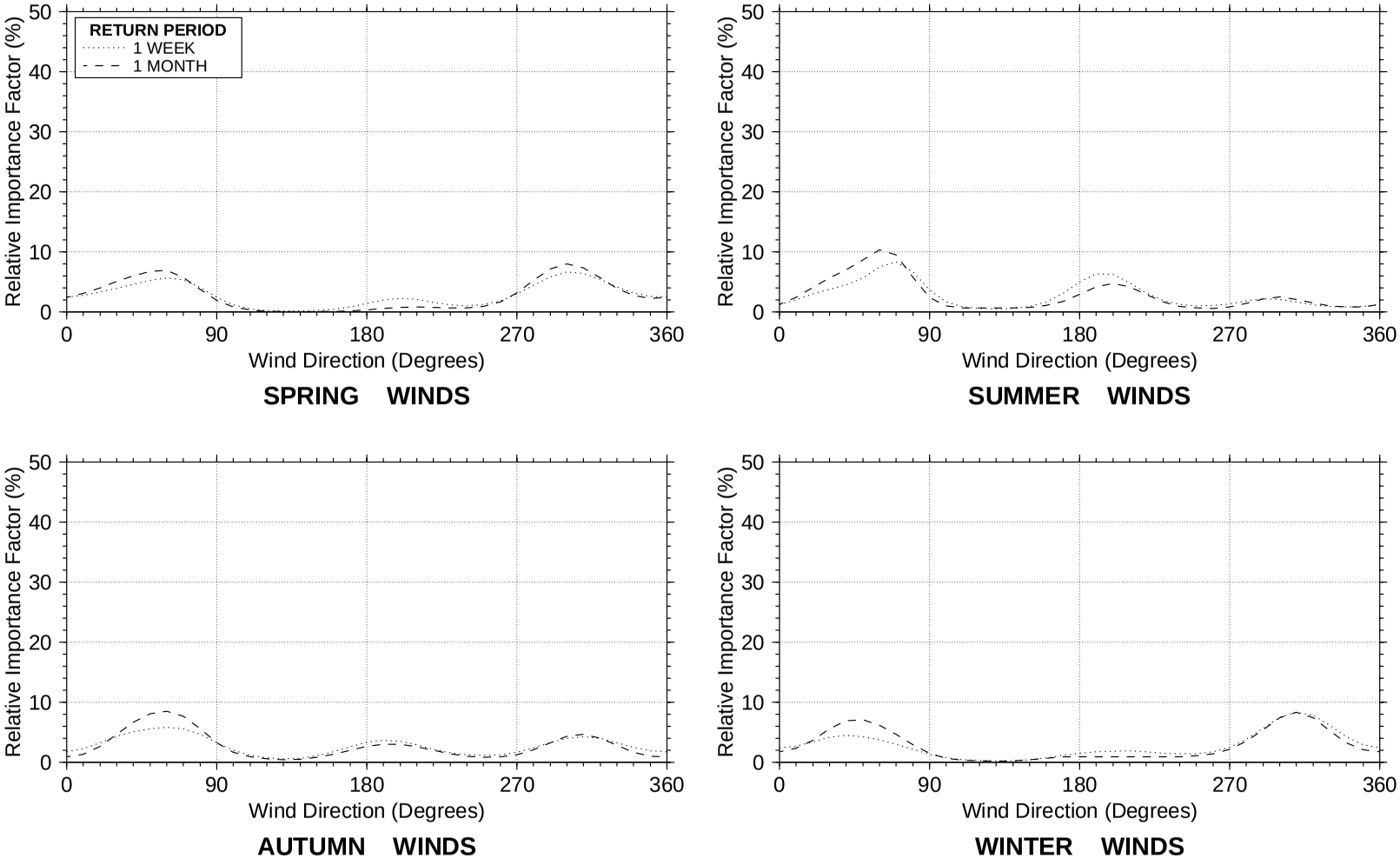

FIGURE 2.13 SEASONAL RELATIVE IMPORTANCE FACTORS FOR VARIOUS WIND DIRECTIONS AND MAXIMUM WIND SPEEDS WITH DIFFERENT RECURRENCE INTERVALS, WALLOPS ISLAND,

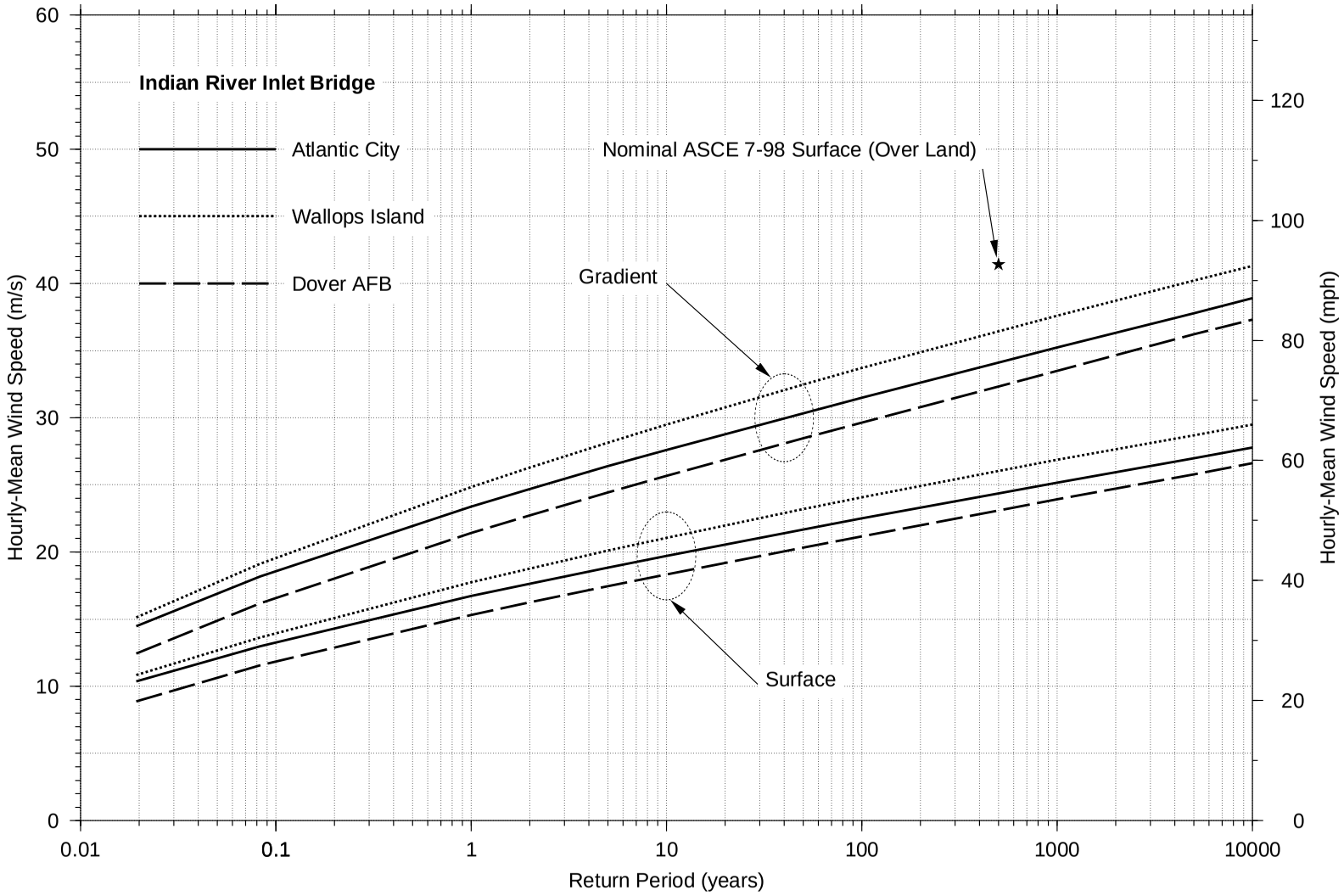

FIGURE 2.14 PREDICTED EXTREME HOURLY-MEAN SURFACE AND GRADIENT WIND SPEEDS FOR VARIOUS RETURN PERIODS AT DOVER AFB, ATLANTIC CITY AND WALLOPS ISLAND

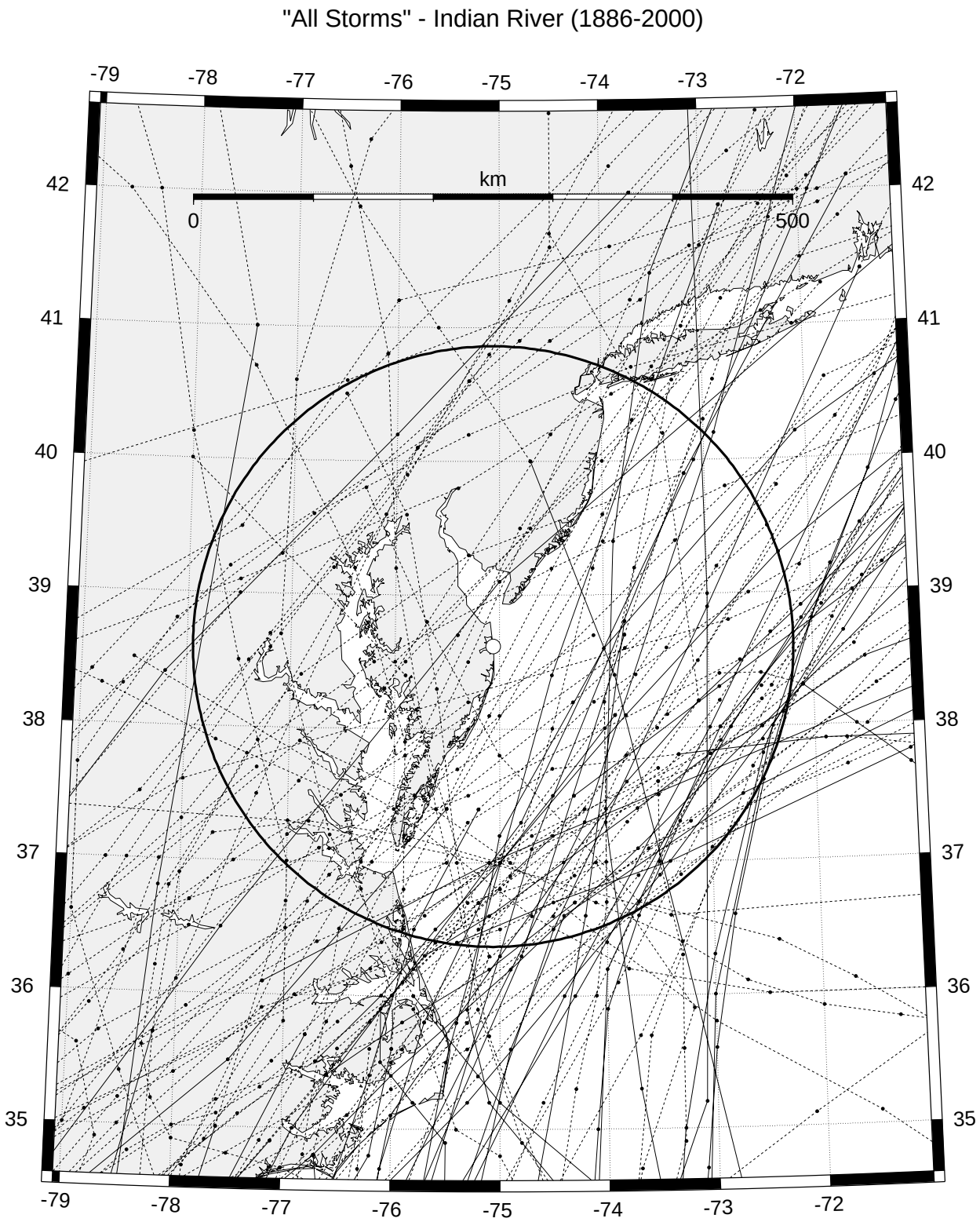

FIGURE 2.15 TROPICAL STORMS PASSING WITHIN A 250 KM RADIUS OF INDIAN RIVER INLET BRIDGE FOR THE RECORD PERIOD 1886-2000 – ALL STORMS CASE

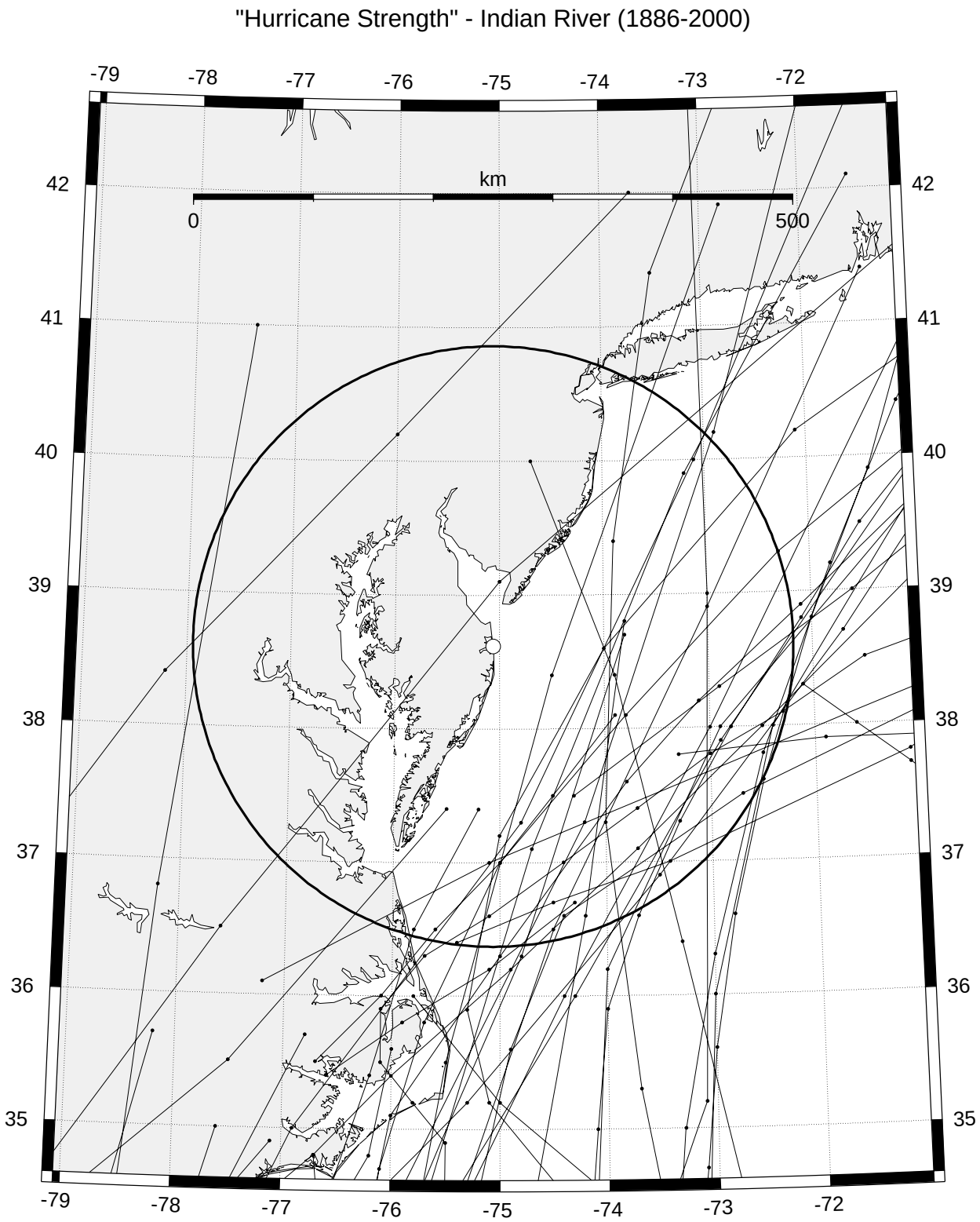

FIGURE 2.16 TROPICAL STORMS PASSING WITHIN A 250 KM RADIUS OF INDIAN RIVER INLET BRIDGE FOR THE RECORD PERIOD 1886-2000 – STORM SEQUENCES REACHING "HURRICANE" STAGE (V>33m/s)

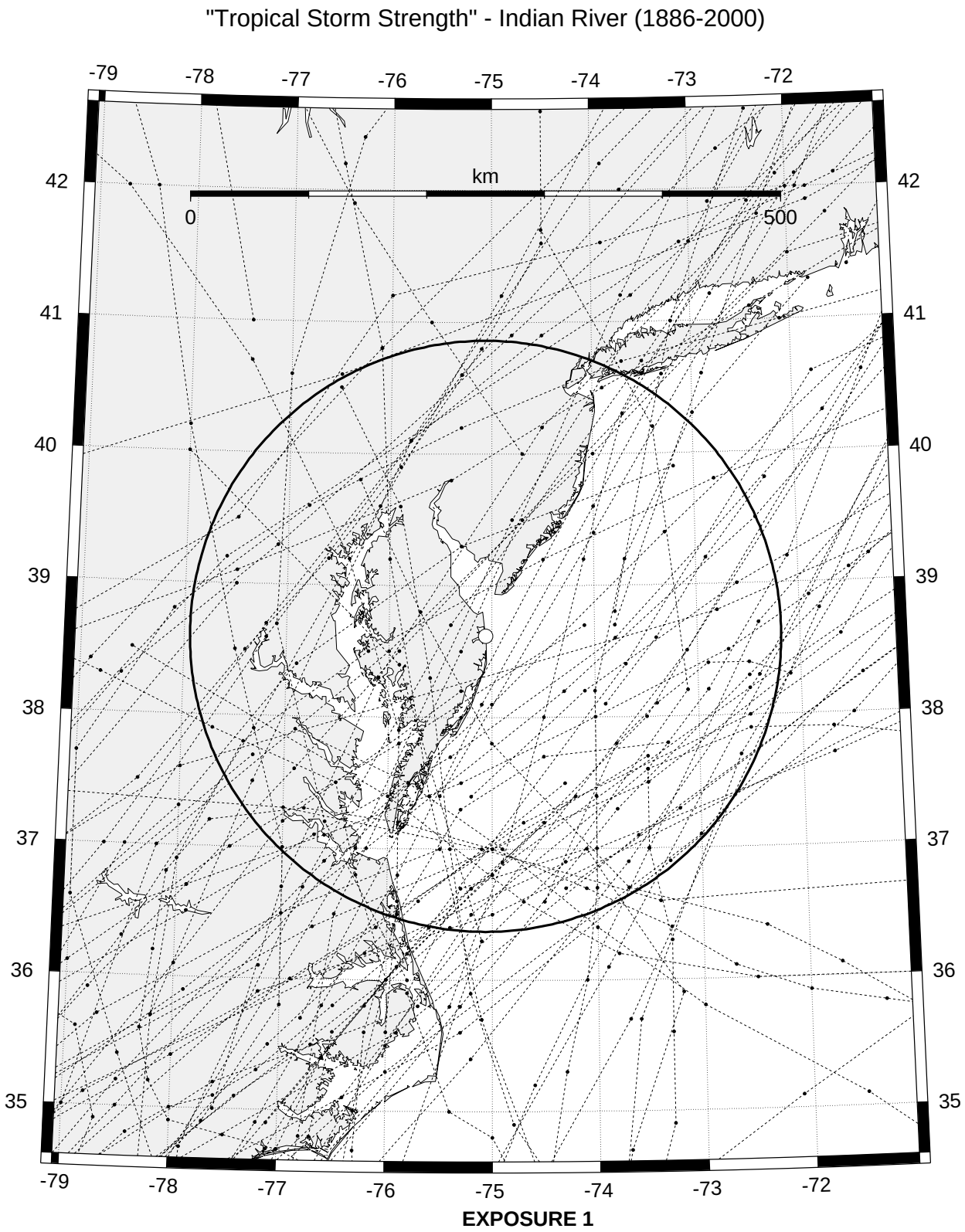

FIGURE 2.17 TROPICAL STORMS PASSING WITHIN A 250 KM RADIUS OF INDIAN RIVER INLET BRIDGE FOR THE RECORD PERIOD 1886-2000 – STORM SEQUENCES REACHING "TROPICAL STORM" STAGE (V<33m/s)

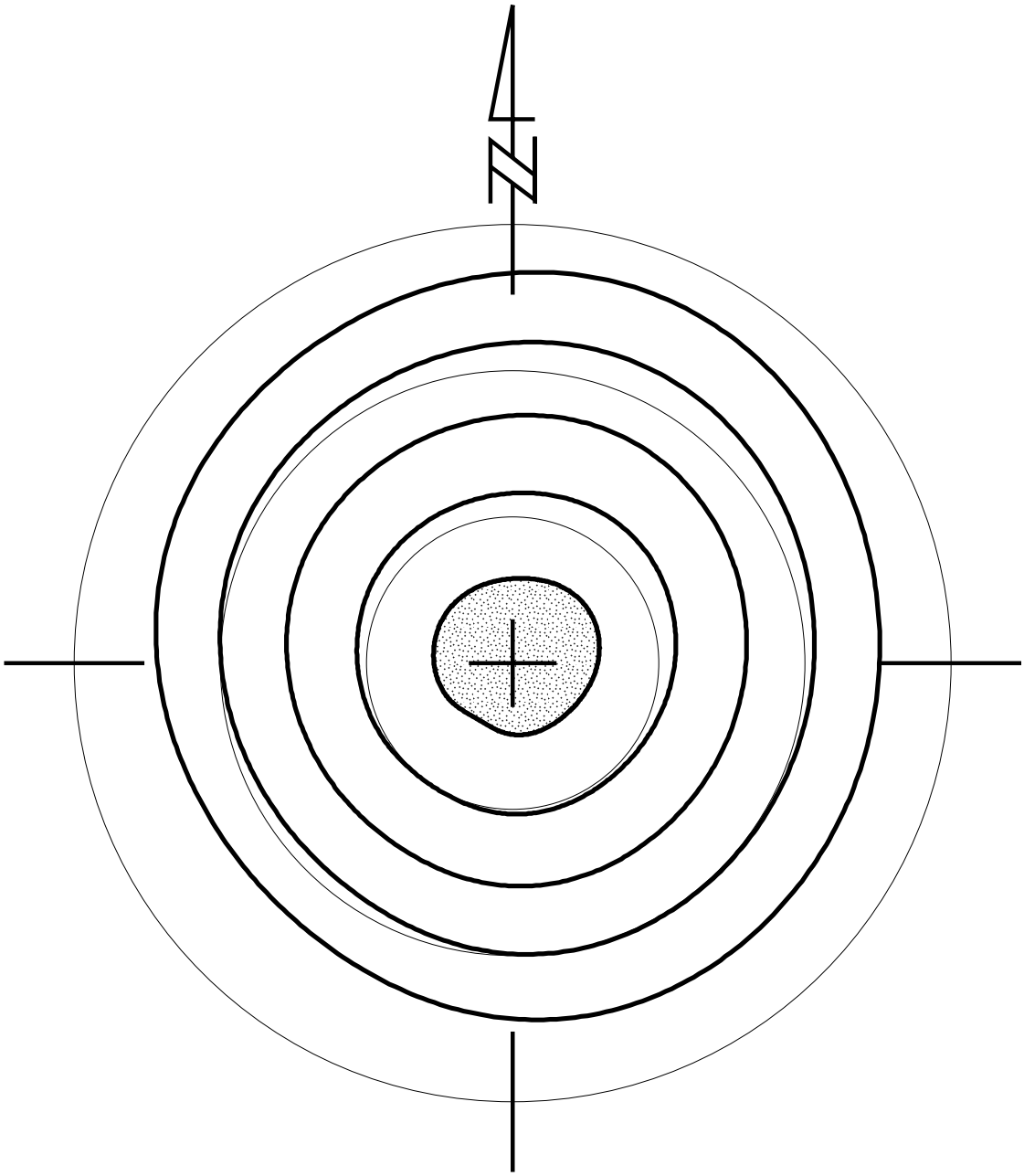

ANNUAL

Radial distances indicate wind speed in m/s

0 40 80

A point along the innermost contour represents the wind speed exceeded on average 1% of the time within a 22.5 degree sector centred on that direction. Other contours represent probability levels of 0.1%, 0.01%, 0.001% and 0.0001%, respectively.

Hurricane Climate at 274 ft Level

FIGURE 2.18 ANNUAL PROBABILITY DISTRIBUTION OF HOURLY-MEAN WIND SPEED AND WIND DIRECTION AT 83.5 m (274 ft) ABOVE WATER LEVEL FOR INDIAN RIVER INLET OBTAINED FROM MONTE CARLO SIMULATION OVER 100,000 YEARS (37,150 STORMS)

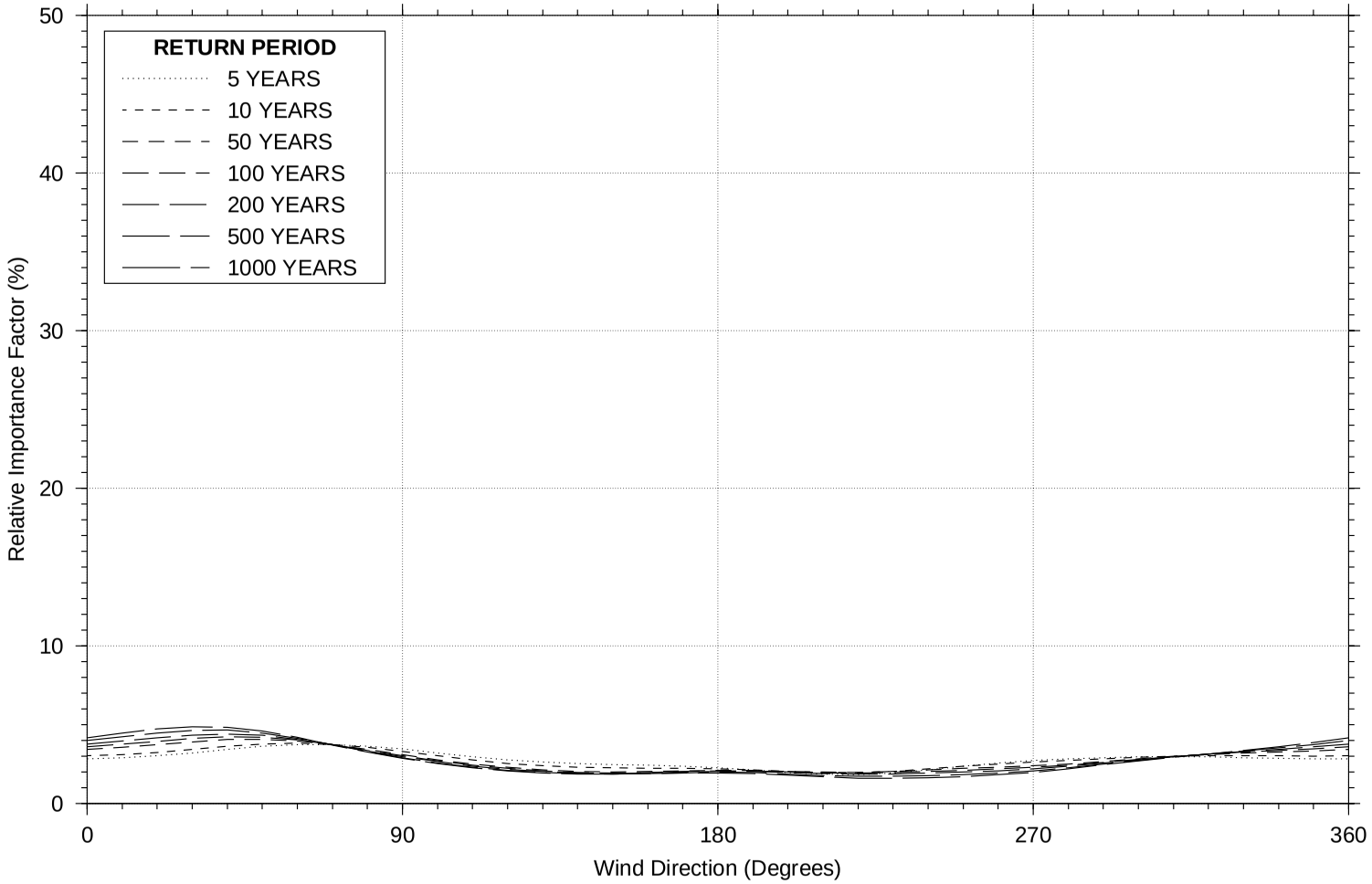

FIGURE 2.19 RELATIVE IMPORTANCE FACTORS FOR VARIOUS WIND DIRECTIONS AND MAXIMUM WIND SPEEDS WITH DIFFERENT RECURRENCE INTERVALS AT 83.5 m (274 ft) ABOVE WATER LEVEL FOR INDIAN RIVER INLET

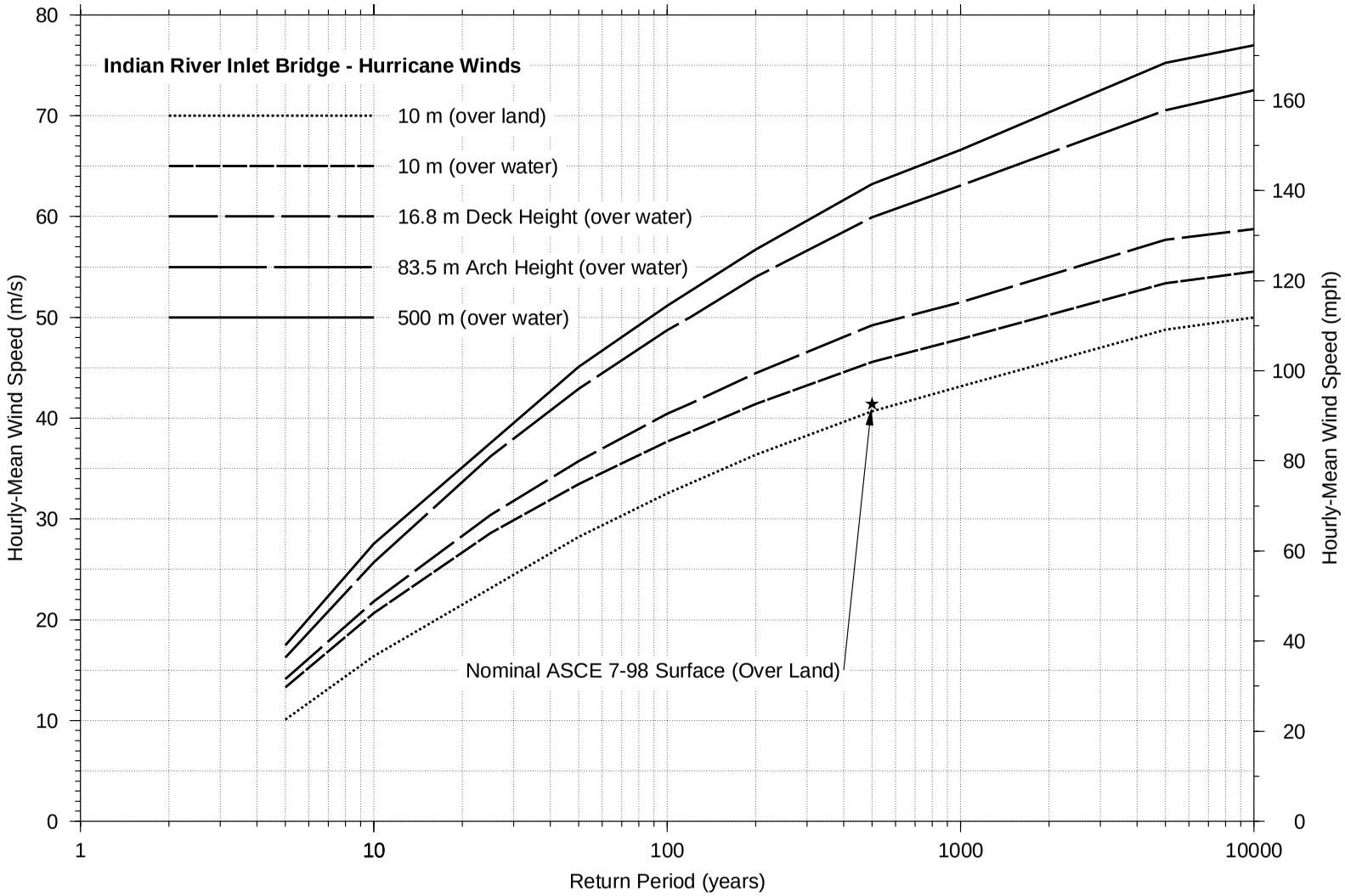

FIGURE 2.20 PREDICTED EXTREME HOURLY-MEAN WIND SPEEDS FOR VARIOUS RETURN PERIODS FOR HURRICANE WINDS AT 10 m (33 ft), 16.8 m (DECK HEIGHT OF 55 ft), 83.5 m (ARCH LEVEL OF 274 ft) AND 500 m LEVEL (1640 ft)

3 SECTION MODEL STUDY – BRIDGE DECK

3.1 General

This section examines the behavior of the Indian River Inlet Bridge under the action of wind using the section model approach.

The bridge was studied using the section model technique at the inlet to the High Speed Section of the Boundary Layer Wind Tunnel II. Testing of the deck section model was conducted under the action of both grid-generated turbulence and uniform flow conditions for comparative purposes. The grid was designed to model the high frequency end of the full scale wind spectrum, critical for the definition of resonant response of the bridge section.

The 7 ft long section model corresponds to a 560 ft long section of the full scale deck at a prototype scale of 1 to 80. A typical section model test setup is shown in Figure 3.1. The turbulence generating grid at the inlet of the wind tunnel can be seen in the background. Close-up views of the model and instrumentation set-up are shown in Figure 3.2.

A summary of the similitude requirements for the design of the basic deck section model is shown in Table 3.1. Further details concerning the design of section model and the approach to testing can be found in Appendix A.

Full scale dynamic properties of the basic deck section were provided by Figg Bridge Engineers, Inc. and are given in Table 3.2. The frequencies associated with the fundamental vertical and torsional symmetrical modes of vibration for the bridge deck were selected as the frequencies to be simulated in the section model tests. These two modes of vibration are expected to provide the highest likelihood of a coupled type of flutter instability. During the test, the model was matched to the scaled mass and mass moment of inertia properties of the bridge deck section. The scaled model properties are also presented in Table 3.2.

3.2 Dynamic Response Testing

3.2.1 General

The section model was mounted on soft springs with adjustable pneumatic dashpots permitting the simulation of the vertical and torsional frequencies of vibration. The sprung model was ballasted with additional mass to represent the dynamically scaled mass and mass moment of inertia.

Historically, the development of section model testing was done in aeronautical wind tunnels in smooth, uniform flow and included testing under conditions of inclined mean flow in an attempt to handle the fluctuating component of turbulence. The use of turbulent flow in the test procedure generally makes it unnecessary to consider the effect of wind inclination in dynamic tests unless the bridge is situated in extreme topography where inclined <u>mean</u> wind conditions may exist.

The dynamic section model tests of the bridge deck were performed in two sequences. The Initial properties of the bridge provided by the Engineers, were used in the first series of tests with a torsional to vertical frequency ratio of 2.22. The second series of tests were conducted after the structural design of the bridge was modified and revised dynamic properties of the bridge were provided. The modified dynamic properties included a torsional to vertical frequency ratio of 1.19.

The section model of the deck was tested in both smooth and turbulent flows at 0° angle of incidence for a nominal structural damping of 0.5% of critical. A ‘low damping’ case was also investigated. Table 3.3 summarizes the test conditions and parameters as well as the corresponding test numbers in the test program.

3.2.2 Modeling of Wind

Turbulence in the wind tunnel was generated by a grid placed upstream of the model. The grid used in this study has a bar size of 2" in width and a spacing of 10" from center to center, which provides a reasonable representation of the natural wind energy levels at the frequency range of interest in the full scale wind spectrum. The vertical I_w, and horizontal I_u turbulence intensities generated using this grid are about 0.04 and 0.05 respectively. Turbulence developed using the fixed grid technique is normally lacking sufficient energy in the low frequency - large scale range to match full scale, resulting in an overall lower turbulence intensity than that expected at the site. The energy in the high frequency end of the spectrum, however, is well modeled using this grid, which is critical for the definition of resonant response and the overall behavior of the structure in turbulent wind. Measured turbulence spectra in the wind tunnel and that suggested by ESDU (z_o =0.025ft) is presented in Figure 3.4. This value of z_o corresponds roughly to ASCE terrain category C and is appropriate for this location.

3.2.3 Dynamic Bridge Response

The extreme mass and exceptional stiffness of the Indian River Bridge structural system makes it very difficult to provide a "well conditioned" experiment, where the entire wind speed range of the wind tunnel is utilized. Prototype bridges with high natural frequencies require models and test rigs with high stiffness and high sprung natural frequencies. This, in general, is not possible with traditional test equipment which is designed for the natural frequencies and mass conditions associated with most cable stayed and suspension bridges. Consequently, test wind speeds associated with common winds are low, small responses are observed and the resolution of instrumentation becomes problematic.

Tests for the Indian River Inlet Bridge deck section were performed in smooth flow to assess its aerodynamic characteristics and any tendency to instability with regard to both vortex induced vibration and flutter. The turbulence intensity in the smooth flow was below 0.5%. In addition, the test in turbulent flow was carried out to assess the effect of turbulent buffeting.

All results from the dynamic section model tests are presented in graphical form in Appendix B. The peak response was formed from a peak factor times the root-mean-square (RMS) response. Thus, the total response is equal to the mean, plus or minus the peak. The peak shown in the plots is formed from the RMS multiplied by an appropriate peak factor. In plotting, for the range of wind speeds where the model is stable, the peak shown is formed from the RMS multiplied by a statistical peak factor of 3.5.

$$y_{\max} = \bar{y} \pm g \cdot y_{RMS}$$

where g is the peak factor and $y_{\max}, \bar{y}$ and y_{RMS} are the maximum, mean and root mean square (RMS) response.

The peak factor during instability decreases to a value approaching 1.4 or $\sqrt{2}$, (i.e. 1/(RMS) of a sinusoidal signal with amplitude of 1.0). Thus, for the range of wind speeds where the model has shown either a large vortex shedding peak or flutter instability, the <u>actual</u> peak factor calculated from the test for the corresponding wind speed is used to obtain the peak shown in the plot. Otherwise, the use of a constant peak factor of 3.5 would tend to overestimate the peak response in the region of the instability. Rotations and full scale displacements in these plots have been plotted against the full scale mean wind speed at deck height in mph. Full scale displacements were obtained from the measured model displacements and converted using the geometric length scaling of 1:80. Rotations need no such scaling. The full scale and model frequencies have been used to determine the conversion factors from model scale velocity to full scale wind speed through the following relationship:

$$V_{\text{full scale}} = V_{\text{model}} \cdot \left(\frac{f_{\text{full scale}}}{f_{\text{model}}} \right) \cdot \left(\frac{1}{\lambda_L} \right)$$

where $(1/\lambda_L) = 80$, the geometric scale of the model and f is the natural frequency of either the vertical or torsional mode of vibration.

In section model testing, the onset of a “Flutter Instability” can be defined as when the character of the response changes from a random type motion to that of a regular, sinusoidal motion, involving either pure torsional or a coupled vertical-torsional vibration. This can be clearly identified through an examination of the “peak factor” which is defined as the ratio of the largest observed reading during the sample period to the Root Mean Square (RMS) of the sample. A random signal has peak factors in the 3-4 range, while a sinusoid has a peak factor of $\sqrt{2}$ or 1.41. For the purpose of this investigation, a peak factor of less than 2 was selected as the governing criteria. A discussion of the peak factor with respect to its use in determining conditions of flutter instability is contained in Appendix D.

During the first series of dynamic testing of the deck section model, no significant motions in either lift or torsion were observed. The mass of the bridge deck is particularly large, while maintaining a relatively small radius of gyration. Typical bridge decks exhibit a radius of gyration to deck width ratio of 0.3 to 0.35, but due to the relatively heavy centrally located tie beam, this ratio is of the order of 0.25, which in combination with the high torsional stiffness of the deck, results in a high natural frequency in torsion (1.71 Hz). The vertical modes of vibration are largely governed by the large contribution to the overall stiffness by the arch and are also comparatively high for a bridge of this span (0.77 Hz). The wind speeds for flutter instability are generally proportional to the torsional natural frequency and given the relatively high frequency and high frequency ratio, this was not expected to occur within practical wind speeds.

The second series of tests test was carried out after the bridge structural properties were modified, resulting in a frequency of the first symmetric lift mode of 0.73Hz and the first symmetric torsional mode of 0.87Hz. This yields a torsional to lift frequency ratio of 1.19, which was significantly lower than the value of 2.22 used in the first series of tests. Ordinarily, a frequency ratio this low would be of some concern for coupled instability, however, the high frequency in general, indicates that any instability would be likely only at very high wind speeds. The mass and mass moment of inertia of the model were the same as in the first series of tests.

The plots in Appendix B indicate that the maximum vertical displacement from both series of tests is well below 0.5 feet. The maximum rotation from the first series of tests is less than 0.1 degrees, and the maximum rotation from the second series is only marginally larger at 0.3 degree. Therefore, no instability or significant buffeting response is likely for the bridge.

3.3 Static Response Testing – Bridge Deck

The model was mounted on the BLWTL Bridge 3-component balance, which is capable of measuring the total forces on the section (X and Z body forces as well as the moment). Tests were performed adjusting the model inclination relative to the mean wind flow. The sign convention for the definition of the force coefficients is given in Figure 3.5.

A typical force coefficient is defined as follows:

$$C_{x,z} = \frac{F_{x,z}}{qB}$$

in which C is an aerodynamic coefficient, F is the mean aerodynamic force per unit span length, $q = \frac{1}{2}\rho V^2$ is the mean wind velocity pressure at deck level, ρ is the density of air (0.00238 slugs/ft^3), V is the mean wind velocity at deck level in ft/s, and B is the bridge deck width. The subscripts x,z refer to the X and Z body force components respectively.

The moment coefficient is defined:

$$C_m = \frac{F_m}{qB^2}$$

Tests were carried out in both smooth flow (I_u= 0.5%) and grid generated turbulent flow (I_u= 7%) for angles of mean vertical inclination between -12 to +12 degrees in 1 degree increments. The tests were

repeated for three different wind speeds to investigate a potential for Reynolds Number effects. A velocity-weighted average was performed using the measurements at the three wind speeds. Due to the asymmetry of the deck, two wind directions were tested and are denoted as sidewalk upstream and sidewalk downstream.

The static aerodynamic coefficients from all tests of the section model are summarized in Tables 3.4 to 3.7. The corresponding curves of force coefficient vs. angle of attack are shown in Figures 3.6 and 3.7 for sidewalk upstream and downstream respectively. A complete data set of the force coefficients as well as the slopes of the Z and torsional forces (based upon the angle of attack in radians) is given in Appendix C.

The coefficients are normalized by deck width to make comparisons with other structures more meaningful. Should the results be desired on a projected area to the wind basis, as is sometimes the case, the $C_{x,z}$ coefficients should be multiplied by the ratio of deck width to overall section height (for example, 110.5/14=7.9), and for C_m by the square of this value ($(110.5/14)^2$=62.3). The centre of measurement of the forces was at 6.5 ft below the upper surface of the tie beam on the tie beam centerline.

There are no significant differences observed between the smooth and turbulent flow test results for any of the coefficients at small angles of attack for either wind direction. For the sidewalk upstream case, the coefficients differ for the two flow conditions at high negative angles of attack. The coefficients show that there a positive slope in the aerodynamic lift and torsional force coefficient curve for small angles attack, which is indicative of good stability characteristics. This observation is consistent with the results of the dynamic tests.

TABLE 3.1 SECTION MODEL SCALING PARAMETERS

PARAMETER	SIMILITUDE REQUIREMENT	VALUE
Length*	$\lambda_L = \mathbf{L}_m / \mathbf{L}_p$	0.0125
Density	$\lambda_\rho = \rho_m / \rho_p$	1.0
Velocity (refer to Table 2.2)	$\lambda_v = \mathbf{V}_m / \mathbf{V}_p = \lambda_L \ \mathbf{f}_m / \mathbf{f}_p$	0.0609
Mass per Unit Length	$\lambda_m = \lambda_\rho \lambda_L^2$	1.56E-04
Mass	$\lambda_M = \lambda_\rho \lambda_L^3$	1.95E-06
Mass Moment of Inertia per Unit Length	$\lambda_i = \lambda_m \lambda_L^2$	2.44E-08
Mass Moment of Inertia	$\lambda_I = \lambda_M \lambda_L^2$	3.05E-10
Time	$\lambda_T = \mathbf{T}_m / \mathbf{T}_p = \lambda_L / \lambda_V$	0.205
Damping	$\lambda_\zeta = \zeta_m / \zeta_p$	1.0

* Length Scale 1: 80

TABLE 3.2 FULL SCALE AND MODEL SCALE PROPERTIES FOR THE BASIC DECK SECTION

	PROTOTYPE	MODEL
Characteristic Length B	110.6 ft	1.38 ft
Mass		
lift	45.6 kip/ft	7.13 lb/ft
torque	34.2E+03 kip-ft^2/ft	.835 lb-ft^2/ft
Frequency		
lift	0.77 Hz	3.75 Hz
torque	1.71 Hz	8.26 Hz
f_t/f_l	2.22	2.20
Stiffness		
lift	33.2 kip/ft/ft	860 lb/ft
torque	2140 kip-ft/ft/degree	8.54 lb-ft/degree
Damping (% of critical)		
lift	~ 0.7%	~ 0.1% and 0.5%
torque	~ 0.7%	~ 0.2% and 0.5%

Velocity Scaling:

Vertical: $$\frac{V_m}{V_p} = \frac{(\mathrm{fB})_m}{(\mathrm{fB})_p} = \frac{3.75}{0.77}\frac{1}{80} = \frac{1}{16.4}$$

Torsional: $$\frac{V_m}{V_p} = \frac{(\mathrm{fB})_m}{(\mathrm{fB})_p} = \frac{8.26}{1.71}\frac{1}{80} = \frac{1}{16.6}$$

Average: $$\frac{V_m}{V_p} = \left(\frac{1}{16.4} + \frac{1}{16.6}\right) \bullet 0.5 = \frac{1}{16.5}$$

TABLE 3.3 RESULTS OF DYNAMIC SECTION MODEL TESTS

Indian River Inlet Bridge, Dynamic Section Model Test Result Summary, 0 Degrees Angle of Attack

SECTION MODEL TESTING with initial frequencies, February 2004

					Prototype Properties *				Vmax at deck height	Flutter instability	Vortex induced vibration
NO.	**Test**	**Flow**	**Damping**	**Walkway Location**	**Mass**	**MMI**	**fv**	**ft**	**mph**		
					Lb/ft	Lb-ft^2/ft	Hz	Hz			
1	EYT301	smooth	0.1% in lift & 0.26% in torsion	upstream	45619	3.42E+07	0.77	1.71	220	Not observed	Not observed
2	DYN101	smooth	0.5% in lift & torsion	upstream	45619	3.42E+07	0.77	1.71	202	Not observed	Not observed
3	EYT201	turbulent	0.1% in lift & 0.26% in torsion	upstream	45619	3.42E+07	0.77	1.71	219	Not observed	Not observed
4	DYT101	turbulent	0.5% in lift & torsion	upstream	45619	3.42E+07	0.77	1.71	218	Not observed	Not observed
5	EYN101	smooth	0.1% in lift & 0.26% in torsion	downstream	45619	3.42E+07	0.77	1.71	229	Not observed	Not observed
6	DYN301	smooth	0.5% in lift & torsion	downstream	45619	3.42E+07	0.77	1.71	219	Not observed	Not observed
7	EYT101	turbulent	0.1% in lift & 0.26% in torsion	downstream	45619	3.42E+07	0.77	1.71	226	Not observed	Not observed
8	DYT102	turbulent	0.5% in lift & torsion	downstream	45619	3.42E+07	0.77	1.71	218	Not observed	Not observed

SECTION MODEL TESTING with modified frequencies, June 2004

					Prototype Properties *				Vmax at deck height	Flutter instability	Vortex induced vibration
NO.	**Test**	**Flow**	**Damping**	**Walkway Location**	**Mass**	**MMI**	**fv**	**ft**	**mph**		
					Lb/ft	Lb-ft^2/ft	Hz	Hz			
1	PWU101	smooth	0.13% in lift & 0.6% in torsion	upstream	45619	3.42E+07	0.73	0.87	231	Not observed	Not observed
2	PWD101	smooth	0.13% in lift & 0.6% in torsion	downstream	45619	3.42E+07	0.73	0.87	230	Not observed	Not observed
3	PWD201	turbulent	0.5% in lift & 0.6% in torsion	downstream	45619	3.42E+07	0.73	0.87	239	Not observed	Not observed
4	PWU201	turbulent	0.5% in lift & 0.6% in torsion	upstream	45619	3.42E+07	0.73	0.87	239	Not observed	Not observed

* Typical properties supplied by the Engineers (actual properties vary along span and with arch coordinate). Mass and structural properties of the deck changed during the course of the study due to evolving design of the bridge. Model design values reflect the prototype properties at the time of the model test.

TABLE 3.4 STATIC FORCE COEFFICIENTS, SIDEWALK UPSTREAM, SMOOTH FLOW

Angle of Attack	Cx	Cz	Cm
-12	0.058	-1.185	-0.141
-11	0.048	-1.188	-0.153
-10	0.031	-1.235	-0.178
-9	0.011	-1.281	-0.209
-8	-0.013	-1.324	-0.250
-7	-0.010	-1.234	-0.243
-6	0.004	-1.102	-0.214
-5	0.019	-0.969	-0.178
-4	0.031	-0.827	-0.139
-3	0.047	-0.686	-0.099
-2	0.059	-0.545	-0.062
-1	0.068	-0.404	-0.025
0	0.072	-0.258	0.010
1	0.073	-0.117	0.041
2	0.073	0.039	0.071
3	0.072	0.201	0.091
4	0.074	0.309	0.097
5	0.078	0.373	0.098
6	0.082	0.406	0.099
7	0.085	0.428	0.101
8	0.088	0.442	0.102
9	0.092	0.474	0.105
10	0.095	0.550	0.113
11	0.098	0.579	0.117
12	0.101	0.598	0.120

Slope of Cz Curve = 8.34
Slope of Cm Curve = 1.91
Cz at 0° = -0.258
Cx at 0° = 0.072
Cm at 0° = 0.010

TABLE 3.5 STATIC FORCE COEFFICIENTS, SIDEWALK UPSTREAM, TURBULENT FLOW

Angle of Attack	Cx	Cz	Cm
-12	0.005	-1.449	-0.231
-11	-0.008	-1.459	-0.251
-10	-0.020	-1.452	-0.271
-9	-0.023	-1.401	-0.276
-8	-0.016	-1.312	-0.263
-7	-0.005	-1.203	-0.240
-6	0.007	-1.081	-0.209
-5	0.019	-0.953	-0.174
-4	0.033	-0.823	-0.138
-3	0.047	-0.682	-0.100
-2	0.060	-0.547	-0.064
-1	0.069	-0.415	-0.029
0	0.075	-0.279	0.005
1	0.078	-0.148	0.037
2	0.081	-0.020	0.067
3	0.082	0.113	0.094
4	0.081	0.244	0.116
5	0.079	0.360	0.128
6	0.079	0.455	0.134
7	0.079	0.520	0.135
8	0.081	0.561	0.133
9	0.083	0.585	0.131
10	0.085	0.599	0.128
11	0.087	0.604	0.126
12	0.089	0.612	0.124

Slope of Cz Curve = 7.57
Slope of Cm Curve = 1.87
Cz at 0° = -0.279
Cx at 0° = 0.075
Cm at 0° = 0.005

TABLE 3.6 STATIC FORCE COEFFICIENTS, SIDEWALK DOWNSTREAM, SMOOTH FLOW

Angle of Attack	Cx	Cz	Cm
-12	-0.151	-1.546	-0.222
-11	-0.135	-1.473	-0.209
-10	-0.108	-1.388	-0.191
-9	-0.081	-1.300	-0.171
-8	-0.055	-1.206	-0.151
-7	-0.029	-1.111	-0.130
-6	-0.006	-1.014	-0.109
-5	0.015	-0.914	-0.087
-4	0.033	-0.813	-0.067
-3	0.048	-0.702	-0.045
-2	0.061	-0.586	-0.023
-1	0.070	-0.475	-0.004
0	0.076	-0.362	0.015
1	0.079	-0.248	0.033
2	0.081	-0.136	0.048
3	0.081	-0.020	0.061
4	0.080	0.089	0.069
5	0.079	0.192	0.073
6	0.078	0.281	0.072
7	0.078	0.351	0.070
8	0.078	0.397	0.067
9	0.079	0.426	0.064
10	0.079	0.443	0.060
11	0.080	0.461	0.057
12	0.080	0.473	0.055

Slope of Cz Curve = 6.46
Slope of Cm Curve = 1.02
Cz at 0° = -0.362
Cx at 0° = 0.076
Cm at 0° = 0.015

TABLE 3.7 STATIC FORCE COEFFICIENTS, SIDEWALK DOWNSTREAM, TURBULENT FLOW

Angle of Attack	Cx	Cz	Cm
-12	-0.154	-1.517	-0.224
-11	-0.138	-1.473	-0.214
-10	-0.112	-1.403	-0.198
-9	-0.086	-1.328	-0.180
-8	-0.060	-1.245	-0.160
-7	-0.036	-1.156	-0.138
-6	-0.012	-1.060	-0.116
-5	0.010	-0.962	-0.094
-4	0.029	-0.860	-0.072
-3	0.046	-0.748	-0.050
-2	0.059	-0.633	-0.029
-1	0.068	-0.515	-0.008
0	0.075	-0.396	0.012
1	0.078	-0.273	0.030
2	0.078	-0.144	0.043
3	0.076	-0.002	0.050
4	0.075	0.105	0.048
5	0.077	0.184	0.046
6	0.079	0.235	0.045
7	0.082	0.267	0.045
8	0.084	0.302	0.046
9	0.085	0.371	0.048
10	0.087	0.373	0.051
11	0.092	0.333	0.054
12	0.093	0.342	0.056

Slope of Cz Curve = 6.99
Slope of Cm Curve = 1.04
Cz at 0° = -0.396
Cx at 0° = 0.075
Cm at 0° = 0.012

a) TURBULENT FLOW

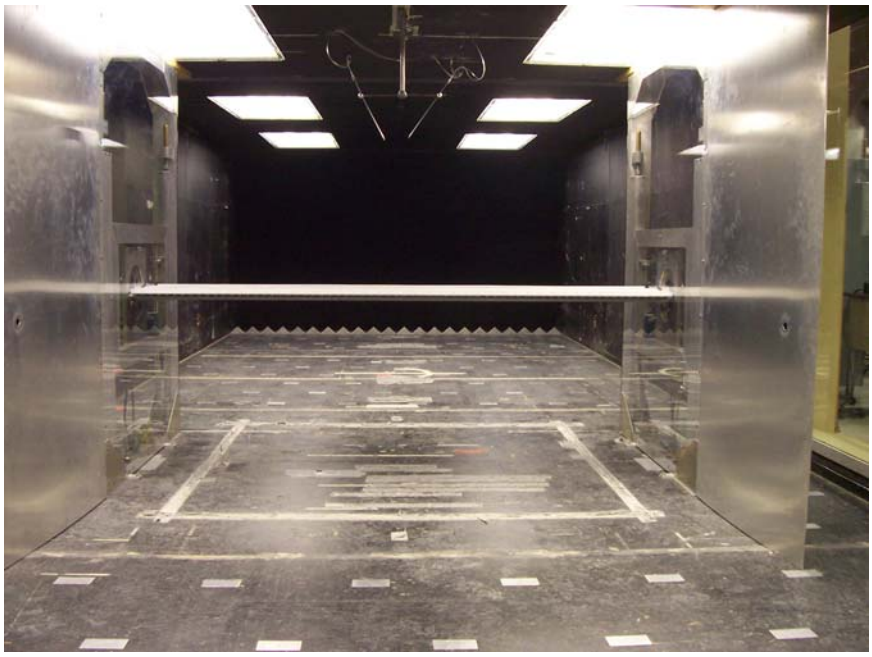

b) SMOOTH FLOW

FIGURE 3.1 SECTION MODEL TEST SET-UP – BRIDGE DECK

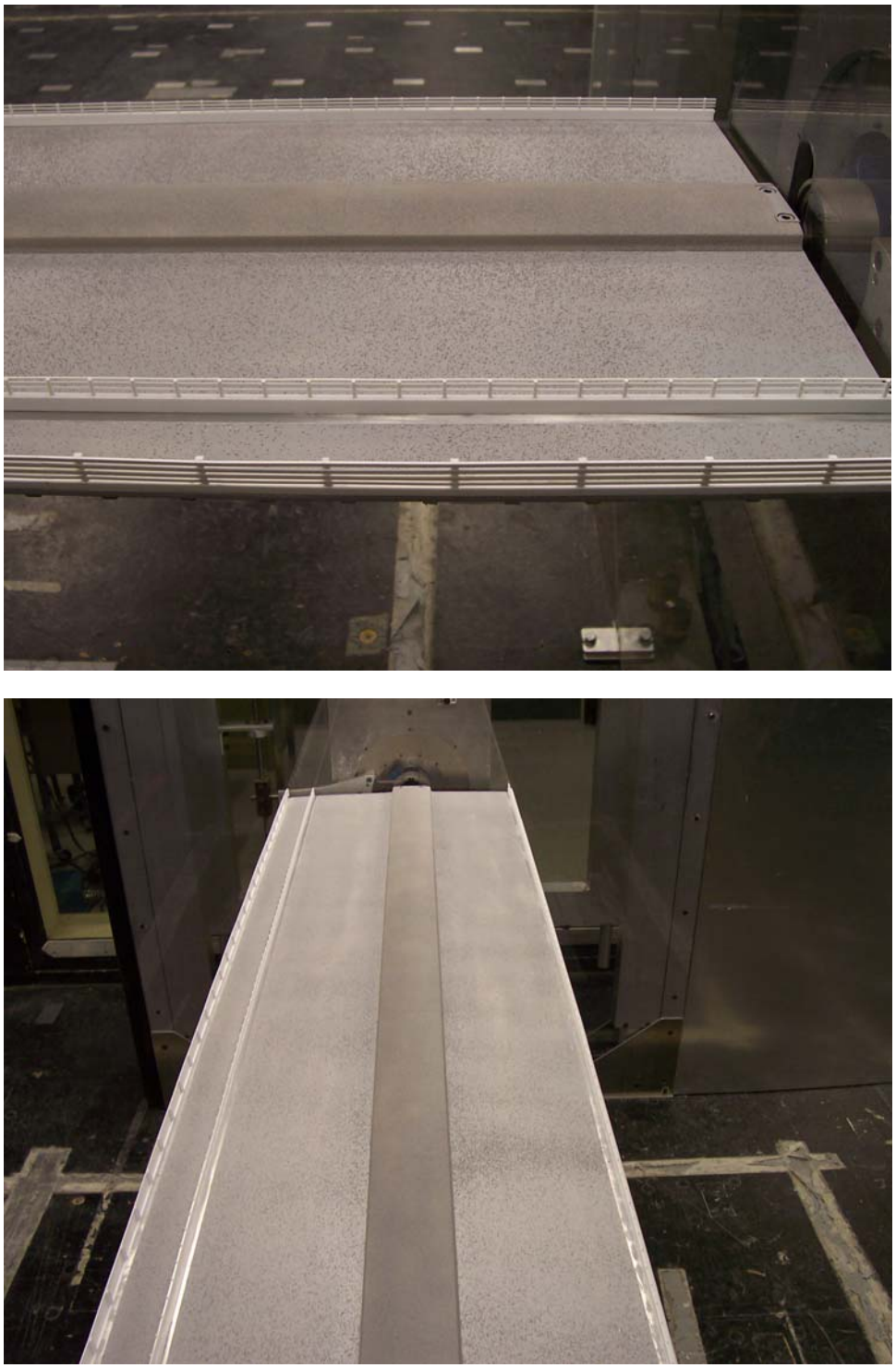

FIGURE 3.2 CLOSE-UP VIEWS OF THE SECTION MODEL

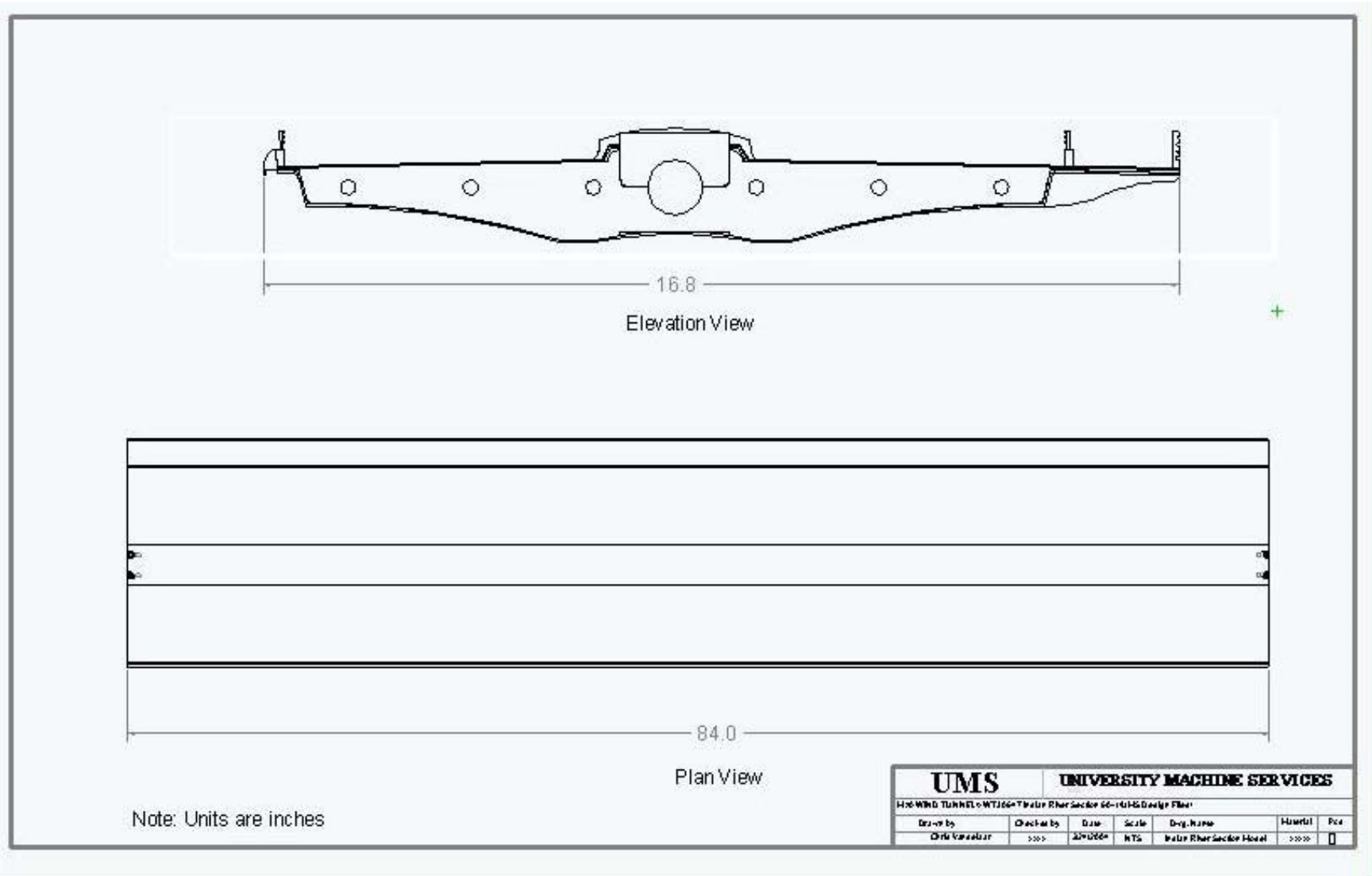

FIGURE 3.3 MODEL DRAWINGS – DECK SECTION

Longitudinal Spectra

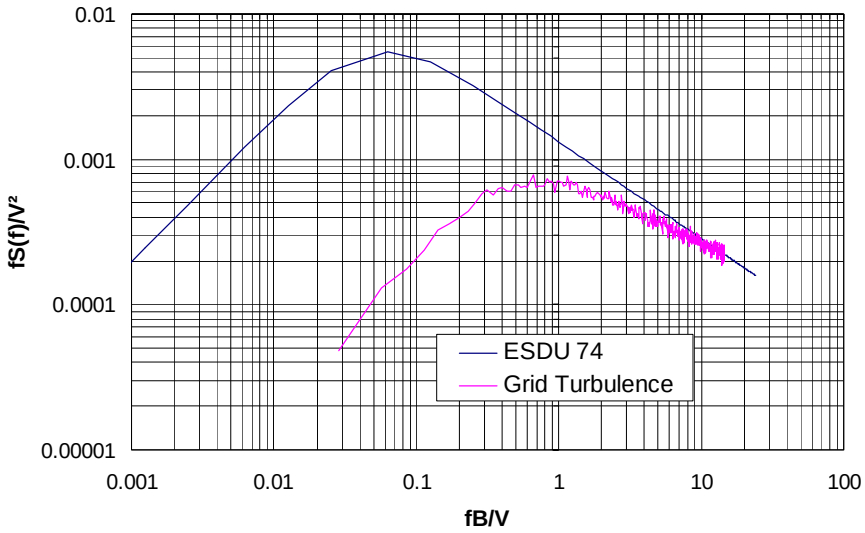

Vertical Spectra

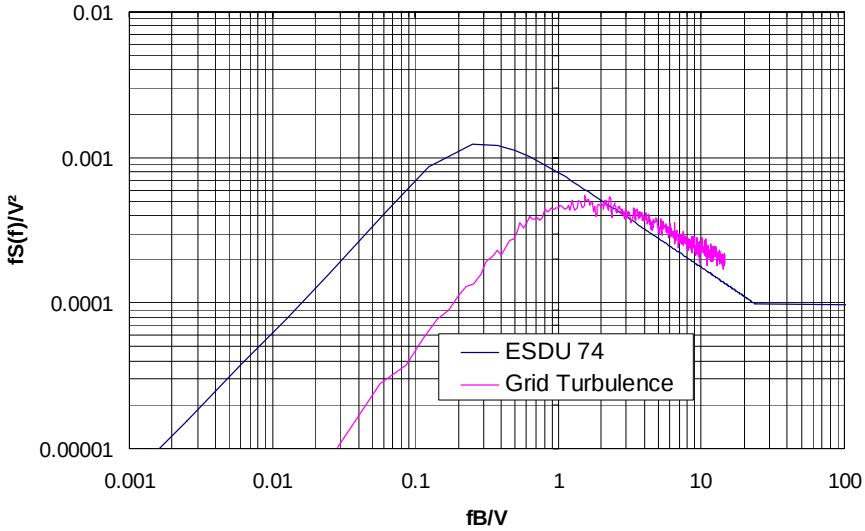

FIGURE 3.4 TURBULENCE SPECTRA (FULL SCALE AND GRID-TURBULENCE)

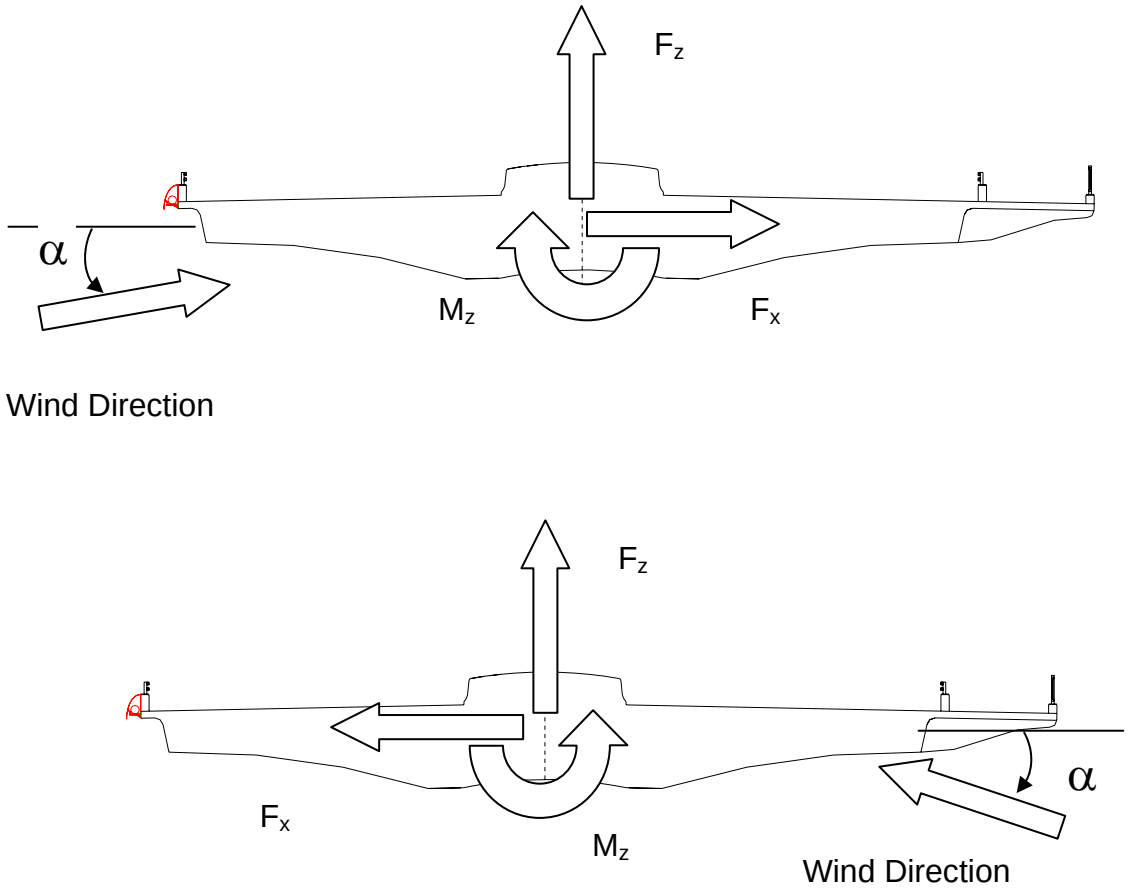

FIGURE 3.5 SKETCH SHOWING SIGN CONVENTION OF FORCES

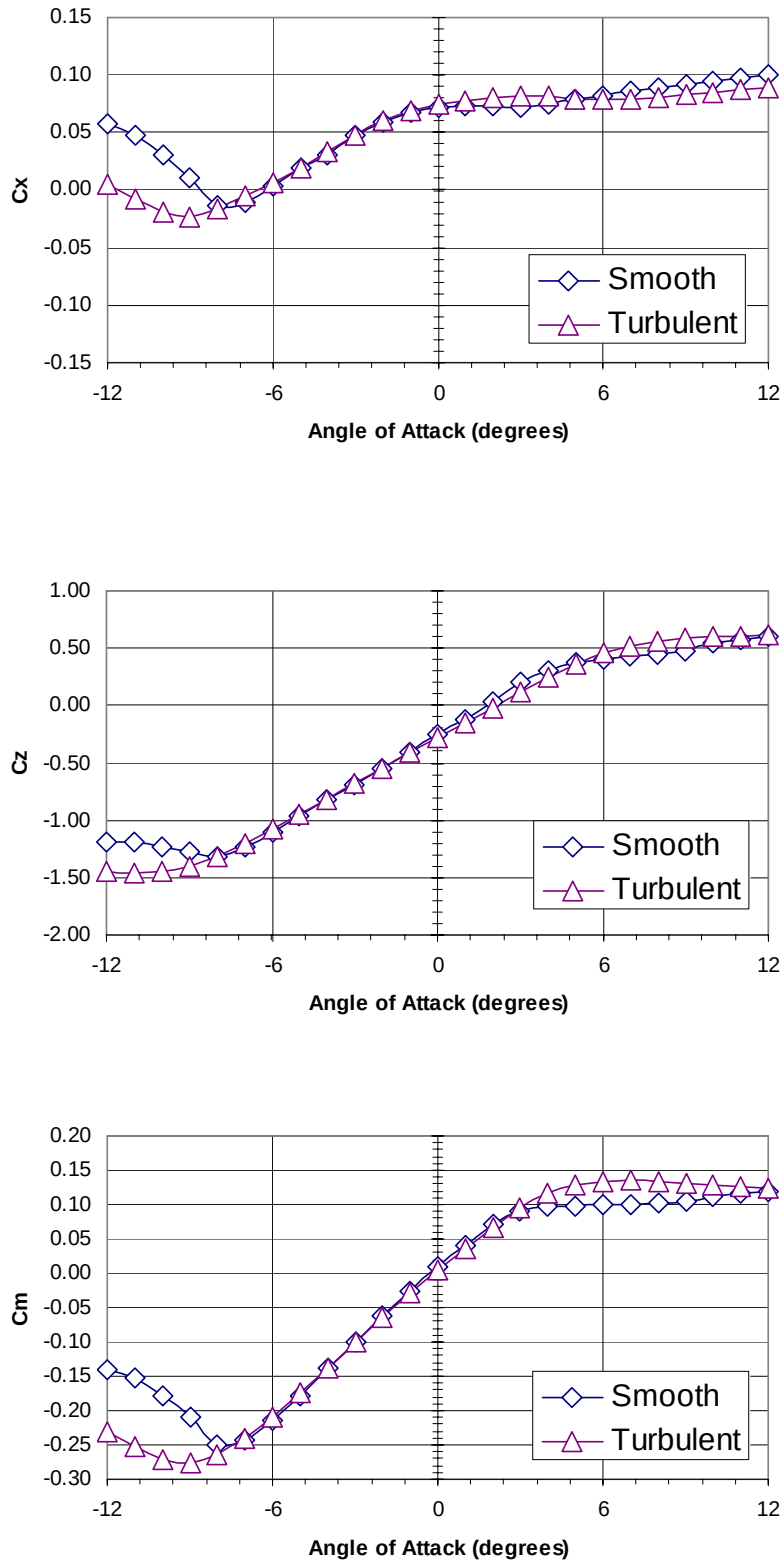

FIGURE 3.6 STATIC FORCE COEFFICIENTS – SIDEWALK UPSTREAM

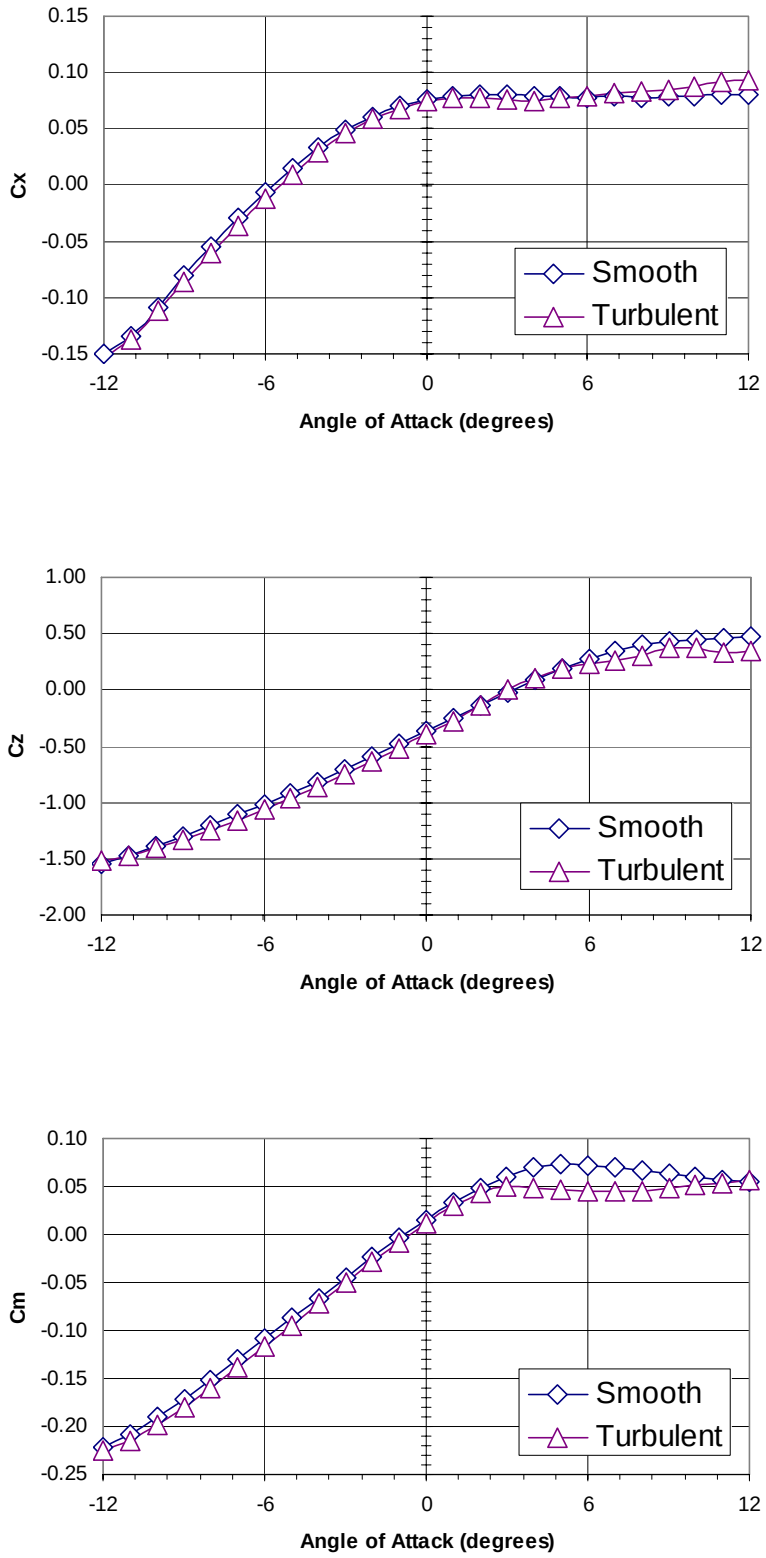

FIGURE 3.7 STATIC FORCE COEFFICIENTS – SIDEWALK DOWNSTREAM

4 EQUIVALENT STATIC LOAD ANALYSIS FOR BRIDGE DECK

4.1 General

The definition of wind loads on the Indian River Bridge follows the approach taken by the Laboratory during the study of wind action on the Sunshine Skyway Bridge, in Tampa, Florida, USA [4, 5]. The definition of wind loads on the structure depends upon the measurements of the dynamic response of a model to turbulent wind and the correction of this response for discrepancies in the intensity and spectrum of turbulence, the damping and the joint acceptance function (a measure of the aerodynamic efficiency of the bridge in its response to turbulence). This approach is described in detail in Appendix E and in References [6, 7].

4.2 Adaptation of Section Model Tests Results

The section model responses shown in Figure 4.1 in turbulent flow were used as the basis for the derivation of the wind loading for the structure. The prototype modes and frequencies used for the prediction of the full scale deck loading were based upon a dynamic analysis of the structure which was supplied by the Engineers. The fundamental symmetric and asymmetric modes of vibration in lift, drag and torque were used in the determination of the equivalent static wind loads. The prototype and model properties used in the analysis are shown in Tables 4.1 and 4.2 respectively.

The turbulence intensities developed in the wind tunnel using grid turbulence is normally lacking sufficient energy in the low frequency - large scale range. While adequate for the definition of resonant response and the overall behavior of the structure to turbulent wind, a slight correction to the loading is made to account for the difference in frequency content. The amplitudes of the spectra of turbulence are matched over the range of reduced frequencies ($f^* = fB/V$) of interest for the deck. The response is adjusted for the deficiency in low frequency turbulence which acts more or less quasi-statically.

The intensities of grid-generated turbulence in the wind tunnel were about 4% and 5% respectively for the vertical and longitudinal components. The responses shown in Figure 4.1 of the Section Model Study are not adjusted for the target level of turbulence (nor the deficiency in low frequency turbulence). The analysis of the dynamic loads includes an adjustment to consider both of these areas, as well as a mode shape correction. A vertical turbulence intensity of 5%, resulted from the selection of the terrain roughness length Z_o (=0.025 ft) at the project site, was used in the analysis (implying an approximate correction of 5/4 or 1.25 on the dynamics).

The equivalent static load analysis was carried out for the completed bridge for a mean wind inclination of 0°. The lowest symmetric and asymmetric deck modes of vibration which are used as the load distribution functions are shown in Figure 4.2. Since the true fundamental asymmetric torque mode of the bridge deck are higher than the 15th mode with frequencies over 1.7Hz, its effect on the overall dynamic responses of the bridge is considered small and not included in this analysis. The equivalent static wind loads resulting from this analysis of the bridge deck are presented in Figure 4.3. A mean hourly wind speed of 91 mph at deck height is used as a reference wind speed, and the loads for this speed are reproduced in equation form below. These loads are summarized for the assumed prototype damping case of 0.5% of critical (or a logarithmic decrement of 0.031). Loads for other wind speeds can be interpolated from the plots.

$$W_x(\eta)\ lb/ft = 177\alpha(\eta) \pm \gamma_{1x} 271\alpha_{1x}(\eta) \pm \gamma_{2x} 129\alpha_{2x}(\eta) \qquad (1)$$

$$W_z(\eta)\ lb/ft = 551\alpha(\eta) \pm \gamma_{1z} 3520\alpha_{1z}(\eta) \pm \gamma_{2z} 4756\alpha_{2z}(\eta) \qquad (2)$$

$$W_\theta(\eta)\ lb\cdot ft/ft = 7947\alpha(\eta) \pm \gamma_{1\theta} 56191\alpha_{1\theta}(\eta) \qquad (3)$$

In the equations, W_x (kN/m), W_z (kN/m) and W_θ (kN-m/m) are the desired wind loads per unit length resulting from the application of: $\overline{W}$ (kN/m), the mean, distributed according to $\alpha(\eta)$ (normally with a

constant value of 1), $\tilde{W}_1$ (kN/m), the symmetric, according to $\alpha_1(\eta)$ and $\tilde{W}_2$ (kN-m/m), the asymmetric, according to $\alpha_2(\eta)$. These distribution functions vary according to the mode shapes presented in Figure 4.2 with a maximum value of 1.0.

To reflect the multitude of combinations with which the fluctuating loads can occur, the load combination factors γ_{1x}, γ_{2x} γ_{1z}, γ_{2z}, $\gamma_{1\theta}$, $\gamma_{2\theta}$ should be used in any combination of the modal terms whose values are taken as follows: γ=±1.0 if only one modal term is included; ±0.8 for two terms; ±0.7 for three terms and ±0.6 for four or more terms. This applies to all modal terms whether they are in X, Z and θ, singly or together.

TABLE 4.1 SUMMARY OF PROTOTYPE PROPERTIES

Deck Height:	A deck height of 50 ft was used in the analysis.
Deck Width:	110.6 ft
Mass:	45619 lb/ft
Mass Moment of Inertia:	3.42E+07 lb-ft^2/ft
Structural Damping:	0.5% of critical (0.031 log. dec.)

	Frequency (Hz)					
	Symmetric			**Anti-symmetric**		
Configuration	**drag**	**lift**	**torque**	**drag**	**lift**	**torque**
Completed Bridge	0.54	0.73	0.87	1.0	0.49	N/A

TABLE 4.2 SUMMARY OF MODEL PROPERTIES

Test data file:	PWU2A001.aer
Frequency:	3.75 Hz (Lift)
	4.74 Hz (Torque)
Mass:	7.11 Lb/ft
Mass moment of Inertia:	0.819 lb-ft^2/ft
Structural Damping:	0.5% of critical (=0.031 log. dec.)
Length:	7 ft
$dC_z / d\alpha$	7.57
C_x at 0°	0.075

TABLE 4.3 SUMMARY OF WIND CHARACTERISTICS

Wind Characteristics

based on ESDU 82026, ESDU 83045, ESDU 85020

Aerodynamic roughness length:	z_o	0.025 ft
Height of deck:	H	50 ft
Reference hourly mean wind speed at deck height:	V_{ref}	91 mph
Latitude:		44.5°
Longitudinal turbulence intensity:	I_u	0.14
Vertical turbulence intensity:	I_w	0.05

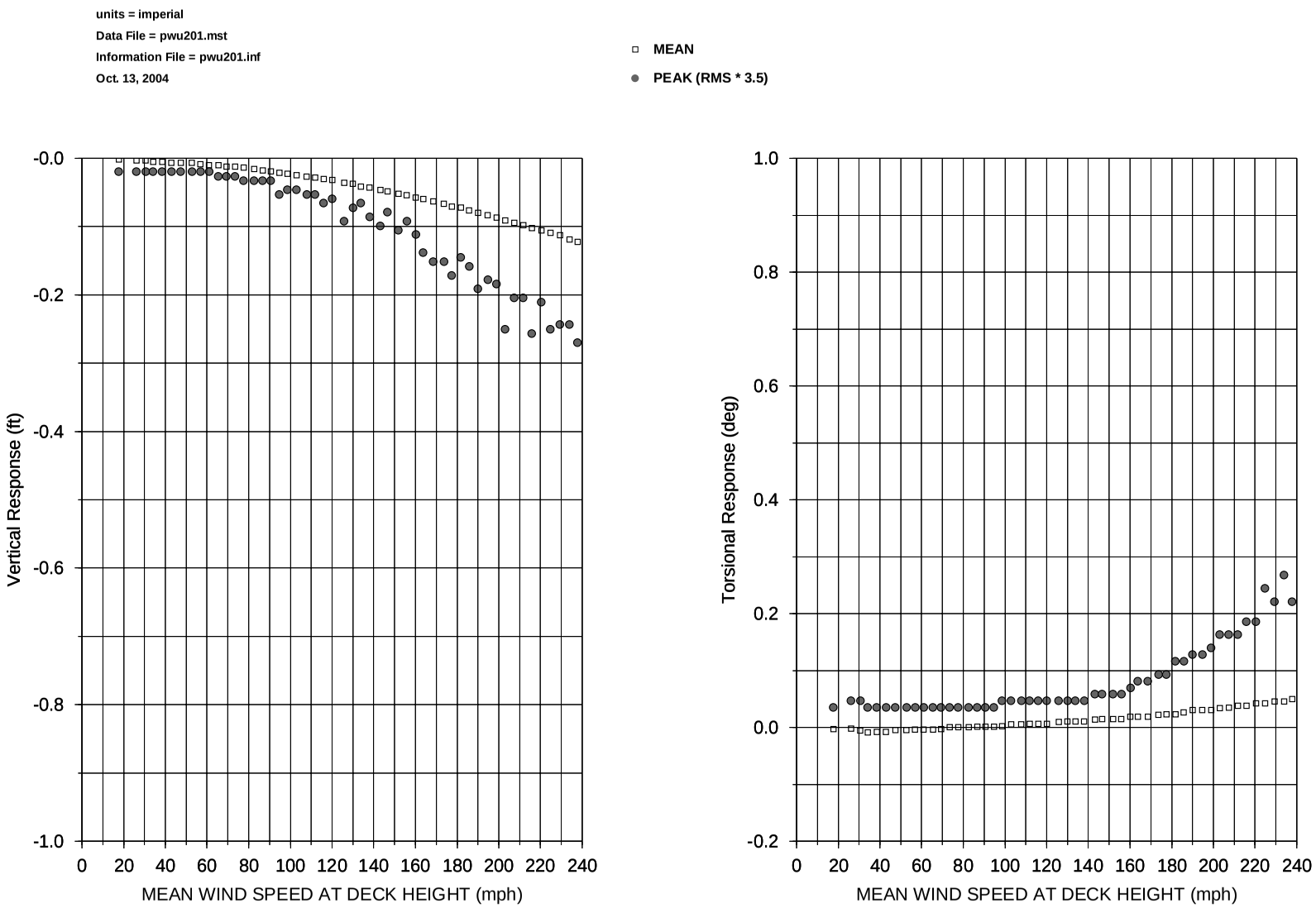

IRIB - Revised Properties, Sidewalk Upstream, Turb Flow, 0.5% Damping

FIGURE 4.1 DYNAMIC TEST RESULT, TURBULENT FLOW AT 0° ANGLE OF ATTACK

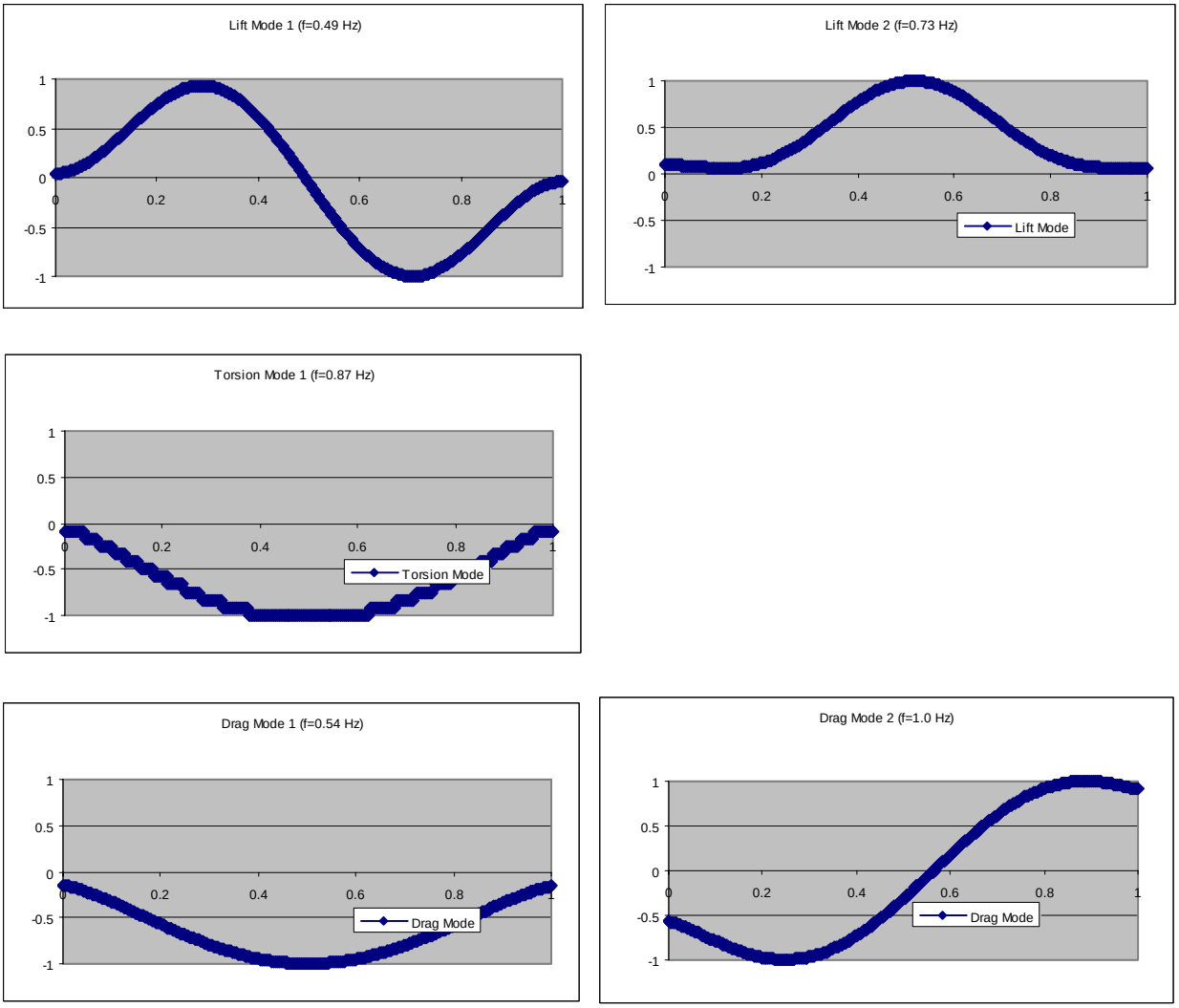

FIGURE 4.2 MODE SHAPES USED IN THE ANALYSIS

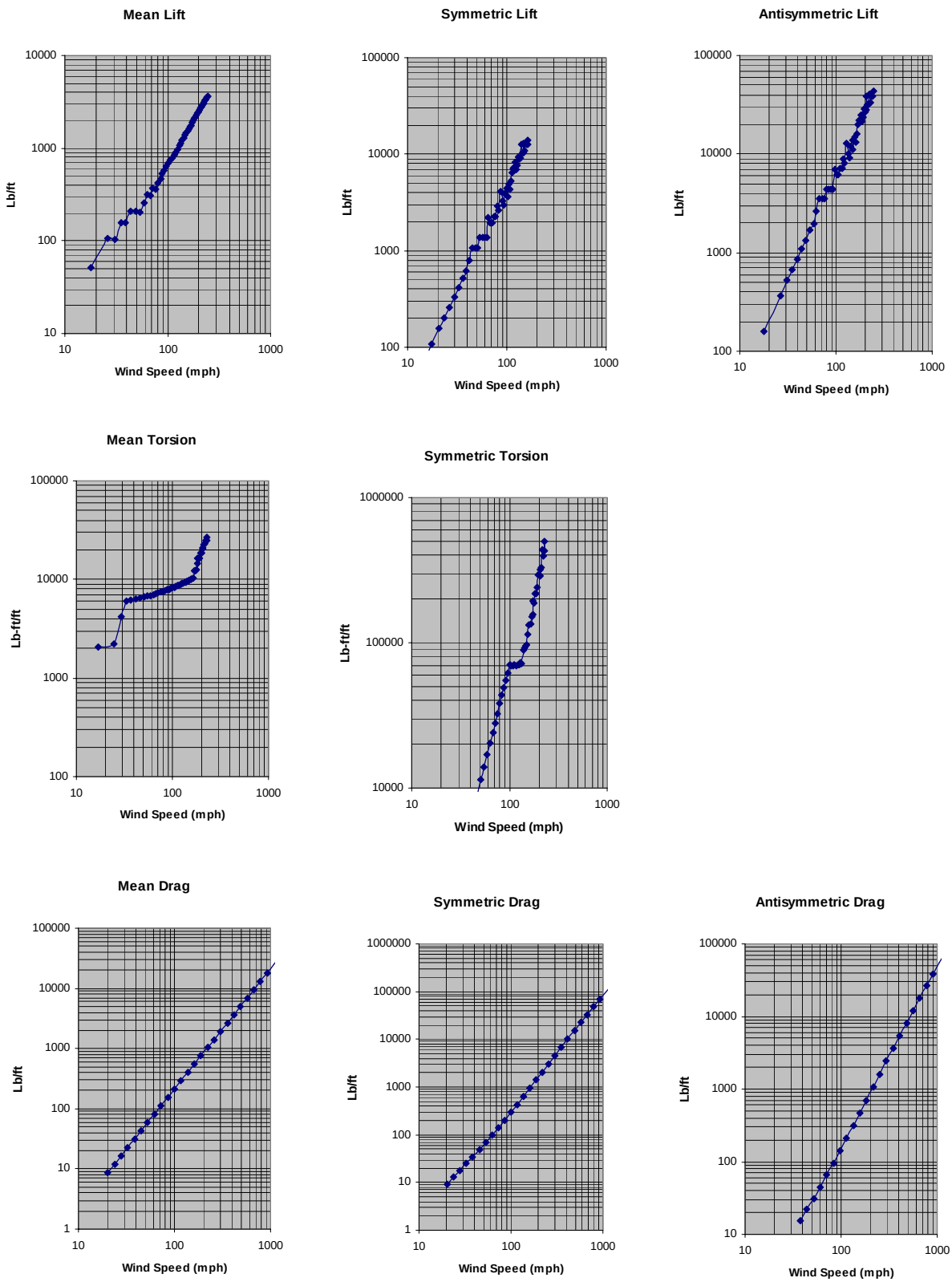

FIGURE 4.3 WIND LOAD COMPONENTS FOR COMPLETED BRIDGE

5 SECTION MODEL STUDY – ARCH SECTION

5.1 General

This section examines the behavior of the Indian River Inlet Bridge arch rib under the action of wind using the section model approach.

The 7 ft long section model corresponds to a uniform 280 ft long section of the full scale arch at a prototype scale of 1 to 40. A typical section model test setup is shown in Figure 5.1. A close up view of the model is shown in Figure 5.2 and the model drawings are shown in Figure 5.3.

The arch rib was studied using the section model technique at the inlet to the High Speed Section of the Boundary Layer Wind Tunnel II. Testing of the deck section model was conducted under the action of both grid-generated turbulence and uniform flow conditions for comparative purposes. The spectrum of the grid generated turbulence was given in Section 3 of the deck section model study and is repeated here as Figure 5.4. The small scales of turbulence (higher frequencies) generated by the grid simulate those in the atmosphere which, in the case of bluff sections, can alter the aerodynamic force coefficients and thus the comparison of the two flow conditions.

The static testing of the arch rib gives force coefficients as a function of angle of attack of the wind which can be used to examine the overall stability of the section and also as an input to a detailed analysis of the response of the overall arch. The latter is discussed in Section 6 of this report

5.2 Static Testing – Arch Rib

The model was mounted on the BLWTL Bridge 3-component balance, which is capable of measuring the total forces on the section (X and Y body forces as well as the torque). Tests were performed adjusting the model inclination relative to the mean wind flow. Lift and Drag were calculated from the measured X and Y body force components. The sign convention for the definition of the force coefficients is given in Figure 5.5.

The force coefficients are similar in definition to those for a bridge deck, but in this case the across-wind dimension, *D* is used because the cross-section is considerably more bluff and the separated flow region dominates the aerodynamic behavior. The definitions are:

$$C_{x,y} = \frac{F_{x,y}}{qD}$$

for and the torque coefficient is defined:

$$C_{Mz} = \frac{F_t}{qBD}$$

Tests were carried out in the same flow fields (smooth and turbulent) as the bridge deck. A similar range of Reynolds numbers was investigated. However, unlike the bridge deck results, a strong Reynolds number dependency in the results was observed. In short, this means that the values of the static force coefficients change with wind speed, making interpretation of the results (i.e. extrapolation to full scale) difficult, if not impossible. The difficulty arises from the degree to which the coefficients change with Reynolds number and is added to by the fact that in general, wind tunnels are unable to achieve full scale Reynolds numbers.

A second series of tests were conducted to investigate the extent of the Reynolds number dependency. While testing to full scale Reynolds number is not practical, the different regimes of behavior (subcritical, critical and supercritical) are all present in the range examined in the model tests and thus give an indication of the coefficient values at full scale. The values for use in design are based on the

tests on the arch model, combined with experience with flow around the circular cylinder, a shape that is reported on extensively in the literature. Due to the attempt to achieve the maximum Reynolds numbers in the testing program, a large model scale was used resulting in significant blockage of the wind tunnel cross section. The effect of blockage or wall confinement effects is to increase the magnitude of the negative pressure in the wake of the arch model. This leads to higher mean forces than would be measured on the same model without the confining effect of the wind tunnel walls. Various methods of correcting the force coefficients for blockage effects have been studied. The method was developed by used here was developed by Modi and El Sherbiny (Reference 8) for circular cylinders. The blockage correction is given by:

$$C_{F_c} = C_F \cdot (1 - 1.404 \cdot C_{Fx} \cdot S)$$

where the subscript c denotes corrected value, C_{Fx} is the measured drag coefficient and S denotes the solid blockage ratio. In this case, S=10%.

The static aerodynamic coefficients from the second series are summarized in Table 5.1 for both turbulent and smooth flows, along with the slopes of the coefficients. The full set of results from the second series is shown in Figure 1.6. The values from Table 5.1 correspond to the asymptotes indicated. The data from the first series of tests is given in Appendix F.

The slopes of the vertical force coefficient curve provide an indication of dynamic stability for cross-wind motion or “galloping”. Using Den Hartog’s criteria, if $(C_x + \frac{\partial C_y}{\partial \alpha}) < 0$, there will be an aerodynamic force in the vertical direction which will be proportional to the velocity of the motion or in other words a negative aerodynamic damping term and hence a cross-wind instability would be the result. This is not the case for the arch due to the large drag force and the near-zero slope in the vertical force coefficient.

It has been shown that the quasi-steady approximation to torsional aerodynamic damping is equal to:

$$\zeta_\theta = \left(\frac{C'_m}{32\pi}\right)\left(\frac{\rho_{air} B^4}{I_o}\right)\left(\frac{V}{fB}\right)$$

In spite of a negative slope in the Moment Coefficient (-0.21), the large mass moment of inertia (I_o) and small characteristic dimension (B) and high natural frequency (f) make this a very small term when compared to the structural damping of the arch rib.

TABLE 5.1 SUMMARY OF RESULTS FROM STATIC TESTS ON INDIAN RIVER INLET BRIDGE ARCH

	Recommended Value for Design	Slope
C_{Fx}	0.95	
C_{Fy}	0.45	~ 0
C_{Mz}	0.07	-0.21

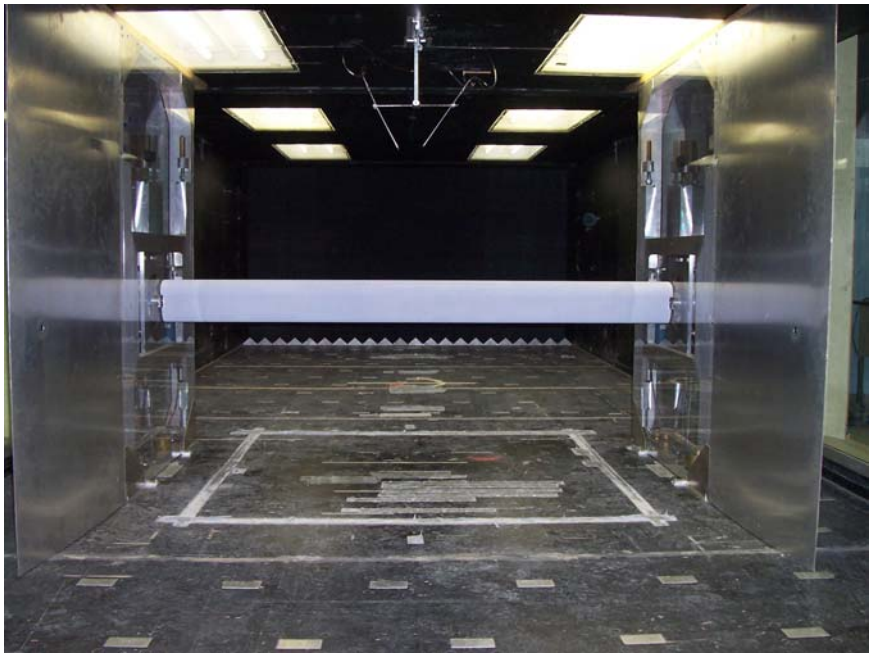

FIGURE 5.1 SECTION MODEL TEST SET-UP – ARCH SECTION

FIGURE 5.2 CLOSE-UP VIEW OF THE ARCH SECTION MODEL

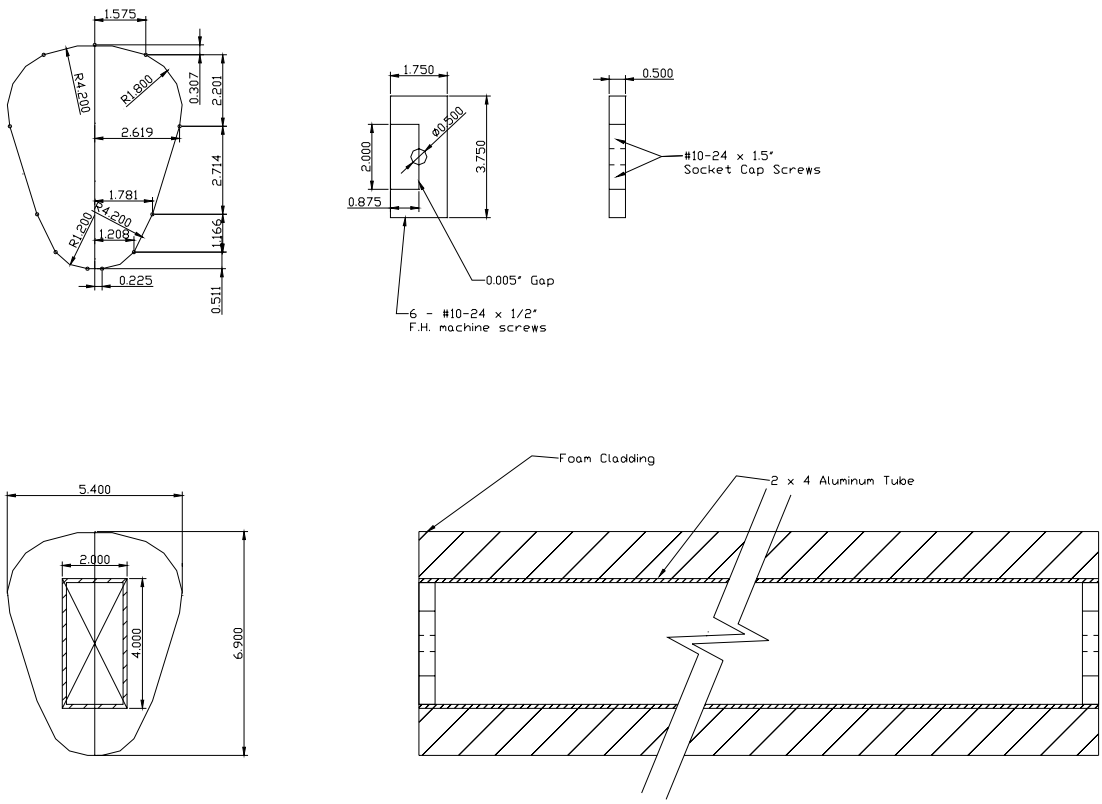

FIGURE 5.3 MODEL DRAWINGS – ARCH SECTION

Longitudinal Spectra

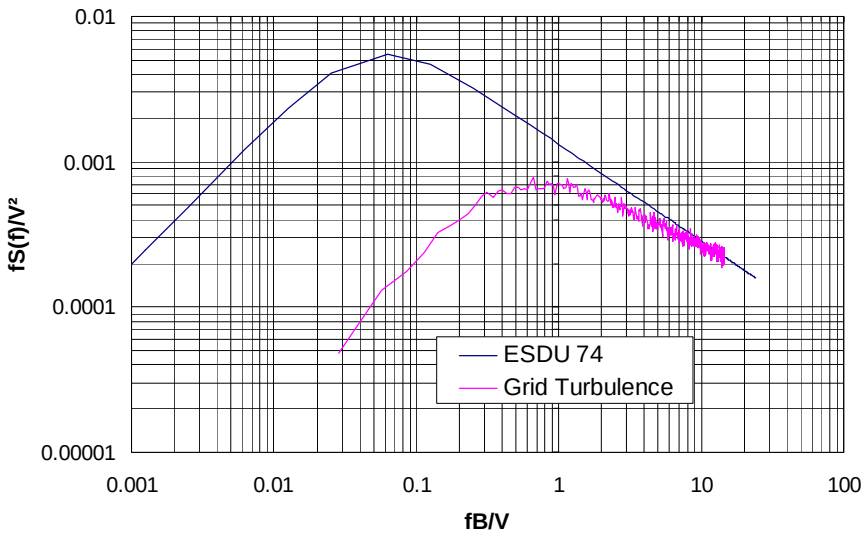

Vertical Spectra

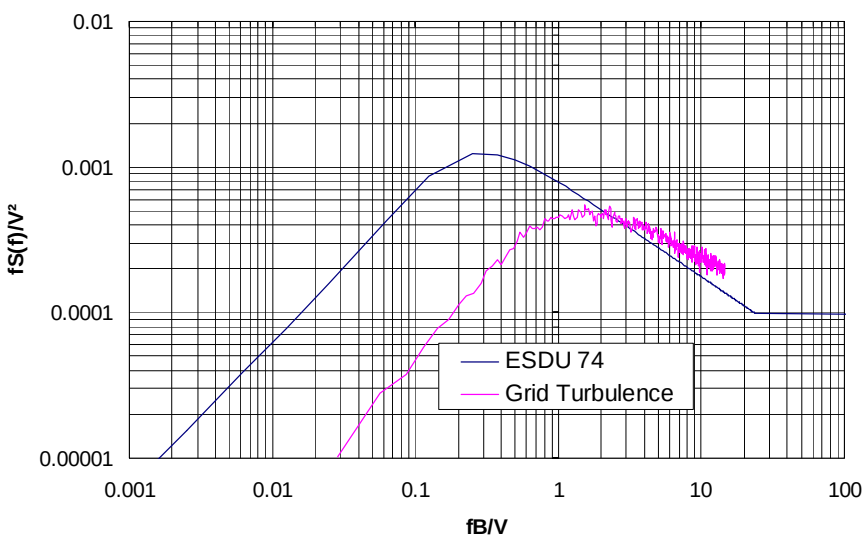

FIGURE 5.4 TURBULENCE SPECTRA (FULL SCALE AND GRID-TURBULENCE)

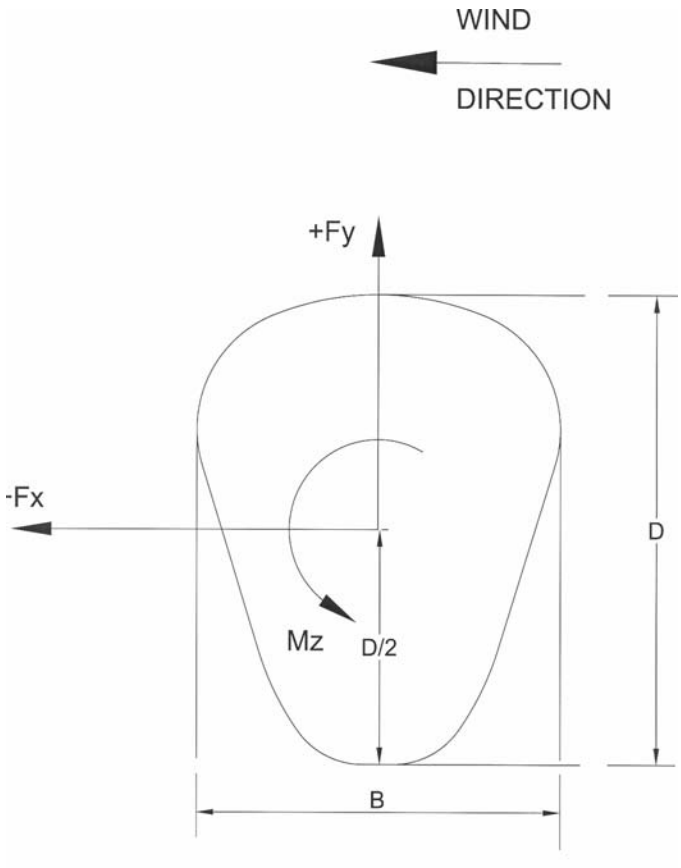

FIGURE 5.5 SKETCH SHOWING SIGN CONVENTION OF FORCES, ARCH SECTION

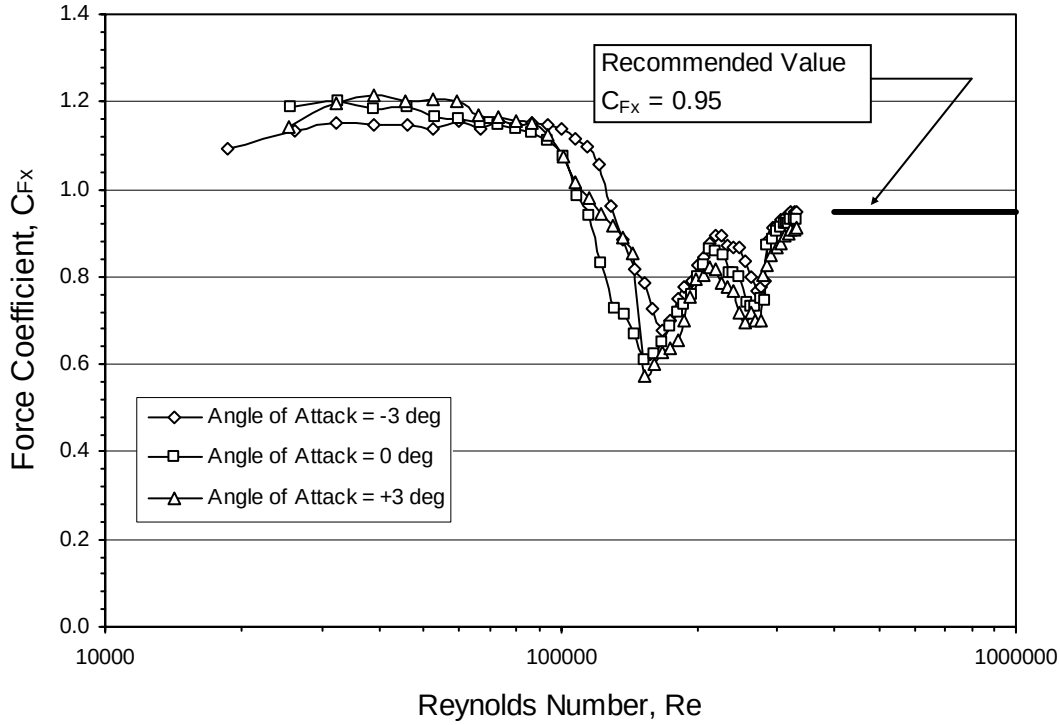

SMOOTH FLOW

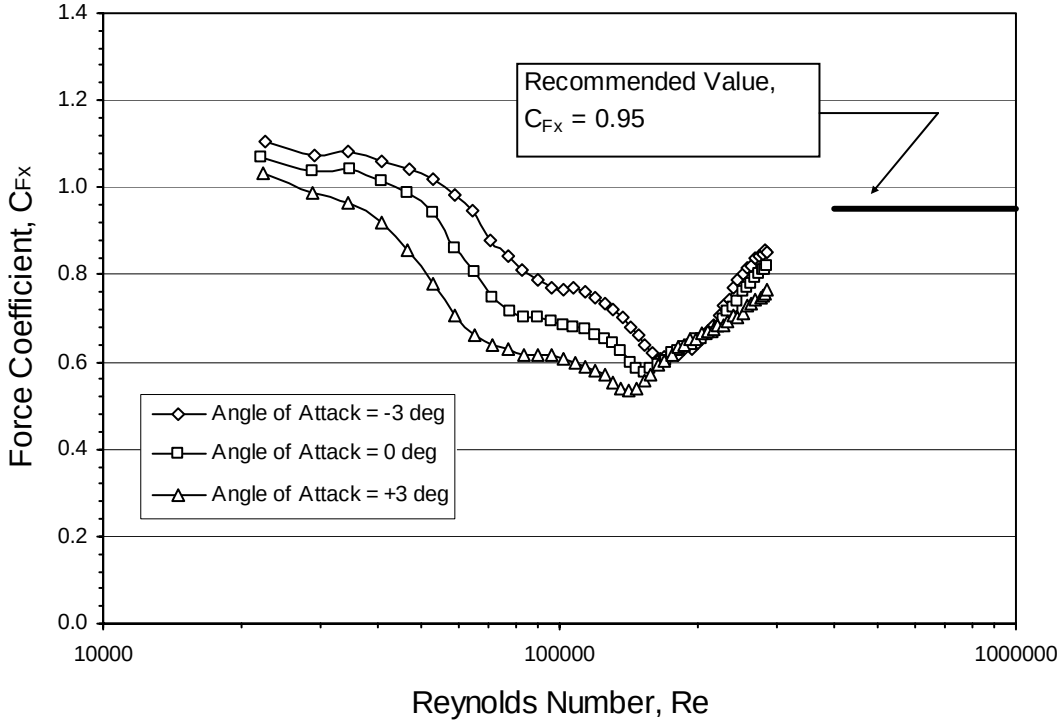

TURBULENT FLOW

FIGURE 5.6 STATIC FORCE COEFFICIENTS, ARCH SECTION

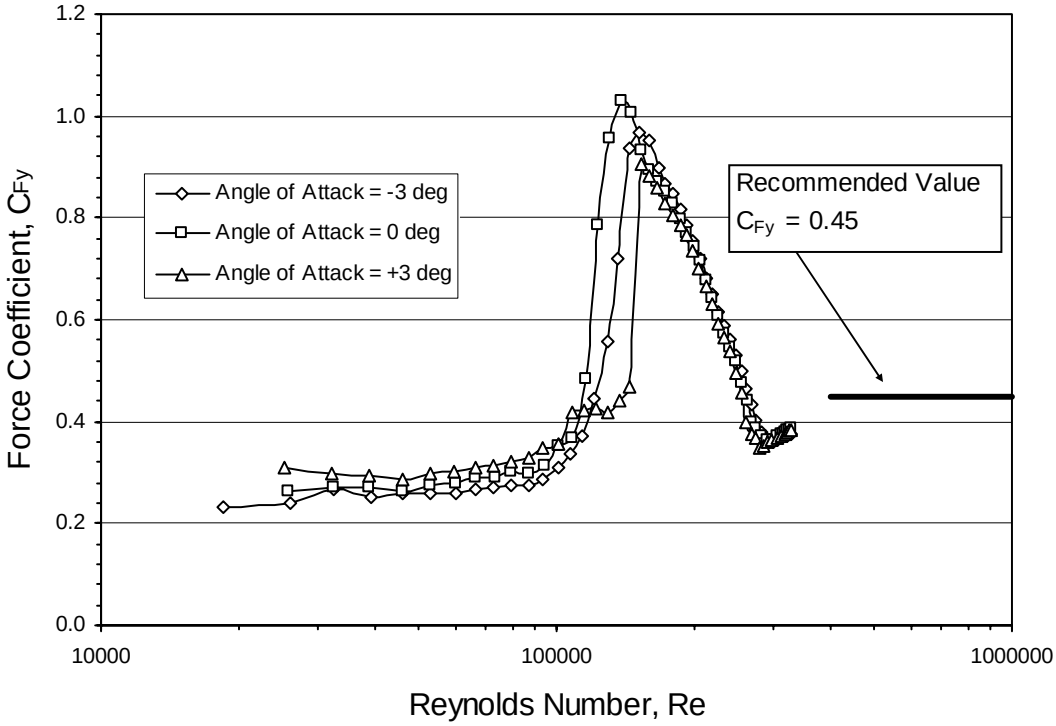

SMOOTH FLOW

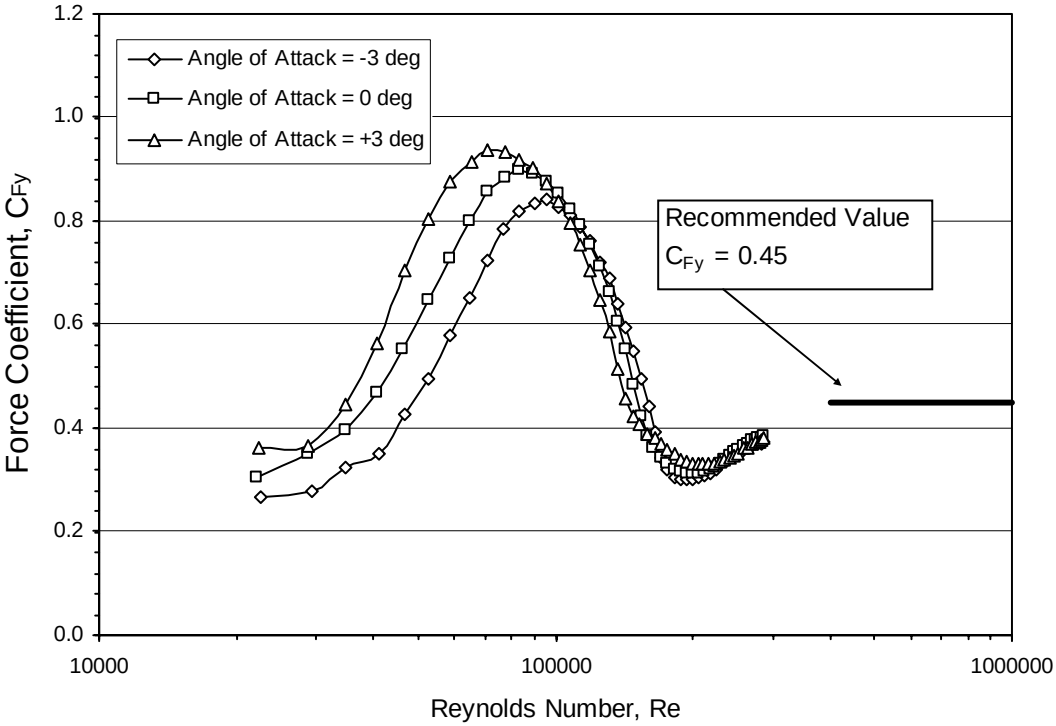

TURBULENT FLOW

FIGURE 5.6 (CONT.) STATIC FORCE COEFFICIENTS, ARCH SECTION

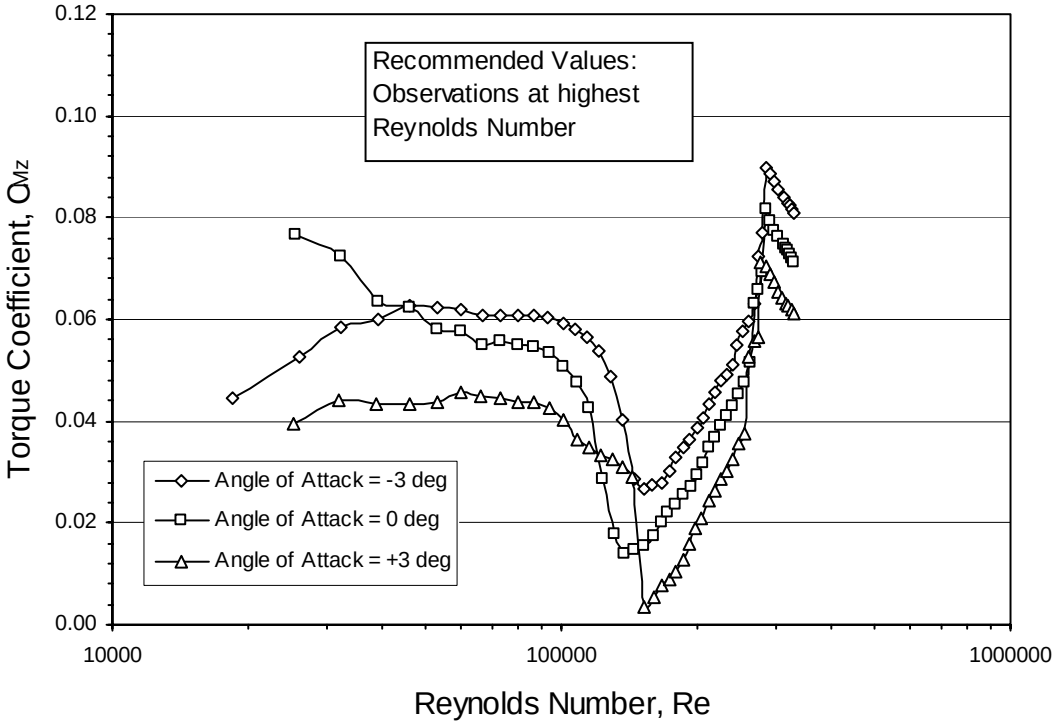

SMOOTH FLOW

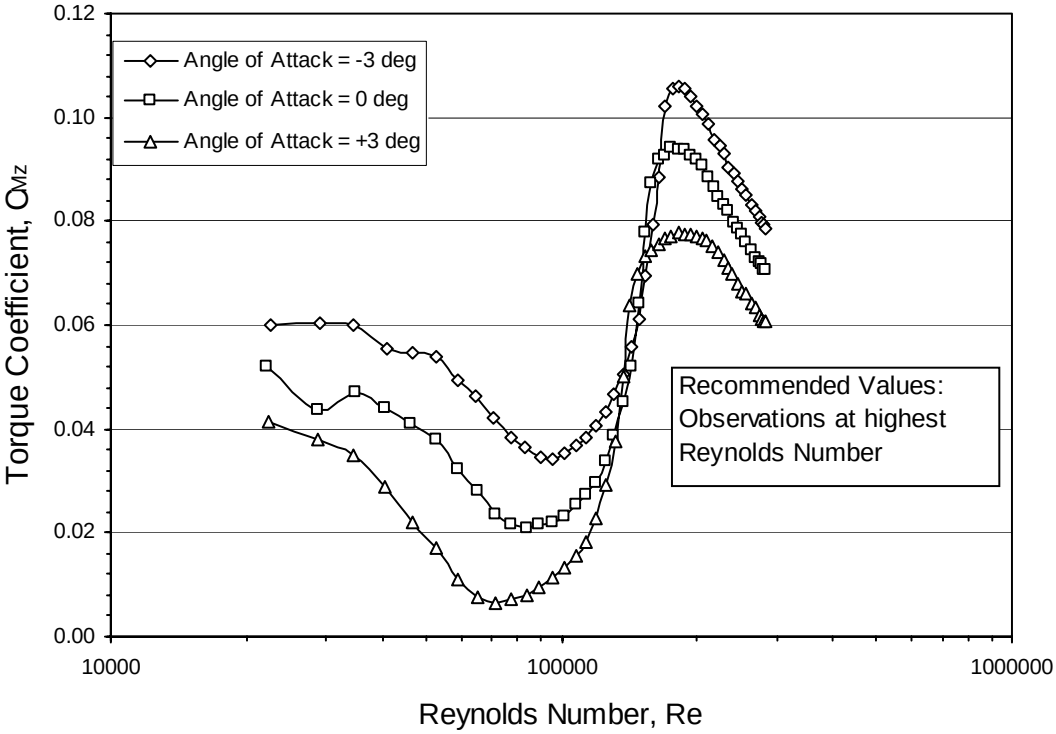

TURBULENT FLOW

FIGURE 5.6 (CONT.) STATIC FORCE COEFFICIENTS, ARCH SECTION

6 STRUCTURAL LOADS ON ARCH RIB

6.1 Approach for Loads Analysis

The structural loads analysis follows the well established procedure for calculating the response of line-like structures to wind action. The details of this procedure are presented in Appendix G.

The coefficients from the static testing were used in conjunction with the arch structural properties provided by Figg Bridge Engineers to calculate the maximum bending moments due to drag. The arch properties included influence functions for bending moment at the base of the arch and the mode shapes for all arch dominated modes with periods longer than 1.0 second. The influence functions are shown in Figures 6.2 and 6.3, while the coordinate system used in defining the influence functions is given in Figure 6.1. These data were combined with the design wind speeds and profiles previously reported. The results are summarized in Table 6.1. The structural damping assumed in the calculations was 2.75%.

6.2 Equivalent Static Loads

Equivalent static loads were derived based on the overall bending moment at the base of the arch. The loads are presented here as statically acting pressures in four components: (1) mean, (2) quasi-steady (slowly varying and hence similar in distribution to the mean), (3) symmetric and (4) anti-symmetric. The maximum magnitudes of the various components are given in Table 6.2. The distributions with height of the components are given in Figure 6.4. The mean, quasi-steady and symmetric load components all vary with the square of the mean wind speed. The anti-symmetric load is simplified and does not have this added complication of wind speed varying with height. The curve in Figure 6.4 is given by:

$$\frac{P(z)}{P(z_{crown})} = \left(\frac{\ln\left(z + z_{deck} / z_o \right)}{\ln\left(z_{deck} + z_{crown} / z_o \right)} \right)^2$$

where $P(z_{crown})$ is given in Table 6.2, z_{deck} is the deck height and z_o is the roughness length. $z_o = 0.024ft$ for the 100-year wind storm off the Atlantic Ocean. The anti-symmetric load component is constant with height.

The distributions with distance along the deck from the arch – deck intersection are given in Figure 6.5. The mean and quasi-steady components are constant along the span, the symmetric component is a half period sine wave and the anti-symmetric component is a full period sine wave. The latter two follow very closely with the first and second ‘arch’ modes of the bridge.

The loads are applied in sequence and the load effects combined as usual with the load combination factor, γ, when more than one load effect is combined. γ equals 1.0 when the load effect due to any one of P_Q, P_{sym} or $P_{antisym}$ is added to the mean load effect, 0.8 when any two are added and 0.7 when all three are added simultaneously.

The change in the equivalent static loads for various return periods is given in Figure 6.6. To account for the change in the roughness for increasing wind speed, revised z_o values are given in Table 6.3.

TABLE 6.1 RESULTS FROM DETAILED ANALYSIS OF WIND-INDUCED RESPONSE OF THE ARCH RIB

	Intersection of Arch Rib and Deck	Joint 1
Peak Moment		
Mx =	131 x 10^3 kip-ft	111 x 10^3 kip-ft
Mz =	140 x 10^3 kip-ft	118 x 10^3 kip-ft
Equivalent Gust Factor	2.48	2.51

TABLE 6.2 MAGNITUDE OF PRESSURES FOR THE VARIOUS COMPONENTS OF THE EQUIVALENT STATIC LOAD DISTRIBUTIONS CORRESPONDING TO A 100-YEAR RETURN PERIOD MEAN HOURLY WIND SPEED AT ARCH CROWN = 110 MPH

Component	Magnitude
Mean, P_{mean} *	30 psf
Quasi-Steady, P_Q	15 psf
Symmetric, P_{sym}	40 psf
Anti-Symmetric, $P_{antisym}$	8.5 psf

TABLE 6.3 VARIATION OF MEAN WIND SPEED AT ARCH HEIGHT ROUGHNESS LENGTH, Z_O WITH RETURN PERIOD

Return Period (Years)	Mean Windspeed at Arch Height (mph)	Roughness Length, z_o (ft)
10	58	.0057
50	96	.018
100	110	.024
500	135	.038
1000	143	.043
10000	165	.058

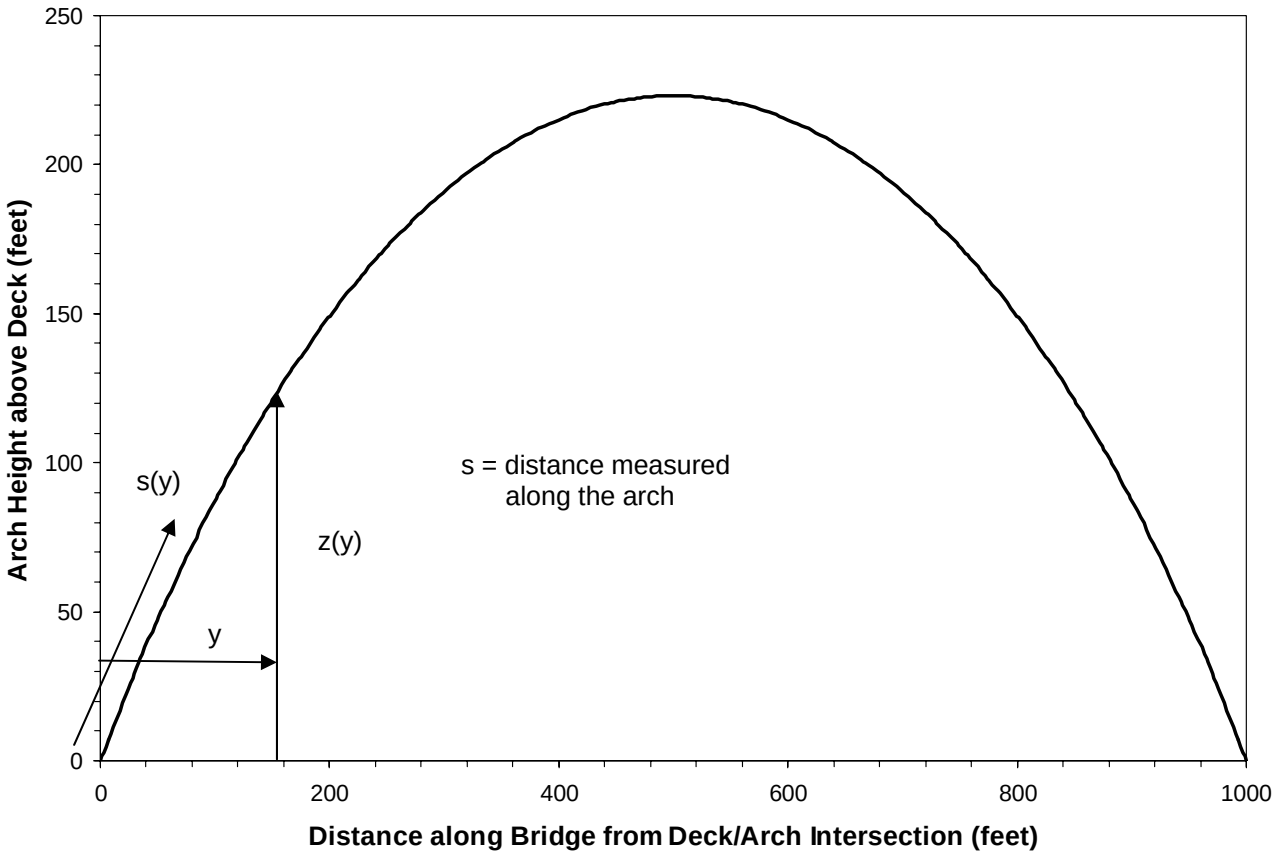

FIGURE 6.1 DEFINITIONS OF GEOMETRY AND COORDINATE SYSTEM

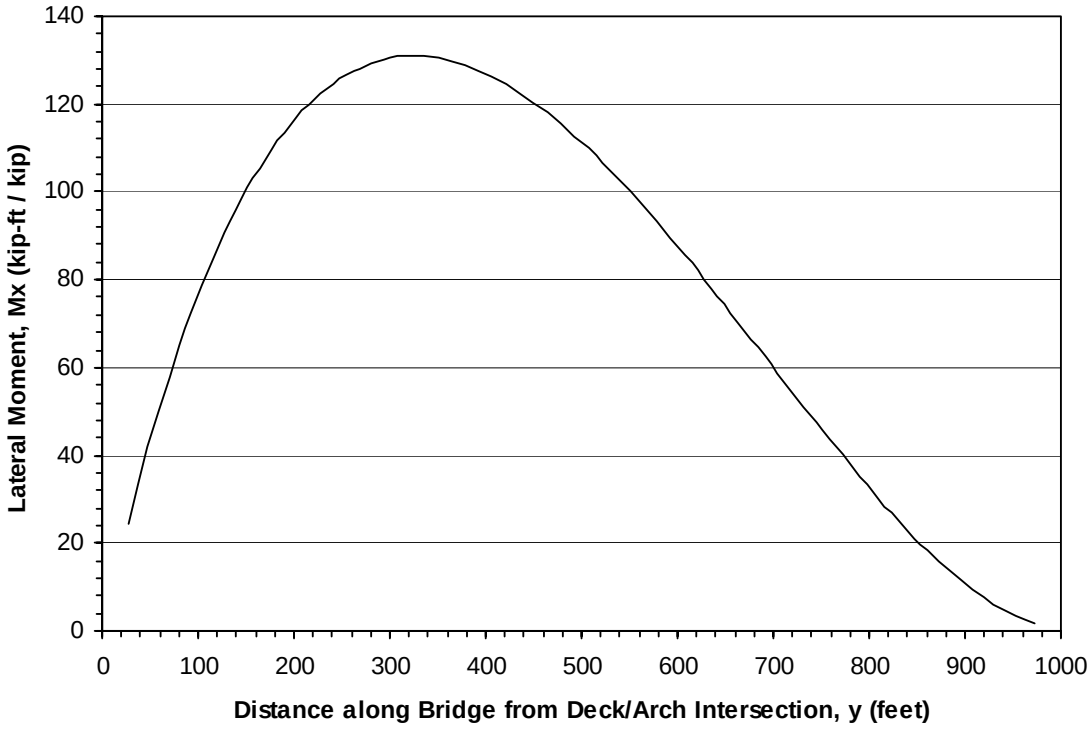

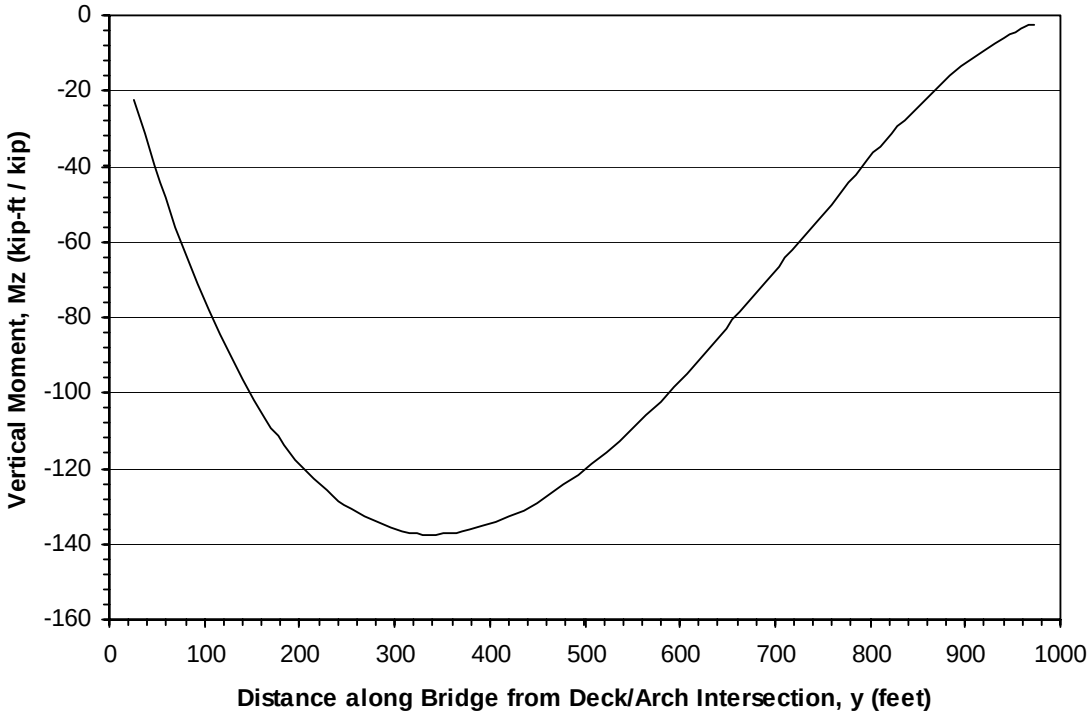

FIGURE 6.2 INFLUENCE FUNCTIONS FOR THE BENDING MOMENT RESPONSE AT THE DECK/ARCH INTERSECTION

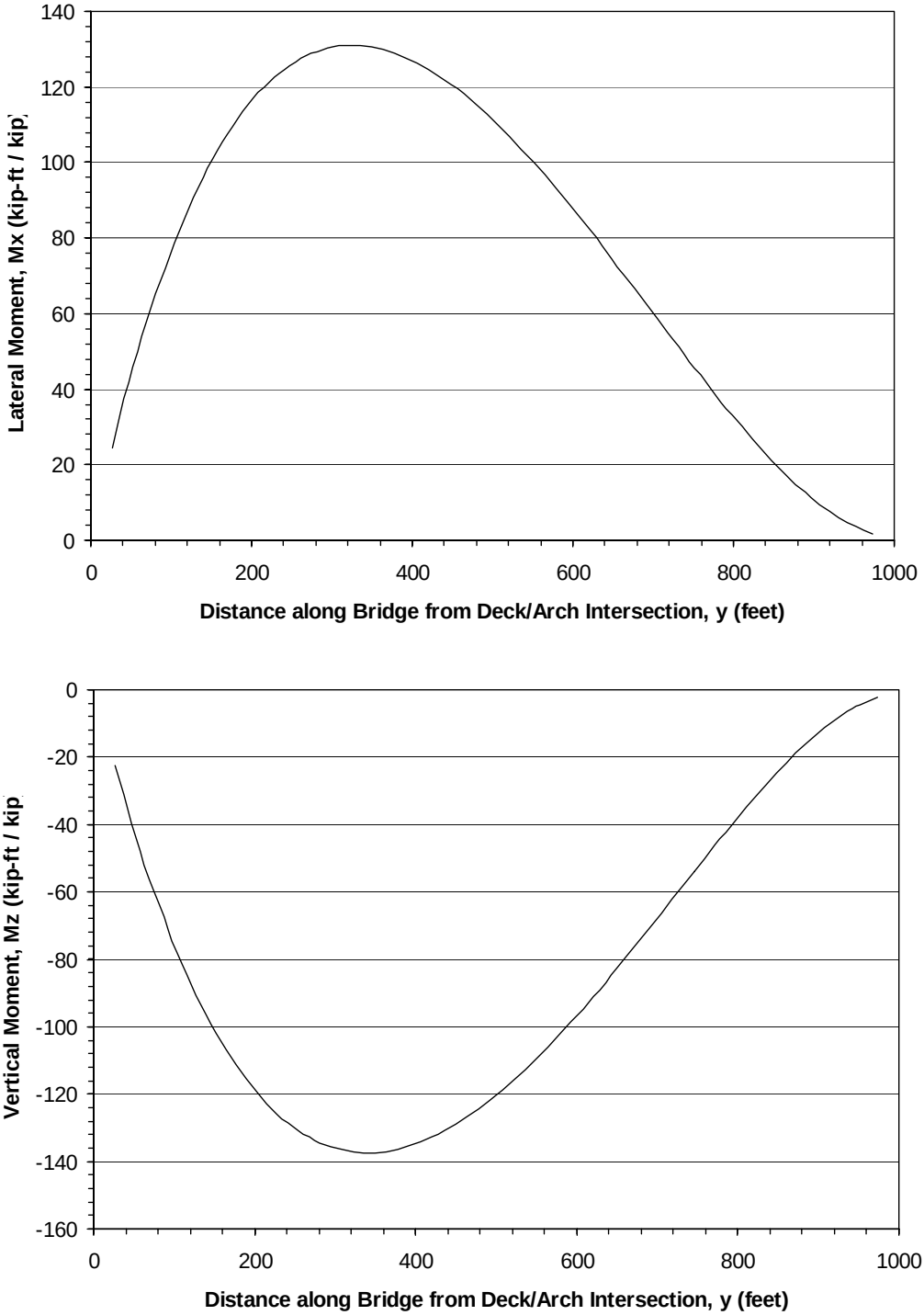

FIGURE 6.3 INFLUENCE FUNCTIONS FOR THE BENDING MOMENT RESPONSE AT THE REDUCTION IN CROSS SECTION ON THE ARCH RIB

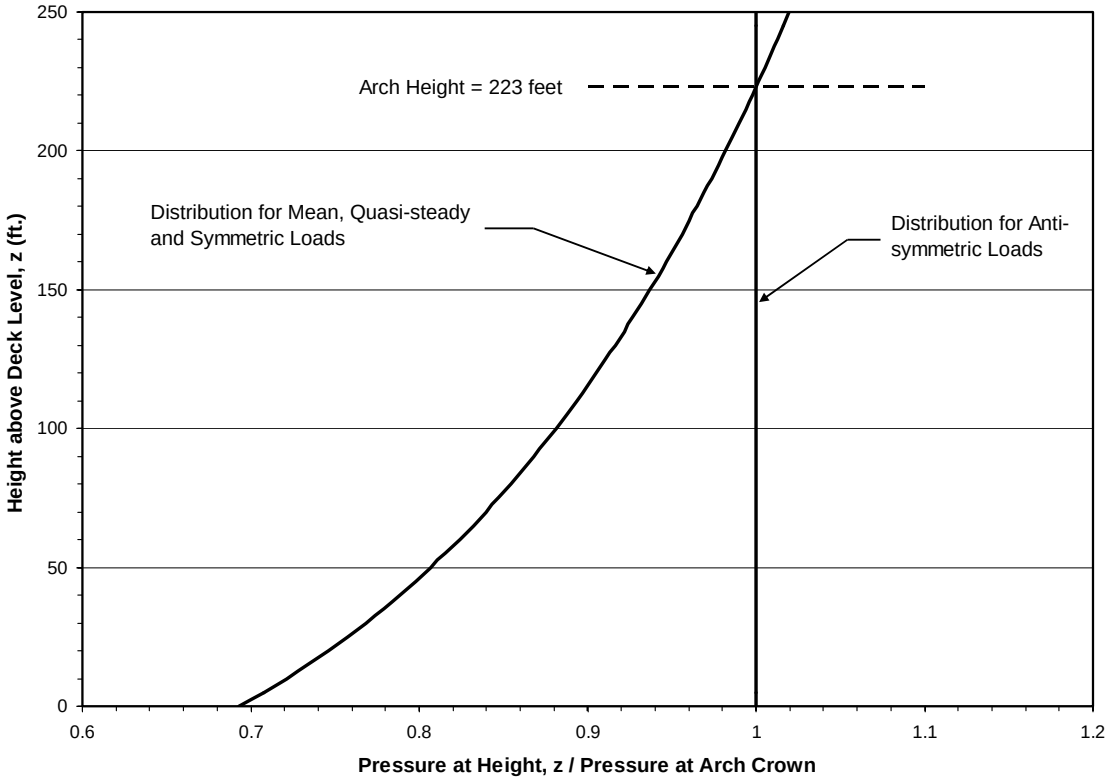

FIGURE 6.4 DISTRIBUTION WITH HEIGHT OF THE VARIOUS COMPONENTS OF EQUIVALENT STATIC LOADS

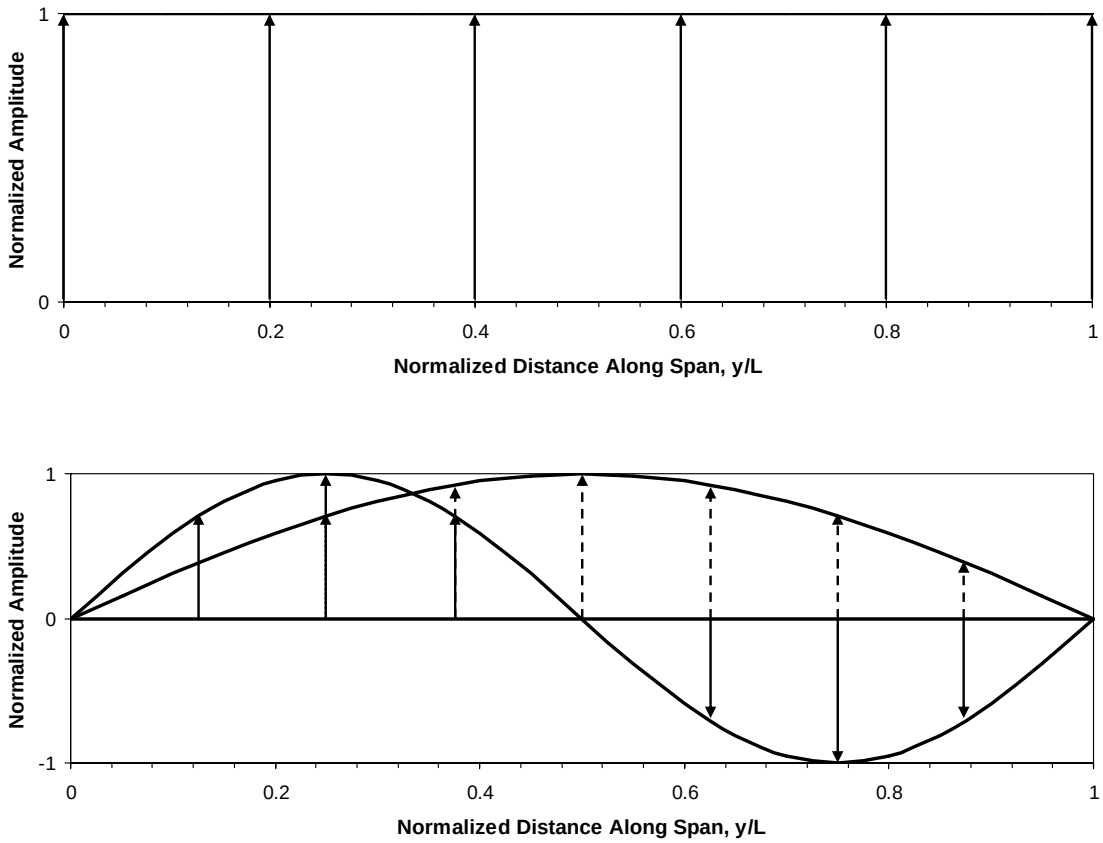

FIGURE 6.5 SPANWISE DISTRIBUTION OF THE MEAN AND QUASI-STEADY (TOP) AND SYMMETRIC AND ANTI- SYMMETRIC COMPONENTS (BOTTOM) OF THE EQUIVALENT STATIC LOADS

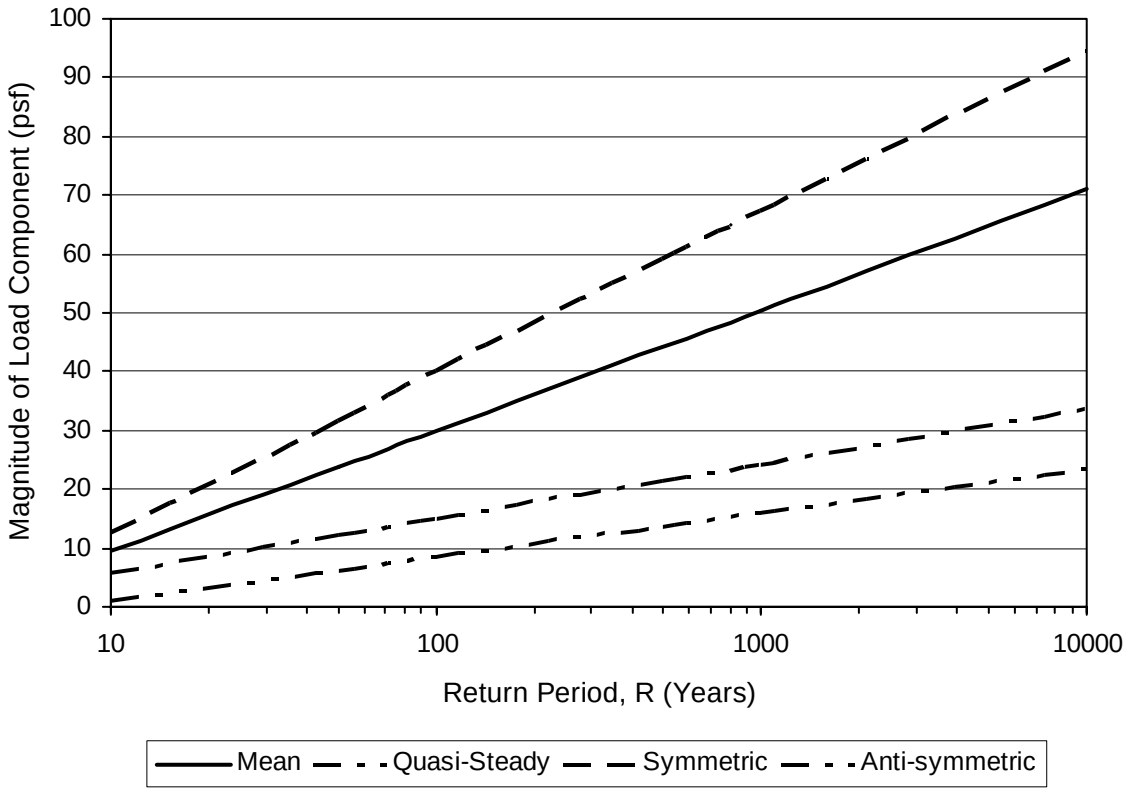

FIGURE 6.6 VARIATION OF EQUIVALENT STATIC LOAD COMPONENTS WITH RETURN PERIOD

7 FULL AEROELASTIC MODEL STUDY

7.1 General

A full bridge aeroelastic model of the Indian River Inlet Bridge was designed and constructed at a geometric scale of 1 to 150 relative to the prototype, in order to place the entire bridge on the turntable at the Low Speed Test Section of BLWTII. This scale was also selected to provide appropriate simulation of full scale turbulence characteristics important for the development of the aerodynamics of the bridge. The total length of the modeled bridge deck along the bridge span is about 1300ft in full scale. The approach taken for the full aeroelastic model study has been discussed in [1], and has been used in a variety of long and short span bridge studies.

Tests were performed for the completed bridge and three under-construction stages. The under-construction stages include the cantilevered tie-beam, cantilevered arch and the bridge prior to final deck completion. For some of the tests in the under-construction stages, mass scaled construction cranes were modeled and installed either on the deck or arch. In addition, two "temporary" construction towers were designed and constructed on both sides of the bridge to support the arch through a simplified system of cables with equivalent stiffness to the scaled prototype.

The behavior of the full bridge aeroelastic model was tested under two wind profiles; firstly, a hurricane profile obtained from GPS dropsonde field measurement [9], corresponding to a roughness length of Z_o=0.025ft as discussed in the wind climate study in Section 2 of this report; secondly, a typical open country exposure corresponding to a roughness length of Z_o=0.1ft. Measurements of bridge responses were taken at five different wind angles of 0°, 30°, 60°, 90° and 270° for both wind profiles. A wind angle of 0° is defined as wind along the longitudinal axis of the bridge, and 90° and 270° as wind perpendicular to the bridge deck. The 90° wind is for the test set-up with the pedestrian walkway on the windward side. The wind characteristics generated in the wind tunnel are considered to be good representation of the wind conditions at the bridge site. In addition, tests were also conducted at 90° wind with the two exposures and with / without the existing bridge upwind to assess its effect on the proposed Indian River Bridge.

In order to identify any potential vortex shedding induced vibration and flutter instability, an additional "smooth flow" test was carried out with the bridge model elevated above the boundary layer of the tunnel floor. These tests were only conducted for wind perpendicular to the bridge at 90°. In the test, the bridge model was elevated about 1.5ft off the tunnel floor, resulting in a uniform smooth flow condition with low turbulence intensities of about 1.7% from the deck level to the arch crown height. In addition, for the completed bridge configuration, a test with a bare wind tunnel floor (resulting in very low turbulence), was performed for comparison.

Photographs of the bridge model at 90° wind in smooth flow, in the low turbulence condition, and in the two modeled exposures (hurricane profile and open country exposure) are given in Figure 7.1. The existing bridge modeled in the test can be seen upwind of the Indian River Bridge in (C) and (D) of Figure 7.1. Close-up views of the bridge model for the completed bridge configuration including some of the instrumentation set-up are given in Figure 7.2. Close-up views of the three under-construction stages are given in Figures 7.3 to 7.5. Examples of the model in other wind directions tested are shown in Figure 7.6 for the hurricane profile and in Figure 7.7 for the open country exposure. The definition of the wind directions used in the tests is sketched in Figure 7.8.

7.2 Dynamic Similarity

A description of the design methodology for full aeroelastic models follows below. The aeroelastic modelling of structures generally requires equality of the following non-dimensional quantities in addition to an overall geometric similarity:

- Froude Number (ratio of the gravitational to the inertia forces);
- Cauchy Number (ratio of the elastic to inertia forces);

- Density Ratio (ratio of the inertia force of the structure to that of the flow);
- Damping Ratio;
- Reynolds Number (based on the dimensions of the structure).

In design of the full bridge aeroelastic model for the Indian River Inlet Bridge, it was decided that Froude Number scaling ($Fr = gL/V^2$) is preserved. This fact requires tests to be conducted at low wind speeds since the velocity scaling is coupled to the length scale. With the selected length scale of 1:150 for the aeroelastic model, the resulting Froude scaled velocity ratio of 12.25:1 between prototype and model is well suited to the scaling of the turbulent boundary layer in the Low Speed Test Section of BLWTII.

Cauchy Number is a non-dimensional parameter which represents the ratio of the elastic forces of the bridge to the inertia forces of the flow ($Ca = E/\rho V^2$). This parameter is preserved in the design of the model.

The density ratio (ρ_{model}/ρ_{air}) fixes the mass of the model with respect to the air in the wind tunnel. Since the air density of the prototype is assumed the same as that of the model, the density of the model must be identical to that of the prototype.

The damping ratio ($\delta_{model}/\delta_{prototype}$) is an important quantity to preserve, since it has a direct effect on the resonant motions. In the majority of cases, the damping is approximately that which may be (conservatively) expected to be found in the prototype bridge (i.e. between 0.4 and 1.0% of critical in different modes of vibration). The design of aeroelastic models does not easily allow for the adjustment of the structural damping and in order to identify possible instabilities under the action of wind, the model is designed to have as low a value of structural damping as possible. This also has the effect of providing conservative estimates of the structural responses. The effect of increased damping in the prototype can be estimated through an analytical correction to the test results if required.

Reynolds number similarity ($Re = VL/\nu$) is not practical in most cases and aeroelastic tests are usually carried out at a Reynolds Number several orders of magnitude lower than that of full scale. For sharp edged bodies such as bridge decks, the effects of this relaxation of *Re* scaling is not severe for overall wind induced forces and responses. Reynolds number effects can be significant in the modelling of circular objects such as cables. In these instances, the model cable diameter is adjusted to equate to the mean drag wind effects using an equivalent C_dDL approach.

7.3 Description of Model Design

The full aeroelastic model was designed using the scaling parameters listed in Table 7.1. Prototype values of the relevant structural and non-structural elements for the completed bridge and the tie-beam configurations, as provided by the Engineers are given in Table 7.2. Since the initial design and fabrication of the full aeroelastic model, the design of the prototype bridge evolved with revisions to the structural properties which were not possible to incorporate into the full aeroelastic model without undue delay in the testing program. The values representing the most recent bridge properties are also listed in Table 7.2 for comparison. Most properties in the model are within 10% of those of the final design, however the two most significant differences are in the main span mass and mass moment of inertia per unit length. The general effect of these two parameters on model response and resulting wind loading is discussed.

The CNC (Computer Numeric Control) and RP-FDM (Rapid Prototyping – Fused Deposition Method) facilities at the University Machine Services were used in the construction of the full aeroelastic model. A complete set of model drawings for the completed bridge configuration is given in Figure 7.9. Model drawings for the under-construction stages are given in Figure 7.10.

7.3.1 Arch

The elastic properties of the arch were modeled by a central "spine" providing the appropriate in-plane, out-of-plane and rotational stiffness of the completed arch. High strength aluminum sections were machined in a channel shape to allow for the simulation of the three degrees of freedom in the primary bending and rotational directions. The bases of the arch provided fixed end conditions for the spines.

The arch cladding modules provide no additional stiffness to the structural spine of the arch, yet provide the necessary mass and geometric shape for the proper simulation of the aerodynamic forces. The individual arch modules are separated from each other through a small gap (0.030”), which has been shown to be aerodynamically insignificant. The arch cladding modules were constructed using the RP-FDM machine and ballasted with proper weights to provide the scaled value of mass per unit length of the arch. The cladding segments were affixed to the spine at each segment centre.

7.3.2 Deck

The elastic properties of the deck were modeled by a central "spine" providing the appropriate vertical, lateral and torsional stiffness of the deck. A high-strength aluminum structural element was machined in a channel shape to allow for the simulation of the three degrees of freedom in lateral, vertical and torsional directions. The deck spine was fabricated in four sections, with splice plate connections located in the main span near the arch and at midspan. In this manner, different construction stages could be simulated by removal of the splice plates and / or replacement of the deck spine and cladding with that of the tie beam alone.

The deck cladding modules were fabricated from acrylic using CNC Milling Machine technology, reflecting the aerodynamic shape of the deck. The detailed prototype railings were simulated in the model using pre-fabricated plastic sections with additional longitudinal members to provide an equivalent porosity to the prototype. Each module was ballasted with additional brass weights to provide the scaled values of mass and mass moment of inertia per unit length of the structure. The cladding segments were affixed to the spine at the appropriate centre of twist of the deck through the use of a machined brass cross beam. The cross beam also provided increased rigidity to the deck and a connection from the cables to the structural spine.

7.3.3 Tie-Beam (Construction Stage)

The elastic properties of the tie-beam were modeled by a central "spine" providing the appropriate vertical, lateral and torsional stiffness. A high-strength aluminum structural element was machined in a channel shape to allow for the simulation of the three degrees of freedom in lateral, vertical and torsional directions. The tie beam was attached to the deck spine near the arch via a full moment capacity splice plate connection. Another splice plate connection located at midspan was used to simulate the cantilevered tie beam as well as the fully connected condition.

The tie-beam cladding modules were fabricated in the same way as described for the deck, reflecting the aerodynamic shape of the tie-beam. Each module was ballasted with additional brass weights to provide the scaled values of mass and mass moment of inertia per unit length of the structure. The cladding segments were affixed to the spine at the appropriate centre of twist of the tie-beam.

An additional stiffness element was required for the deck in order to simulate the condition where the tie beam was fully completed and the deck was at its maximum length, immediately prior to the deck completion. In this condition, the deck spine was installed to its maximum length, simulating the stiffness properties of the completed deck, however, the central splice was not installed. In its place, a small link element, simulating the stiffness properties of the tie beam alone was used to connect the ends of the deck spine.

7.3.4 Connections and Bearings

The appropriate bearing conditions at the abutments of the side spans were accomplished in the model by the use of vertically oriented leaf springs allowing longitudinal displacement, however, providing a restraint to vertical motion and deck torsion. Fixed restraints were used between the deck and arch.

7.3.5 Cables

The stay cables were modeled by 0.017" flexible aircraft cables with additional foam cylindrical cladding to approximate the mean drag force of the prototype cable. The equivalent axial stiffness (AE) of each group of prototype stay cables was provided by extension springs. The drag forces on the cables were well simulated with the combination of the wind drag on the aircraft cable plus that on the foam cladding. The simulation was aimed above an equivalent prototype wind speed at which the prototype cables can be assumed to be in the supercritical Reynolds Number region (with an approximate C_d of 0.7). The model cable, if scaled directly via the Length Scale would be in the subcritical region with a C_d of 1.2. The mass per unit length of the cables was not simulated in this approach, as the response of the cables at the extremely small scale of the full aeroelastic model is not representative of full scale behavior.

During the test of the cantilevered arch configuration, the hanger cables were not removed. These hangers were fixed into the arch cladding segments and to remove them from the model would destroy the integrity of the arch cladding. Since the mass of these hangers would be a small fraction of the generalized mass of the structure, it was felt that the effect of this slight overestimation on the overall dynamic response of the structure should be small. The aerodynamic effect of these hangers would be a slight increase in the mean aerodynamic drag as well as a potential increase in the aerodynamic damping. These changes were not considered to be significant enough to warrant the remanufacture of the arch cladding segments.

7.3.6 Construction Equipment

Temporary construction towers at both sides of the bridge were used in the construction stage tests to support the arch. Each tower was assumed to provide a fixed, immobile plane in which equivalent tie stiffness cables could be attached to support the arch. Struts were placed on the back span side of the towers to ensure that the "tower" was sufficiently stiff to provide this fixed plane during the tests. An analysis was performed by the Engineers in order to define the equivalent stiffness of each cable which includes the equivalent effect of tower displacement and anchor cable extensional stiffness. The extensional stiffness of the "equivalent" was concentrated in a coil spring connected to cross-beams at the appropriate location on the arch cross-section. The temporary construction cables were in place for each construction stage that was examined. This system of cables can best be seen in Figure 7.4.

Mass and geometrically scaled construction cranes were installed for three construction stages of the cantilevered arch (a single crane on one side of the arch at midspan), cantilevered deck (one crane on only one side of the deck midspan) and bridge prior to deck completion (one crane each on both sides of the deck midspan). Both the supporting towers and construction cranes can be seen in some of the close-up views of the construction stages in Figures 7.3 to 7.6. In cases where the instrumentation was not present on one half of the bridge and hence there would be limited effect on the instrumented half, then only one construction crane was included on the model.

7.3.7 Effect of Revision to Prototype Properties

The response of the bridge is a complex interaction between the wind and the structure. When the design of the full aeroelastic model becomes fixed in order to provide the test results in a timely manner, often the properties of the prototype evolve beyond that point in time when the model design cannot be changed. Small changes to stiffness and mass can usually be tolerated resulting in small, inconsequential effects on the model response and hence the full scale predictions can be relied on with no modifications.

The final design of the Indian River Inlet Bridge has changed since the design and fabrication of the full bridge aeroelastic model. In addition to modifications to the deck structural and mass properties, the foundation conditions in the final design are flexible, whereas those of the model are rigid. The deck stiffness properties appear to be within 10% of the final design values, however the mass properties of the deck are approximately 25% lighter in mass and 30% smaller MMI than the prototype. These changes to mass and stiffness have resulted in differences in the natural frequencies between the prototype and that of the scaled model, using conventional Froude number scaling.

Although it is desirable to use Froude number scaling, it is not essential, and estimates of the prototype behavior can be scaled from the model response using revised scaling parameters. Table 7.1 indicates that the Bending and Torsional Moment and Force scaling parameters are proportional to the square of the velocity scale. Therefore, if a revised velocity scale is adopted which would be based on the length and frequency ratios between model and prototype, then the measured model response will be unchanged, if the response follows a V^2 relationship. This V^2 relationship between wind speed and response is an accepted behavior and deviations from this would most likely result through strong aerodynamic damping (either positive or negative).

It is expected that underestimating the mass and MMI of the deck will have the effect of underestimating the aerodynamic damping, resulting in conservative estimates of the model response. The analysis of the model response data which follow below, the original Froude number scaling between Model and Prototype response has been used (as shown in Table 7.1). No modification has been attempted to correct for the changes in prototype properties as it is believed that the response estimates as presented are conservative estimates of the prototype behavior. Unfortunately, it is not possible to alter the stiffness properties without a redesign and manufacture of the stiffness elements in the model. However, in order to verify the assumed effects of modifications to the mass and MMI, a limited retest of the model could be performed, in which the model mass properties were adjusted to the final design values.

7.4 Instrumentation

The model deck spine was instrumented with strain gages at three main cross sections for the completed bridge configuration. Lift and drag bending moments, as well as deck torque were measured at locations close to the deck-arch connection, at the quarter point of the span and near midspan. The arch spine was instrumented with strain gages in the in-plane, out-of-plane and torsional degrees of freedom at the end of the arch. Transverse and vertical bending moments were also measured at the crown of the arch. The strain gages close to the deck midspan were not used for the construction stages of cantilevered deck and bridge prior to deck completion.

The model of completed bridge was fitted with six non-contacting laser displacement transducers to monitor deck displacements. These transducers were located at the quarter points and at midspan. Two transducers were oriented in a vertical manner separated by a fixed distance at each cross section. The time history output of these two channels was digitally summed and differenced to provide measures of the deck vertical motion and rotation. A third transducer was placed at each cross section downwind of the model to yield drag displacements. The resolution of the displacement measuring system was 0.002” in model scale (or 0.295” in full scale). This translates into a resolution of the angular motion of approximately 0.03 degrees. All displacements and rotations presented in the plots are well within the resolution of the instrumentation.

Four pairs of high sensitivity accelerometers were placed at four locations of the completed bridge model; at the crown and ¼ point of the arch (oriented to provide in-plane and out-of-plane accelerations), at the quarter and midpoints of the deck (oriented to provide vertical accelerations at the edge of the deck). The time history outputs of the two pairs of accelerometers on the deck were summed and differenced to obtain the vertical and rotational accelerations. Additional accelerometers were located at the quarter point and midspan of the deck in the transverse direction to provide a measure of the lateral accelerations.

Strain gages were located at three sections in the simulation of the cantilevered tie-beam, in addition to the existing arch strain gaging. These were: deck end and arch end lift, drag and torsional moments, as well as arch midspan drag and lift bending moments. Four pairs of accelerometers were placed at arch midspan, deck midspan and the two deck 1/4 points to measure drag and lift accelerations. In addition, four pairs of laser deflection transducers were installed near the accelerometers to obtain the corresponding drag and lift displacements.

The wind speed at deck height was monitored throughout the tests and used as the reference wind speed for subsequent analyses of the experimental data. In addition, wind speeds at the level of the arch crown were also recorded during the tests.

In summary, a total number of 35 channels were used in the tests for the completed bridge configuration. An additional 10 channels were formed during the analysis using the time history recorded. These formed channels include, the lift displacement and torsion at the deck midspan and at both ¼ points, the lift and torsional accelerations at the deck midspan and at one of the ¼ points. Details of the instrumentation used and their locations for the completed bridge configuration are summarized in Table 7.3. They are also given schematically in Figure 7.11. Details of the instrumentation and their locations for the under-construction stages, are given in Appendices I, J and K.

Revisions to the instrumentation layout were necessary for each stage of construction in the tests. The construction stage representing the bridge prior to deck completion omitted the bending moments at the deck midspan, however measurements of the lateral and vertical displacements were added at the arch crown location. The deck instrumentation was removed along with the deck spine and cladding for the cantilevered arch construction stage. Two additional lasers were installed at the two arch ¼ points to measure arch drag displacements.

7.5 Wind Simulation

The turbulent boundary layer profile and turbulence characteristics used for the testing of the full aeroelastic bridge model were expected to be similar to wind over the terrain approaching the actual bridge site. The 1:150 scale aeroelastic model was tested in two terrain conditions; a hurricane profile for wind from the ocean side corresponding to a Z_o of about 0.025ft, and an open country exposure from the land with a Z_o of 0.1ft. In addition, the bridge model was also tested in a low turbulent flow (bare tunnel floor) and in smooth flow with the bridge deck elevated about 1.5 ft off the tunnel floor. In the smooth flow set-up, a fairing plate of about 2 ft long is added to the supporting beam of the bridge model in order to guide the flow over the model.

Hot-wire measurements of the vertical variation in the mean wind speed and turbulence intensity were made. Figure 7.12 presents the vertical profiles of the mean wind speed and of the intensity of the longitudinal component of turbulence obtained in the tunnel for each of the two upstream terrain conditions. The target mean wind speed profiles and turbulence intensities at the bridge site are also plotted for comparison. The mean profile for the open country exposure and the longitudinal turbulence intensities for both exposures are from ESDU [10, 11]. The mean profile for the hurricane exposure an accepted standard and is based on GPS dropsonde field measurements discussed in [9]. Figure 7.12 shows that both the mean profiles and the longitudinal turbulence intensities compare very well between the wind tunnel data and the target values over the range from the deck height to the arch crown level. As discussed in [3], the surface roughness Z_o varies with the mean wind speed in hurricane winds, a Z_o of 0.025ft was selected based on the analysis of the wind data at the bridge site. Table 7.7 summarizes the longitudinal and vertical turbulence intensities measured at the deck and arch crown heights of 55 ft and 275ft in the tunnel. Target values from ESDU are also presented in the table.

Measured power spectra of the longitudinal and vertical components of turbulence at the deck level are given in Figure 7.13 for the hurricane profile and in Figure 7.14 for the open country exposure, along with the empirical ESDU spectra. The data is normalized by V^2. The ESDU spectra presented are consistent with 1) a hurricane profile with a Z_o of 0.025ft at the deck elevation of 55 ft; and 2) an open country exposure with a Z_o of 0.1ft at the deck elevation. The ESDU spectra in the figures show similar shape or distribution of energy with frequency, indicating a good simulation of the full scale wind conditions in the wind tunnel tests.

Five wind angles, 0° (along the deck), 30°, 60°, 90° (perpendicular to deck with pedestrian walkway on the windward side) and 270° (perpendicular to deck with pedestrian walkway on the leeward side), were selected in the tests for the two upstream terrain conditions each configuration of the bridge. The effect of the existing bridge was investigated with wind at 90° for the two exposures. In addition, the low turbulence condition test with the bare wind tunnel floor (for the completed bridge configuration) and the smooth flow test with the elevated bridge model were also conducted at 90° wind.

7.6 Wind Speed Measurements

The deck height wind speed used in the analysis and plotting for this project corresponds to a full scale wind speed averaged over a time period of 15 minutes, which is very close to the mean hourly wind speed.

The definition of mean wind speed used in the study is the arithmetic average wind speed over the specified time period and at a specified height above ground level. The international standard (WMO) is at the 10m level for an average time of 10 minutes in an open country terrain condition.

The fastest-mile wind speed is the average wind speed in miles per hour for a 'mile of wind' to pass a particular point. For example, a fastest-mile speed of 60 mph would have an averaging time of 60 seconds (i.e. 3600/60 = 60 seconds), while a 100 mph fastest mile speed would have an averaging time of 36 seconds (i.e. 3600/100 = 36 seconds). The use of the fastest-mile speed was discontinued with the introduction of ASCE 7-95.

The instantaneous gust speed is a wind speed with an averaging time of 1-3 seconds typically. The current ASCE 7-98 [2] uses a 3-second gust.

The relationship between wind speeds with various averaging times, ranging from 1 second and longer is shown in relation to a 1-hour average in the curve by Durst [12] for the open country exposure, as shown in Figure 7.15 from ASCE 7-98. Figure 7.16 also shows this relationship. For other terrain conditions other than the open country exposure, this ratio can be estimated from the following equation,

$$\frac{U_t(Z)}{U_{3600}(Z)} = 1 + c(t) \times I_u$$

where, I_u is the turbulence intensity in the longitudinal direction at the specified height and $C(t)$ takes the values from the following table depending on the time duration.

t	1	10	20	30	50	100	200	300	600	1000	3600
$C(t)$	3.00	2.32	2.00	1.73	1.35	1.02	0.70	0.54	0.36	0.16	0.00

Two exposures were modeled in the test for the Indian River Bridge study; namely, a hurricane and an open country profile. Using the above equation for each exposure (with corresponding turbulence intensities) and height, different factors result for 3-second gust to mean wind speed ratio. However, the variation is not large and an average factor of 1.43 can be used to convert the mean wind speed at deck height reported in Appendices H, I, J and K to a 3-second gust wind speed.

7.7 Aeroelastic Model Test Procedure

The tests of the full aeroelastic model was comprised of taking measurements and records of time histories of all channels for various responses at each wind speed for a selected range of wind speeds. The responses at approximately 40 to 80 wind speeds were examined in each test. The mean, root-mean-square (RMS), maximum and minimum values of all measured bridge responses were obtained in a subsequent analysis of the time histories. A total of 35 channels, including wind speeds at deck height and the arch crown level, as well as various bridge deck and arch responses were recorded for a scaled time period of more than 15 minutes at each wind speed.

As described in Section 7.2, the design of aeroelastic models does not easily allow for the adjustment of the structural damping and in order to identify possible aerodynamic instabilities under the action of wind, the model is designed to have as low a value of structural damping as possible. This also has the effect of providing conservative estimates of the structural responses. The damping values of the first drag, lift and torsional modes of the deck, as well as the first arch drag mode of the bridge model for the completed bridge configuration are given in Table 7.6. These values are compatible with bridges of similar precast concrete construction. In order to assess the effect of higher damping on the lateral response of the arch, an additional test was carried out at an increased damping value of 0.7% in the first arch drag mode.

The responses as presented contain all responses up to 40 Hz in model scale or 3.3 Hz prototype. The peak response was formed from the root-mean-square (RMS) response multiplied by a peak factor. Thus, the total response is equal to the mean, plus or minus the peak. In these plots, the peak response equals to the RMS multiplied by a statistically-based peak factor for random response (i.e. turbulent buffeting) of 3.5. Since the peak factor at the vortex peak location decreases, the use of a constant value of 3.5 for these wind speeds would over-estimate the dynamic response when vortex induced peak occurs. Thus, for the range of wind speeds where the model has shown a large vortex shedding peak, the actual peak factor calculated from the test for the corresponding wind speed was used rather than the random response peak factor of 3.5.

7.8 Response of Completed Bridge and Construction Stage Configurations

7.8.1 General

All tests performed in this study are summarized in Table 7.4. Table 7.5 lists the tests performed for the completed bridge configuration. Similar summary tables for the three under-construction stages are given respectively at the beginning of Appendices I, J and K. The test conditions corresponding to each test are also described in the tables. The maximum wind speeds tested in each condition and the vortex shedding peaks observed in the test are also given in the tables. A complete set of response plots for all tests performed for the completed bridge configuration is contained in Appendix H. Results for each under-construction stage are included in Appendices I, J and K respectively.

The wind criteria for the proposed Indian River Bridge require that the bridge should not exhibit any instability up to the 10,000 year return period wind speed. From Figure 7.12 of the mean wind speed profiles, the ratios of deck to arch height wind speeds are about 0.85 and 0.80 for the hurricane profile and the open country exposure respectively. The wind climate study in Section 2 shows that the mean hourly wind speed at the arch height for the 10000 year return period is about 163mph. Therefore the mean hourly wind speed for the 10,000 year return period at deck height, using the larger ratio of 0.85 for the hurricane profile, is $163 \times 0.85 = 139$ mph (3-second gust of 199 mph).

Peak responses and corresponding peak factors for 90° wind for hurricane and open country profiles are tabulated in Tables 7.8 through 7.11. The responses are compiled for selected critical responses and given for the 100-year mean hourly wind speed at deck height of 91 m/h (or a 3-second gust wind speed of 130 mph). Tables are presented for the completed bridge as well as the three under construction stages of the bridge that were tested. This provides some measure of the variability of the magnitude of the peak response that may be expected. In general, the measured peak factors fall within a range between 3.0 and 4.0, consistent with the generalized peak factor of 3.5 which was used in the plots of bridge response found in Appendices I,J and K.

7.8.2 Completed Bridge

All tests conducted in this study for the completed bridge configuration passed this target wind speed with no flutter instability observed. In all tests, the mean wind speed at deck height reached at least 139 mph (3-second gust of 199 mph).

Tests conducted in the hurricane profile and the open country profile do not show any significant vortex shedding peaks, apart from a small peak at about 45 mph (3-second gust of 64 mph).

A test in “smooth flow” (with the bridge elevated above the boundary layer of the tunnel floor) was conducted for comparative purposes and to provide upper bound estimates of stability and vortex shedding induced response. Four vortex shedding peaks appear in the response plots; at 45 mph (3-second gust of 64 mph), 80 mph (3-second gust of 114 mph), 110 mph (3-second gust of 157 mph) and 140 mph (3-second gust of 200 mph). It has been identified that the vortex peak at 45 mph (3-second gust of 64 mph) is associated with the deck first asymmetric lift mode, and the vortex peak at 80 mph (3-second gust of 114 mph) is related to the deck first symmetric torsional mode. The peaks at 110 mph (3-second gust of 157 mph) and 140 mph (3-second gust of 200 mph) are related to the deck higher lift modes. All of these vortex shedding-induced response peaks are considered to be small and are not expected to appear in the response of the prototype bridge.

Figures 7.17 and 7.18 present the coherences of the lift displacements and the torsions respectively at the two ¼ span locations on the deck for the completed bridge configuration in smooth flow at 90°. Both figures include the auto-spectra, the cross-spectra, the phase angles and the coherences of the two lift or torsion channels used. Figure 7.17 shows clearly the dominant peak at the frequency of 7.5 Hz from both channels 42 and 46 of the ¼ span lift displacements. The figure also shows that these two channels are perfectly correlated, but move in opposite directions. Similarly in Figure 7.18, the responses of the two torsion channels at the deck ¼ span locations are dominated by the frequency of 13.7 Hz. These two channels are not only perfectly correlated, but also move in the same direction, indicating a symmetric mode of vibration.

Bridge buffeting responses are generally proportional to the turbulence intensity level in the wind. Bridge lateral (drag direction) responses are governed by the longitudinal turbulence intensity, while the vertical (lift direction) and torsional responses are determined by the vertical turbulence intensity. As shown in the plots, buffeting responses in the open country exposure (with larger turbulence intensity) are generally higher than the responses observed in the hurricane profile. However, the mean values are about the same for both exposures.

In order to see the effect of higher arch drag damping on the lateral responses of the arch, an extra test was carried out with the arch drag damping increased to 0.70% from the original value of 0.22%. The test was only performed in the open country exposure in 90° wind. The results show that the various arch lateral responses were reduced by about 20% at wind speeds around 120 mph (3-second gust of 172 mph). Generally, the model responses are inversely proportional to the square root of the total damping (structural + aerodynamic) (i.e. $\propto 1/\sqrt{\xi_s + \xi_a}$). Using quasi-steady analysis [13], the aerodynamic damping for the first arch symmetric drag mode in the along wind direction of the arch can be estimated as: $\xi_{dragj} = (\frac{C_x}{4\pi})(\frac{\rho B^2}{m})(\frac{\overline{V}}{f_j B})$. Using a drag coefficient for the arch of 0.8, ξ_{drag} is estimated to be about 0.5% at a wind speed of 120 mph. Therefore, the arch lateral responses after the increase of the damping should be approximately $\sqrt{\frac{0.5+0.22}{0.5+0.70}} = 0.77$ of the response before the increase in damping, which is comparable to the observed test results.

The behavior of the completed bridge configuration can be summarized as follows,

- No flutter instability was observed in any of the tests performed up to a full scale wind speed of 139 mph (3-second gust of 199 mph) at deck height.
- No vortex shedding induced instability was observed in any of the tests with either the hurricane profile or the open country profile, except a small vortex peak at about 45 mph (3-second gust of 64 mph).
- Several vortex shedding induced peaks were observed in the lift and torsional deck responses in the smooth flow test (raised floor) and test in low turbulence boundary layer flow (bare tunnel floor) at a deck height wind speed of about 45 mph (3-second gust of 64 mph), 80 mph (3-second gust of 114 mph), 110 mph (3-second gust of 157 mph) and 140 mph (3-second gust of 200 mph). These vortex peaks are not considered significant. The vortex peak

at 45 mph (3-second gust of 64 mph) corresponds to the deck first lift asymmetric mode, while the vortex peak at 80 mph (3-second gust of 114 mph) corresponds to the deck first symmetric torsional mode. The peaks at 110 mph (3-second gust of 157 mph) and 140 mph (3-second gust of 200 mph) are related to the deck higher lift modes.

- At 60° wind, a small vortex peak can be seen at about 50 mph (3-second gust of 72 mph). At other smaller wind angles of 30° and 0°, all vortex peaks were eliminated.

- The effect of the existing bridge, placed upstream of the proposed Indian River Bridge, is small at both terrain conditions of hurricane and open country exposures.

- With higher structural damping of 0.7% in the first arch drag mode, the lateral responses of the arch were reduced by about 20%. The higher arch drag damping has almost no effect on other measured deck and arch responses.

- As shown in the plots, buffeting responses in the open country exposure (with larger turbulence intensity) are generally higher than the responses in the hurricane profile (smoother and less turbulent).

- The effect of increased mass and mass moment of inertia is complicated. Since the bridge frequencies are also changed, the first deck lift and torque frequencies are used to obtain the new velocity scaling. With the new smaller frequencies, the velocity scaling becomes smaller, thus the corresponding full scale wind speed is also small. Since the scaling of the bending moments and accelerations are proportional to the square of the velocity scaling, these responses become also smaller by the square of the velocity ratio. However, since the length scale is fixed, the displacement would be higher at the same wind speed.

7.8.3 Bridge Under Construction

All tests conducted with the under-construction stages also passed the target wind speed of 139 mph (3-second gust of 199 mph) with no occurrence of flutter instability.

No significant vortex shedding peaks were observed in any of the tests conducted in the hurricane and the open country exposures. The conservative tests performed in smooth flow with the bridge configuration prior to deck completion shows a small vortex shedding peak at about 50 mph (3-second gust of 72 mph) in 90° wind, similar to that which was observed for the completed bridge. This peak was eliminated with added turbulence at deck height in the boundary layer flows. The tests in smooth flow with the cantilevered tie-beam configuration showed an additional small peak at 85 mph (3-second gust of 122 mph) range in the arch lift response, which also was eliminated in the boundary layer flows. The tests in smooth flow for the cantilevered arch configuration also shows a somewhat larger vortex peak at 90 mph (3-second gust of 129 mph) for the arch vertical response. Again, this peak is reduced significantly in both the hurricane and open country profiles. Another small vortex peak can be also found at about 35 mph (3-second gust of 50 mph) for this bridge configuration.

The behavior of the bridge while under construction can be summarized as follows,

- No flutter instability was observed in any of the tests performed up to a full scale wind speed of 139 mph (3-second gust of 199 mph) at deck height.

- No significant vortex shedding peaks were observed in any of the tests conducted in the hurricane and the open country exposures. The various vortex shedding peaks, though small, are summarized below.

- The bridge configuration prior to final deck completion shows a vortex peak at 50 mph (3-second gust of 72 mph) similar to that which was observed in the test for the completed bridge in smooth flow. However, the peak was eliminated in the open country and hurricane profiles.

- The cantilevered tie-beam configuration had two small vortex peaks, one at 50 mph (3-second gust of 72 mph) similar to the one observed in the response of the bridge configuration prior to deck completion and an additional peak at 85 mph (3-second gust of 122 mph) in the arch lift response.

- The arch lift response in smooth flow for the cantilevered arch configuration also indicated a small vortex peak at a wind speed of 85 mph (3-second gust of 122 mph). Again, this peak was reduced significantly in the simulated boundary layer flows. Another small vortex peak was found at about 35 mph (3-second gust of 50 mph) in the arch lift.

- The effect of the presence of the construction cranes was examined during the tests of the construction stages. The vortex peak at about 85 mph (3-second gust of 122 mph) was completely eliminated in the testing of the cantilevered arch, while the vortex peak at 35 mph (3-second gust of 50 mph) was slightly reduced. Otherwise, the effect of the presence of construction cranes on the various deck and arch responses is small.

- The effect of the existing bridge upwind of the model, was small at both terrain conditions of hurricane and open country exposures.

- Buffeting responses in the open country exposure (with a larger turbulence intensity) are generally higher than the responses in the hurricane profile.

.

TABLE 7.1 AEROELASTIC SCALING PARAMETERS (FROUDE SCALED)

Parameter	Similitude Requirement	Value
Length*	$\lambda_L = L_m / L_P$	6.67E-03
Density	$\lambda_\rho = \rho_m / \rho_P$	1
Velocity**	$\lambda_V = V_m / V_P$	8.16E-02
Mass per Unit Length	$\lambda_m = \lambda_\rho \lambda_L^2$	4.44E-05
Mass	$\lambda_M = \lambda_\rho \lambda_L^3$	2.96E-07
Mass Moment of Inertia per Unit Length	$\lambda_i = \lambda_m \lambda_L^2$	1.98E-09
Mass Moment of Inertia	$\lambda_I = \lambda_M \lambda_L^2$	1.32E-11
Time	$\lambda_T = T_m / T_P = \lambda_L / \lambda_V$	8.17E-02
Damping	$\lambda_\xi = \xi_m / \xi_P$	1
Elastic Stiffness	$\lambda_{EI} = \lambda_{GC} = \lambda_V^2 \lambda_L^4$	1.32E-11
	$\lambda_{EA} = \lambda_V^2 \lambda_L^2$	2.96E-07
Force per Unit Length	$\lambda_f = \lambda_V^2 \lambda_L = \lambda_L^3 / \lambda_T^2$	4.44E-05
Force	$\lambda_F = F_m / F_P = \lambda_V^2 \lambda_L^2$	2.96E-07
Bending and Torsional Moment	$\lambda_{BM} = \lambda_V^2 \lambda_L^3$	1.97E-09
Warping Stiffness	$\lambda_{CwE} = \lambda_V^2 \lambda_L^6$	5.85E-16

*Length Scale = 1:150

**Velocity Scale = 1:12.25

** $\lambda_V = \lambda_T = \sqrt{\lambda_L}$

(Froude Scaling)

TABLE 7.2 PARAMETERS FOR DESIGN OF THE AEROELASTIC MODEL

	Parameter		Prototype Value Final Design	Prototype Value Used in Model Design*	Scaled Target Value for Model
Deck Main Span	Moment of Inertia - Vertical	I_x	3.85×10^3 ft^4	4.23×10^3 ft^4	6.27×10^{-4} in^4
	Moment of Inertia - Lateral	I_y	1.78×10^5 ft^4	1.73×10^5 ft^4	2.56×10^{-2} in^4
	Torsional Constant	C	1.28×10^4 ft^4	1.12×10^4 ft^4	1.80×10^{-3} in^4
	Mass per unit length	m	57.70 kips/ft	45.62 kips/ft	0.169 lb/in
	Mass Moment of Inertia per unit length	I_θ	41007 kip-ft²/ft	34197 kip-ft²/ft	1.394 lb-in²/in
	Elastic Modulus – deck and arch	E_d	Concrete: 5.42×10^6 lb/in²	Concrete: 5.42×10^6 lb/in²	Aluminum: 1.00×10^7 lb/in²
	Shear Modulus – deck and arch	E_d	Concrete: 2.26×10^6 lb/in²	Concrete: 2.26×10^6 lb/in²	Aluminum: 3.85×10^6 lb/in²
Deck Back Span	Moment of Inertia - Vertical	I_x	3.85×10^3 ft^4	3.93×10^3 ft^4	5.82×10^{-4} in^4
	Moment of Inertia - Lateral	I_y	1.78×10^5 ft^4	1.72×10^5 ft^4	2.55×10^{-2} in^4
	Torsional Constant	C	1.28×10^4 ft^4	1.05×10^4 ft^4	1.68×10^{-3} in^4
	Mass per unit length	m	57.70 kips/ft	42.31 kips/ft	0.157 lb/in
	Mass Moment of Inertia per unit length	I_θ	41007 kip-ft²/ft	29431 kip-ft²/ft	1.395 lb-in²/in
Tie Beam	Moment of Inertia - Vertical	I_x	2.194×10^3 ft^4	2.194×10^3 ft^4	3.25×10^{-4} in^4
	Moment of Inertia - Lateral	I_y	4.505×10^3 ft^4	4.505×10^3 ft^4	6.67×10^{-4} in^4
	Torsional Constant	C	4.700×10^3 ft^4	4.366×10^3 ft^4	6.47×10^{-4} in^4
	Mass per unit length	m	19.18 kips/ft	19.18 kips/ft	0.071 lb/in
	Mass Moment of Inertia per unit length	I_θ	1016 kip-ft²/ft	1016 kip-ft²/ft	0.048 lb-in²/in
Cables	Area	A	15.84 in²	15.84 in²	
	Length	L	25.12 ft to 206.08 ft	25.12 ft to 206.08 ft	
	Elastic Modulus – cable	E_c	28.5×10^6 lb/in^2	28.5×10^6 lb/in^2	
	Stiffness – cable	K_c	1.50×10^6 to 1.83×10^5 lb/in per cable	1.50×10^6 to 1.83×10^5 lb/in per cable	a spring with a stiffness 66.6 to 8.11 lb/in

* Typical properties supplied by the Engineers (actual properties vary along span and with arch coordinate). Mass and structural properties of the deck changed during the course of the study due to evolving design of the bridge. Model design values reflect the prototype properties at the time of the model test.

TABLE 7.2 (CONT.) PARAMETERS FOR DESIGN OF THE AEROELASTIC MODEL

	Parameter		Prototype Value Final design	Prototype Value Used in Model Design*	Scaled Target Value for Model
Bottom of Base of Arch	Moment of Inertia - Vertical	I_x	1.38×10^6 ft^4	1.41×10^6 ft^4	2.09×10^{-1} in^4
(Below Deck	Moment of Inertia - Lateral	I_y	6.37×10^5 ft^4	6.68×10^5 ft^4	9.89×10^{-2} in^4
h=0 ft)	Torsional Constant	C	1.72×10^6 ft^4	1.74×10^{10} ft^4	2.79×10^3 in^4
	Mass per unit length	m	509.10 kips/ft	5186.41 kips/ft	19.209 lb/in
	Mass Moment of Inertia per unit length	I_θ	302302 kip-ft²/ft	312232 kip-ft²/ft	7.384 lb-in²/in
Mid Base of Arch	Moment of Inertia - Vertical	I_x	4.22×10^5 ft^4	4.12×10^5 ft^4	6.10×10^{-2} in^4
(Below deck	Moment of Inertia - Lateral	I_y	1.95×10^5 ft^4	1.95×10^5 ft^4	2.88×10^{-2} in^4
h=15.9 ft)	Torsional Constant	C	5.00×10^5 ft^4	5.07×10^5 ft^4	8.12×10^{-2} in^4
	Mass per unit length	m	281.60 kips/ft	279.90 kips/ft	1.037 lb/in
	Mass Moment of Inertia per unit length	I_θ	92499 kip-ft²/ft	90941 kip-ft²/ft	2.150 lb-in²/in
Top Base of Arch	Moment of Inertia - Vertical	I_x	6.07×10^4 ft^4	5.93×10^4 ft^4	8.78×10^{-3} in^4
(Below deck	Moment of Inertia - Lateral	I_y	2.81×10^4 ft^4	2.80×10^4 ft^4	4.15×10^{-3} in^4
h=37.8 ft)	Torsional Constant	C	7.20×10^4 ft^4	7.29×10^4 ft^4	1.17×10^{-2} in^4
	Mass per unit length	m	106.9 kips/ft	106.2 kips/ft	0.393 lb/in
	Mass Moment of Inertia per unit length	I_θ	13318 kip-ft²/ft	13093 kip-ft²/ft	0.311 lb-in²/in
Transition of Arch	Moment of Inertia - Vertical	I_x	8.71×10^3 ft^4	8.71×10^3 ft^4	1.29×10^{-3} in^4
	Moment of Inertia - Lateral	I_y	5.26×10^3 ft^4	5.26×10^3 ft^4	7.79×10^{-4} in^4
	Torsional Constant	C	1.09×10^4 ft^4	1.37×10^4 ft^4	2.20×10^{-3} in^4
	Mass per unit length	m	31.20 kips/ft	30.39 kips/ft	0.113 lb/in
	Mass Moment of Inertia per unit length	I_θ	2143 kip-ft²/ft	2095 kip-ft²/ft	0.0492 lb-in²/in
Typical Arch	Moment of Inertia - Vertical	I_x	7.62×10^3 ft^4	7.62×10^3 ft^4	1.13×10^{-3} in^4
	Moment of Inertia - Lateral	I_y	4.50×10^3 ft^4	4.50×10^3 ft^4	6.67×10^{-4} in^4
	Torsional Constant	C	0.98×10^4 ft^4	1.00×10^4 ft^4	1.60×10^{-3} in^4
	Mass per unit length	m	24.40 kips/ft	23.46 kips/ft	0.087 lb/in
	Mass Moment of Inertia per unit length	I_θ	1881 kip-ft²/ft	1819 kip-ft²/ft	0.0426 lb-in²/in

*Typical properties supplied by the Engineers

TABLE 7.3 INSTRUMENTATION LOCATIONS, INDIAN RIVER INLET BRIDGE, COMPLETED BRIDGE

Instrumentation **x – longitudinal, y – lateral (Drag), z – vertical (Lift)**	**Instrumentation Locations**
Strain Gages:	
M_x, M_y and M_z at **Deck** End (marked **A**)	Lift and Drag Moments, as well as Torque at 438ft from Midspan
M_x, M_y and M_z at **Deck** 1/4 Point (marked **B**)	Lift and Drag Moments, as well as Torque at 238ft from Midspan
M_x, M_y and M_z at **Deck Midspan** (marked **C**)	Lift and Drag Moments, as well as Torque at 38ft from Midspan
M_x, M_y and M_z at **Arch** End (marked **D**)	Lift and Drag Moments, as well as Torque at 42ft from Arch-Deck connection
M_y and M_z at **Arch** Crown (marked **E**)	Lift and Drag Moments at 44ft from Arch Crown
Accelerometers:	
y, z and θ accel. at **Deck** Midspan (marked **C**)	Lift, Drag and Torsional Accelerations at Midspan
y, z and θ accel. at **Deck** 1/4 Point (marked **B**)	Lift, Drag and Torsional Accelerations at 225ft from Midspan
y and z accel. at **Arch** ¼ Point (marked **G**)	Lift and Drag Accelerations at the ¼ point on the Arch (235ft from the arch crown in the deck longitudinal direction)
y and z accel. at **Arch** Crown (marked **E**)	Lift and Drag Accelerations at 14ft from Arch Crown
Displacements:	
y, z and θ displacements at **Deck** Midspan (marked **C**)	Lift and Drag Displacements, as well as Deck Rotation at 12ft from Midspan
y, z and θ displacements at **Deck** 1/4 point (marked **B**)	Lift and Drag Displacements, as well as Deck Rotation at 225ft from Midspan
y, z and θ displacements at **Deck** other 1/4 point (marked **F**)	Lift and Drag Displacements, as well as Deck Rotation at 240ft from Midspan
Wind Speeds:	
Deck Level	Deck Height
Arch Level	Arch Crown Height

TABLE 7.4 SUMMARY OF FULL BRIDGE AEROELASTIC MODEL TESTS, INDIAN RIVER INLET BRIDGE

Bridge Configuration	No. of Tests	Flow Conditions	Wind Directions	Existing Bridge and Construction Cranes
Completed Bridge	15	Smooth flow, low turbulent flow, hurricane exposure and open country exposure	0° (along deck), 30°, 60°, 90° (perpendicular to deck) and 270°	Existing bridge
Cantilevered Tie-Beam*	11	Smooth flow, hurricane exposure and open country exposure	0° (along deck), 30°, 60°, 90° (perpendicular to deck) and 270°	Existing bridge
Cantilevered Arch*	12	Smooth flow, hurricane exposure and open country exposure	0° (along deck), 30°, 60°, 90° (perpendicular to deck) and 270°	Existing bridge and one construction crane on arch
Bridge Prior to Deck Completion*	13	Smooth flow, hurricane exposure and open country exposure	0° (along deck), 30°, 60°, 90° (perpendicular to deck) and 270°	Existing bridge and two construction cranes on deck

***** Supporting towers were used at both sides of the bridge in the under-construction stages in the test to support the arch.

TABLE 7.5 SUMMARY OF FULL BRIDGE AEROELASTIC MODEL TESTS, COMPLETED BRIDGE CONFIGURATION

Test File	Test No.	Flow condition	Existing bridge	Wind direction (Test angle)	V_{deck} (mph) Maximum wind speed at deck height	Vortex Peak Locations
IFA102	1	Bare tunnel floor (low turbulent flow)	No	Perpendicular to bridge (90°)	155	40 ~ 50 mph, 80 mph, 105 mph, 135 mph
ITA201	2	Hurricane profile	Yes	Perpendicular to bridge (90°)	142	40 ~ 50 mph
IFA201	3	Hurricane profile	No	Perpendicular to bridge (90°)	141	40 ~ 50 mph
IFB201	4	Hurricane profile	No	60° to the bridge	141	50 mph
IFC201	5	Hurricane profile	No	30° to the bridge	143	N/A
IFD201	6	Hurricane profile	No	Along the bridge (0°)	144	N/A
IFE201	7	Hurricane profile	No	Perpendicular to bridge (270°)	141	40 mph
IFA301	8	Open Country profile	Yes	Perpendicular to bridge (90°)	143	40 mph
IFA302	9	Open Country profile	No	Perpendicular to bridge (90°)	143	40 mph
IFB302	10	Open Country profile	No	60° to the bridge	141	N/A
IFC302	11	Open Country profile	No	30° to the bridge	146	N/A
IFD302	12	Open Country profile	No	Along the bridge (0°)	145	N/A
IFE302	13	Open Country profile	No	Perpendicular to bridge (270°)	144	40 mph
IFA303	14	Open Country Profile (higher arch damping)	No	Perpendicular to bridge (90°)	144	N/A
IFA402	15	Smooth Flow (bridge elevated)	No	Perpendicular to bridge (90°)	148	45 mph, 80 mph, 110 mph, 140 mph

TABLE 7.6 SUMMARY OF FULL BRIDGE MODEL PROPERTIES, COMPLETED BRIDGE

Mode No.	Type	Model Frequency	Damping Values	Model Scaled to Prototype **(Fixed Foundation)**	Dec. 2004 Values **(Flexible Foundations)**
1	Arch Symmetric Drag	2.3	0.22%	0.19	0.18
2, 5	Deck Asymmetric Lift	7.4	0.25%	0.60	0.49
3	Arch Asymmetric Drag	6.8	-	0.55	0.52
4	Deck Symmetric Drag	11.3	0.69%	0.92	0.54
6	Deck Symmetric Lift	12.4	0.49%	1.01	0.73
7	Deck Symmetric Torsion	13.4	0.18%	1.09	0.87

Note: some of the modes involve mixed deck and arch motions.

TABLE 7.7 SUMMARY OF TURBULENCE INTENSITIES (IN TEST AND TARGET VALUES)

		Hurricane Exposure (Zo=0.025ft)		Open Country Exposure (Zo=0.1ft)		Bare Tunnel Floor	Smooth Flow
Height		**Longitudinal Turbulence**	**Vertical Turbulence**	**Longitudinal Turbulence**	**Vertical Turbulence**	**Longitudinal Turbulence**	**Longitudinal Turbulence**
Deck Height (55 ft)	Values in Test	15.0%	6.2%	18.2%	8.3%	7.2%	1.7%
	Target Values from ESDU	14.7%	6.3%	17.8%	7.6%	N/A	N/A
Arch Crown (275ft)	Values in Test	12.2%	5.5%	14.5%	7.8%	1.7%	1.7%
	Target Values from ESDU	11.8%	5.3%	13.4%	6.2%	N/A	N/A

TABLE 7.8 PEAK RESPONSES AND PEAK FACTORS FOR SELECTED TESTS AND CHANNELS, COMPLETED BRIDGE

			Peak Responses & Peak Factors at mean wind design speed of 91 mph at deck height			
			Test IFA201		Test IFA302	
Channel No.	Channel Name	Unit	Peak Responses	Peak Factor	Peak Responses	Peak Factor
1	Deck End Lift Moment	kip-ft	19590	3.7	19480	3.6
2	Deck End Drag Moment	kip-ft	46880	3.9	51040	3.8
3	Deck End Torque	kip-ft	21600	3.7	23830	4.0
7	Deck Midspan Lift Moment	kip-ft	16050	4.0	15880	3.9
8	Deck Midspan Drag Moment	kip-ft	67930	3.9	68260	3.7
9	Deck Midspan Torque	kip-ft	7930	4.2	8330	3.9
10	Arch End Lift Moment	kip-ft	42700	3.7	42950	3.6
11	Arch End Drag Moment	kip-ft	161890	3.3	153020	3.2
37	Arch End Torque	kip-ft	2050	3.6	1980	3.4
12	Arch Mid Pt. Lift Moment	kip-ft	19680	3.9	19470	3.8
13	Arch Mid Pt. Drag Moment	kip-ft	90080	3.3	85160	3.1
40	Deck Midspan Lift Accel.	milli-g	84.5	3.8	84.1	3.9
41	Deck Midspan Torsional Accel.	deg/s^2	3.654	3.4	3.936	3.7
19	Deck Midspan Drag Accel.	milli-g	25.2	3.8	26.7	3.7
22	Arch Mid Pt. Lift Accel.	milli-g	71.1	3.9	68.7	3.9
23	Arch Mid Pt. Drag Accel.	milli-g	126.8	3.5	121.3	3.3
44	Deck Midspan Lift Displ.	ft	0.082	3.8	0.088	3.9
45	Deck Midspan Rotation	degree	0.101	3.6	0.111	3.9
29	Deck Midspan Drag Displ.	ft	0.065	3.9	0.074	4.0

Notes:

1. Test IFA201: hurricane profile without existing bridge, wind perpendicular to deck (90 degrees).

2. Test IFA302: open country profile without existing bridge, wind perpendicular to deck (90 degrees).

TABLE 7.9 PEAK RESPONSES AND PEAK FACTORS FOR SELECTED TESTS AND CHANNELS, CANTILEVERED TIE BEAM

			Peak Responses & Peak Factors at mean wind design speed of 91 mph at deck height			
			Test CPA202		Test CPA304	
Channel No.	Channel Name	Unit	Peak Responses	Peak Factor	Peak Responses	Peak Factor
1	Tie Beam End Lift Moment	kip-ft	8860	3.3	11610	3.4
2	Tie Beam End Drag Moment	kip-ft	74600	3.1	92960	3.1
3	Tie Beam End Torque	kip-ft	940	3.5	1070	3.4
4	Arch End Lift Moment	kip-ft	29750	3.3	38760	3.4
5	Arch End Drag Moment	kip-ft	78730	3.3	91730	3.3
6	Arch End Torque	kip-ft	1890	3.5	1950	3.3
7	Arch Mid Pt. Lift Moment	kip-ft	27050	3.4	26200	3.5
8	Arch Mid Pt. Drag Moment	kip-ft	36580	3.3	43620	3.3
11	Tie Beam Midspan Lift Accel.	milli-g	168.6	3.6	N/A	N/A
12	Tie Beam Midspan Drag Accel.	milli-g	85.2	3.4	88.8	3.2
13	Arch Mid Pt. Lift Accel.	milli-g	76.2	3.4	65.4	3.4
14	Arch Mid Pt. Drag Accel.	milli-g	63.0	3.3	72.3	3.3
20	Tie Beam Midspan Lift Displ.	ft	0.118	3.6	0.121	3.5
19	Tie Beam Midspan Drag Displ.	ft	1.232	3.1	1.565	3.0
23	Arch Midspan Lift Displ.	ft	0.09	3.3	0.098	3.4
24	Arch Midspan Drag Displ.	ft	0.924	3.2	1.146	3.3

Notes:

1. Test CPA202: hurricane profile without existing bridge, wind perpendicular to deck (90 degrees).

2. Test CPA304: open country profile without existing bridge, wind perpendicular to deck (90 degrees).

TABLE 7.10 PEAK RESPONSES AND PEAK FACTORS FOR SELECTED TESTS AND CHANNELS, CANTILEVERED ARCH

			Peak Responses & Peak Factors at mean wind design speed of 91 mph at deck height			
			Test CPB201		Test CPB302	
Channel No.	Channel Name	Unit	Peak Responses	Peak Factor	Peak Responses	Peak Factor
4	Arch End Lift Moment	kip-ft	55490	3.5	55240	3.3
5	Arch End Drag Moment	kip-ft	102870	3.3	105580	3.2
6	Arch End Torque	kip-ft	22200	3.4	21170	3.2
7	Arch Mid Pt. Lift Moment	kip-ft	2970	3.5	3080	3.3
8	Arch Mid Pt. Drag Moment	kip-ft	1090	3.7	1050	3.7
13	Arch Mid Pt. Lift Accel.	milli-g	208.7	3.6	203.3	3.4
14	Arch Mid Pt. Drag Accel.	milli-g	106.7	3.5	106.8	3.4
23	Arch Midspan Lift Displ.	ft	0.334	3.7	0.318	3.2
24	Arch Midspan Drag Displ.	ft	2.344	3.3	2.206	3.1

Notes:

1. Test CPB201: hurricane profile without existing bridge, wind perpendicular to deck (90 degrees).

2. Test CPB302: open country profile without existing bridge, wind perpendicular to deck (90 degrees).

TABLE 7.11 PEAK RESPONSES AND PEAK FACTORS FOR SELECTED TESTS AND CHANNELS, BRIDGE PRIOR TO FINAL DECK COMPLETION

			Peak Responses & Peak Factors at mean wind design speed of 91 mph at deck height			
			Test CPD202		Test CPD304	
Channel No.	Channel Name	Unit	Peak Responses	Peak Factor	Peak Responses	Peak Factor
1	Deck End Lift Moment	kip-ft	14270	3.6	21130	3.7
2	Deck End Drag Moment	kip-ft	42100	3.5	48770	3.5
3	Deck End Torque	kip-ft	17240	4.0	20550	4.0
4	Arch End Lift Moment	kip-ft	33370	3.6	51780	3.7
5	Arch End Drag Moment	kip-ft	89910	3.1	104750	3.1
6	Arch End Torque	kip-ft	5270	6.7	5150	6.0
7	Arch Mid Pt. Lift Moment	kip-ft	15690	3.6	21720	3.7
8	Arch Mid Pt. Drag Moment	kip-ft	44410	3.1	51680	3.1
40	Deck Midspan Lift Accel.	milli-g	50.3	3.9	93.1	3.8
41	Deck Midspan Torsional Accel.	deg/s^2	1.969	3.9	2.683	3.7
17	Deck Midspan Drag Accel.	milli-g	N/A	N/A	19.9	3.7
18	Arch Mid Pt. Lift Accel.	milli-g	N/A	N/A	46.3	3.6
19	Arch Mid Pt. Drag Accel.	milli-g	103.2	3.5	108.3	3.1
44	Deck Midspan Lift Displ.	ft	0.064	3.4	0.081	3.7
45	Deck Midspan Rotation	degree	0.079	3.4	0.092	3.6
27	Deck Midspan Drag Displ.	ft	0.059	3.5	0.068	3.6
33	Arch Midspan Lift Displ.	ft	0.066	3.5	0.248	3.9
34	Arch Midspan Drag Displ.	ft	1.029	3.0	1.077	3.0

Notes:

1. Test CPD202: hurricane profile without existing bridge, wind perpendicular to deck (90 degrees).

2. Test CPD304: open country profile without existing bridge, wind perpendicular to deck (90 degrees).

(A) BARE TUNNEL FLOOR (LOW TURBULENT FLOW), 90° WIND, COMPLETED BRIDGE

(B) SMOOTH FLOW WITH BRIDGE MODEL ELEVATED, 90° WIND, COMPLETED BRIDGE

FIGURE 7.1 THE FULL BRIDGE AEROELASTIC MODEL IN THE WIND TUNNEL

(C) HURRICANE EXPOSURE, WITH EXISTING BRIDGE, 90° WIND, COMPLETED BRIDGE

(D) OPEN COUNTRY EXPOSURE, WITH EXISTING BRIDGE, 90° WIND, COMPLETED BRIDGE

FIGURE 7.1 (CONT.) THE FULL BRIDGE AEROELASTIC MODEL IN THE WIND TUNNEL

(E) HURRICANE EXPOSURE, WITHOUT EXISTING BRIDGE, 90° WIND, COMPLETED BRIDGE

(F) OPEN COUNTRY EXPOSURE, WITHOUT EXISTING BRIDGE, 90° WIND, COMPLETED BRIDGE

FIGURE 7.1 (CONT.) THE FULL BRIDGE AEROELASTIC MODEL IN THE WIND TUNNEL

FIGURE 7.2 FULL BRIDGE AEROELASTIC MODEL - DETAILS OF MODEL AND INSTRUMENTATION, COMPLETED BRIDGE

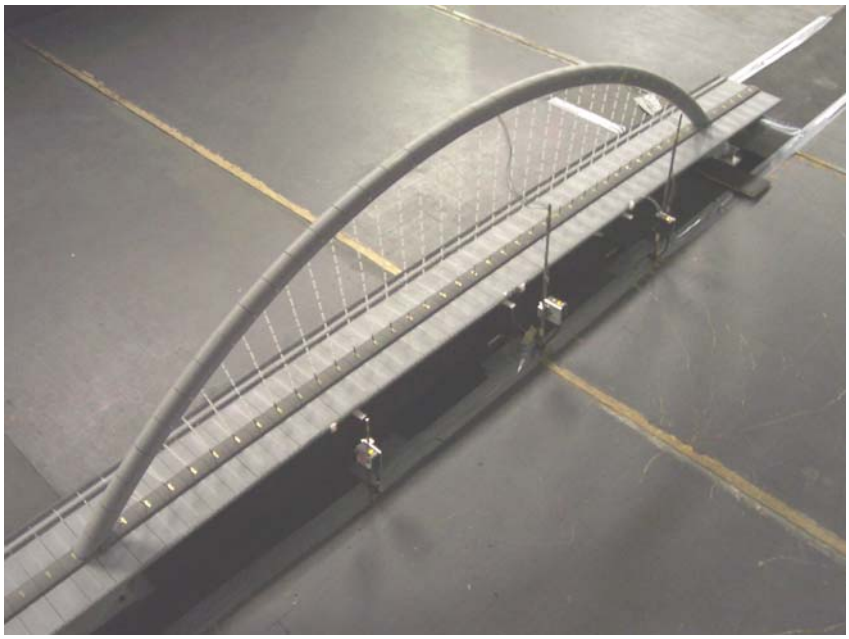

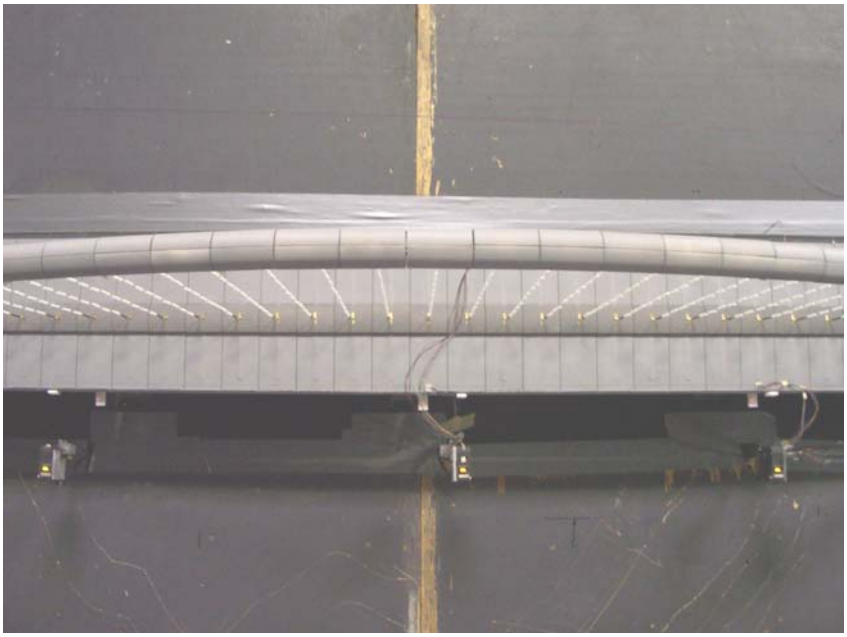

FIGURE 7.2 (CONT.) CLOSE-UP VIEWS OF THE FULL BRIDGE AEROELASTIC MODEL - DETAILS OF MODEL AND INSTRUMENTATION, COMPLETED BRIDGE

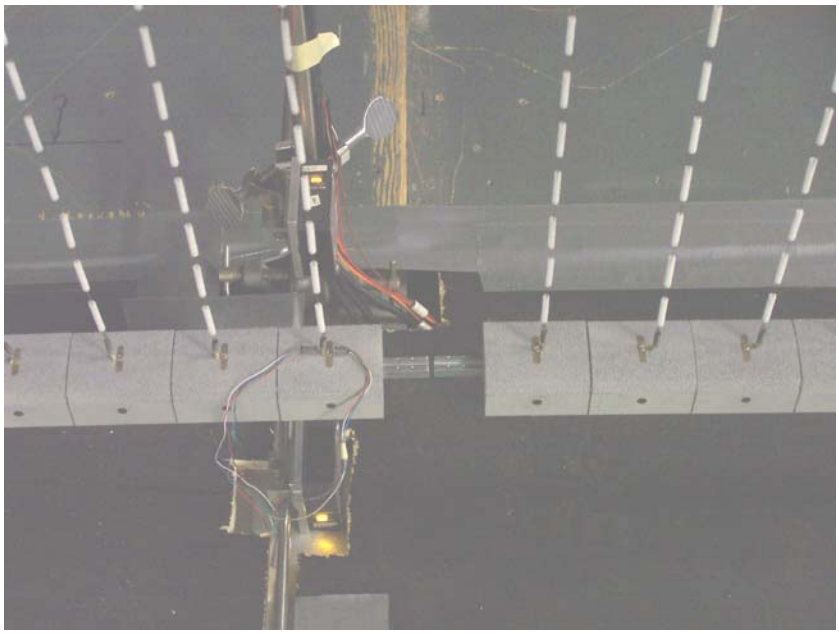

FIGURE 7.3 FULL BRIDGE AEROELASTIC MODEL, CONSTRUCTION STAGE – CANTILEVERED TIE BEAM

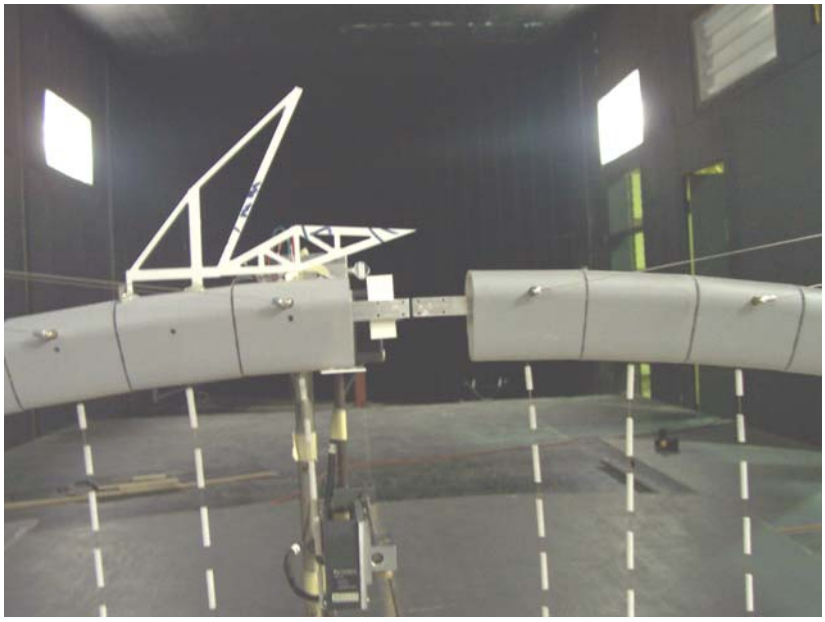

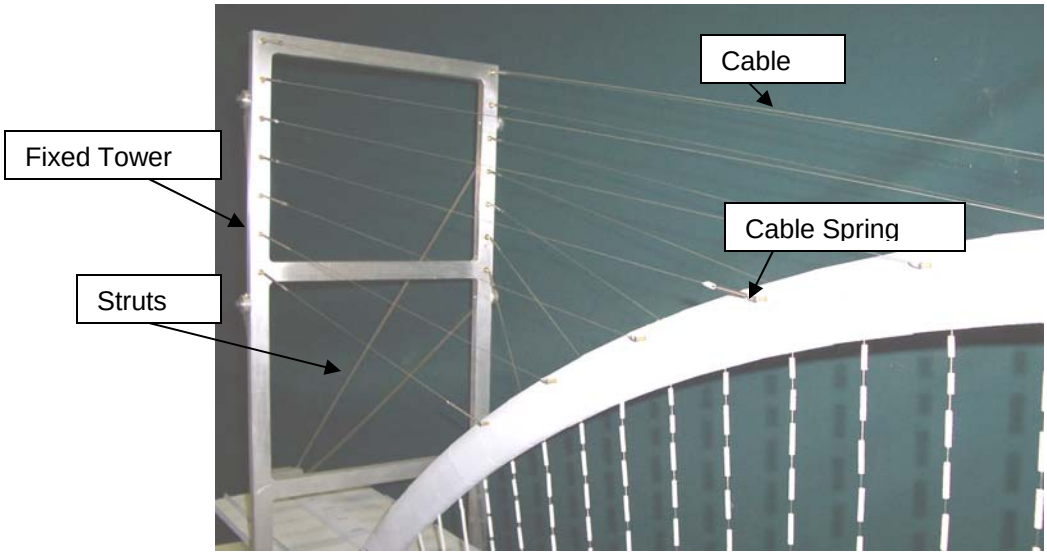

FIGURE 7.4 FULL BRIDGE AEROELASTIC MODEL, CONSTRUCTION STAGE – CANTILEVERED ARCH

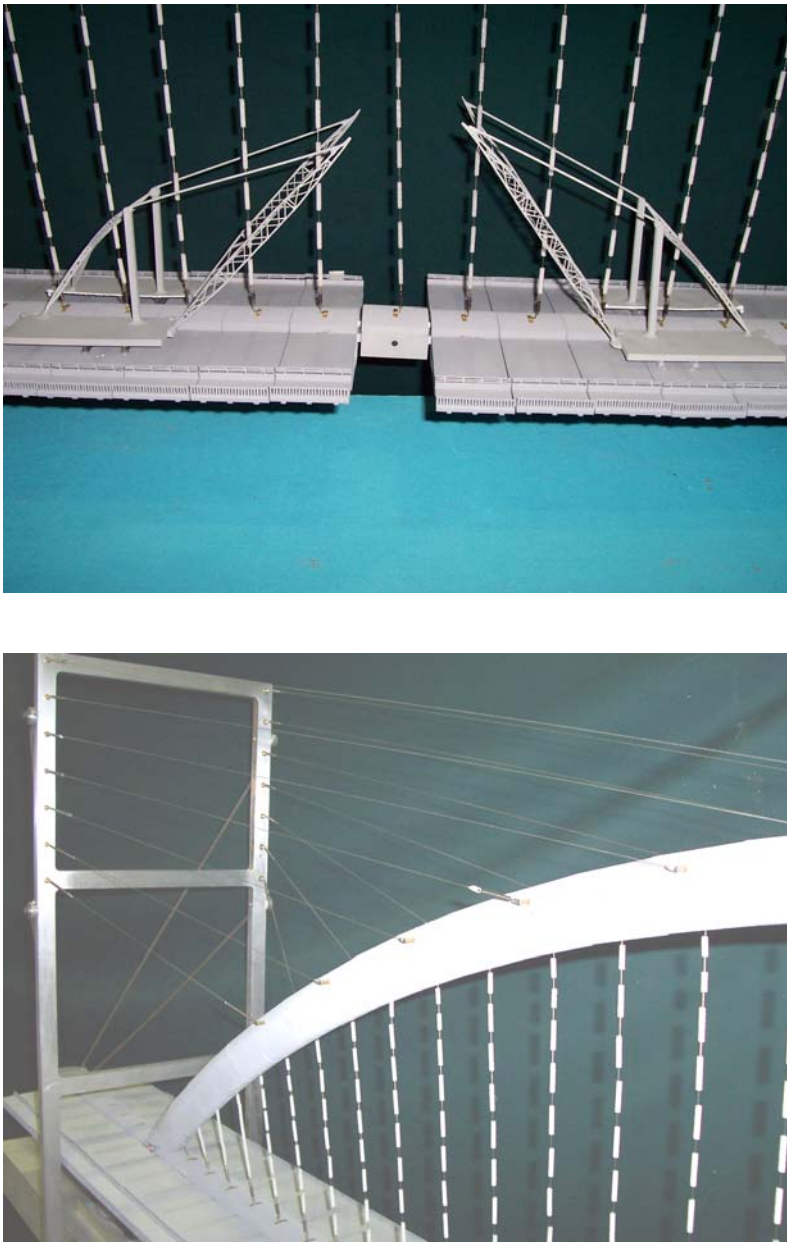

FIGURE 7.5 FULL BRIDGE AEROELASTIC MODEL, CONSTRUCTION STAGE – BRIDGE PRIOR TO DECK COMPLETION

(A) HURRICANE PROFILE, 60° WIND, COMPLETED BRIDGE

(B) HURRICANE PROFILE, 30° WIND, COMPLETED BRIDGE

FIGURE 7.6 THE FULL BRIDGE AEROELASTIC MODEL - HURRICANE EXPOSURE

(C) HURRICANE PROFILE, 0° WIND, COMPLETED BRIDGE

FIGURE 7.6 (CONT.) THE FULL BRIDGE AEROELASTIC MODEL - HURRICANE EXPOSURE

(A) OPEN COUNTRY PROFILE, 60° WIND, COMPLETED BRIDGE

(B) OPEN COUNTRY PROFILE, 30° WIND, COMPLETED BRIDGE

FIGURE 7.7 THE FULL BRIDGE AEROELASTIC MODEL - OPEN COUNTRY EXPOSURE

(C) OPEN COUNTRY PROFILE, 0° WIND, COMPLETED BRIDGE

FIGURE 7.7 (CONT.) THE FULL BRIDGE AEROELASTIC MODEL - HURRICANE EXPOSURE

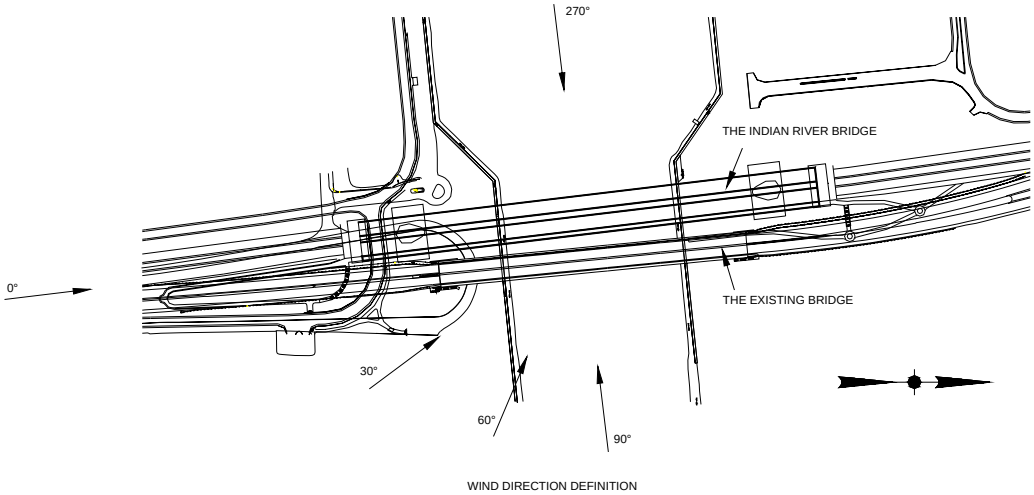

FIGURE 7.8 DEFINITION OF LOCAL WIND AZIMUTH

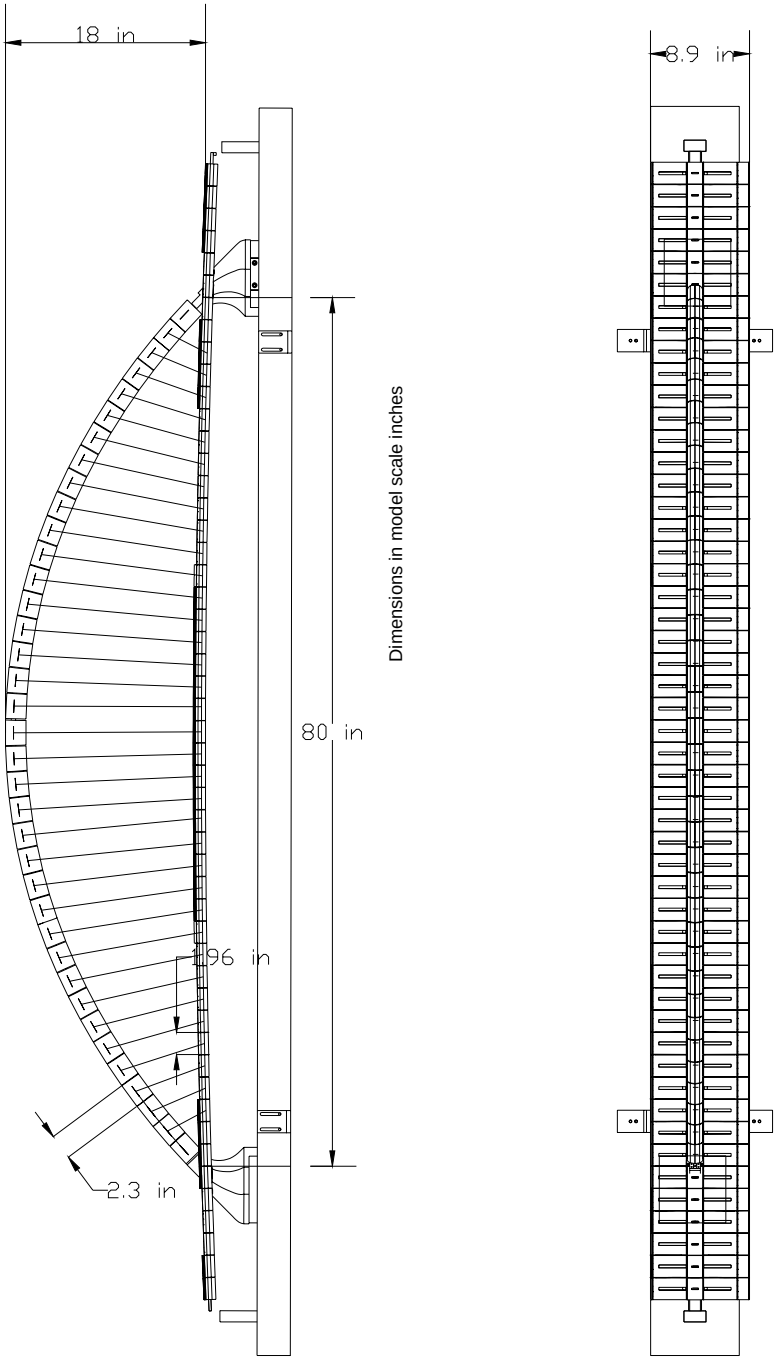

FIGURE 7.9 THE 1:150 SCALE AEROELASTIC MODEL, COMPLETED BRIDGE

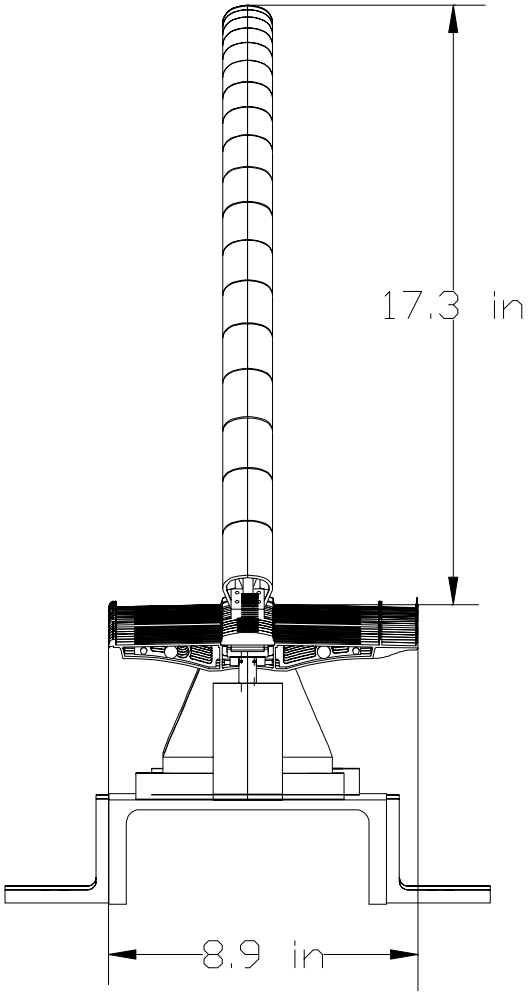

FIGURE 7.9 (CONT.) THE 1:150 SCALE AEROELASTIC MODEL, COMPLETED BRIDGE

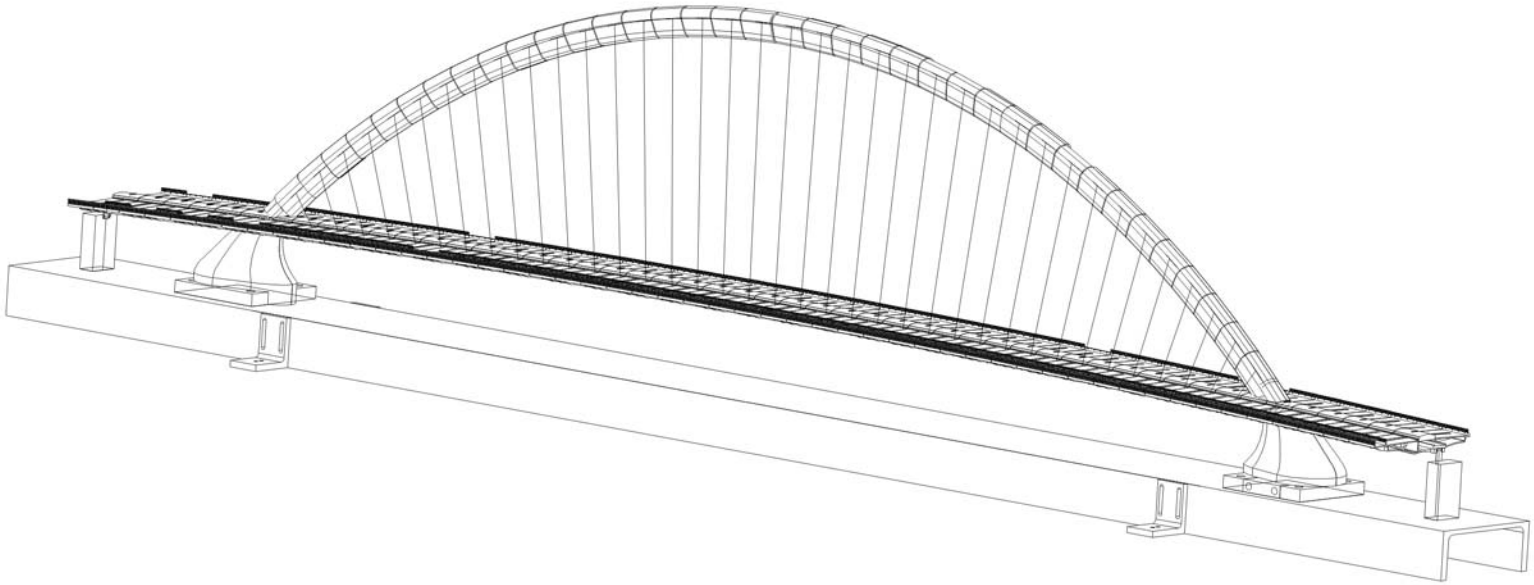

FIGURE 7.9 (CONT.) THE 1:150 SCALE AEROELASTIC MODEL, COMPLETED BRIDGE

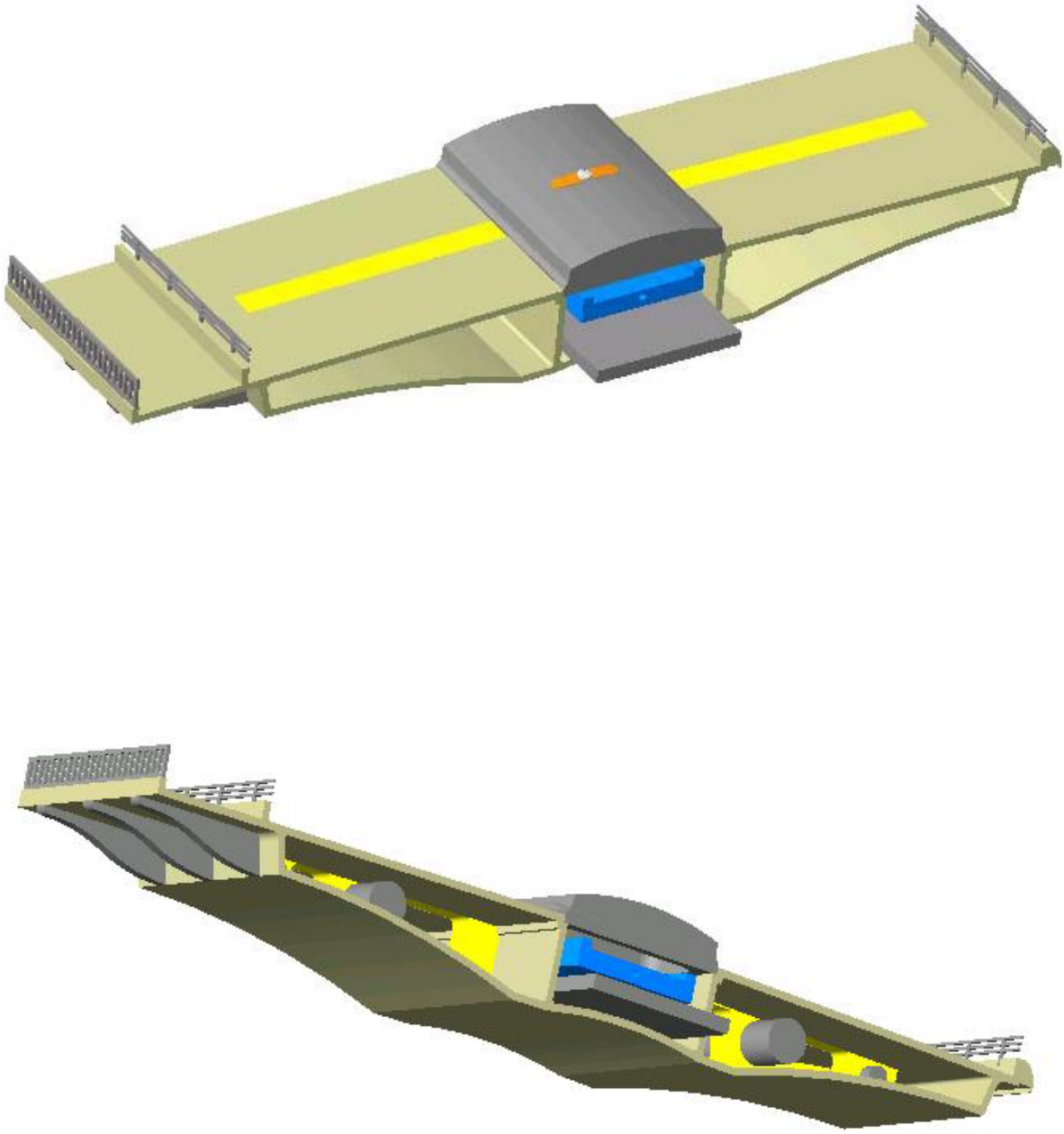

FIGURE 7.9 (CONT.) THE 1:150 SCALE AEROELASTIC MODEL (DECK MODULE) , COMPLETED BRIDGE

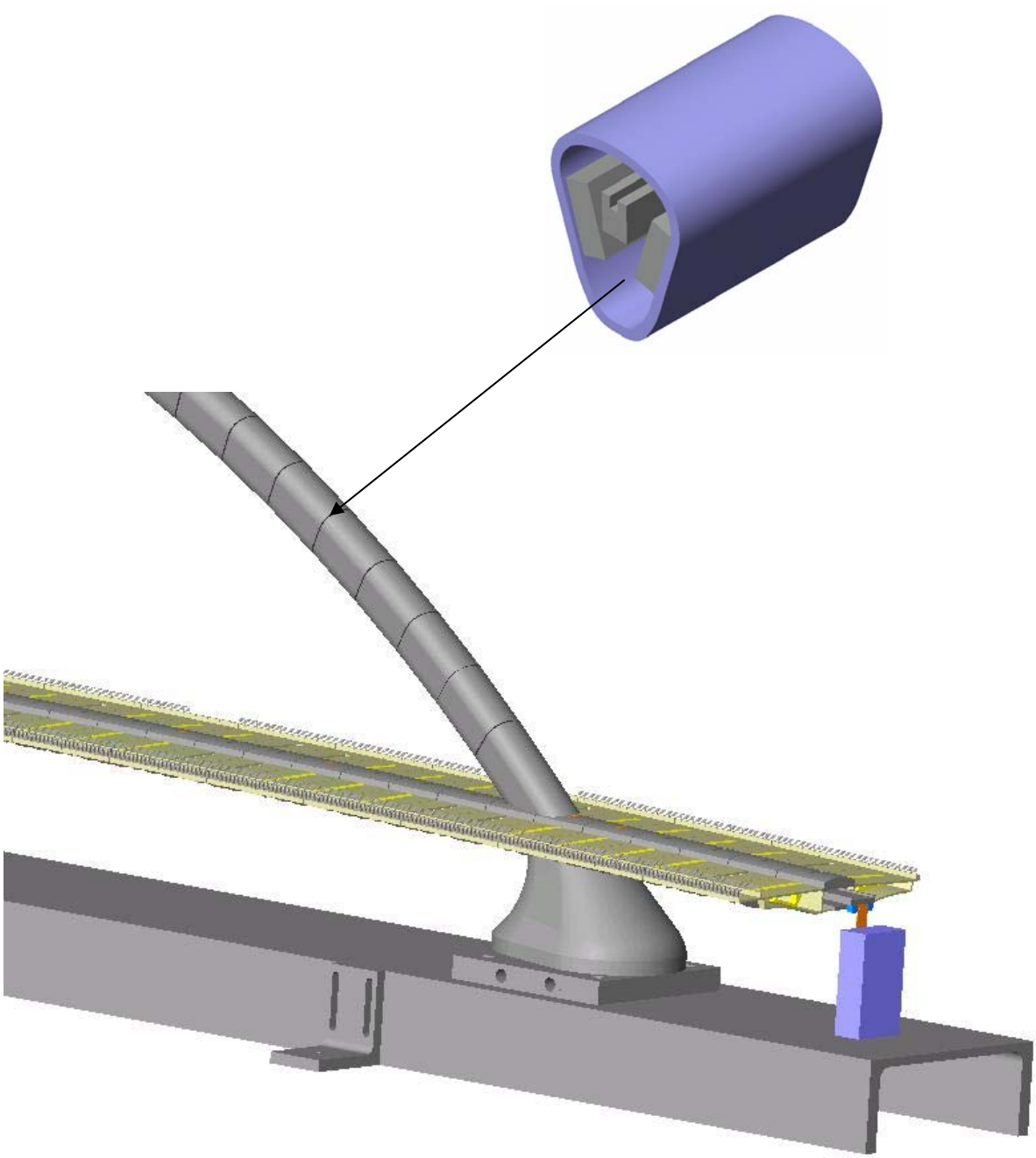

FIGURE 7.9 (CONT.) THE 1:150 SCALE AEROELASTIC MODEL (ARCH MODULE), COMPLETED BRIDGE

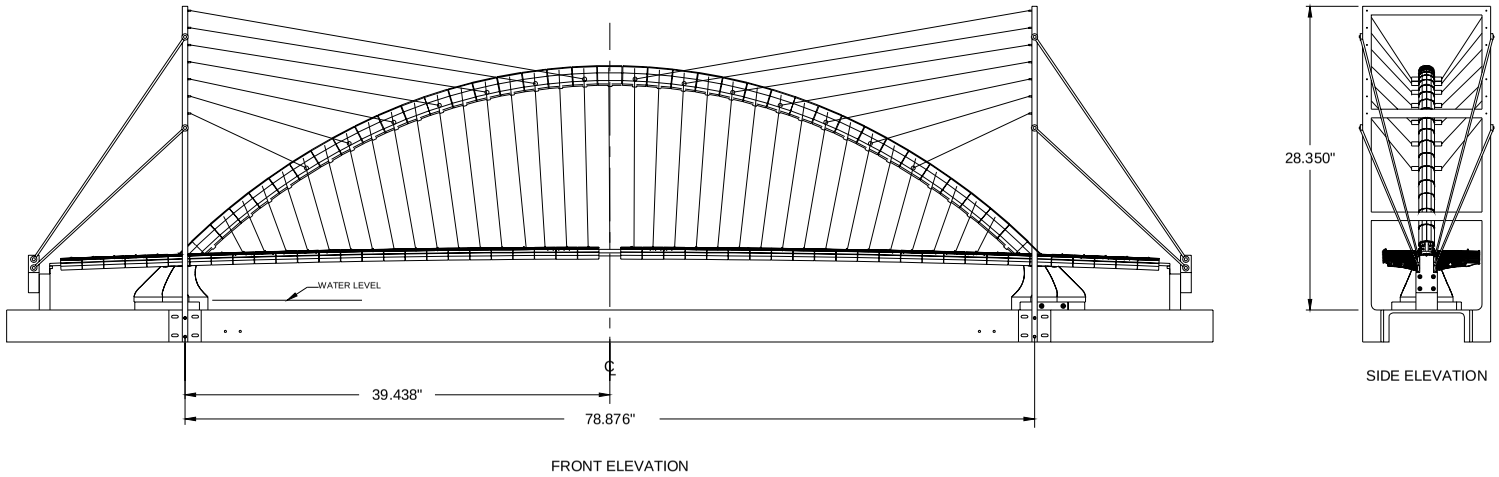

INDIAN RIVER BRIDGE - CONSTRUCTION STAGE

FIGURE 7.10 THE 1:150 SCALE AEROELASTIC MODEL, CONSTRUCTION STAGE, BRIDGE PRIOR TO DECK COMPLETION

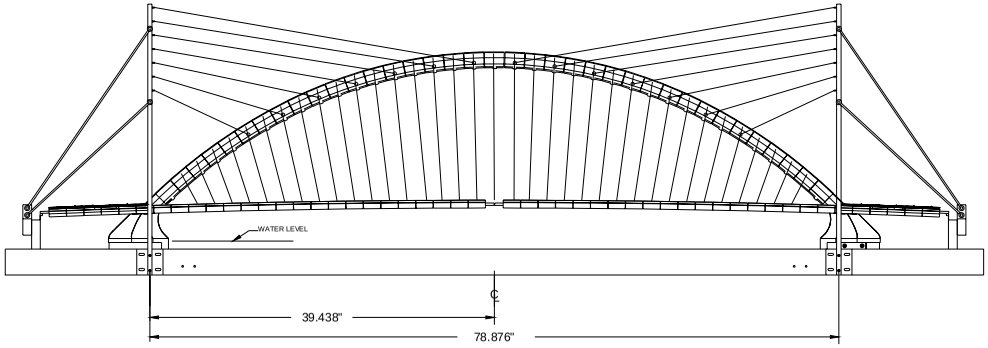

FRONT ELEVATION

INDIAN RIVER BRIDGE - CONSTRUCTION STAGE

FIGURE 7.10 (CONT.) THE 1:150 SCALE AEROELASTIC MODEL, CONSTRUCTION STAGE, CANTILEVERED TIE-BEAM

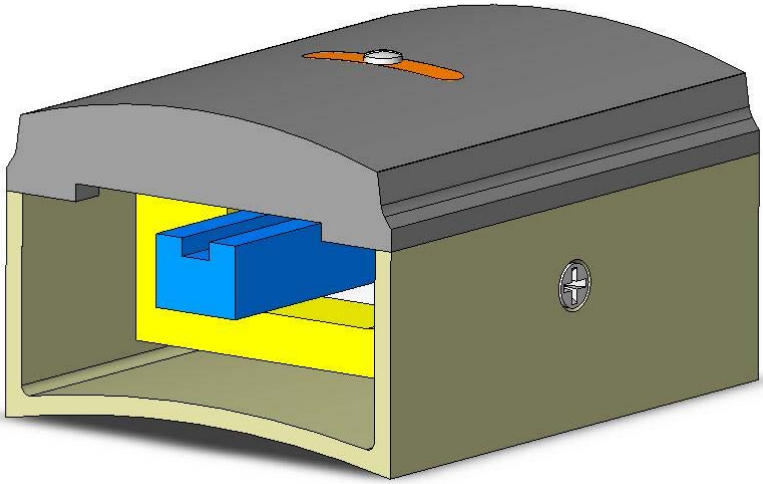

FIGURE 7.10 (CONT.) THE 1:150 SCALE AEROELASTIC MODEL (TIE-BEAM MODULE), CONSTRUCTION STAGE

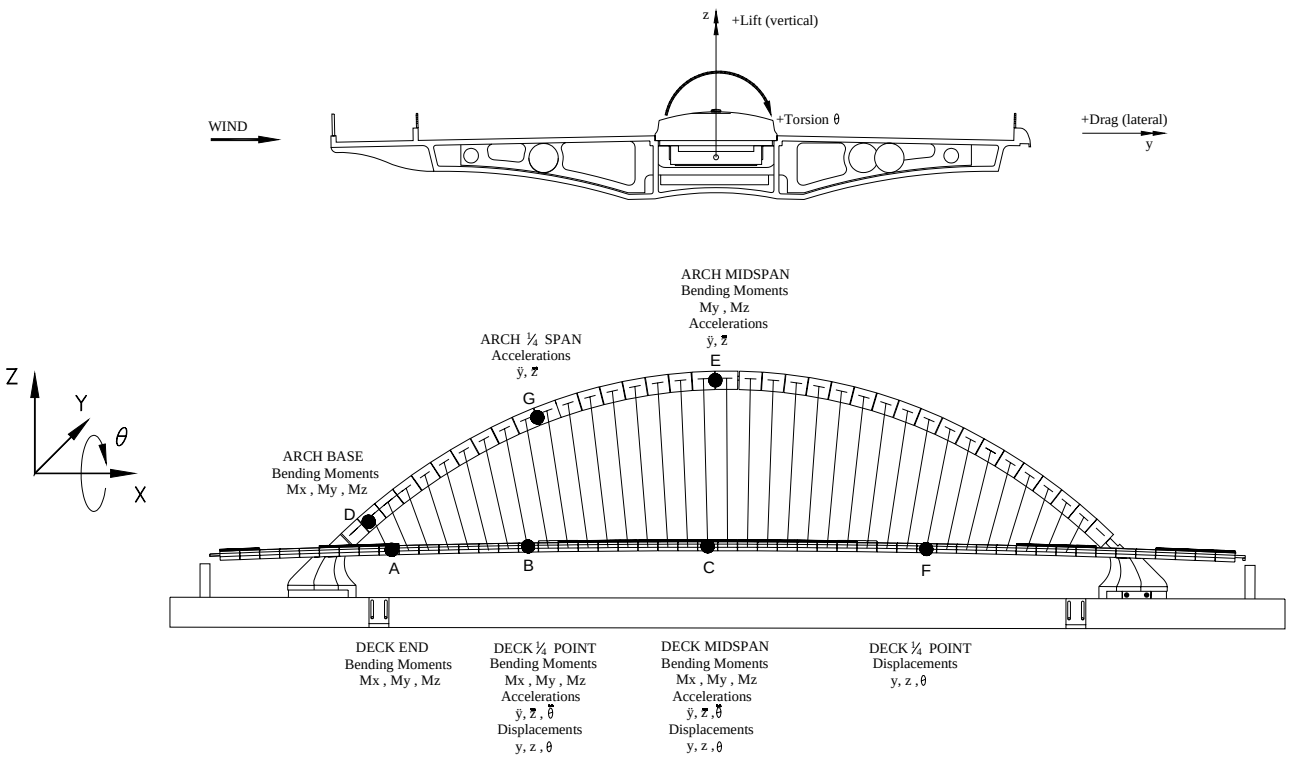

FIGURE 7.11 BRIDGE SIGN CONVENTION AND INSTRUMENTATION LOCATIONS

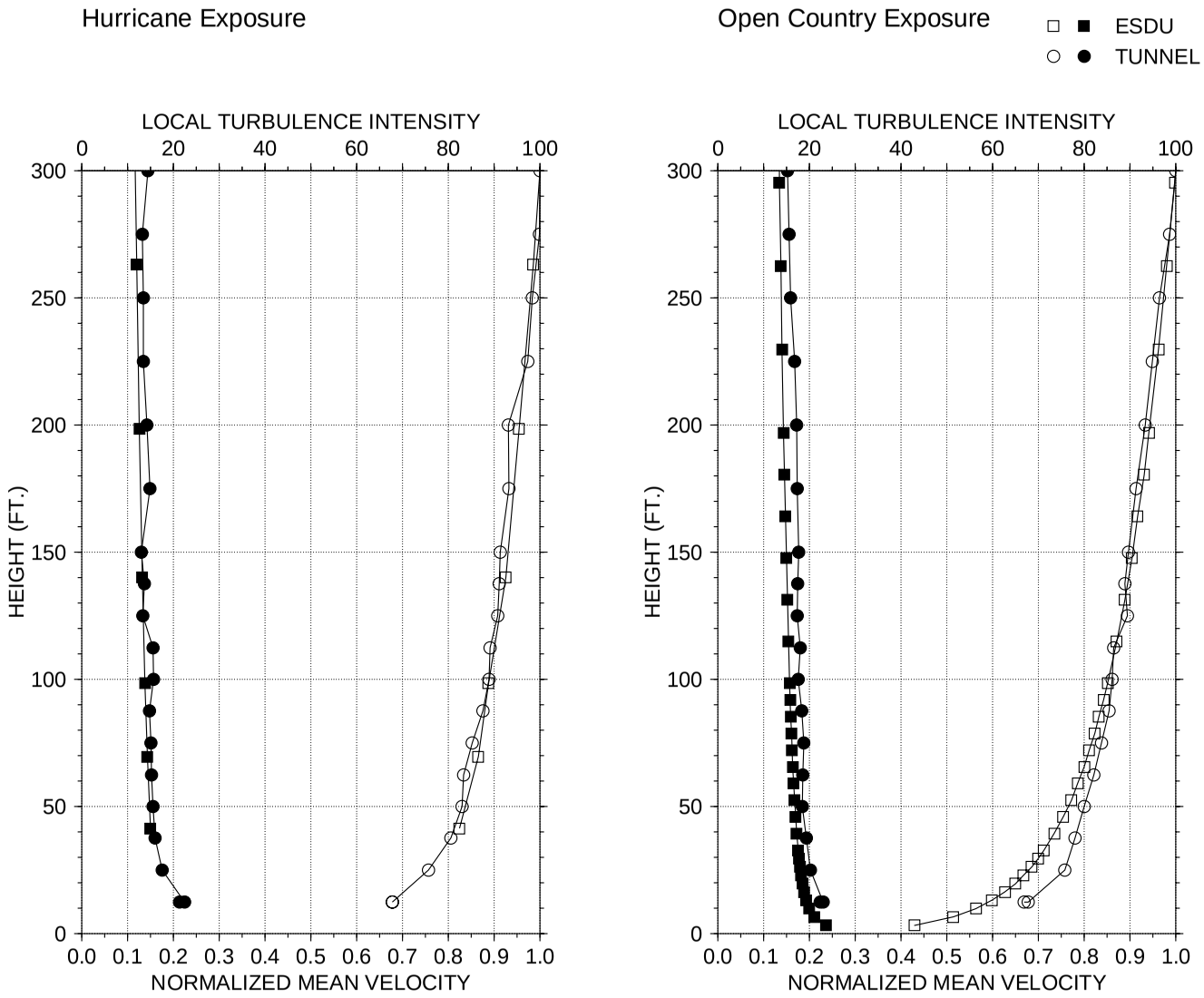

FIGURE 7.12 WIND PROFILES USED IN THE FULL BRIDGE MODEL TESTS, OPEN COUNTRY AND SUBURBAN EXPOSURES

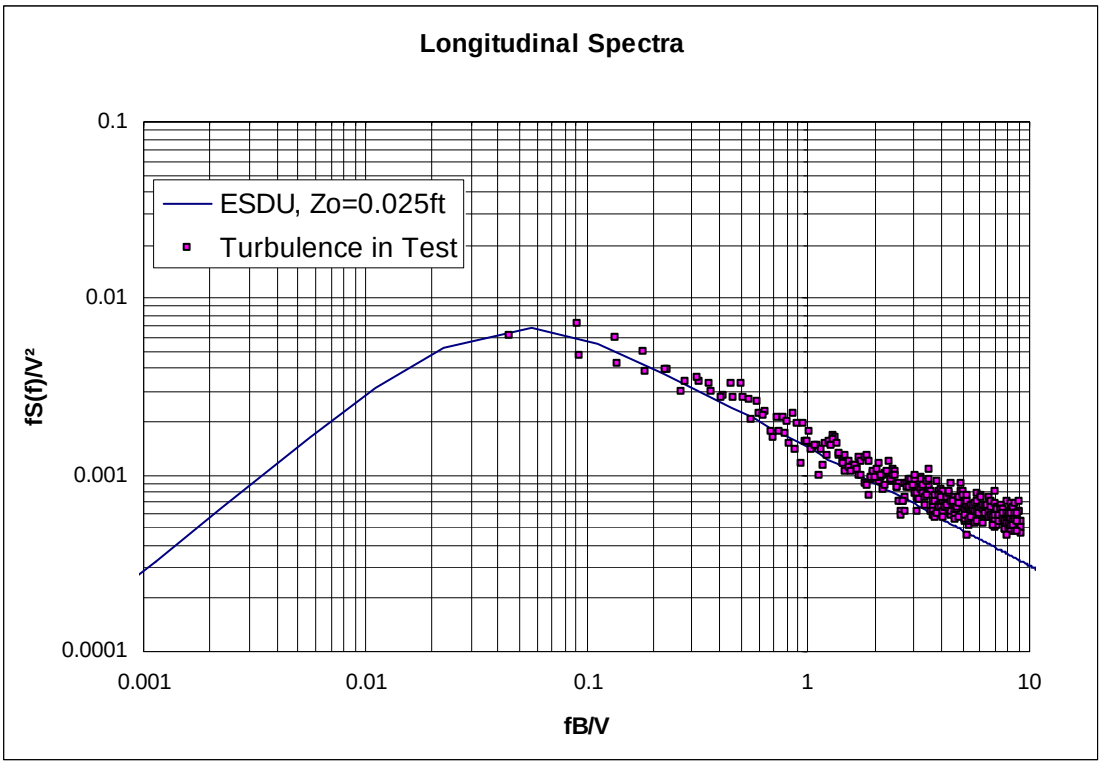

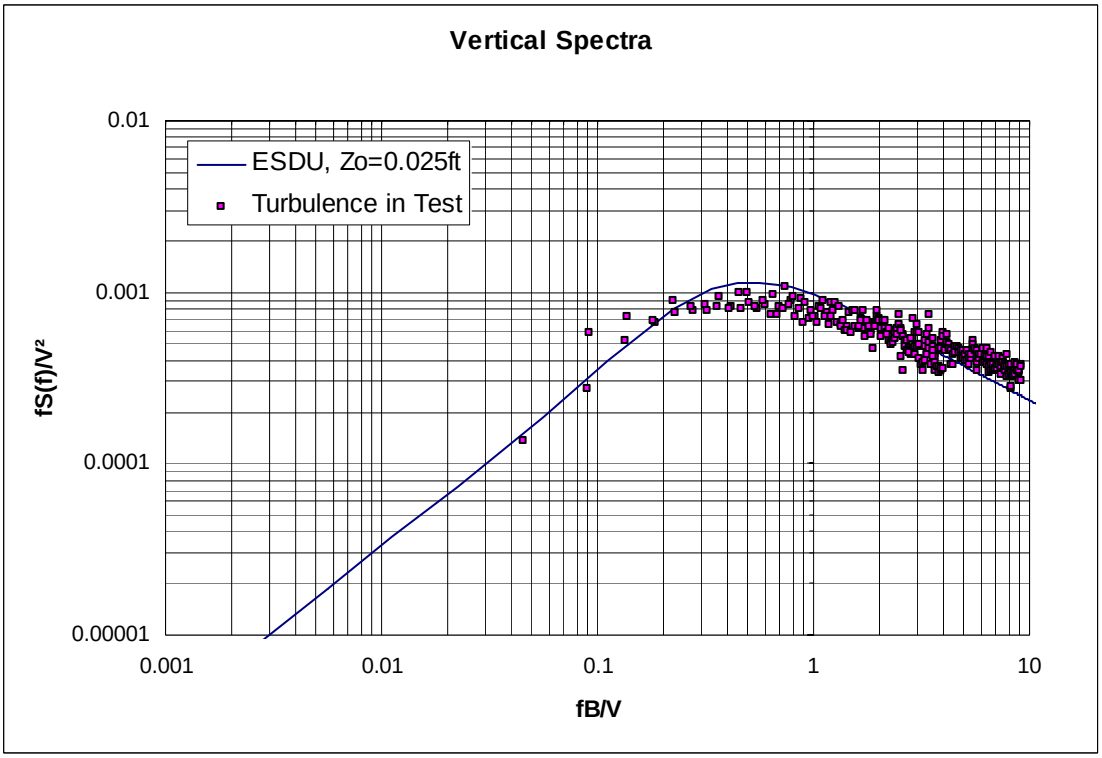

FIGURE 7.13 WIND SPECTRA AT DECK HEIGHT, HURRICANE EXPOSURE

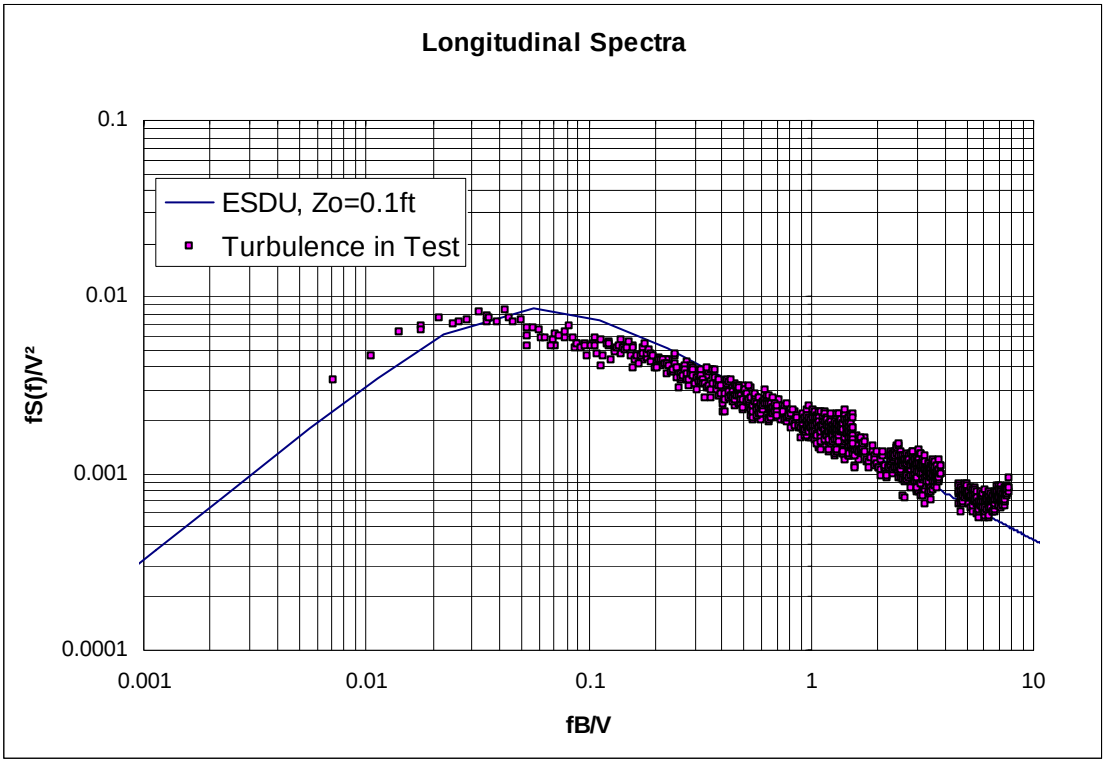

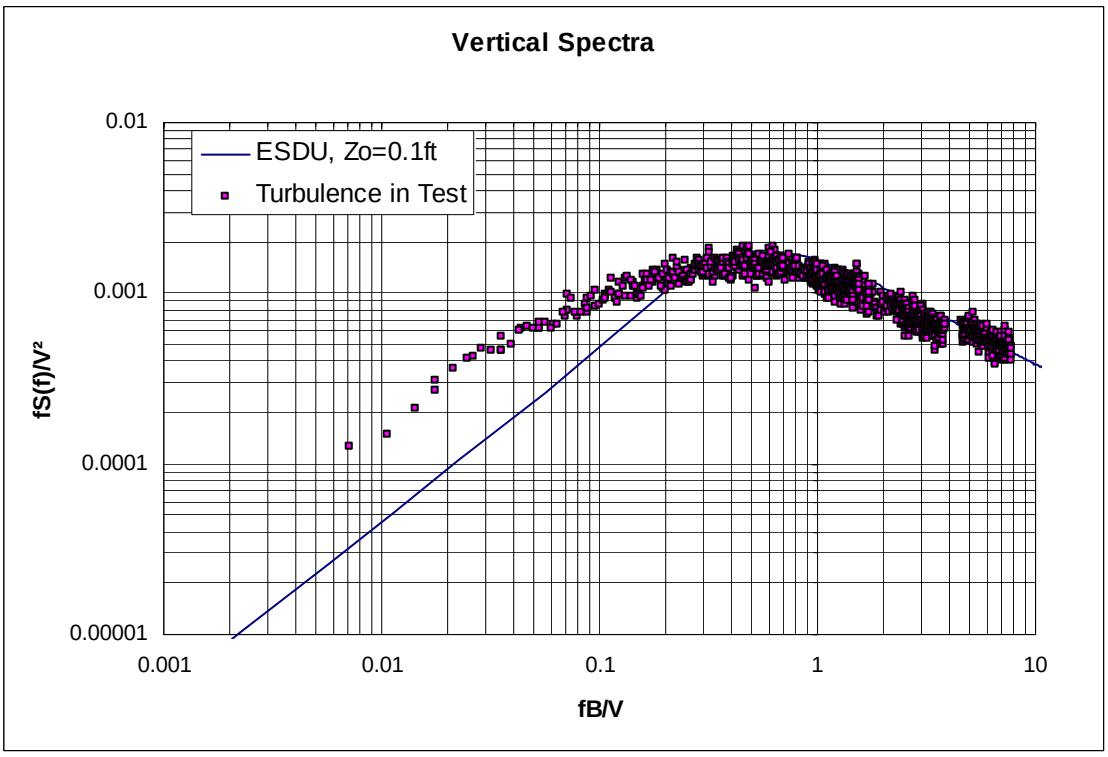

FIGURE 7.14 WIND SPECTRA AT DECK HEIGHT, OPEN COUNTRY EXPOSURE

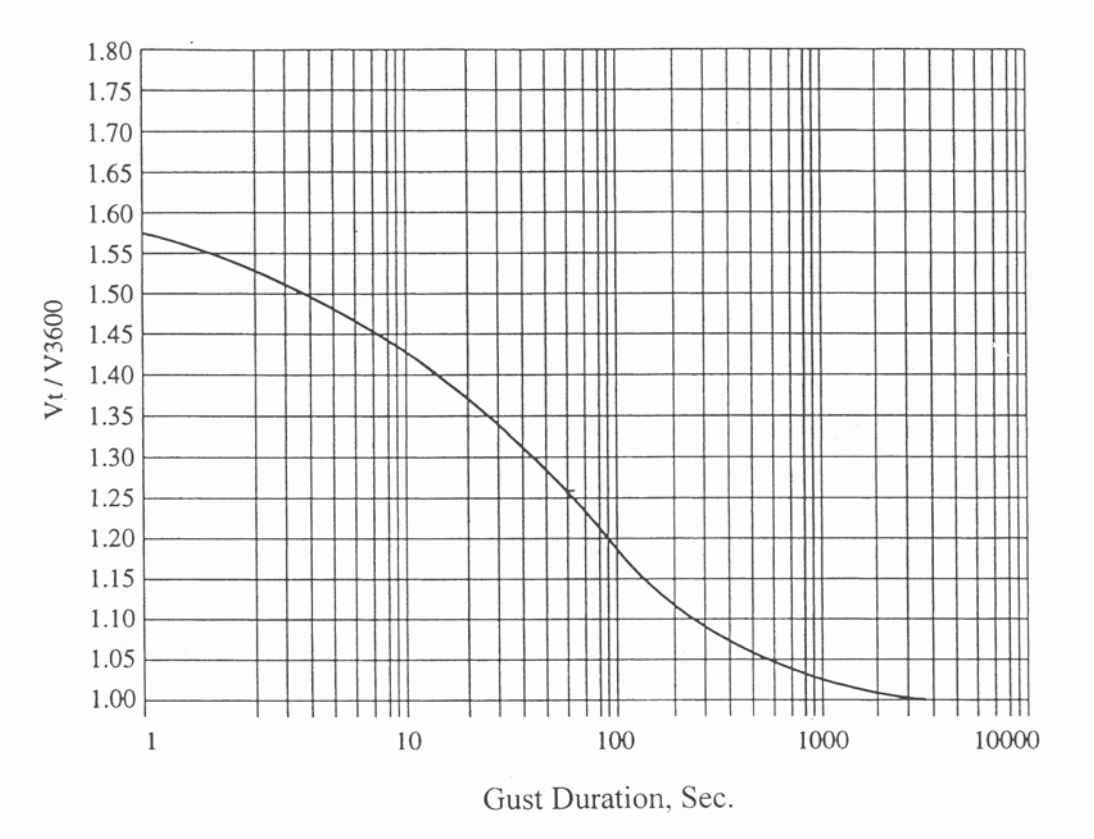

FIGURE 7.15 RATIO OF PROBABLE MAXIMUM SPEED AVERAGED OVER t SECONDS TO HOURLY MEAN SPEED

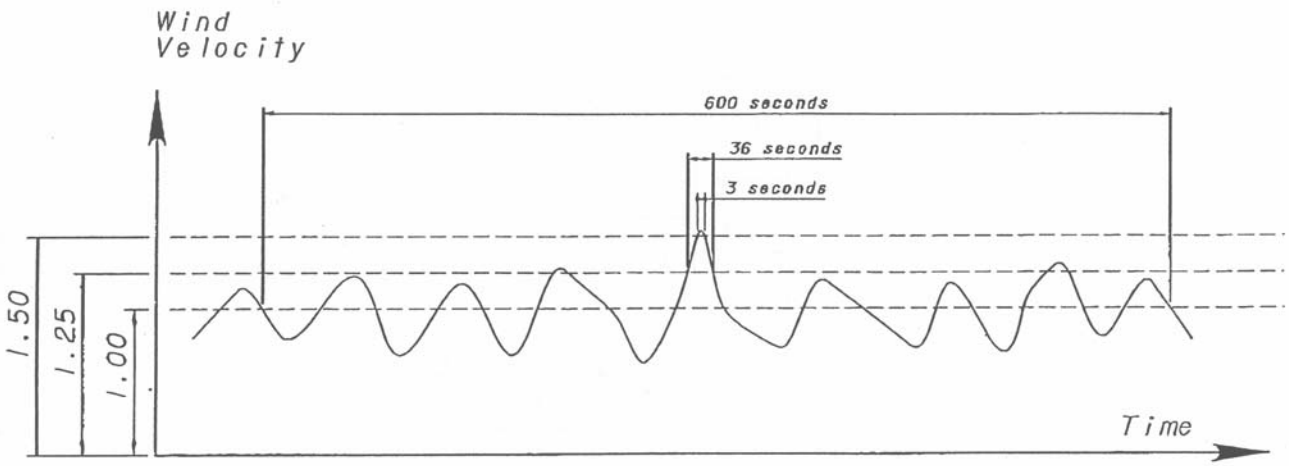

Mean Wind Speed = 10 minute (600 seconds) average

Fastest Mile = 36 seconds (AASHTO 100 mph definition)

Instantaneous Speed = peak 3 second speed

FIGURE 7.16 DEFINITION OF WIND SPEEDS FOR VARIOUS AVERAGING TIME

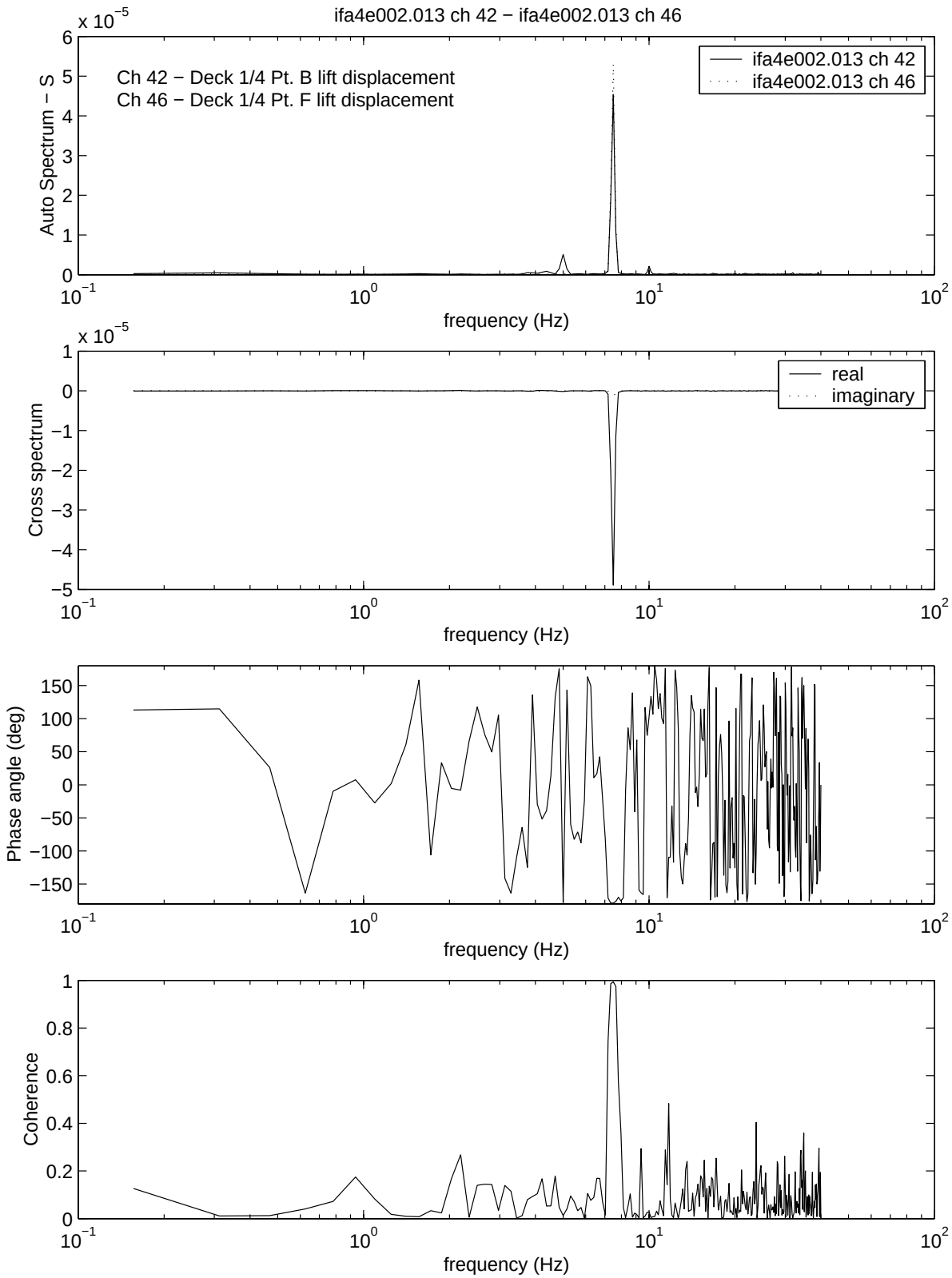

FIGURE 7.17 COHERENCE OF THE DECK LIFT DISPLACEMENTS AT THE TWO ¼ POINTS (B AND F) FOR THE FIRST VORTEX PEAK (DECK ASYMMETRIC LIFT MODE AT 7.5 HZ) AT 45 MPH DECK HEIGHT, SMOOTH FLOW

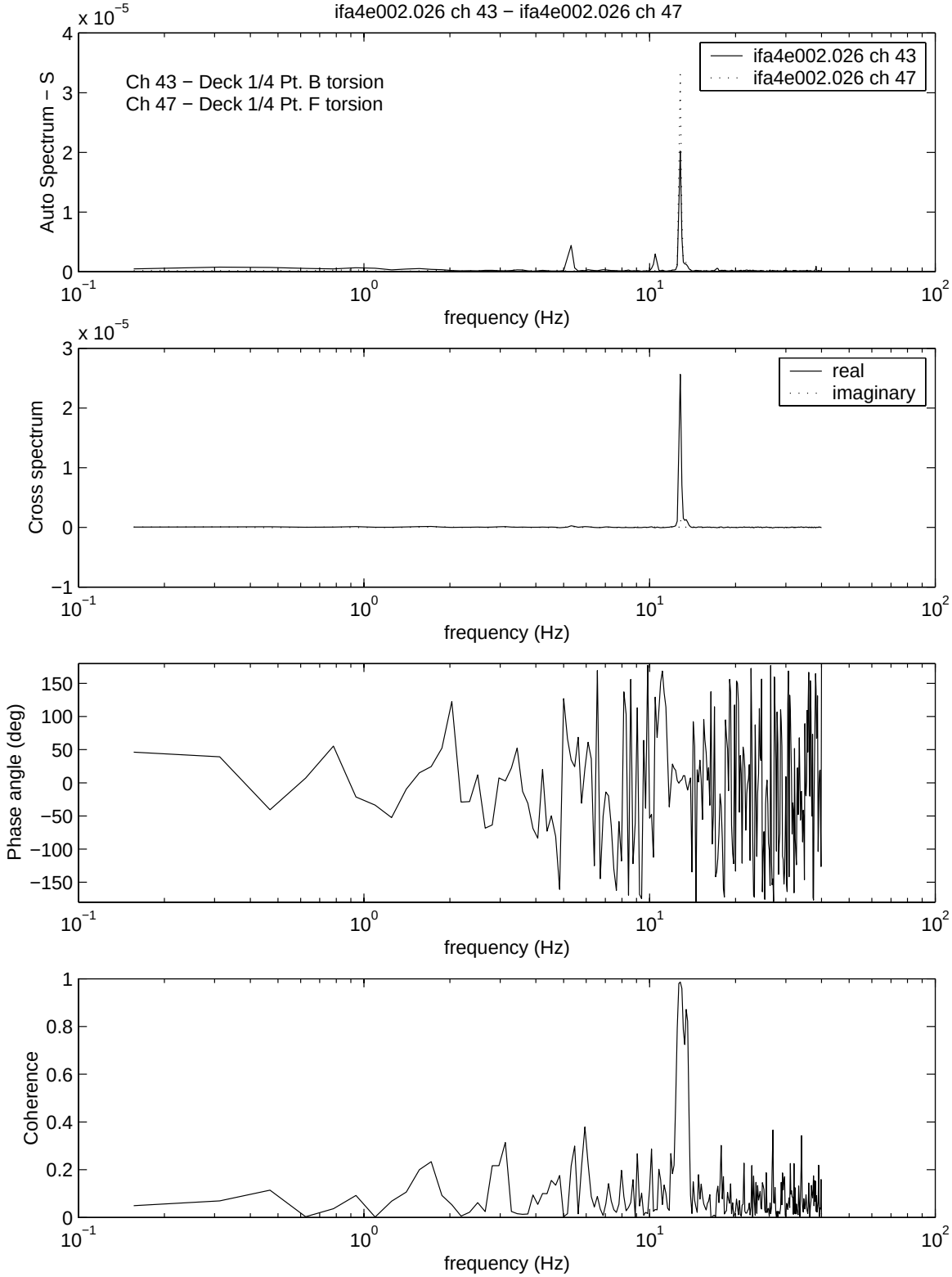

FIGURE 7.18 COHERENCE OF THE DECK TORSION AT THE TWO ¼ POINTS (B AND F) FOR THE SECOND VORTEX PEAK (DECK SYMMETRIC TORSION MODE AT 13.7 HZ) AT 80 MPH (DECK HEIGHT), SMOOTH FLOW

REFERENCES

1) "Wind Tunnel Testing: A General Outline", The University of Western Ontario, Boundary Layer Wind Tunnel Laboratory General Outline Report, May 1999.

2) ASCE, "Minimum Design Loads for Buildings and Other Structures – ASCE 7-98", American Society of Civil Engineers, New York, N.Y., January, 2000.

3) Vickery, P.J., Skerlj, P.F., Steckley, A.C. And Twisdale, L.A., "Hurricane Wind-Field Model for use in Hurricane Simulation", Journal of Structural Engineering, ASCE, 126(10), pp. 1203-1222, 2000.

4) Davenport, A.G. and King, J.P.C., "A Study of Wind Effects for the Sunshine Skyway Bridge, Tampa, Florida - Concrete Alternate", The University of Western Ontario, Faculty of Engineering Science Research Report, BLWT-SS24-1982, London, Ontario, Canada, 1982.

5) Davenport, A.G. and King, J.P.C., "A Study of Wind Effects for the Sunshine Skyway Bridge, Tampa, Florida - Steel Alternate", The University of Western Ontario, Faculty of Engineering Science Research Report, BLWT-SS25-1982, The University of Western Ontario, London, Ontario, Canada, 1982.

6) Davenport, A.G. and King, J.P.C., "The Incorporation of Dynamic Wind Loads into the Design Specifications for Long Span Bridges", ASCE Fall Convention: Structures Congress, New Orleans, La., October 1982.

7) Davenport, A.G. and King, J.P.C., "Dynamic Wind Forces on Long Span Bridges", 12th IABSE Congress, Vancouver, Canada, September 1984.

8) Modi, V.J. and El-Sherbiny, S. 1971. Effect of wall confinement on aerodynamics of stationary circular cylinders. Proceedings of the 3rd International Conference on Wind Effects on Buildings and Structures, Tokyo. pp. 365-375.

9) Powell, M.D., Reinhold T.A. and Vickery P.J., "Engineering Implications of New Information on Boundary Layer Profiles in Hurricanes", Americas Conference on Wind Engineering 2001.

10) Engineering Sciences Data Unit, "Strong Winds in the Atmospheric Boundary Layer", Data Items 82026, 83045, London, 1982, 1983.

11) Engineering Sciences Data Unit, "Characteristics of Atmospheric Turbulence Near the Ground", Data Item 74031, October, 1974.

12) Davenport, A.G., "Reliability of Long Span Bridges under Wind Loading", Proc. of ICOSSAR 81, Trondheim, Norway 1981.

13) Durst, C.S., "Wind Speeds over Short Periods of Time", Meteor. Mag. 89, 181-187, 1960.

APPENDIX A

THE SECTION MODEL APPROACH FOR THE STUDY OF WIND ACTION ON LONG SPAN BRIDGES

A1 DESIGN OF THE SECTION MODEL

The most elementary of the tools available to the wind engineer for the study of the aerodynamics of long span bridges is the section model. It is also, perhaps the most productive and economical of these tools [A1,A2].

The section model consists of a typical rigid section of the deck, geometrically and aerodynamically similar to the prototype, mounted in the wind tunnel in such a way as to measure the wind produced static and dynamic lift, drag and moment. The model is usually located within the parallel walls of the wind tunnel, or equipped with end plates in order to channel the wind over the deck in a two-dimensional manner.

In a fixed position, the section model can be instrumented to measure lift, drag and torsion either through the mounting of the model on a three component force balance, or on stiff springs to reduce the dynamic motions. The bridge deck is rotated with respect to the oncoming flow to measure the variation in the forces with angle of attack, usually between +15° and -15°. The force coefficients are typically specified as follows:

Lift force per unit length: $$L = \frac{1}{2}\rho V^2 B C_L \quad \text{(A1)}$$

Drag force per unit length: $$D = \frac{1}{2}\rho V^2 B C_D \quad \text{(A2)}$$

Torsional force per unit length: $$T = \frac{1}{2}\rho V^2 B^2 C_T \quad \text{(A3)}$$

Where ρ is the air density, B is the model deck width and C_L, C_D, C_T are dimensionless lift, drag and torsional force coefficients, respectively.

As first used in early applications, the section model was conceived as a substitute for the prototype bridge. Since its dynamics and aerodynamics cannot fully duplicate those of the full scale bridge, interpretation of the results of any section model test is required. Research in recent years has better defined the limited but important role of the section model.

Mounted on springs, with scaled mass per unit length, mass moment of inertia per unit length, structural damping and natural frequencies, the section model is commonly used to investigate the following:

- the dynamic response to vortex shedding
- to ensure that the section is aerodynamically stable to an acceptably high wind speed, given the meteorology of the bridge site
- to determine the response to turbulence

Usually, the effect of turbulence is to reduce the response of the bridge deck to vortex shedding. Consequently, tests are conducted in flow conditions with low turbulence intensity (or, so-called “smooth flow”) in order to conservatively estimate the amplitudes of motion. Various edge treatments can be

investigated to improve the response to vortex shedding. The model is also tested with the same low turbulence flow to provide conservative estimates of flutter behaviour of the section. The response is often investigated with several structural damping ratios.

A uniform grid or spires are used to provide simulations of the scaled atmospheric turbulence. Measured response to turbulent buffeting can be interpreted using an appropriate theory to provide estimates of the prototype wind loading that can be used in the design of the bridge.

The section model can also be used to measure the motion-related forces. Mounted on springs, or driven through sinusoidal motions, the section model experiences aerodynamic forces proportional to the bridge motion and the time derivatives of the motion. These so-called "flutter" forces can be measured and used in a dynamic theoretical model of the bridge in order to predict its performance and aerodynamic stability.

A2 DESIGN OF THE SECTION MODEL

Aeroelastic modeling of structures generally requires equality of the following non-dimensional quantities, in addition to an overall geometric similarity [A3, A4, A5]:

- Froude Number (ratio of the gravitational to the inertia forces);
- Cauchy Number (ratio of the elastic to inertia forces);
- Density Ratio (ratio of the inertia force of the structure to that of the flow);
- Damping Ratio
- Reynolds Number (based on the dimensions of the structure)

Froude Number scaling ($F_r = gL/V^2$) is not necessary in section model studies, since the stiffness is supplied by external springing and not due to gravitational effects. L is a characteristic dimension, V is the wind speed and g is the acceleration due to gravity. Cauchy Number is rewritten in terms of $V/(fB)$ and provides the link in the wind speeds between model and prototype. f is a natural frequency and B is the bridge deck width. Density scaling (ρ_s/ρ_α) is important, where the subscripts s and a refer to the structure and air respectively. This ensures that the mass is scaled correctly, in relation to the added mass of air due to the moving bridge. Equal modal damping (ζ_s in a ratio to critical or δ_s in logarithmic decrement) between model and prototype is required, but exploratory tests are often performed with lower model damping in order to ensure that any instability can readily be identified.

Reynolds Number similarity ($R_e=VL/\nu$, where ν is the kinematic viscosity of the air) is not practical in most cases and section model tests are usually carried out at a Reynolds Number several orders of magnitude lower than that of full scale. For sharp edged bodies such as bridge decks, the effects of this relaxation of R_e scaling is not severe for overall wind induced forces and responses. In the case of the geometric modeling of circular objects such as the cables and handrails, however, R_e effects can be significant and an "equivalent force effect" approach should be taken.

The full scale data that is needed to design the model and springing system consists of:

- a constant mass ($m_v = \rho_s B^2$) per unit length of span, or a calculated value, giving the correct modal mass in the case of a non-uniform span-wise distribution
- a mass moment of inertia ($I_T = \rho_s B^4$) per unit length of span, or a calculated value, as for the mass, in the case of a non-uniform span-wise distribution, or a radius of gyration, r, of the mass, m_v
- target values of modal damping for the modes of vibration to be examined (nominally the fundamental vertical and torsional modes)

- natural frequencies of the modes to be examined
- location of the rotation centre of the deck cross section which determines the torsional mode

Most section model rigs have two dominant modes of vibration, namely, vertical and torsional motion. It is through the selection of the springs and the spring spacing that the above scaling is applied. Firstly, the geometric scale factor is selected, along with the model length. Typical geometric scales are in the order of 1:40 to 1:80, in order that deck details are well simulated. The length of the model should be of the order of 4-5 times the deck width in order that correlation effects of the wind on the structure are correct.

The target mass and mass moment of inertia are determined through the expressions above. Before selecting the model support stiffness a target value for the velocity scale factor, $V_{prototype}/V_{model} = (fB)_{prototype}/(fB)_{model}$, is set such that the range of wind speed available in the wind tunnel corresponds to a satisfactory range of wind speeds in the prototype.

It is important to include the model support mass as part of the moving mass of the model as well as providing sufficient model stiffness such that internal flexing or twisting of the model does not occur.

A typical arrangement of springs for the section model rig in use at the Boundary Layer Wind Tunnel Laboratory at the University of Western Ontario is as shown in Figure A1. The arrangement of the model mounting system incorporates radial bearings at the ends of the model at the K_3 support, which allow the locking of vertical or torsional motion to perform single degree of freedom tests.

The following spring stiffnesses are considered:

- k_1 is four main springs above the model, at a spacing X
- k_2 is four main springs below the model
- k_3 is four leaf springs in pairs on each end of the model which provide a drag restraint and allows only vertical motion (in other section model rigs, this spring system has often been modelled using a very long drag-wire fore and aft of the model)
- k_{lc} is four load cell transducers

The simplified equation for the natural frequencies of vertical and torsional modes of vibration is:

$$f_V = \frac{1}{2\pi}\sqrt{\frac{k_V}{m}} \qquad \text{(A4)}$$

and:

$$k_V \approx 4k_1 + 2k_3 + 4\frac{1}{\frac{1}{k_2} + \frac{1}{k_k}} \qquad \text{(A5)}$$

also: $f_T = f_V\left(\frac{X}{2r}\right)$ (where r is the radius of gyration and X is the spring spacing)

Dashpots are installed at appropriate locations on the main arms of the rig to provide the desired structural damping in the vertical and torsional modes of vibration. Although with this arrangement of spring supports it is not possible to prevent the model from undesirable rocking modes of vibration, by summing and differencing the load cell outputs, the electrical output from this type of mode can be eliminated.

The spring system is mounted on a frame structure which is independent of the wind tunnel and can accommodate virtually any length of model. The section model test set-up is shown in the wind tunnel in Figure A2 with the turbulence generating grid at the inlet to the test section. The frame structure is enclosed in an aerodynamic fairing system which minimizes the wall boundary layers and helps to ensure homogeneous flow conditions across the span of the model. The springing and dashpot system are shown in Figure A3. With this design, the model can be installed on the rig and calibrated outside of the wind tunnel, providing clear efficiencies in the test procedure. Both static and dynamic calibrations are performed on the model, ensuring that the modal mass and mass moment of inertia are as desired. A relationship between the dynamic deflection and the load cell output is obtained through this calibration, as well as a confirmation of the stiffness of the springing system.

A3 THE SECTION MODEL TEST AND ANALYSIS

The dynamic section model tests are usually comprised of a manual and automatic run. The manual run allows the wind tunnel operator to gradually increase the wind speed, while carefully noting any visual signs of instabilities and establishing a safe upper bound wind speed for the test. A set of wind speeds (~50) are selected and the test repeated under automatic control. Measurements include the time history of the vertical and torsional motions of the model as well as the wind speed. The time history is analyzed on-line and the instantaneous maximum, minimum, root-mean-square (RMS) and mean value is recorded. A Leiblein analysis of the peaks is also performed. This is repeated for each of the desired wind speeds. Additional wind speeds are set in the vicinity of any vortex shedding peaks in order to establish the response peak.

The presence of a vortex shedding peak or flutter instability is obvious from an examination of the response data. This type of instability is marked as a change in the response from a random motion to a sinusoidal motion. An examination of the “peak factor” (or the ratio of the peak to RMS value) clearly indicates this change. The peak factor for random motion is of the order of 3-4 while that for a pure sinusoid is $\sqrt{2}$.

The tests are performed both for uniform flow and for grid-generated turbulent flow conditions. The results in turbulent flow are often used in an analysis of Equivalent Static Loads, which effectively translate the results from the section model tests into effective loads which can be used for design [A6].

REFERENCES - APPENDIX A

A1. “Manual of Practice for Wind Tunnel Tests of Buildings and Structures”, American Society of Civil Engineers - Aerospace Division, New York, NY, June 1997.

A2. Hjorth-Hansen, E., "Section Model Tests", Proc. Aerodynamics of Large Bridges, Balkema, Rotterdam, 1992.

A3. Davenport, A.G. and Isyumov, N., "The Application of the Boundary Layer Wind Tunnel to the Prediction of Wind Loading", Proceedings of the Int. Res. Sem., N.R.C., Ottawa, Canada, September 1967, Vol. 1, Univ. of Toronto Press.

A4. Davenport, A.G. and King, J.P.C., "A Study of Wind Effects for the Sunshine Skyway Bridge, Tampa, Florida - Concrete Alternate", The University of Western Ontario, Faculty of Engineering Science Research Report, BLWT-SS24-1982, London, Ontario, Canada, 1982.

A5. Davenport, A.G. and King, J.P.C., "A Study of Wind Effects for the Sunshine Skyway Bridge, Tampa, Florida - Steel Alternate", The University of Western Ontario, Faculty of Engineering Science Research Report, BLWT-SS25-1982, The University of Western Ontario, London, Ontario, Canada, 1982.

A6. Davenport, A.G. and King, J.P.C., "Dynamic Wind Forces on Long Span Bridges", 12th IABSE Congress, Vancouver, Canada, September 1984.

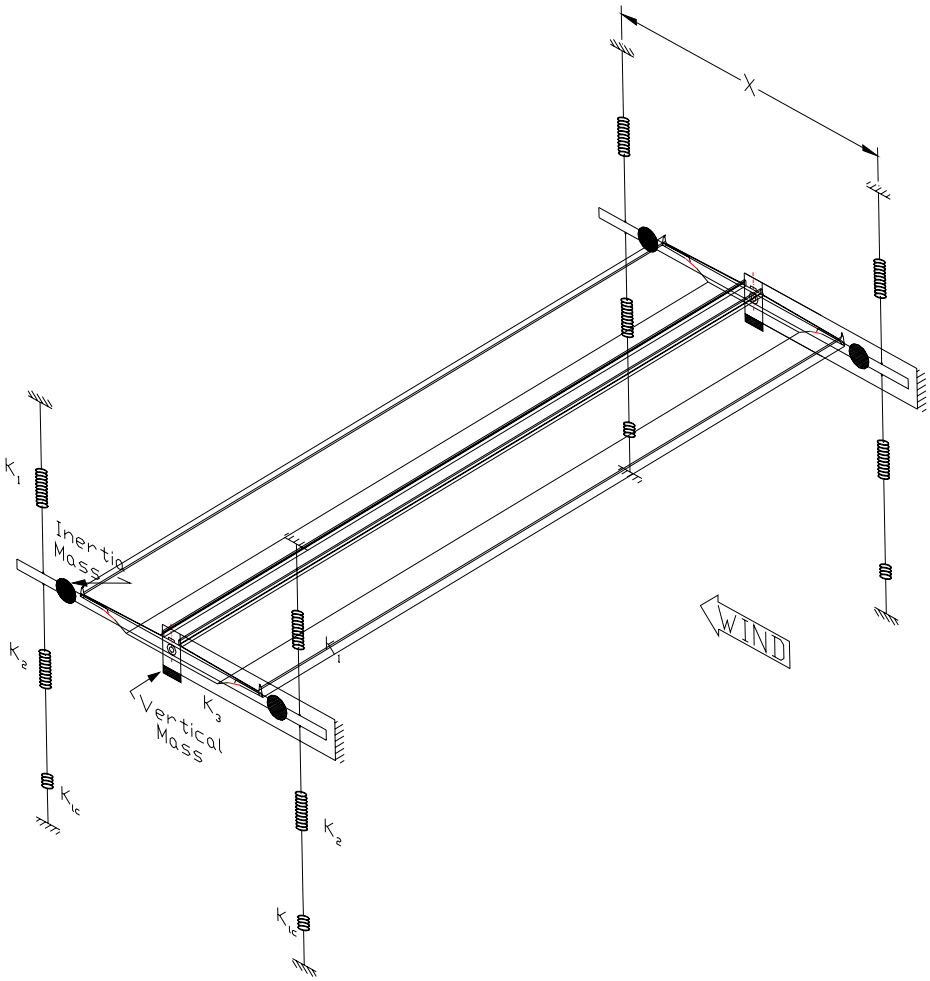

FIGURE A1 DYNAMIC SECTION MODEL RIG

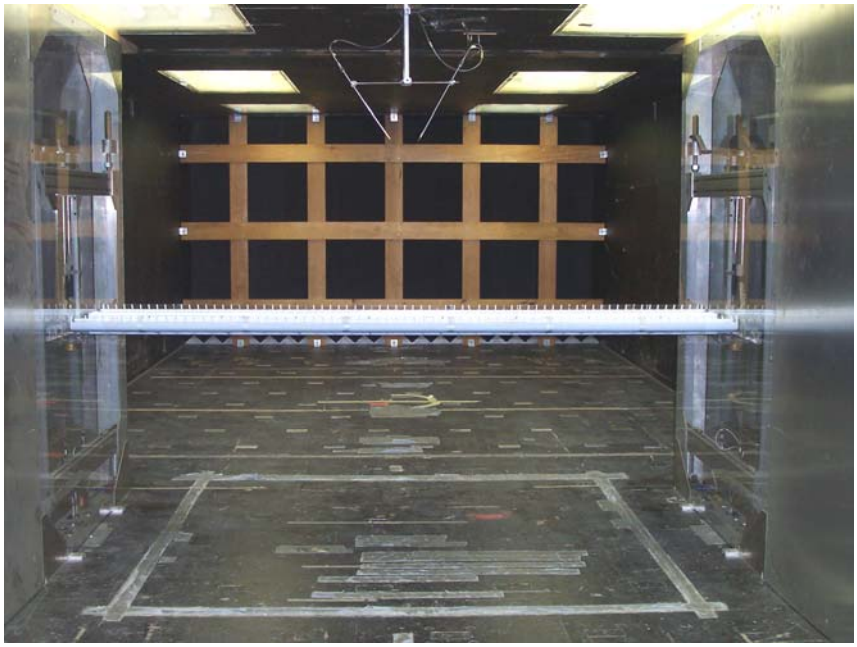

FIGURE A2 2.13m LONG DYNAMIC SECTION MODEL

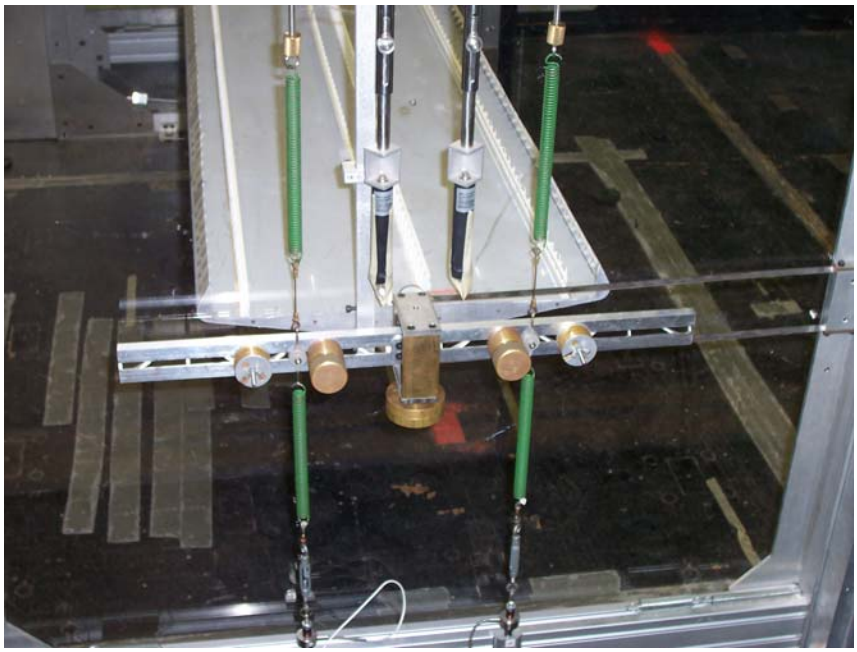

FIGURE A3 DETAILS OF DYNAMIC TEST RIG

APPENDIX B

RESULTS OF DYNAMIC SECTION MODEL TESTS – BRIDGE DECK

TABLE B1 RESULTS OF DYNAMIC SECTION MODEL TESTS

Indian River Inlet Bridge, Dynamic Section Model Test Result Summary, 0 Degree Angle of Attack

SECTION MODEL TESTING with initial frequencies, February 2004

					Prototype Properties				Vmax at deck height	Flutter instability	Vortex induced vibration
NO.	**Test**	**Flow**	**Damping**	**Walkway Location**	**Mass**	**MMI**	**fv**	**ft**	**mph**		
					Lb/ft	Lb-ft^2/ft	Hz	Hz			
1	EYT301	smooth	0.1% in lift & 0.26% in torsion	upstream	45619	3.42E+07	0.77	1.71	220	Not observed	Not observed
2	DYN101	smooth	0.5% in lift & torsion	upstream	45619	3.42E+07	0.77	1.71	202	Not observed	Not observed
3	EYT201	turbulent	0.1% in lift & 0.26% in torsion	upstream	45619	3.42E+07	0.77	1.71	219	Not observed	Not observed
4	DYT101	turbulent	0.5% in lift & torsion	upstream	45619	3.42E+07	0.77	1.71	218	Not observed	Not observed
5	EYN101	smooth	0.1% in lift & 0.26% in torsion	downstream	45619	3.42E+07	0.77	1.71	229	Not observed	Not observed
6	DYN301	smooth	0.5% in lift & torsion	downstream	45619	3.42E+07	0.77	1.71	219	Not observed	Not observed
7	EYT101	turbulent	0.1% in lift & 0.26% in torsion	downstream	45619	3.42E+07	0.77	1.71	226	Not observed	Not observed
8	DYT102	turbulent	0.5% in lift & torsion	downstream	45619	3.42E+07	0.77	1.71	218	Not observed	Not observed

SECTION MODEL TESTING with modified frequencies, June 2004

					Prototype Properties				Vmax at deck height	Flutter instability	Vortex induced vibration
NO.	**Test**	**Flow**	**Damping**	**Walkway Location**	**Mass**	**MMI**	**fv**	**ft**	**mph**		
					Lb/ft	Lb-ft^2/ft	Hz	Hz			
1	PWU101	smooth	0.13% in lift & 0.6% in torsion	upstream	45619	3.42E+07	0.73	0.87	231	Not observed	Not observed
2	PWD101	smooth	0.13% in lift & 0.6% in torsion	downstream	45619	3.42E+07	0.73	0.87	230	Not observed	Not observed
3	PWD201	turbulent	0.5% in lift & 0.6% in torsion	downstream	45619	3.42E+07	0.73	0.87	239	Not observed	Not observed
4	PWU201	turbulent	0.5% in lift & 0.6% in torsion	upstream	45619	3.42E+07	0.73	0.87	239	Not observed	Not observed

units = imperial
Data File = eyt301.mst
Information File = eyt301.inf
Feb. 26, 2004

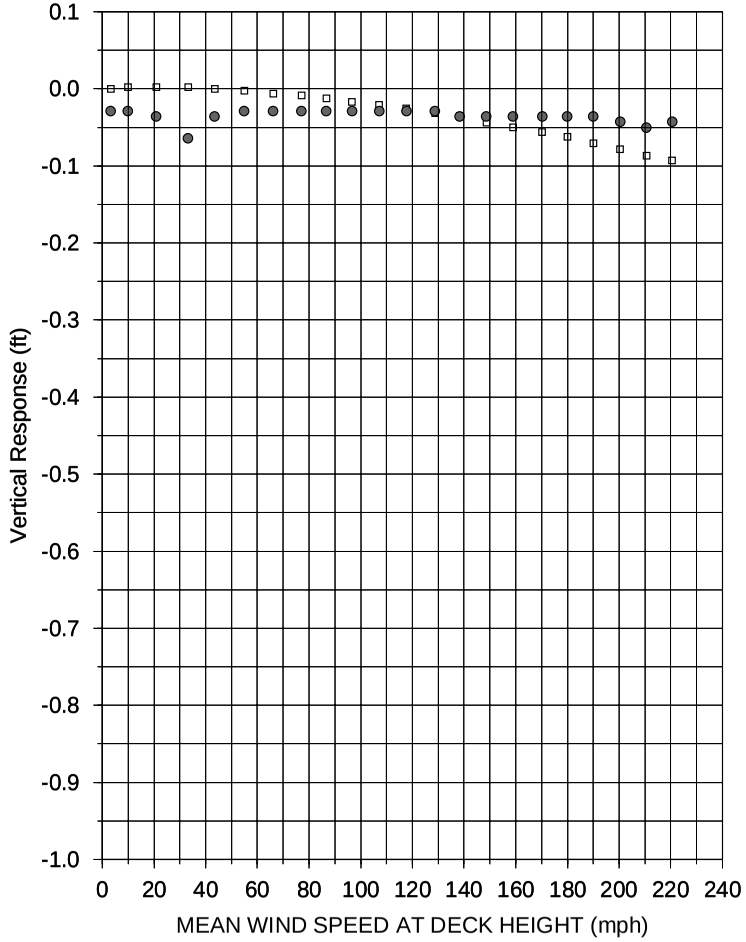

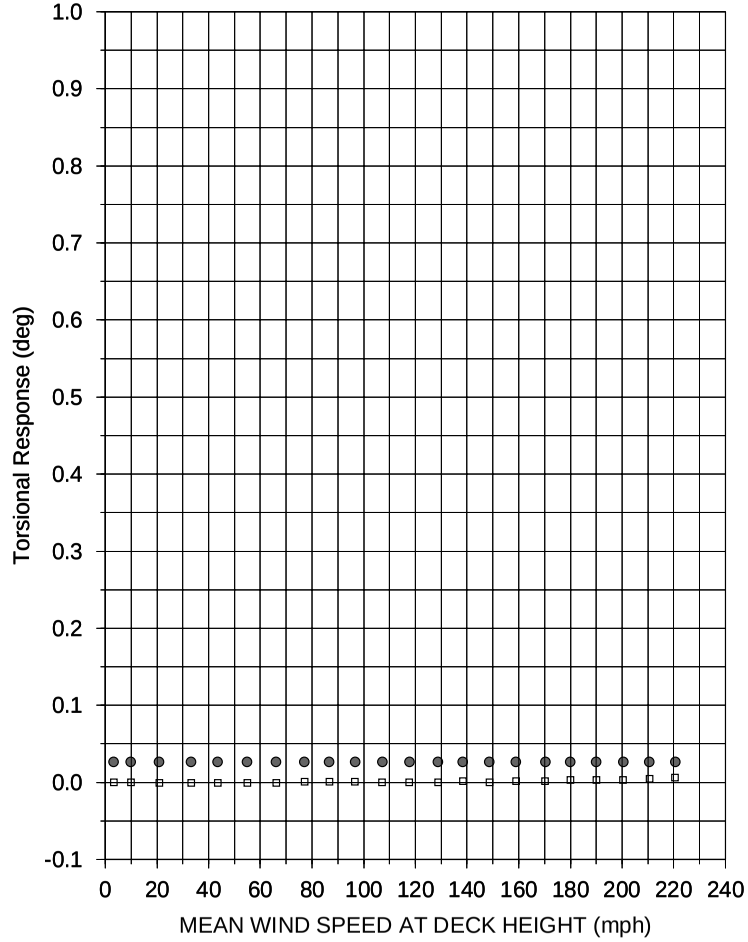

Indian River Bridge, Sidewalk Upstream, Smooth Flow, Low Damping

units = imperial
Data File = dyn101.mst
Information File = dyn101.inf
Feb. 26, 2004

MEAN
PEAK (RMS * 3.5)

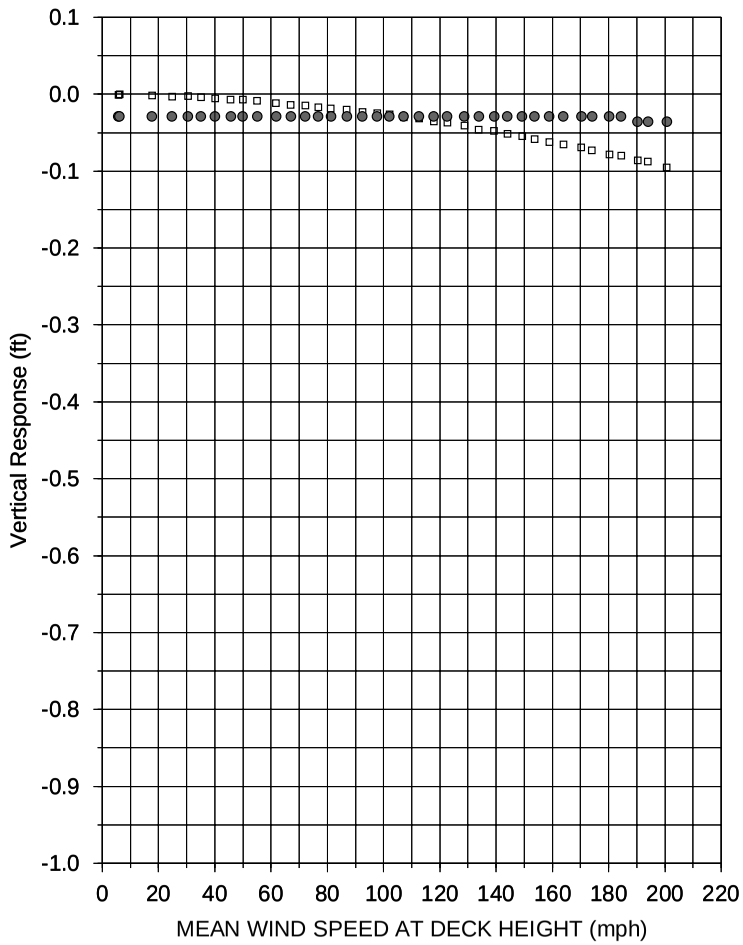

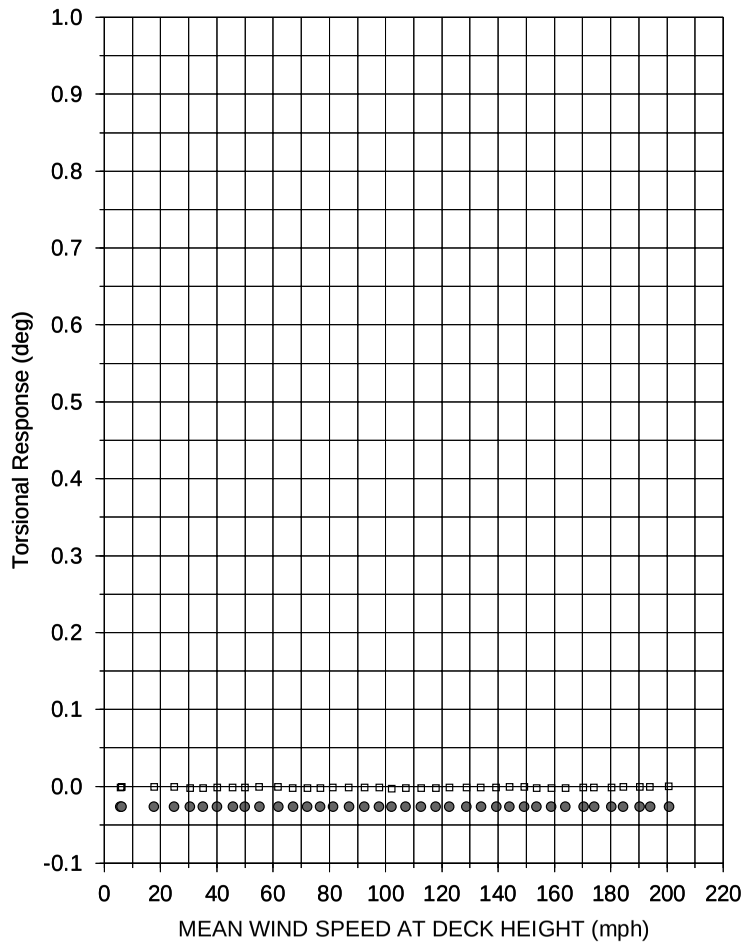

Indian River Bridge, Sidewalk Upstream, Smooth Flow, Damping=0.5%

units = imperial
Data File = eyt201.mst
Information File = eyt201.inf
Feb. 26, 2004

MEAN
PEAK (RMS * 3.5)

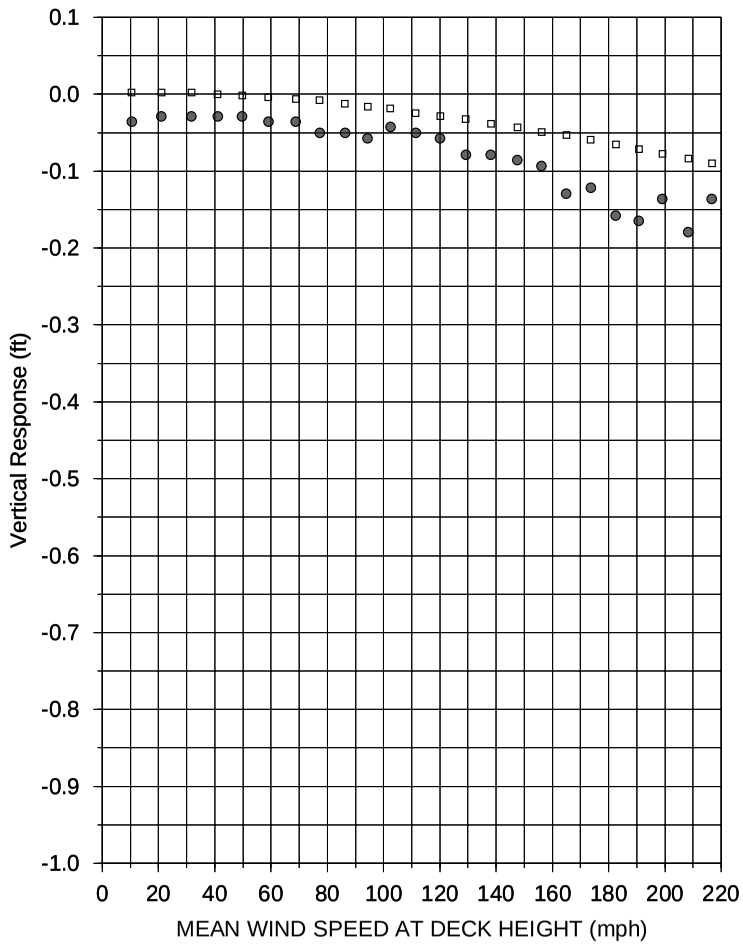

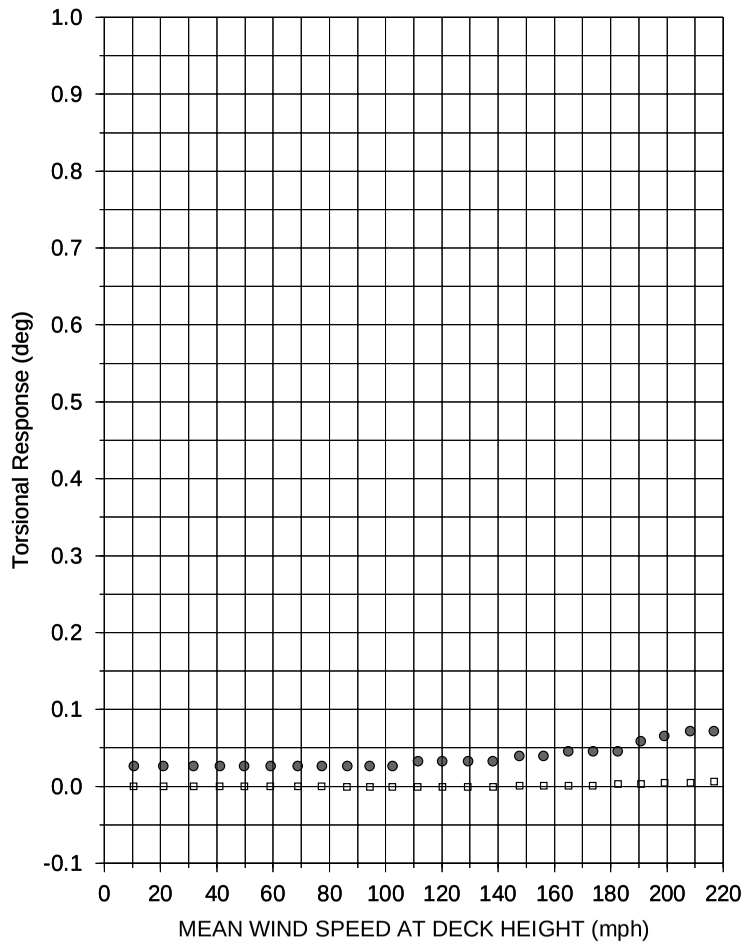

Indian River Bridge, Sidewalk Upstream, Turb. Flow, Low Damping

units = imperial
Data File = dyt101.mst
Information File = dyt101.inf
Feb. 26, 2004

MEAN
PEAK (RMS * 3.5)

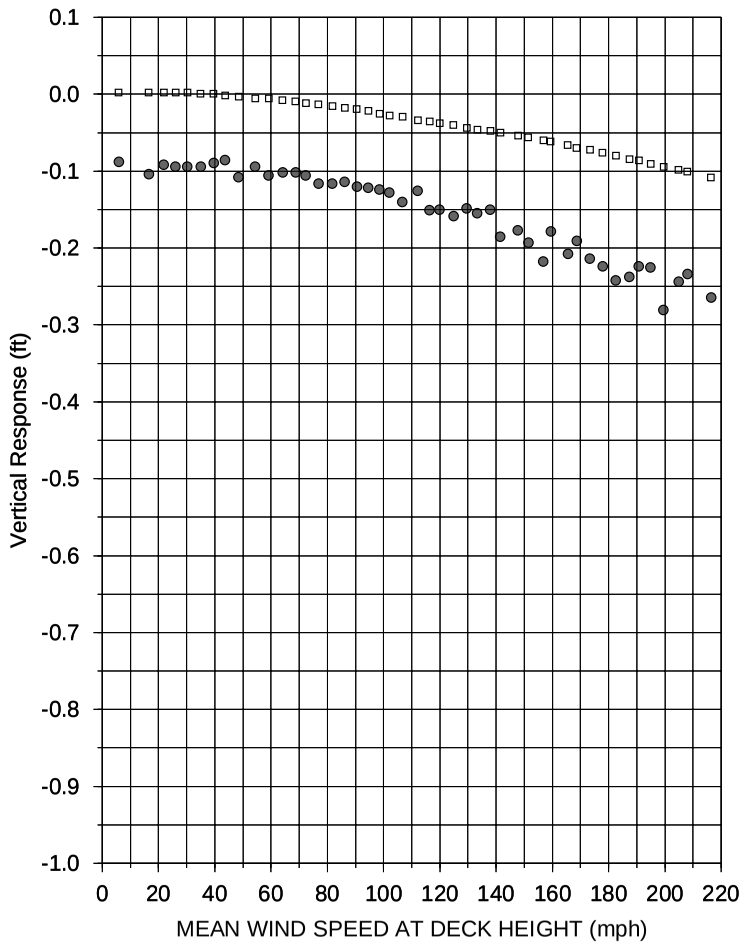

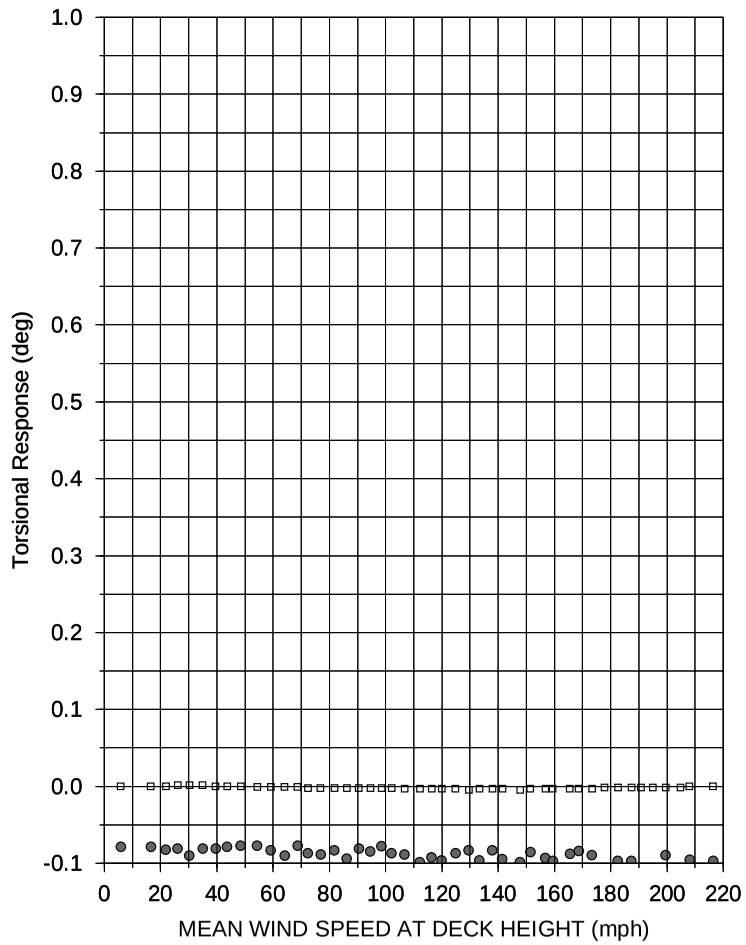

Indian River Bridge, Sidewalk Upstream, Turb. Flow, Damping=0.5%

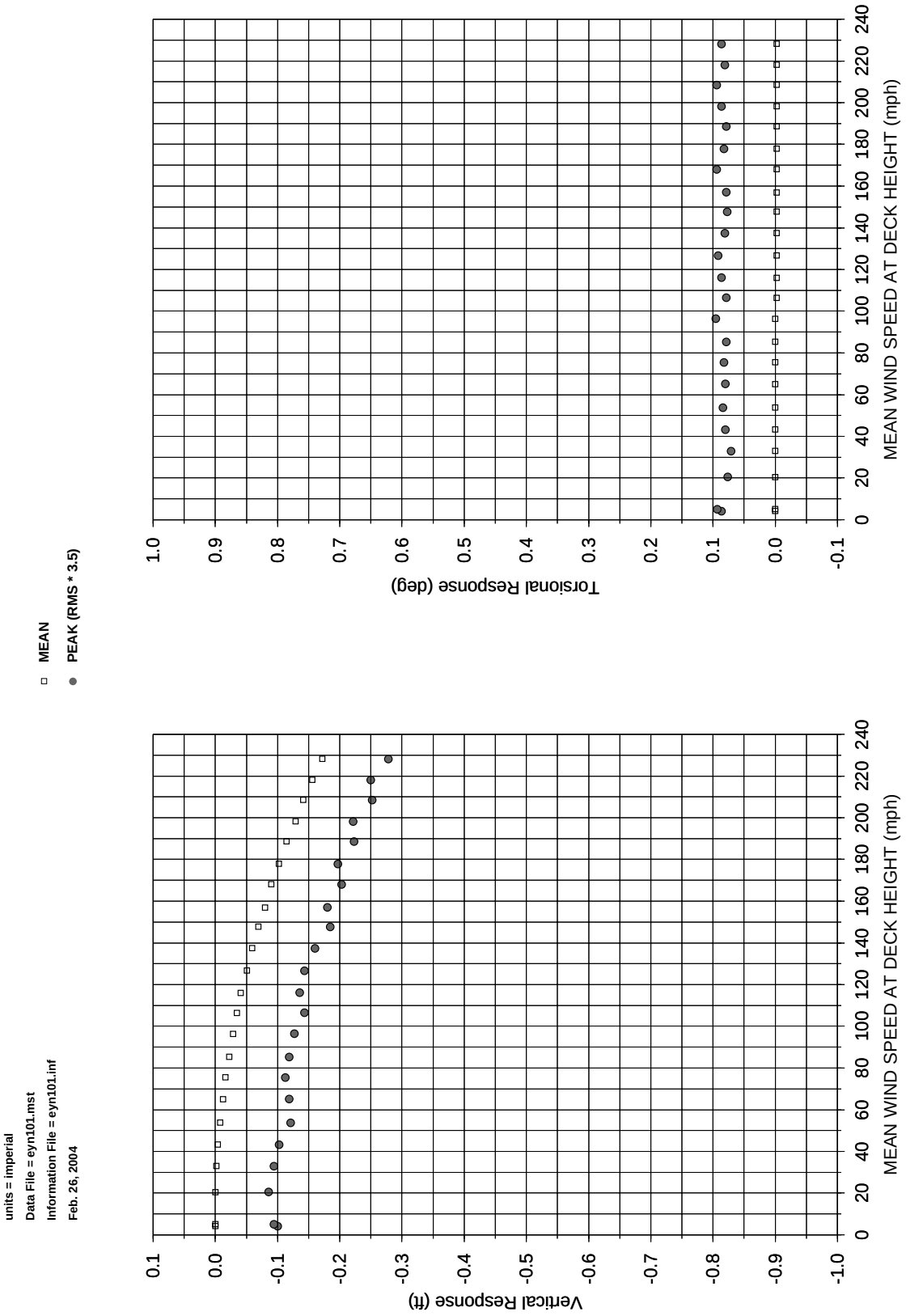

Indian River Bridge, Sidewalk Downstream, Smooth Flow, Low Damping

units = imperial
Data File = dyn301.mst
Information File = dyn301.inf
Feb. 26, 2004

MEAN
PEAK (RMS * 3.5)

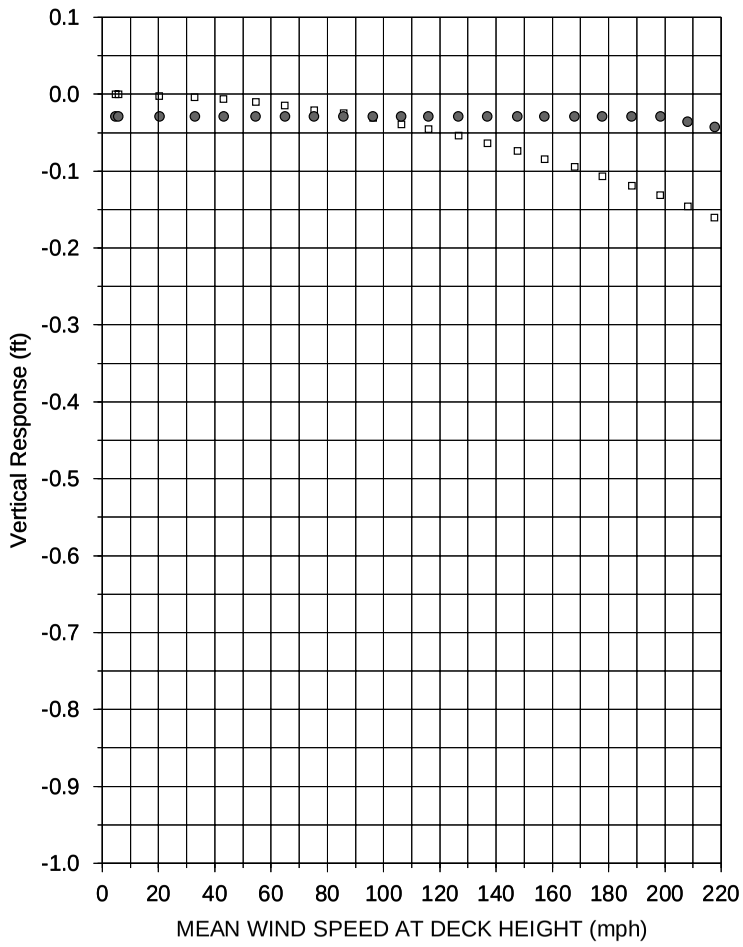

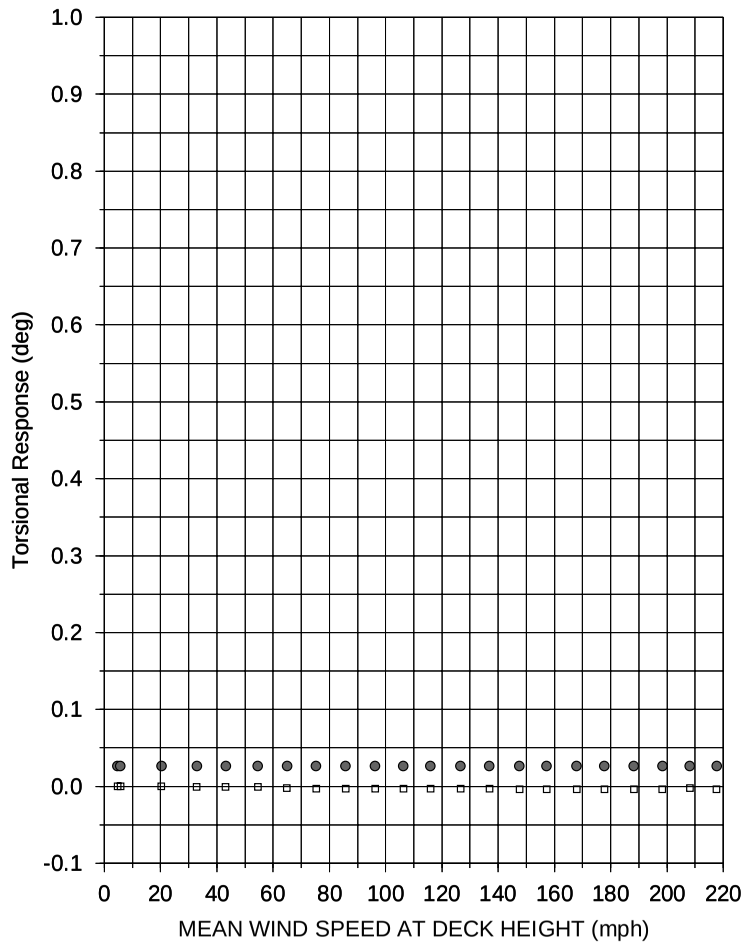

Indian River Bridge, Sidewalk Downstream, Smooth Flow, Damping=0.5%

units = imperial
Data File = eyt101.mst
Information File = eyt101.inf
Feb. 26, 2004

MEAN
PEAK (RMS * 3.5)

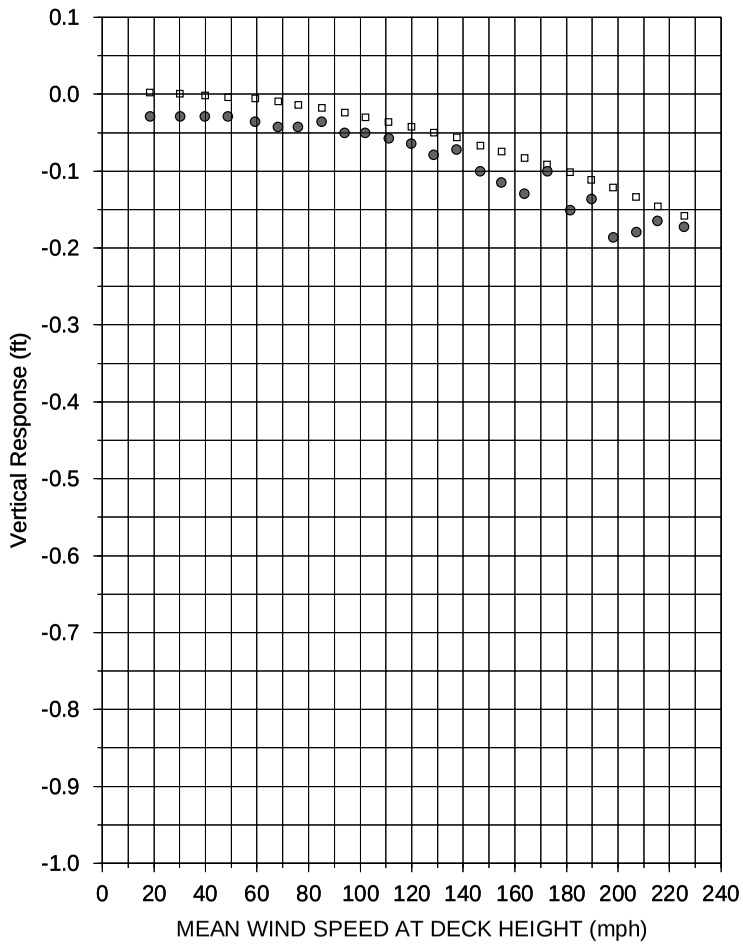

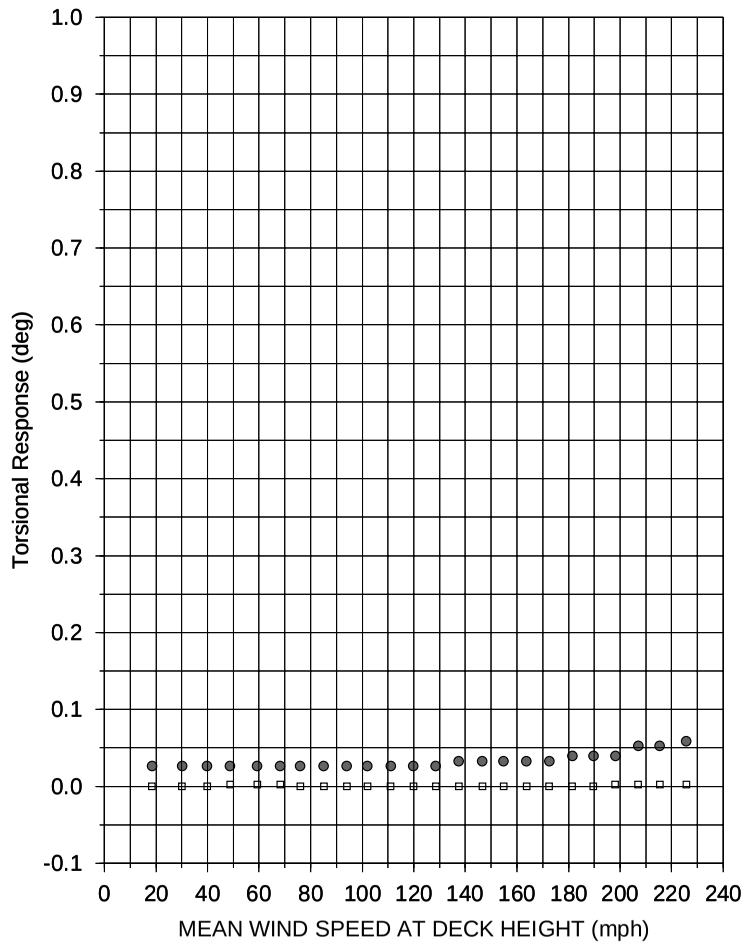

Indian River Bridge, Sidewalk Downstream, Turb. Flow, Low Damping

units = imperial
Data File = dyt102.mst
Information File = dyt102.inf
Feb. 26, 2004

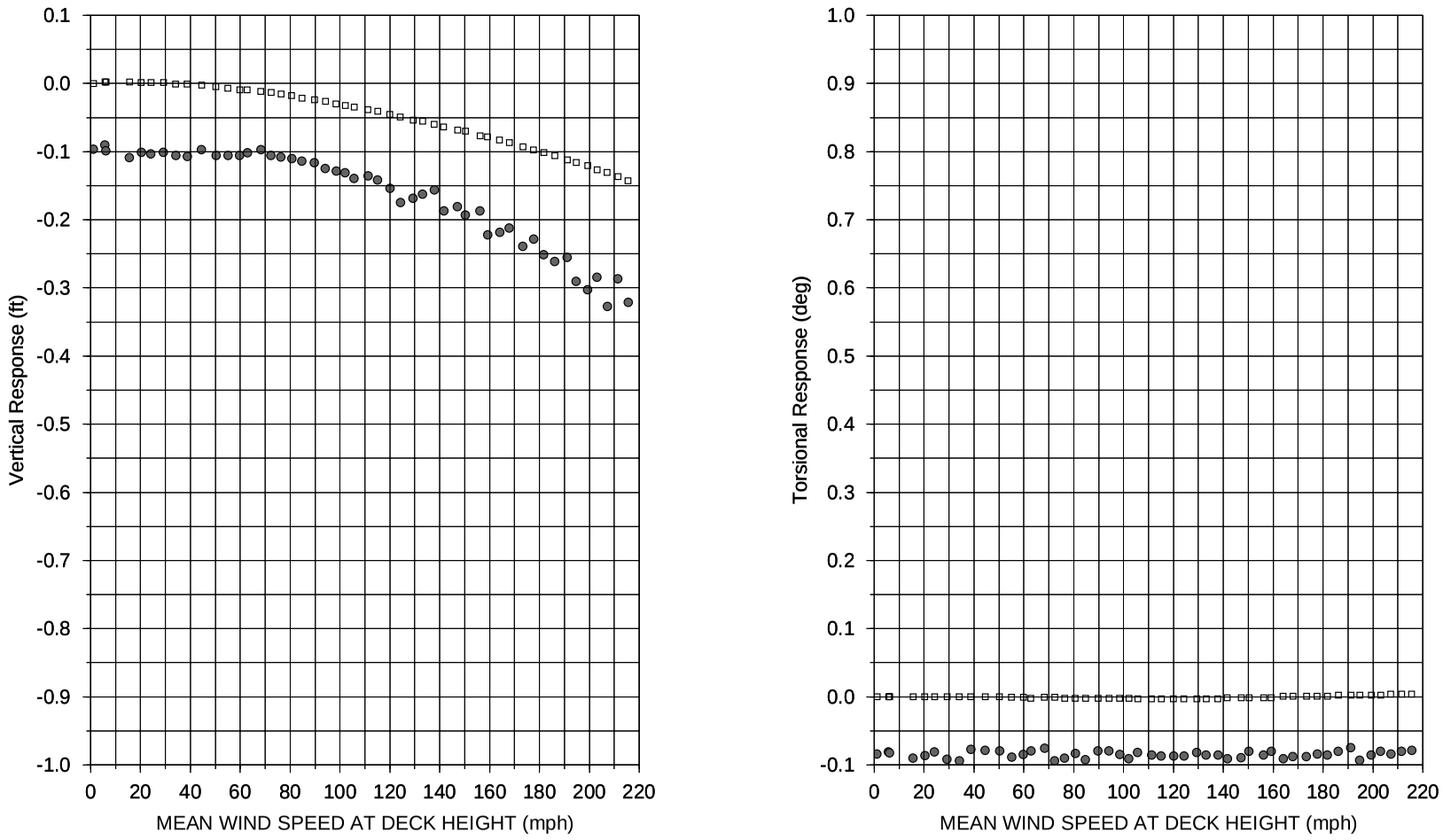

Indian River Bridge, Sidewalk Downstream, Turb. Flow, Damping=0.5%

units = imperial
Data File = pwu101.mst
Information File = pwu101.inf
Jan. 31, 2005

MEAN
PEAK (RMS * 3.5)

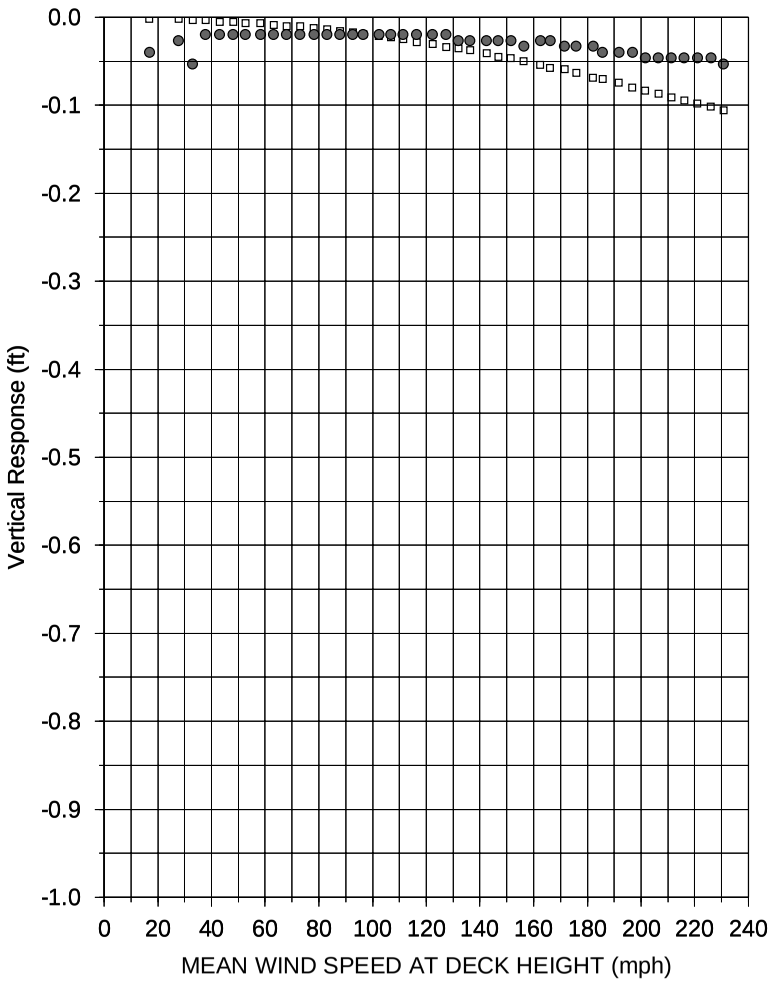

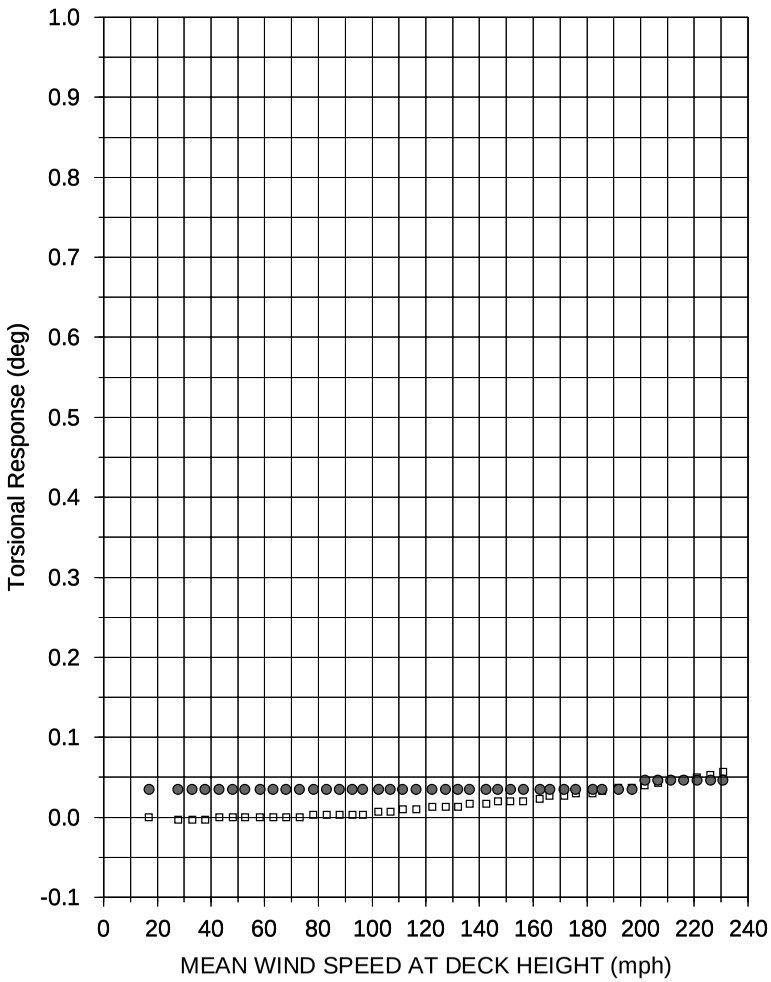

IRIB - Revised Properties, Sidewalk Upstream, Smooth Flow, Low Damping

units = imperial
Data File = pwd101.mst
Information File = pwd101.inf
Jan. 31, 2005

MEAN
PEAK (RMS * 3.5)

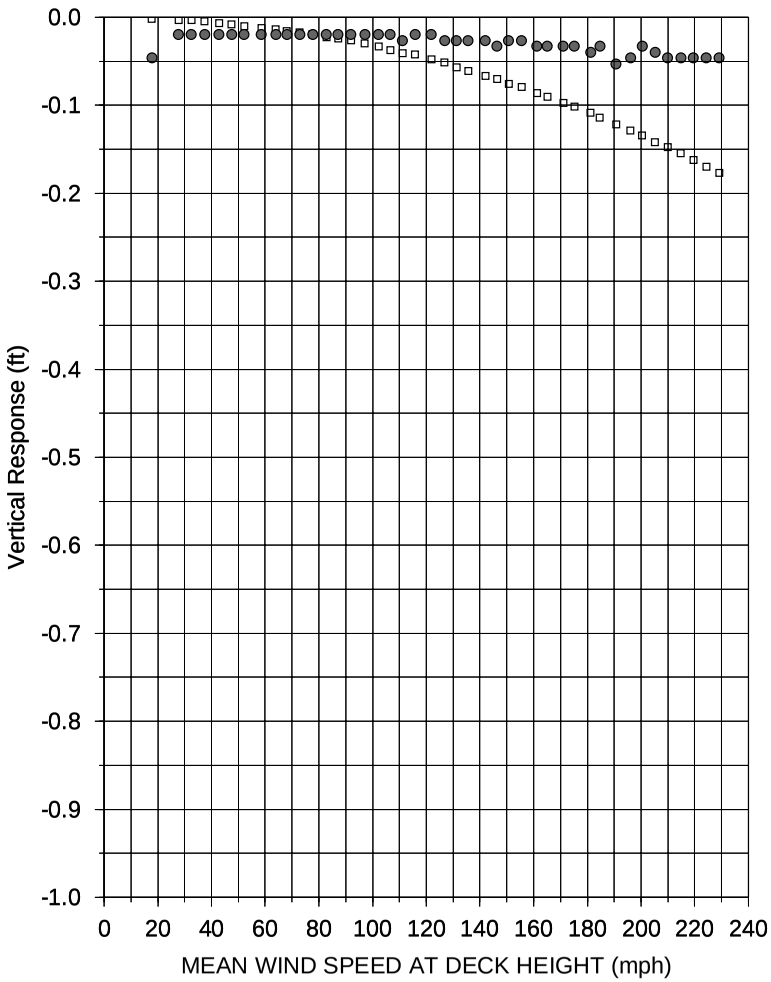

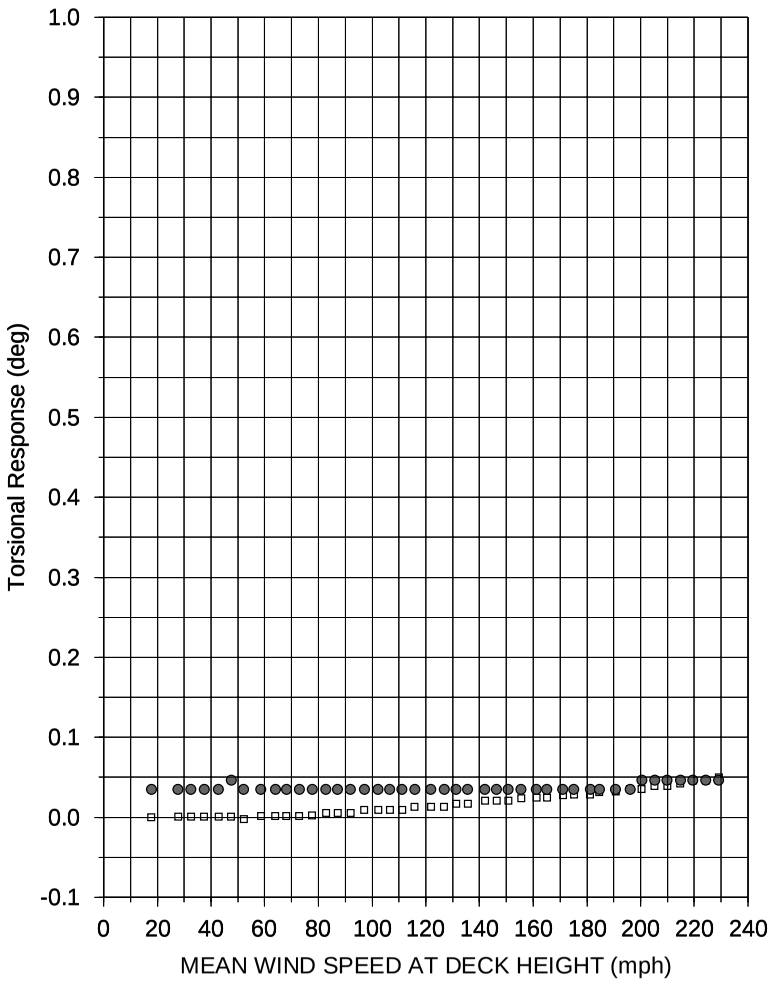

IRIB - Revised Properties, Sidewalk Downstream, Smooth Flow, Low Damping

units = imperial
Data File = pwd201.mst
Information File = pwd201.inf
Jan. 31, 2005

MEAN
PEAK (RMS * 3.5)

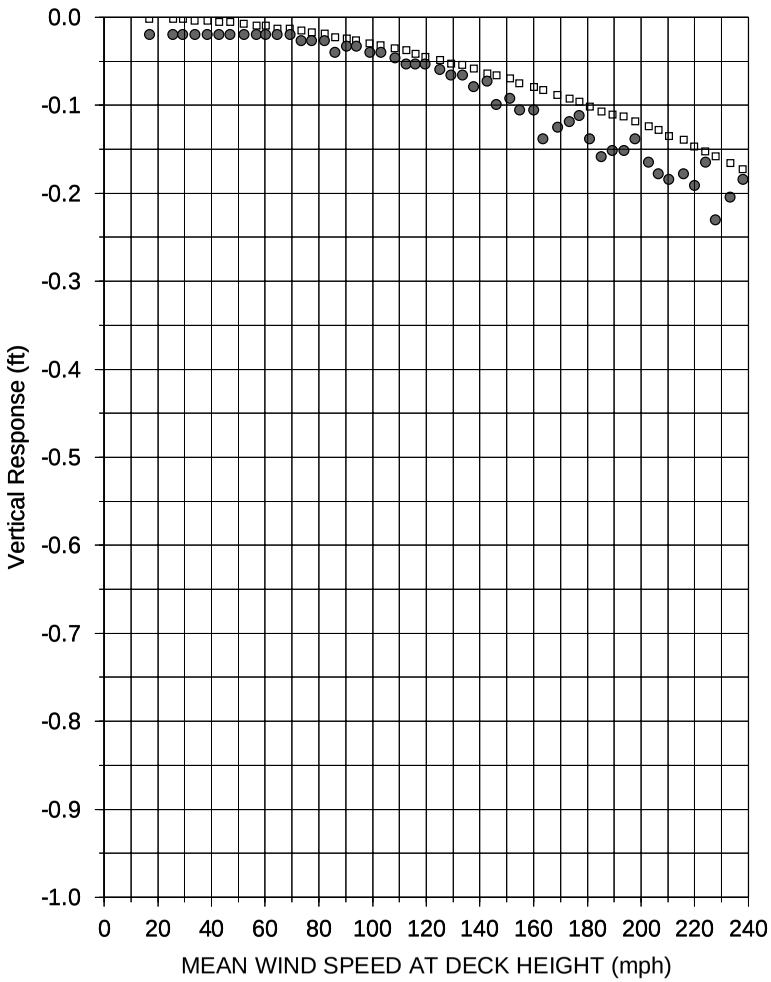

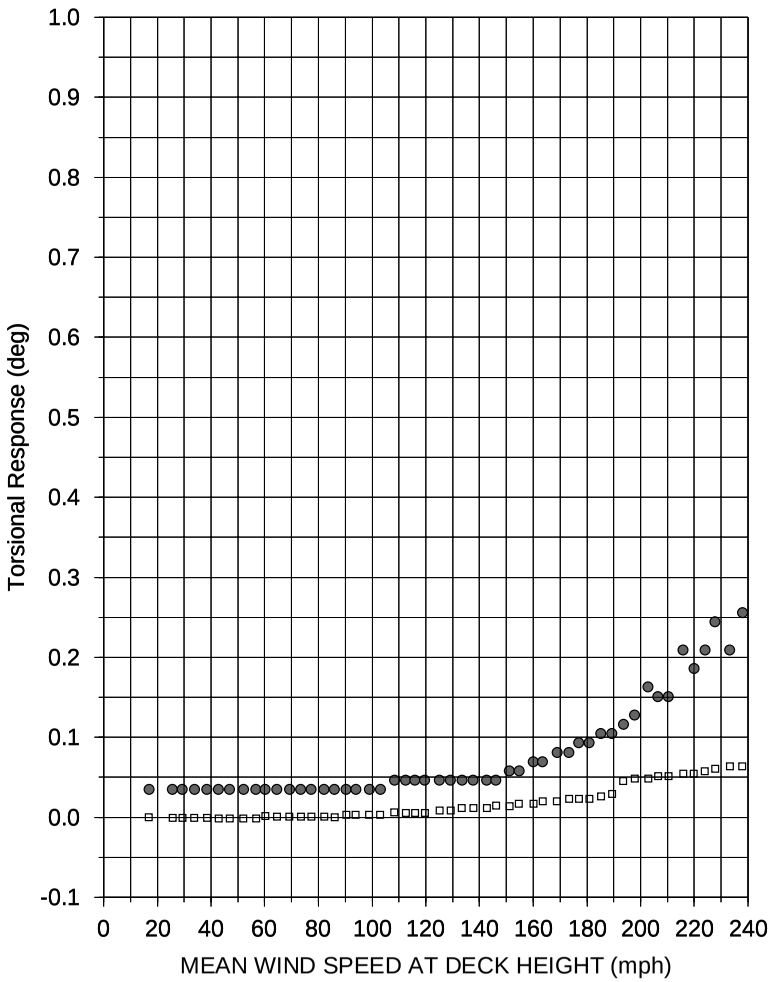

IRIB - Revised Properties, Sidewalk Downstream, Turb Flow, 0.5% Damping

units = imperial
Data File = pwu201.mst
Information File = pwu201.inf
Jan. 31, 2005

MEAN
PEAK (RMS * 3.5)

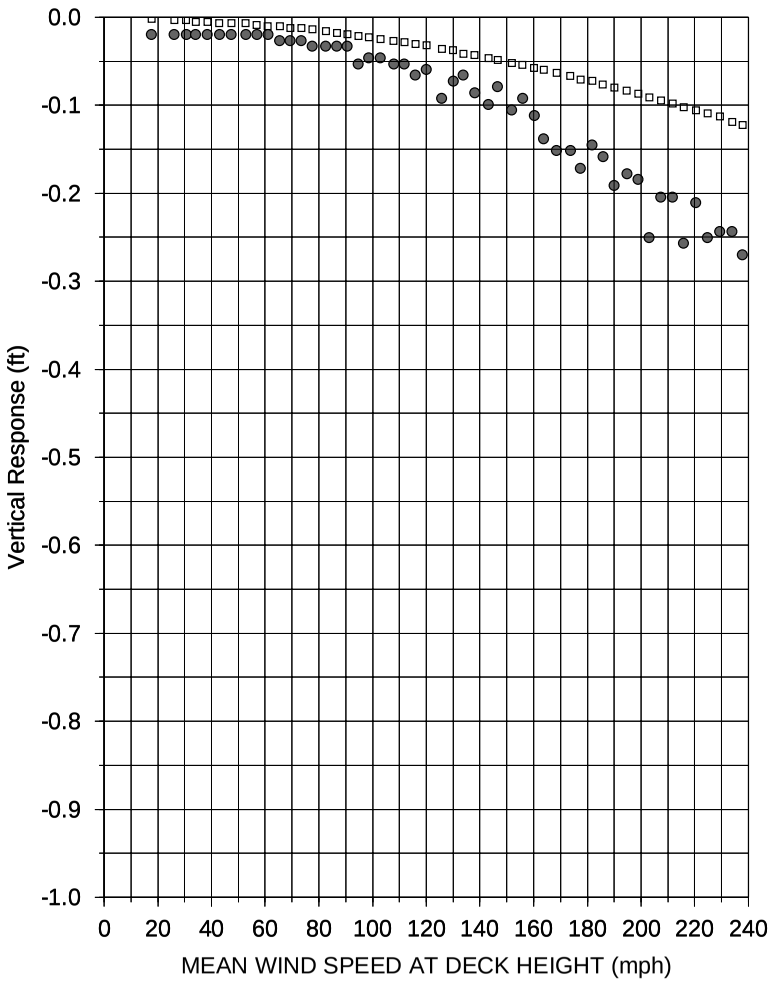

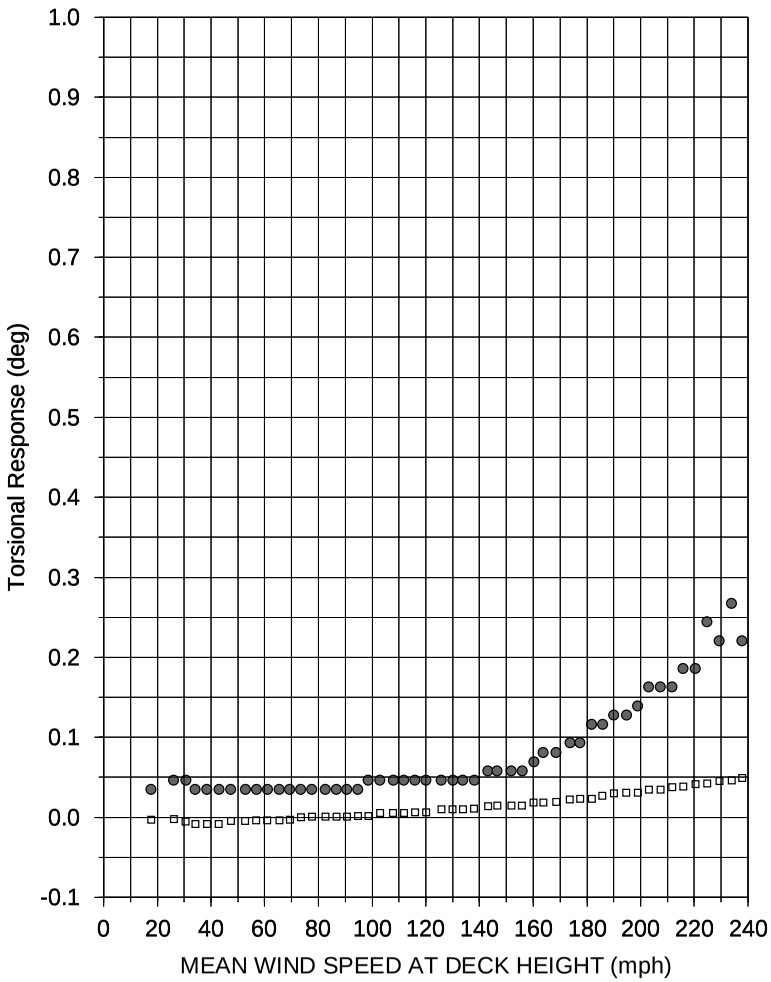

IRIB - Revised Properties, Sidewalk Upstream, Turb Flow, 0.5% Damping

APPENDIX C

RESULTS OF STATIC SECTION MODEL TESTS – BRIDGE DECK

TABLE C1 INDIAN RIVER - SIDEWALK UPSTREAM, SMOOTH FLOW

Angle of Attack	Cx	Cz	Cm
-12	0.058	-1.185	-0.141
-11	0.048	-1.188	-0.153
-10	0.031	-1.235	-0.178
-9	0.011	-1.281	-0.209
-8	-0.013	-1.324	-0.250
-7	-0.010	-1.234	-0.243
-6	0.004	-1.102	-0.214
-5	0.019	-0.969	-0.178
-4	0.031	-0.827	-0.139
-3	0.047	-0.686	-0.099
-2	0.059	-0.545	-0.062
-1	0.068	-0.404	-0.025
0	0.072	-0.258	0.010
1	0.073	-0.117	0.041
2	0.073	0.039	0.071
3	0.072	0.201	0.091
4	0.074	0.309	0.097
5	0.078	0.373	0.098
6	0.082	0.406	0.099
7	0.085	0.428	0.101
8	0.088	0.442	0.102
9	0.092	0.474	0.105
10	0.095	0.550	0.113
11	0.098	0.579	0.117
12	0.101	0.598	0.120

Slope of Cz Curve = 8.34
Slope of Cm Curve = 1.91
Cz at 0° = -0.258
Cx at 0° = 0.072
Cm at 0° = 0.010

TABLE C2 INDIAN RIVER - SIDEWALK UPSTREAM, TURBULENT FLOW

Angle of Attack	Cx	Cz	Cm
-12	0.005	-1.449	-0.231
-11	-0.008	-1.459	-0.251
-10	-0.020	-1.452	-0.271
-9	-0.023	-1.401	-0.276
-8	-0.016	-1.312	-0.263
-7	-0.005	-1.203	-0.240
-6	0.007	-1.081	-0.209
-5	0.019	-0.953	-0.174
-4	0.033	-0.823	-0.138
-3	0.047	-0.682	-0.100
-2	0.060	-0.547	-0.064
-1	0.069	-0.415	-0.029
0	0.075	-0.279	0.005
1	0.078	-0.148	0.037
2	0.081	-0.020	0.067
3	0.082	0.113	0.094
4	0.081	0.244	0.116
5	0.079	0.360	0.128
6	0.079	0.455	0.134
7	0.079	0.520	0.135
8	0.081	0.561	0.133
9	0.083	0.585	0.131
10	0.085	0.599	0.128
11	0.087	0.604	0.126
12	0.089	0.612	0.124

Slope of Cz Curve = 7.57
Slope of Cm Curve = 1.87
Cz at 0° = -0.279
Cx at 0° = 0.075
Cm at 0° = 0.005

TABLE C3 INDIAN RIVER - SIDEWALK DOWNSTREAM, SMOOTH FLOW

Angle of Attack	Cx	Cz	Cm
-12	-0.151	-1.546	-0.222
-11	-0.135	-1.473	-0.209
-10	-0.108	-1.388	-0.191
-9	-0.081	-1.300	-0.171
-8	-0.055	-1.206	-0.151
-7	-0.029	-1.111	-0.130
-6	-0.006	-1.014	-0.109
-5	0.015	-0.914	-0.087
-4	0.033	-0.813	-0.067
-3	0.048	-0.702	-0.045
-2	0.061	-0.586	-0.023
-1	0.070	-0.475	-0.004
0	0.076	-0.362	0.015
1	0.079	-0.248	0.033
2	0.081	-0.136	0.048
3	0.081	-0.020	0.061
4	0.080	0.089	0.069
5	0.079	0.192	0.073
6	0.078	0.281	0.072
7	0.078	0.351	0.070
8	0.078	0.397	0.067
9	0.079	0.426	0.064
10	0.079	0.443	0.060
11	0.080	0.461	0.057
12	0.080	0.473	0.055

Slope of Cz Curve = 6.46
Slope of Cm Curve = 1.02
Cz at 0° = -0.362
Cx at 0° = 0.076
Cm at 0° = 0.015

TABLE C4 INDIAN RIVER - SIDEWALK DOWNSTREAM, TURBULENT FLOW

Angle of Attack	Cx	Cz	Cm
-12	-0.154	-1.517	-0.224
-11	-0.138	-1.473	-0.214
-10	-0.112	-1.403	-0.198
-9	-0.086	-1.328	-0.180
-8	-0.060	-1.245	-0.160
-7	-0.036	-1.156	-0.138
-6	-0.012	-1.060	-0.116
-5	0.010	-0.962	-0.094
-4	0.029	-0.860	-0.072
-3	0.046	-0.748	-0.050
-2	0.059	-0.633	-0.029
-1	0.068	-0.515	-0.008
0	0.075	-0.396	0.012
1	0.078	-0.273	0.030
2	0.078	-0.144	0.043
3	0.076	-0.002	0.050
4	0.075	0.105	0.048
5	0.077	0.184	0.046
6	0.079	0.235	0.045
7	0.082	0.267	0.045
8	0.084	0.302	0.046
9	0.085	0.371	0.048
10	0.087	0.373	0.051
11	0.092	0.333	0.054
12	0.093	0.342	0.056

Slope of Cz Curve = 6.99
Slope of Cm Curve = 1.04
Cz at 0° = -0.396
Cx at 0° = 0.075
Cm at 0° = 0.012

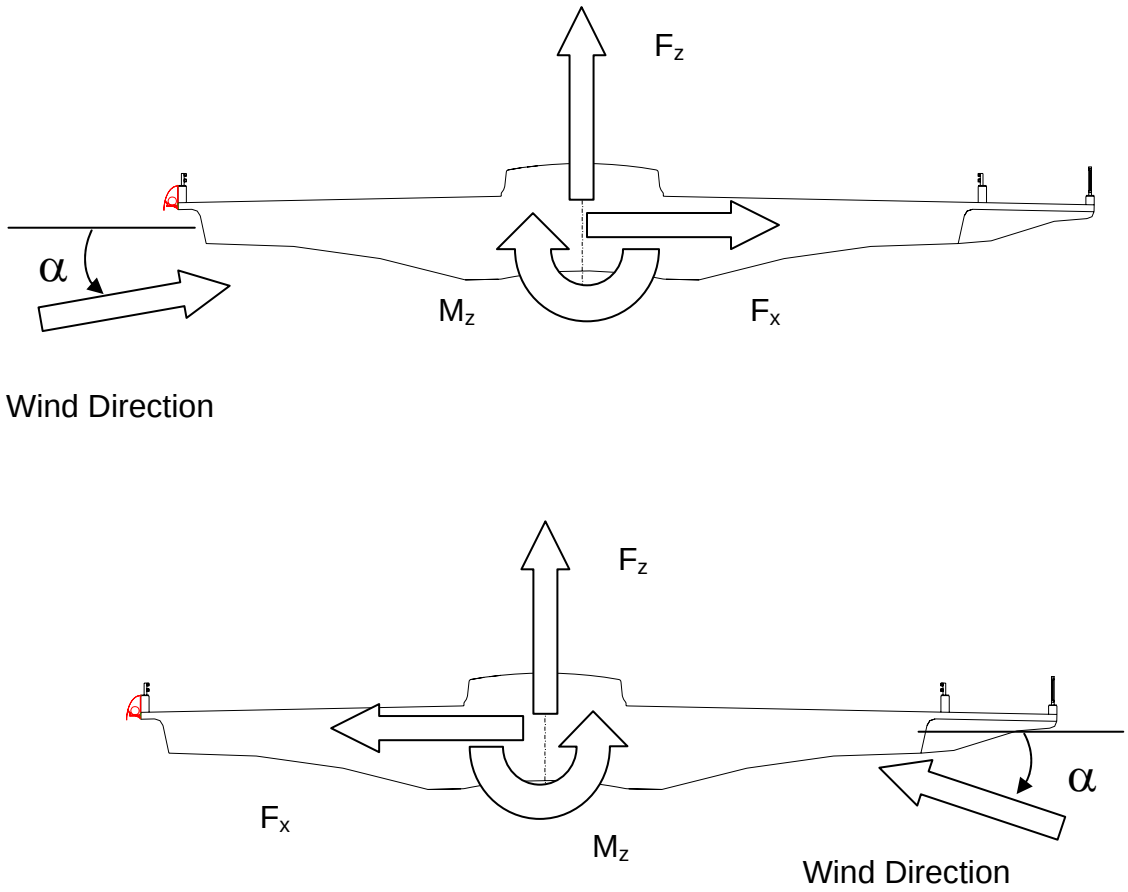

FIGURE C1 SKETCH SHOWING SIGN CONVENTION OF FORCES

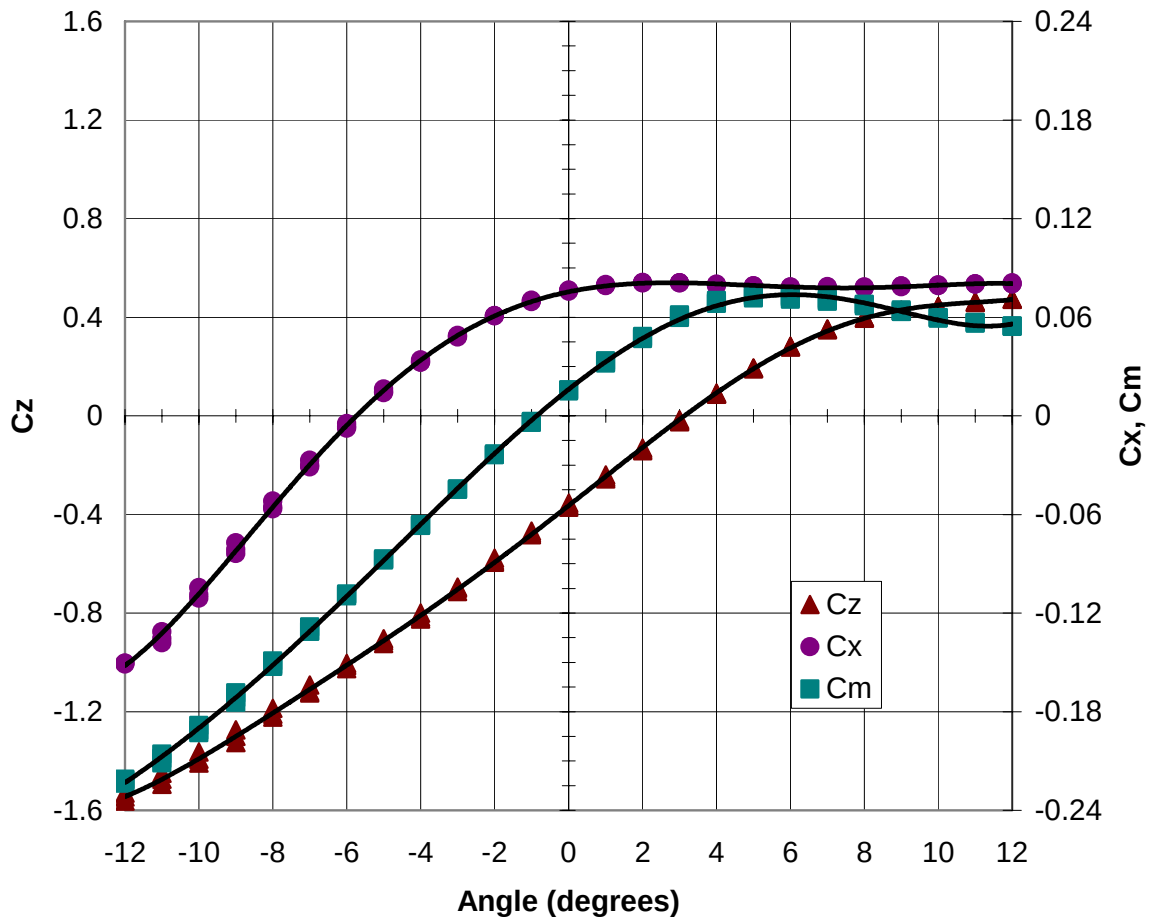

Indian River - Sidewalk Downstream, Smooth Flow

FIGURE C2 SIDEWALK DOWNSTREAM, SMOOTH FLOW

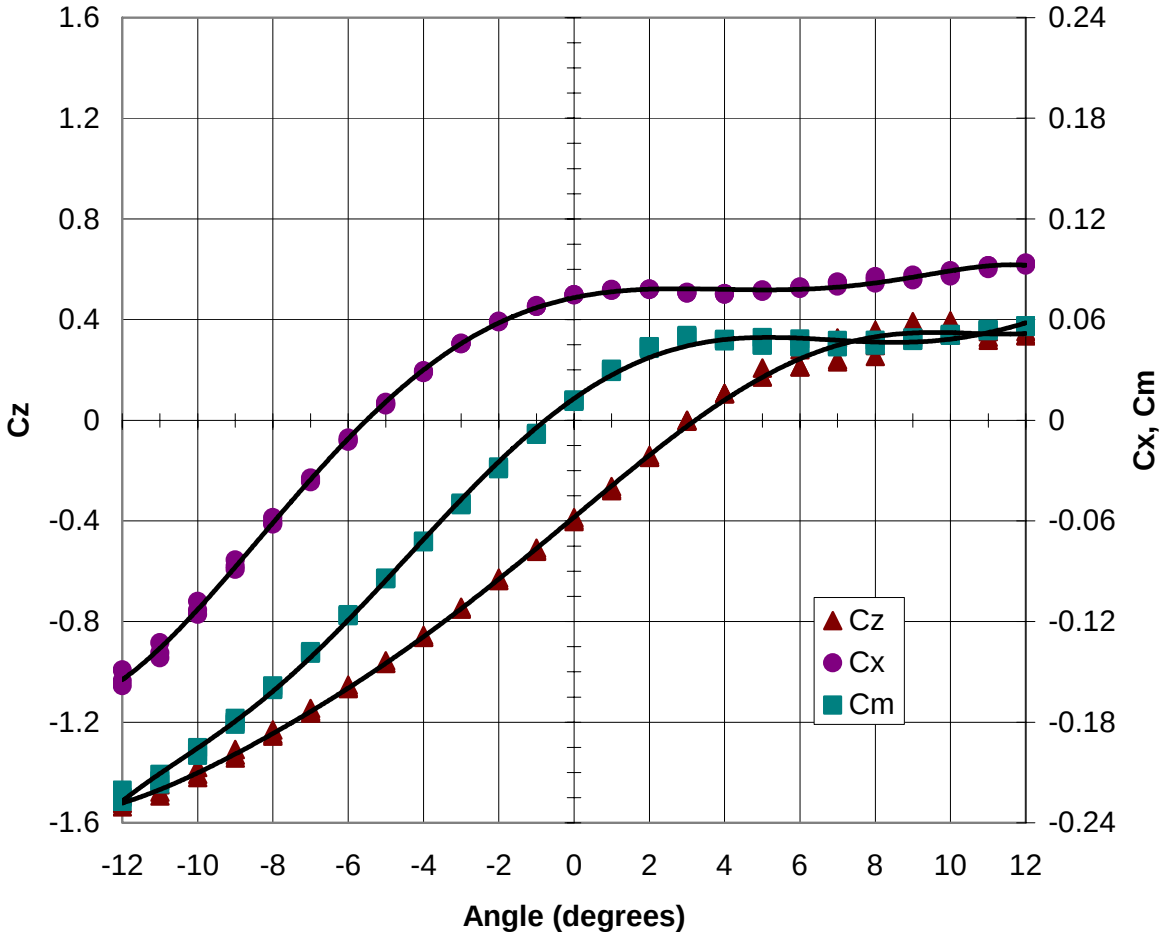

Indian River - Sidewalk Downstream, Turbulent Flow

FIGURE C3 SIDEWALK DOWNSTREAM, TURBULENT FLOW

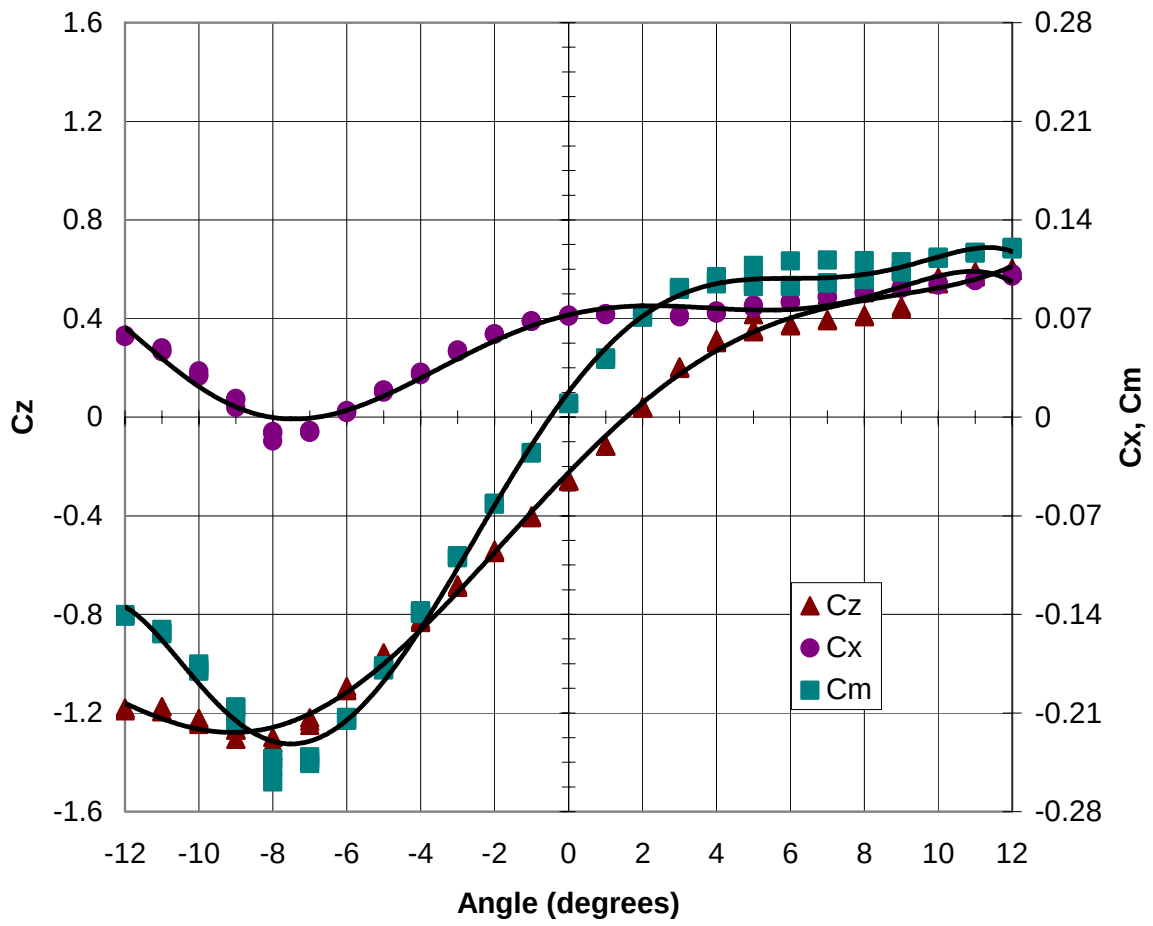

Indian River - Sidewalk Upstream, Smooth Flow

FIGURE C4 SIDEWALK UPSTREAM, SMOOTH FLOW

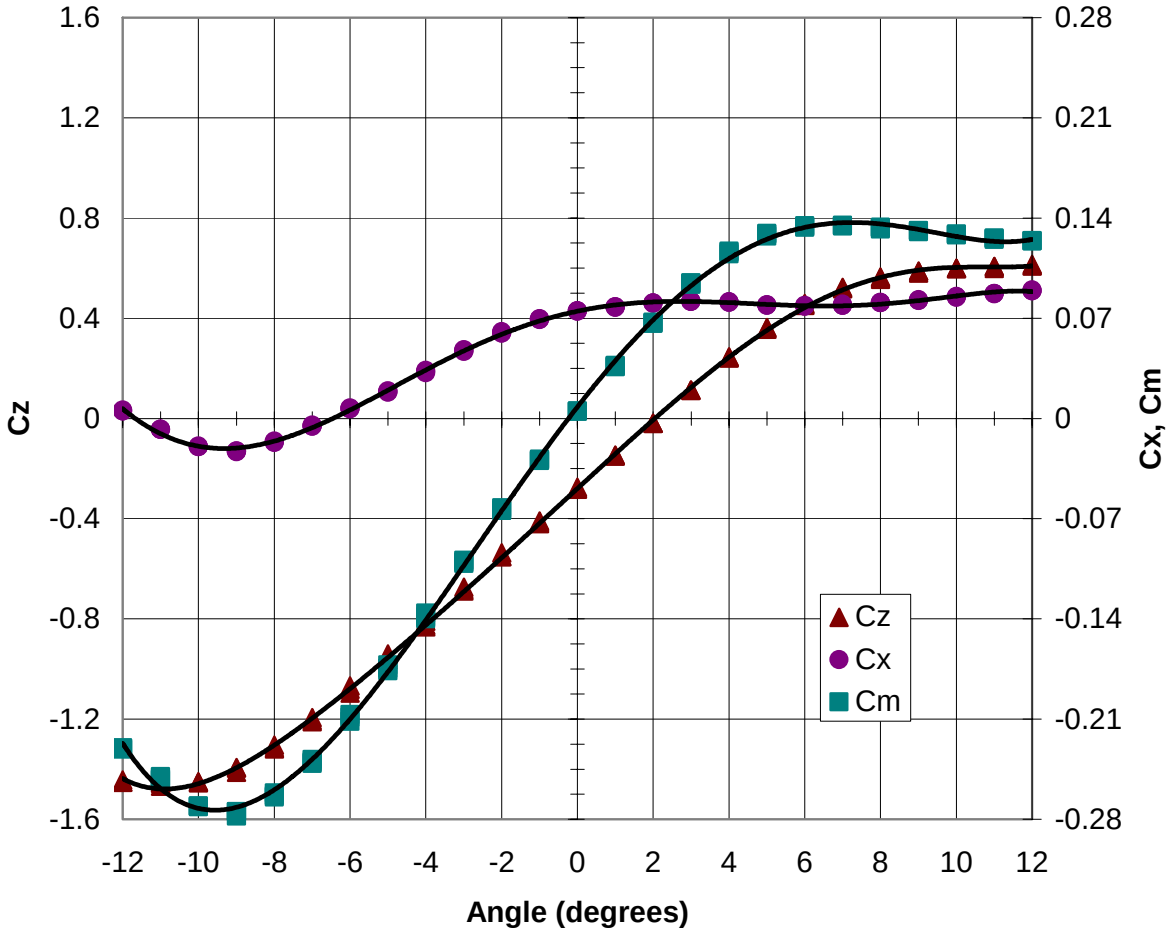

Indian River - Sidewalk Upstream, Turbulent Flow

FIGURE C5 SIDEWALK UPSTREAM, TURBULENT FLOW

APPENDIX D

FLUTTER INSTABILITY CRITERIA

The definition of “flutter” used in this report is related to the “peak factor”, which is defined as the ratio of the largest observed reading during the sample period to the Root Mean Square (RMS) of the sample. Each of the data points on the response plots result from the measurements of real, stable, limited amplitude motion as opposed to a negative total damping case where the amplitude continues to grow in magnitude for the same wind speed. The peak factor can be used to see whether the motion is in a “locked-in” state of sinusoidal motion or only a random type motion.

The onset of a “flutter instability” is defined as when the character of the response changes from a random type motion to that of a regular, sinusoidal motion, involving either pure torsional or a coupled vertical-torsional vibration. This can be clearly identified through an examination of the peak factor. A random signal has peak factors in the 3-4 range, while a sinusoid has a peak factor of $\sqrt{2}$ or 1.41. For the purposes of this investigation, a peak factor of less than 2 was selected as the governing criteria.

There are other definitions of flutter that have been used by this Laboratory and other researchers. One could determine a limiting amplitude beyond which the response is unacceptable. This criterion was used for the Tsing Ma Bridge [D1] and Ting Kau Bridge [D2] studies with a limiting RMS torsional amplitude of 0.5^0 (or a peak amplitude of 3.5^0 on the response plots).

Another method, has been also used, is based on the steepness of the response curves with wind speed to determine flutter instability. This has some logic associated with it since there is a very definite chance in the character of the response from a uniform, steady growth with wind speed to that which is becoming alarmingly violent. However, the steepness of the curves is highly dependent on the total damping of the structure (structure plus aerodynamic damping). In the low wind speed areas, the structural term dominates (or the aerodynamic term is positive). In the high wind speed range, the aerodynamic term dominates and is negative, but does not yet exceed the structural term in magnitude. Infinite amplitudes occur when the total damping becomes equal to zero or negative, since response is inversely proportional to the total damping.

REFERENCES - APPENDIX D

D1. King, J.P.C. and Davenport, A.G., "Lantau Fixed Crossing - Tsing Ma Bridge, Full Aeroelastic Model Tests of Completed Bridge", The University of Western Ontario, Faculty of Engineering Science Research Report, BLWT-SS11-1997, London, Ontario, Canada, 1997.

D2. King, J.P.C. and Davenport, A.G., "Ting Kau Bridge - Wind Tunnel Report", The University of Western Ontario, Faculty of Engineering Science Research Report, BLWT-SS29-1995, London, Ontario, Canada, 1995.

APPENDIX E

DYNAMIC WIND FORCES ON LONG SPAN BRIDGES USING EQUIVALENT STATIC LOADS

E1: INTRODUCTION

The conventional treatment of wind loading on long span bridges has tended to consider the static design wind loading used in normal strength design, and the aerodynamic stability as two separate and distinct aspects. The procedure described in this appendix takes a more unified approach. It depends on the measurement of the dynamic response of section models to grid turbulence rather than smooth flow. The response is corrected for discrepancies in the intensity and spectrum of turbulence, the damping, and the Joint Acceptance Function for the mode shape. A small correction is also added for the deficiency in low frequency excitation from grid turbulence. The design loads are found from the estimates of dynamic motion in the lowest symmetric and asymmetric modes as well as the mean load. This approach is an outgrowth of earlier studies in turbulent flow on the Murray MacKay Bridge(E1), the Bronx-Whitestone Bridge(E2), and Sunshine Skyway Bridge(E3).

E2: THE DESCRIPTION OF DESIGN LOADS

The persistent movements of any long span bridge (E4, E5) in strong wind are organized through its various mode shapes - horizontal, vertical, and torsional. They cover a range of frequencies but take place mostly at or near the individual modes and have a random character due to the continual shifts in phase and amplitude. To summarize the variety of load actions which the dynamic movements will produce in a severe wind storm, a wind load description for design has been proposed as in Figure E1. In this, *x, z* and θ denote the horizontal (downwind), vertical (upward) and torsional (nose-up) components; (see Figure E2); $\overline{W}$, W_1 and W_2 are the mean, symmetric and antisymmetric components per unit length of deck; $\overline{\alpha}, \alpha_1(\eta)$ and $\alpha_2(\eta)$ are the mean and modal load distribution functions; γ_1 and γ_2 are statistical load combination factors and take on ± 1.0 if only one modal term is included; ± 0.8 for two terms; ± 0.7 for three terms and ± 0.6 for four or more terms.

The description of the mean time average wind load components produced by the mean wind is straightforward. They are defined through the force coefficients $C_x(\alpha), C_z(\alpha)$ and $C_\theta(\alpha)$ which may be measured for a range of angles of attack α, the deck width *B*, and the mean reference velocity pressure at deck height *H*, $q_H = \frac{1}{2}\rho U_H^2$. The three mean forces per unit length are then:

$$\overline{W}_x = q_H B C_x(0^0), \overline{W}_z = q_H B C_z(0^0), \overline{W}_\theta = q_H B^2 C_\theta(0^0) \qquad \text{(E1)}$$

Two points should be made. First the coefficients in turbulent flow may differ from those in smooth flow. Second, normally only horizontal mean winds need to be considered. Only in steep mountainous valleys is there likely to be any appreciable inclination to the mean flow.

E3: EVALUATION OF THE MODAL LOAD COMPONENTS W_1 AND W_2

Although the response of a suspension bridge has been represented by coupled vertical and torsional equations of motion (E6, E7), in fact the aerodynamic coupling terms are usually negligible, and the aerodynamic stiffness terms are usually small in comparison to the stiffness of the bridge itself. This leaves the aerodynamic damping as the most significant aerodynamic force induced by motion. If this is negative and numerically greater than the structural damping, large motion will result. The response of

each uncoupled mode of vibration to the turbulent wind can be studied separately and superimposed at the end; usually, only the lowest modes are significant.

We can represent the peak modal load amplitude by the following:

$$W = g\sqrt{\sigma_{wb}^2 + \sigma_{wr}^2} \qquad \text{(E2)}$$

where g is a statistical peak factor, σ_{wb}^2 is the mean square background excitation acting quasi-statically, and σ_{wr}^2 is the mean square excitation at or near the resonant frequency.

The two components of the excitation can be identified in the typical power spectrum shown in Figure E3. The background excitation covers a broad frequency band below the natural frequency; the resonant excitation is concentrated in a peak at the natural frequency, the height of which is controlled by the damping. The two components can be estimated from the following expressions:

$$\sigma_{wbx,z,\theta}^2 = \int_0^\infty f^* S_{Fx,z,\theta}\left(f^*\right) \bullet \left|J_{x,z,\theta}\left(f^*\right)\right|^2 \bullet d\left(ln\, f^*\right) \qquad \text{(E3a)}$$

$$\sigma_{wrx,z,\theta}^2 = \frac{(\pi/4)}{\left(\zeta_s + \zeta_a\left(f_o^*\right)\right)} \bullet f_o^* S_{Fx,z,\theta}\left(f_o^*\right) \bullet \left|J_{x,z,\theta}\left(f_o^*\right)\right|^2 \qquad \text{(E3b)}$$

In the above, the subscripts x,z,θ imply the equations are written for each variable in turn; f* and f_o^* are the reduced frequencies fB/U_H and f_0B/U_H ; ζ_s and $\zeta_s(f^*)$ are the structural damping and aerodynamic damping at frequency f*; $f^* S_{Fx,z,\theta}(f^*)$ is the power spectral density of the externally induced x, z, θ components on a cross-section of the bridge deck at the reduced frequency f*; $\left|J_{x,z,\theta}\left(f^*\right)\right|$ is the "Joint Acceptance Function", relating the generalized modal force component with the mode shape and the force components at frequency f* at cross-sections of the bridge and involves the spanwise correlation of the forces.

The external forces on a bridge cross-section arise from either the direct action of turbulence in the wind or through the action of flow fluctuations in the wake. The latter are commonly described as vortex shedding. We can write:

$$f^* S_F\left(f^*\right) = \left(f^* S_F\left(f^*\right)\right)_{turb} + \left(f^* S_F\left(f^*\right)\right)_{wake} \qquad \text{(E4)}$$

The turbulent term can be written:

$$\left(f^* S_F\left(f^*\right)\right)_{turb} = \left(q_H B\right)^2 \bullet \left(C_{x.z.\theta}^2 \left|A\left(f^*\right)\right|^2\right) \bullet \left(f^* S_{u,v,w}\left(f^*\right)\right) \qquad \text{(E5)}$$

where:

$f^* S_{u,v,w}\left(f^*\right)$ = the power spectra of the turbulent velocity fluctuations u,v,w

$A\left(f^*\right)$ = the "Aerodynamic Admittance" which translates the turbulent velocity fluctuations into forces on a cross section;

$C_{x,z,\theta}$ = a reference aerodynamic coefficient.

The contributions of the turbulence to the expressions for σ_{wb}^2 and σ_{wr}^2 can be written as follows. To simplify the notation we will consider the lift *(z)* force and only include the vertical *(w)* component of turbulence, which normally will dominate.

$$\left(\sigma_{wbz}^2\right) = \left(q_H B C_z'\right) \bullet \left(\frac{\sigma_w}{\overline{U}_H}\right)^2 \bullet \int_0^\infty \frac{f^* S_w\left(f^*\right)}{\sigma_w^2} \bullet \left|A\left(f^*\right)\right|^2 \bullet \left|J_z\left(f^*\right)\right|^2 d\left(ln\, f^*\right) \qquad \text{(E6)}$$

$$\left(\sigma_{wrz}^2\right) = \left(q_H B C_z'\right) \bullet \left(\frac{\sigma_w}{\overline{U}_H}\right)^2 \bullet \frac{f_0^* S_w\left(f_0^*\right)}{\sigma_w^2} \bullet \left|A\left(f_0^*\right)\right|^2 \bullet \left|J_z\left(f_0^*\right)\right|^2 \frac{(\pi/4)}{\left(\zeta_s + \zeta_s\left(f_0^*\right)\right)} \qquad \text{(E7)}$$

The coefficient C_z' denotes ($aC_z/a\alpha$). Similar expressions for the torsion can be written with θ replacing *z* and introducing an additional factor B^2. For the drag direction, $2C_x$ replaces C_z' and *u* replaces *w*.

If the left hand terms are normalized by the $\left(q_H B C_z'\right)^2$ term, the response is a function primarily of the reduced frequency f* and the intensity of turbulence $\left(\sigma_w / \overline{U}_h\right)$, two homologous quantities which link the full-scale bridge behavior with any dynamically scaled model. Otherwise, the turbulence controlled response is bound up in the functional form of the turbulence spectrum, S_w, the aerodynamic admittance, A_z, the Joint Acceptance Function, J_z, and the aerodynamic damping .

The Aerodynamic Admittance reflects the efficiency of the bridge deck as a lift generator, as well as the correlation of the flow in the vicinity of the deck. The theoretical and observed form of this function is shown in Figure E8. The Joint Acceptance Function can be written:

$$\left|J_z\left(f^*\right)\right|^2 = \int_0^L \int_0^L R_{F1F2}\left(\eta_1, \eta_2; f^*\right) \mu(\eta_1) \mu(\eta_2) d\eta_1 d\eta_2 \qquad \text{(E8)}$$

where $\mu(\eta) =$ the mode shape with unit mean square amplitude; and

$$R_{F1F2}\left(\eta_1, \eta_2; f^*\right) = exp\left(-cf^* \frac{L}{B} \frac{|\eta_1 - \eta 2|}{L}\right) \qquad \text{(E9)}$$

In which *c* is a constant which defines the effective width of the correlation. A similar expression can be written for the spanwise cross-correlation of the velocity component in which case *c*=8 is representative. It is reasonable to assume the same value holds for the forces F_1 and F_2 on the basis of the "strip assumption".

Equations (E6) and (E7) apply to both the full scale bridge and a model in a turbulent wind tunnel flow. Ideally the latter should be an exact scaling of the former. This ideal, however, is difficult to satisfy in the wind tunnel and some compromises may have to be made. There are significant advantages to using an elongated section model in a turbulent flow generated behind a coarse grid. Although the turbulence scale and intensity cannot be made to exactly correspond to full scale, the values can be made sufficiently close.

To adapt the results of the dynamic section model testing to full scale, corrections need to be applied as follows: (a) Corrections of the low frequency quasi-static, "background" response, σ_{wb}^2, largely omitted from the section model due to the deficit in the vertical velocity spectrum generated by the grid. This can be estimated with reasonable accuracy from equation (E6) using either theoretical or

experimental data as outlined below. (b) Correction of the terms in the resonant response $\sigma_{w_r}^2$ for the discrepancies in the turbulence intensity, vertical velocity spectrum, Joint Acceptance Function and damping. No correction is needed in the Aerodynamic Admittance. The following formula encompasses these corrections:

$$\left(\sigma_{w_r}^2\right)_{full\ scale} = \left(\sigma_{w_r}^2\right)_{mod\ el} \bullet \phi_{\sigma w} \bullet \phi_{Sw} \bullet \phi_J \bullet \phi_\zeta \qquad \text{(E10)}$$

Where the terms $\phi_{\sigma w}, \phi_{Sw}, \phi_J$ *and* ϕ_ζ reflect corrections to the terms in the response due to the discrepancies between the section model and the full scale. These correction factors are found from the ratios of the quantities involved for model and full-scale. Through the appropriate selection of turbulence characteristics in the section model test and the model length, these corrections are relatively small. This last fact should lead to satisfactory reliability.

E4: EXPERIMENTAL DETERMINATION OF DESIGN LOAD COMPONENTS

The wind tunnel testing of the section models of the two Sunshine Skyway Bridge alternates provided an opportunity to apply the proposed method. The proposed structure, over Tampa Bay in Tampa, Florida is a cable-stayed design with a 366m main span. The concrete alternate used a precast, segmental box girder 29.03m wide and 4.27m deep. Two single strut pylons carry a system of radiating stays located on the longitudinal axis of the bridge (Figure E4).

The model of the 1 in 80 scale bridge section shown in Figure E5 is 7 ft. (~2m) in length corresponding to a 170m section of the full scale structure. The model was tested with spring mounting giving the correct frequency ratio in lift and torque and 0.5% damping. Measurements of mean and peak dynamic motion are plotted in Figure E6, and show marked differences between smooth and turbulent flow. With smooth flow there is evidence of some coupling between static lift and torque (i.e. the twisting of the deck due to torque modifies the lift). Although not essential to the method, aerodynamic damping and admittance functions were also measured in the experiments.

The large mesh size and bar spacing of the turbulence grid were selected to give a close representation of the natural wind. The measured vertical turbulence intensity behind this grid is found to be 0.05 compared to the expected full scale value of 0.06 over open water. The grid turbulence spectrum and the target full scale spectrum are drawn together in Figure E10 on a double logarithmic scale. Both have similar form, although the full scale has slightly more energy than does the grid turbulence at lower frequency.

E5: DETERMINATION OF DESIGN WIND LOADS

Following equation (E6), the wind load from the background turbulence excitation is found through the integration with reduced frequency of the product of the vertical wind spectrum (Figure E7), Aerodynamic Admittance Function (Figure E8) (assuming the Sears function), and the Joint Acceptance Function for the particular mode (Figure E9). The form of these functions is such that the bulk of the energy is in the range of reduced frequency f^* between 0.01 and 0.1 and any uncertainty of the functional values at these low frequencies generally introduce little error. Added to this is the resonant component following equation (E7). The resonant modal response, measured in terms of deflection has been converted to an equivalent static load through the modal stiffness:

$$\sigma_{w_{rz}} = m(2\pi f_o)^2 \sigma_z \,; \qquad \sigma_{w_{r\theta}} = I_o (2\pi f_o)^2 \sigma_\theta \qquad \text{(E11)}$$

The correction terms are determined from the ratios of the quantities involved between full scale and model scale. The correction factor for the turbulence intensity, $\phi_{\sigma w}$ is a constant equal to $(.06/.05)^2$ = 1.44 (i.e. this is the ratio of target full scale to model values). Similarly, the correction factor for the vertical

velocity spectrum ϕ_{S_W} is shown in Figure E7, the Joint Acceptance Function, ϕ_J, in Figure E9, and the damping, ϕ_ζ, in Figure E10. The addition of the background and resonant components as in equation (E2), results in the loading shown in Figures E11a and b. The final wind speed scaling will depend upon the final design frequencies of the structure. Thus the example wind loads have been determined for a nominal wind speed at deck height based on the estimates of vertical and torsional frequencies noted in the figures. Verification of this procedure, using 1:350 scale aeroelastic models of both the steel and concrete bridges tested in a turbulent boundary layer were excellent (E3).

E6: CONCLUSIONS

A method has been presented whereby wind tunnel section model test results can be incorporated directly into a load format suitable for the definition of the design wind loads of long span structures. The procedure has been verified experimentally with the satisfactory prediction of the response of two full bridge aeroelastic models to boundary layer shear flow.

REFERENCES - APPENDIX E

E1. Davenport, A.G., Isyumov, N., Fader, D.J. and Bowen, C.F.P., "A Study of Wind Action on a Suspension Bridge During Erection and Completion", University of Western Ontario, Faculty of Engineering Science, Research Report BLWT-3-1969, London, Ontario, Canada, May 1969 and March 1970.

E2. Davenport, A.G., Isyumov, N., Rothman, H. and Tanaka, H., "Wind Induced Response of Suspension Bridges, Wind Tunnel Model and Full Scale Observations", Proc. 5th Int. Conf. Wind Engineering, Ft. Collins, Colorado, 1979, pp. 807-824.

E3. Davenport, A.G. and King, J.P.C., "The Incorporation of Dynamic Wind Loads into the Design Specifications For Long Span Bridges", ASCE Fall Convention, New Orleans, La., 1982.

E4. Tanaka, H. and Davenport, A.G., "Wind Induced Response of Golden Gate Bridge", University of Western Ontario, Faculty of Engineering Science Research Report, BLWT-1-1982, Paper accepted for publication by JSD, ASCE, June 1982.

E5. Melbourne, W.H., "Model and Full Scale Response to Wind Action of the Cable Stayed Box Girder West Gate Bridge", Practical Experience With Flow Induced Vibrations, Symposium Karlsruhe, Germany, 1979, pp. 625-652.

E6. Ukeguchi, N., Sakata, H. and Nishitani, H., "An Investigation of Aeroelastic Instability of Suspension Bridges", Proc. International Symposium on Suspension Bridges, Lisbon, 1966, pp. 273-284.

E7. Scanlan, R.H., "An Examination of Aerodynamic Response Theories and Model Testing Relative to Suspension Bridges", Proc. Wind Effects on Buildings and Structures, Tokyo, 1971, pp. 941-951.

$$W_x(\eta) = \overline{W}_x\,\overline{a}(\eta) + \gamma_{1_x} W_{1_x}\, a_1(\eta) + \gamma_{2_x} W_{2_x}\, a_2(\eta)$$

$$W_z(\eta) = \overline{W}_z\,\overline{a}(\eta) + \gamma_{1_z} W_{1_z}\, a_1(\eta) + \gamma_{2_z} W_{2_z}\, a_2(\eta)$$

$$W_\theta(\theta) = \overline{W}_\theta\,\overline{a}(\eta) + \gamma_{1_\theta} W_{1_\theta}\, a_1(\eta) + \gamma_{2_\theta} W_{2_\theta}\, a_2(\eta)$$

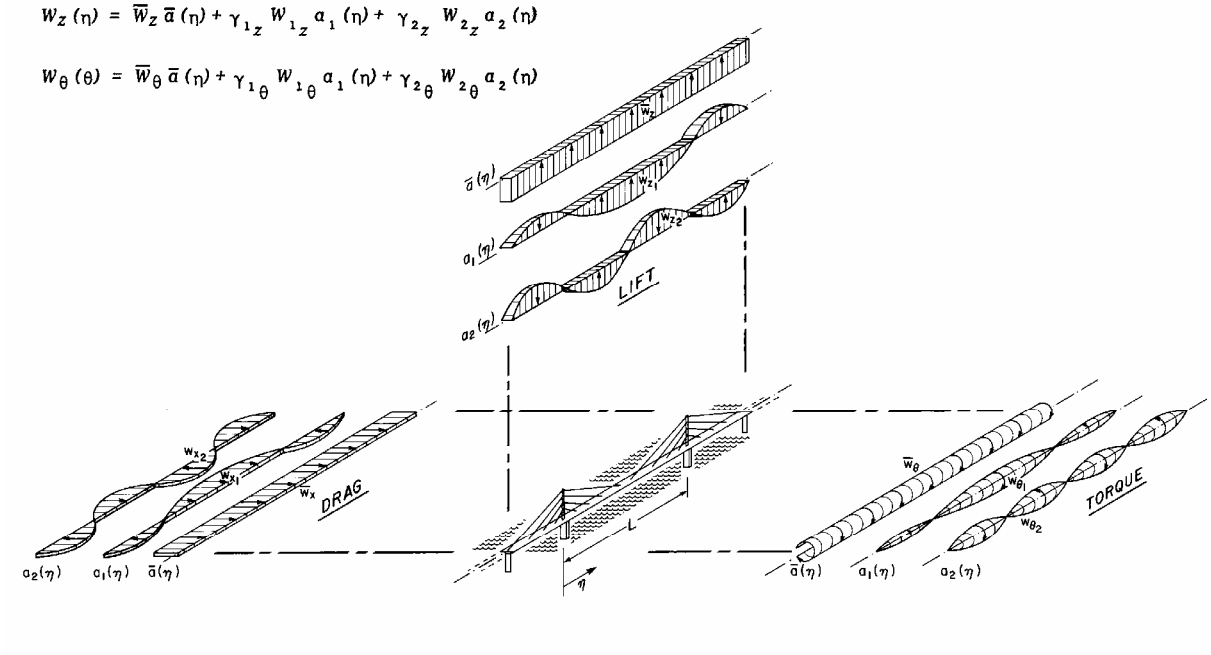

FIGURE E1 DISTRIBUTED WIND LOAD COMPONENTS

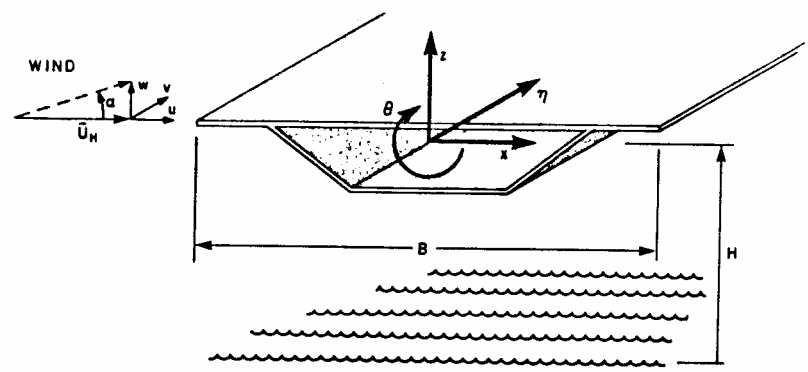

FIGURE E2 NOTATION

$$W_r = g\sqrt{\sigma^2_{W_B} + \sigma^2_{W_R}}$$

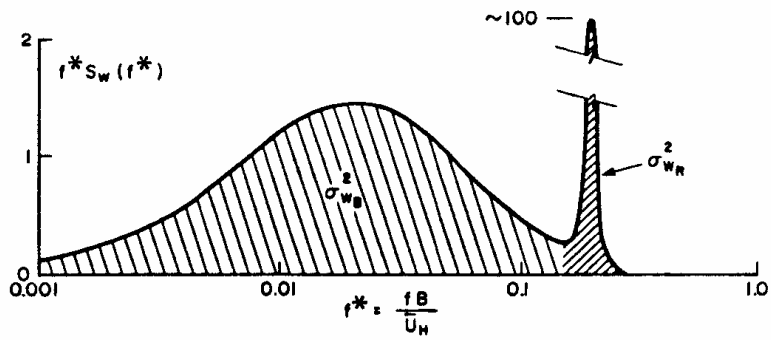

FIGURE E3 SPECTRUM OF MODAL LOAD AMPLITUDE

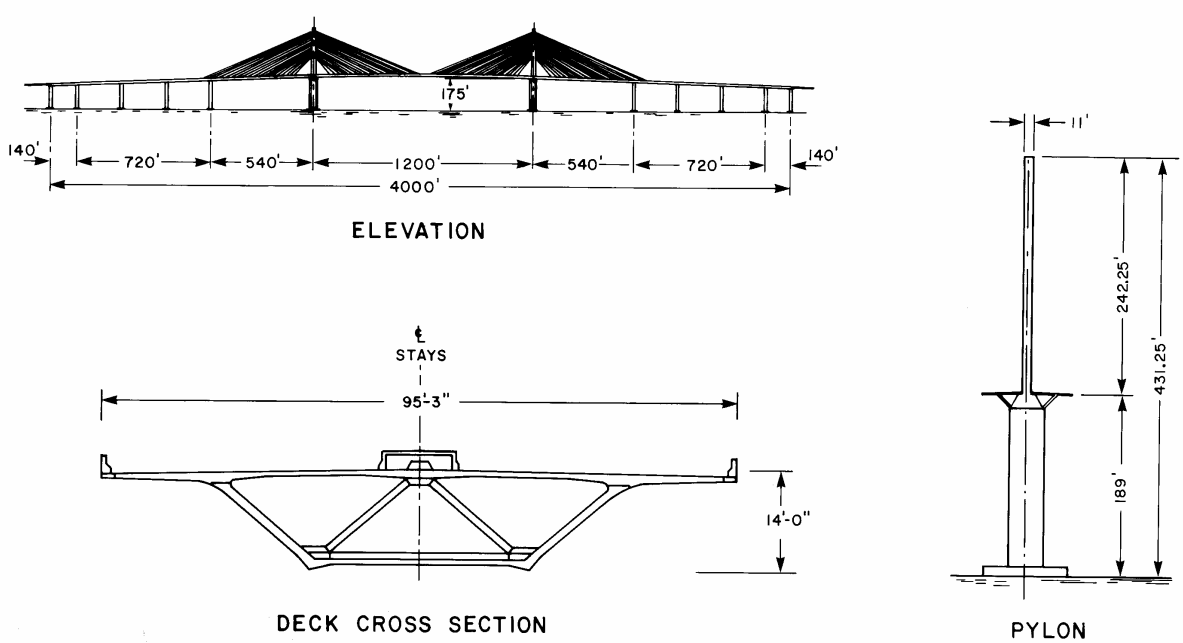

FIGURE E4 THE SUNSHINE SKYWAY BRIDGE

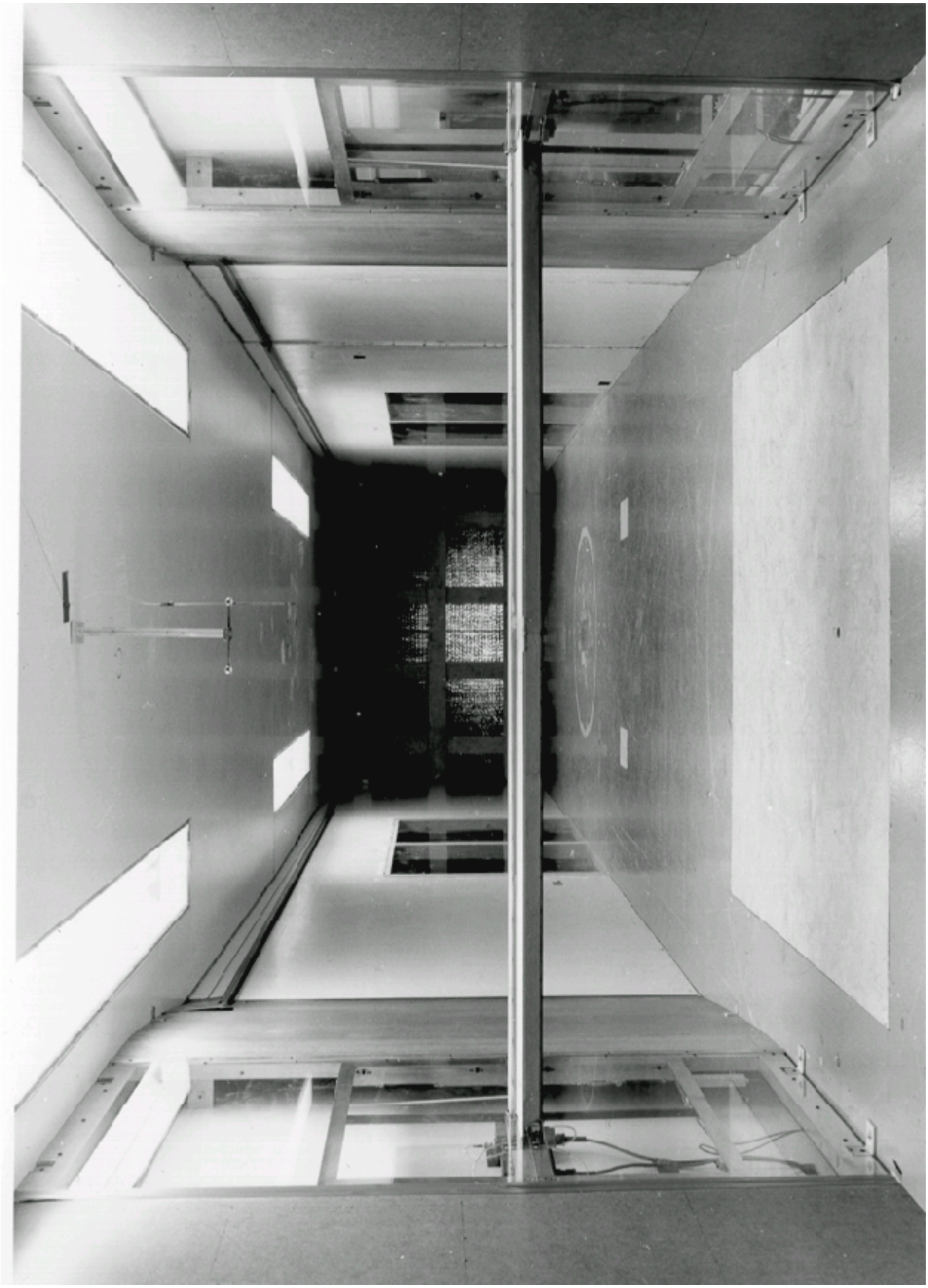

FIGURE E5 SECTION MODEL IN WIND TUNNEL WITH TURBULENCE GRID AT INLET

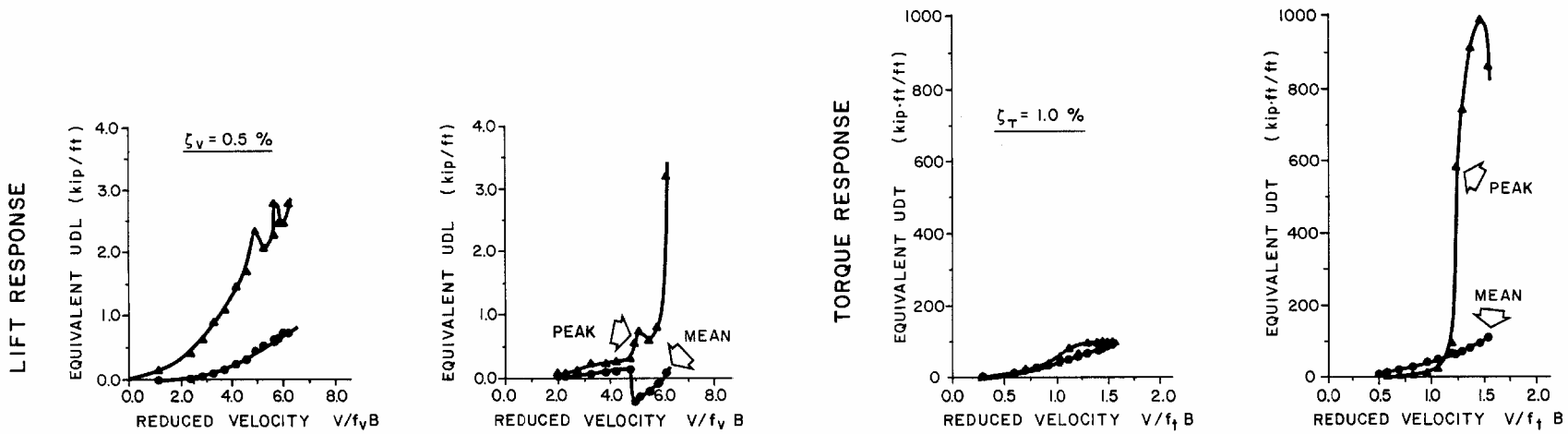

FIGURE E6 SECTION MODEL RESPONSE (UNCORRECTED)

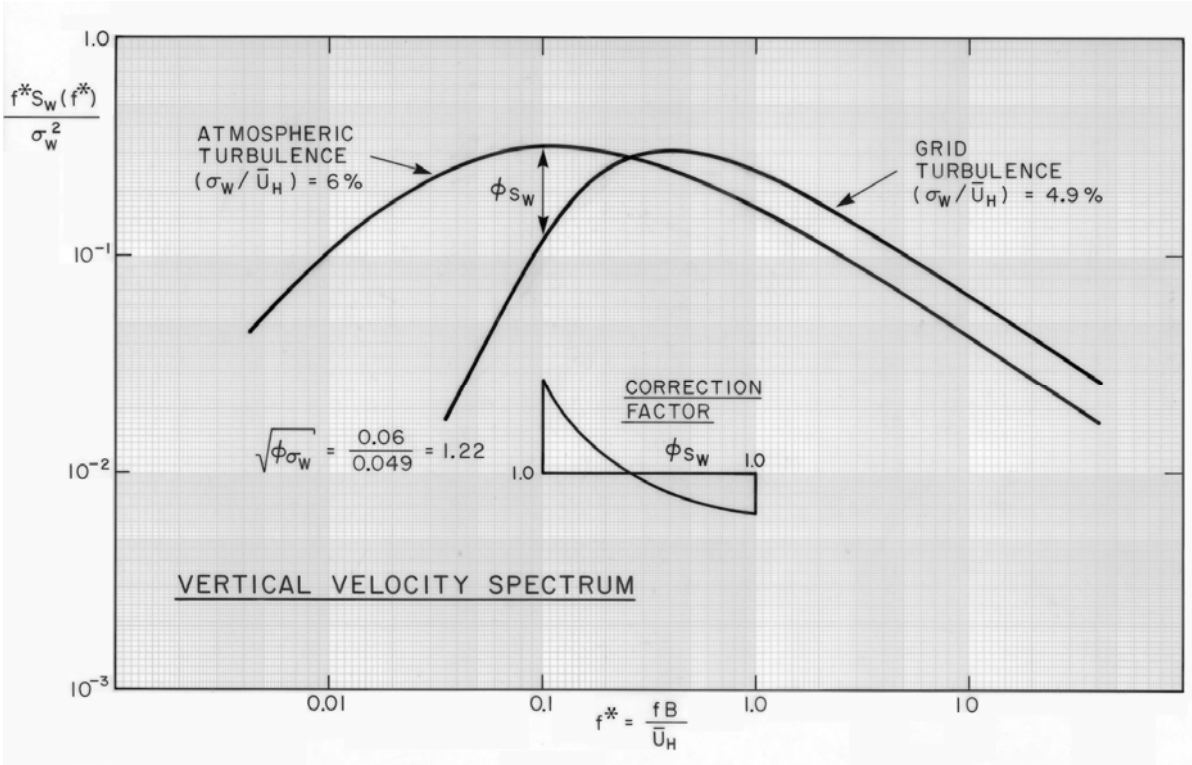

FIGURE E7 SPECTRUM OF VERTICAL COMPONENT OF TURBULENCE

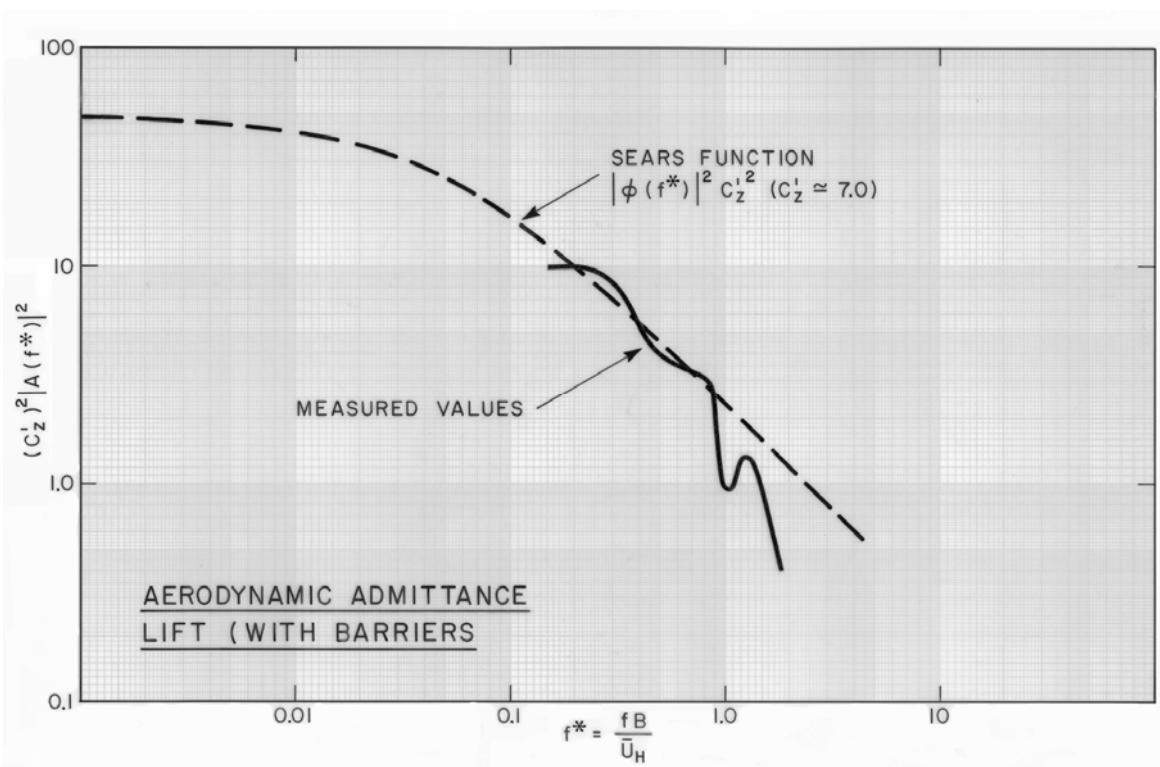

FIGURE E8 AERODYNAMIC ADMITTANCE

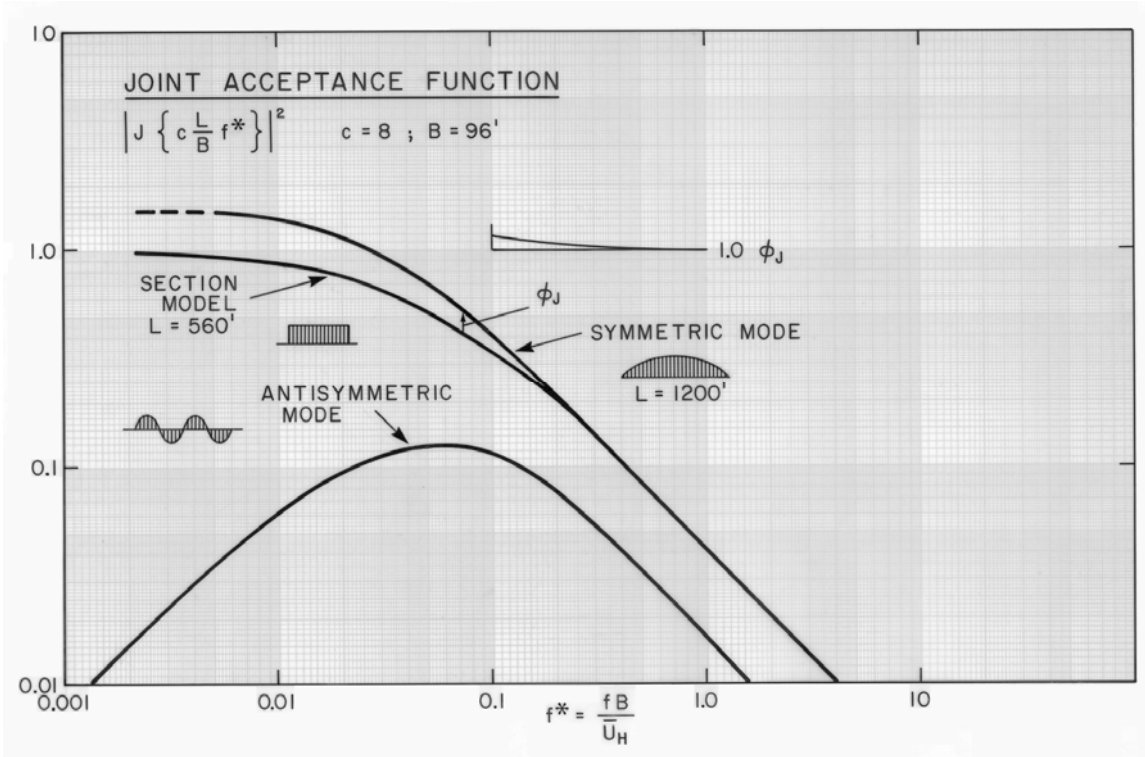

FIGURE E9 JOINT ACCEPTANCE FUNCTION

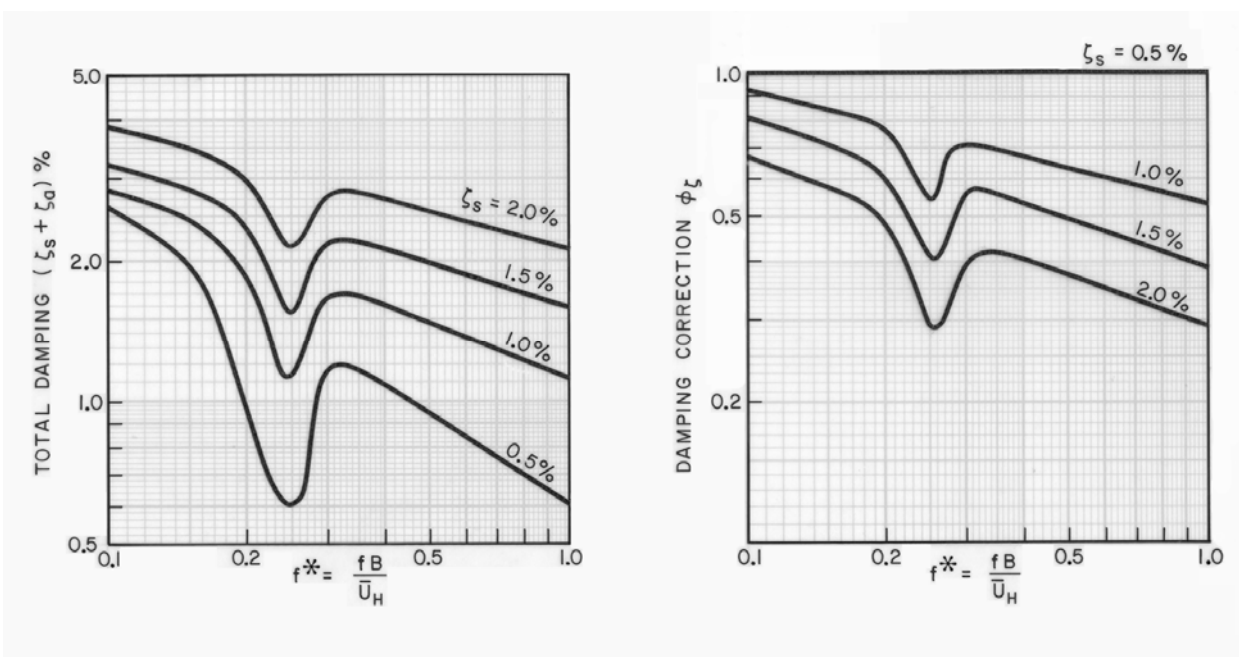

FIGURE E10 DAMPING FUNCTIONS

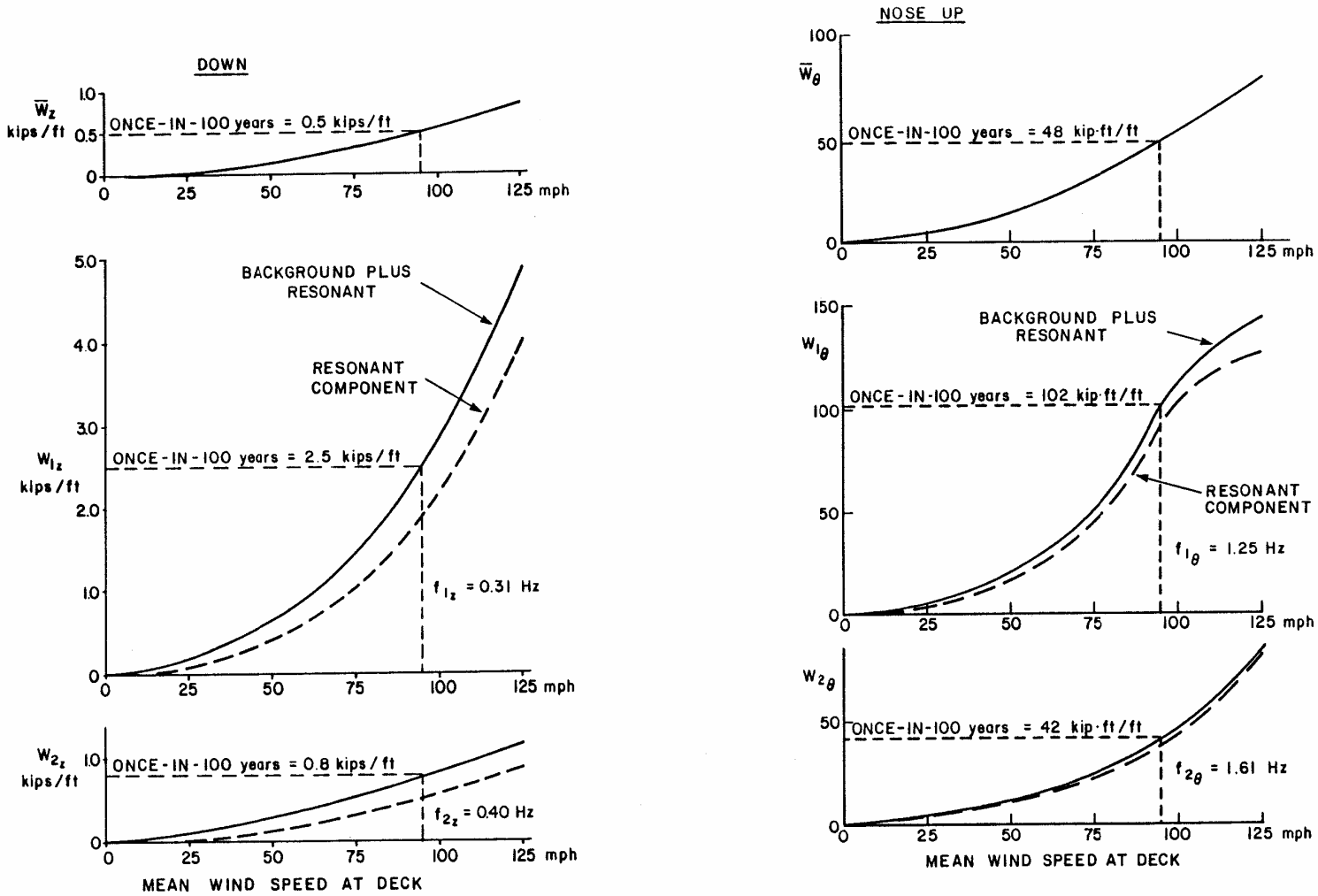

FIGURE E11 WIND LOAD COMPONENTS ON COMPLETED BRIDGE

APPENDIX F

RESULTS OF STATIC SECTION MODEL TESTS – ARCH SECTION

- The results shown in this appendix are not corrected for wall confinement effects.

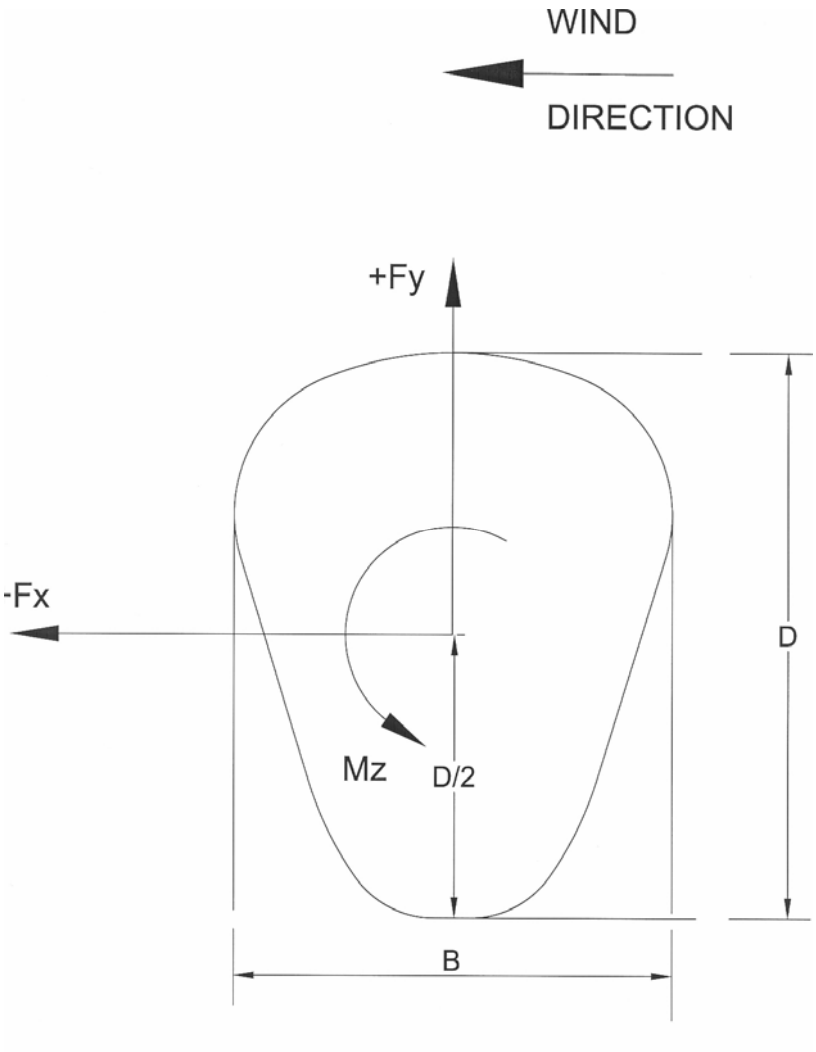

FIGURE F1 SKETCH SHOWING SIGN CONVENTION OF FORCES

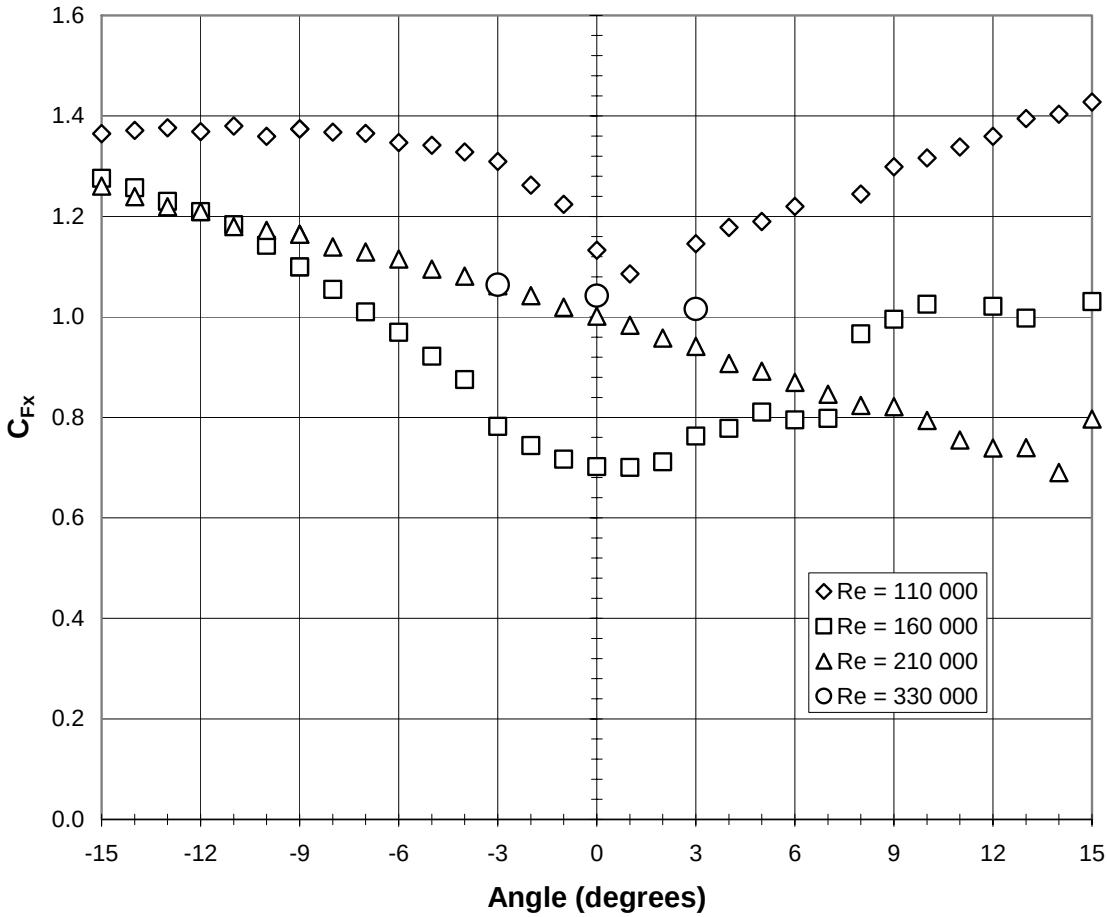

Static Force Coefficients in Smooth Flow

FIGURE F2 STATIC FORCE COEFFICIENTS, SMOOTH FLOW

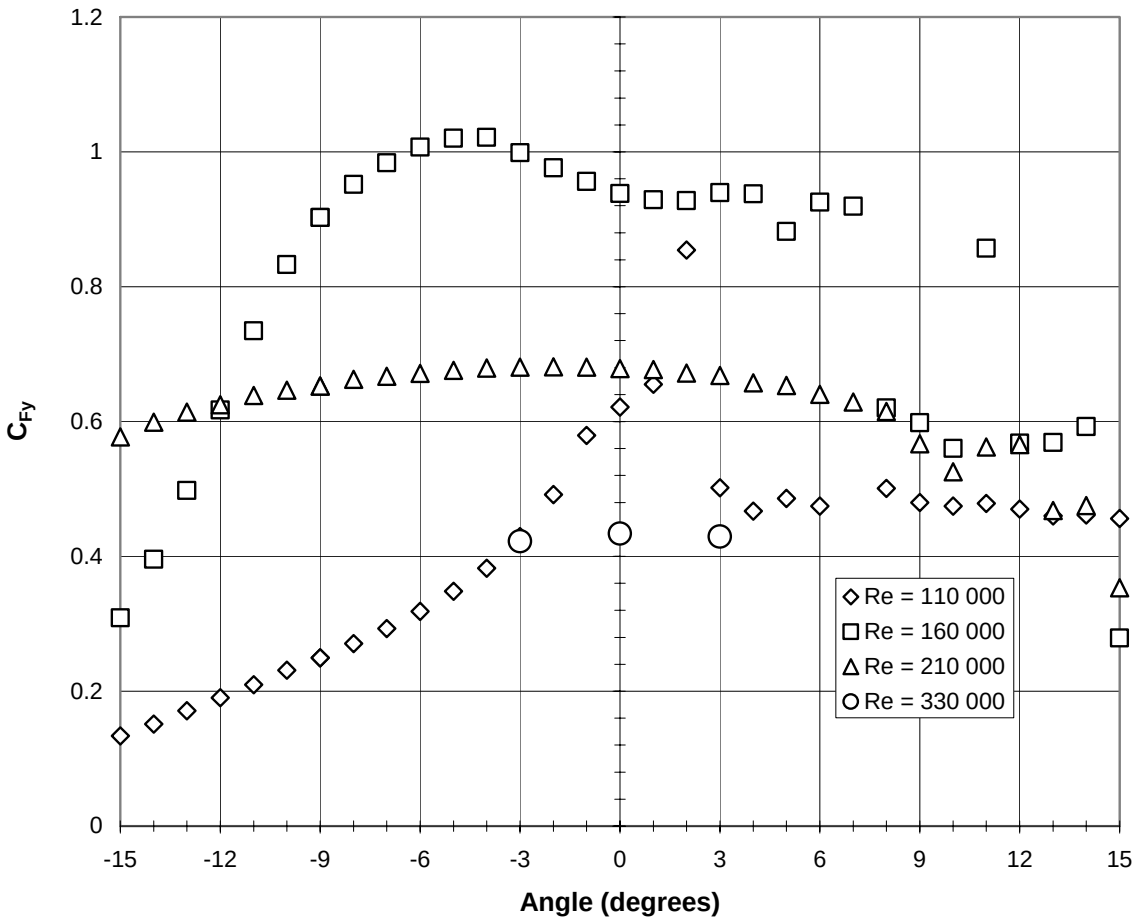

Static Force Coefficients in Smooth Flow

FIGURE F2 (CONT.) STATIC FORCE COEFFICIENTS, SMOOTH FLOW

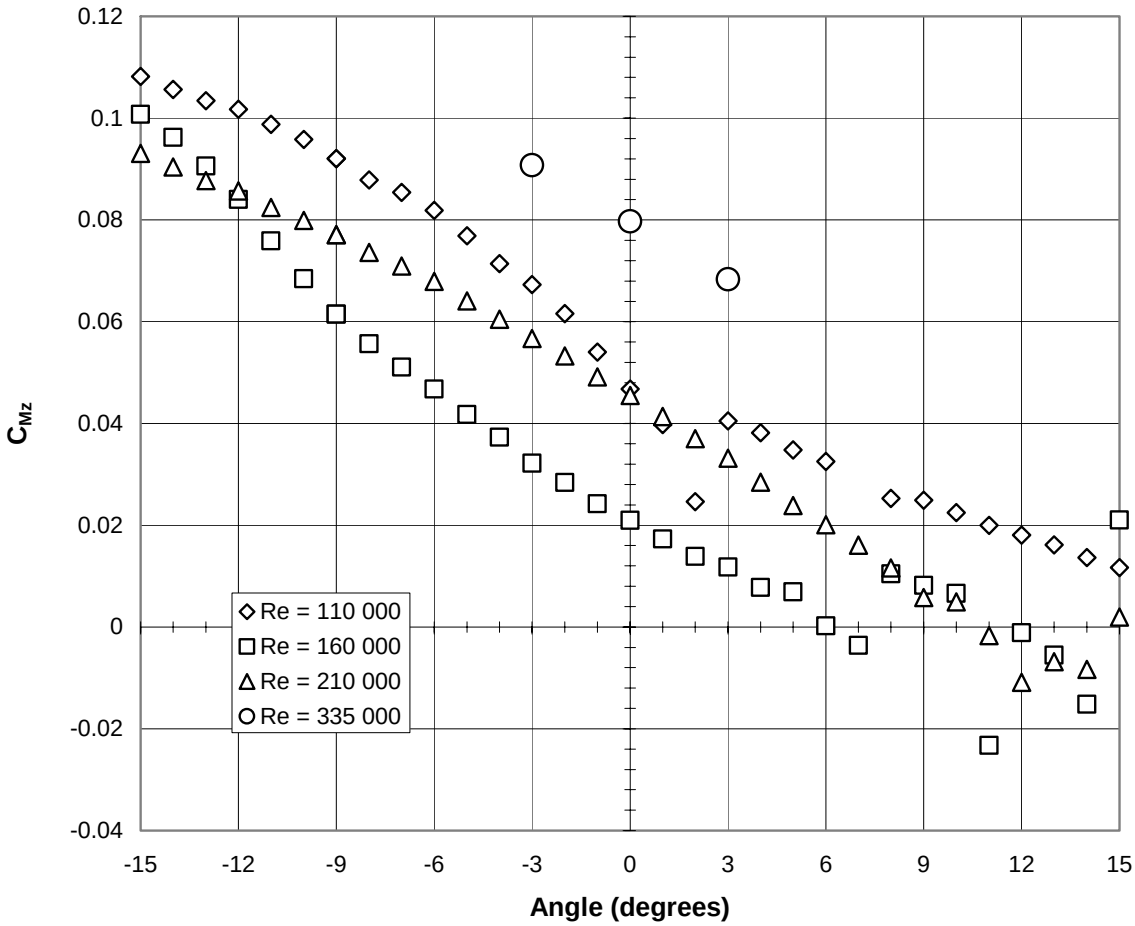

Static Force Coefficients in Smooth Flow

FIGURE F2 (CONT.) STATIC FORCE COEFFICIENTS, SMOOTH FLOW

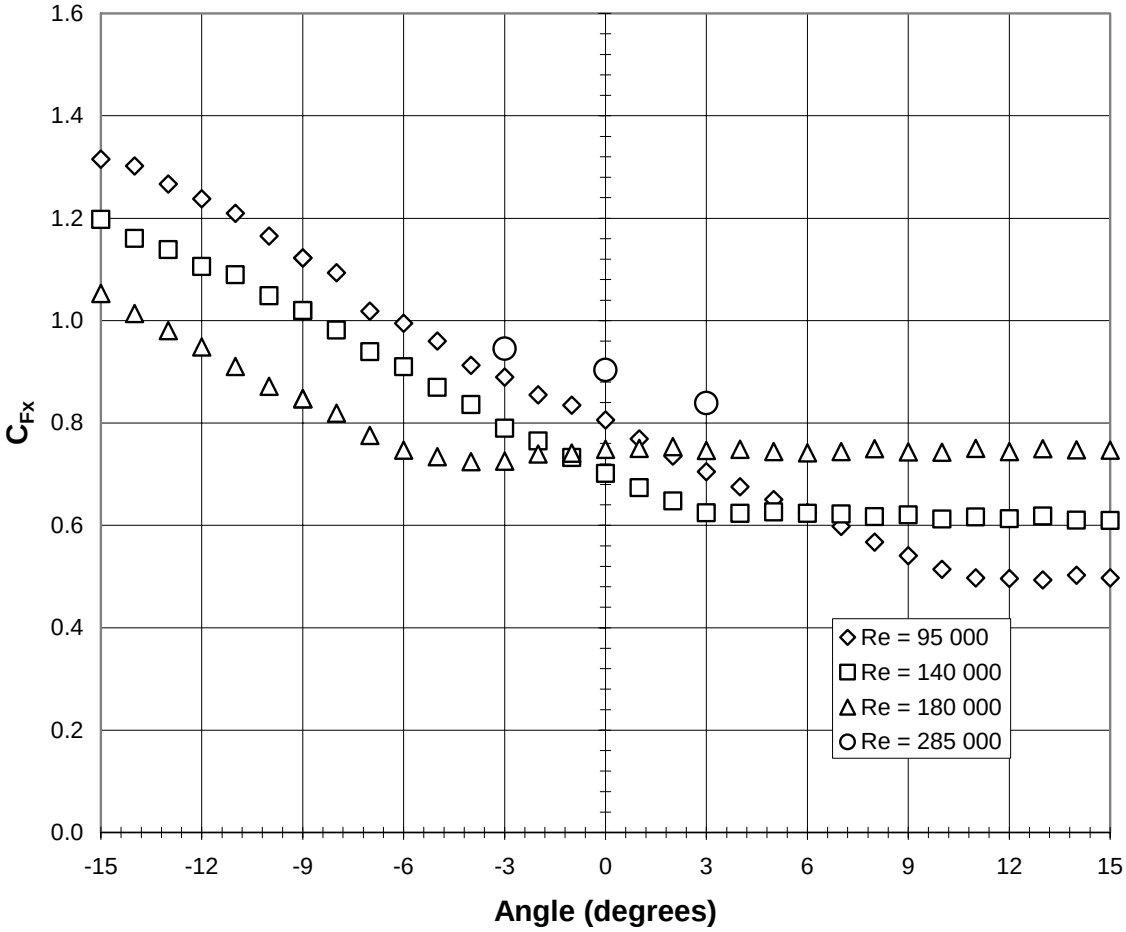

Static Force Coefficients in Turbulent Flow

FIGURE F3 STATIC FORCE COEFFICIENTS, TURBULENT FLOW

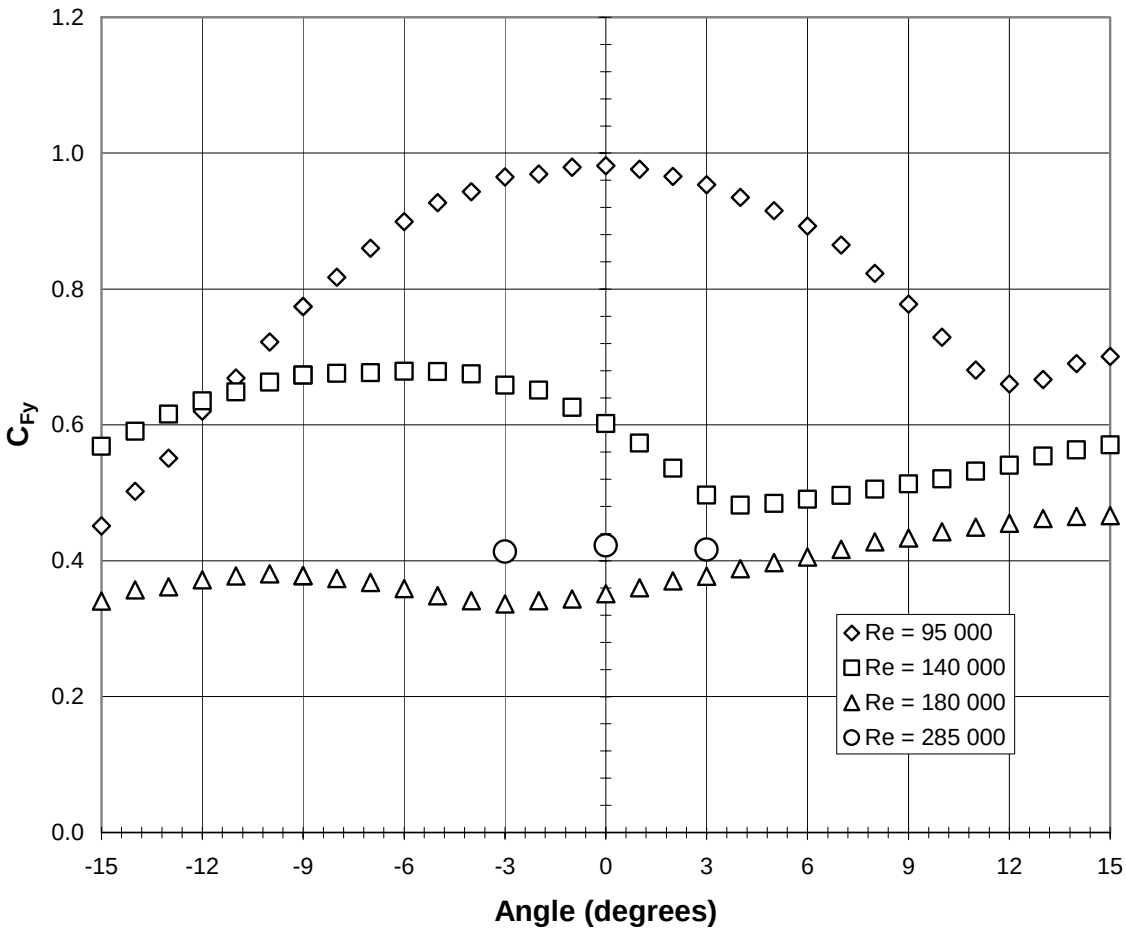

Static Force Coefficients in Turbulent Flow

FIGURE F3 (CONT.) STATIC FORCE COEFFICIENTS, TURBULENT FLOW

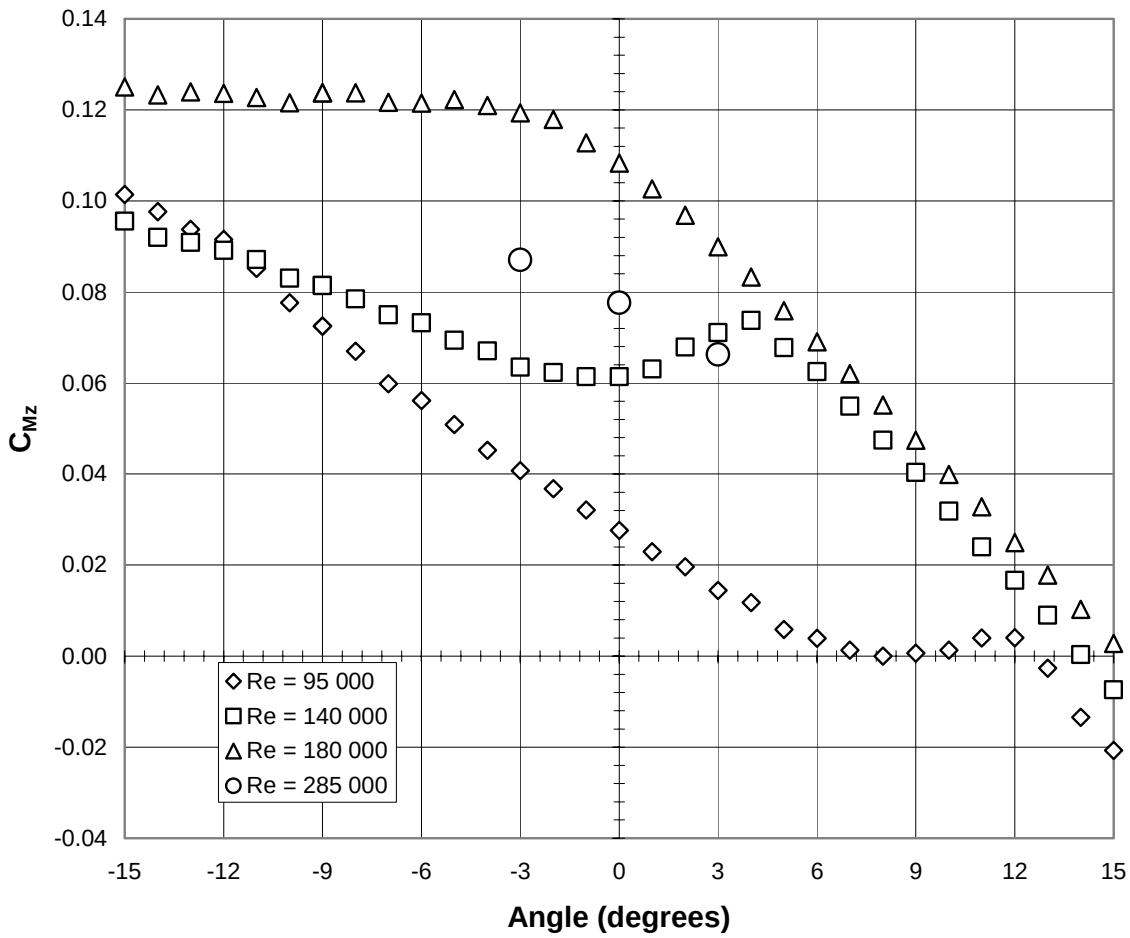

Static Force Coefficients in Turbulent Flow

FIGURE F3 (CONT.) STATIC FORCE COEFFICIENTS, TURBULENT FLOW

APPENDIX G

DEVELOPMENT OF THE PEAK RESPONSE DUE TO ALONG-WIND LOADING OF THE ARCH RIB

The theory presented below is a general form of that used to develop various codes including NBCC, ASCE-7 and AS1170. It follows the usual component breakdown of the response into mean, quasi-steady (background) and resonant components. The various functions required to define the structure of the wind are from Engineering Science Data Units (ESDU) with the exception of the distribution of mean wind speed with height and roughness length, z_o. These items are taken from the BLWTL wind speed report. The applicable ESDU data items are 74031 for the spectral density function of turbulence and longitudinal integral length scale, and 86010 for the spatial distribution of the longitudinal component of turbulence, that is; covariance function and the root coherence function. The theory is described in more detail in References 1 and 2.

Figure G1 describes the configuration of the arch and defines the coordinate system. The responses correspond to influence functions provided by Figg Engineers and these are shown in Figure G2 and Figure G3. In both cases, these are bending moments in the arch.

The peak bending moment, $\hat{M}$ at a given cross-section is given by:

$$\hat{M} = \overline{M} + \sqrt{g_Q^2 \ \tilde{M}_Q^2 + g_R^2 \ \tilde{M}_R^2} \qquad \text{(G1)}$$

where $\overline{M}$ = mean bending moment

$\tilde{M}_Q$ = rms quasi-steady fluctuating moment

g_Q = peak factor for quasi-steady fluctuations

$\tilde{M}_R$ = rms resonant component

g_R = peak factor for resonant component

Following a traditional gust factor approach, the gust factor is defined as:

$$G = \frac{\hat{M}}{\overline{M}} = \left(1 + \sqrt{g_Q^2 \frac{\tilde{M}_Q^2}{\overline{M}^2} + g_R^2 \frac{\tilde{M}_R^2}{\overline{M}^2}}\right) \qquad \text{(G2)}$$

The above is derived from an integration of the drag force per unit length, weighted by the appropriate function. The drag force per unit length is given by:

$$w(s,t) = \frac{1}{2} \rho_{air} \ U^2(s,t) C_D \ D \qquad \text{(G3)}$$

where ρ_{air} = density of air

C_D = local drag coefficient

D = local breadth

$U(s,t) = \overline{U}(s,t) + U(s,t)$

$U^2(s,t) = \overline{U}^2(s) + 2\,\overline{U}(s)\,u(s,t) +$ 2nd order terms

therefore

$w(s,t) = \overline{W}(s) + w(s,t)$

with $\overline{W}(s) = q\,C_D\,D$

$w(s,t) = 2qC_D D \dfrac{u}{\overline{U}}$

$q = \dfrac{1}{2}\,\rho_{air}\,\overline{U}^2$

The mean moment, $\overline{M}$ is defined through the influence function, I_M as the following:

$$\overline{M} = \int_{arch} \overline{W}\,I_M\,ds \qquad \text{(G4)}$$

The variance of the quasi-steady moment is defined as:

$$\tilde{Q}_M^2 = \iint_{arch} \tilde{w}_{s_1 s_2}^2\,I_M(s_1)\,I_M(s_2)\,ds_1\,ds_2 \qquad \text{(G5)}$$

where $\tilde{w}_{s_1 s_2}^2$ is the covariance of the force per unit length. The variance (when s_1 equals s_2) is defined as:

$\tilde{w}^2 = 4\,q^2\,C_D^2\,D^2\,i_u^2$

where i_u = local intensity of turbulence

$= \dfrac{\tilde{u}}{\overline{U}}$

The peak factor for the quasi-steady fluctuations is given by:

$$g_Q = g_u\left(1 + g_u\sqrt{B}\,i_u\right) \qquad \text{(G6)}$$

where g_u = statistical peak factor for wind speed

$= \dfrac{\hat{U} - \overline{U}}{\tilde{u}}$

$\approx$ 3.7

B is the ratio of the actual quasi-steady variance to the quasi-steady variance for a fully correlated gust. This is sometimes referred to as a size effect factor. Mathematically,

$$B = \frac{\tilde{M}_Q^2}{\tilde{w}^2 \iint\limits_{arch} I_M(s_1)\, I_M(s_2)\, ds_1\, ds_2} \tag{G7}$$

where $\tilde{w}^2$ is taken at the same location as i_u in the equation describing g_Q, typically the top of a structure.

The resonant moment, $\tilde{M}_R^2$ is given as:

$$\tilde{M}_R^2 = \sum_{modes} \tilde{a}_i^2\, M_i^2 \tag{G8}$$

where $\tilde{a}_i$ = rms modal coefficient

M_i = moment for a unit modal deflection

M_i is defined mathematically as:

$$M_i = \int\limits_{arch} m(s)\,(2\,\pi\, f_i)^2\, \phi_i(s)\, I_M\, ds \tag{G9}$$

where m = mass per unit length

f_i = ith natural frequency

ϕ_i = ith mode shape

The modal coefficient is defined as:

$$\tilde{a}_i^2 = \frac{1}{K_i^2}\, \frac{\pi}{4\beta}\, f_i\, S(f_i) \tag{G10}$$

where K_i = generalized stiffness

= $(2\,\pi\, f_i)^2\, M_i$

β = net damping

= structural + aerodynamic

$S(f_i)$ = generalized force spectrum at f_i

The generalized force spectrum is given by:

$$S(f_i) = \iint\limits_{arch} S_w\,(s_1, s_2, f_i)\, \phi_i(s_1)\, \phi_i(s_2)\, ds_1\, ds_2 \tag{G11}$$

where S_w = co-spectrum of the drag force per unit length

The aerodynamic damping in a given mode is given by:

$$\beta_{aero} = \frac{\int_{arch} \rho_{air} \; C_D \; D \, \overline{U} \; \phi_i^2 \; ds}{4 \quad \pi \; M_i \; f_i} \tag{G12}$$

References:

[G1] Davenport, A.G. (1962). Response of slender line like structures to a gusty wind. Proc. Of Institute of Civil Engineers. Vol. 23, pp. 389-408.

[G2] Vickery, B.J. (1995). The response of chimneys and tower-like structures to wind loading. In A State of the Art in Wind Engineering, Ninth International Conference on Wind Engineering. Wiley, pp. 205-233.

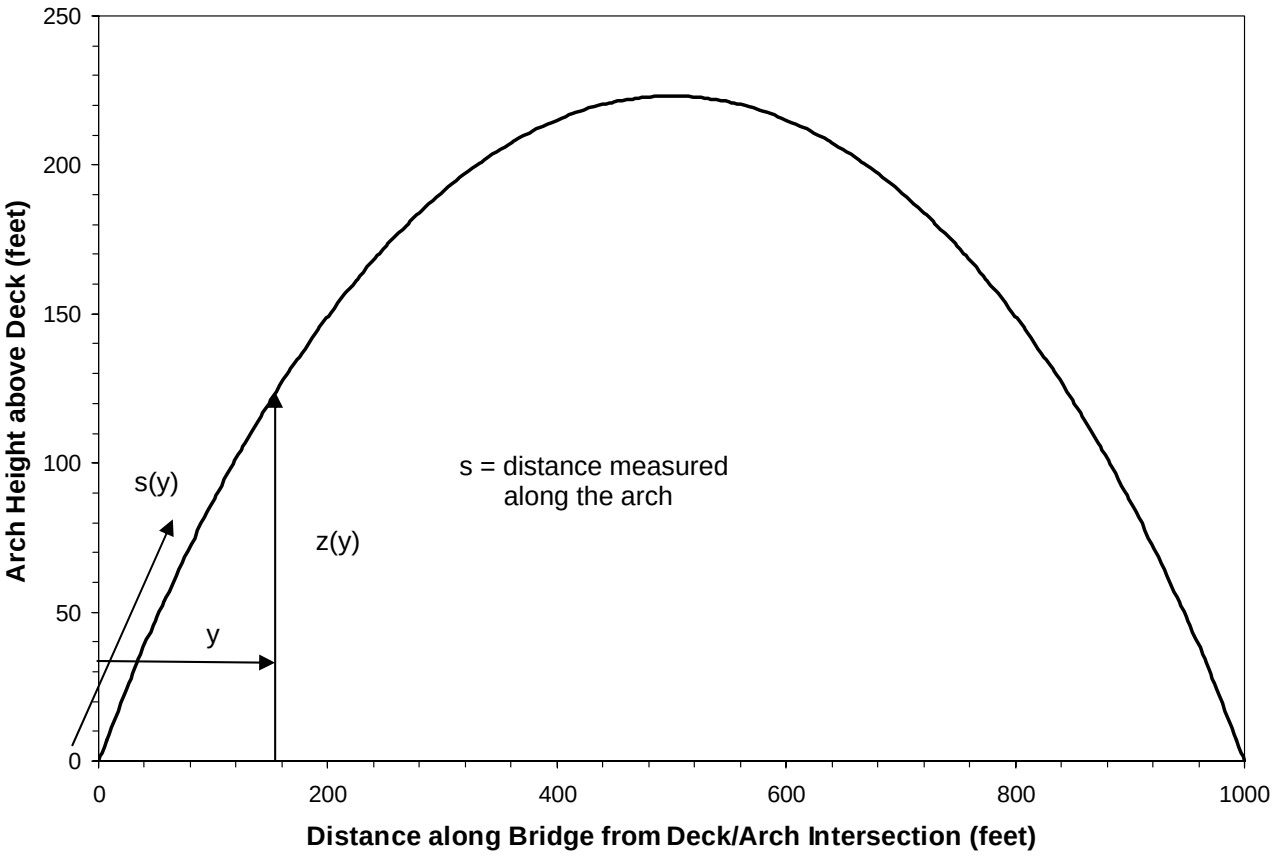

FIGURE G1 DEFINITION OF GEOMETRY AND COORDINATE SYSTEM

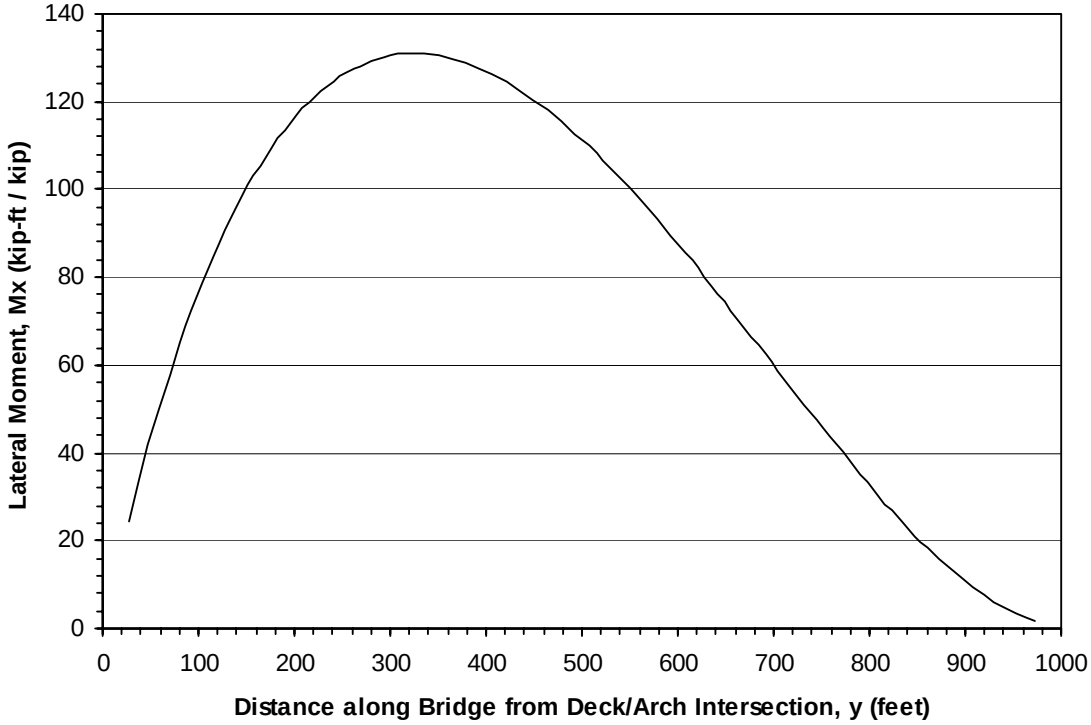

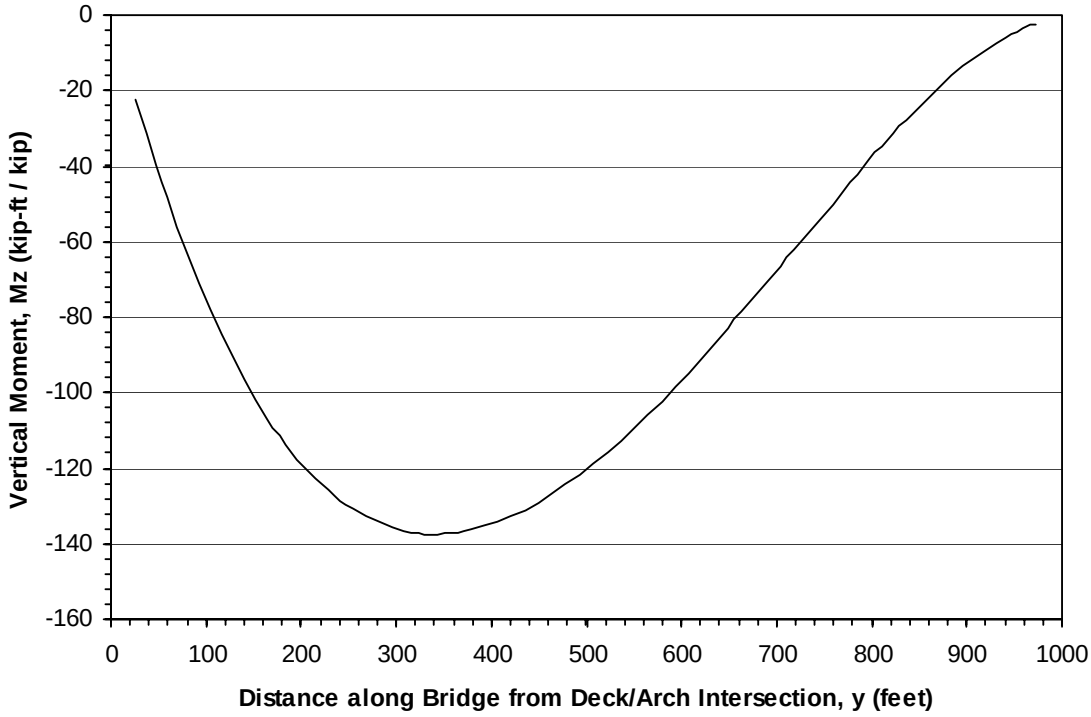

FIGURE G2 INFLUENCE FUNCTIONS FOR THE BENDING MOMENT RESPONSE AT THE DECK/ARCH INTERSECTION

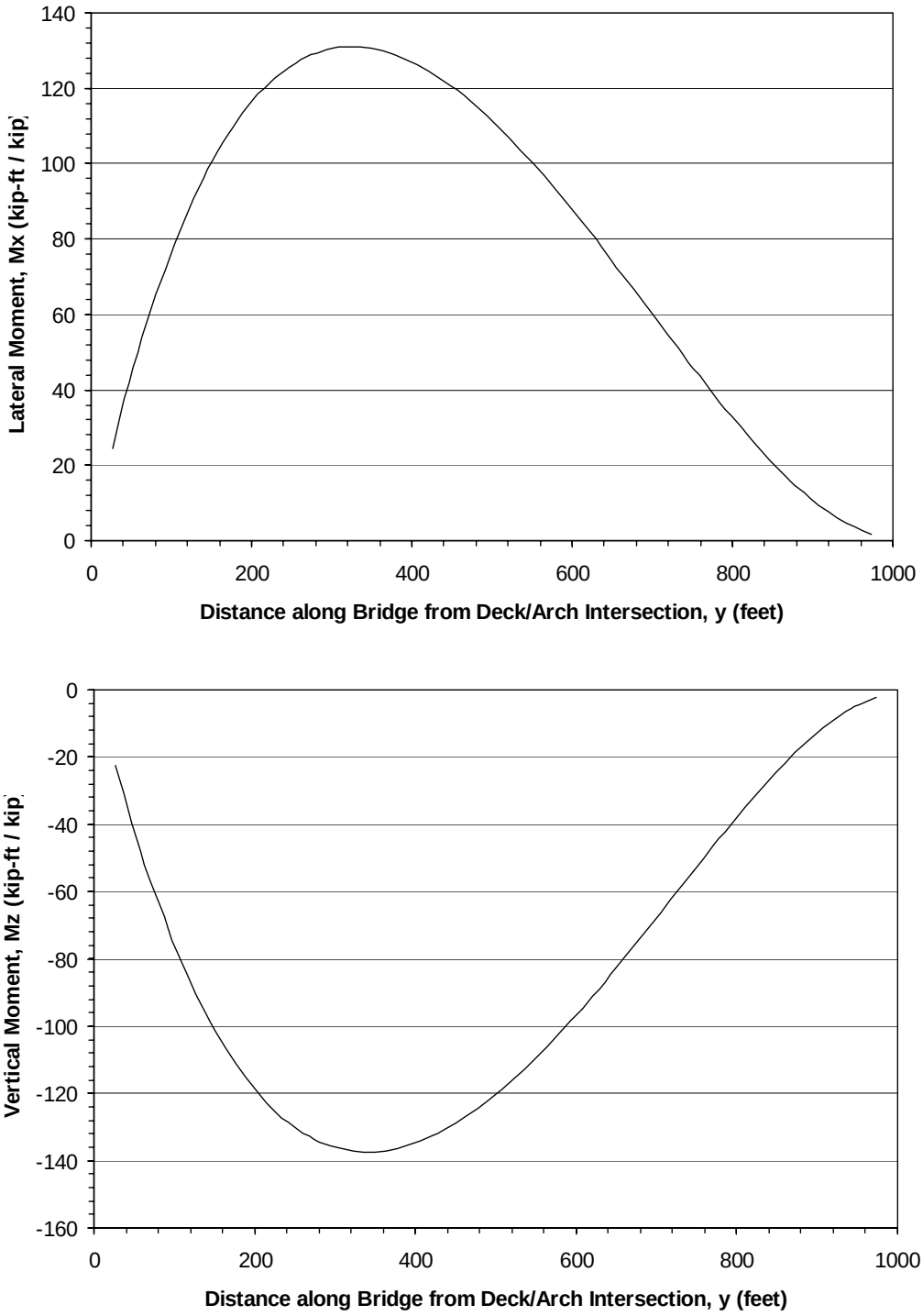

FIGURE G3 INFLUENCE FUNCTIONS FOR THE BENDING MOMENT RESPONSE AT THE REDUCTION IN CROSS SECTION ON THE ARCH RIB

APPENDIX H

RESULTS OF FULL BRIDGE AEROELASTIC TESTS, COMPLETED BRIDGE

Notes:

1. The bending moments given in the plots have the unit of kip-ft. The numbers read directly from the plots should be multiplied by 10^5 to obtain the actual bending moments in kip-ft. For example on page H8 of the Deck Midspan Drag Moment (the lower right figure on that page), both the mean and peak drag moments at about 160mph are approximately 1.0×10^5 kip-ft (not 1.0 kip-ft).

2. The total response is equal to the mean, plus or minus the peak.

3. X is along the longitudinal direction, Y is the lateral direction (drag direction), and Z is the vertical direction (lift direction). Thus M_x is the torque, M_y is the lift moment (generated by the lift) and M_z is the drag moment (generated by the drag).

TABLE H1 INSTRUMENTATION LOCATIONS FOR THE FULL BRIDGE AEROELASTIC MODEL, COMPLETED BRIDGE

Instrumentation **x – longitudinal, y – lateral (Drag), z – vertical (Lift)**	**Instrumentation Locations**
Strain Gages:	
M_x, M_y and M_z at **Deck** End (marked **A**)	Lift and Drag Moments, as well as Torque at 438ft from Midspan
M_x, M_y and M_z at **Deck** 1/4 Point (marked **B**)	Lift and Drag Moments, as well as Torque at 238ft from Midspan
M_x, M_y and M_z at **Deck Midspan** (marked **C**)	Lift and Drag Moments, as well as Torque at 38ft from Midspan
M_x, M_y and M_z at **Arch** End (marked **D**)	Lift and Drag Moments, as well as Torque at 42ft from Arch-Deck connection
M_y and M_z at **Arch** Crown (marked **E**)	Lift and Drag Moments at 44ft from Arch Crown
Accelerometers:	
y, z and θ accel. at **Deck** Midspan (marked **C**)	Lift, Drag and Torsional Accelerations at Midspan
y, z and θ accel. at **Deck** 1/4 Point (marked **B**)	Lift, Drag and Torsional Accelerations at 225ft from Midspan
y and z accel. at **Arch** ¼ Point (marked **G**)	Lift and Drag Accelerations at about the ¼ point on the Arch (235ft from the arch crown in the deck longitudinal direction)
y and z accel. at **Arch** Crown (marked **E**)	Lift and Drag Accelerations at 14ft from Arch Crown
Displacement Lasers:	
y, z and θ displacements at **Deck** Midspan (marked **C**)	Lift and Drag Displacements, as well as Deck Rotation at 12ft from Midspan
y, z and θ displacements at **Deck** 1/4 point (marked **B**)	Lift and Drag Displacements, as well as Deck Rotation at 225ft from Midspan
y, z and θ displacements at **Deck** other 1/4 point (marked **F**)	Lift and Drag Displacements, as well as Deck Rotation at 240ft from Midspan
Wind Speeds:	
Deck Level	Deck Height
Arch Level	Arch Crown Height

TABLE H2 SUMMARY OF TESTS FOR FULL BRIDGE AEROELASTIC MODEL, COMPLETED BRIDGE CONFIGURATION

Test File	Test No.	Flow condition	Existing bridge	Wind direction (Test angle)	V_{deck} (mph) Maximum wind speed at deck height	Vortex Peak Locations
IFA102	1	Bare tunnel floor (low turbulent flow)	No	Perpendicular to bridge (90°)	155	40 ~ 50 mph, 80 mph, 105 mph, 135 mph
ITA201	2	Hurricane profile	Yes	Perpendicular to bridge (90°)	142	40 ~ 50 mph
IFA201	3	Hurricane profile	No	Perpendicular to bridge (90°)	141	40 ~ 50 mph
IFB201	4	Hurricane profile	No	60° to the bridge	141	50 mph
IFC201	5	Hurricane profile	No	30° to the bridge	143	N/A
IFD201	6	Hurricane profile	No	Along the bridge (0°)	144	N/A
IFE201	7	Hurricane profile	No	Perpendicular to bridge (270°)	141	40 mph
IFA301	8	Open Country profile	Yes	Perpendicular to bridge (90°)	143	40 mph
IFA302	9	Open Country profile	No	Perpendicular to bridge (90°)	143	40 mph
IFB302	10	Open Country profile	No	60° to the bridge	141	N/A
IFC302	11	Open Country profile	No	30° to the bridge	146	N/A
IFD302	12	Open Country profile	No	Along the bridge (0°)	145	N/A
IFE302	13	Open Country profile	No	Perpendicular to bridge (270°)	144	40 mph
IFA303	14	Open Country Profile (higher arch damping)	No	Perpendicular to bridge (90°)	144	N/A
IFA402	15	Smooth Flow (bridge elevated)	No	Perpendicular to bridge (90°)	148	45 mph, 80 mph, 110 mph, 140 mph

TABLE H3 SUMMARY OF FULL BRIDGE MODEL PROPERTIES, COMPLETED BRIDGE CONFIGURATION

	Symmetric				**Anti-symmetric**
	Deck Lateral (Drag)	Deck Vertical (Lift)	Deck Torsion	Arch Lateral (Drag)	Deck Vertical (Lift)
Model Frequency (Hz)	11.3	12.8	13.7	2.3	7.5
Model Damping (% of critical)	0.69%	0.49%	0.18%	0.22%	0.25%
Increased Arch Lateral Damping (% of critical)				0.70%	

TABLE H4 SUMMARY OF TURBULENCE INTENSITIES (IN TEST AND TARGET VALUES)

		Hurricane Exposure (Zo=0.025ft)		Open Country Exposure (Zo=0.1ft)		Bare Tunnel Floor	Smooth Flow
Height		**Longitudinal Turbulence**	**Vertical Turbulence**	**Longitudinal Turbulence**	**Vertical Turbulence**	**Longitudinal Turbulence**	**Longitudinal Turbulence**
Deck Height (55 ft)	Values in Test	15.0%	6.2%	18.2%	8.3%	7.2%	1.7%
	Target Values from ESDU	14.7%	6.3%	17.8%	7.6%	N/A	N/A
Arch Crown (270ft)	Values in Test	12.2%	5.5%	14.5%	7.8%	1.7%	1.7%
	Target Values from ESDU	11.8%	5.3%	13.4%	6.2%	N/A	N/A

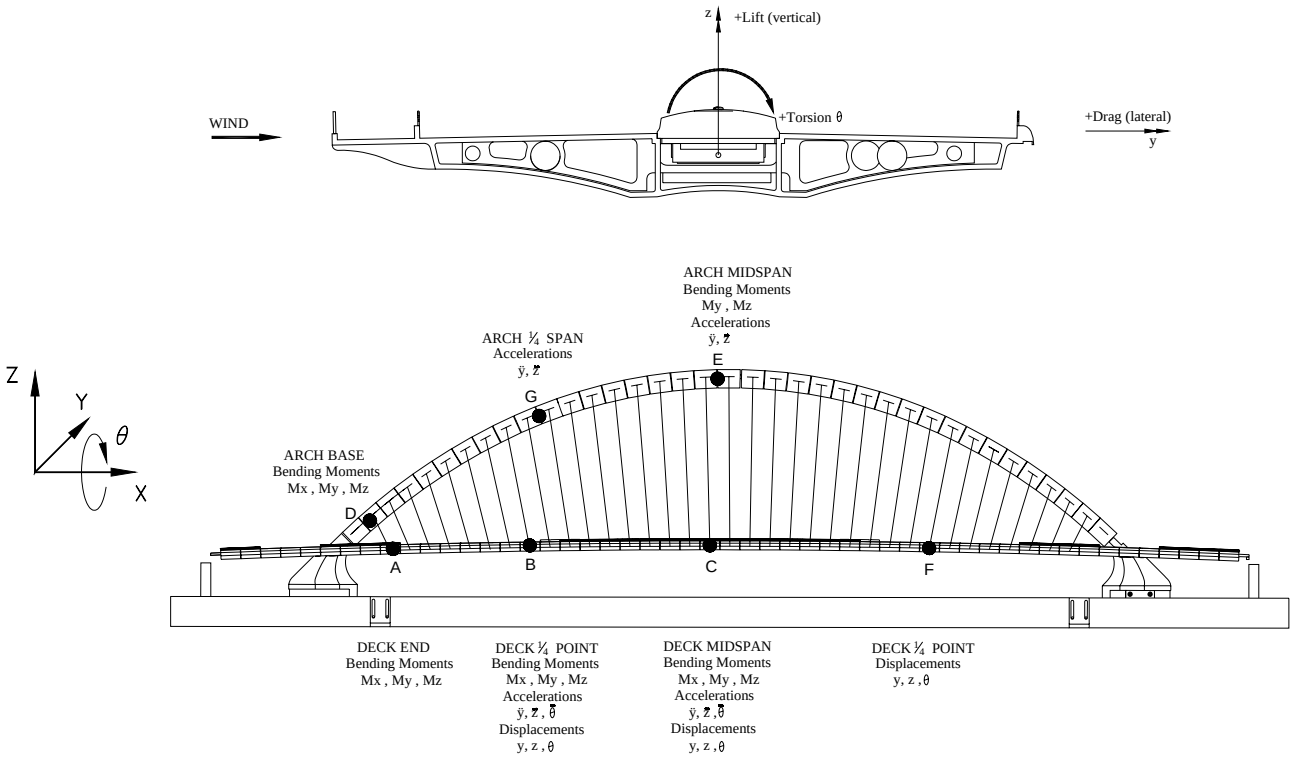

FIGURE H1 BRIDGE SIGN CONVENTION AND INSTRUMENTATION LOCATIONS, COMPLETED BRIDGE

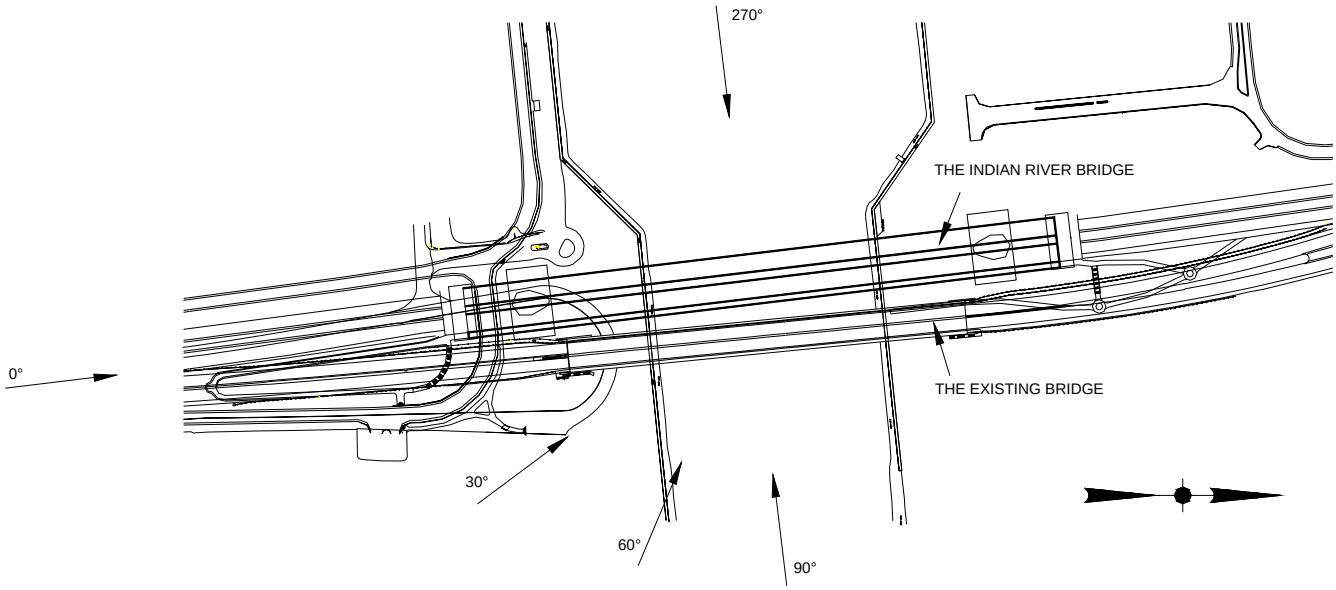

WIND DIRECTION DEFINITION

FIGURE H2 WIND ANGLES DEFINED IN WIND TUNNEL TESTS

May 21, 2004
Data File =ifa102.mst
Information File =ifa102.inf

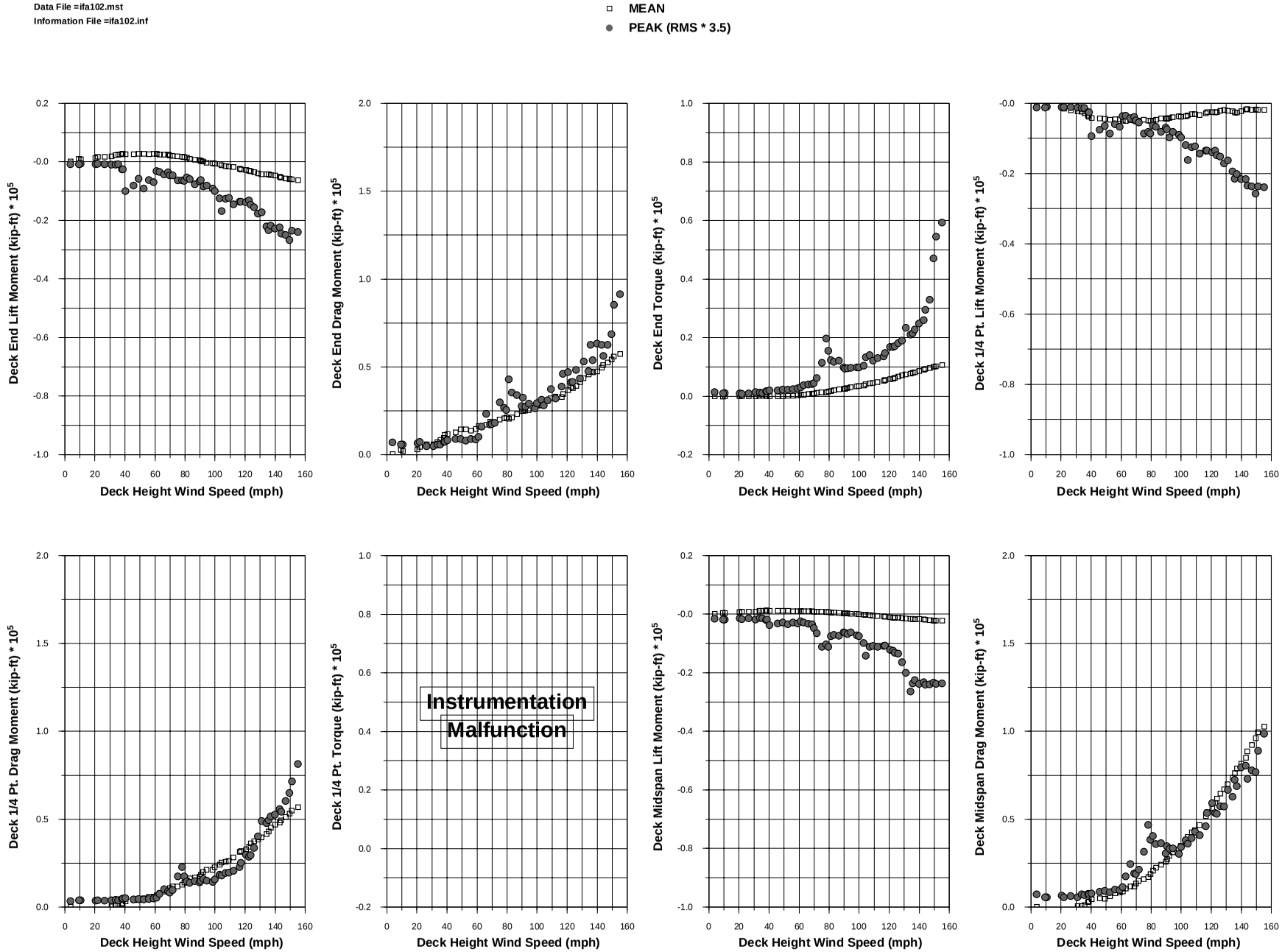

Indian River Bridge, bare tunnel floor, wind perpendicular to deck (90 degrees)

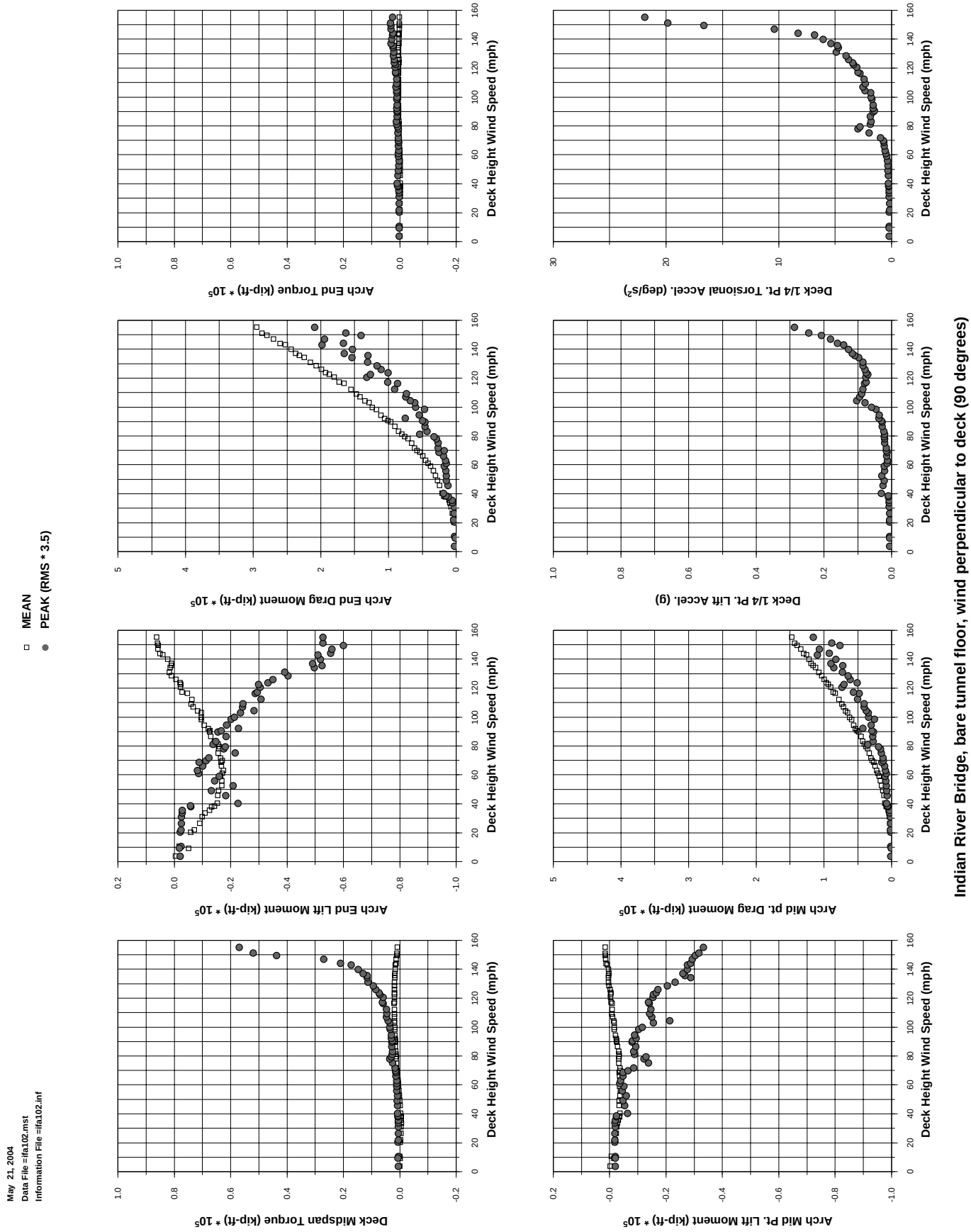

Indian River Bridge, bare tunnel floor, wind perpendicular to deck (90 degrees)

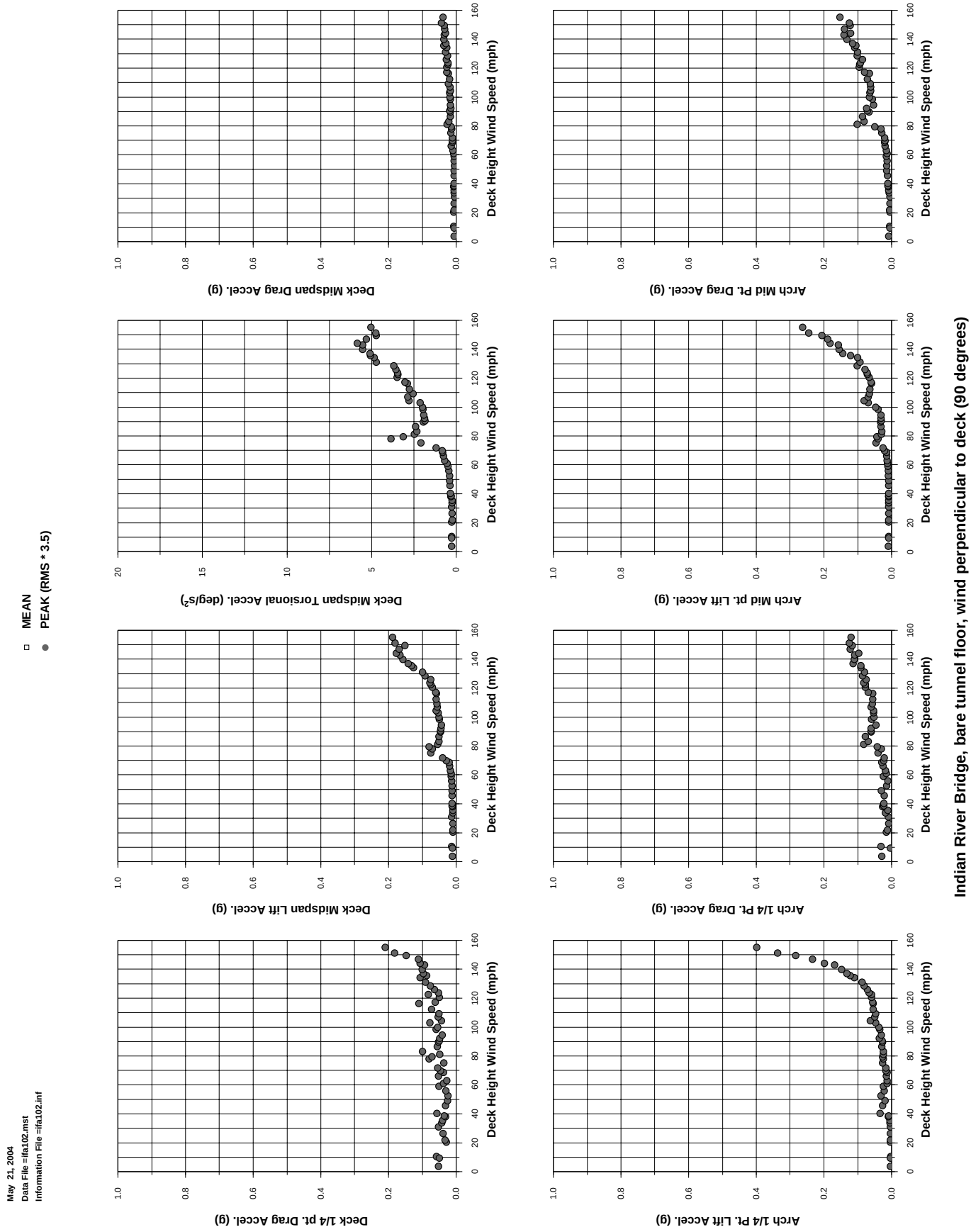

Indian River Bridge, bare tunnel floor, wind perpendicular to deck (90 degrees)

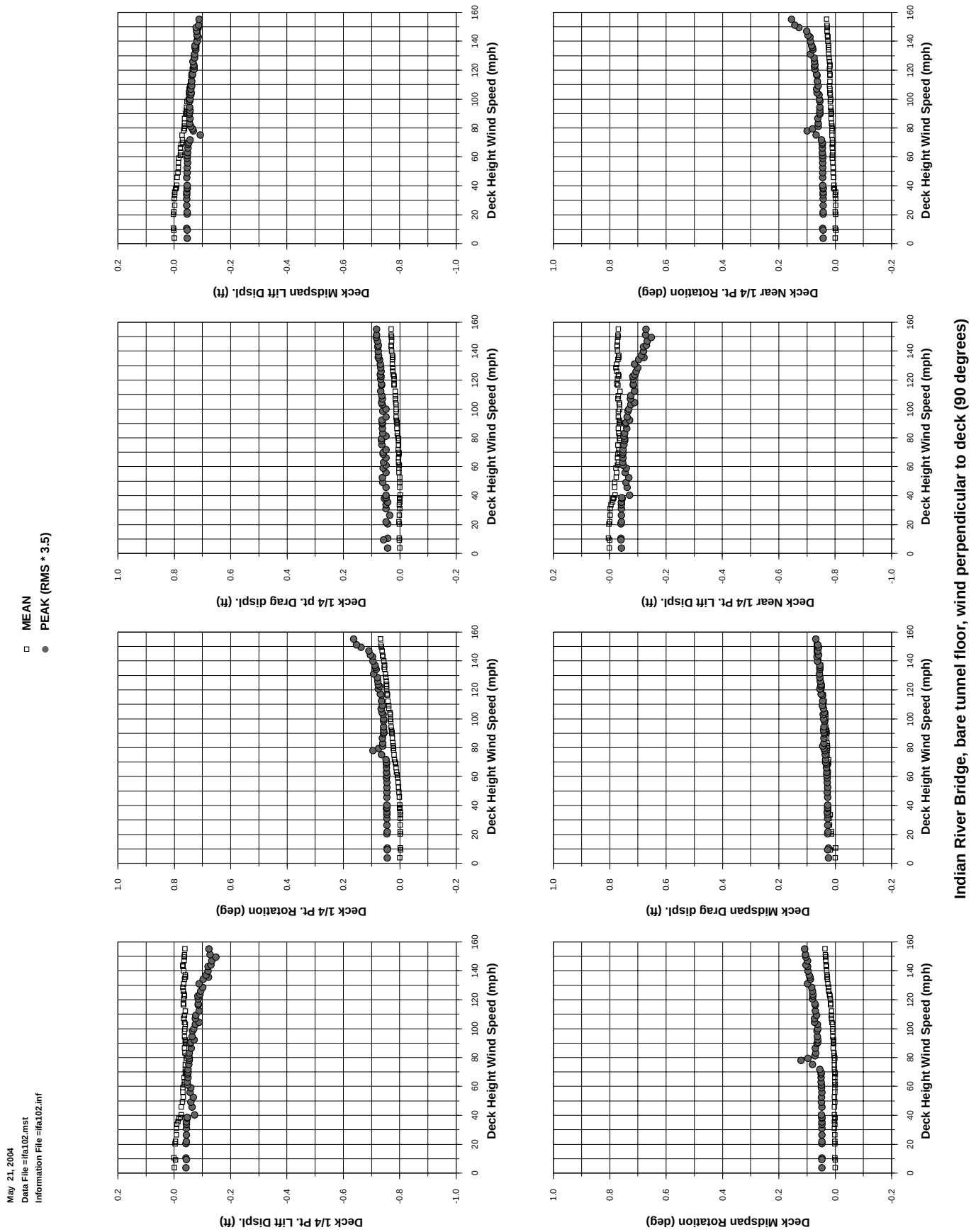

Indian River Bridge, bare tunnel floor, wind perpendicular to deck (90 degrees)

May 21, 2004
Data File =ifa102.mst
Information File =ifa102.inf

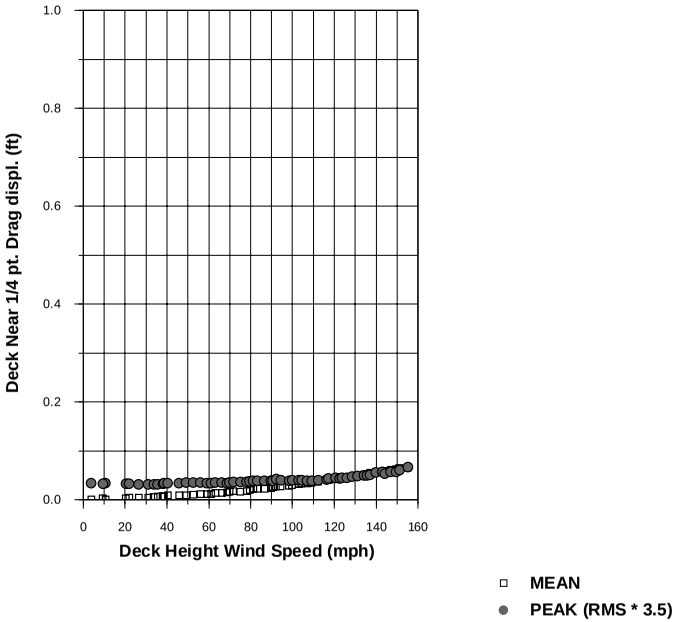

Indian River Bridge, bare tunnel floor, wind perpendicular to deck (90 degrees)

May 25, 2004
Data File =ita201.mst
Information File =ita201.inf

MEAN
PEAK (RMS * 3.5)

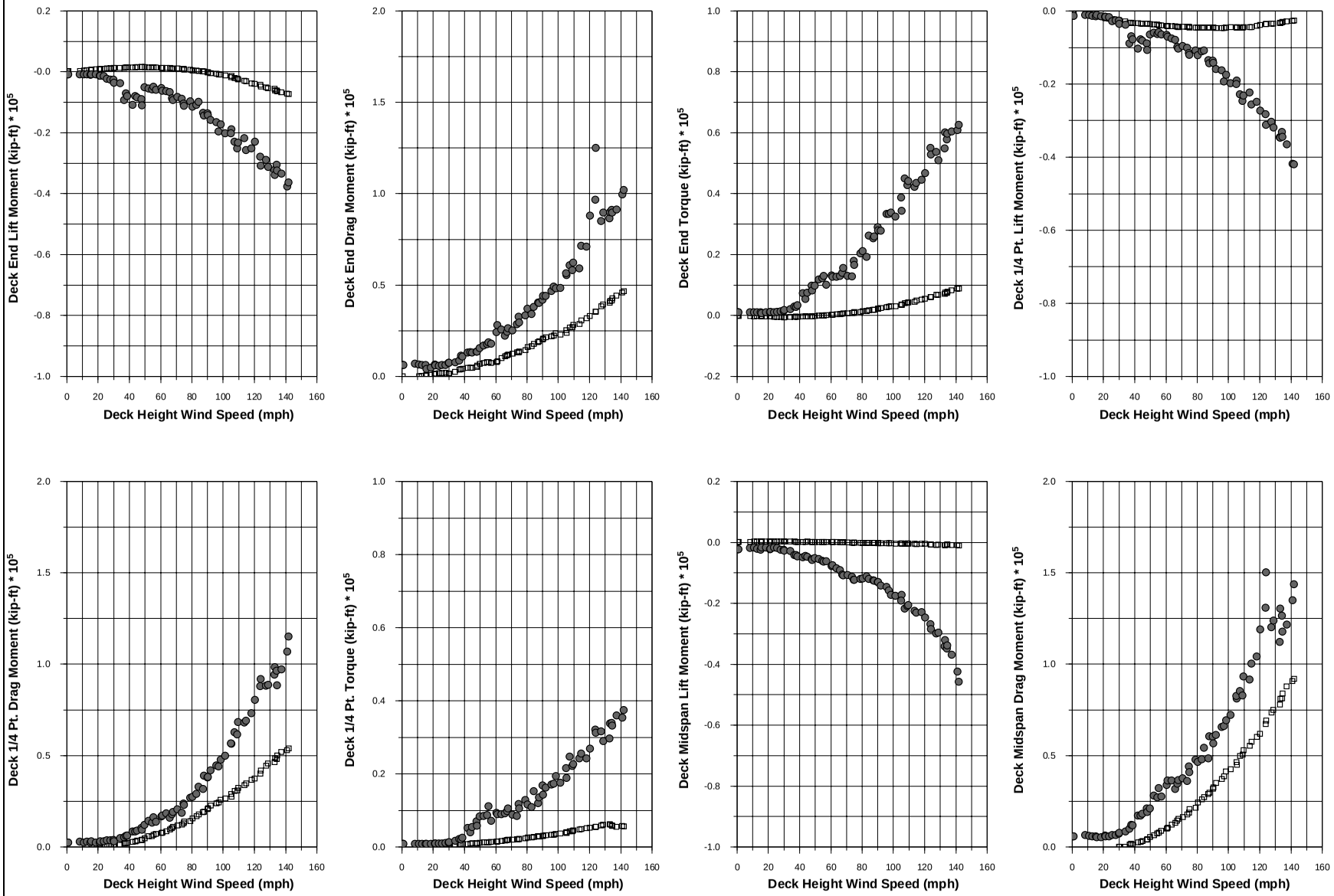

Indian River Bridge, hurricane profile with existing bridge upstream, wind perpendicular to deck (90 degrees)

May 25, 2004
Data File =ita201.mst
Information File =ita201.inf

MEAN
PEAK (RMS * 3.5)

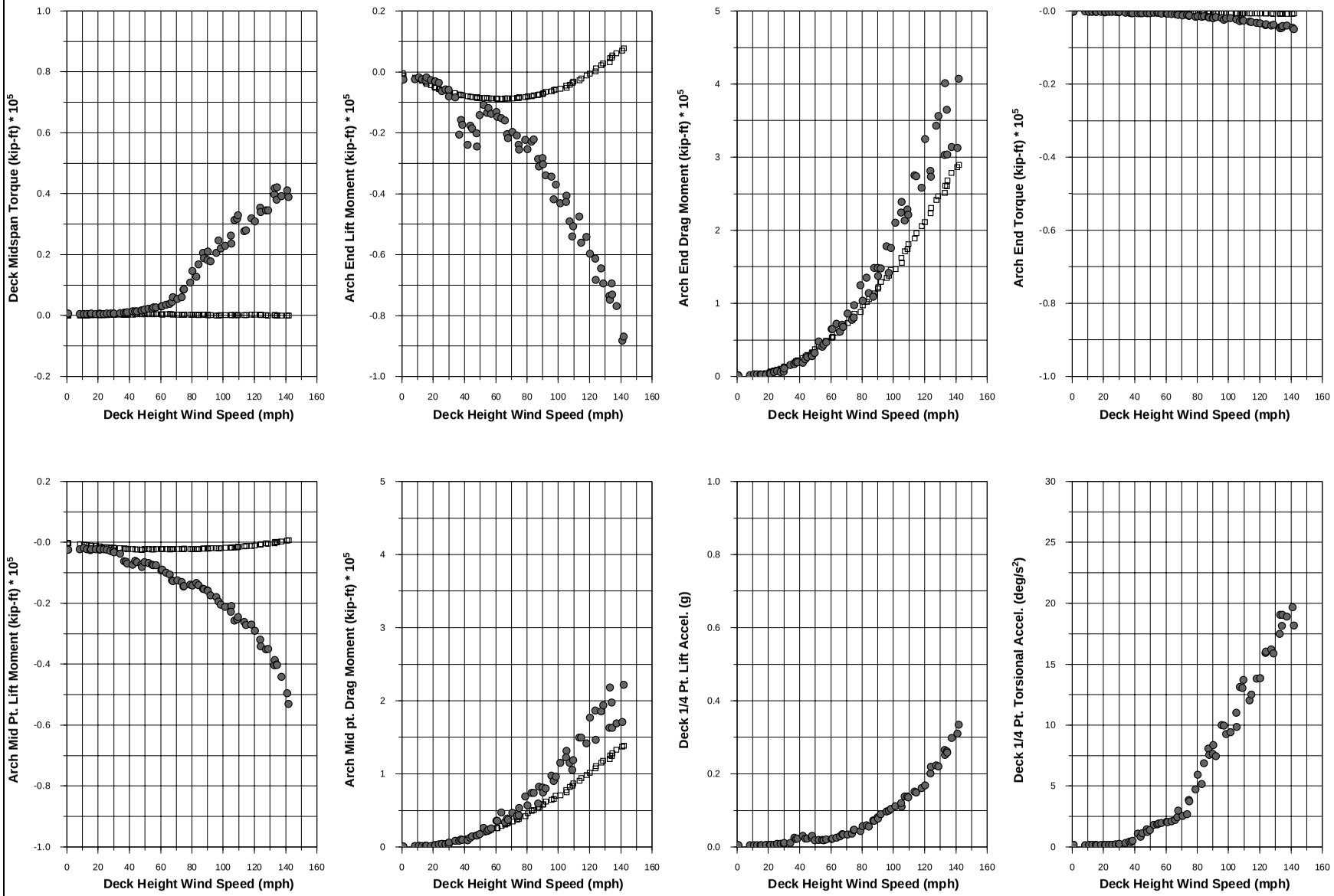

Indian River Bridge, hurricane profile with existing bridge upstream, wind perpendicular to deck (90 degrees)

May 25, 2004
Data File =ita201.mst
Information File =ita201.inf

MEAN
PEAK (RMS * 3.5)

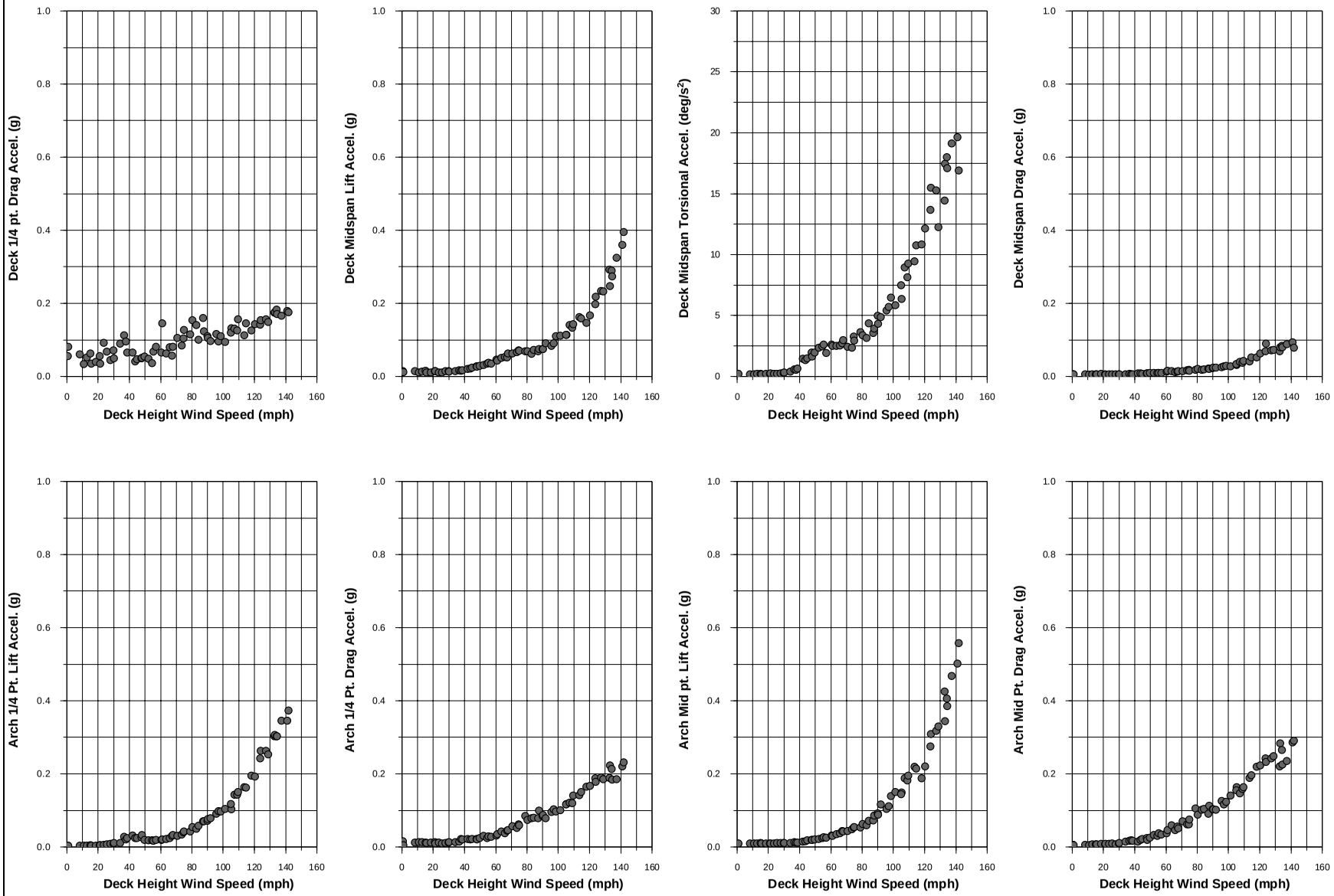

Indian River Bridge, hurricane profile with existing bridge upstream, wind perpendicular to deck (90 degrees)

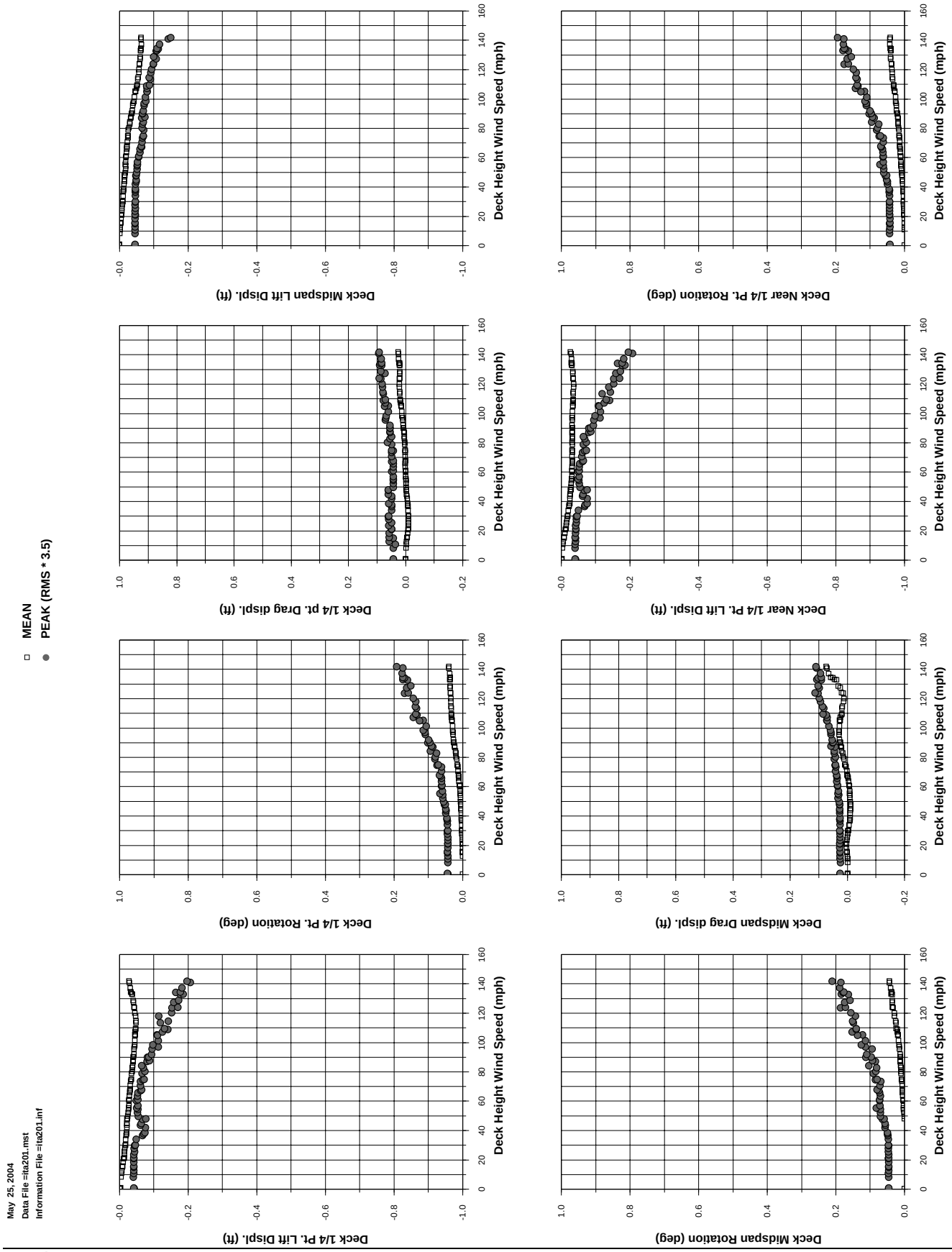

Indian River Bridge, hurricane profile with existing bridge upstream, wind perpendicular to deck (90 degrees)

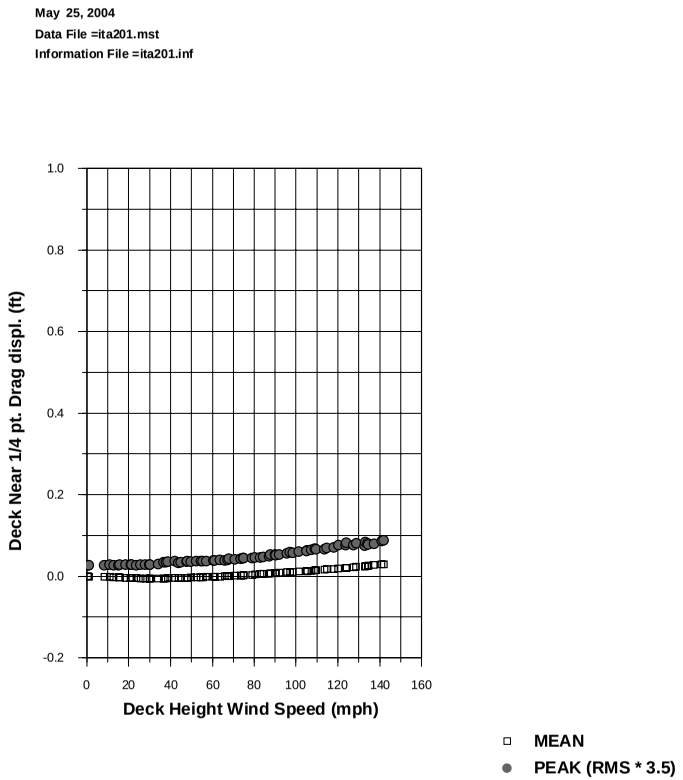

Indian River Bridge, hurricane profile with existing bridge upstream, wind perpendicular to deck (90 degrees)

May 25, 2004
Data File =ifa201.mst
Information File =ifa201.inf

MEAN
PEAK (RMS * 3.5)

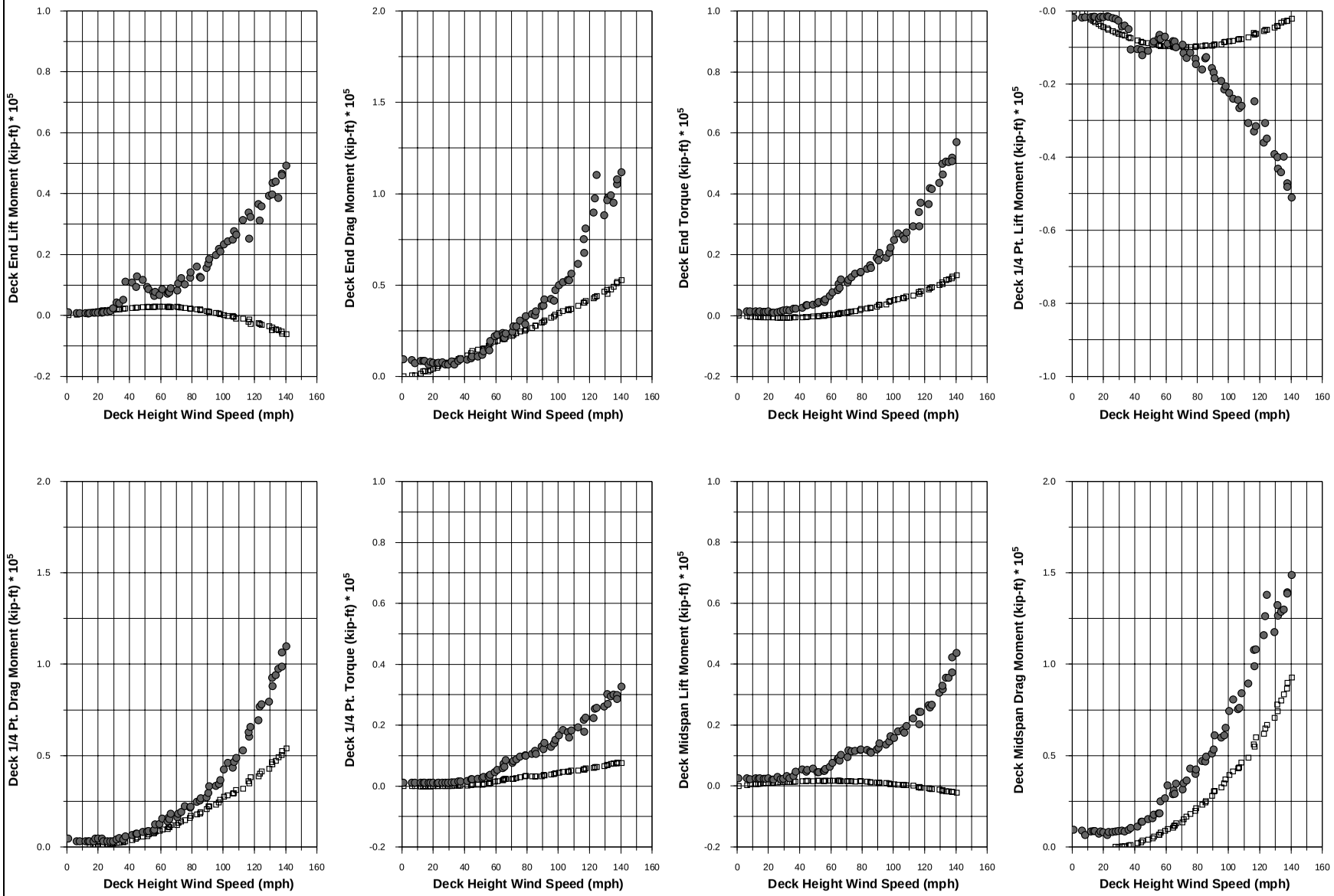

Indian River Bridge, hurricane profile without existing bridge, wind perpendicular to deck (90 degrees)

May 25, 2004
Data File =ifa201.mst
Information File =ifa201.inf

MEAN
PEAK (RMS * 3.5)

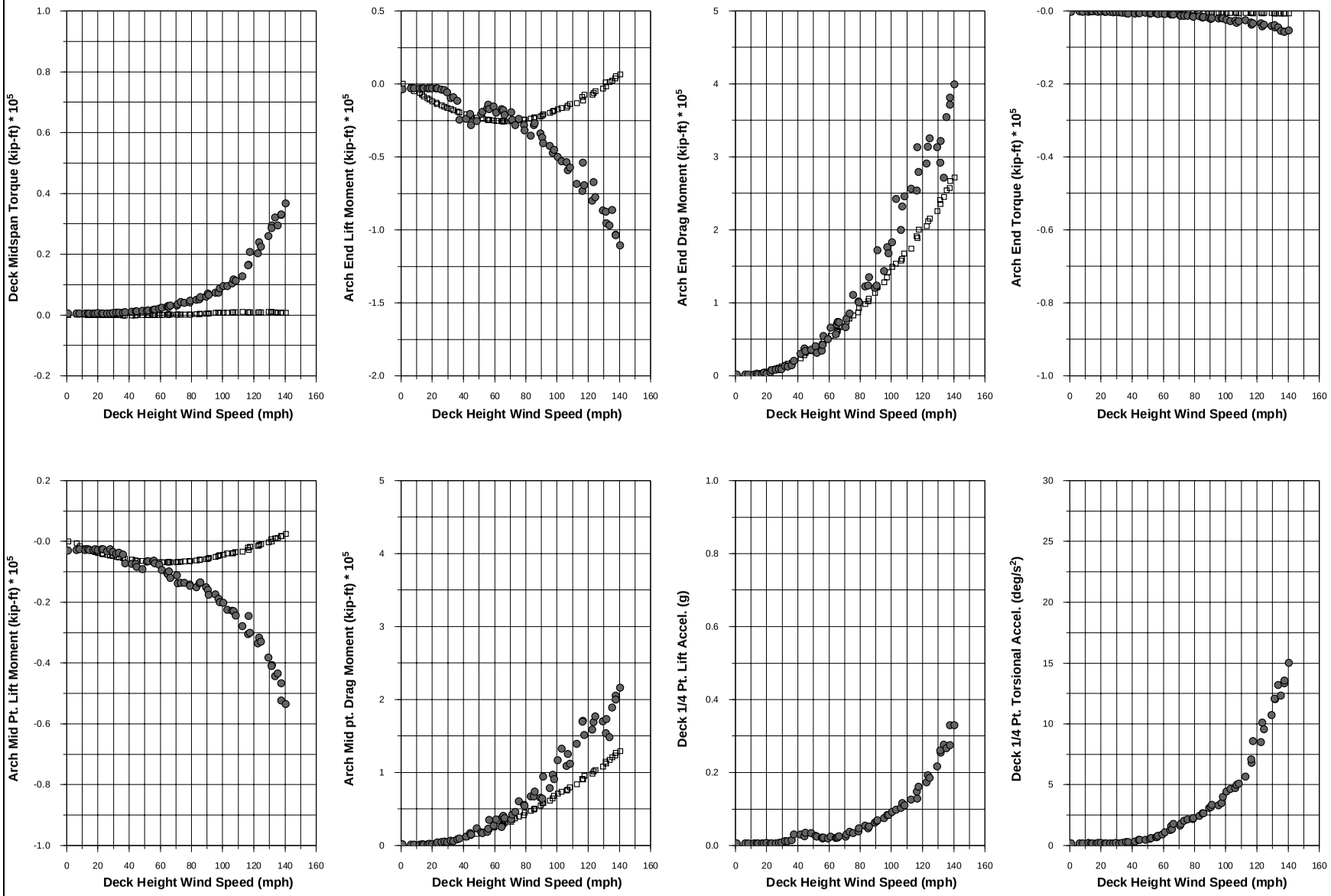

Indian River Bridge, hurricane profile without existing bridge, wind perpendicular to deck (90 degrees)

May 25, 2004
Data File =ifa201.mst
Information File =ifa201.inf

MEAN
PEAK (RMS * 3.5)

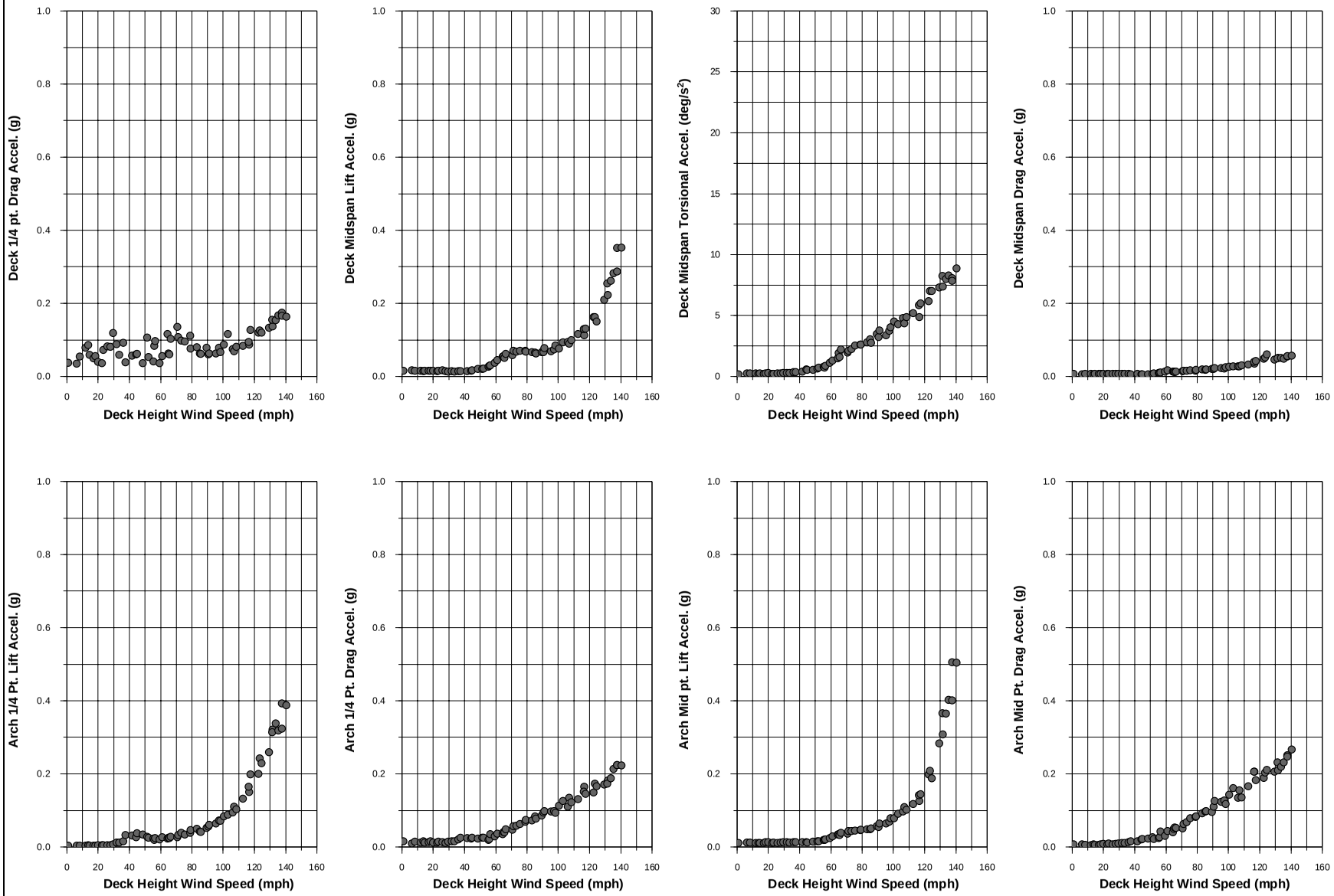

Indian River Bridge, hurricane profile without existing bridge, wind perpendicular to deck (90 degrees)

May 25, 2004
Data File =ifa201.mst
Information File =ifa201.inf

MEAN
PEAK (RMS * 3.5)

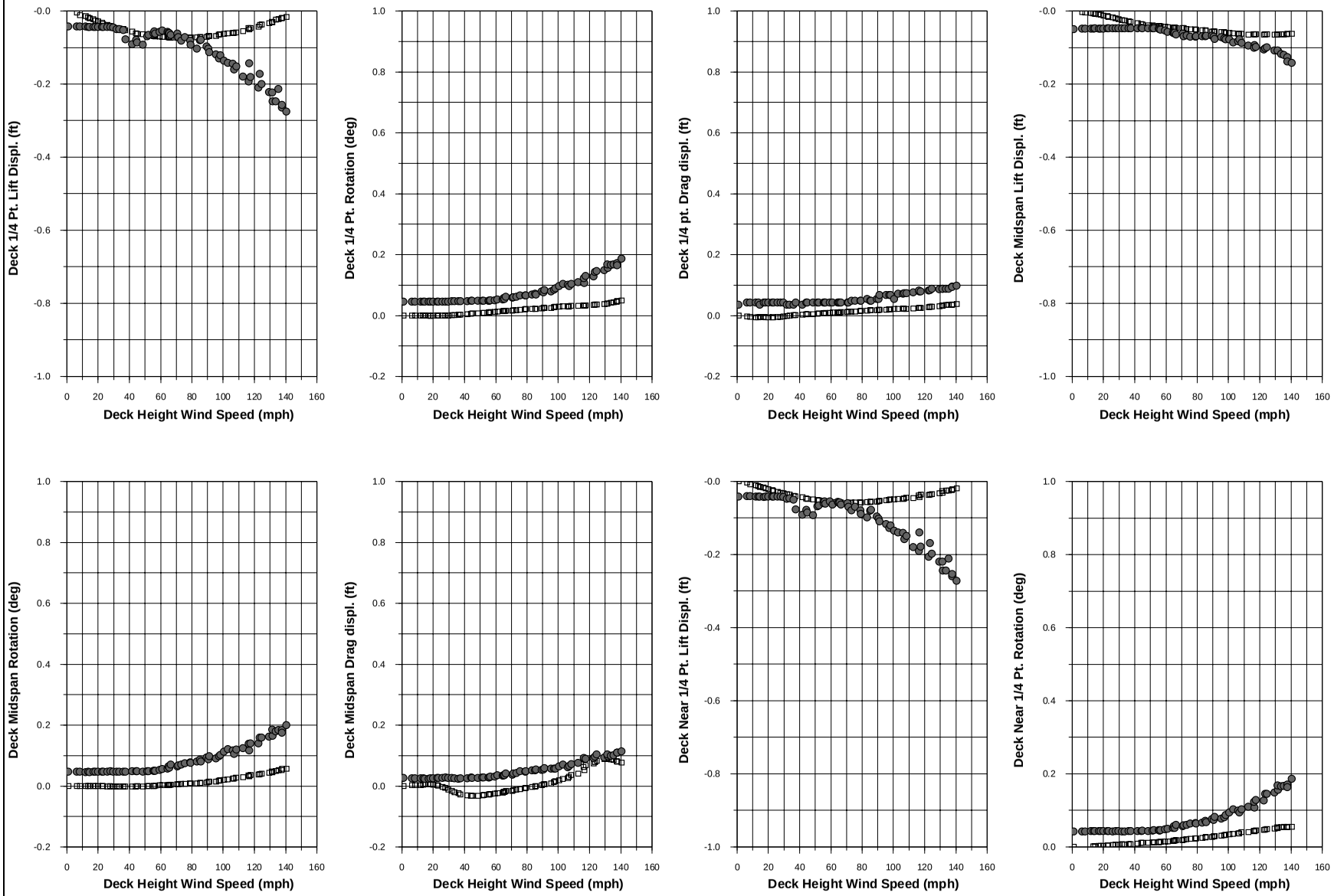

Indian River Bridge, hurricane profile without existing bridge, wind perpendicular to deck (90 degrees)

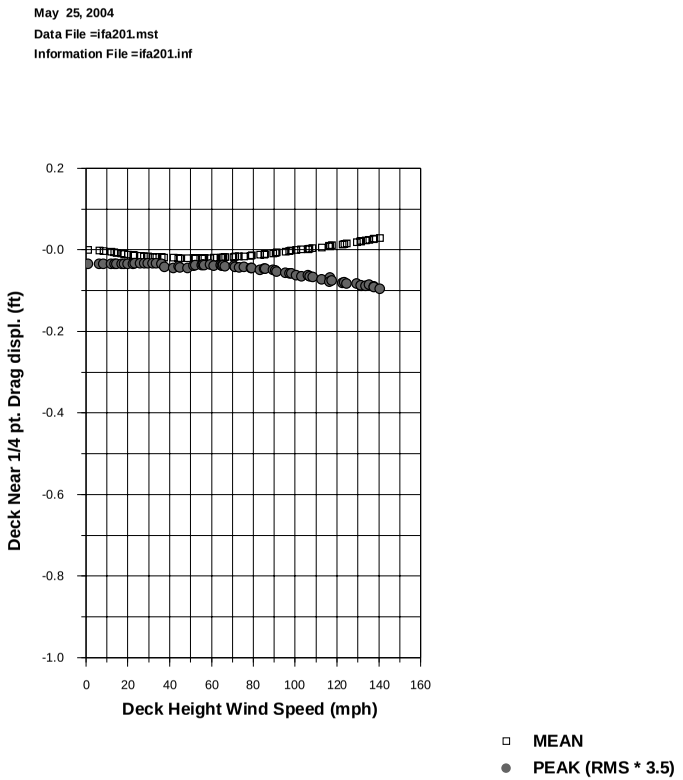

Indian River Bridge, hurricane profile without existing bridge, wind perpendicular to deck (90 degrees)

May 25, 2004
Data File =ifb201.mst
Information File =ifb201.inf

MEAN
PEAK (RMS * 3.5)

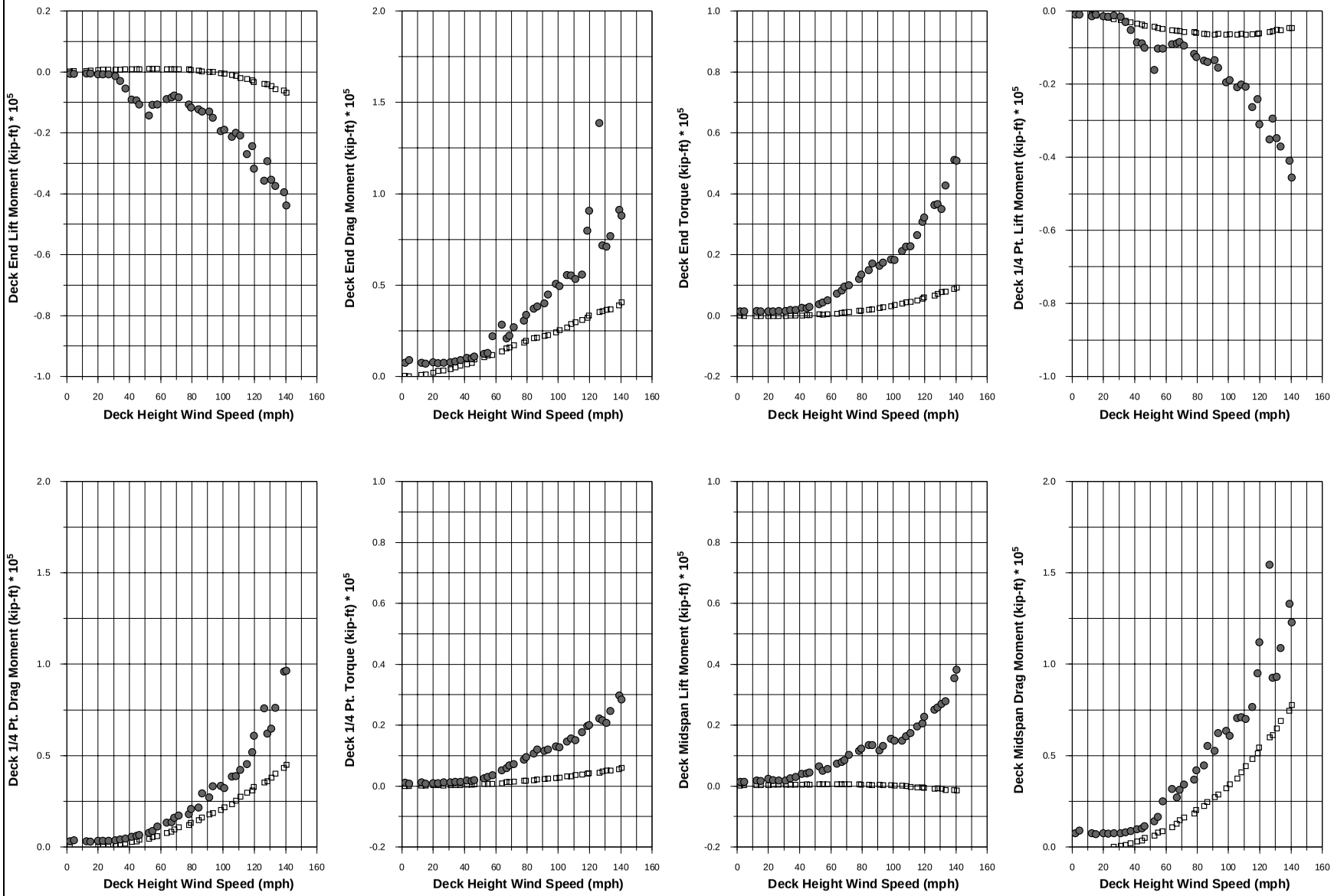

Indain River Bridge, hurricane profile, wind at 60 degrees to deck

May 25, 2004
Data File =ifb201.mst
Information File =ifb201.inf

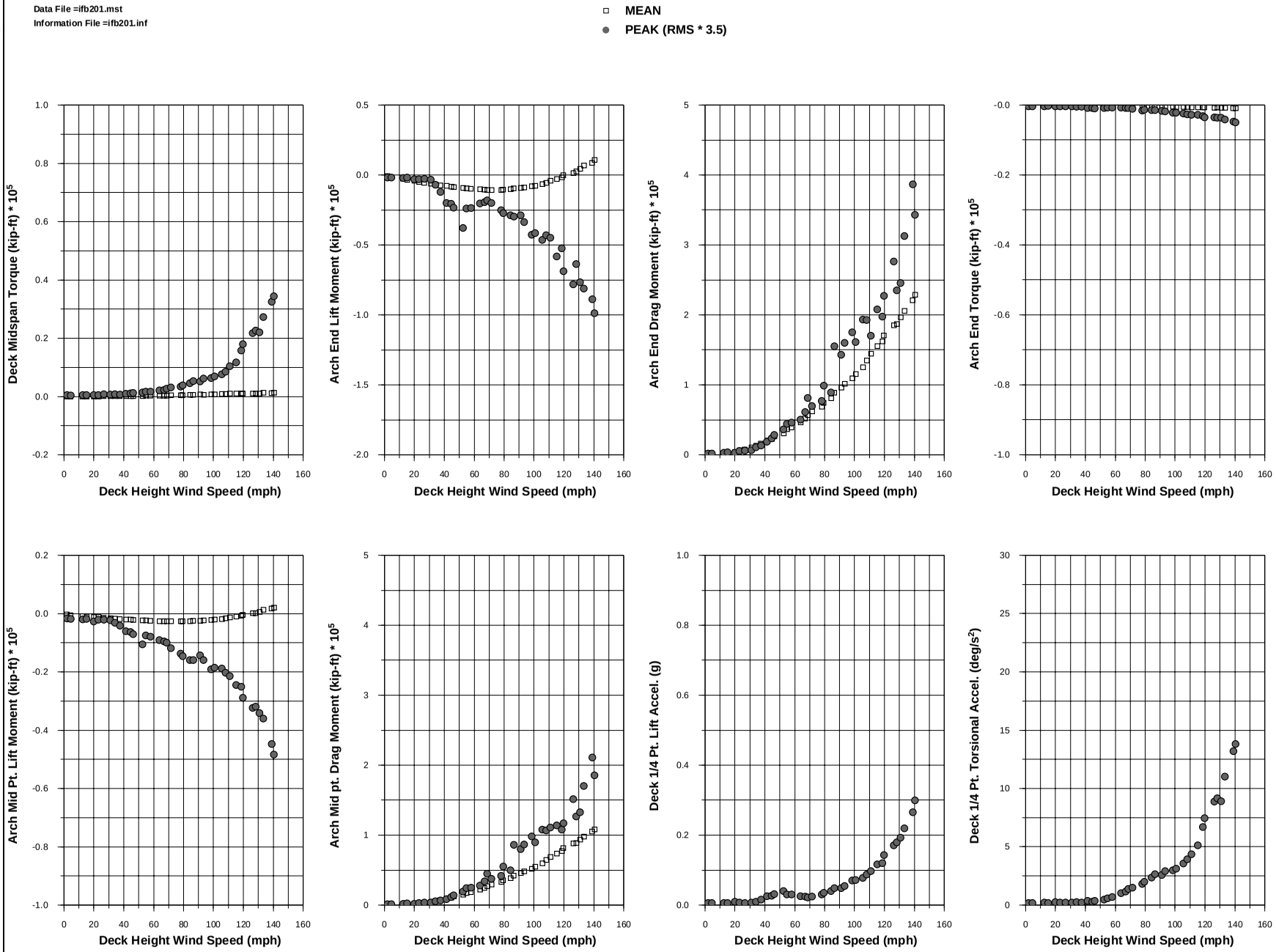

Indain River Bridge, hurricane profile, wind at 60 degrees to deck

May 25, 2004
Data File =ifb201.mst
Information File =ifb201.inf

MEAN
PEAK (RMS * 3.5)

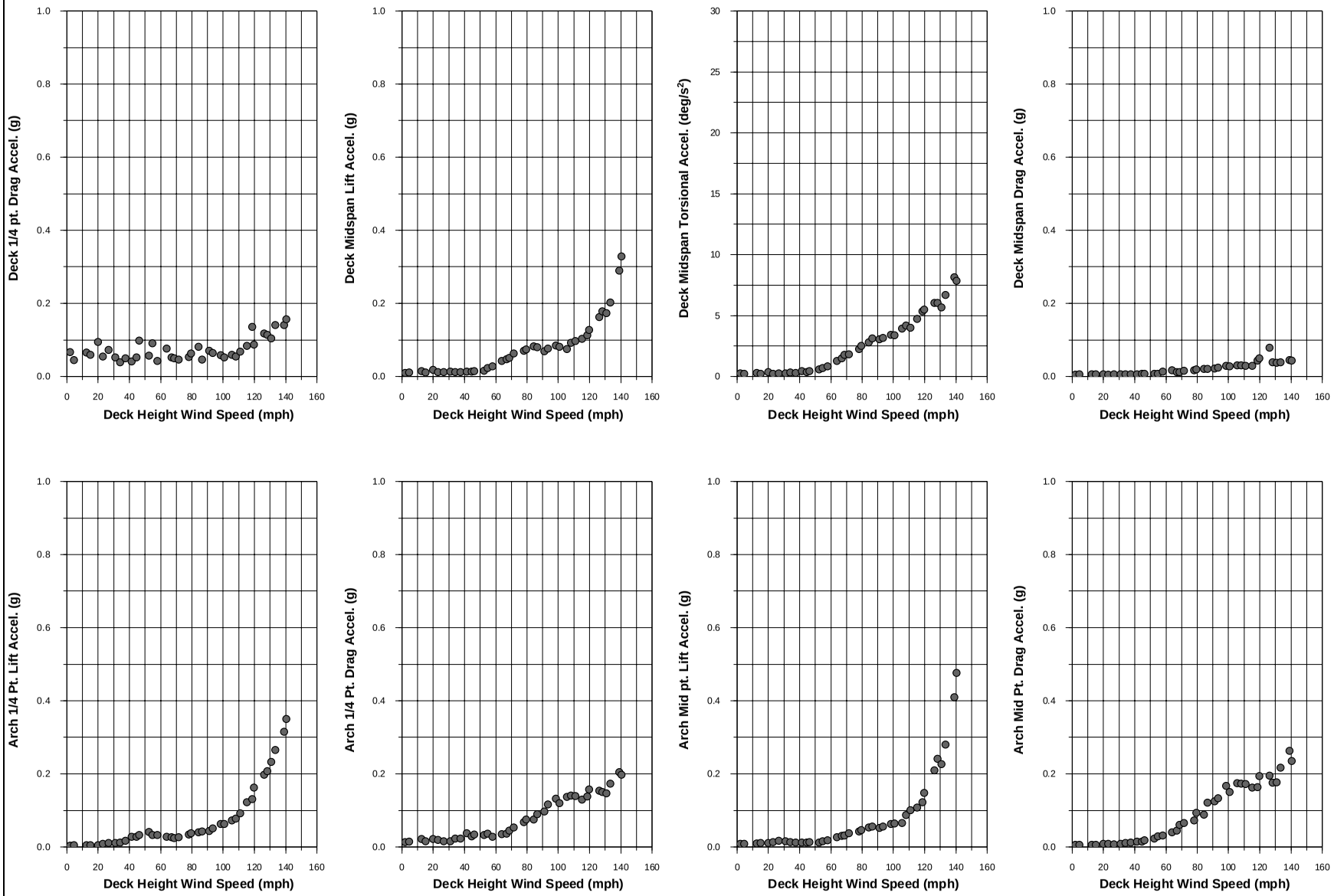

Indain River Bridge, hurricane profile, wind at 60 degrees to deck

May 25, 2004
Data File =ifb201.mst
Information File =ifb201.inf

MEAN
PEAK (RMS * 3.5)

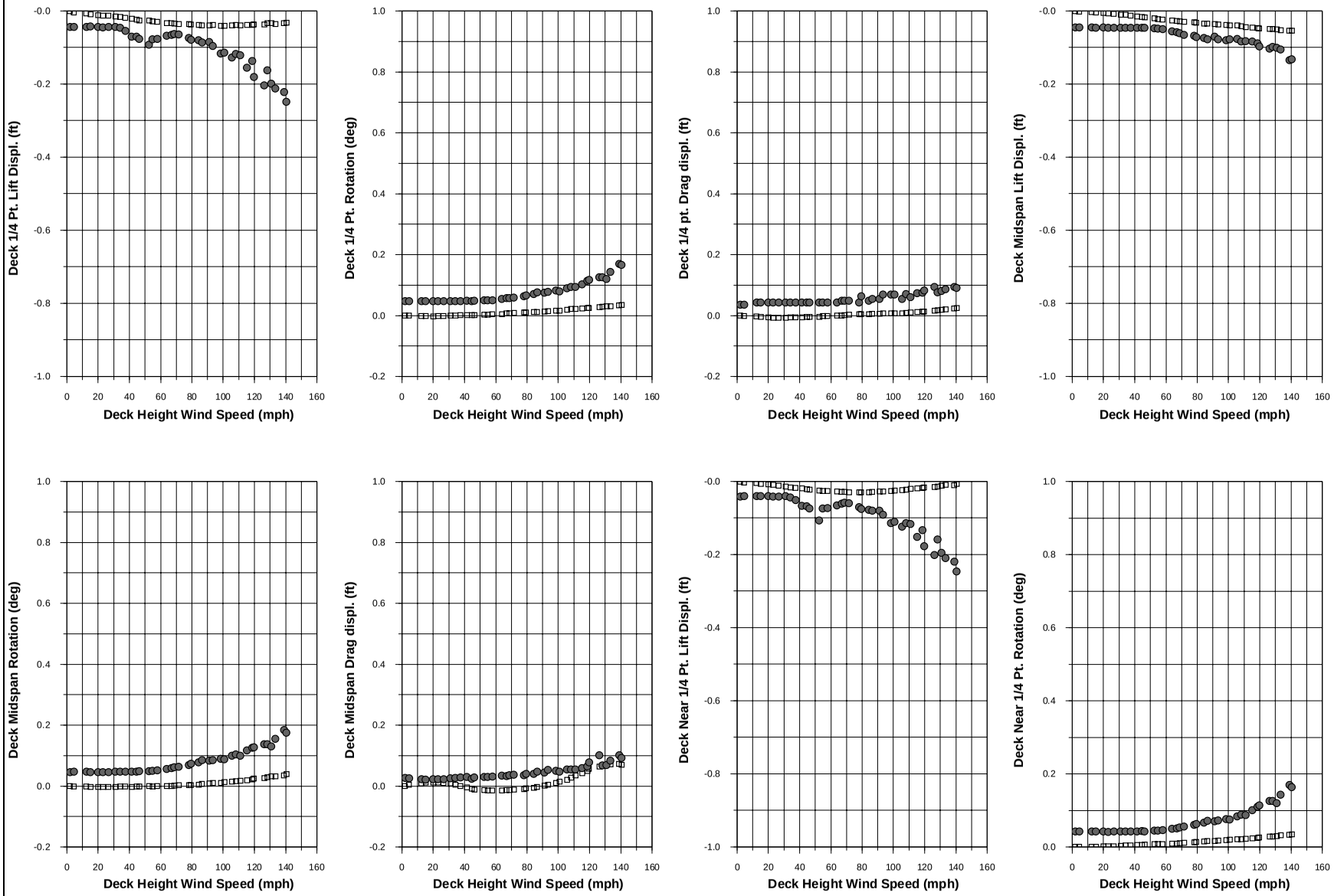

Indain River Bridge, hurricane profile, wind at 60 degrees to deck

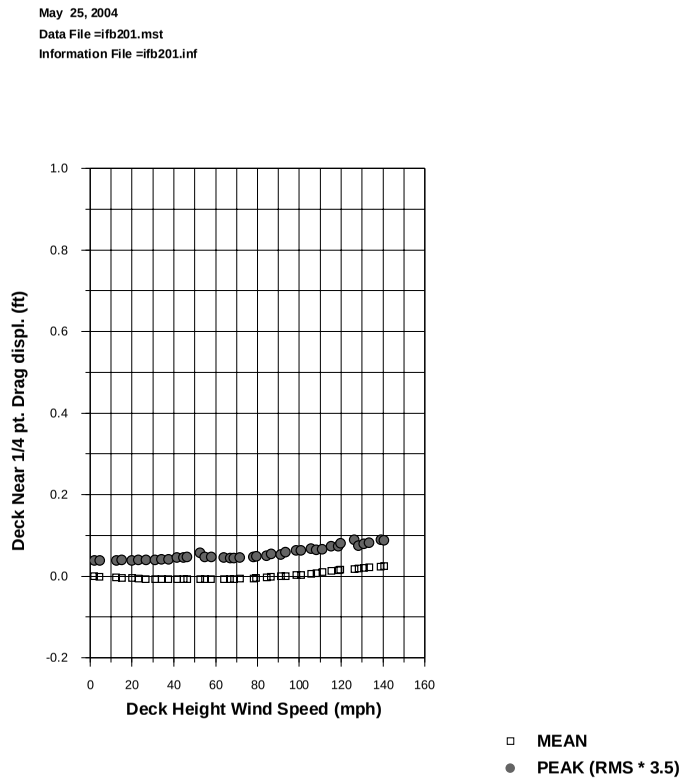

Indain River Bridge, hurricane profile, wind at 60 degrees to deck

May 25, 2004
Data File =ifc201.mst
Information File =ifc201.inf

MEAN
PEAK (RMS * 3.5)

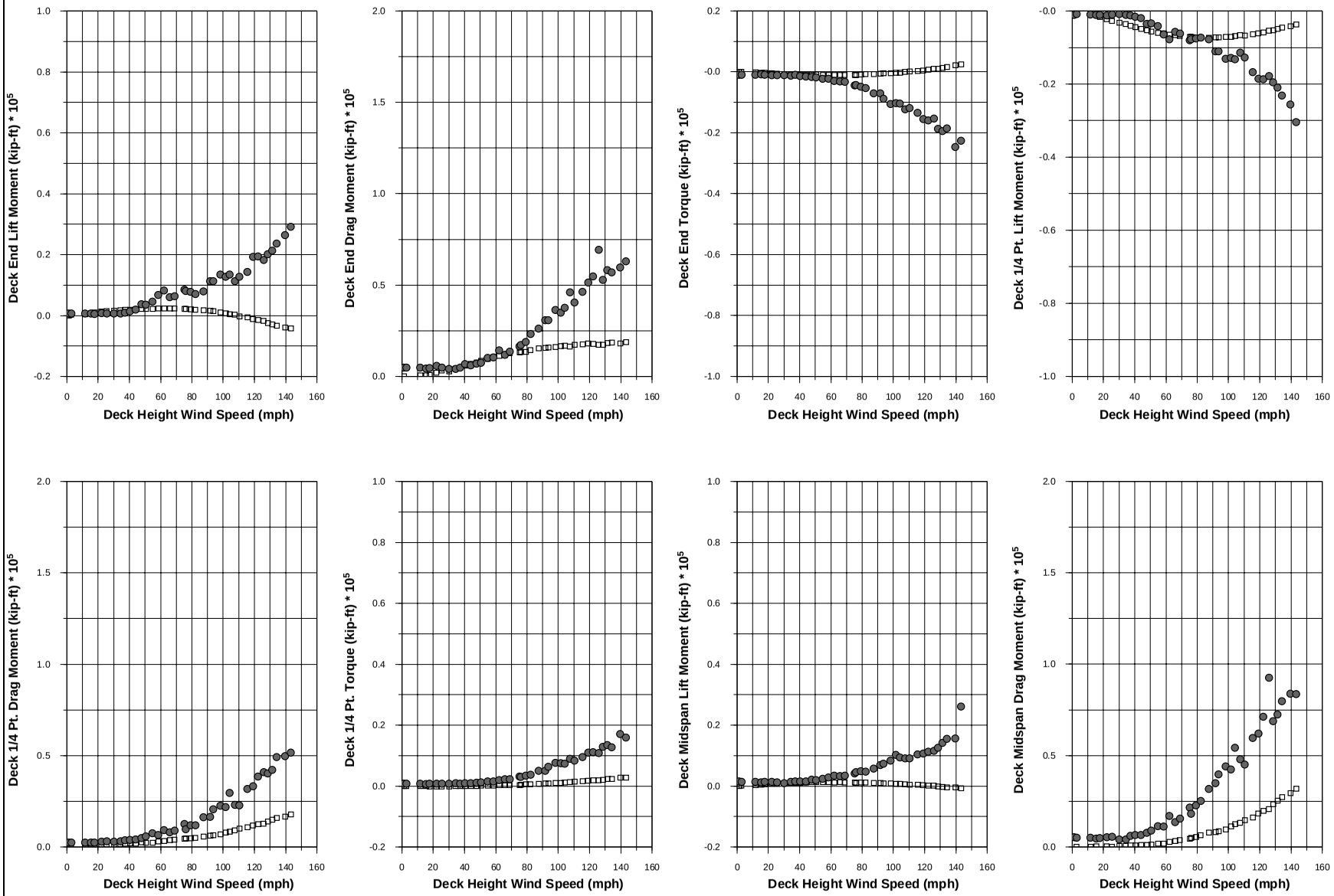

Indian River Bridge, hurricane profile, wind at 30 degrees to deck

May 25, 2004
Data File =ifc201.mst
Information File =ifc201.inf

MEAN
PEAK (RMS * 3.5)

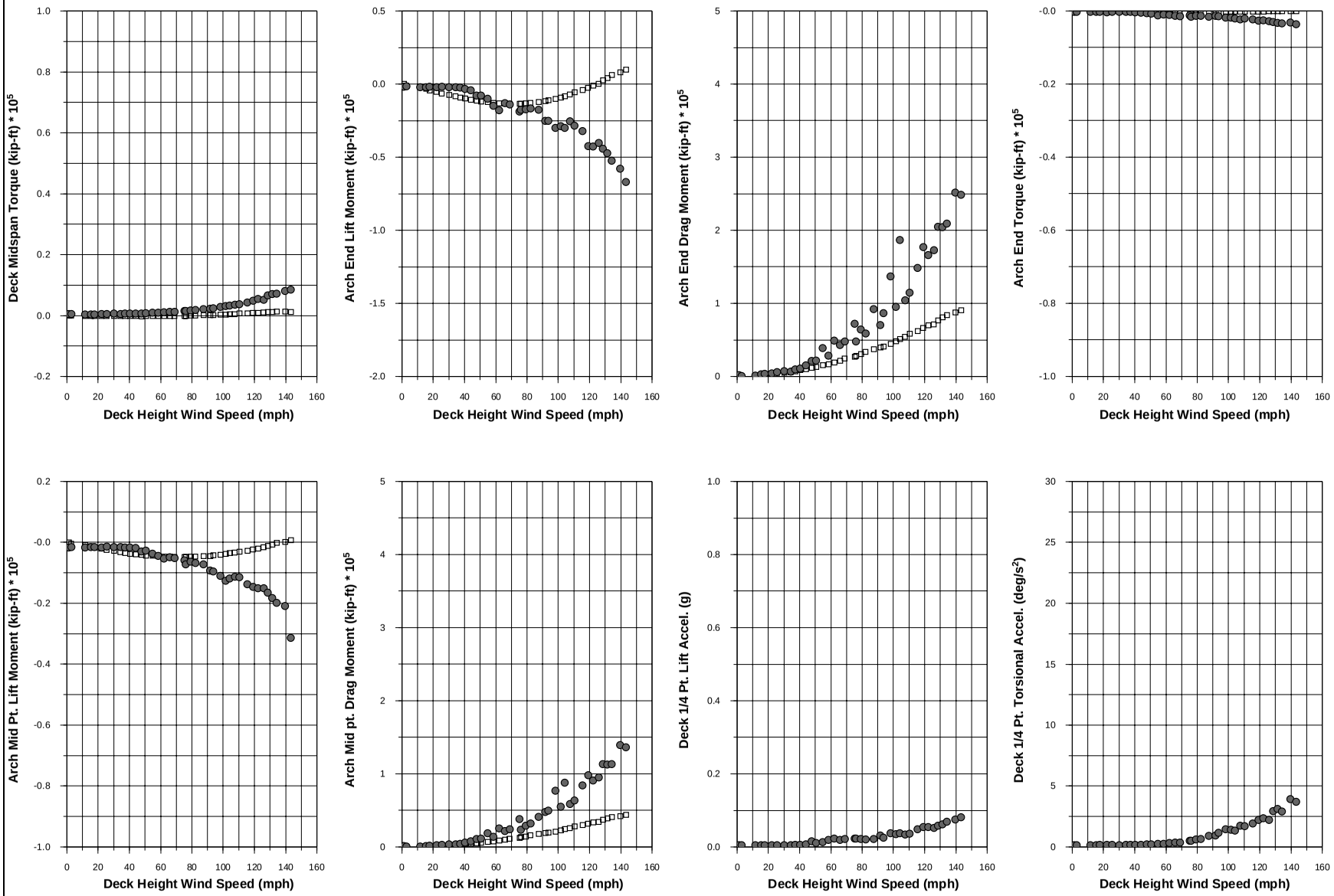

Indian River Bridge, hurricane profile, wind at 30 degrees to deck

May 25, 2004
Data File =ifc201.mst
Information File =ifc201.inf

MEAN
PEAK (RMS * 3.5)

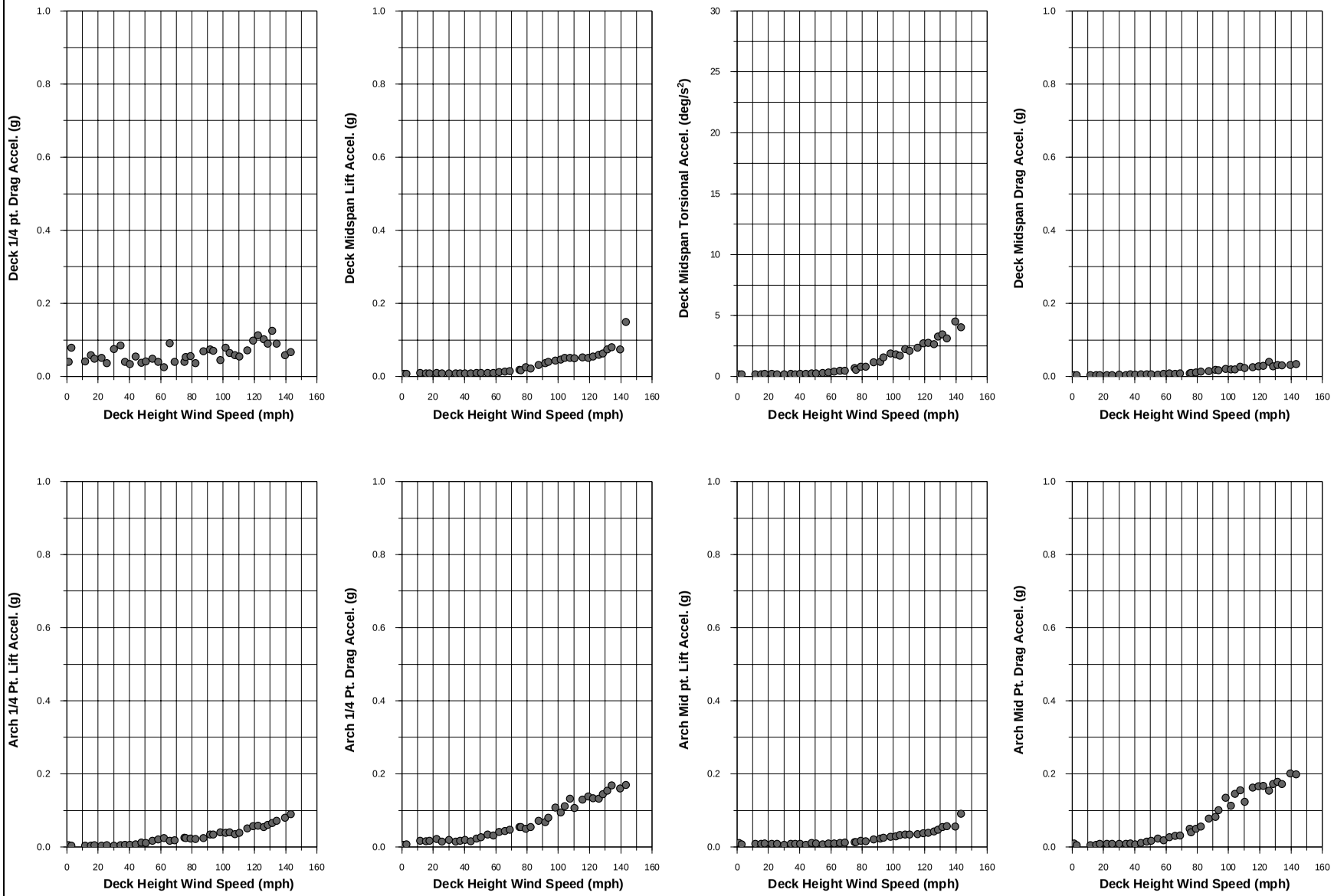

Indian River Bridge, hurricane profile, wind at 30 degrees to deck

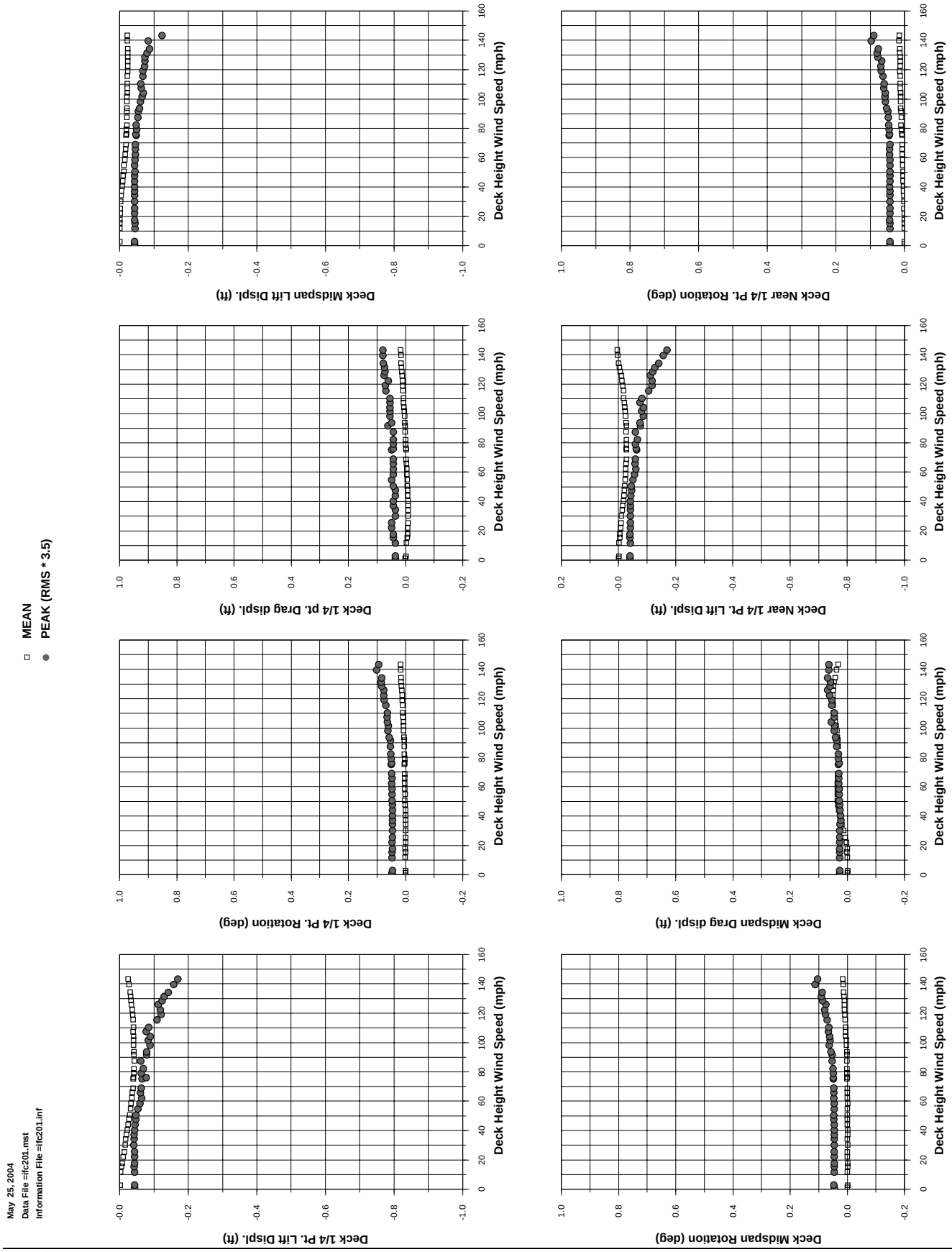

Indian River Bridge, hurricane profile, wind at 30 degrees to deck

May 25, 2004
Data File =ifc201.mst
Information File =ifc201.inf

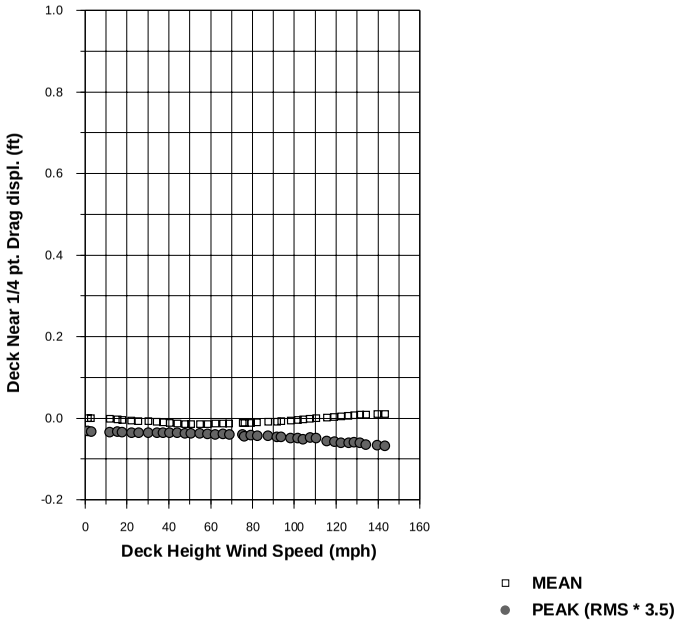

Indian River Bridge, hurricane profile, wind at 30 degrees to deck

May 25, 2004
Data File =ifd201.mst
Information File =ifd201.inf

MEAN
PEAK (RMS * 3.5)

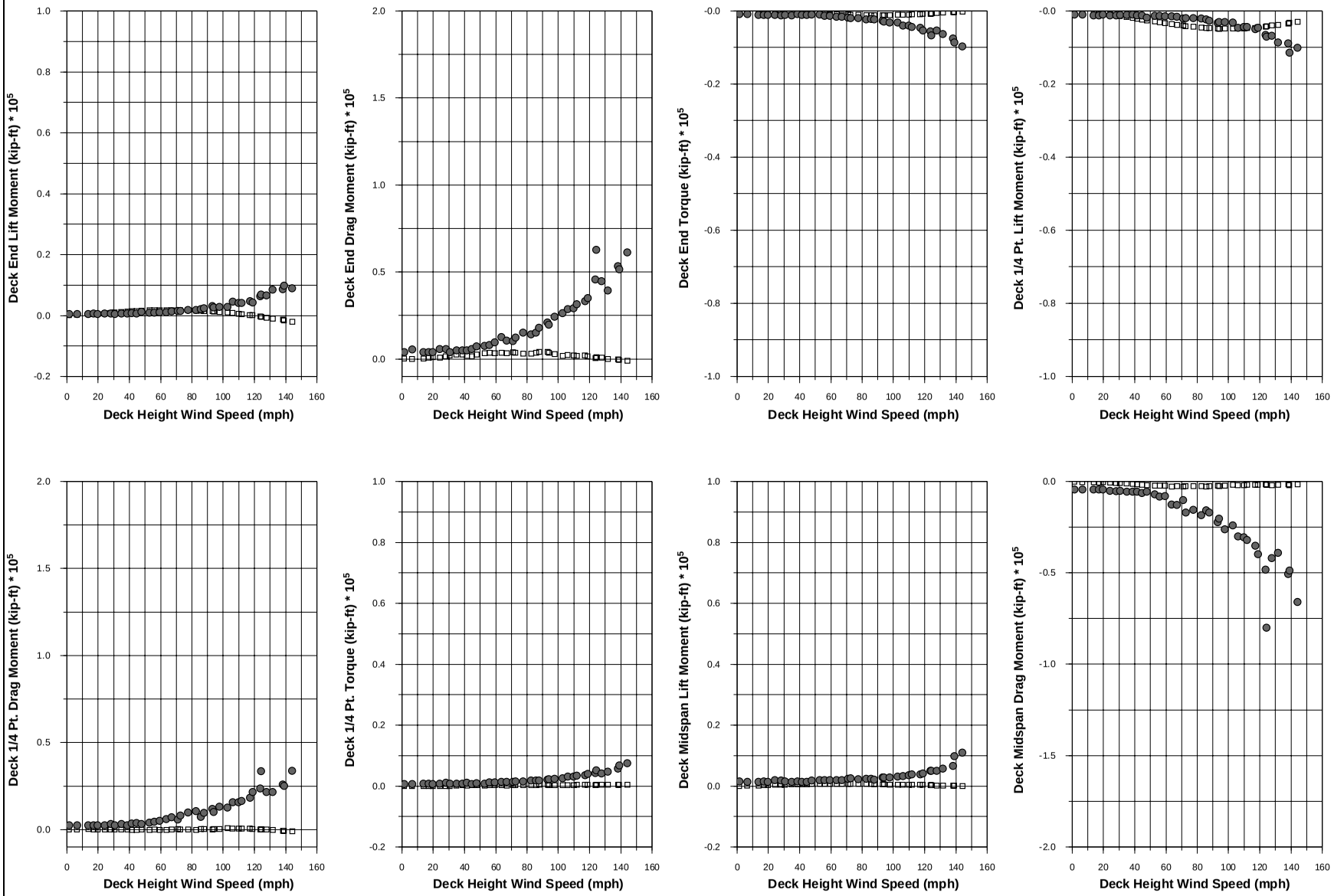

Indian River Bridge, hurricane profile, wind along the deck (0 degree)

May 25, 2004
Data File =ifd201.mst
Information File =ifd201.inf

MEAN
PEAK (RMS * 3.5)

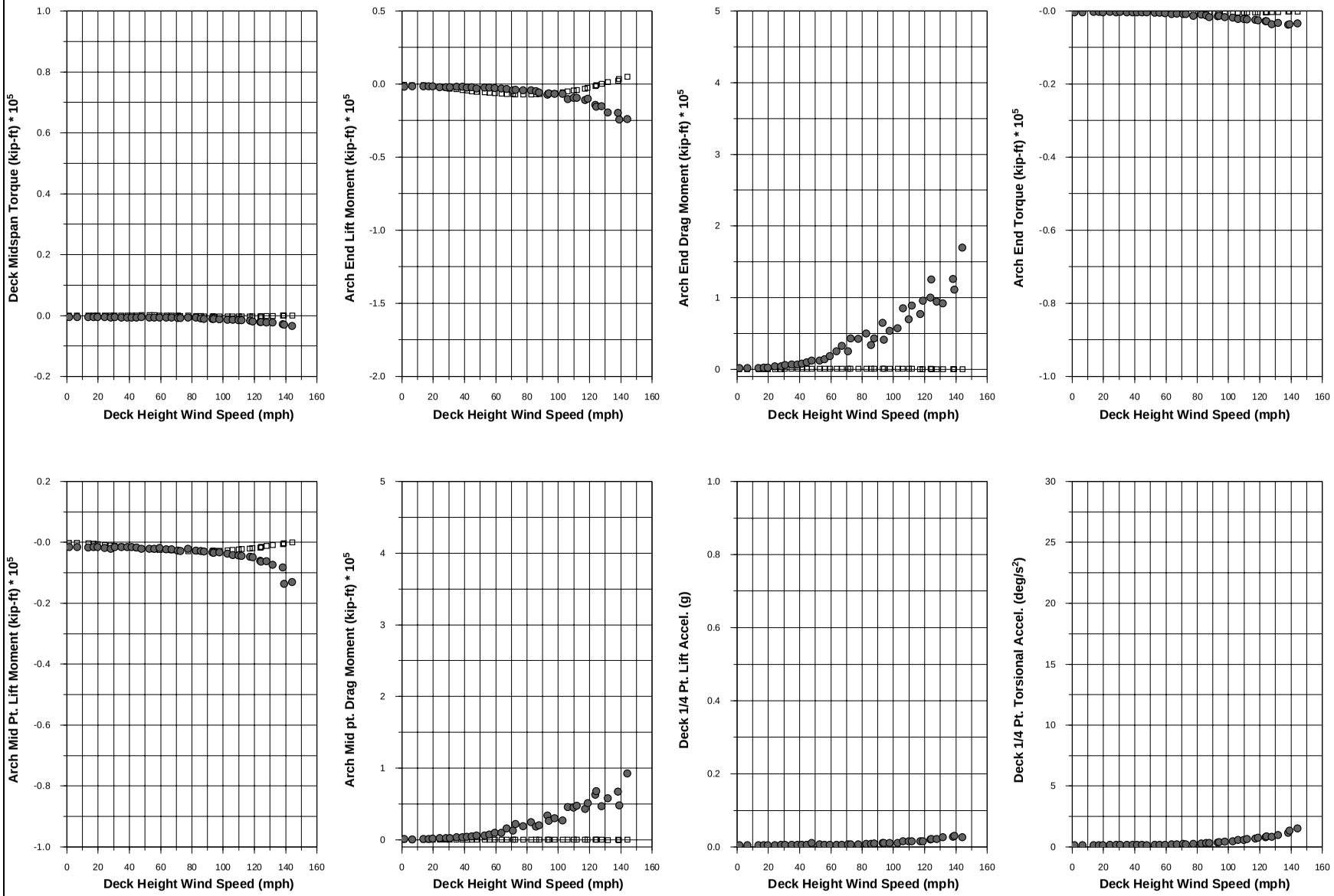

Indian River Bridge, hurricane profile, wind along the deck (0 degree)

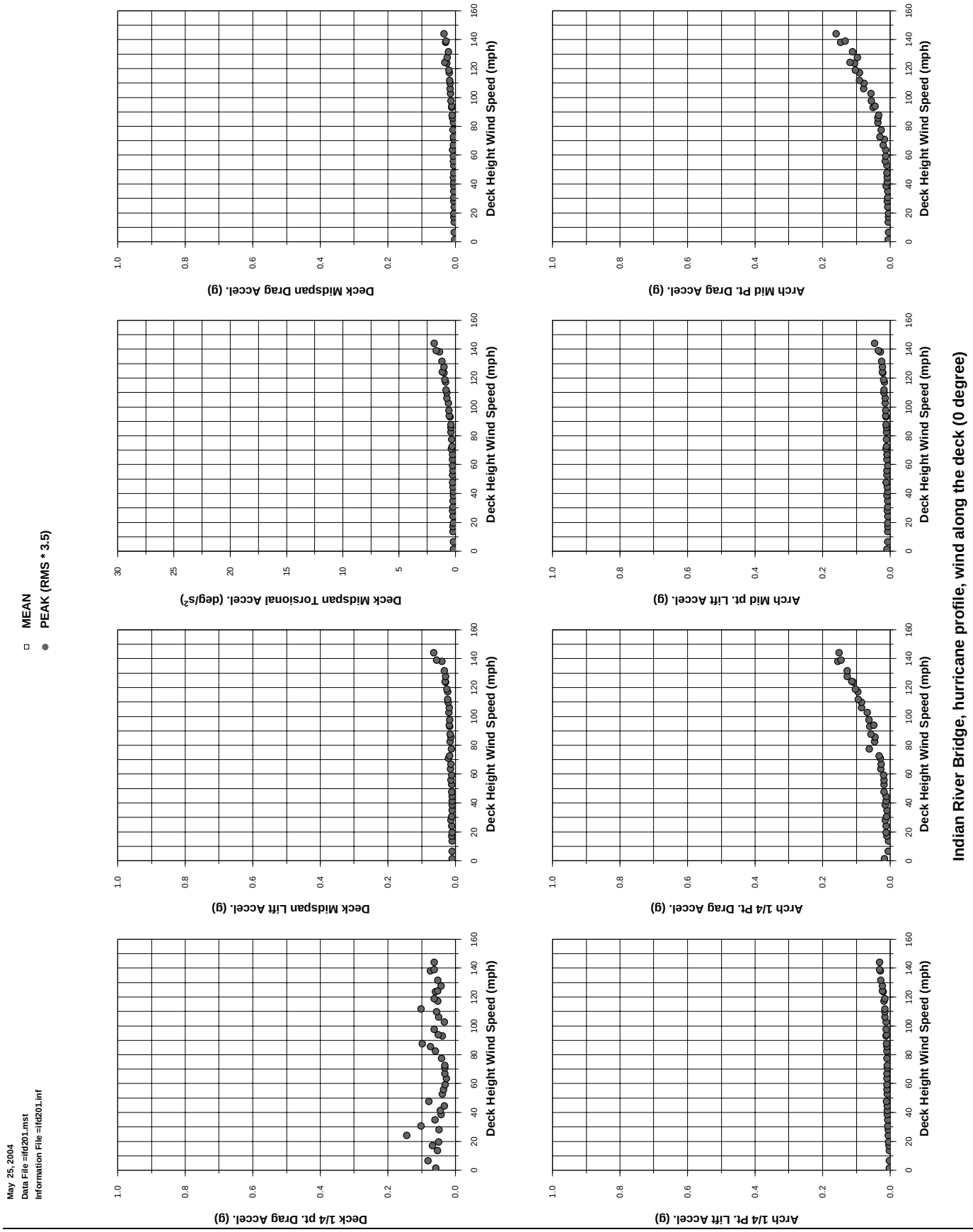

Indian River Bridge, hurricane profile, wind along the deck (0 degree)

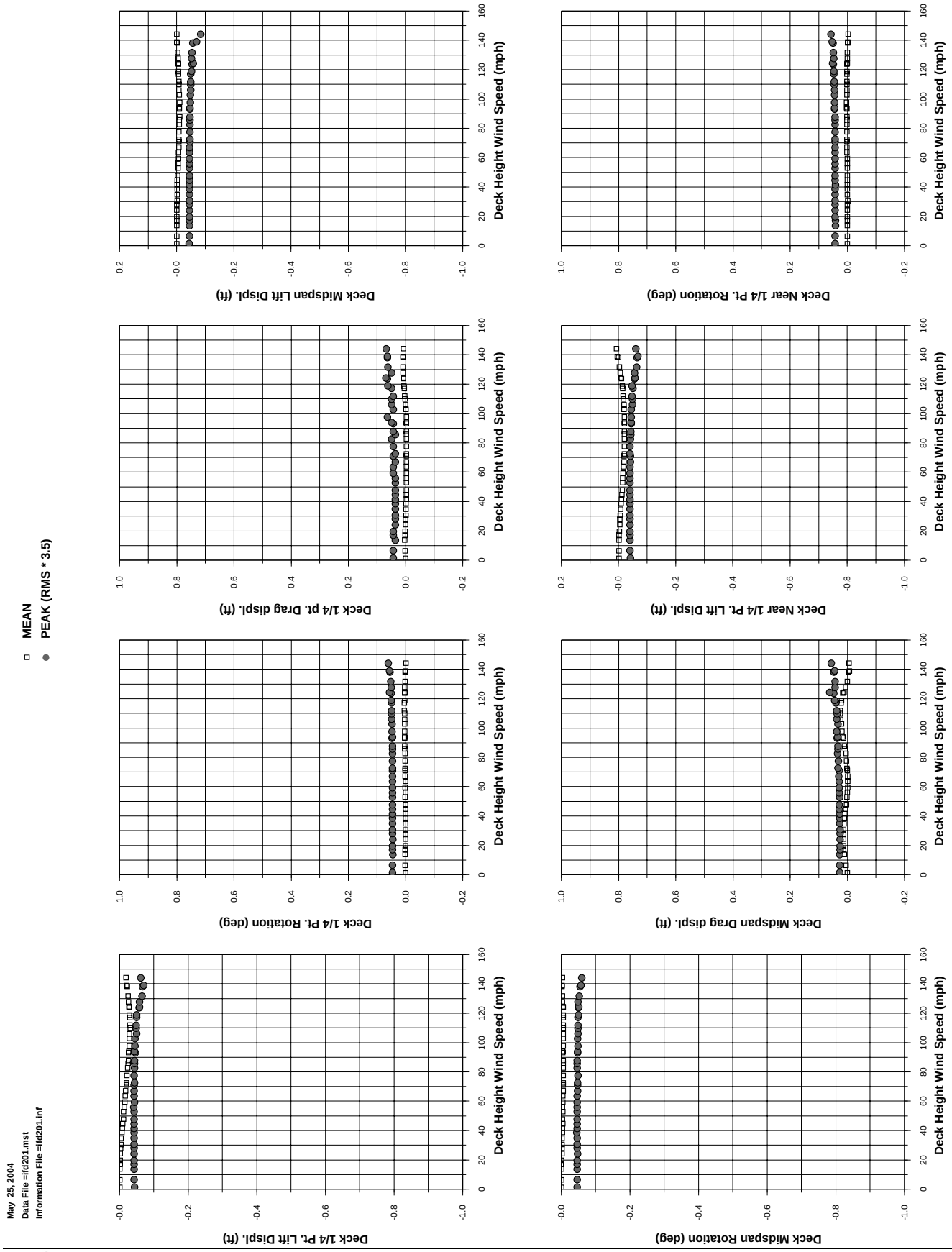

Indian River Bridge, hurricane profile, wind along the deck (0 degree)

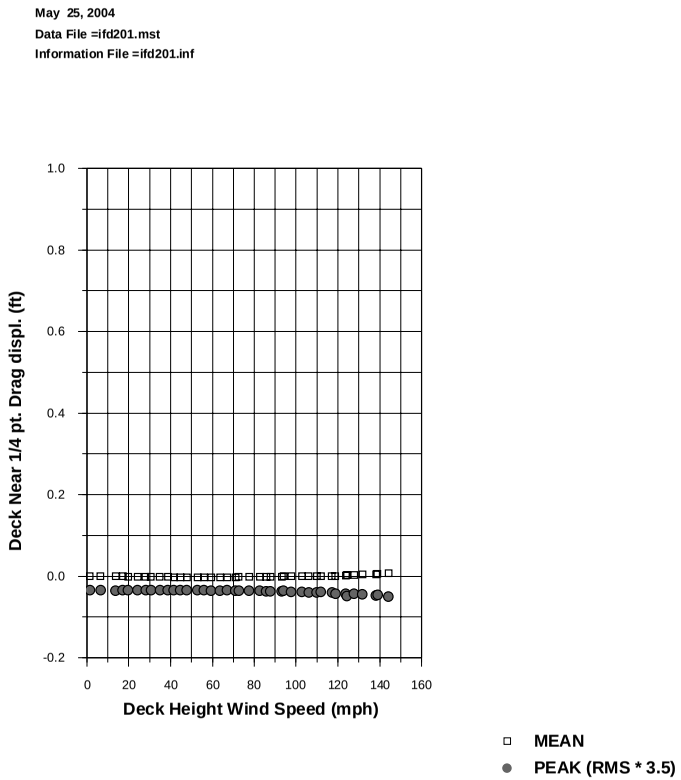

Indian River Bridge, hurricane profile, wind along the deck (0 degree)

May 25, 2004
Data File =ife201.mst
Information File =ife201.inf

MEAN
PEAK (RMS * 3.5)

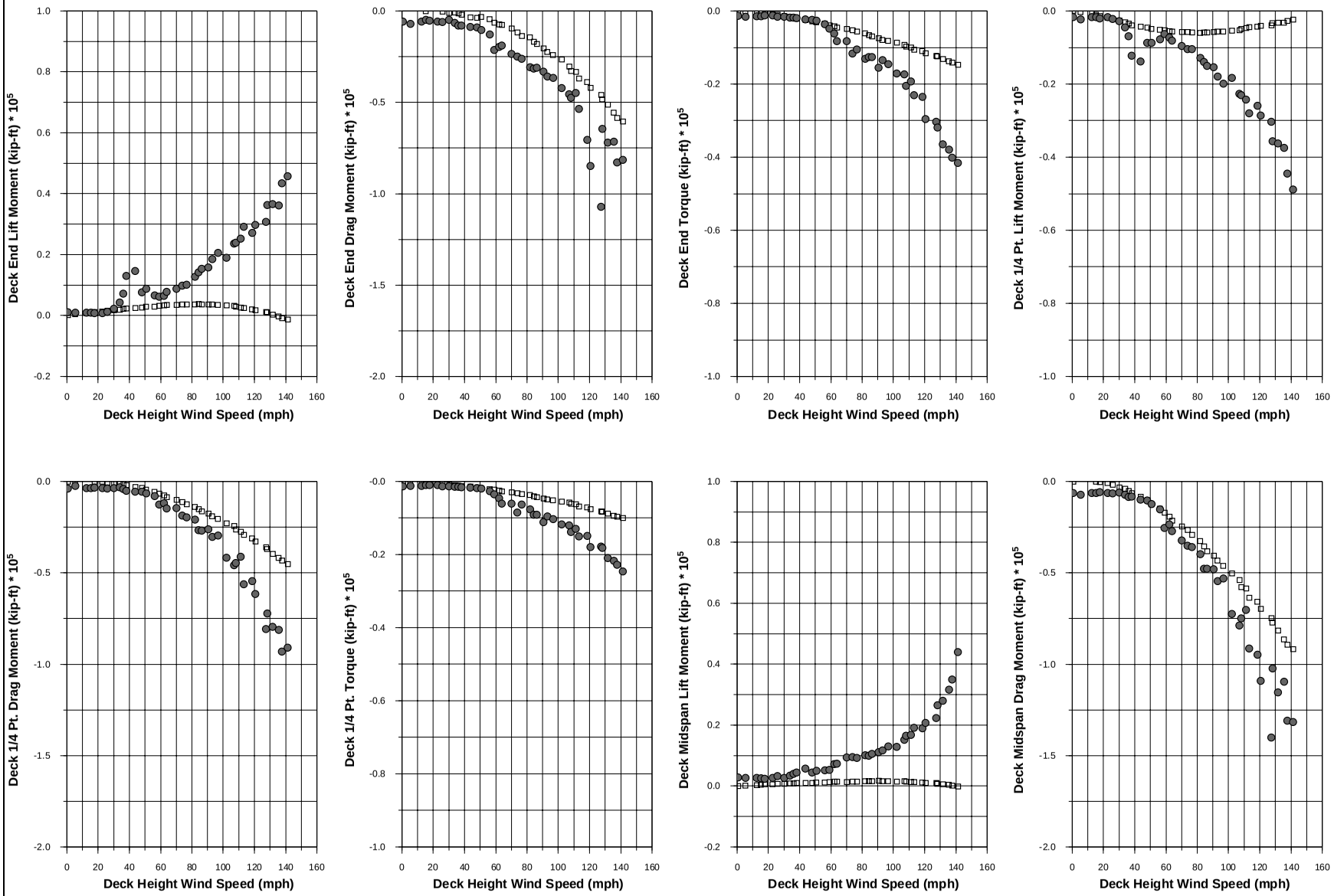

Indian River Bridge, hurricane profile without existing bridge, wind perpendicular to deck (270 degrees)

May 25, 2004
Data File =ife201.mst
Information File =ife201.inf

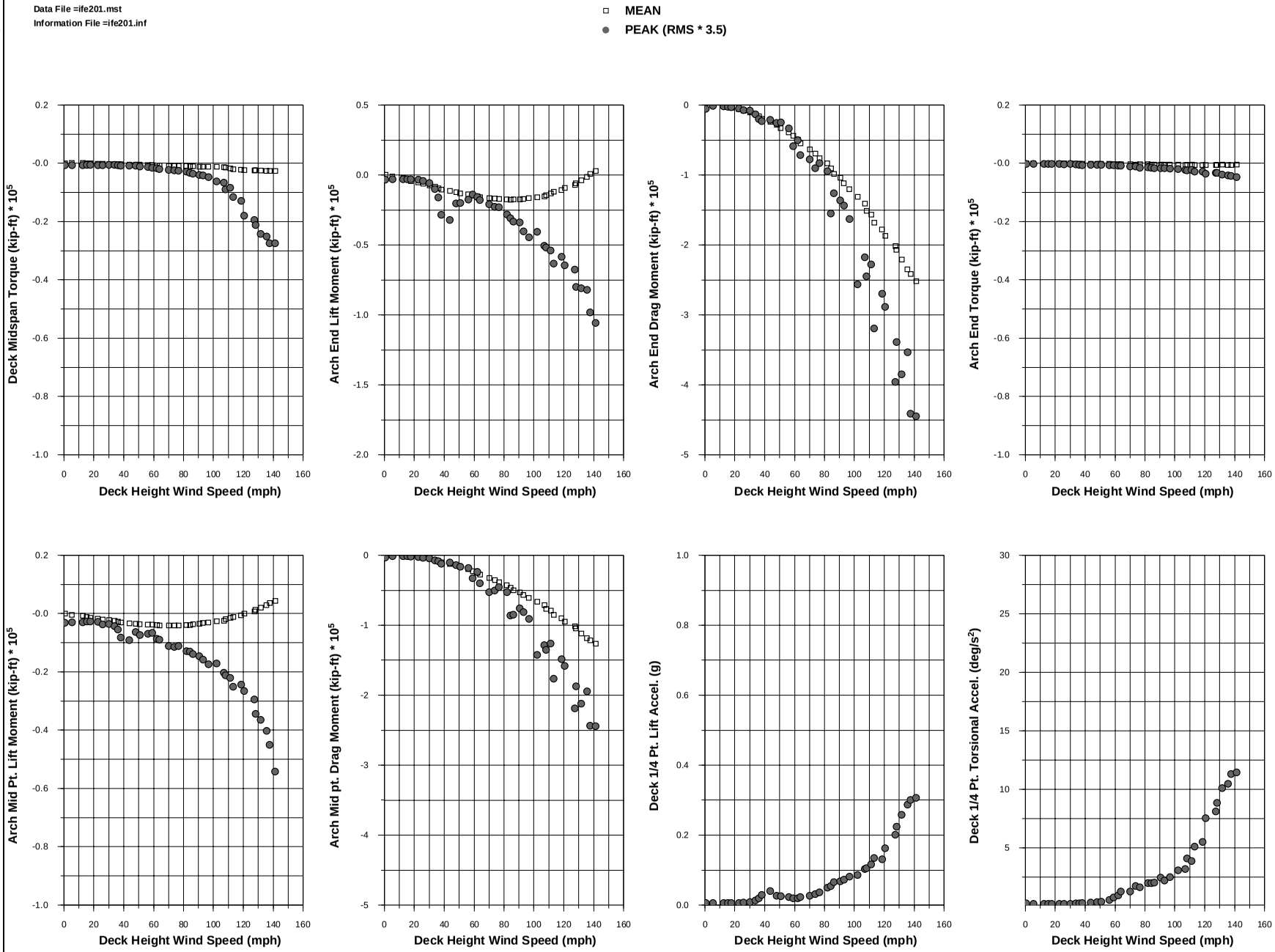

Indian River Bridge, hurricane profile without existing bridge, wind perpendicular to deck (270 degrees)

May 25, 2004
Data File =ife201.mst
Information File =ife201.inf

MEAN
PEAK (RMS * 3.5)

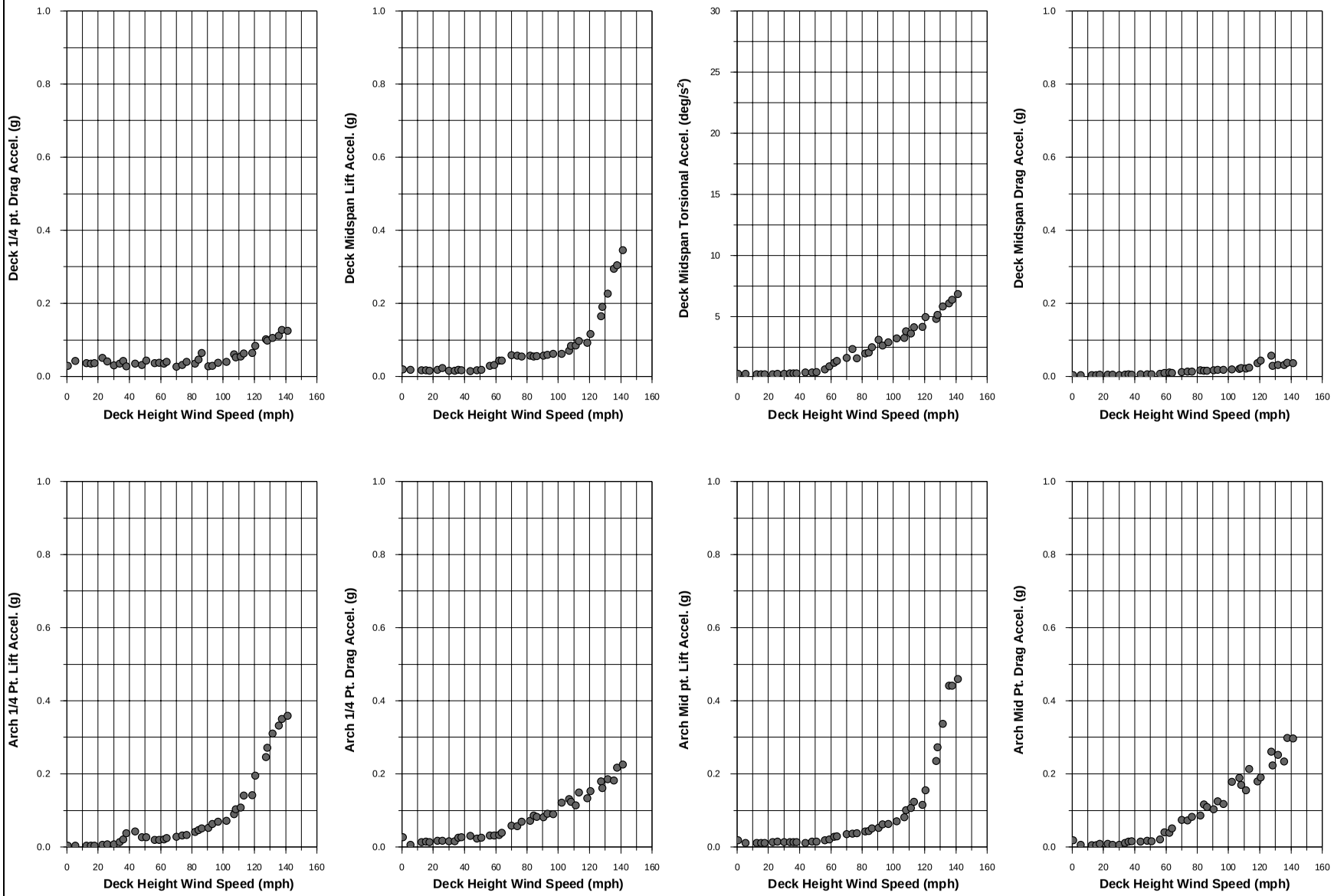

Indian River Bridge, hurricane profile without existing bridge, wind perpendicular to deck (270 degrees)

May 25, 2004
Data File =ife201.mst
Information File =ife201.inf

MEAN
PEAK (RMS * 3.5)

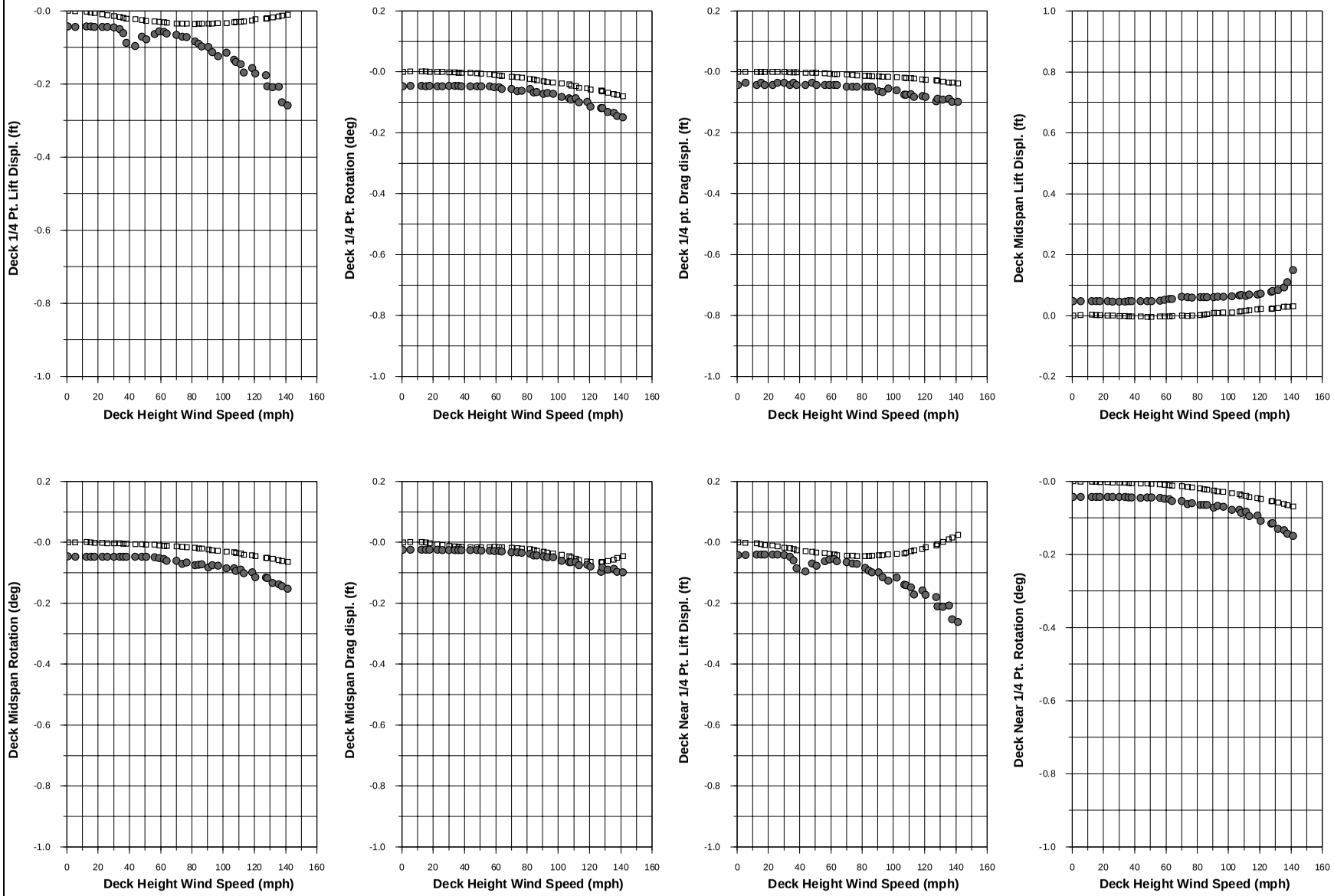

Indian River Bridge, hurricane profile without existing bridge, wind perpendicular to deck (270 degrees)

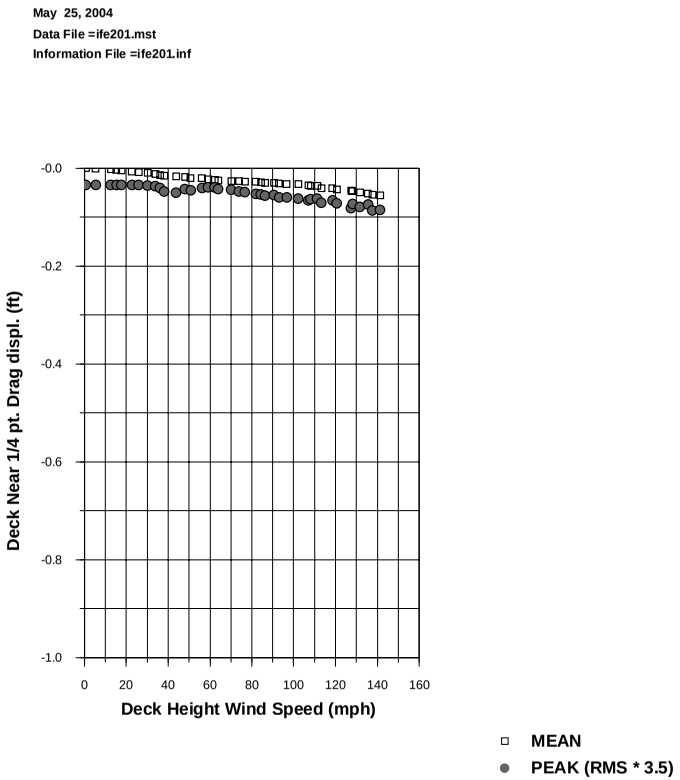

Indian River Bridge, hurricane profile without existing bridge, wind perpendicular to deck (270 degrees)

May 28, 2004
Data File =ifa301.mst
Information File =ifa301.inf

MEAN
PEAK (RMS * 3.5)

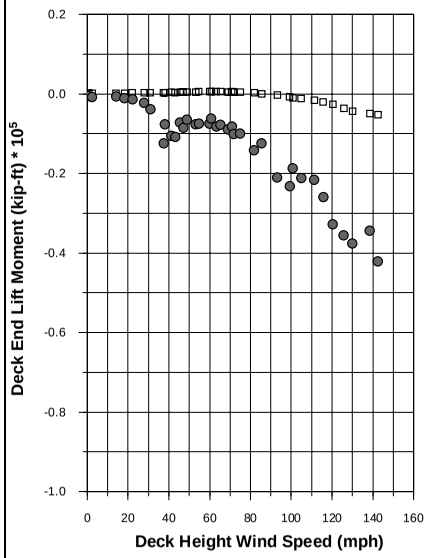

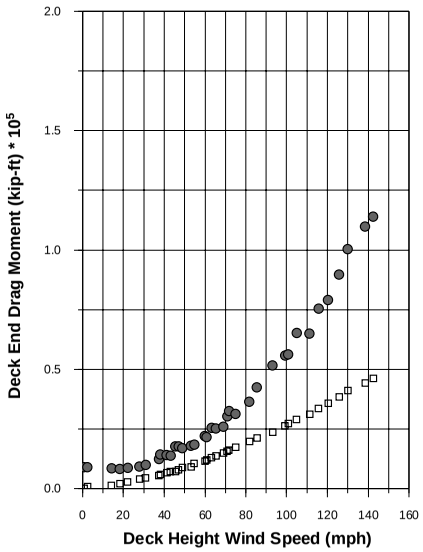

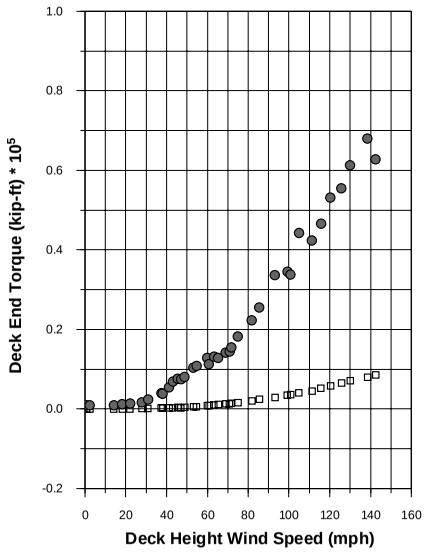

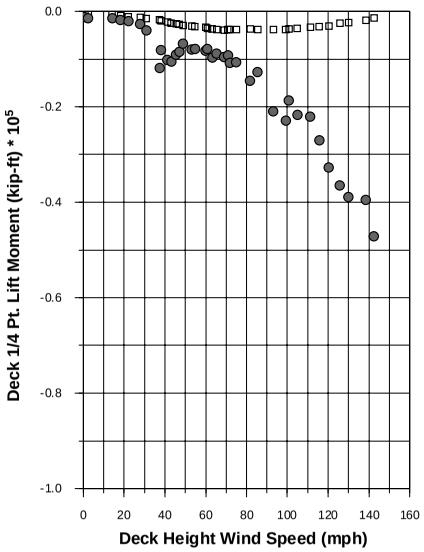

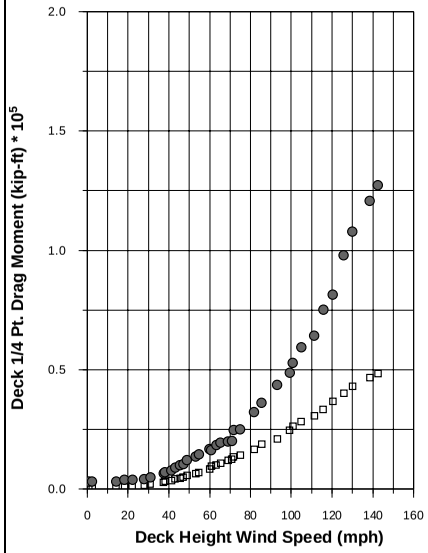

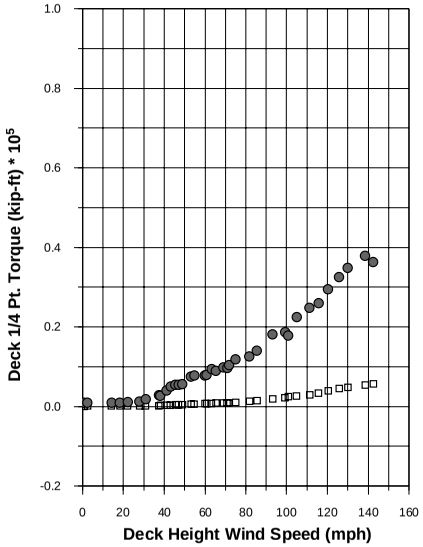

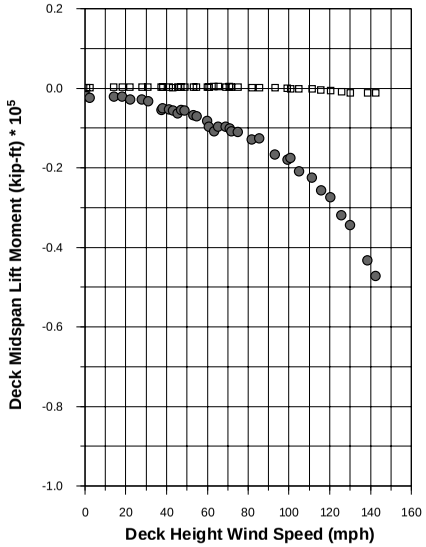

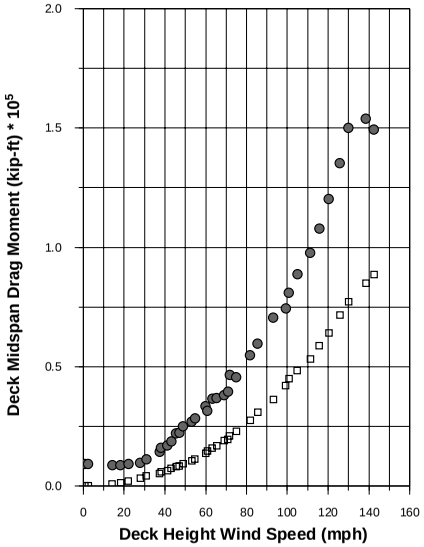

Indian River Bridge, open country profile with existing bridge, wind perpendicular to deck (90 degrees)

May 28, 2004
Data File =ifa301.mst
Information File =ifa301.inf

MEAN
PEAK (RMS * 3.5)

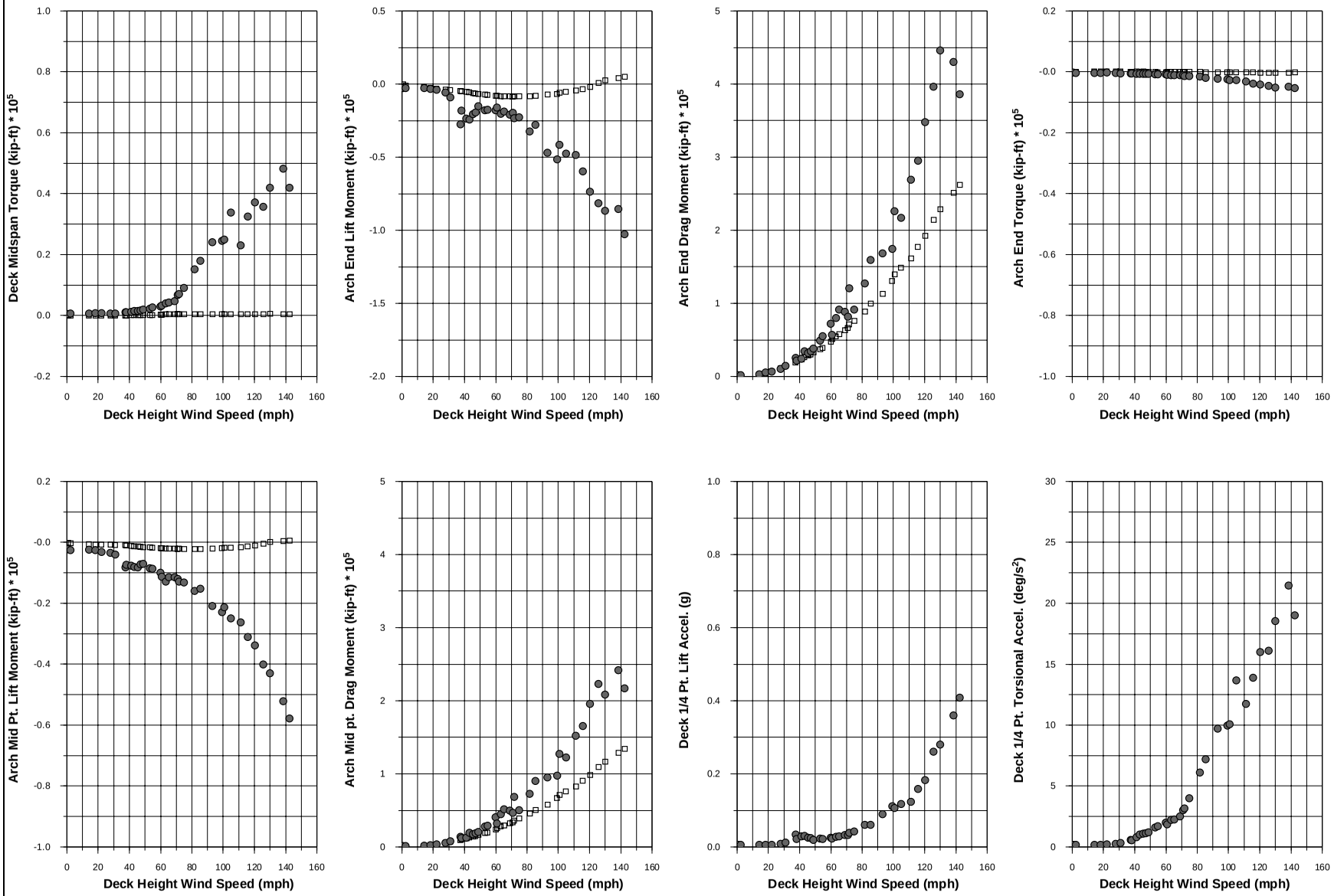

Indian River Bridge, open country profile with existing bridge, wind perpendicular to deck (90 degrees)

May 28, 2004
Data File =ifa301.mst
Information File =ifa301.inf

MEAN
PEAK (RMS * 3.5)

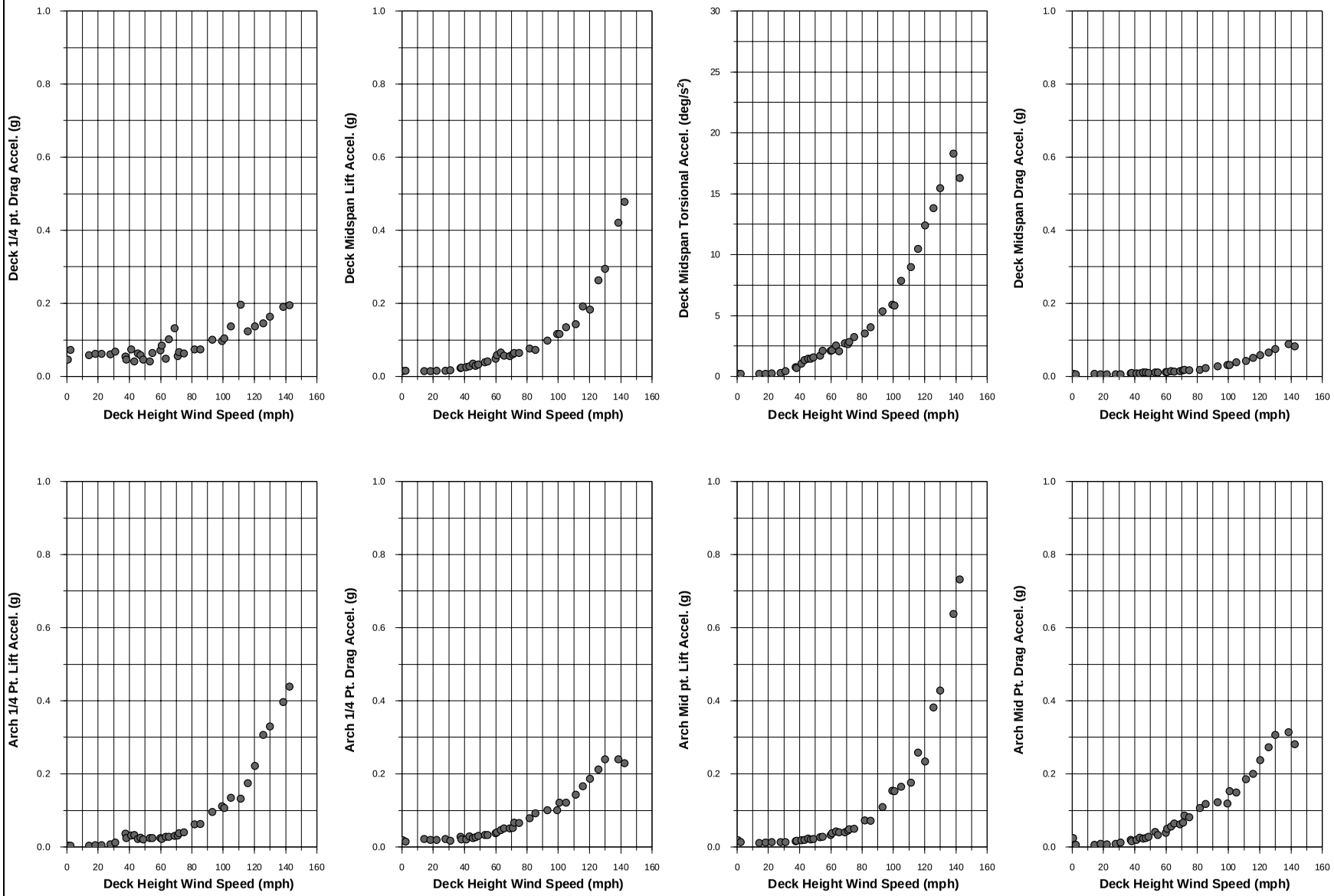

Indian River Bridge, open country profile with existing bridge, wind perpendicular to deck (90 degrees)

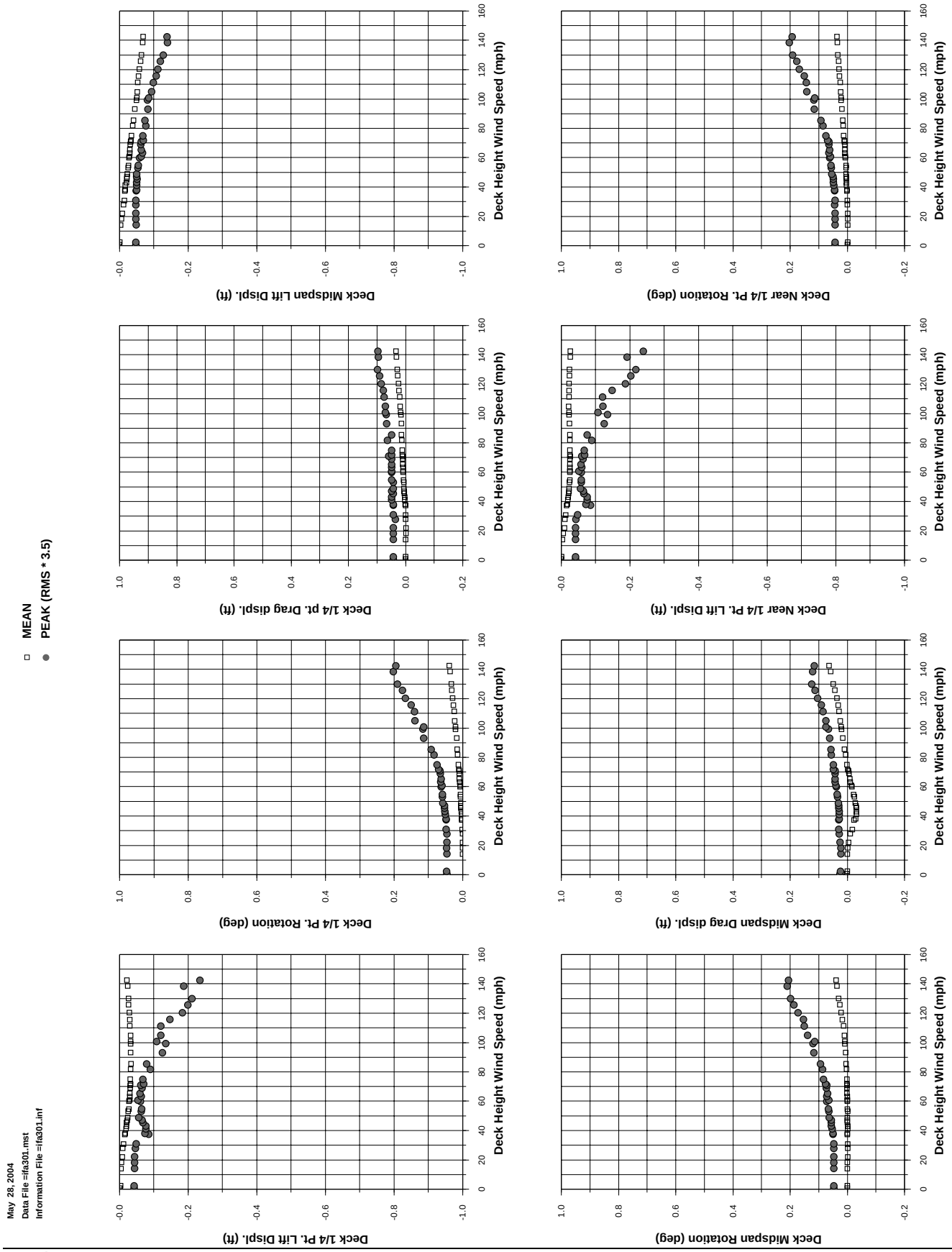

Indian River Bridge, open country profile with existing bridge, wind perpendicular to deck (90 degrees)

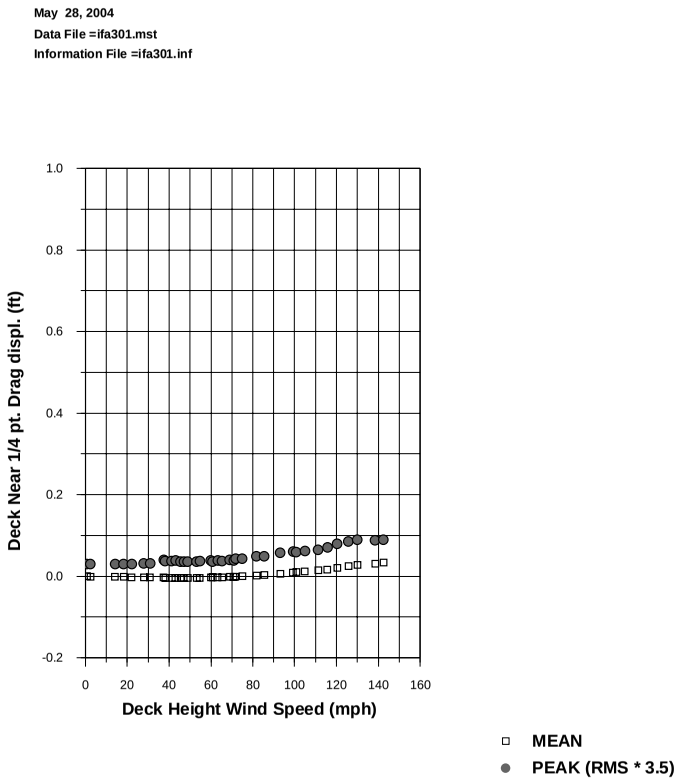

Indian River Bridge, open country profile with existing bridge, wind perpendicular to deck (90 degrees)

May 28, 2004
Data File =ifa302.mst
Information File =ifa302.inf

MEAN
PEAK (RMS * 3.5)

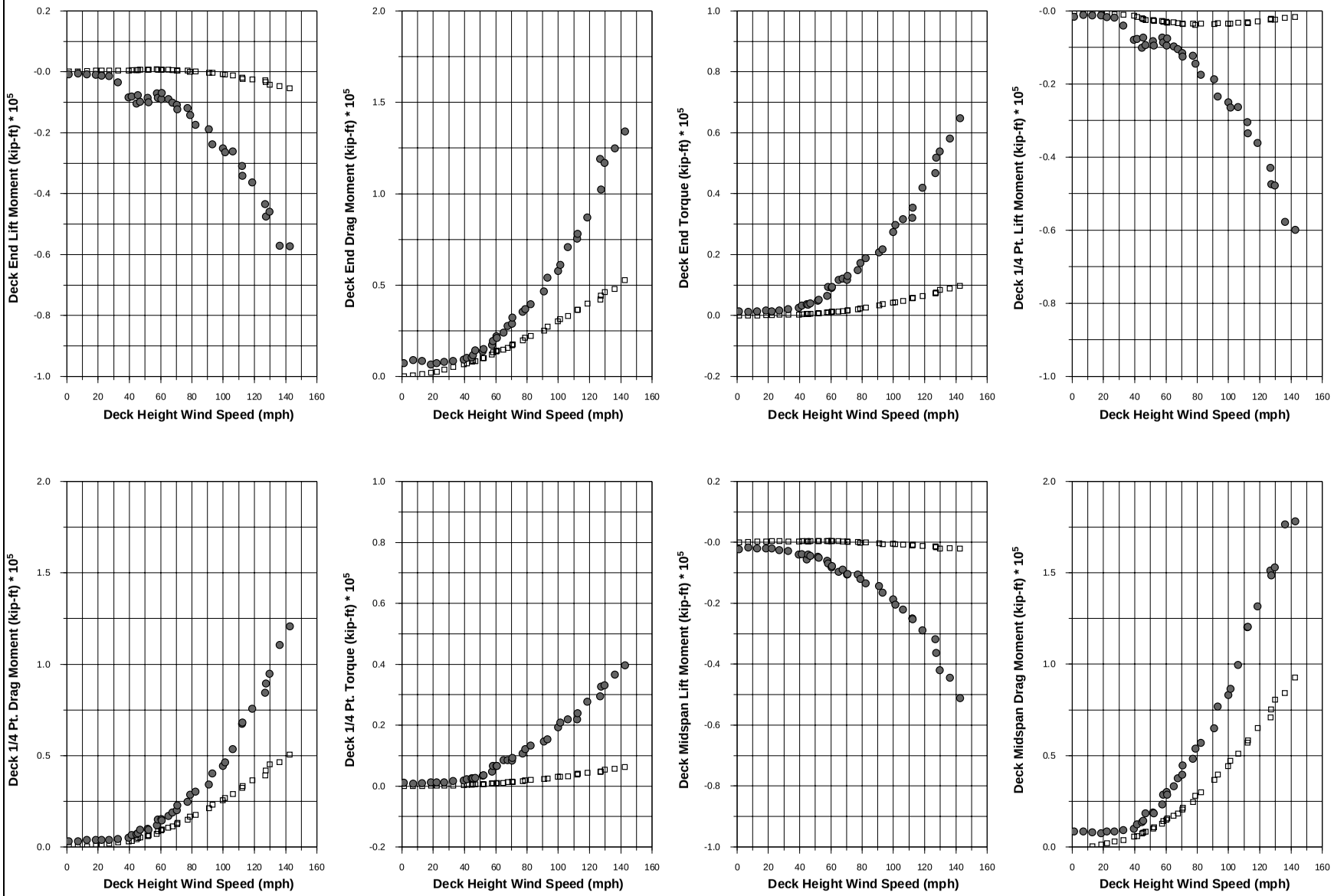

Indian River Bridge, open country profile without existing bridge, wind perpendicular to deck (90 degrees)

May 28, 2004
Data File =ifa302.mst
Information File =ifa302.inf

MEAN
PEAK (RMS * 3.5)

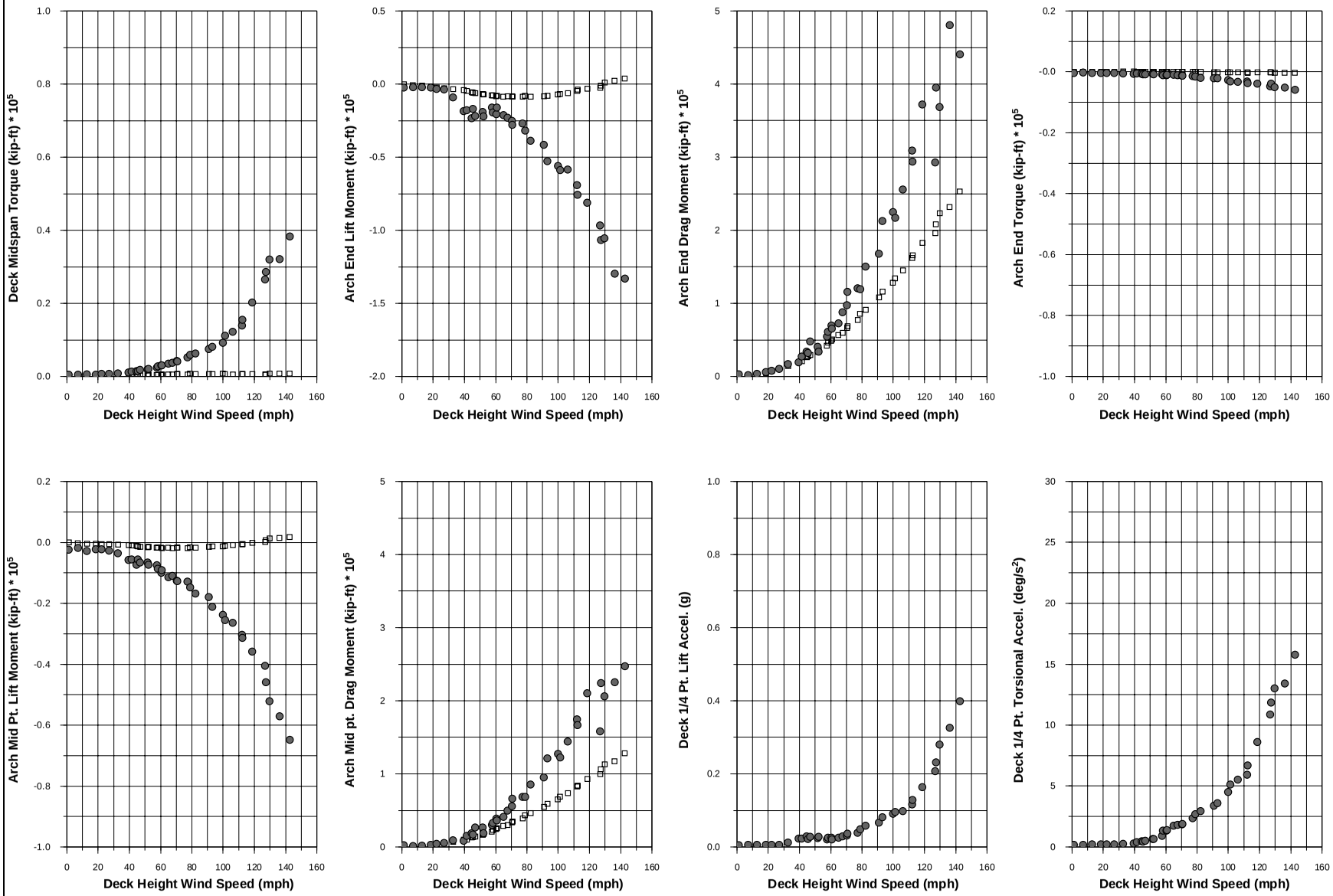

Indian River Bridge, open country profile without existing bridge, wind perpendicular to deck (90 degrees)

May 28, 2004
Data File =ifa302.mst
Information File =ifa302.inf

MEAN
PEAK (RMS * 3.5)

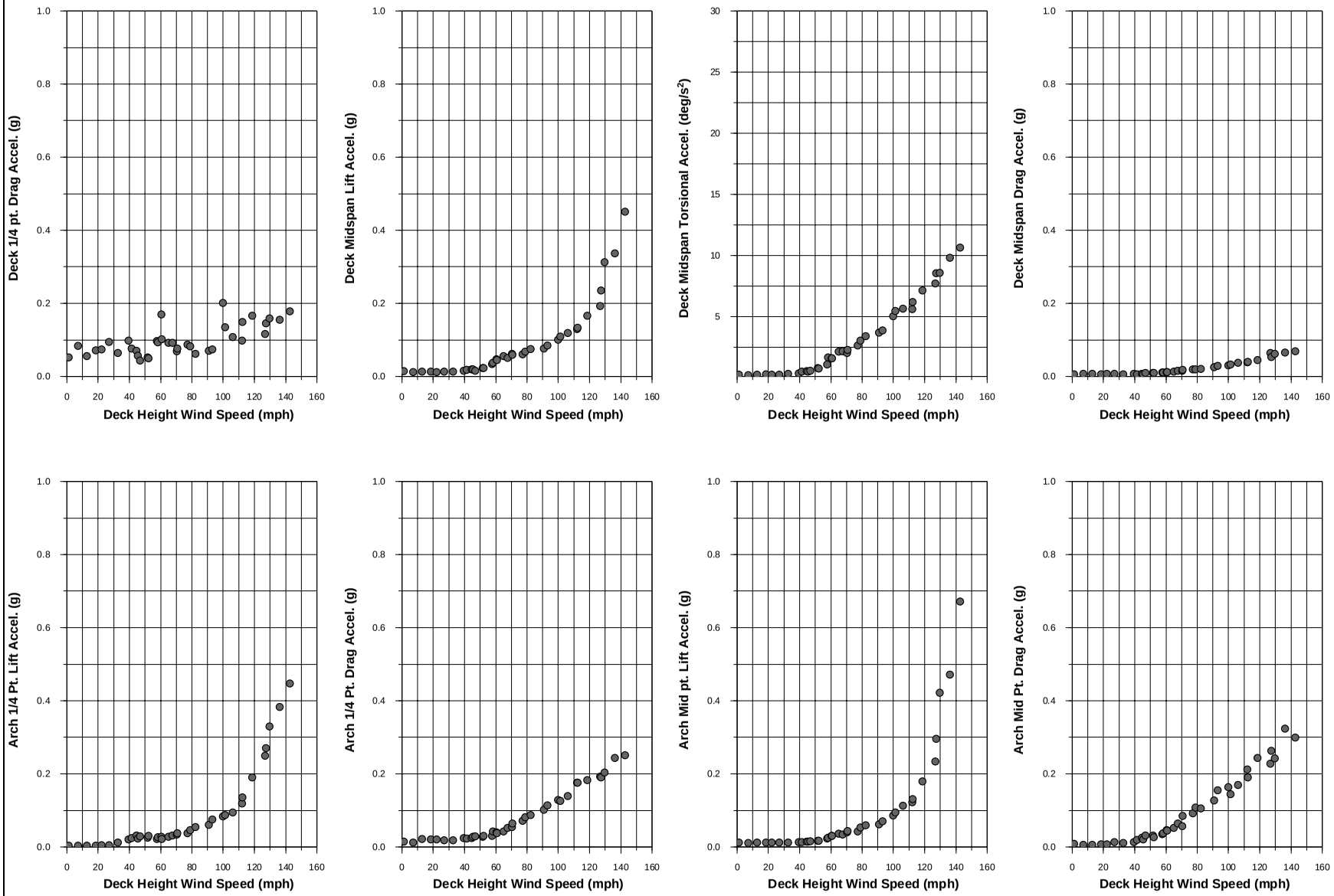

Indian River Bridge, open country profile without existing bridge, wind perpendicular to deck (90 degrees)

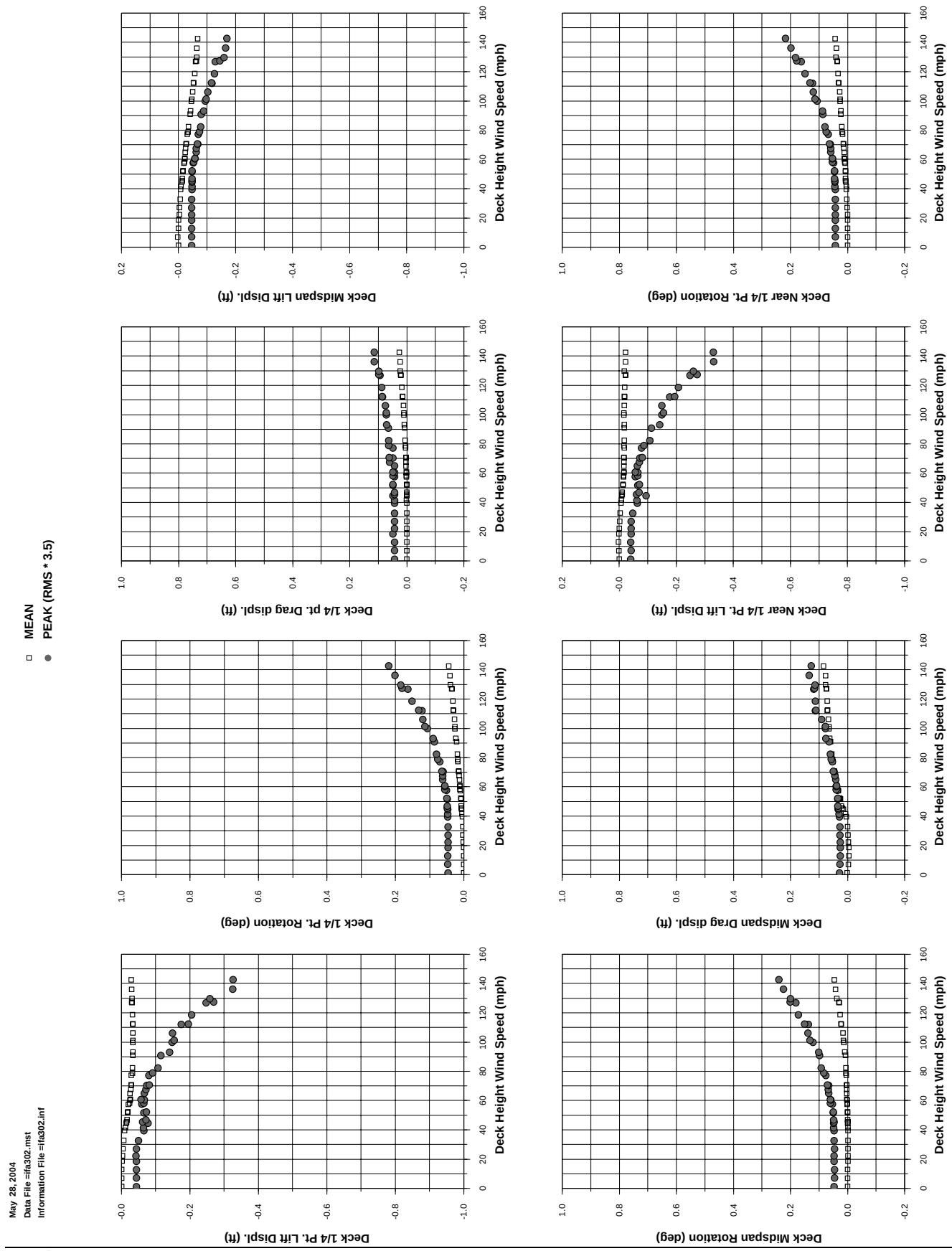

Indian River Bridge, open country profile without existing bridge, wind perpendicular to deck (90 degrees)

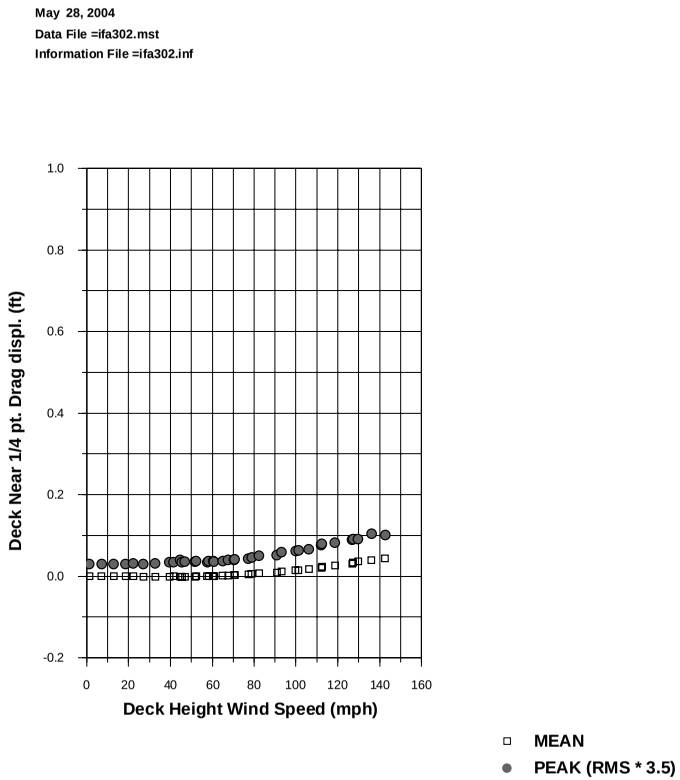

Indian River Bridge, open country profile without existing bridge, wind perpendicular to deck (90 degrees)

May 28, 2004
Data File =ifb302.mst
Information File =ifb302.inf

MEAN
PEAK (RMS * 3.5)

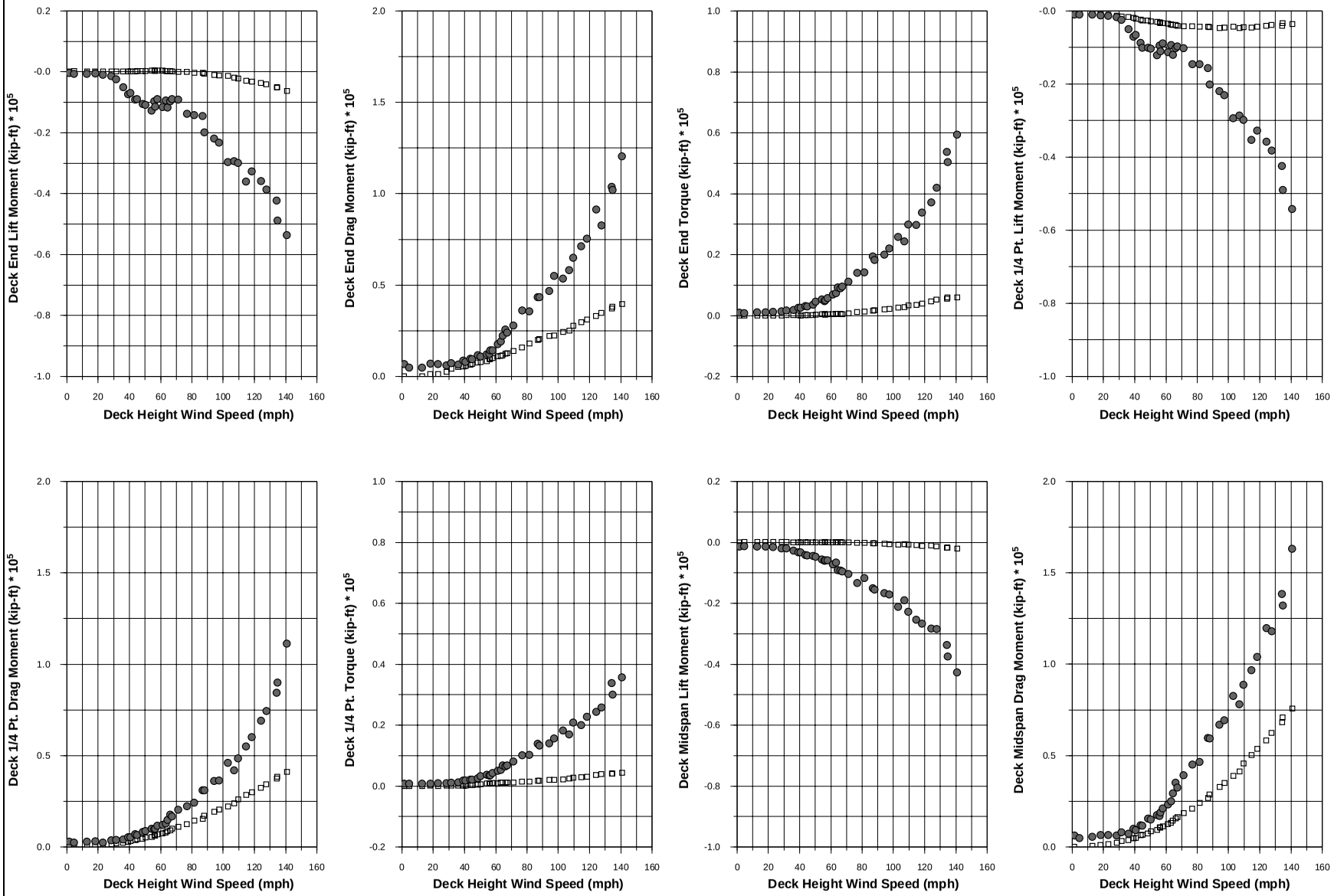

Indian River Bridge, open country profile, wind at 60 degrees to deck

May 28, 2004
Data File =ifb302.mst
Information File =ifb302.inf

MEAN
PEAK (RMS * 3.5)

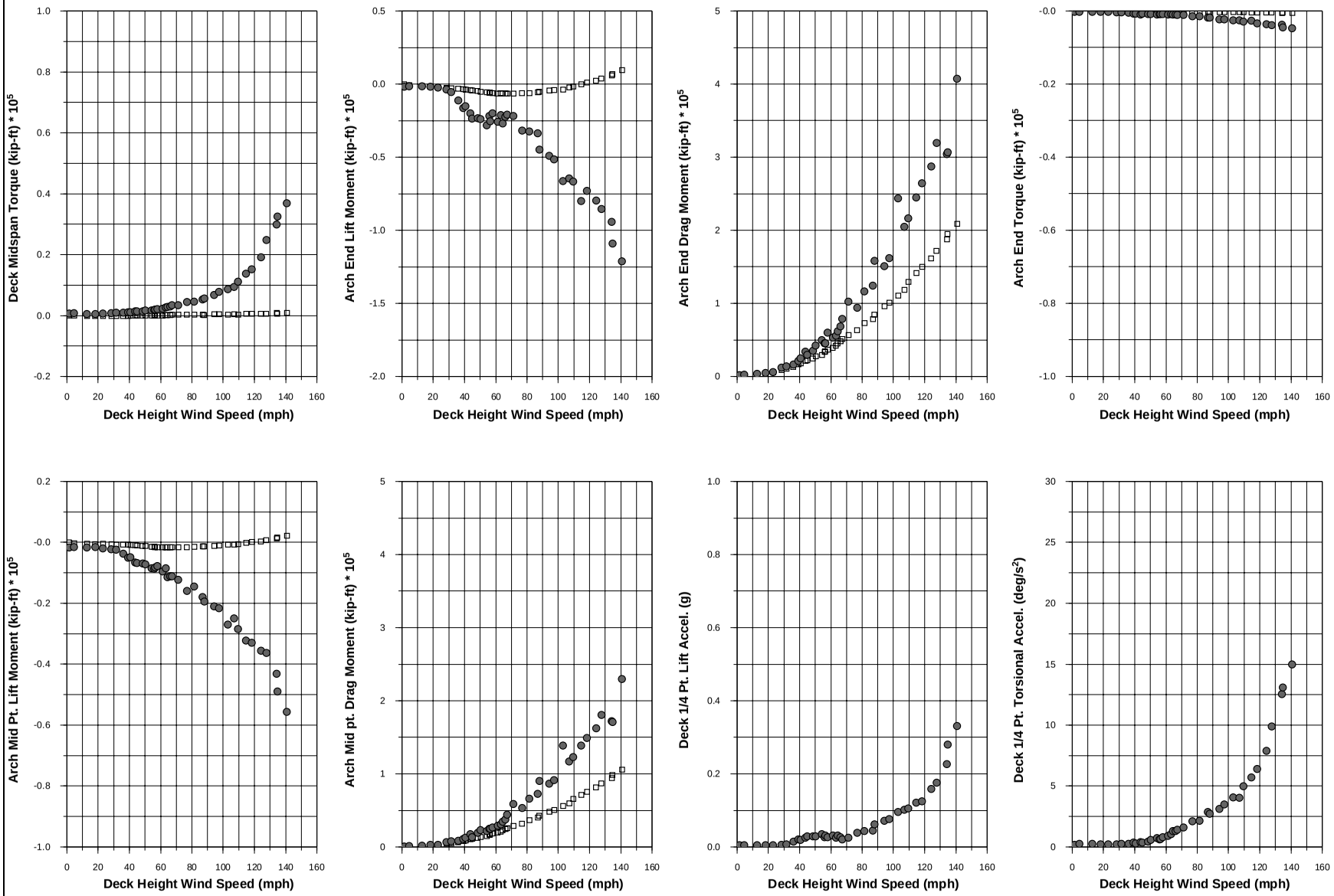

Indian River Bridge, open country profile, wind at 60 degrees to deck

May 28, 2004
Data File =ifa302.mst
Information File =ifa302.inf

MEAN
PEAK (RMS * 3.5)

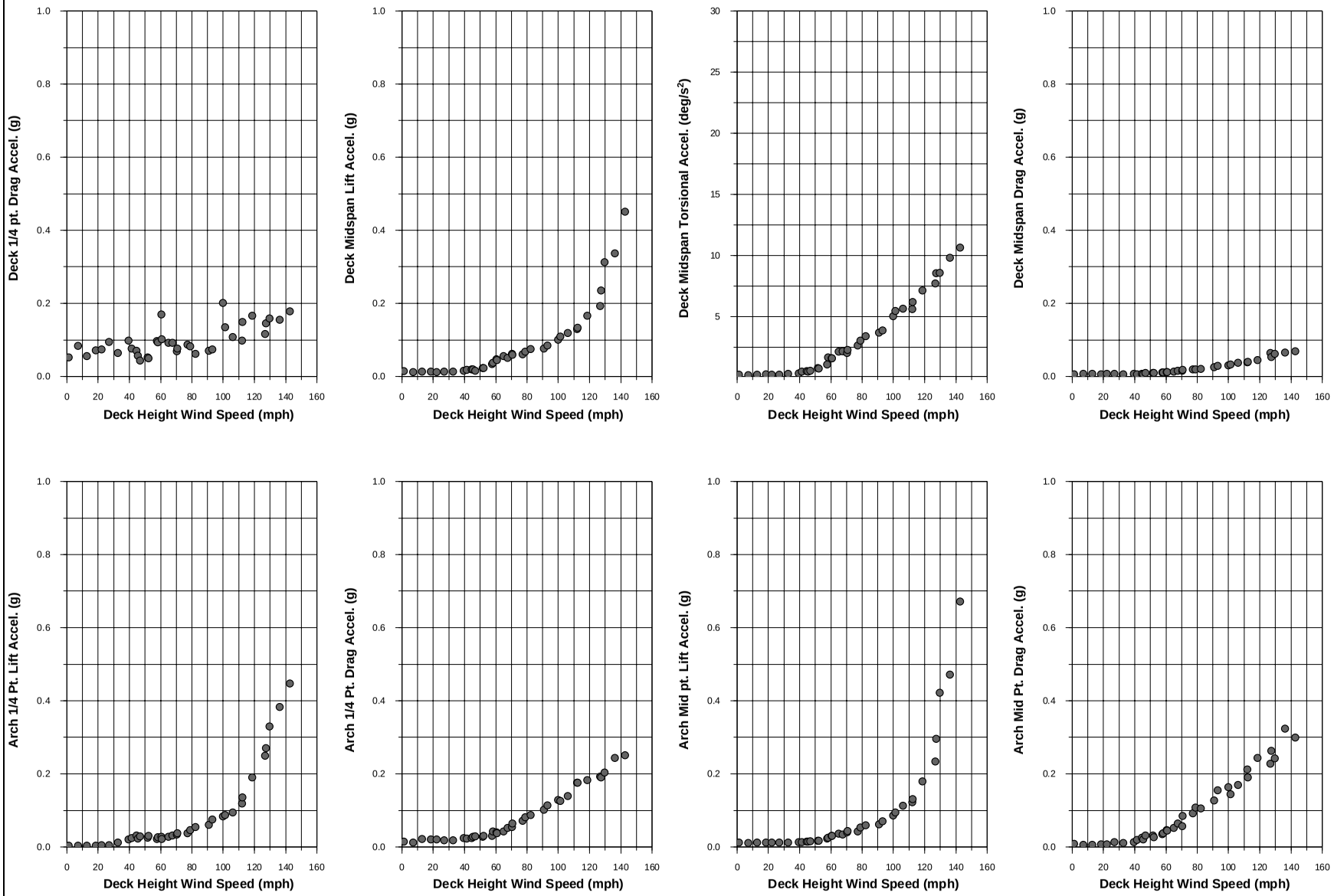

Indian River Bridge, open country profile without existing bridge, wind perpendicular to deck (90 degrees)

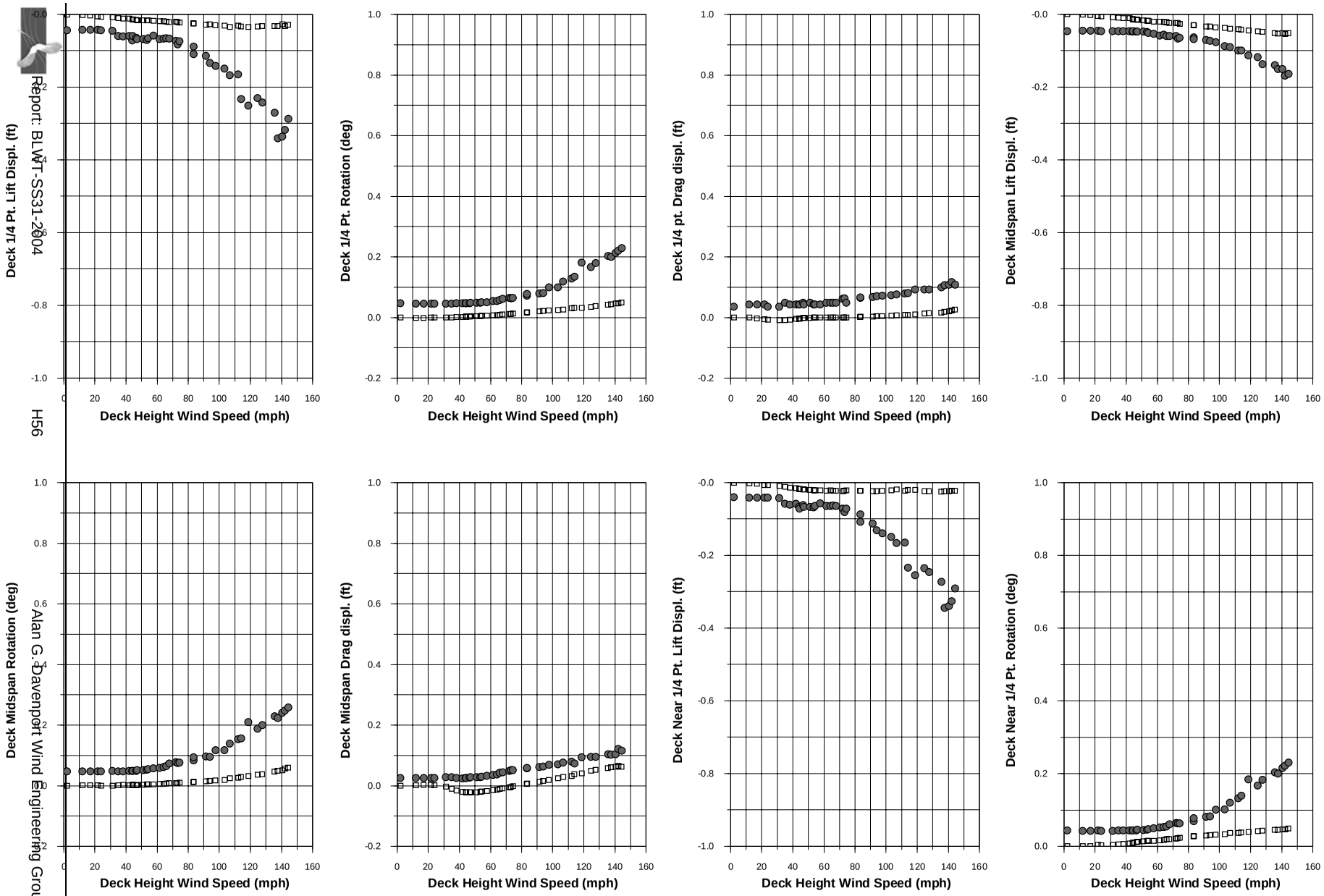

Indian River Bridge, open country profile, wind perpendicular to deck (90 degrees) with higher arch damping

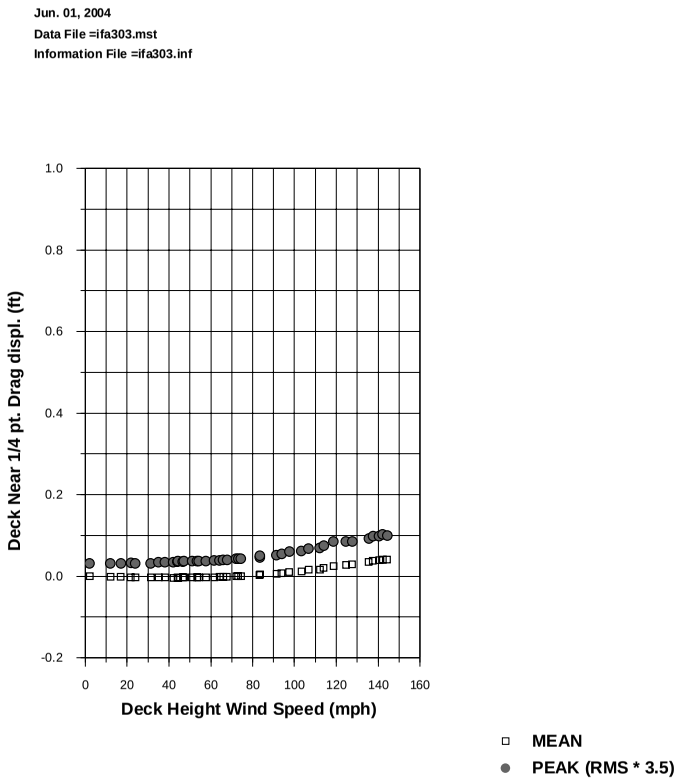

Indian River Bridge, open country profile, wind perpendicular to deck (90 degrees) with higher arch damping

May 28, 2004
Data File =ifc302.mst
Information File =ifc302.inf

MEAN
PEAK (RMS * 3.5)

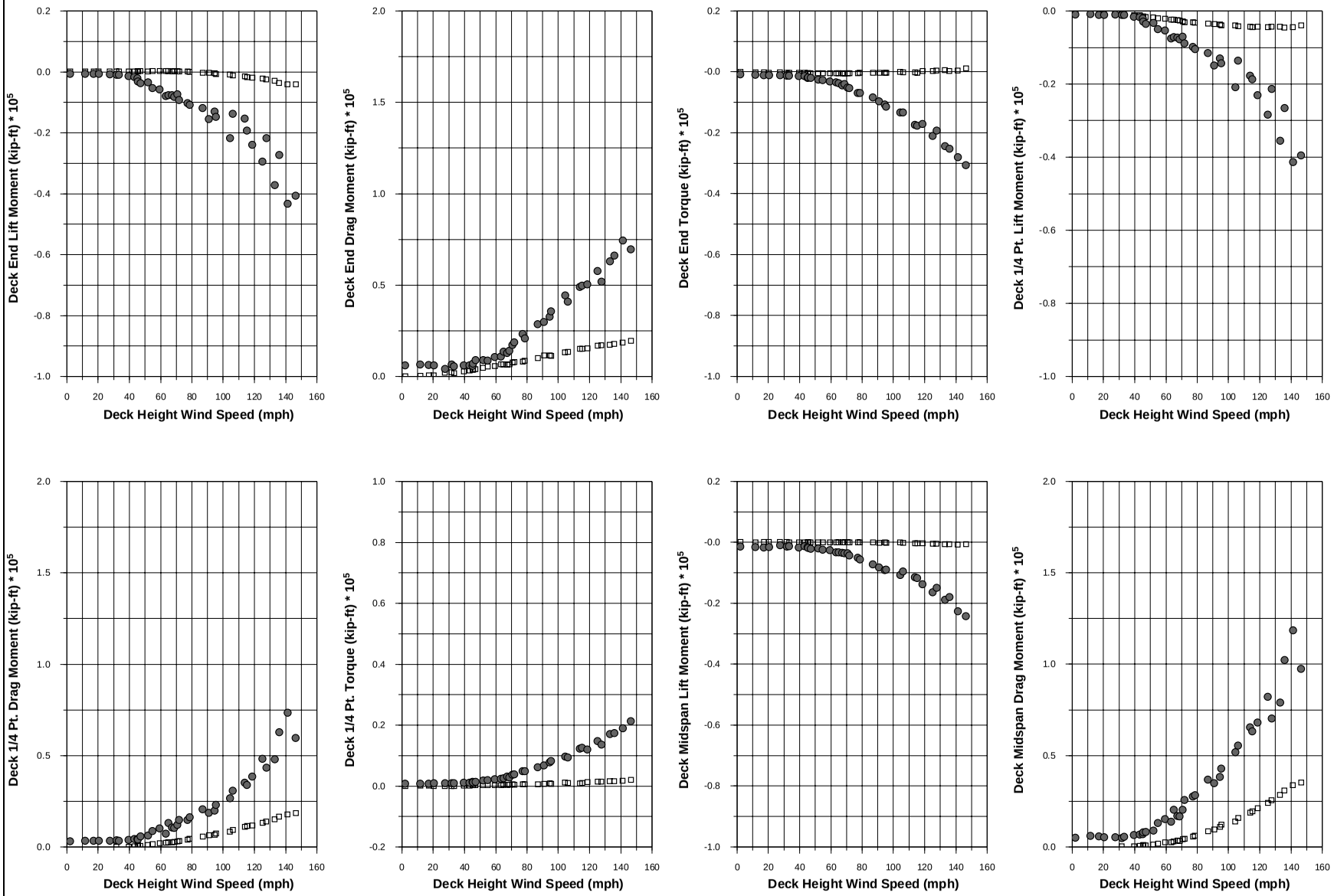

Indian River Bridge, open country exposure, wind at 30 degrees to deck

May 28, 2004
Data File =ifc302.mst
Information File =ifc302.inf

MEAN
PEAK (RMS * 3.5)

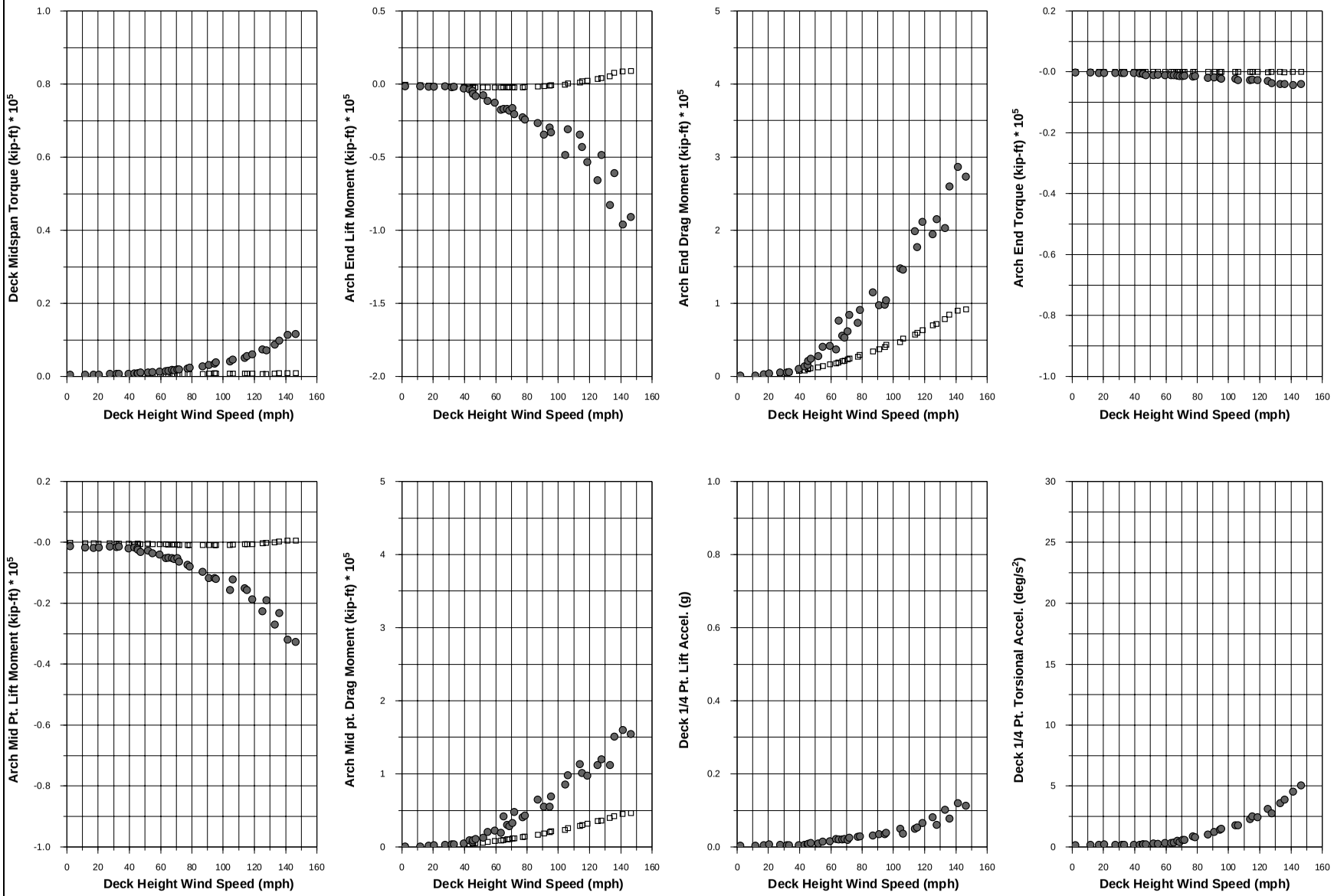

Indian River Bridge, open country exposure, wind at 30 degrees to deck

May 28, 2004
Data File =ifc302.mst
Information File =ifc302.inf

MEAN
PEAK (RMS * 3.5)

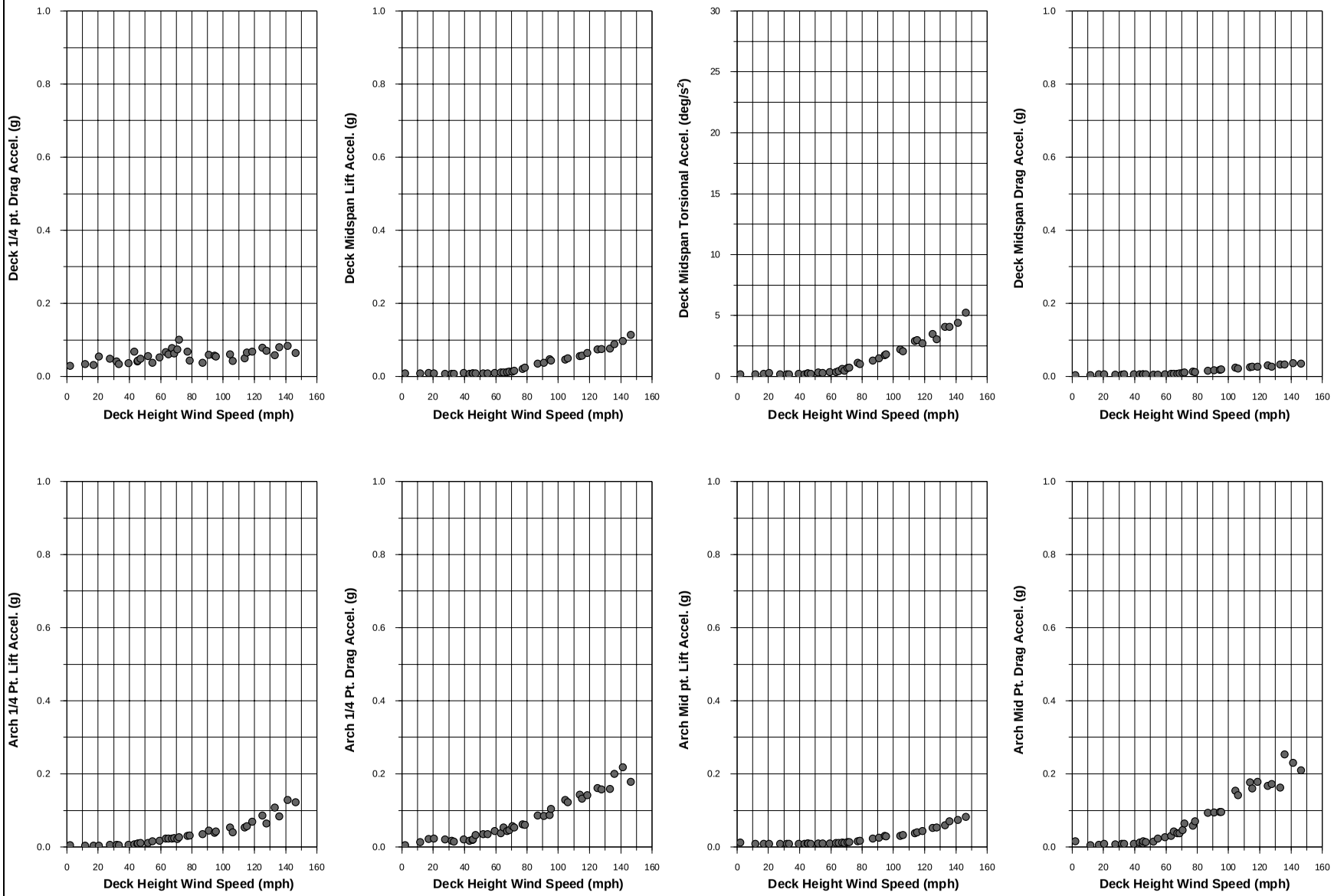

Indian River Bridge, open country exposure, wind at 30 degrees to deck

May 28, 2004
Data File =ifc302.mst
Information File =ifc302.inf

MEAN
PEAK (RMS * 3.5)

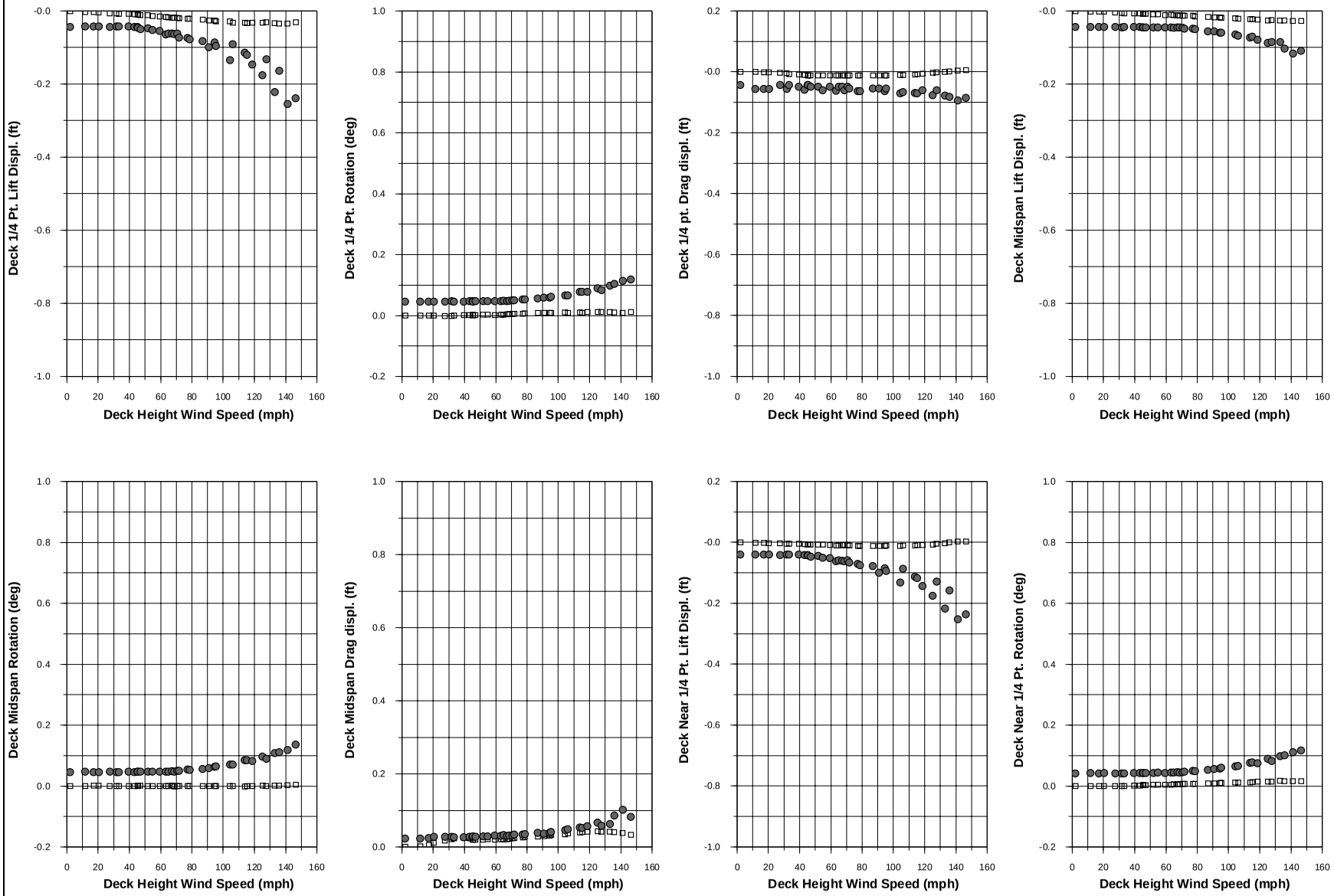

Indian River Bridge, open country exposure, wind at 30 degrees to deck

May 28, 2004
Data File =ifc302.mst
Information File =ifc302.inf

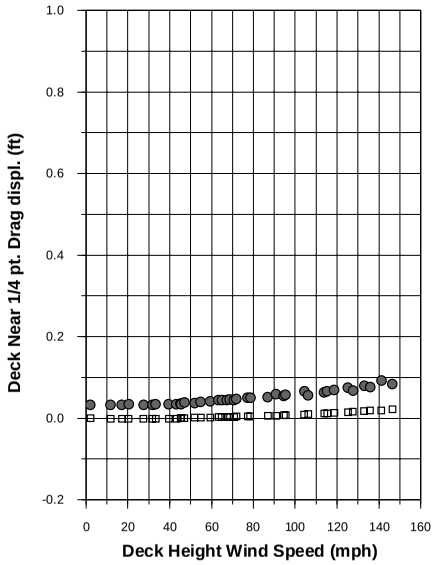

MEAN
PEAK (RMS * 3.5)

Indian River Bridge, open country exposure, wind at 30 degrees to deck

May 31, 2004
Data File =ifd302.mst
Information File =ifd302.inf

MEAN
PEAK (RMS * 3.5)

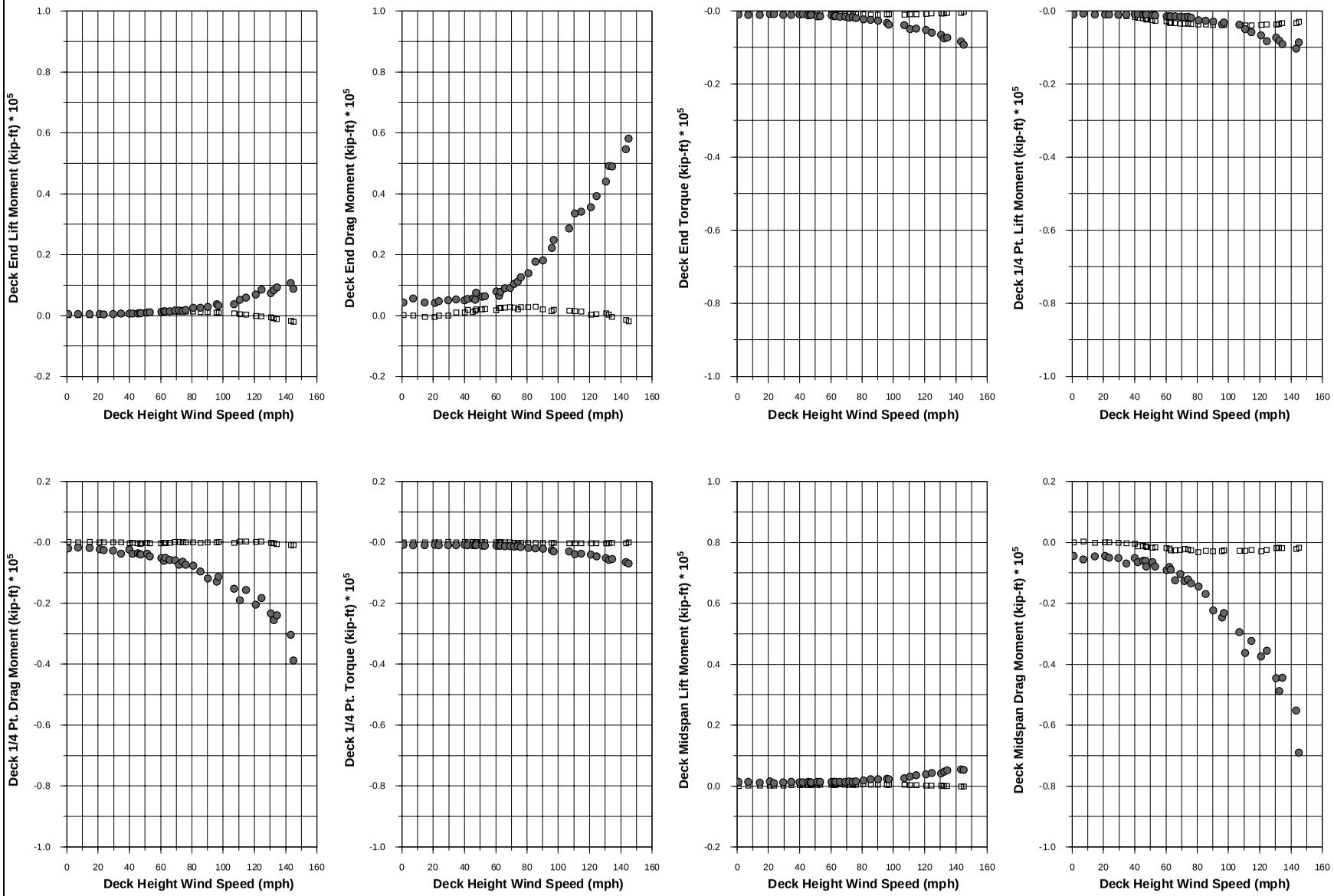

Indian River Bridge, open country exposure, wind along the deck (0 degrees)

May 31, 2004
Data File =ifd302.mst
Information File =ifd302.inf

MEAN
PEAK (RMS * 3.5)

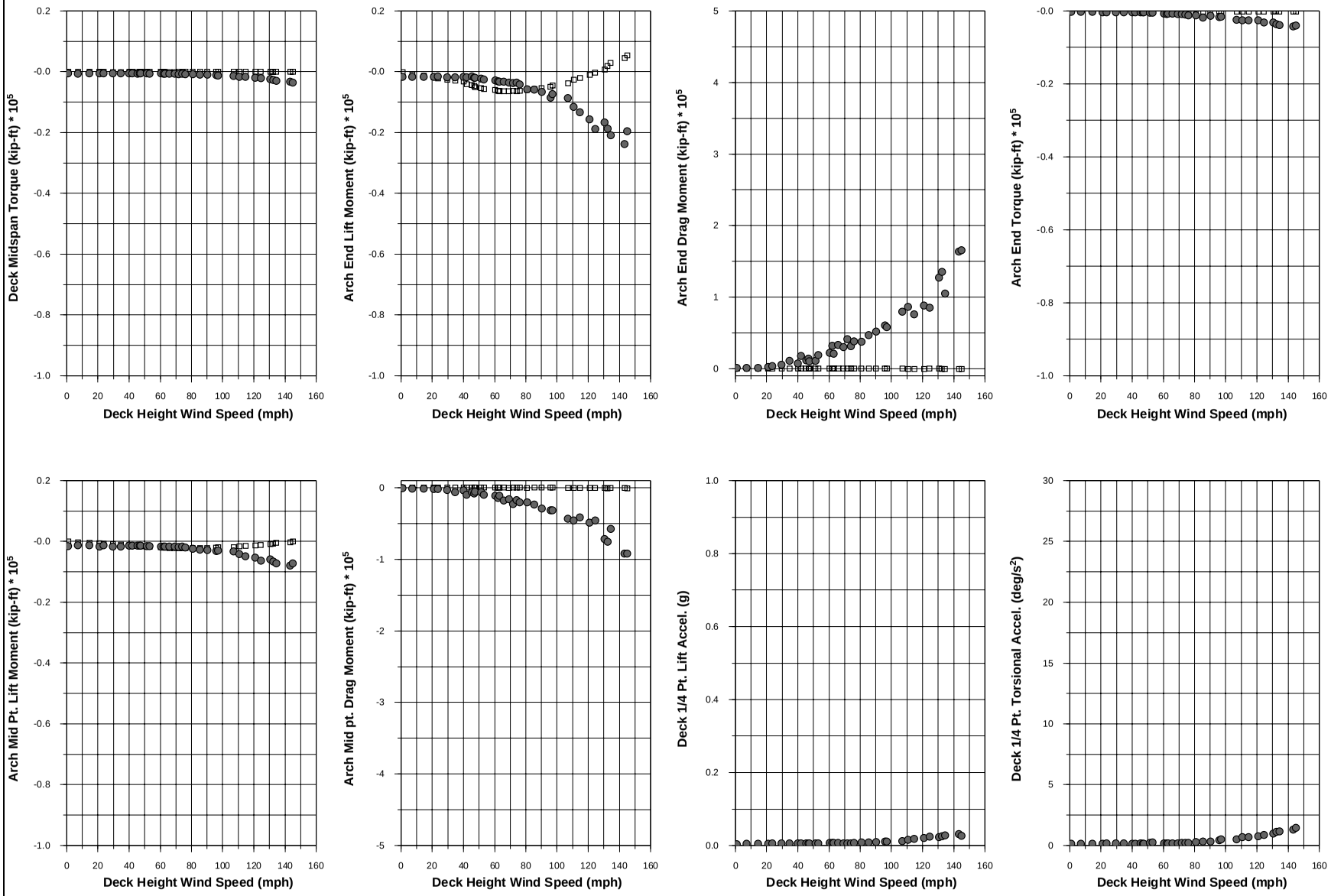

Indian River Bridge, open country exposure, wind along the deck (0 degrees)

May 31, 2004
Data File =ifd302.mst
Information File =ifd302.inf

MEAN
PEAK (RMS * 3.5)

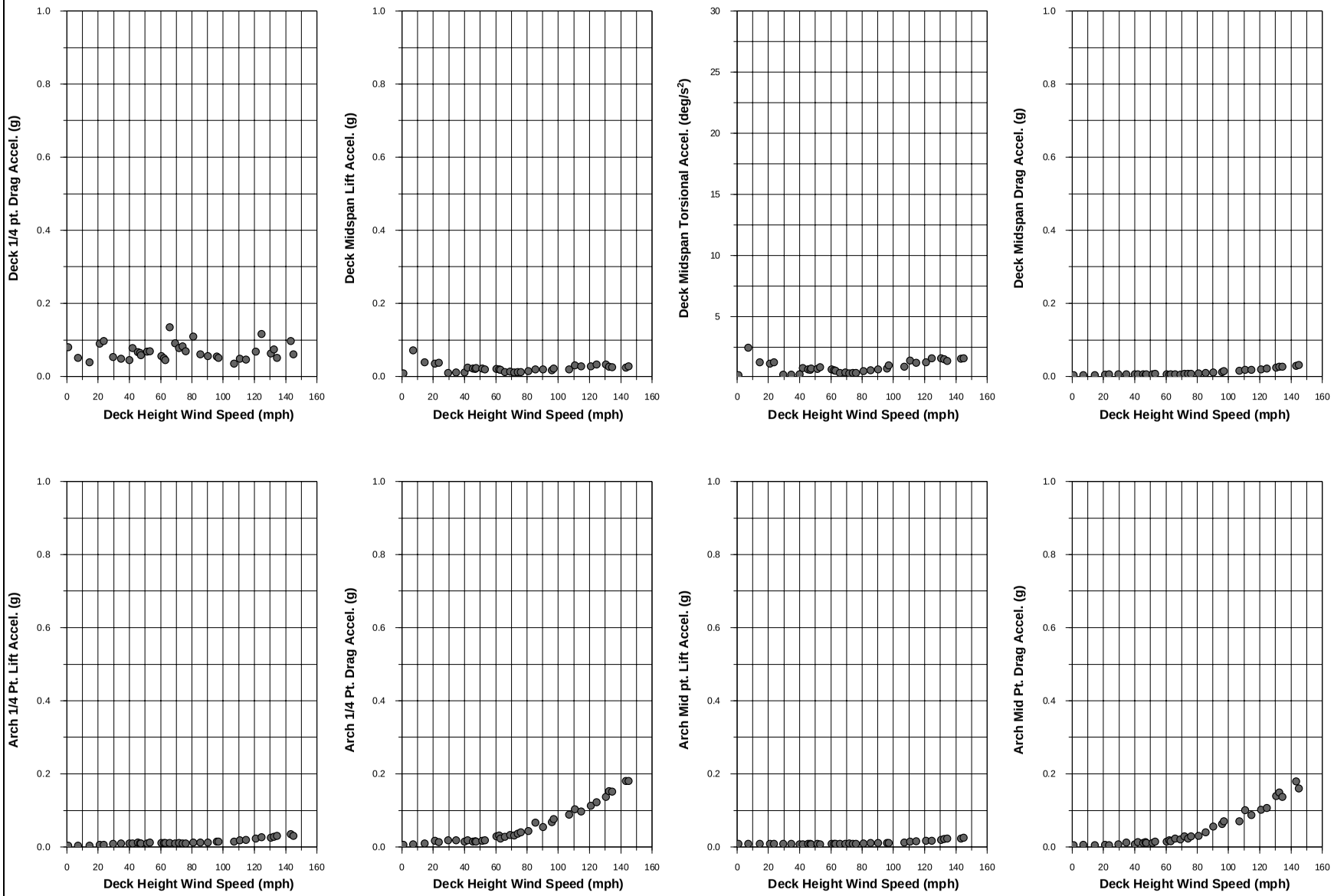

Indian River Bridge, open country exposure, wind along the deck (0 degrees)

May 31, 2004
Data File =ifd302.mst
Information File =ifd302.inf

MEAN
PEAK (RMS * 3.5)

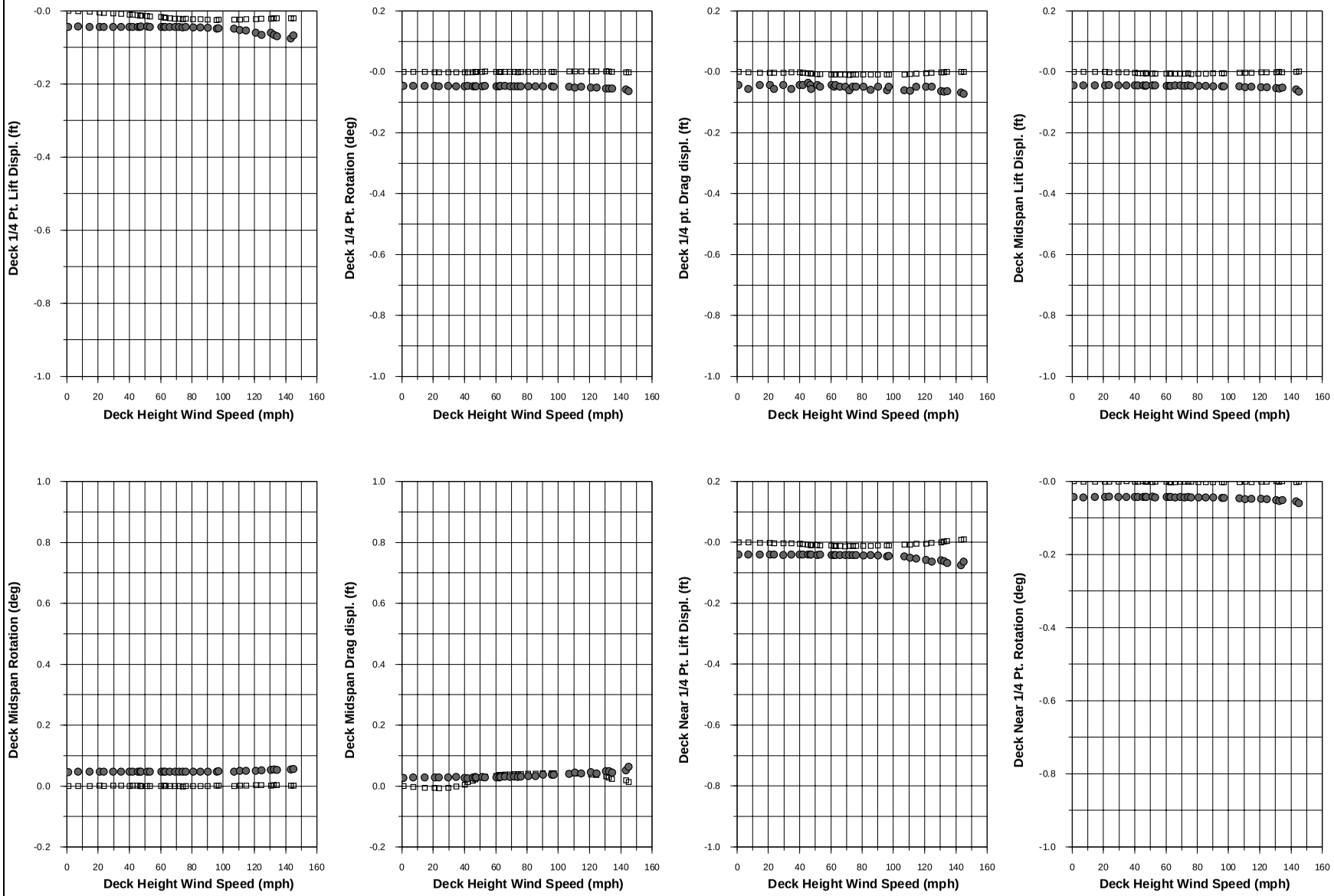

Indian River Bridge, open country exposure, wind along the deck (0 degrees)

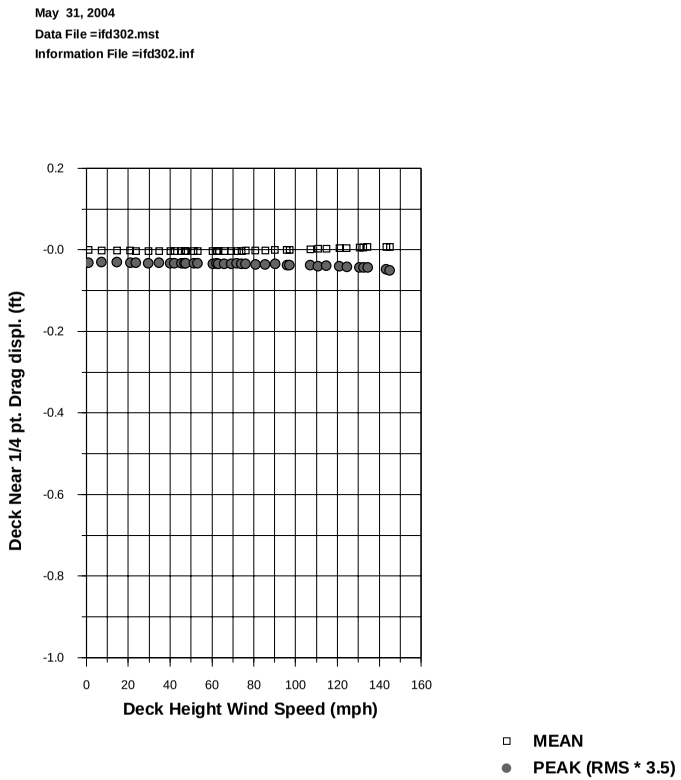

Indian River Bridge, open country exposure, wind along the deck (0 degrees)

May 31, 2004
Data File =ife302.mst
Information File =ife302.inf

MEAN
PEAK (RMS * 3.5)

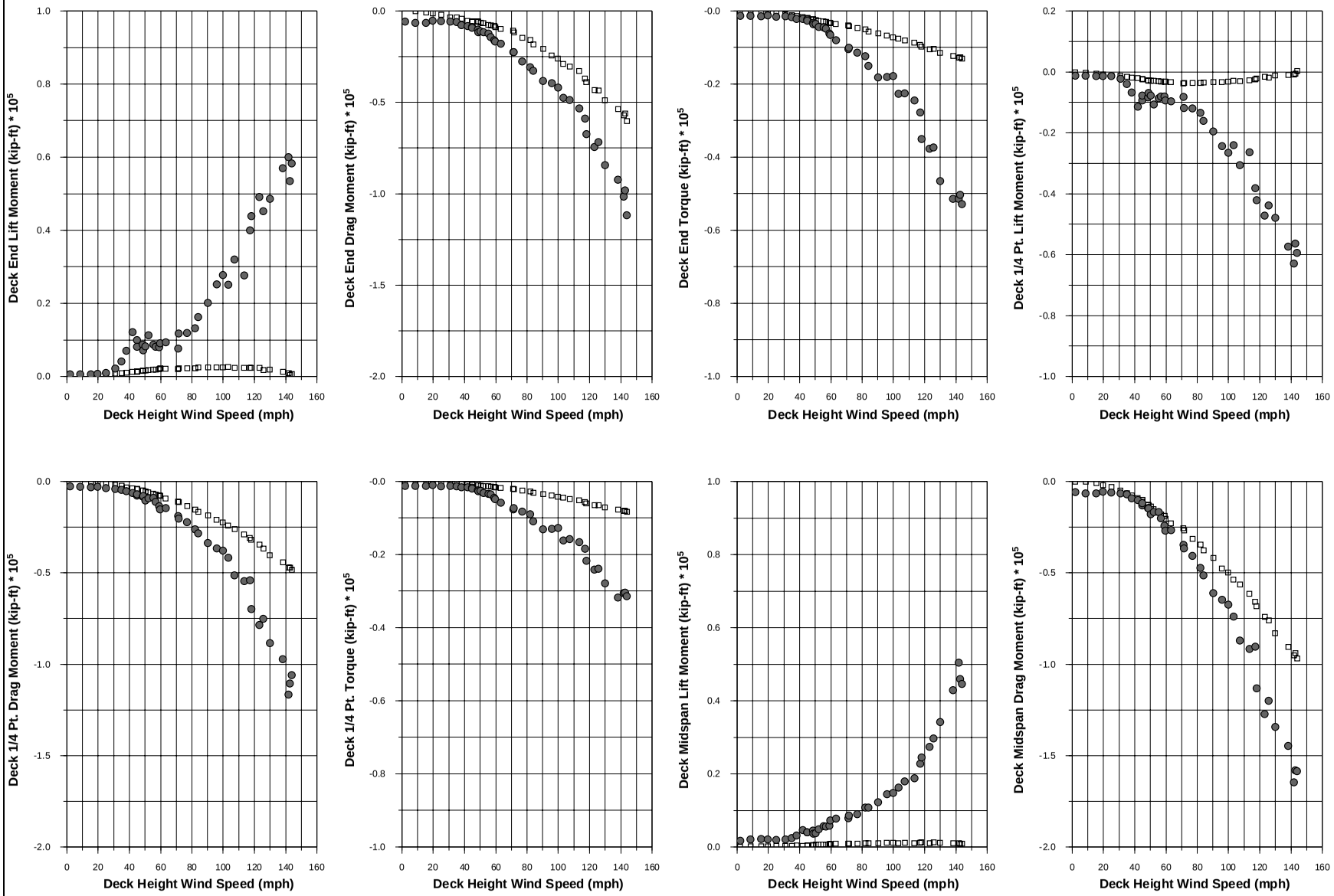

Indian River Bridge, open country profile without existing bridge, wind perpendicular to deck (270 degrees)

May 31, 2004
Data File =ife302.mst
Information File =ife302.inf

MEAN
PEAK (RMS * 3.5)

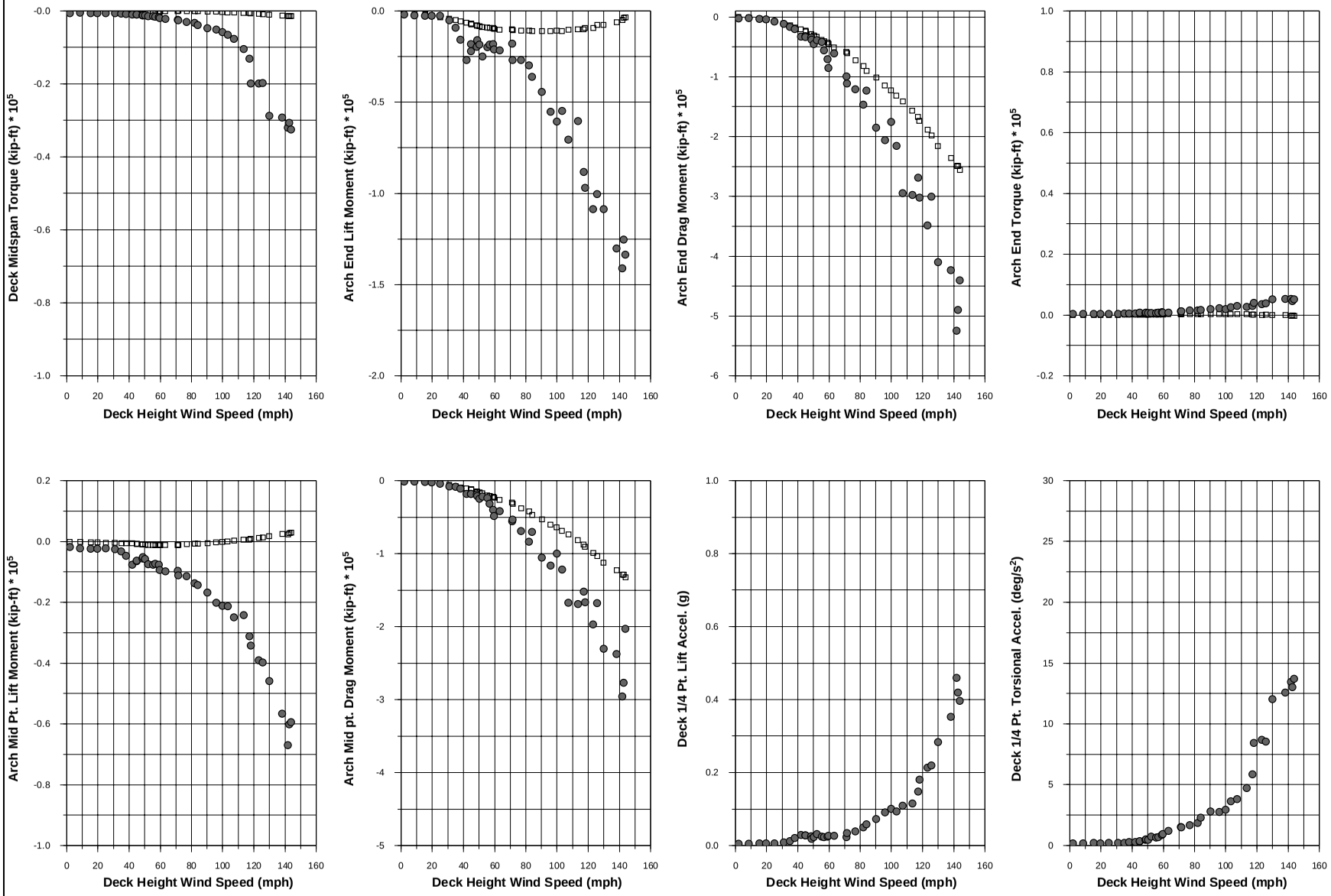

Indian River Bridge, open country profile without existing bridge, wind perpendicular to deck (270 degrees)

May 31, 2004
Data File =ife302.mst
Information File =ife302.inf

MEAN
PEAK (RMS * 3.5)

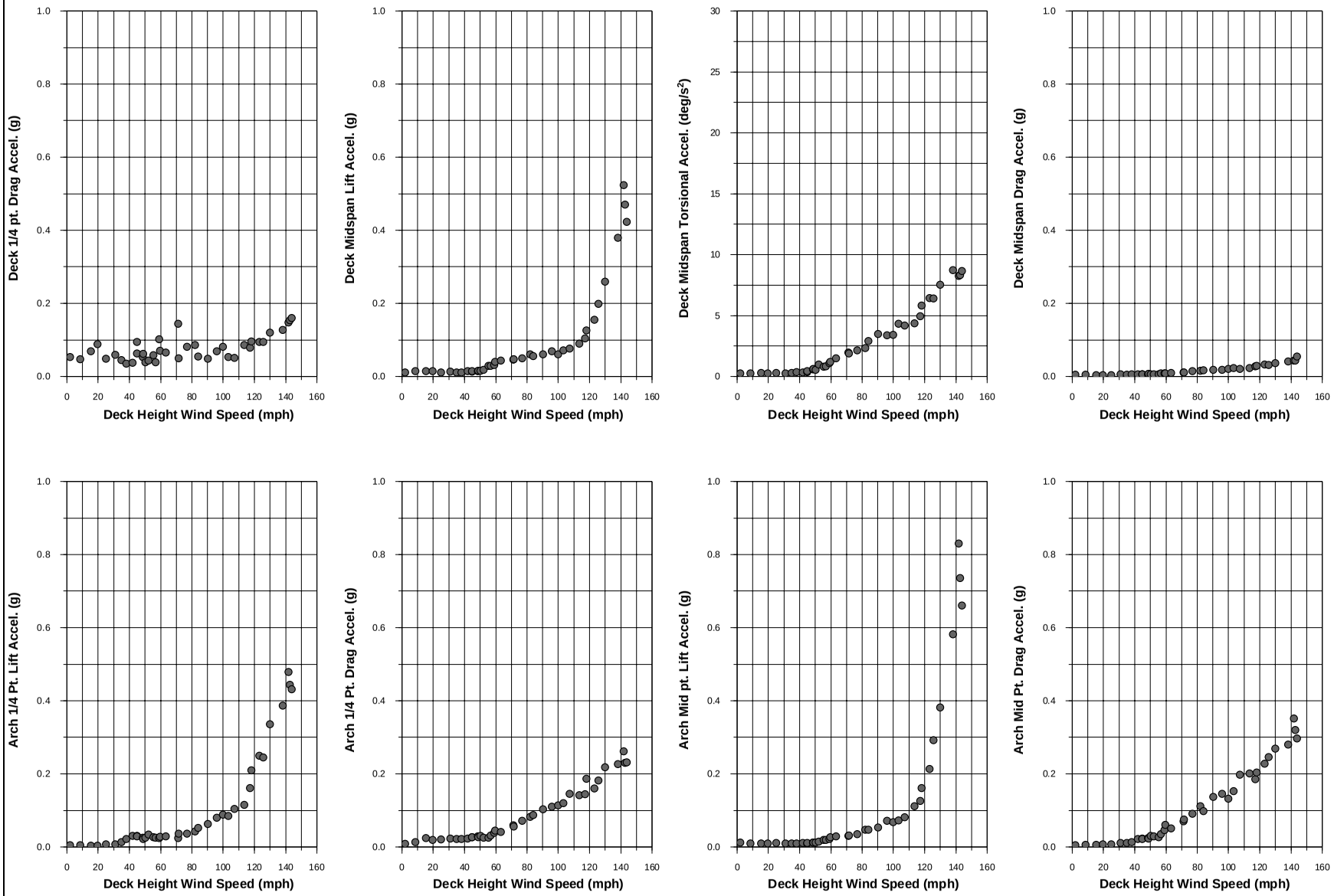

Indian River Bridge, open country profile without existing bridge, wind perpendicular to deck (270 degrees)

May 31, 2004
Data File =ife302.mst
Information File =ife302.inf

MEAN
PEAK (RMS * 3.5)

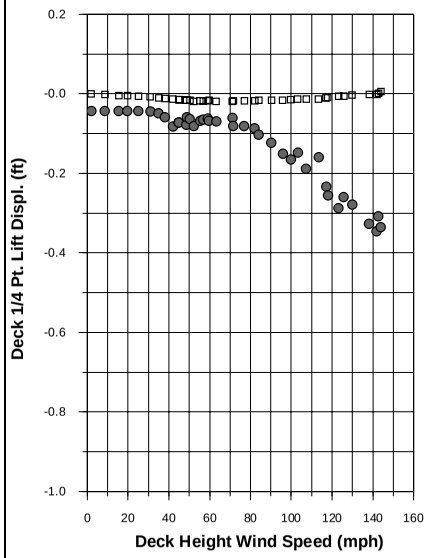

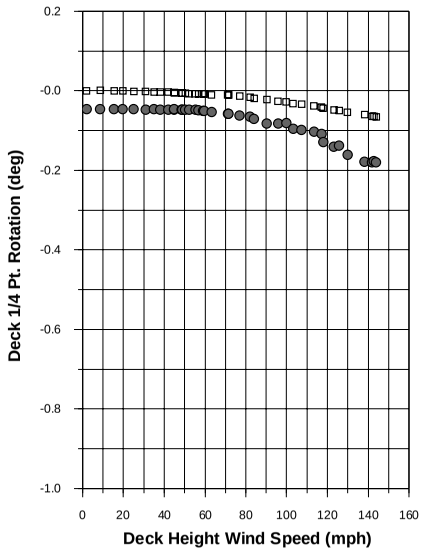

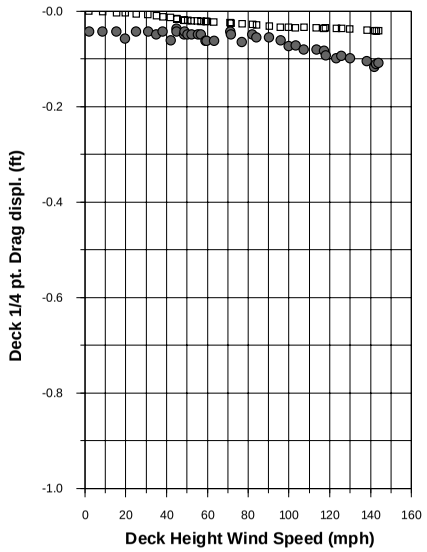

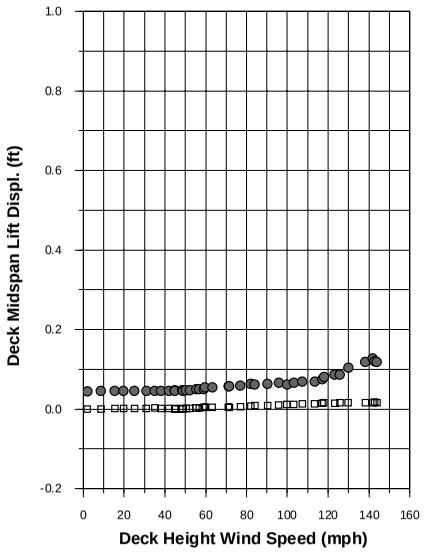

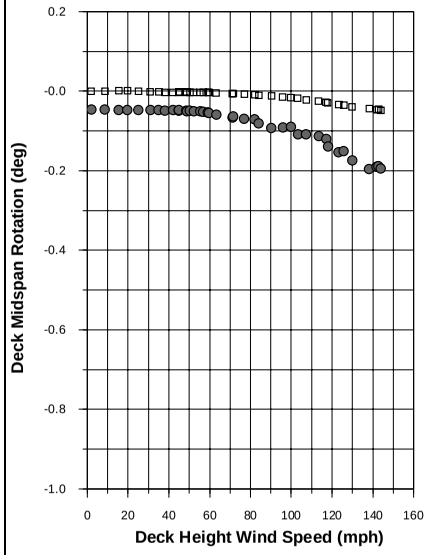

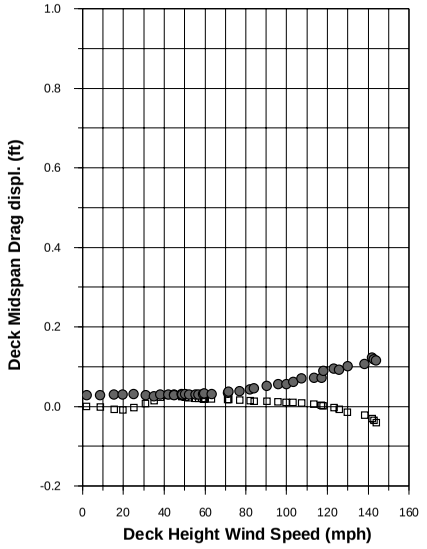

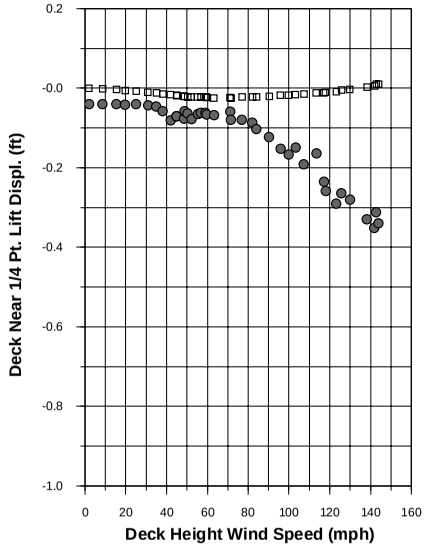

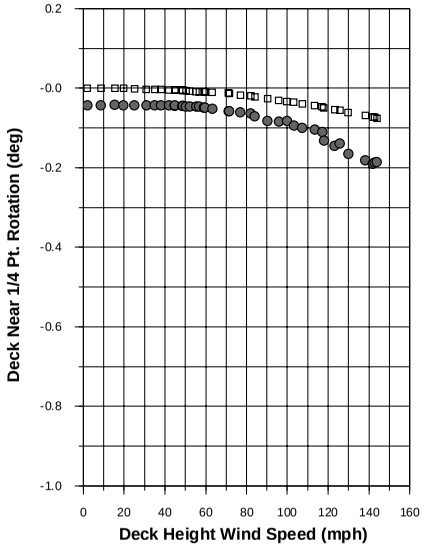

Indian River Bridge, open country profile without existing bridge, wind perpendicular to deck (270 degrees)

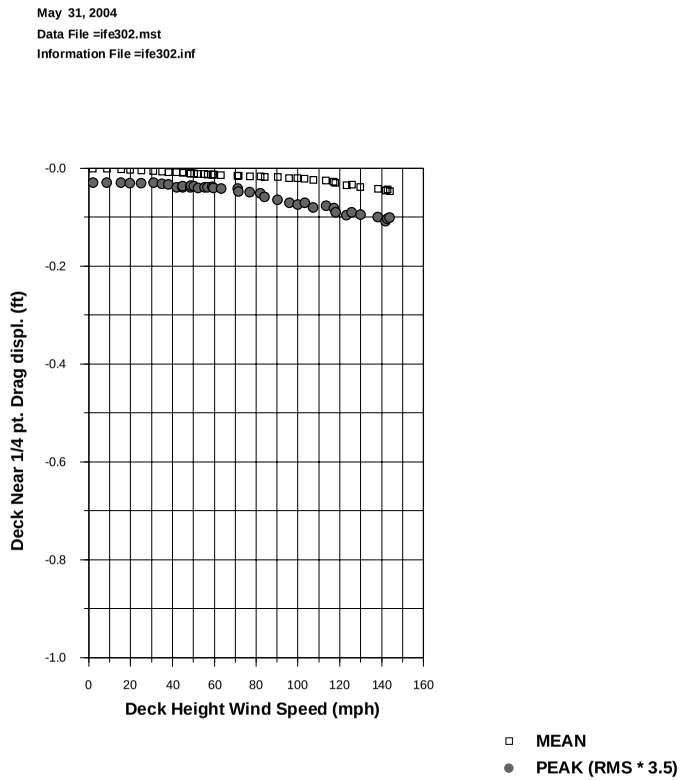

Indian River Bridge, open country profile without existing bridge, wind perpendicular to deck (270 degrees)

Jun. 01, 2004
Data File =ifa303.mst
Information File =ifa303.inf

MEAN
PEAK (RMS * 3.5)

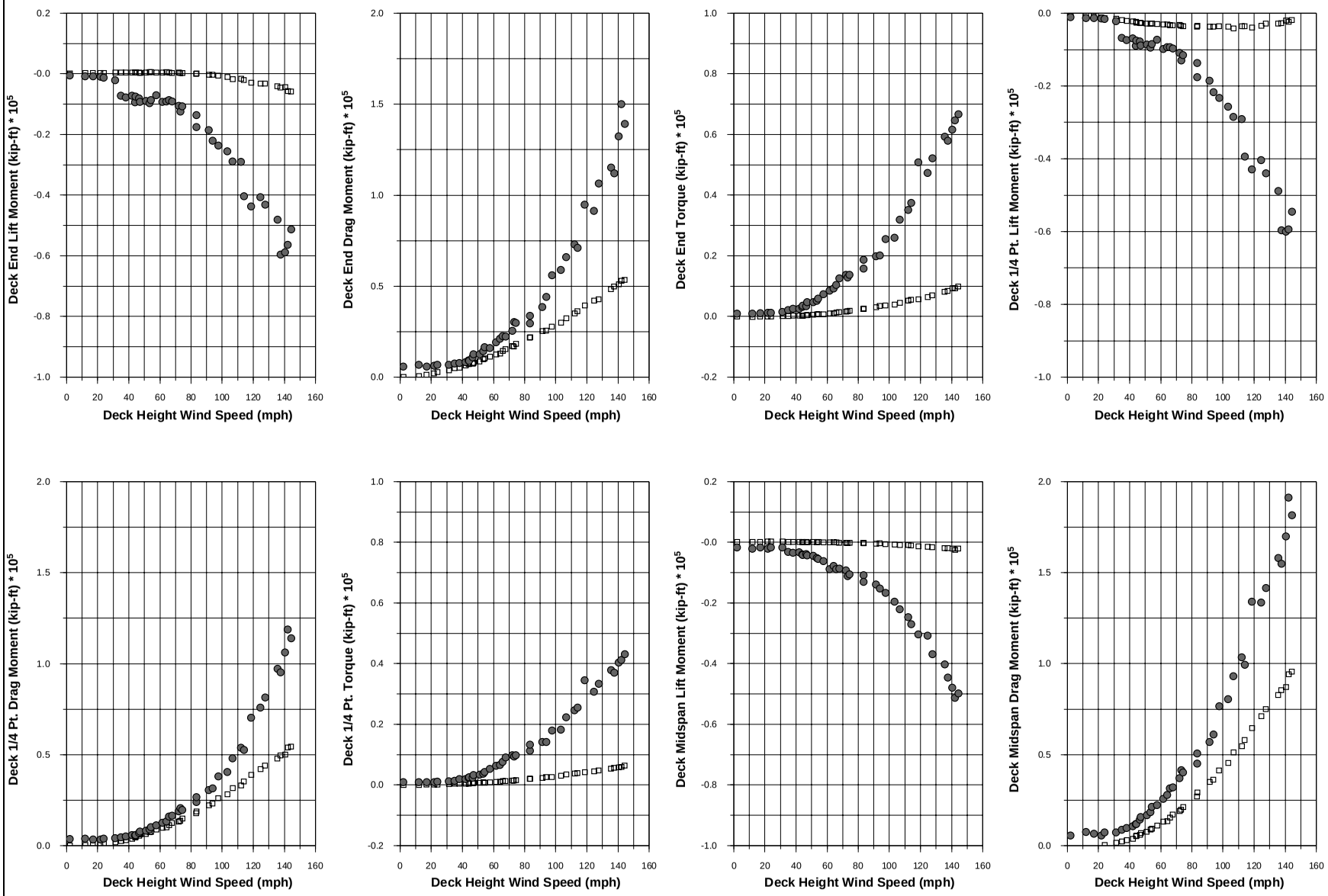

Indian River Bridge, open country profile, wind perpendicular to deck (90 degrees) with higher arch damping

Jun. 01, 2004
Data File =ifa303.mst
Information File =ifa303.inf

MEAN
PEAK (RMS * 3.5)

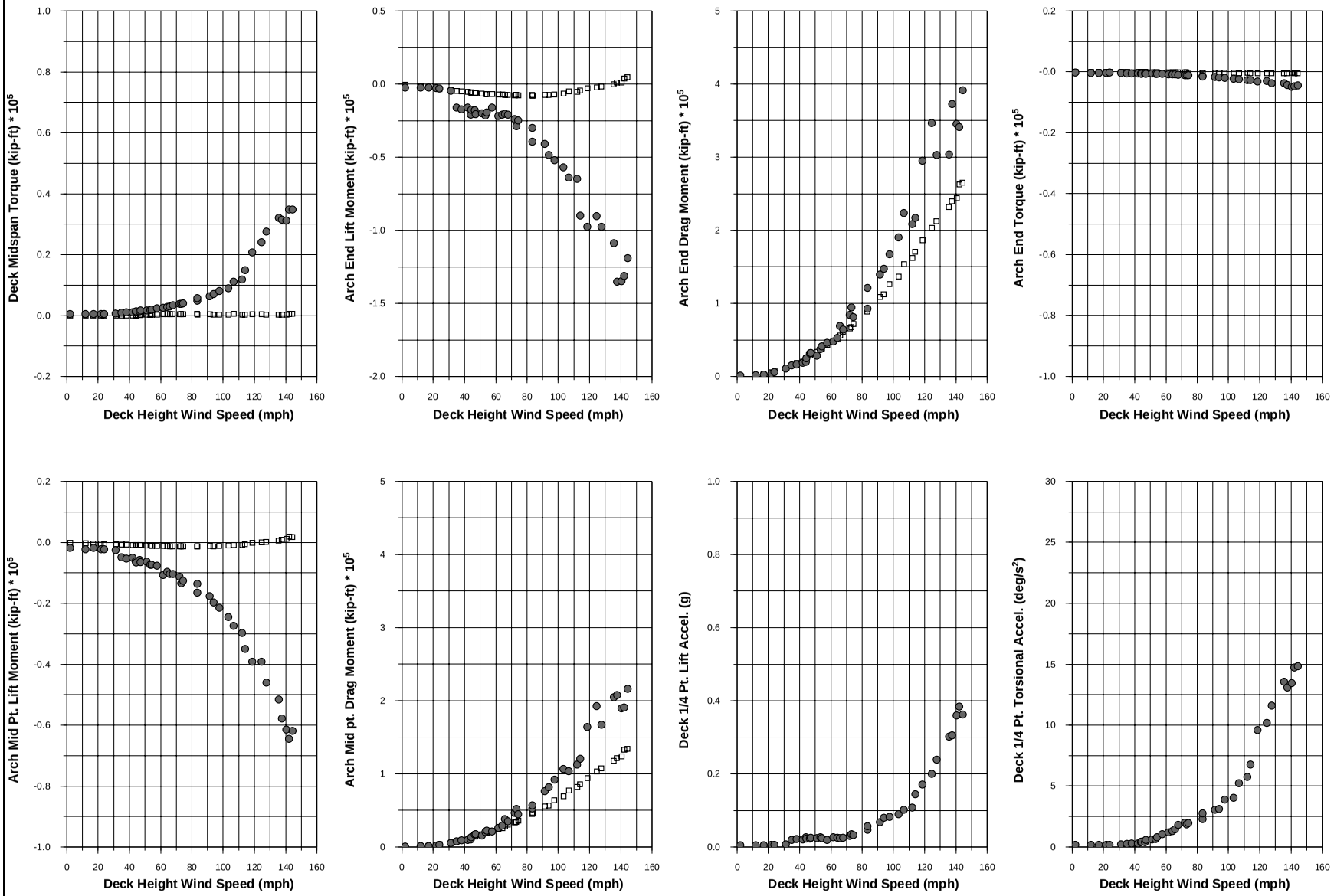

Indian River Bridge, open country profile, wind perpendicular to deck (90 degrees) with higher arch damping

Jun. 01, 2004
Data File =ifa303.mst
Information File =ifa303.inf

MEAN
PEAK (RMS * 3.5)

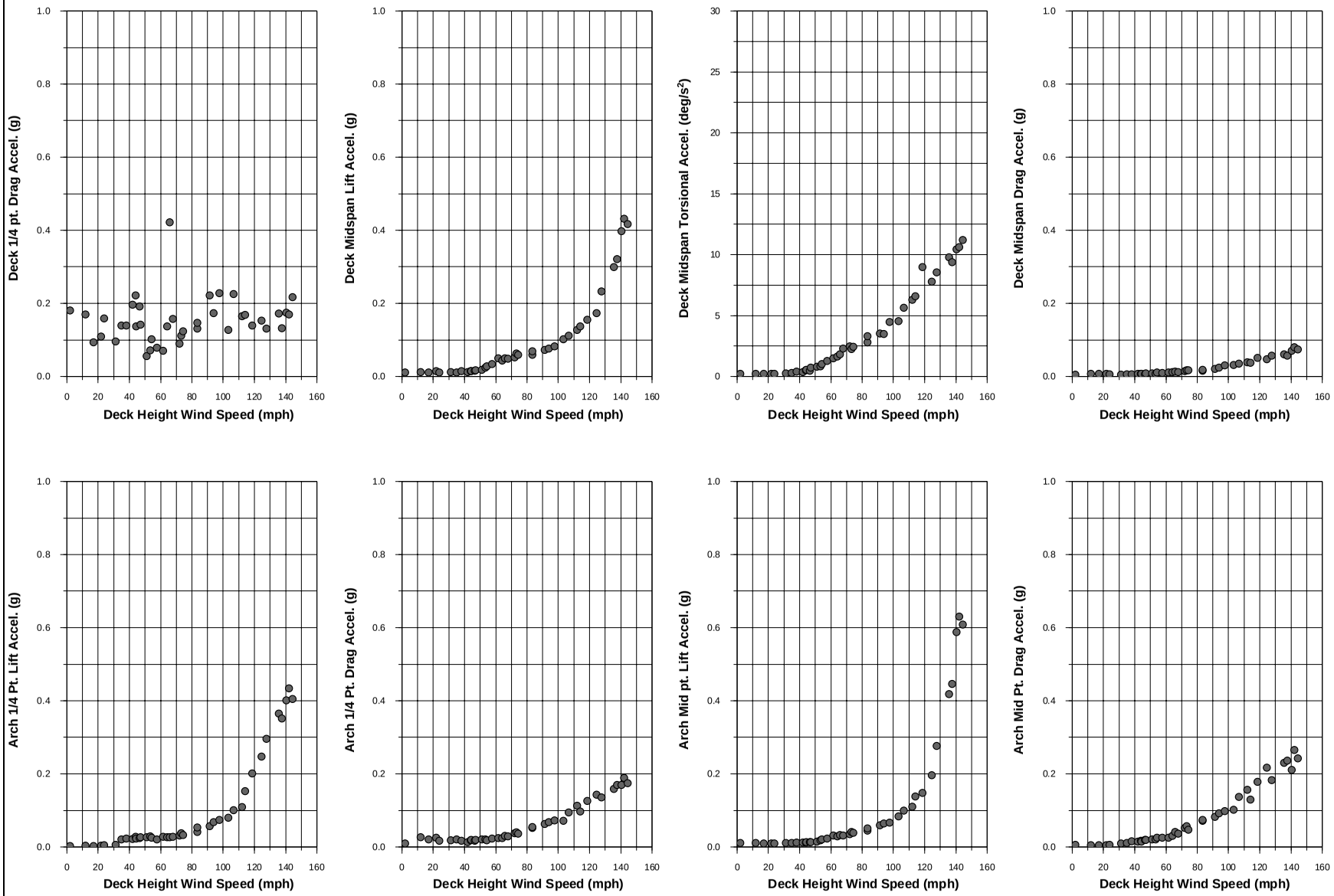

Indian River Bridge, open country profile, wind perpendicular to deck (90 degrees) with higher arch damping

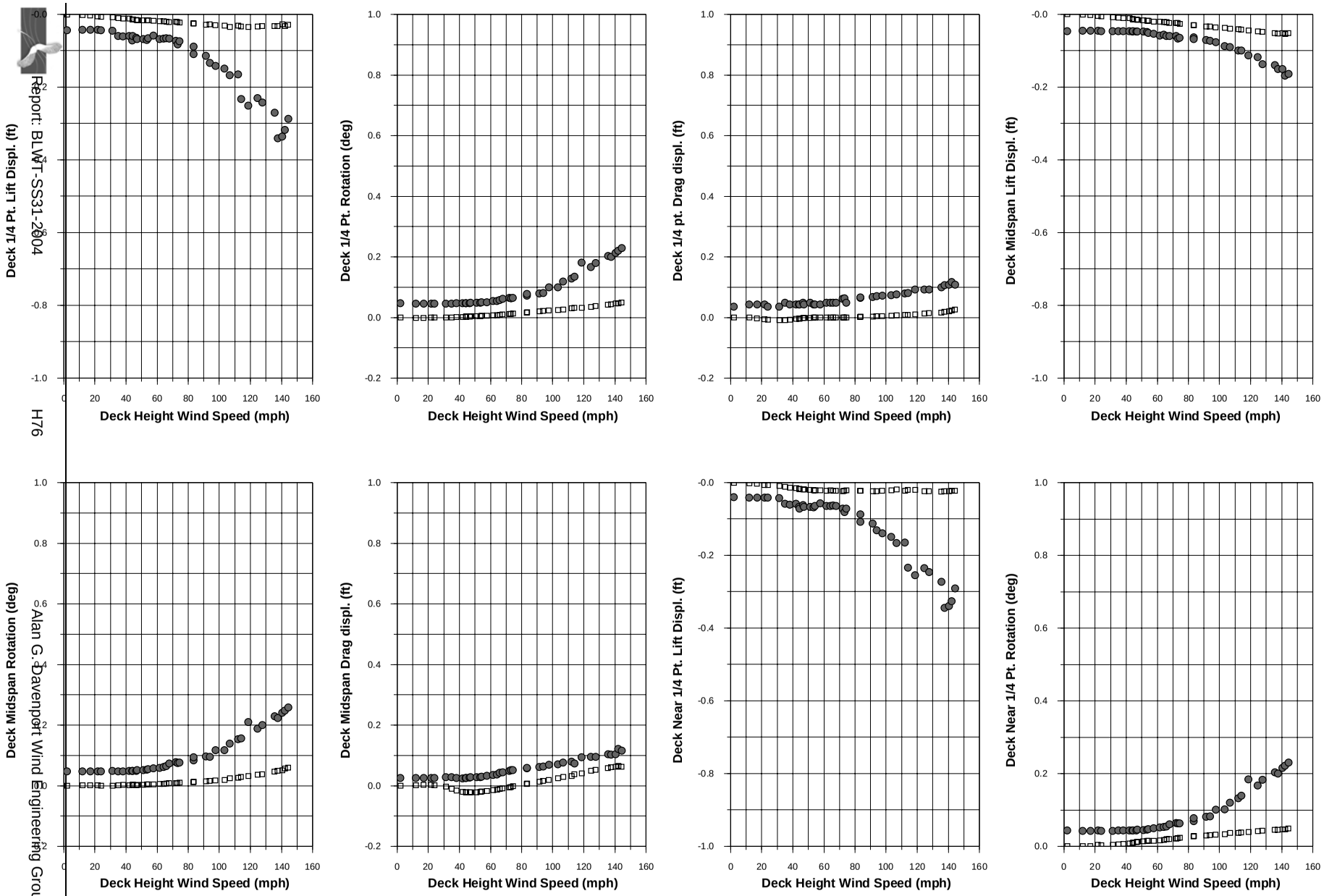

Indian River Bridge, open country profile, wind perpendicular to deck (90 degrees) with higher arch damping

Jun. 01, 2004
Data File =ifa303.mst
Information File =ifa303.inf

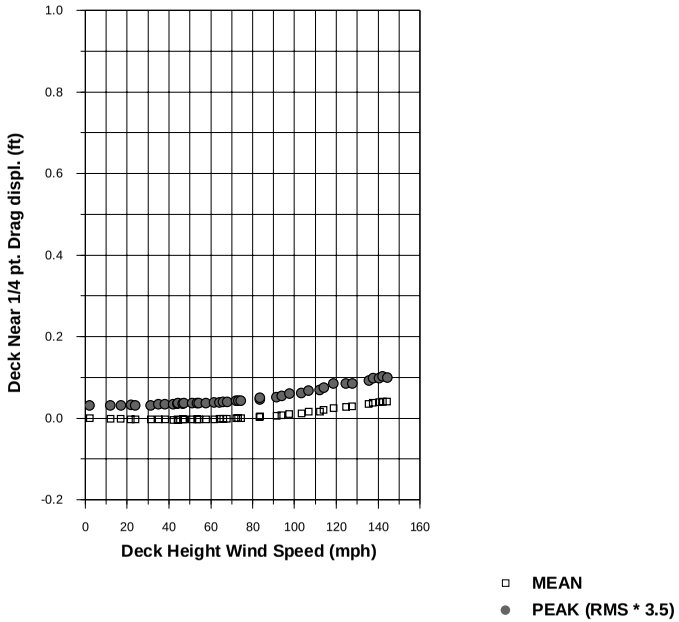

Indian River Bridge, open country profile, wind perpendicular to deck (90 degrees) with higher arch damping

Jun. 09, 2004
Data File =ifa402.mst
Information File =ifa402.inf

MEAN
PEAK (RMS * 3.5)

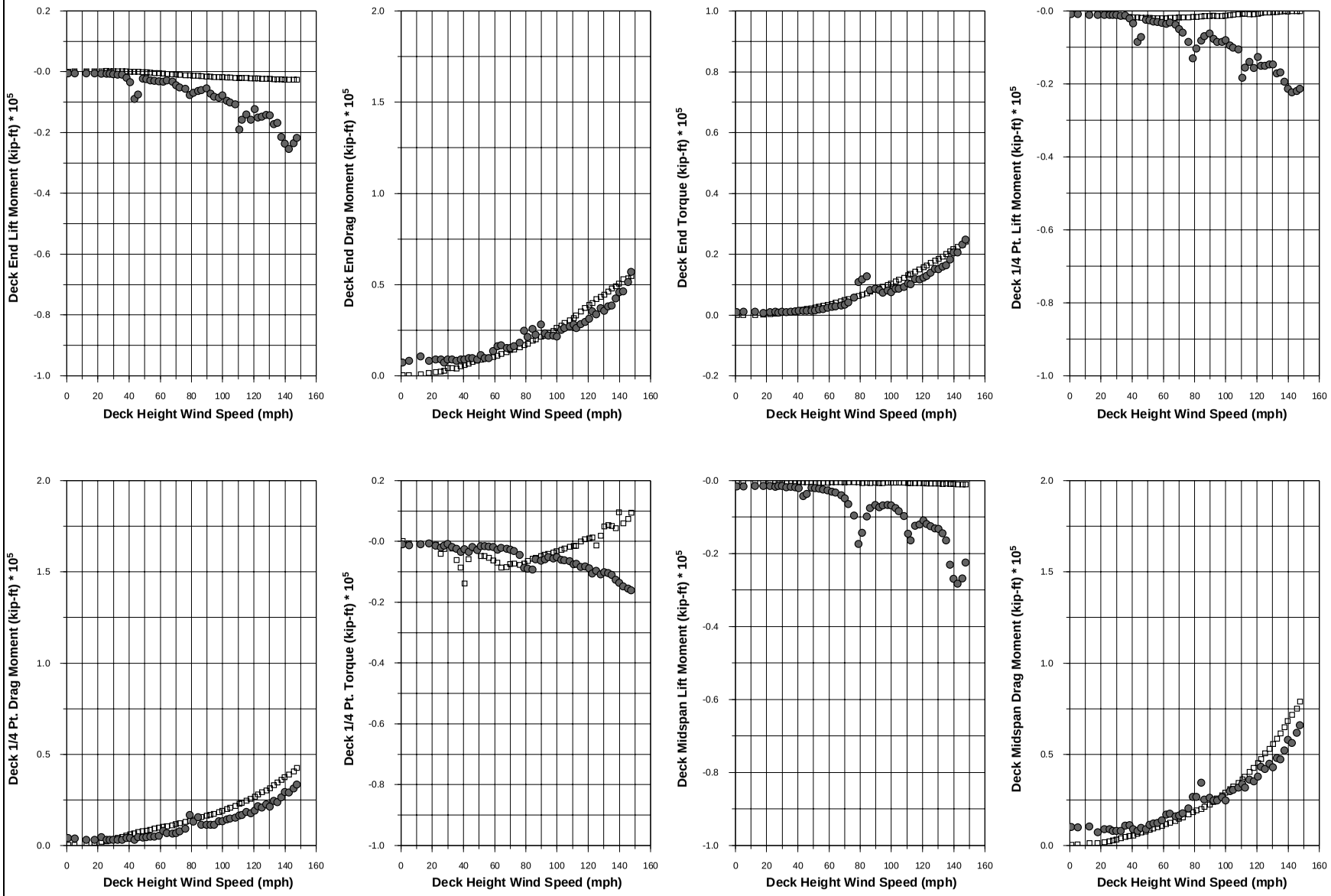

Indian River Bridge, smooth flow, wind perpendicular to deck (90 degrees)

Jun. 09, 2004
Data File =ifa402.mst
Information File =ifa402.inf

MEAN
PEAK (RMS * 3.5)

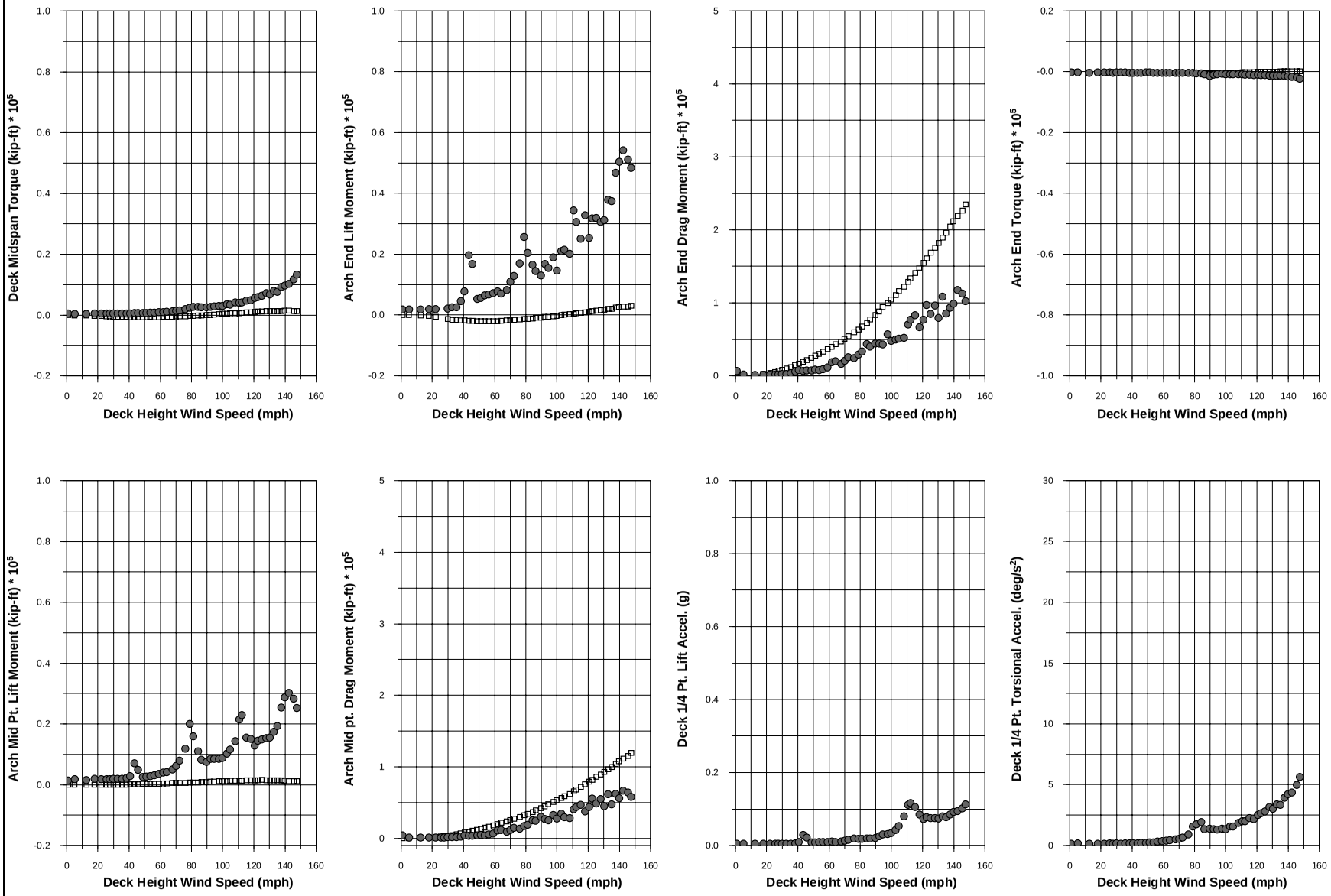

Indian River Bridge, smooth flow, wind perpendicular to deck (90 degrees)

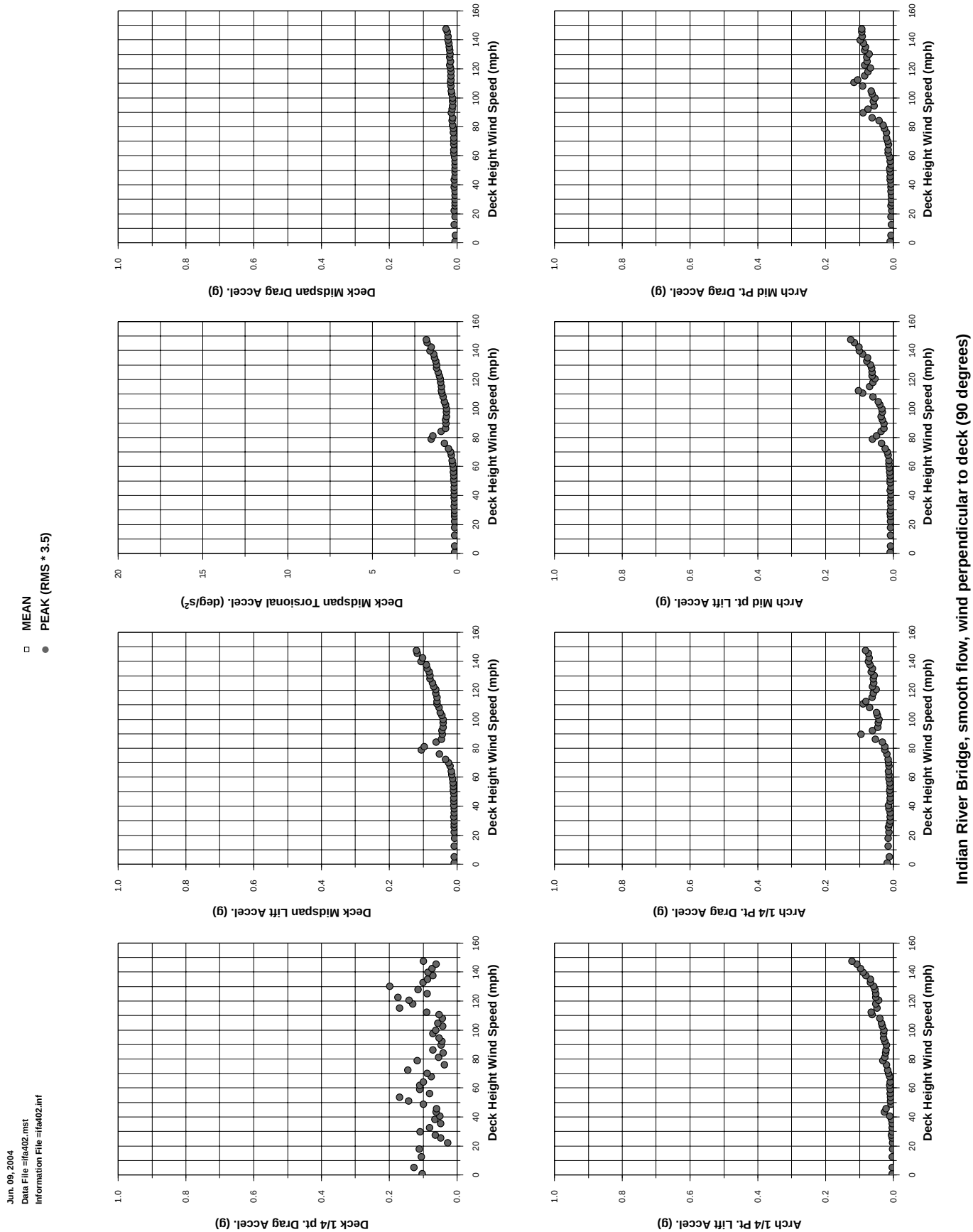

Indian River Bridge, smooth flow, wind perpendicular to deck (90 degrees)

Jun. 09, 2004
Data File =ifa402.mst
Information File =ifa402.inf

MEAN
PEAK (RMS * 3.5)

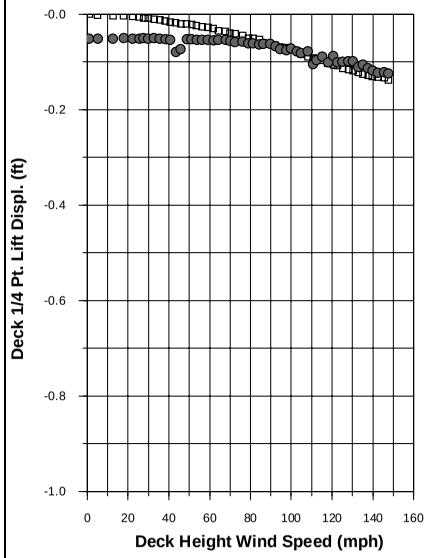

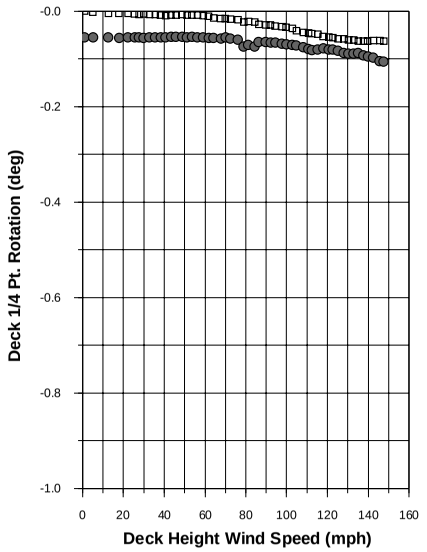

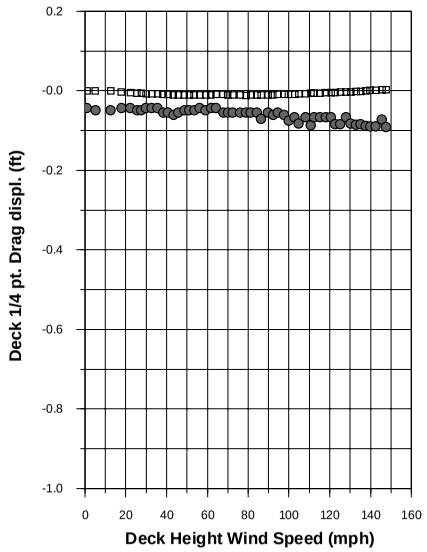

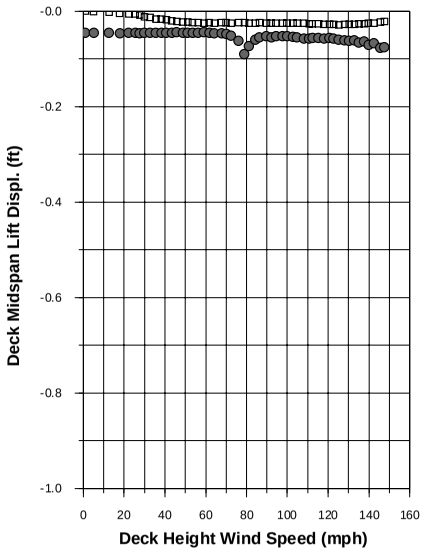

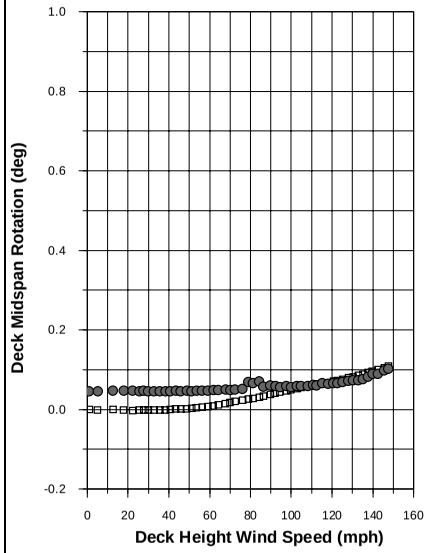

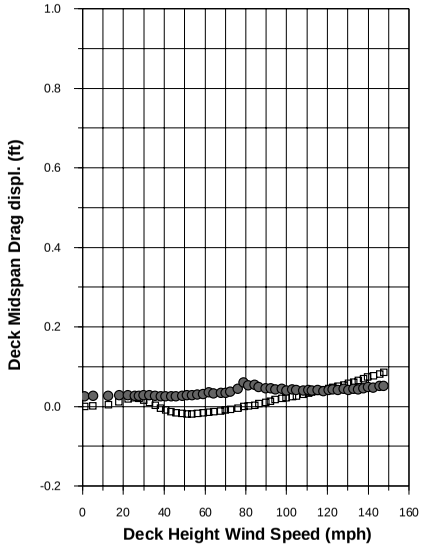

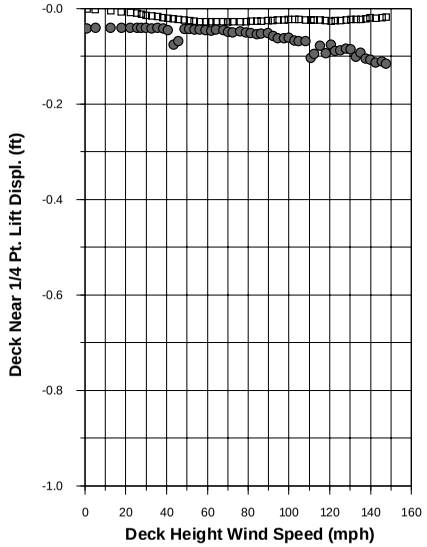

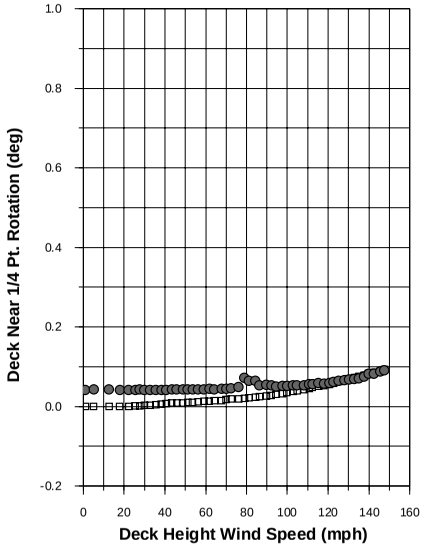

Indian River Bridge, smooth flow, wind perpendicular to deck (90 degrees)

Jun. 09, 2004
Data File =ifa402.mst
Information File =ifa402.inf

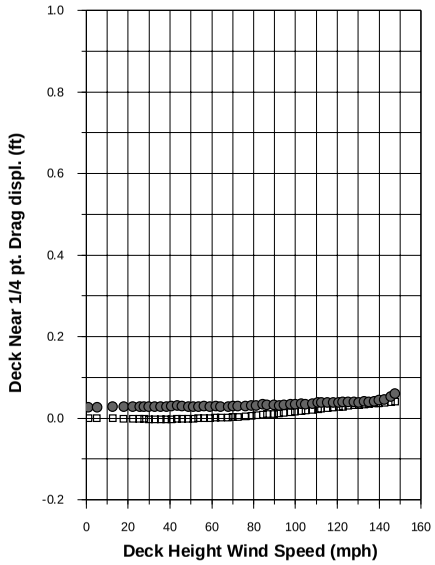

MEAN
PEAK (RMS * 3.5)

Indian River Bridge, smooth flow, wind perpendicular to deck (90 degrees)

APPENDIX I

RESULTS OF FULL BRIDGE AEROELASTIC TESTS, CONSTRUCTION STAGE – CANTILEVERED TIE BEAM

Notes:

1. The bending moments given in the plots have the unit of kip-ft. The numbers read directly from the plots should be multiplied by 10^5 to obtain the actual bending moments in kip-ft. For example on page I9 of the Arch End Drag Moment (the lower left figure on that page), both the mean and peak drag moments at about 100mph are approximately 1.0×10^5 kip-ft (not 1.0 kip-ft).

2. The total response is equal to the mean, plus or minus the peak.

3. X is along the longitudinal direction, Y is the lateral direction (drag direction), and Z is the vertical direction (lift direction). Thus M_x is the torque, M_y is the lift moment (generated by the lift) and M_z is the drag moment (generated by the drag).

TABLE I1 INSTRUMENTATION LOCATIONS, CONSTRUCTION STAGE – CANTILEVERED TIE BEAM

Instrumentation **x – longitudinal, y – lateral (Drag), z – vertical (Lift)**	**Instrumentation Locations** **(Refer to Figure I1)**
Strain Gages:	
M_x, M_y and M_z at **Tie-Beam** End	Lift and Drag Moments, as well as Torque at 438ft from Midspan
M_x, M_y and M_z at **Arch** End	Lift and Drag Moments, as well as Torque at 42ft from Arch-Deck connection
M_y and M_z at **Arch** Crown	Lift and Drag Moments at 44ft from Arch Crown
Accelerometers:	
y and z at **Tie-Beam** Midspan	Lift and Drag Accelerations at 20ft from Midspan
y and z at **Tie-Beam** 1/4 Point	Lift and Drag Accelerations at 225ft from Midspan
y and z at **Tie-Beam** other 1/4 Point	Lift and Drag Accelerations at 235ft from Midspan
y and z accel. at **Arch** Crown	Lift and Drag Accelerations at 14ft from Arch Crown
Displacement Lasers:	
y and z displacements at **Tie-Beam** Midspan	Lift and Drag Displacements at 12ft from Midspan
y and z at **Tie-Beam** 1/4 point	Lift and Drag Displacements at 225ft from Midspan
y and z displacements at **Tie-Beam** other 1/4 point	Lift and Drag Displacements at 240ft from Midspan
y and z displacements at **Arch** Crown	Lift and Drag Displacements at 14ft from Arch Crown
Wind Speeds:	
Deck Level	Deck Height
Arch Level	Arch Crown Height

TABLE I2 SUMMARY OF TESTS, CONSTRUCTION STAGE – CANTILEVERED TIE BEAM, INDIAN RIVER BRIDGE

Test File	Test No.	Flow condition	Existing bridge	Wind direction (Test angle)	V_{deck} (mph) Maximum wind speed at deck height	Vortex shedding peaks at wind speeds
CPA201	1	Hurricane profile	No	Along the bridge (0°)	141	Not observed
CPA202	2	Hurricane profile	No	Perpendicular to bridge (90°)	142	50 mph
CPA203	3	Hurricane profile	Yes	Perpendicular to bridge (90°)	142	Not observed
CPA204	4	Hurricane profile	No	60° to the bridge	144	50 and 90 mph
CPA205	5	Hurricane profile	No	30° to the bridge	144	80 mph
CPA301	6	Open Country profile	No	30° to the bridge	161	80 mph
CPA302	7	Open Country profile	No	Along the bridge (0°)	161	Not observed
CPA303	8	Open Country profile	No	60° to the bridge	148	50 and 90 mph
CPA304	9	Open Country profile	No	Perpendicular to bridge (90°)	140	50 mph
CPA305	10	Open Country profile	Yes	Perpendicular to bridge (90°)	140	Not observed
CPA101	11	Smooth Flow	No	Perpendicular to bridge (90°)	148	50 and 90 mph

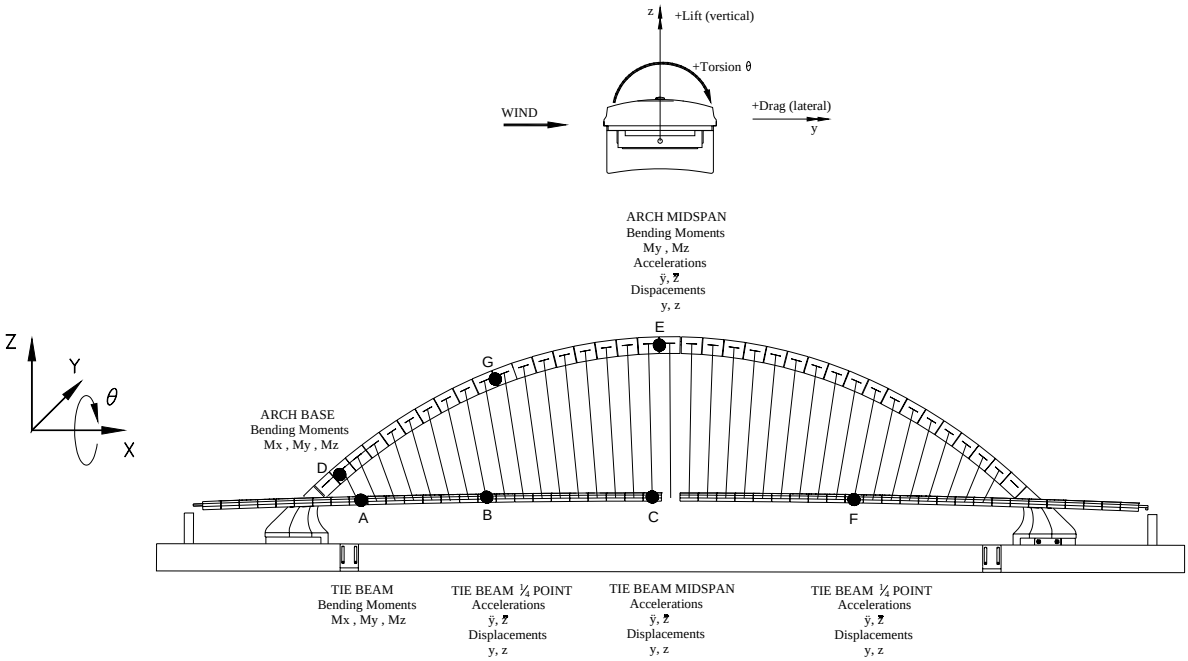

FIGURE I1 BRIDGE SIGN CONVENTION AND INSTRUMENTATION LOCATIONS, CONSTRUCTION STAGE – CANTILEVERED TIE BEAM

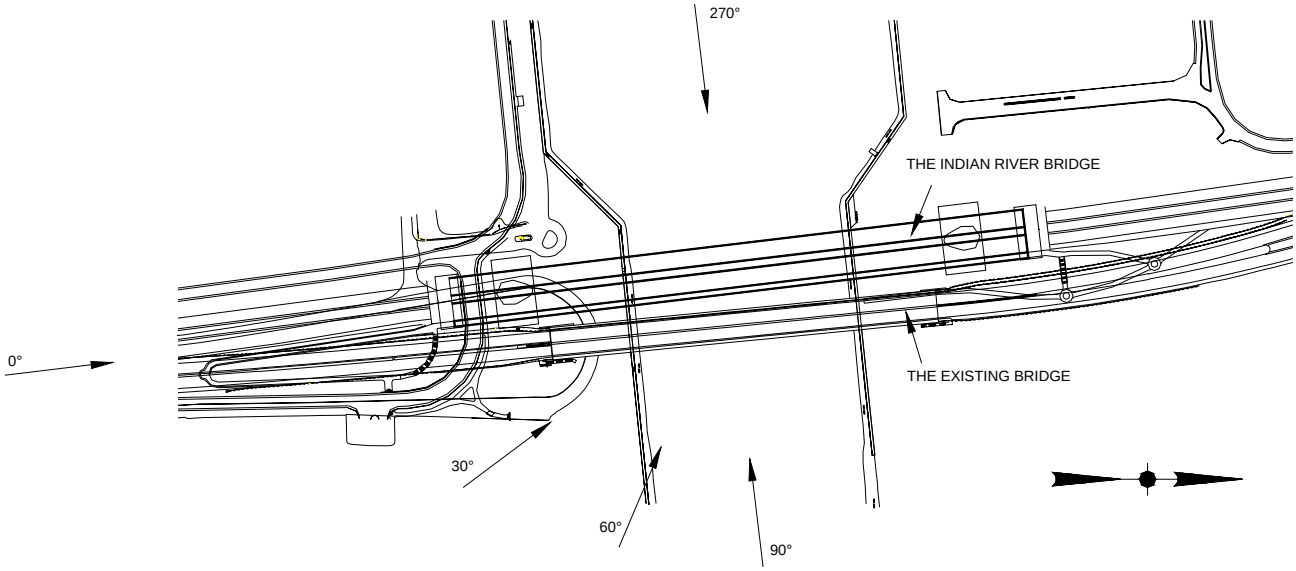

WIND DIRECTION DEFINITION

FIGURE I2 WIND ANGLES DEFINED IN WIND TUNNEL TESTS

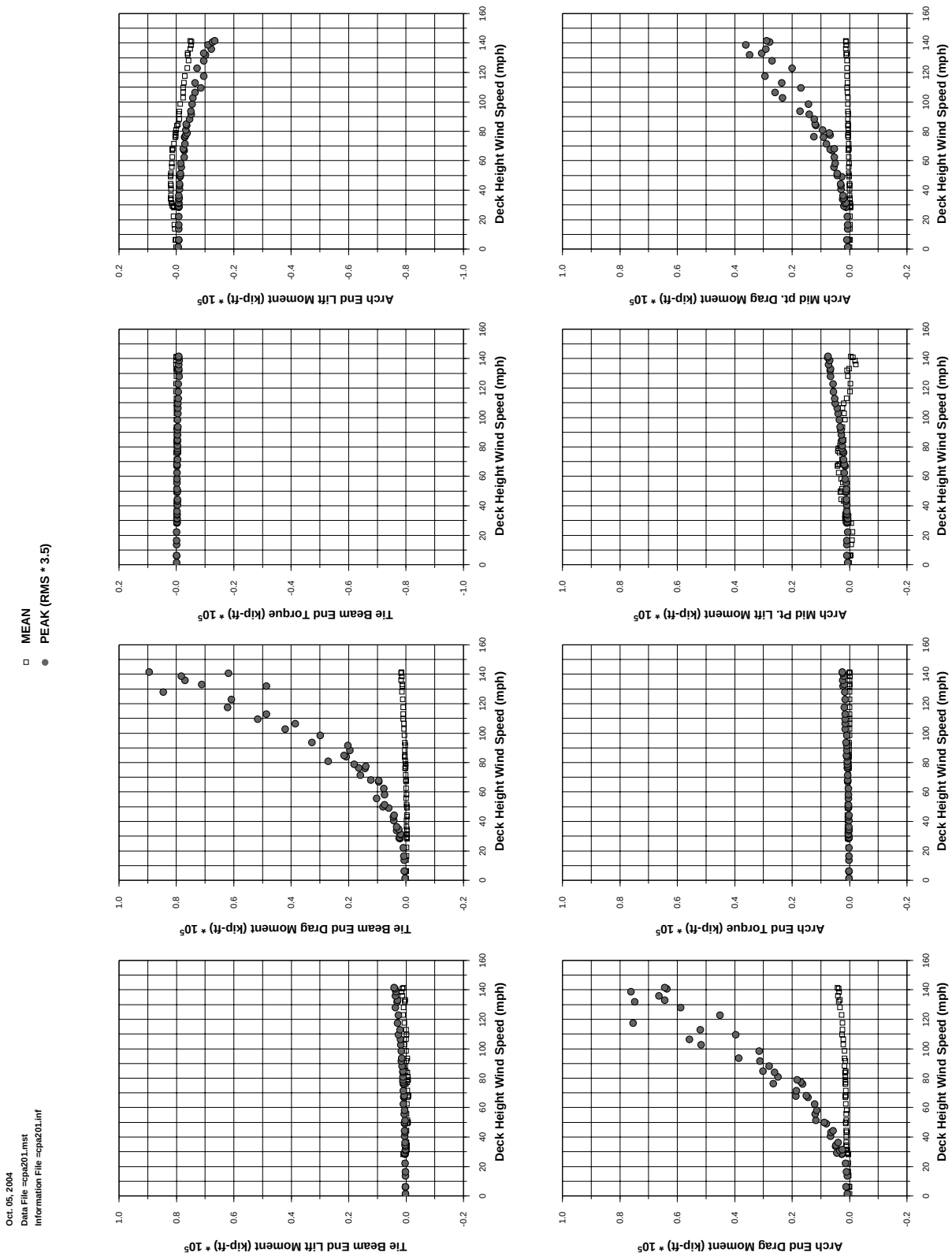

Indian River Bridge, Cantilevered Tie Beam, hurricane profile, 0 degrees

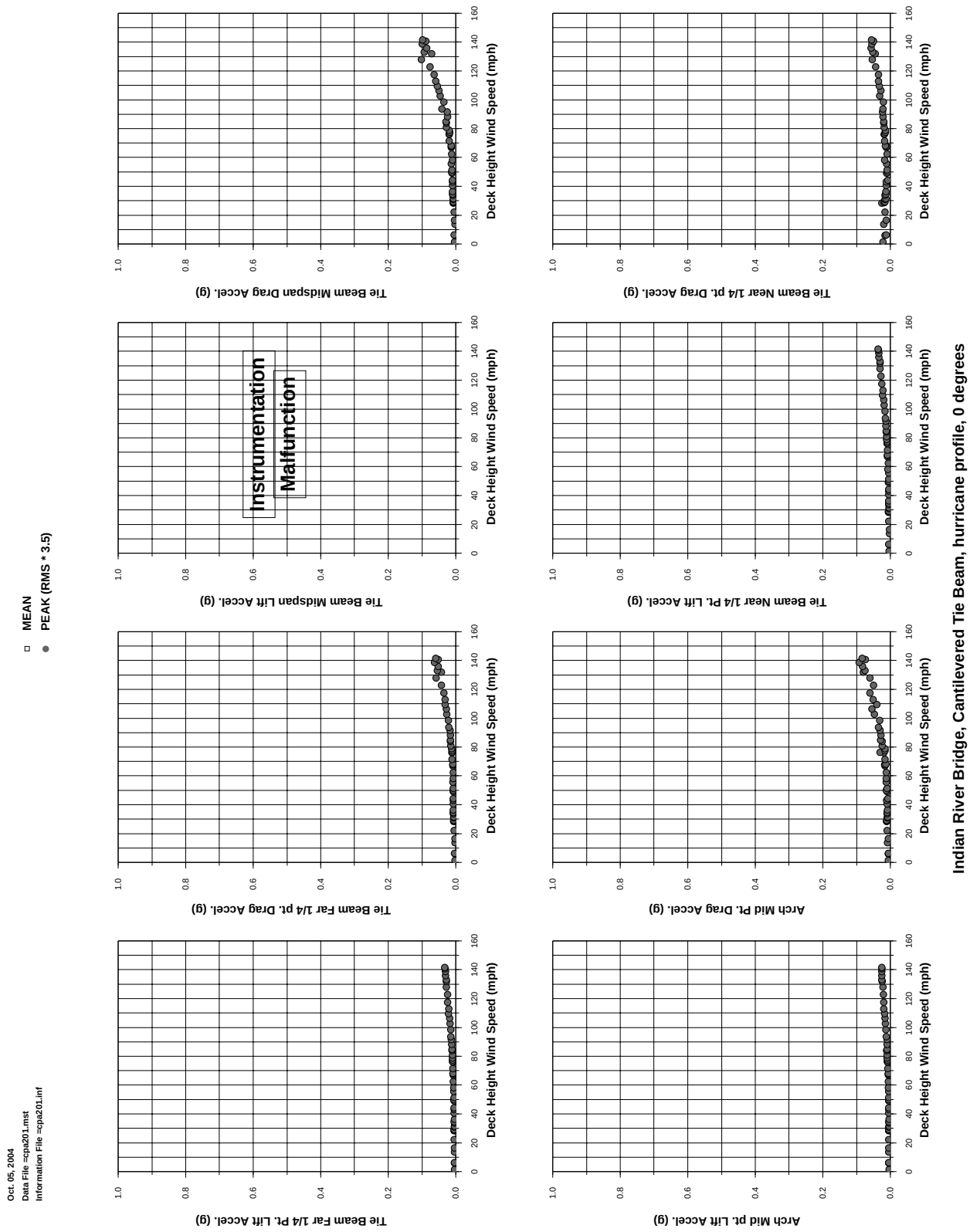

Indian River Bridge, Cantilevered Tie Beam, hurricane profile, 0 degrees

Oct. 05, 2004
Data File =cpa201.mst
Information File =cpa201.inf

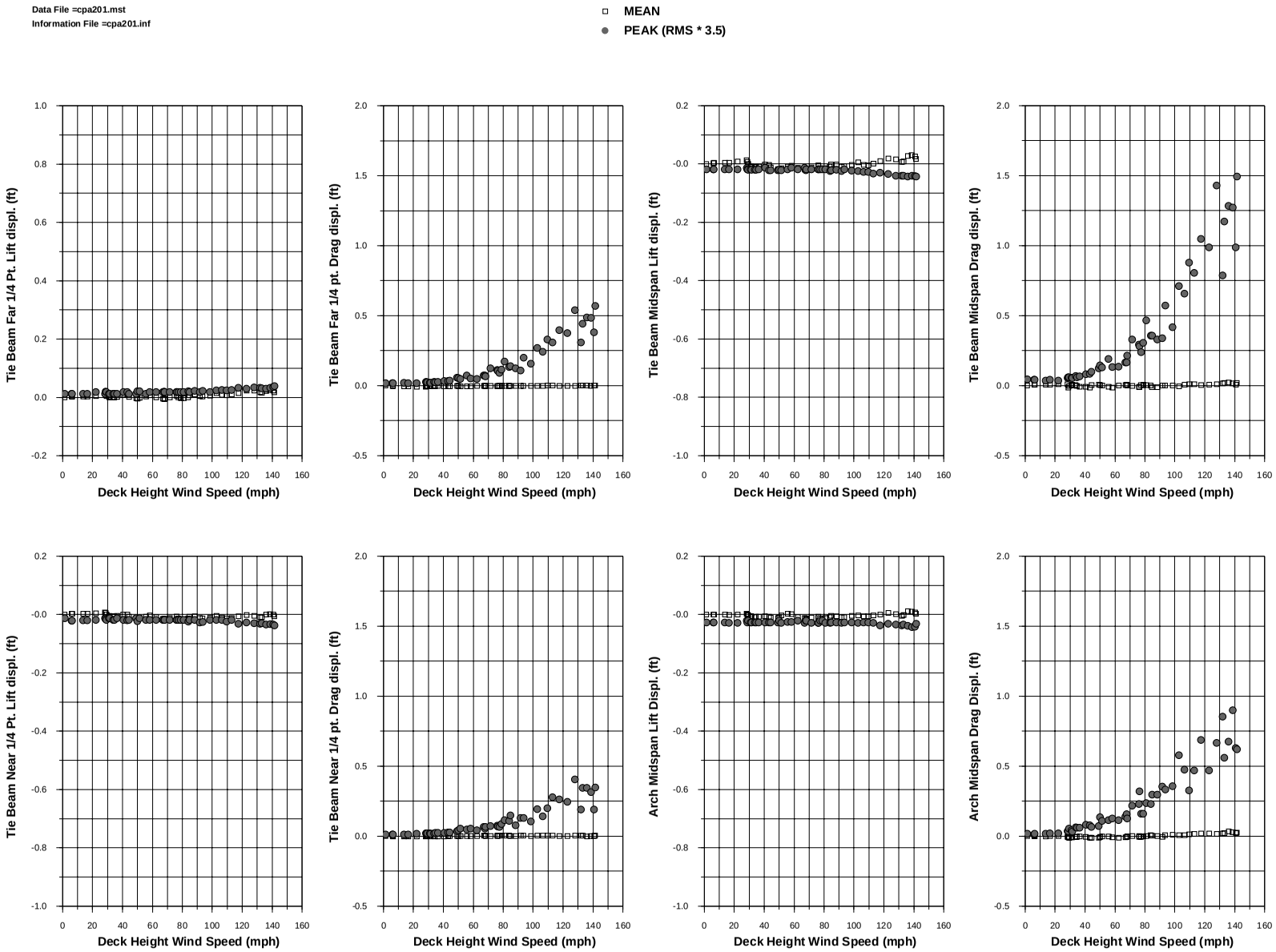

Indian River Bridge, Cantilevered Tie Beam, hurricane profile, 0 degrees

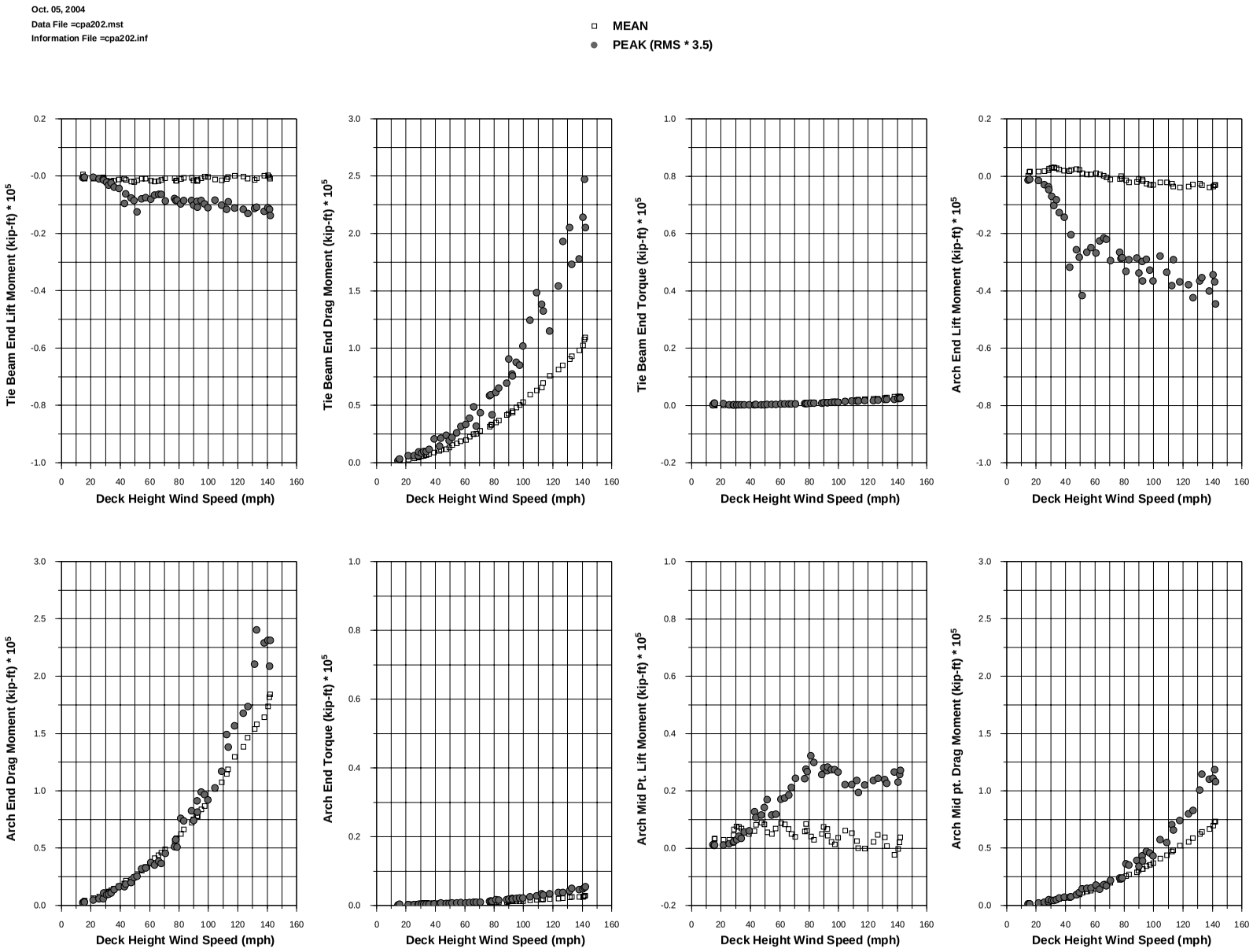

Indian River Bridge, Cantilevered Tie Beam, hurricane profile, 90 degrees, without existing bridge

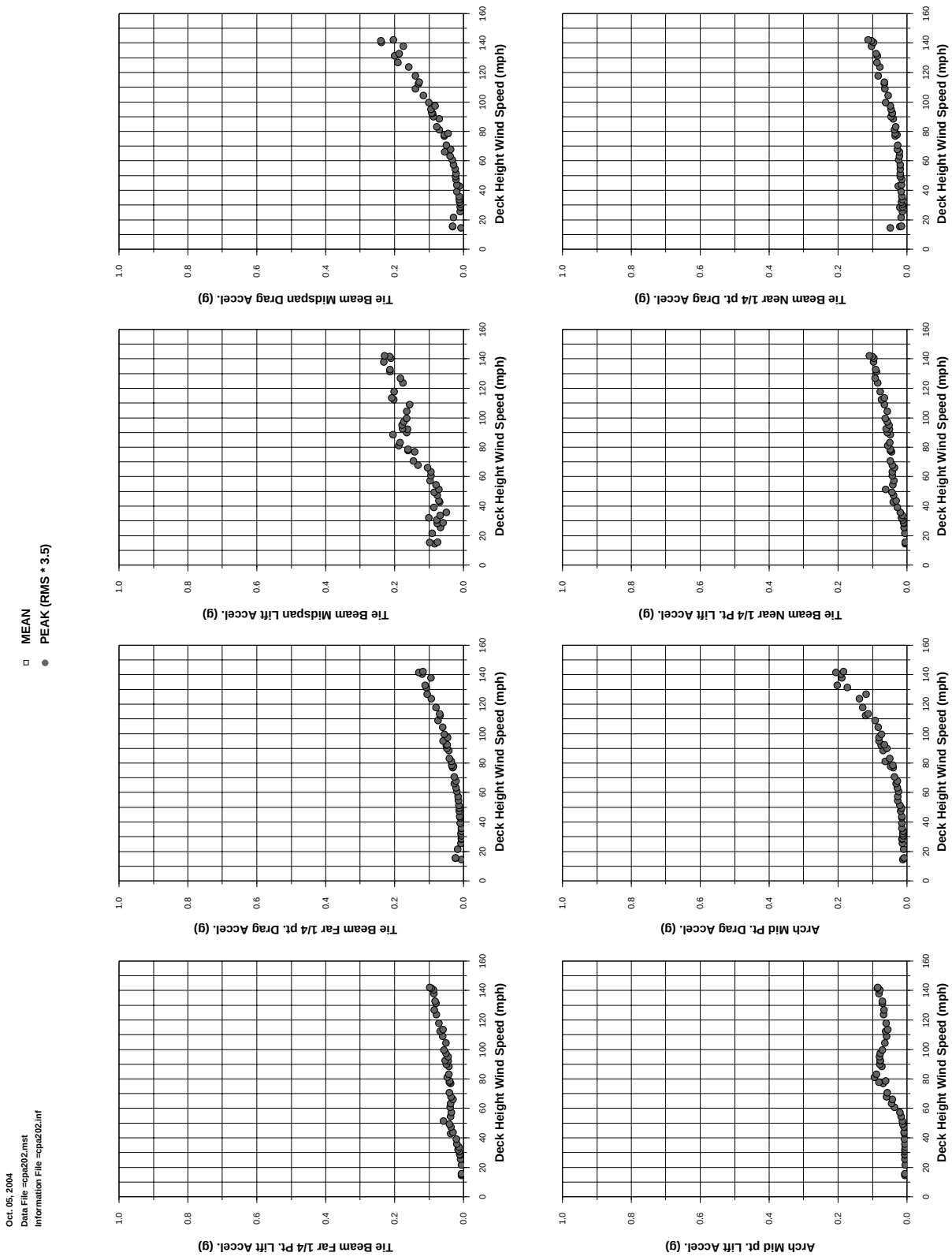

Indian River Bridge, Cantilevered Tie Beam, hurricane profile, 90 degrees, without existing bridge

Oct. 05, 2004
Data File =cpa202.mst
Information File =cpa202.inf

MEAN
PEAK (RMS * 3.5)

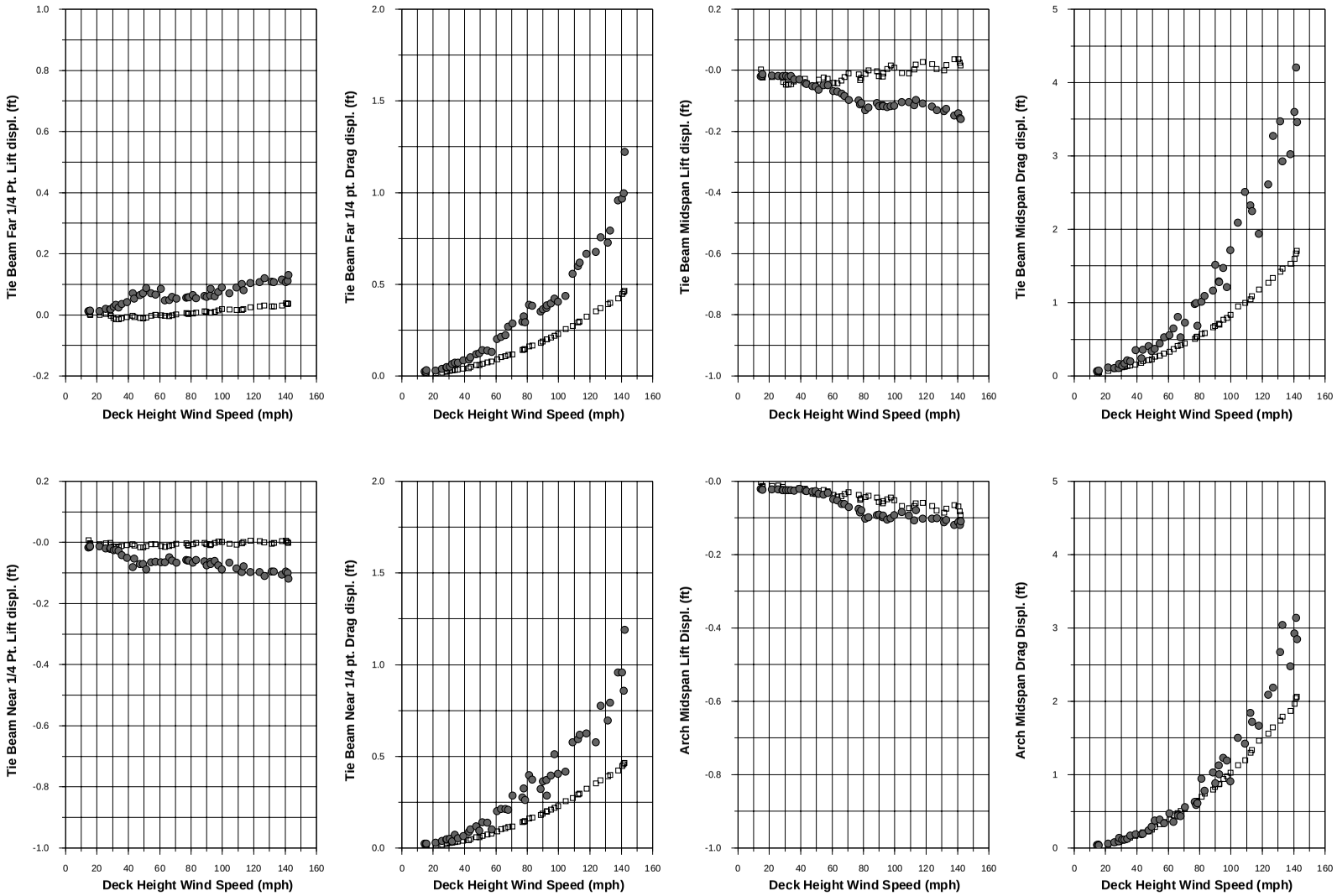

Indian River Bridge, Cantilevered Tie Beam, hurricane profile, 90 degrees, without existing bridge

Oct. 05, 2004
Data File =cpa203.mst
Information File =cpa203.inf

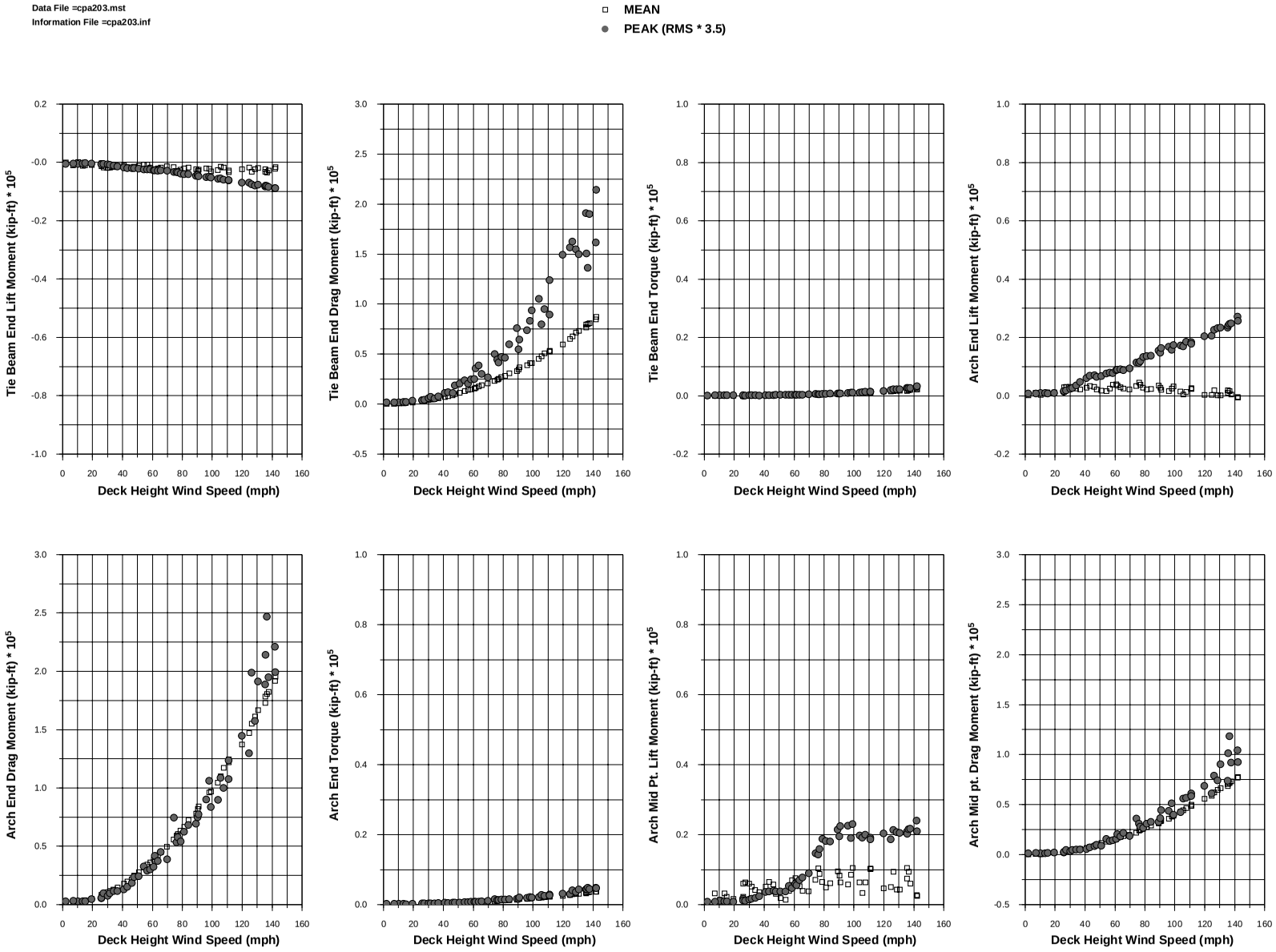

Indian River Bridge, Cantilevered Tie Beam, hurricane profile, 90 degrees, with existing bridge

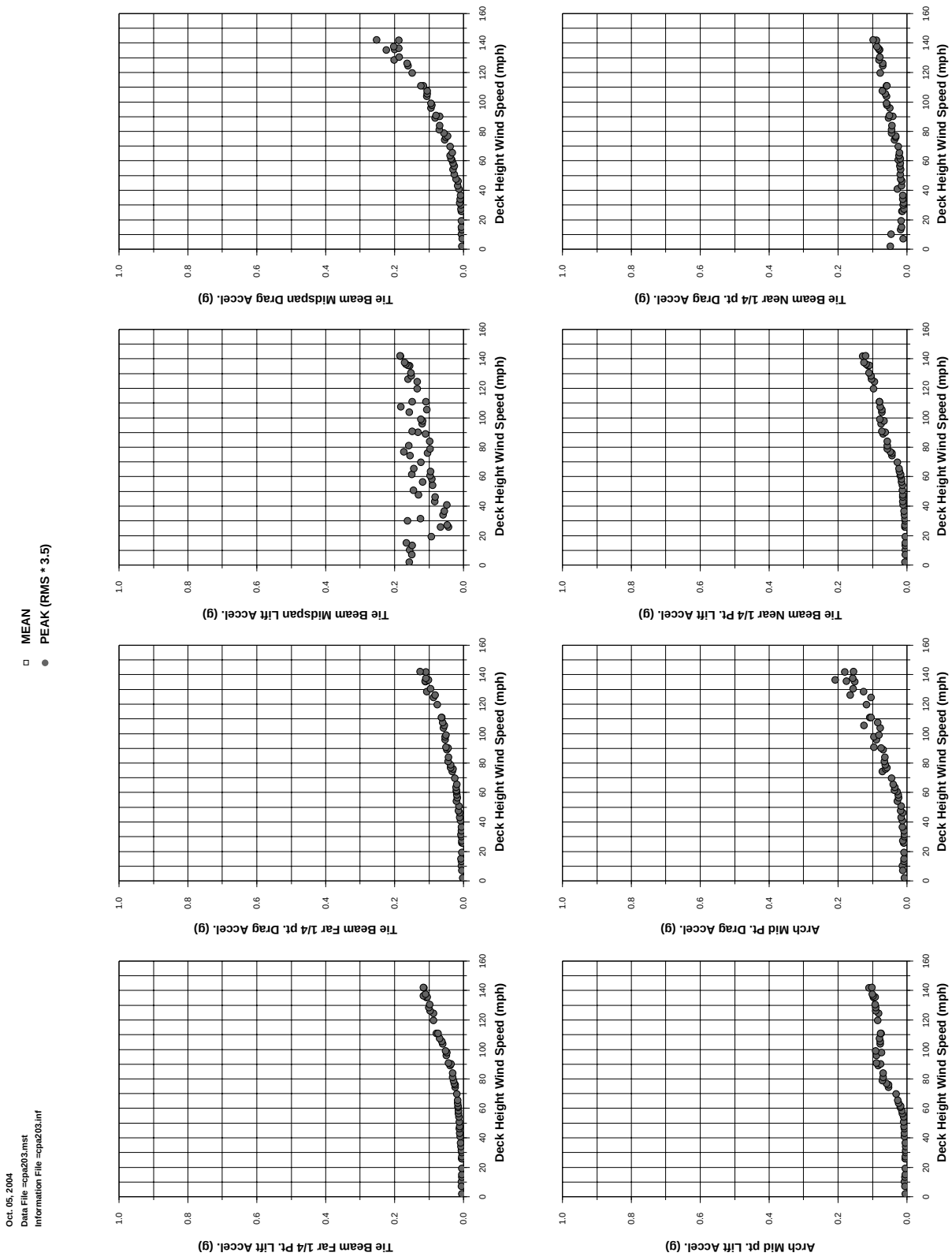

Indian River Bridge, Cantilevered Tie Beam, hurricane profile, 90 degrees, with existing bridge

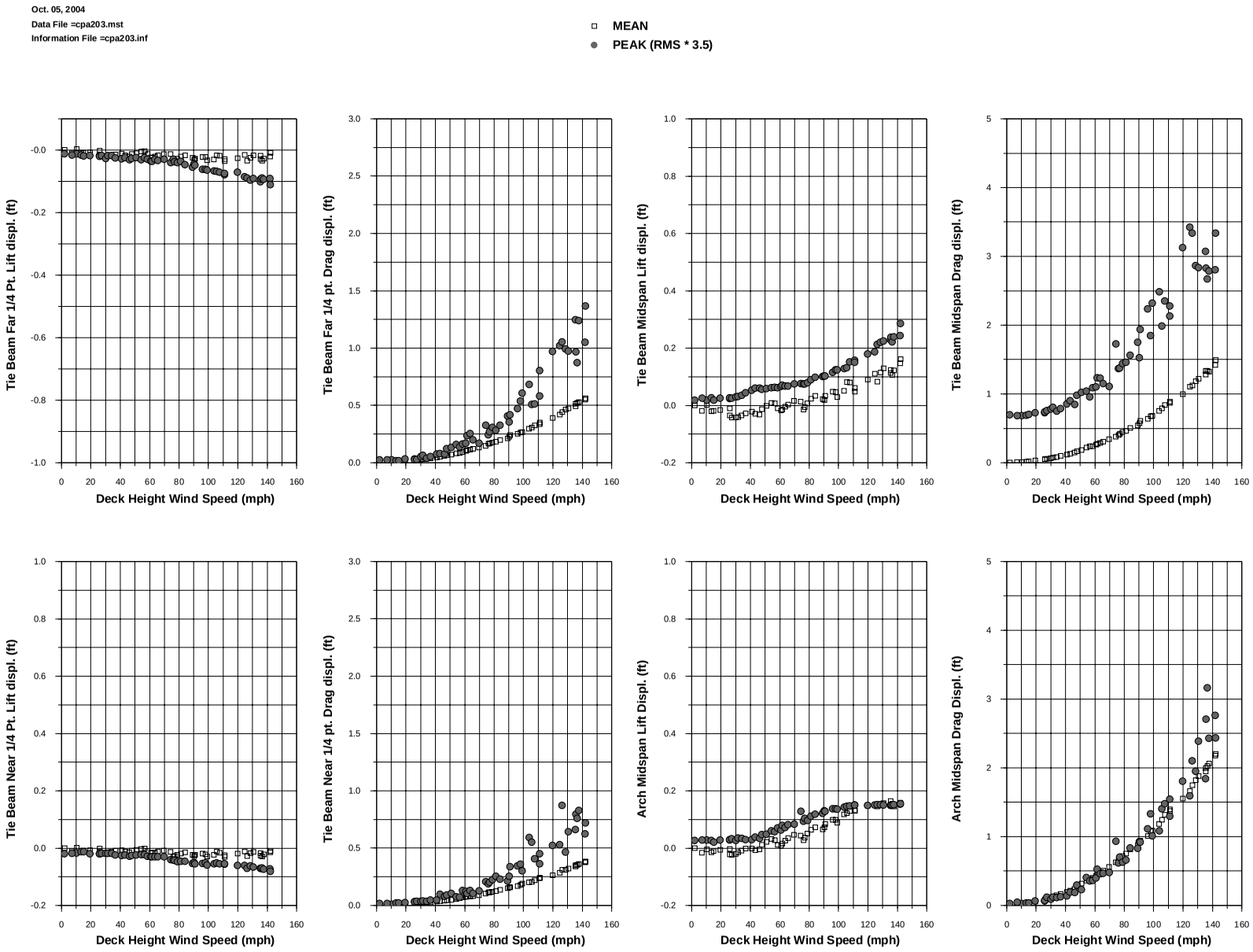

Indian River Bridge, Cantilevered Tie Beam, hurricane profile, 90 degrees, with existing bridge

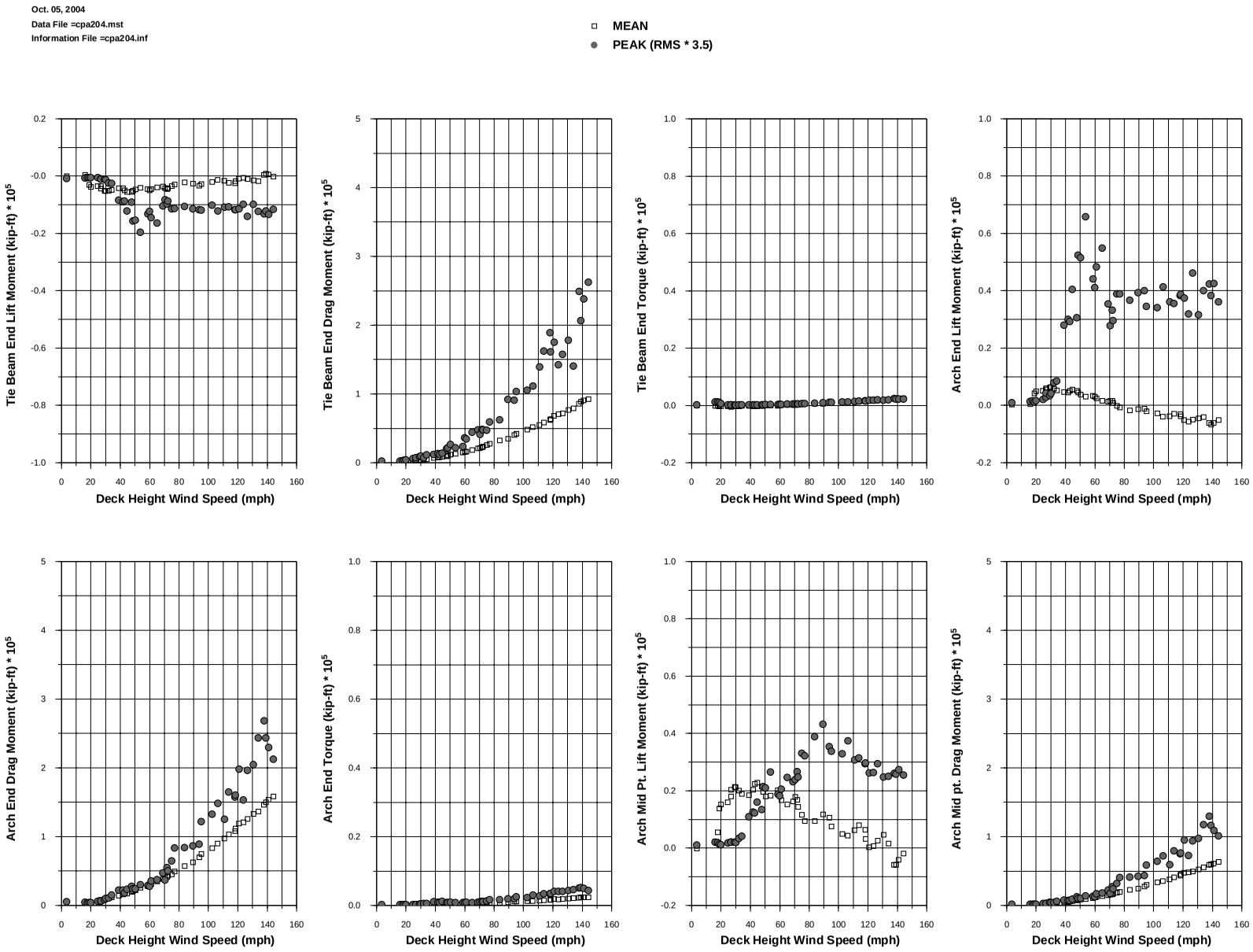

Indian River Bridge, Cantilevered Tie Beam, hurricane profile, 60 degrees,

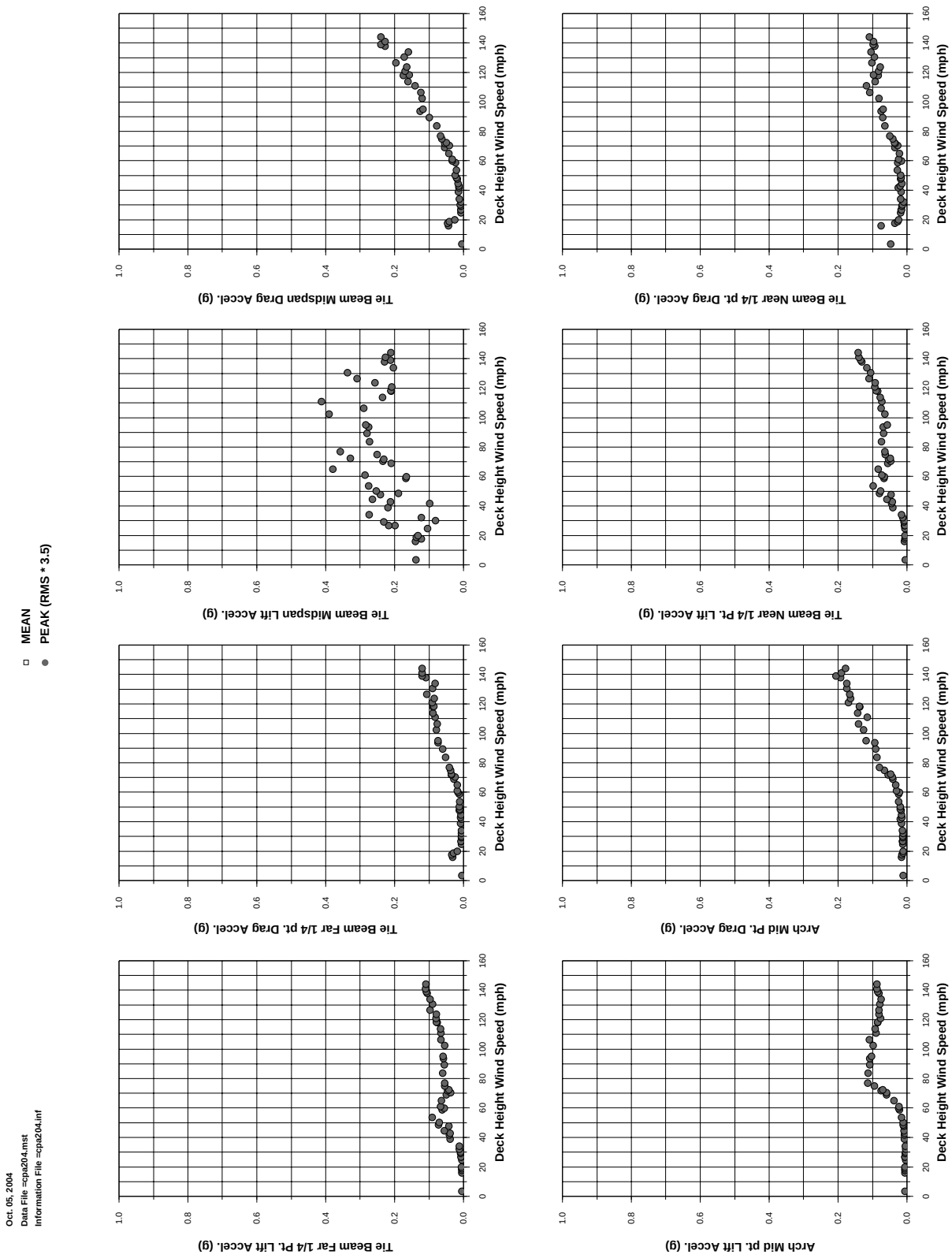

Indian River Bridge, Cantilevered Tie Beam, hurricane profile, 60 degrees,

Oct. 05, 2004
Data File =cpa204.mst
Information File =cpa204.inf

MEAN
PEAK (RMS * 3.5)

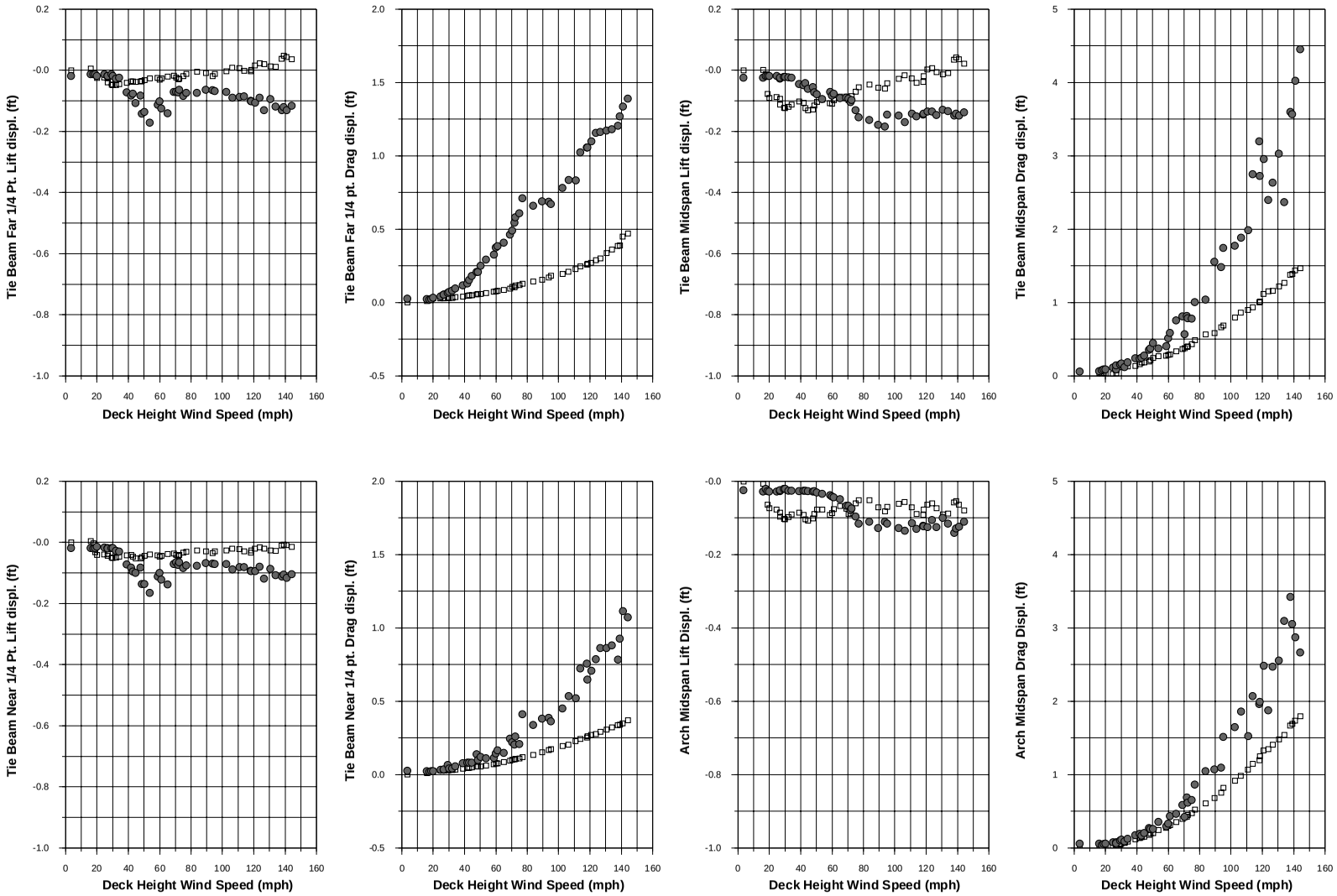

Indian River Bridge, Cantilevered Tie Beam, hurricane profile, 60 degrees,

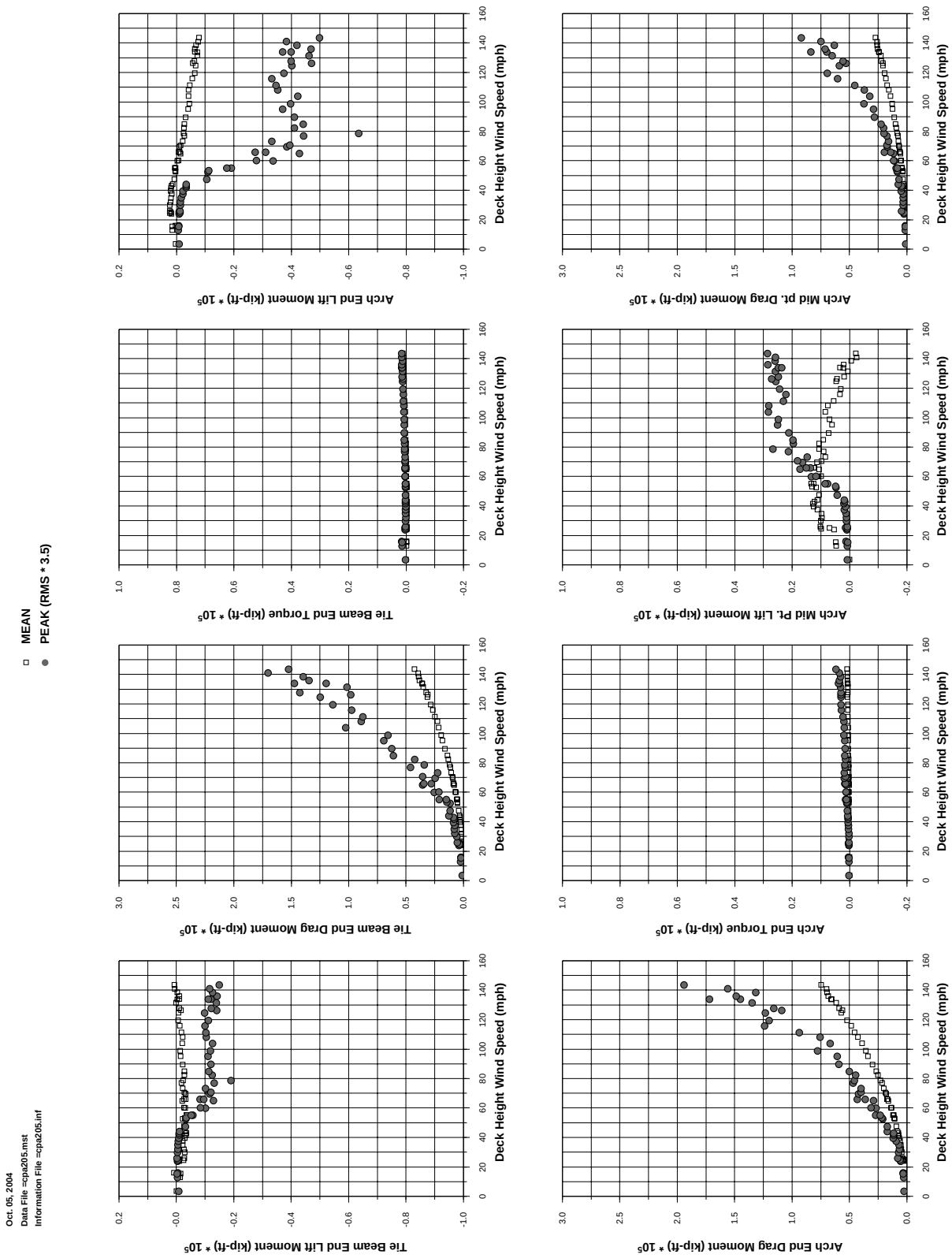

Indian River Bridge, Cantilevered Tie Beam, hurricane profile, 30 degrees

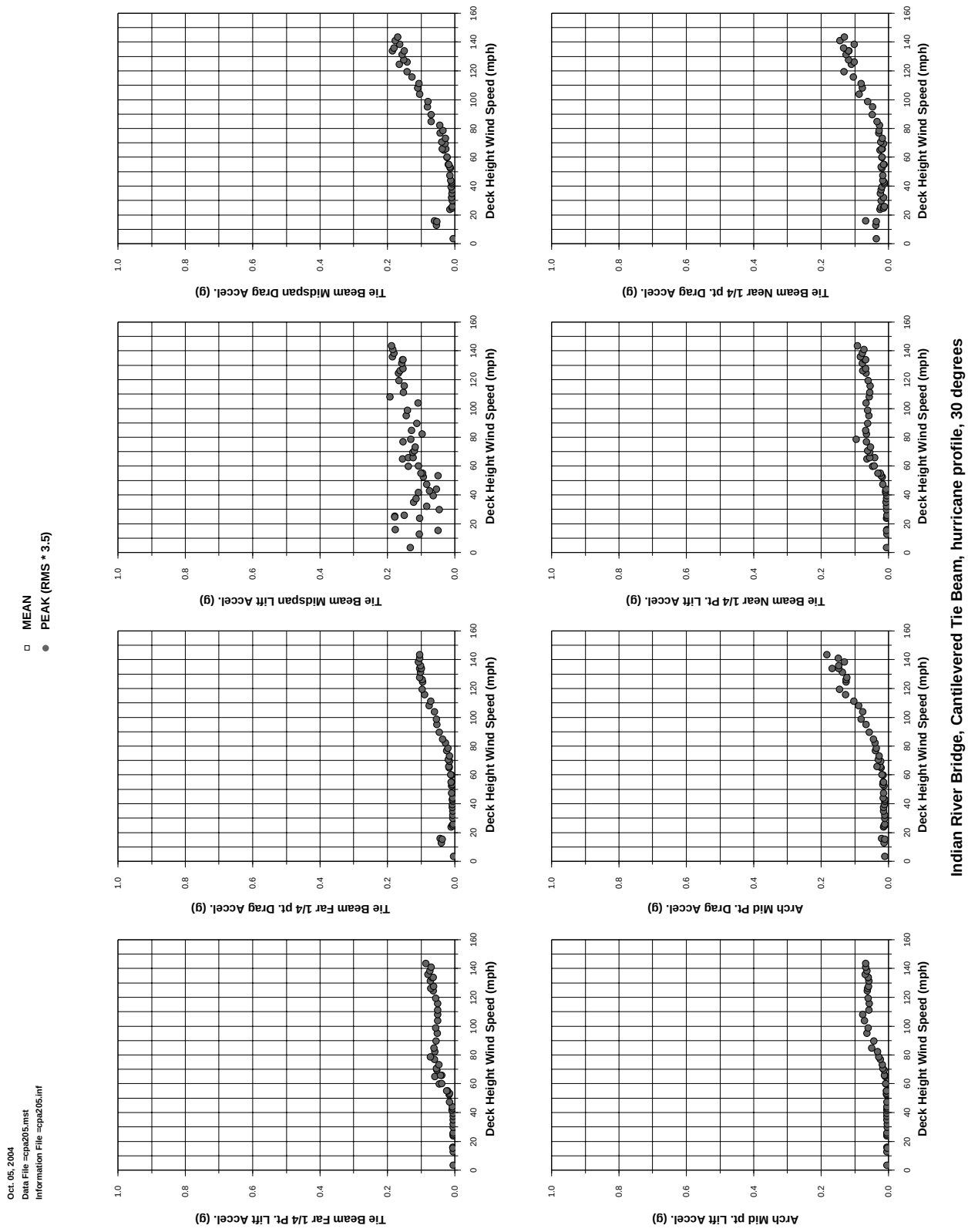

Indian River Bridge, Cantilevered Tie Beam, hurricane profile, 30 degrees

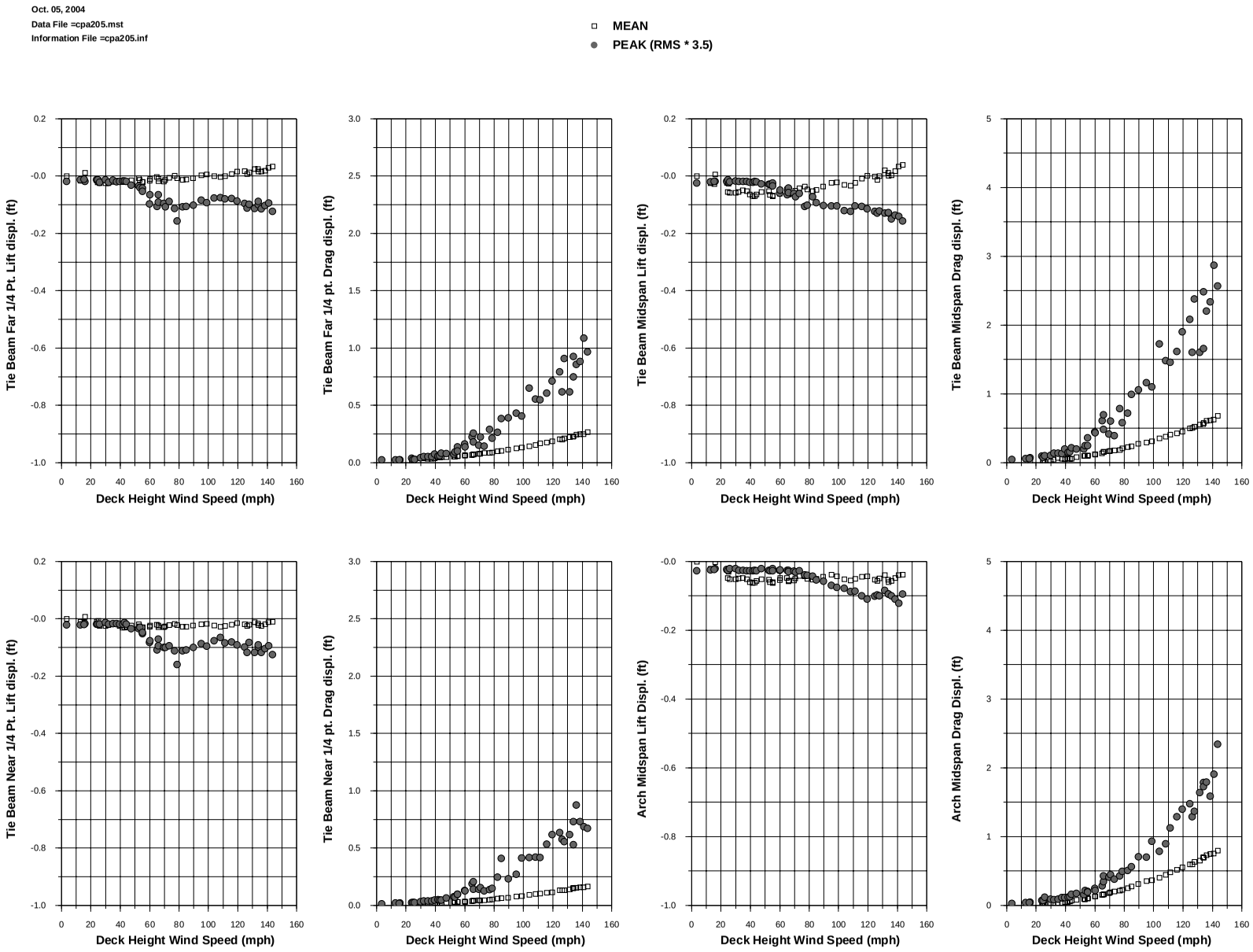

Indian River Bridge, Cantilevered Tie Beam, hurricane profile, 30 degrees

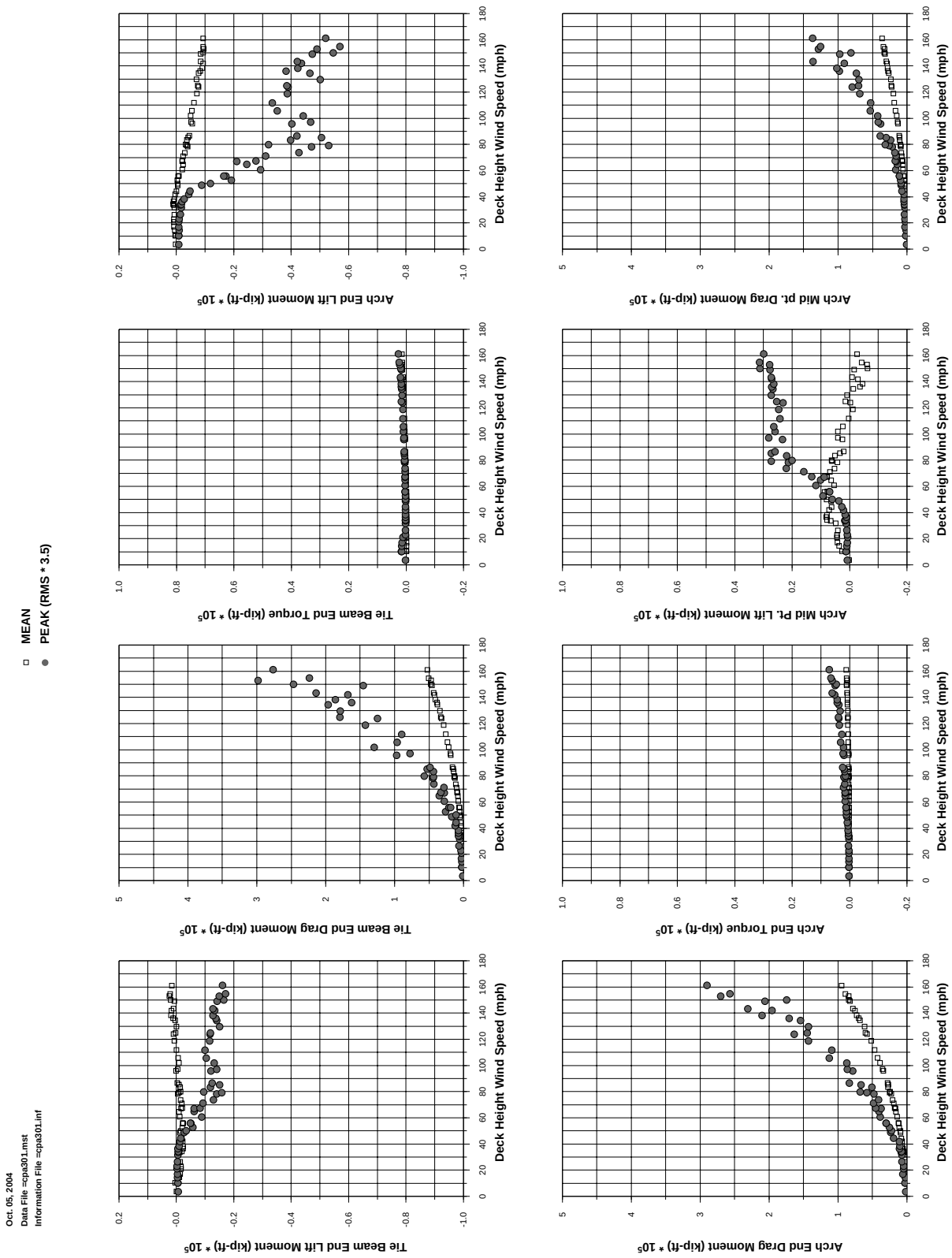

Indian River Bridge, Cantilevered Tie Beam, open country profile, 30 degrees

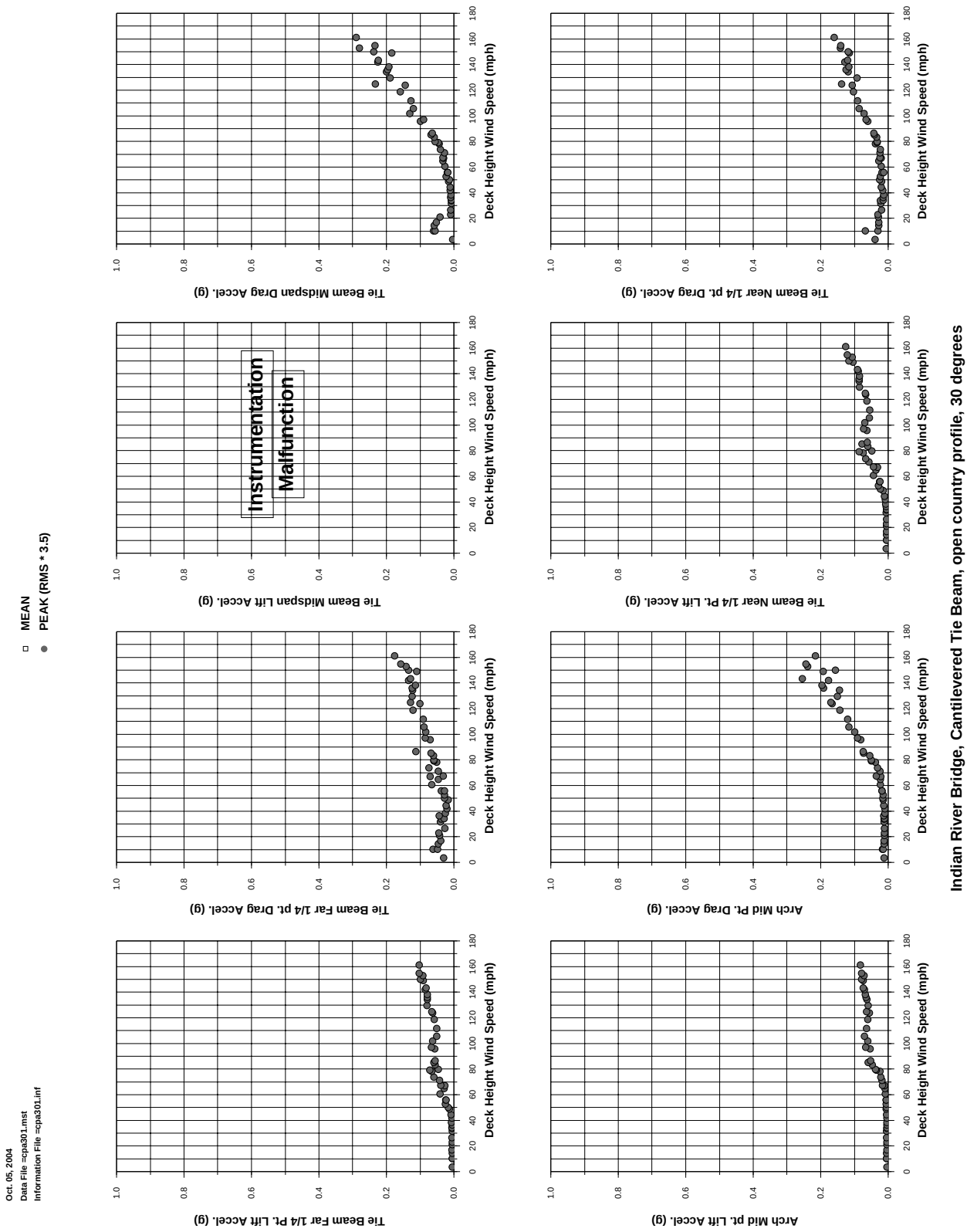

Indian River Bridge, Cantilevered Tie Beam, open country profile, 30 degrees

Oct. 05, 2004
Data File =cpa301.mst
Information File =cpa301.inf

MEAN
PEAK (RMS * 3.5)

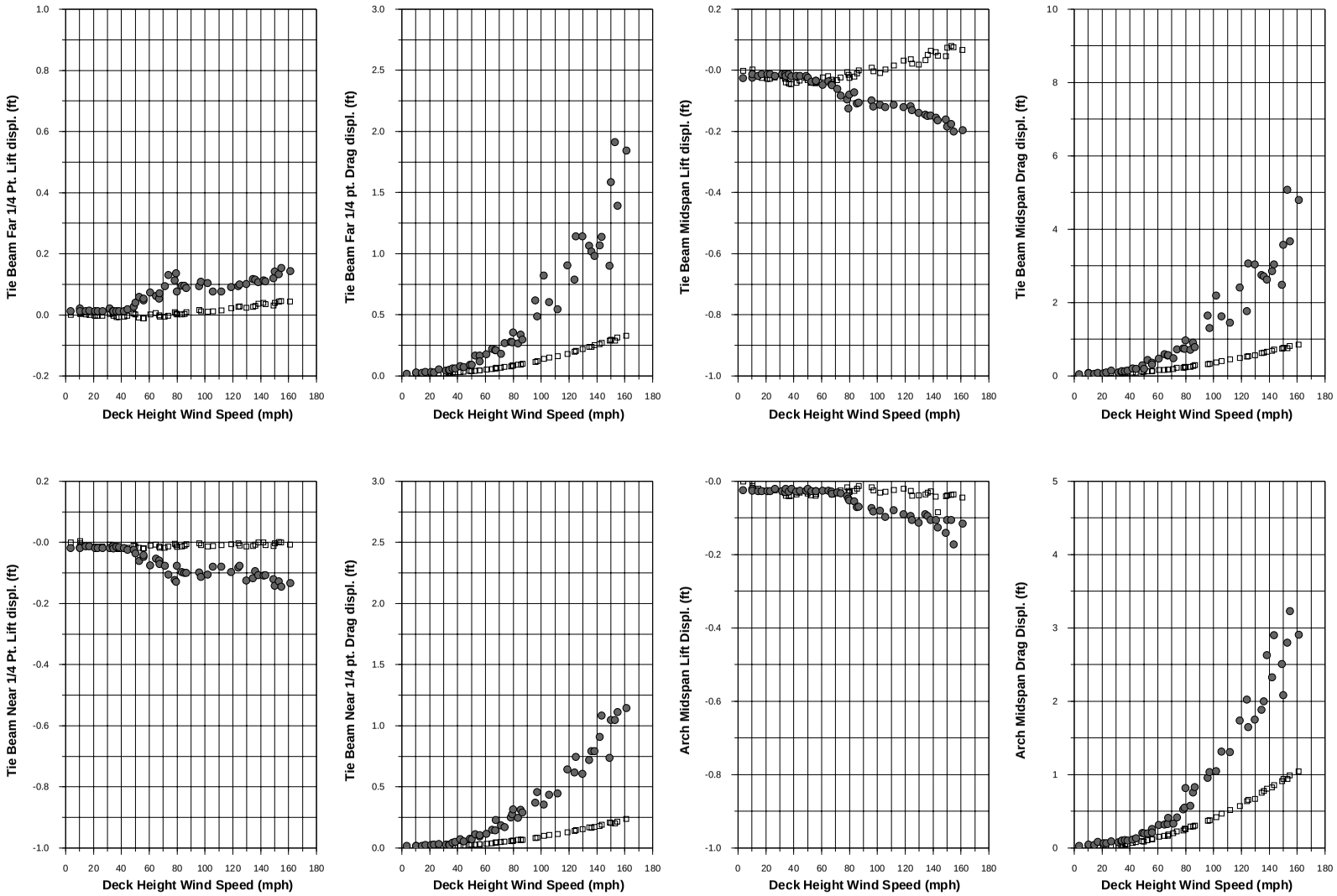

Indian River Bridge, Cantilevered Tie Beam, open country profile, 30 degrees

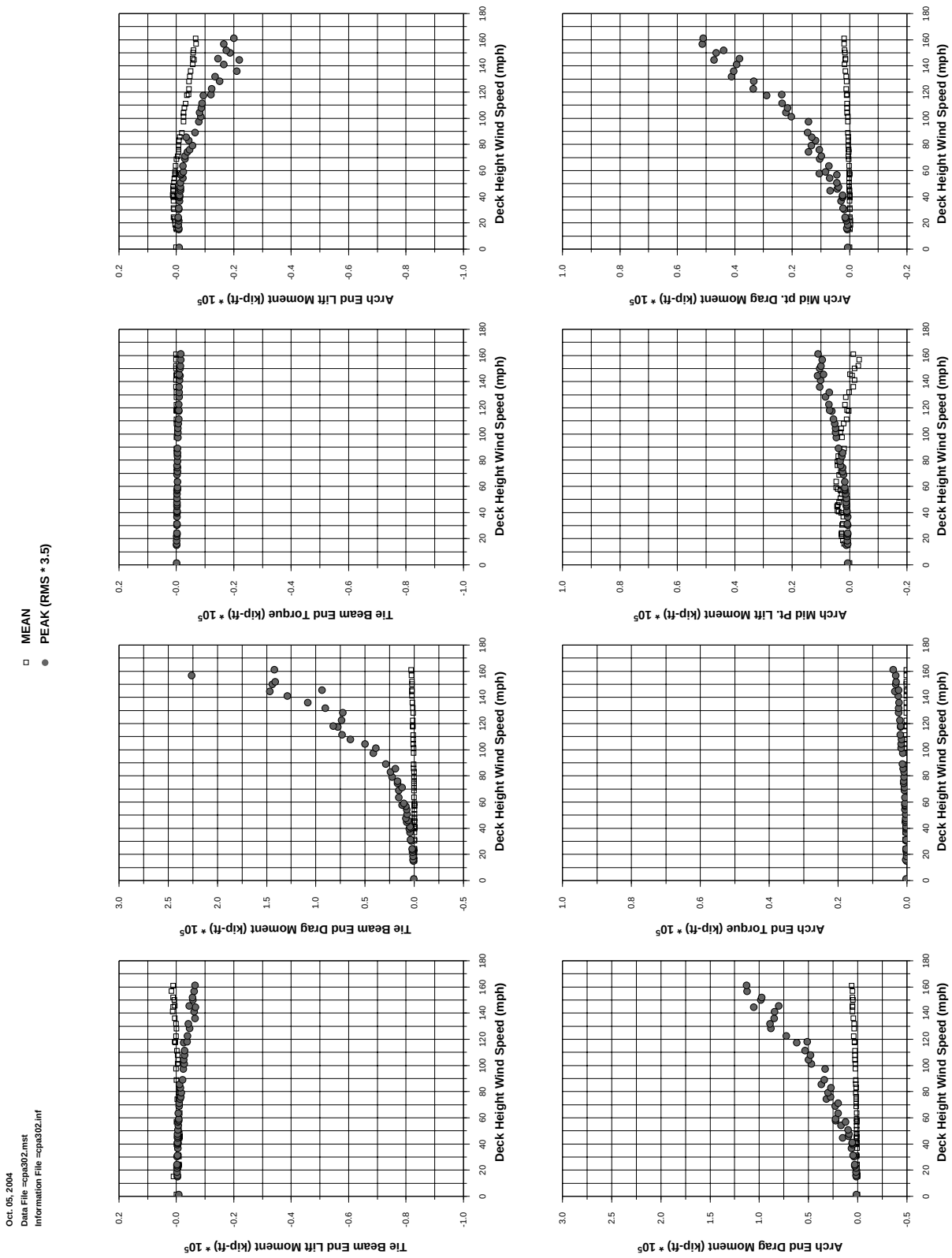

Indian River Bridge, Cantilevered Tie Beam, open country profile, 0 degrees

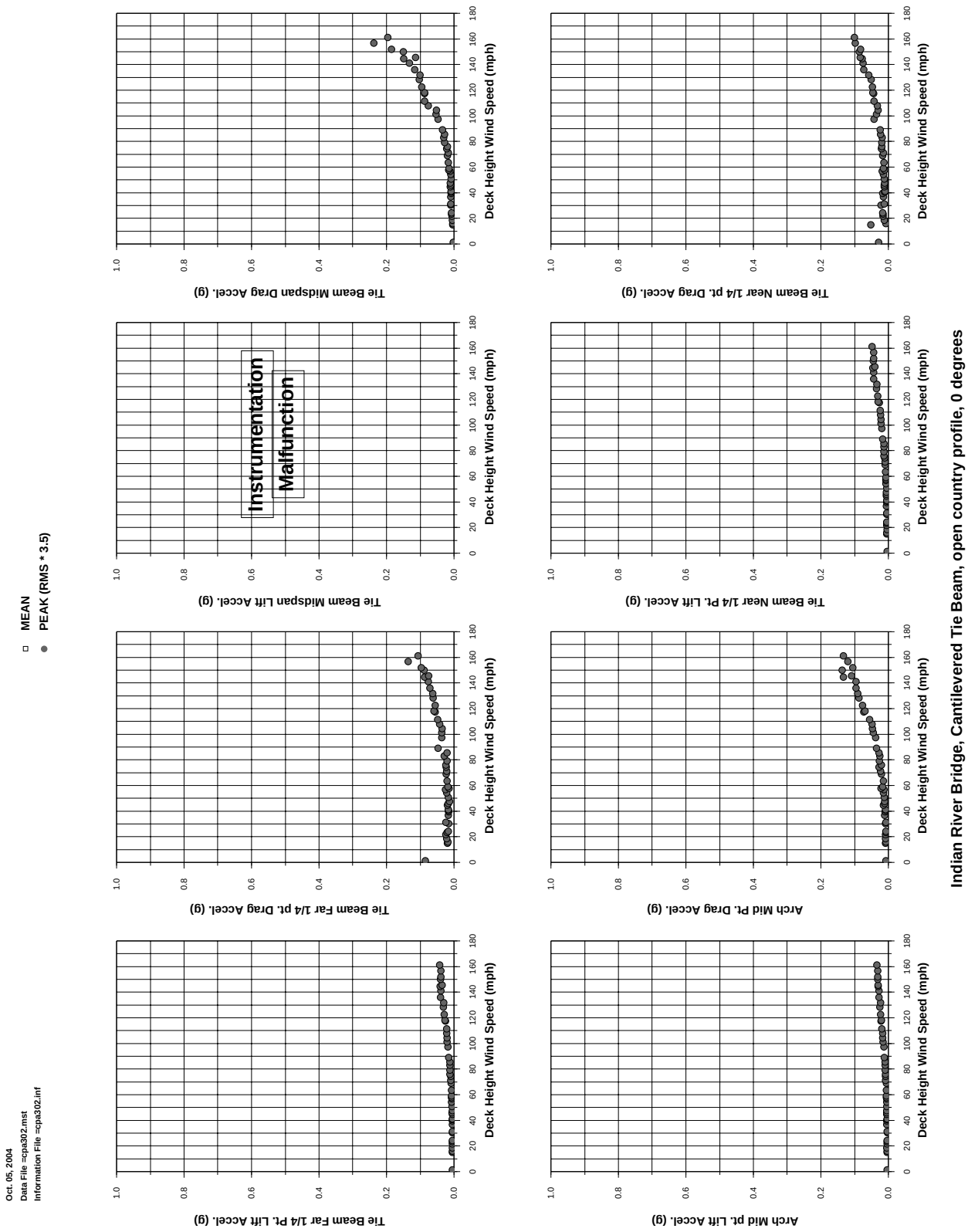

Indian River Bridge, Cantilevered Tie Beam, open country profile, 0 degrees

Oct. 05, 2004
Data File =cpa302.mst
Information File =cpa302.inf

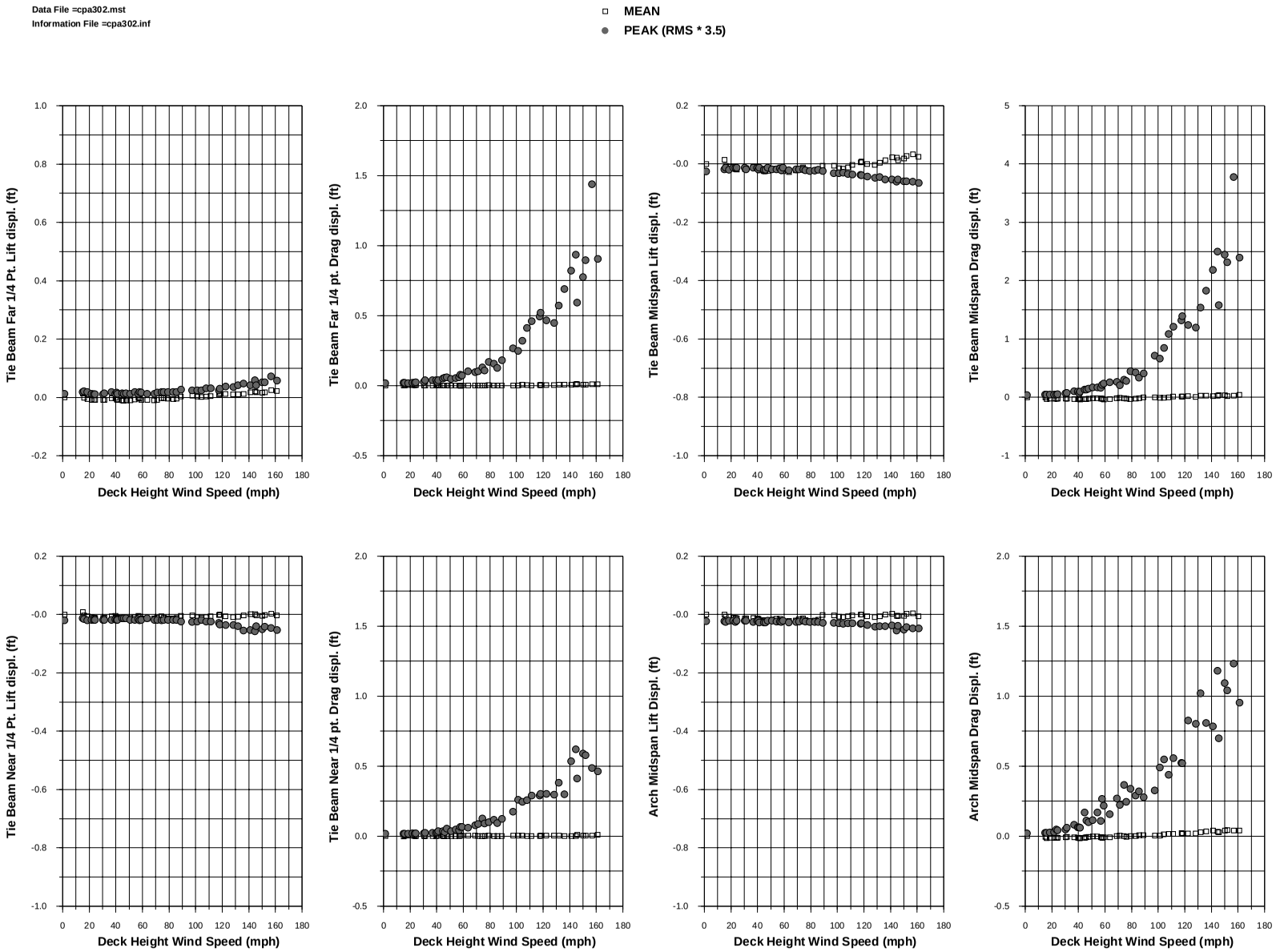

Indian River Bridge, Cantilevered Tie Beam, open country profile, 0 degrees

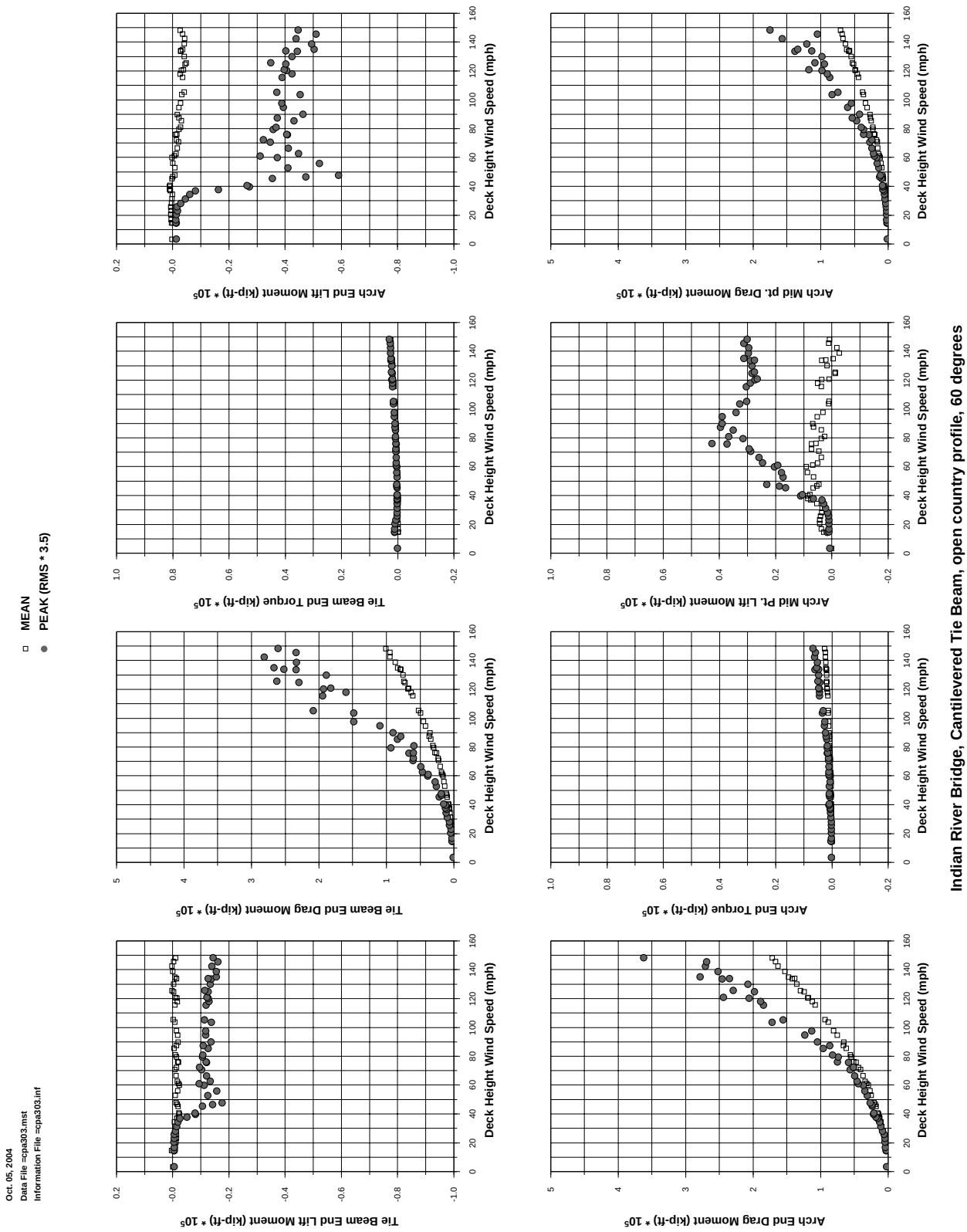

Indian River Bridge, Cantilevered Tie Beam, open country profile, 60 degrees

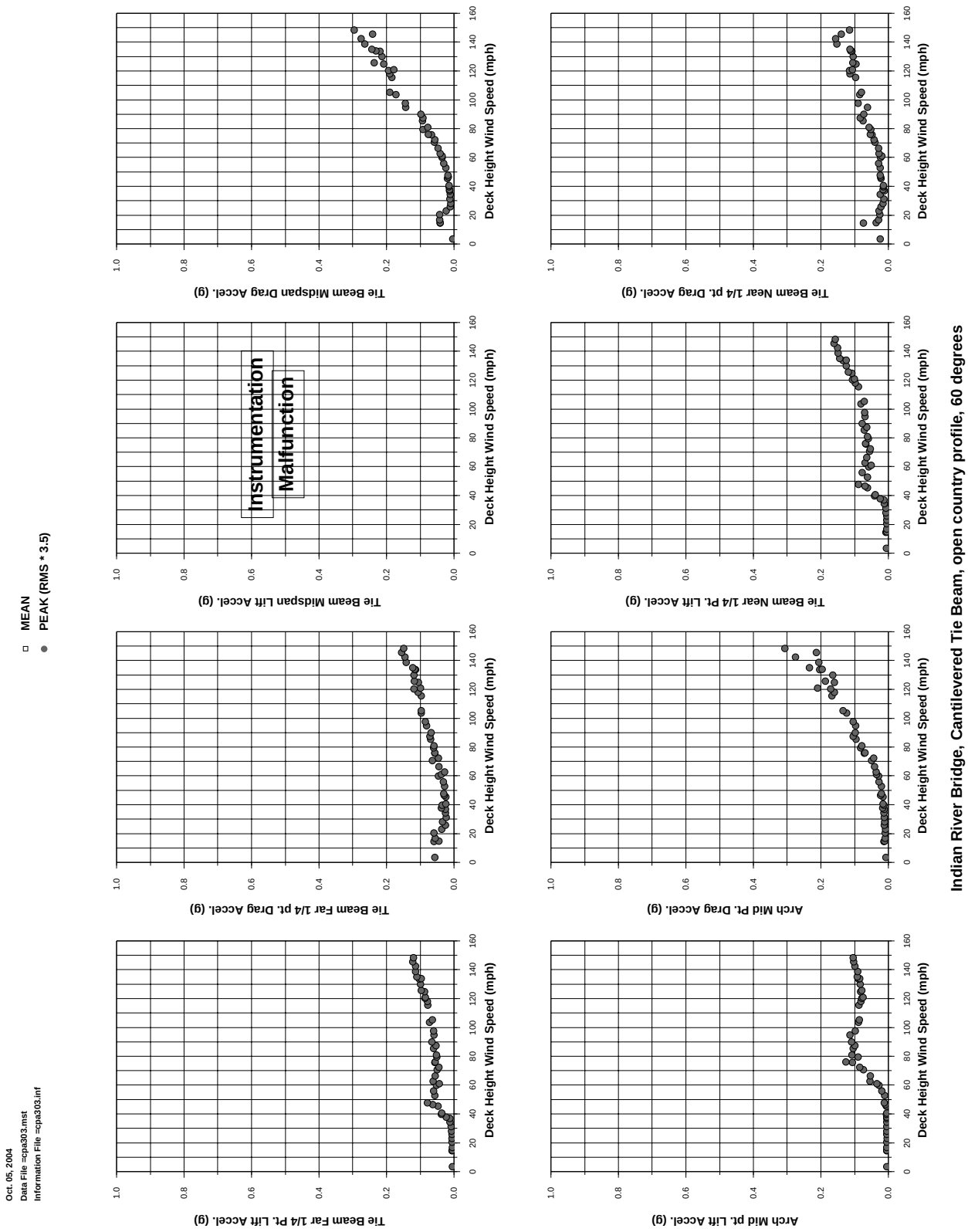

Indian River Bridge, Cantilevered Tie Beam, open country profile, 60 degrees

Oct. 05, 2004
Data File =cpa303.mst
Information File =cpa303.inf

MEAN
PEAK (RMS * 3.5)

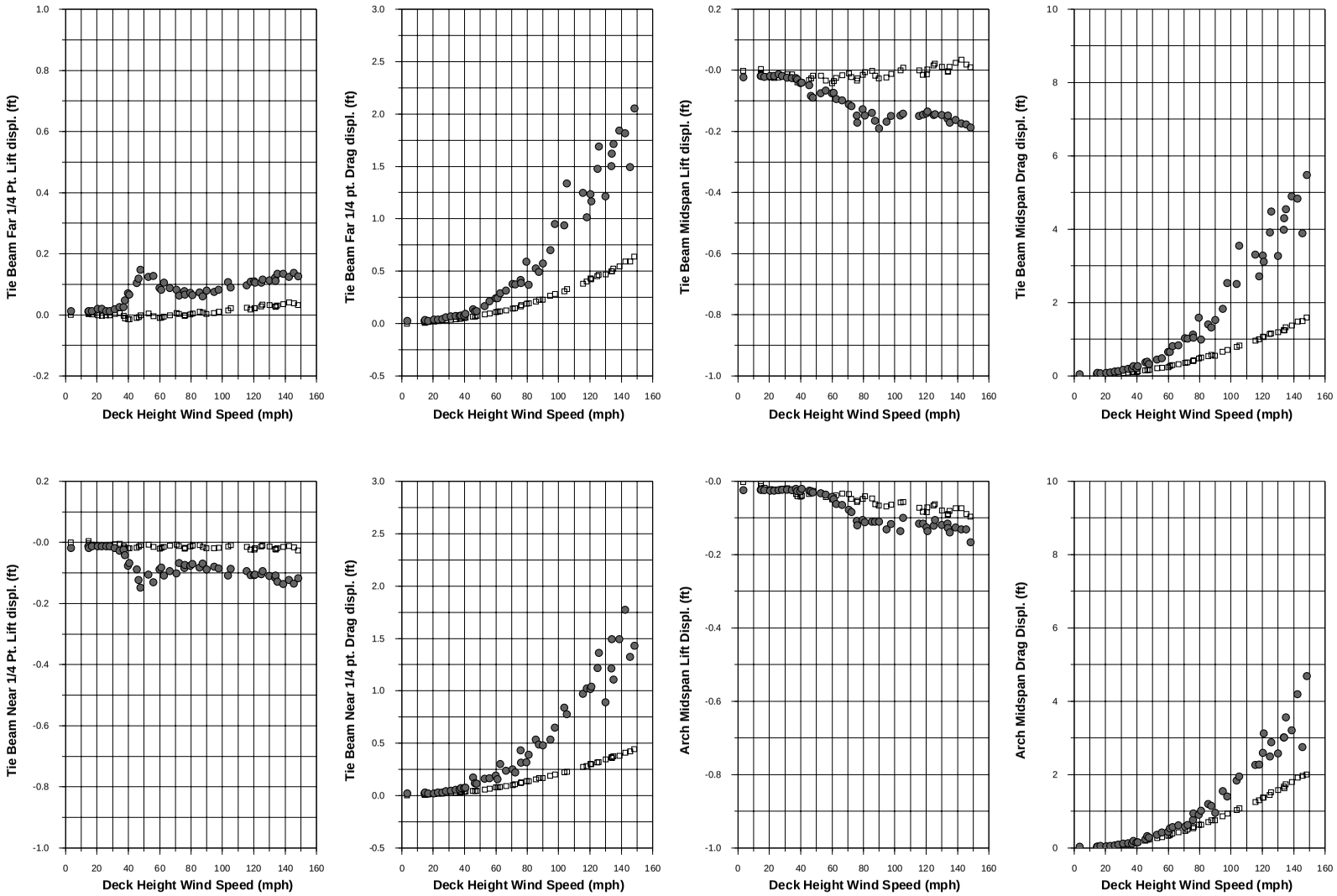

Indian River Bridge, Cantilevered Tie Beam, open country profile, 60 degrees

Oct. 05, 2004
Data File =cpa304.mst
Information File =cpa304.inf

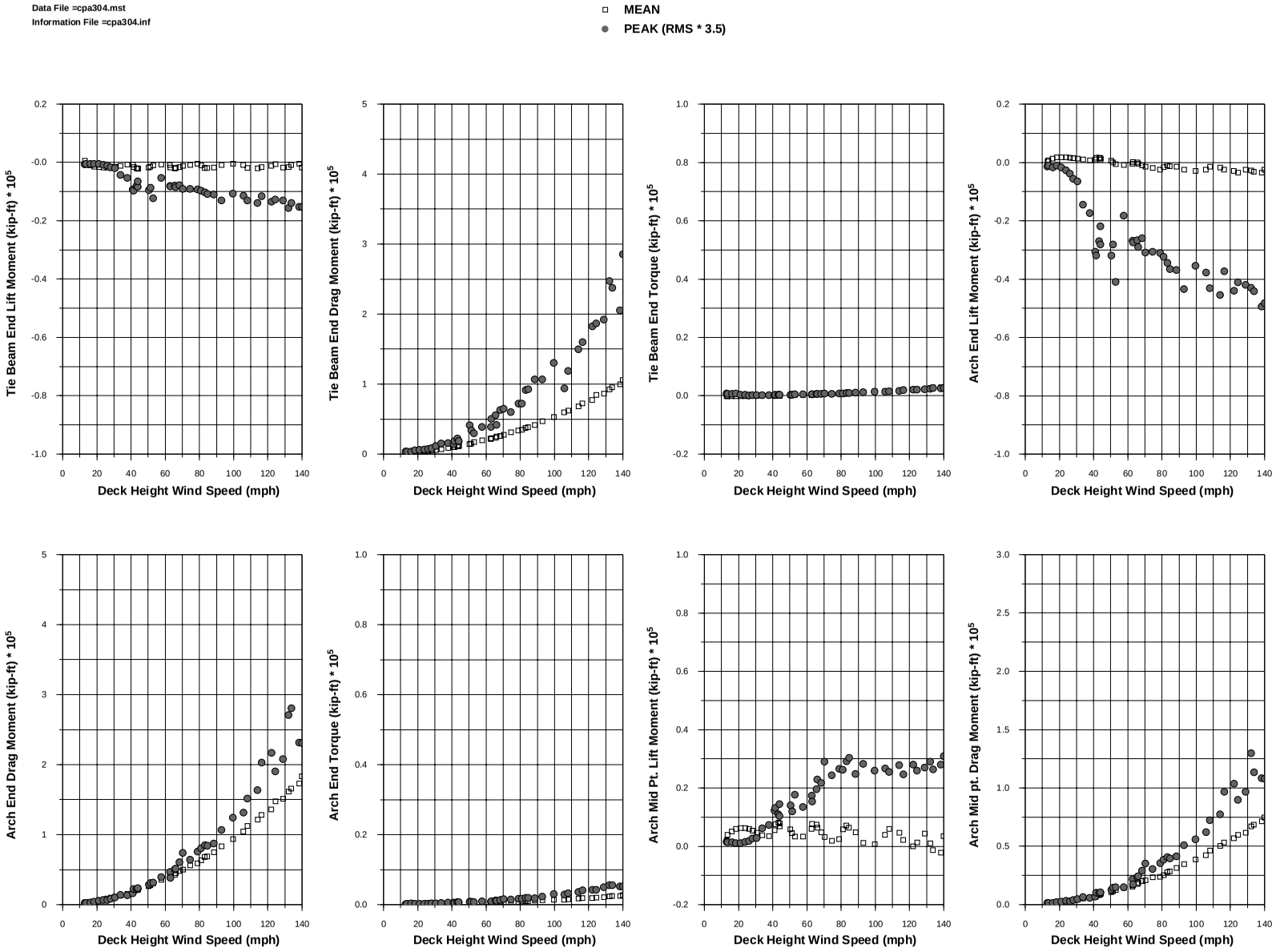

Indian River Bridge, Cantilevered Tie Beam, open country profile, 90 degrees, without existing bridge

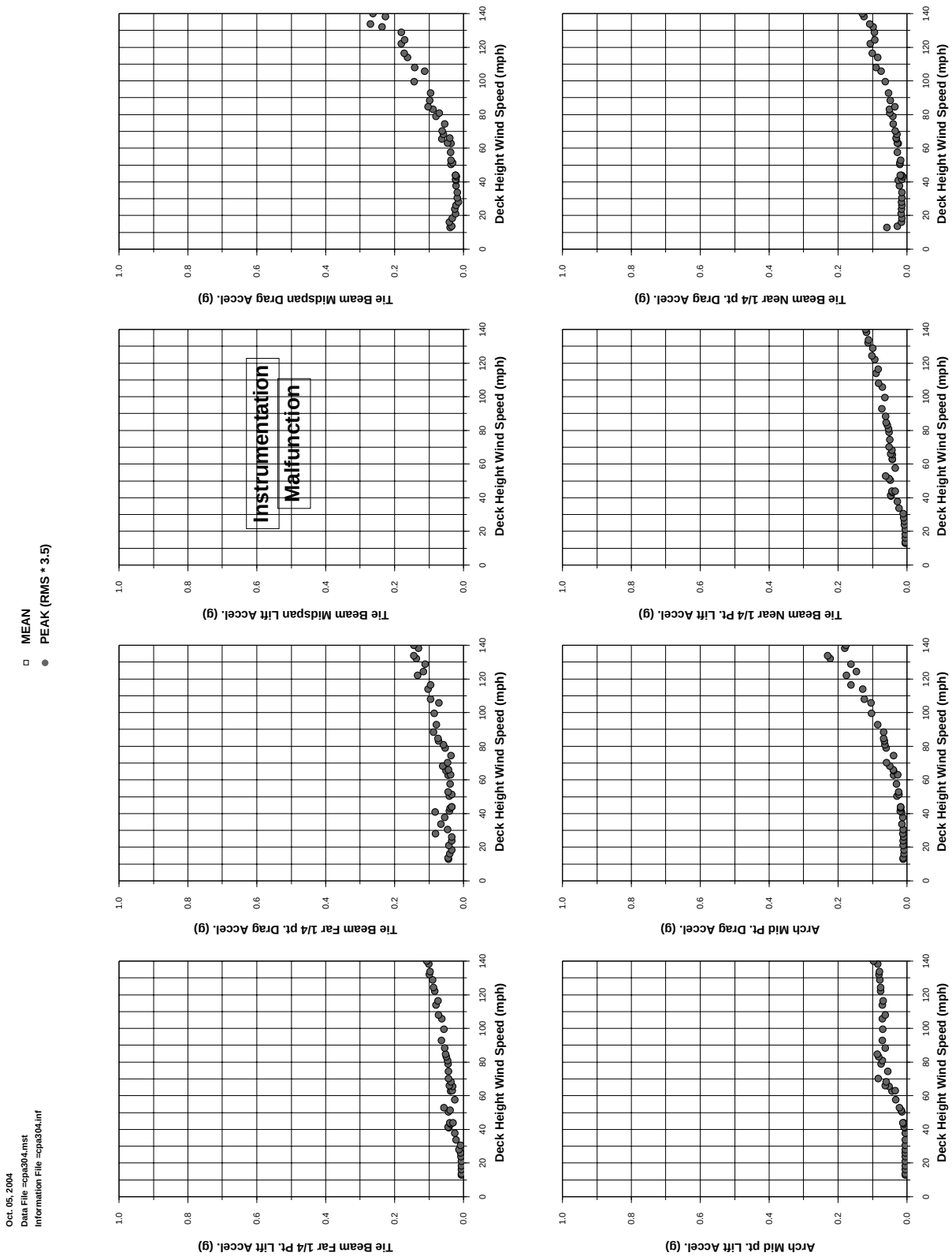

Indian River Bridge, Cantilevered Tie Beam, open country profile, 90 degrees, without existing bridge

Oct. 05, 2004
Data File =cpa304.mst
Information File =cpa304.inf

MEAN
PEAK (RMS * 3.5)

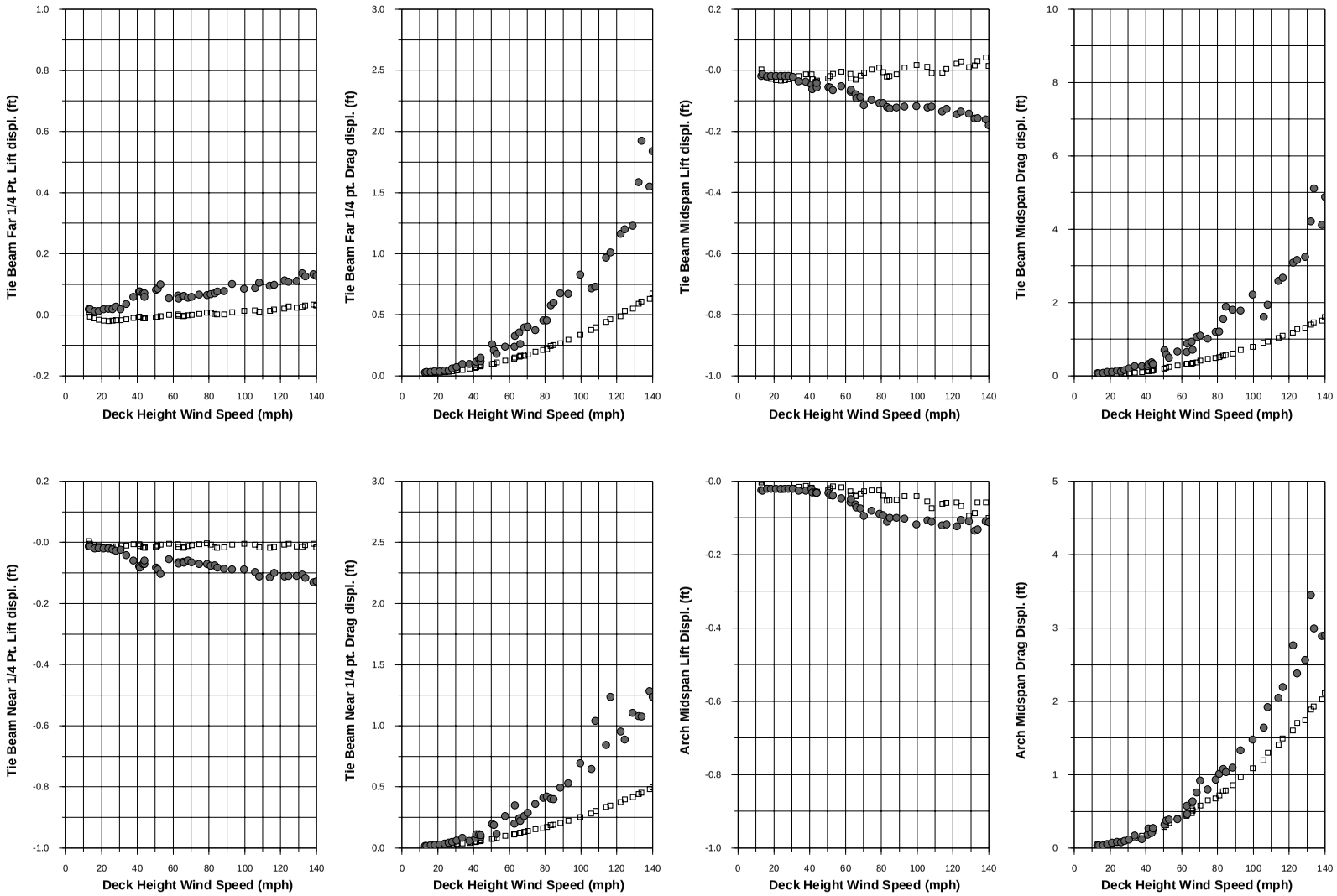

Indian River Bridge, Cantilevered Tie Beam, open country profile, 90 degrees, without existing bridge

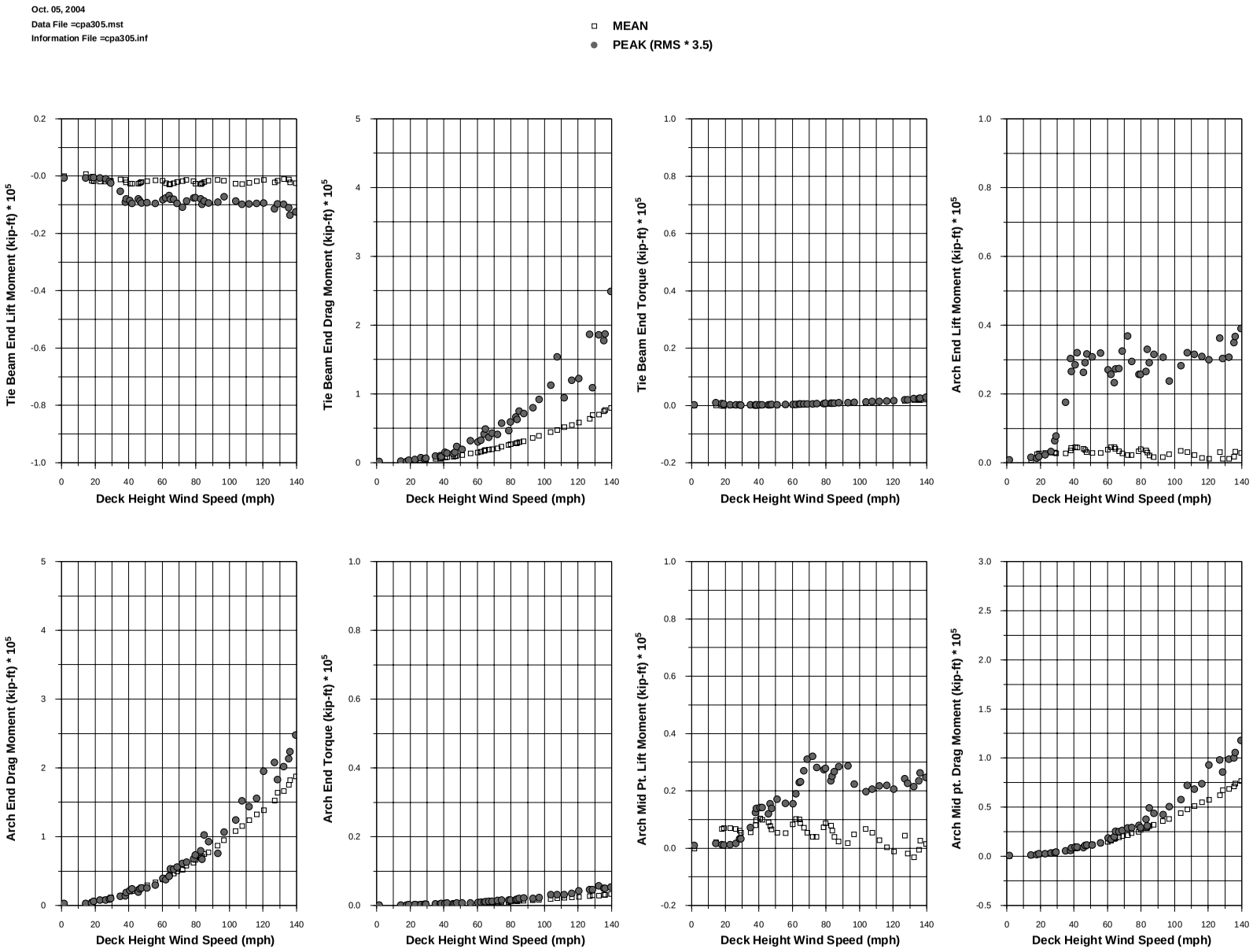

Indian River bridge, Cantilevered Tie Beam, open country profile, 90 degrees, with existing bridge

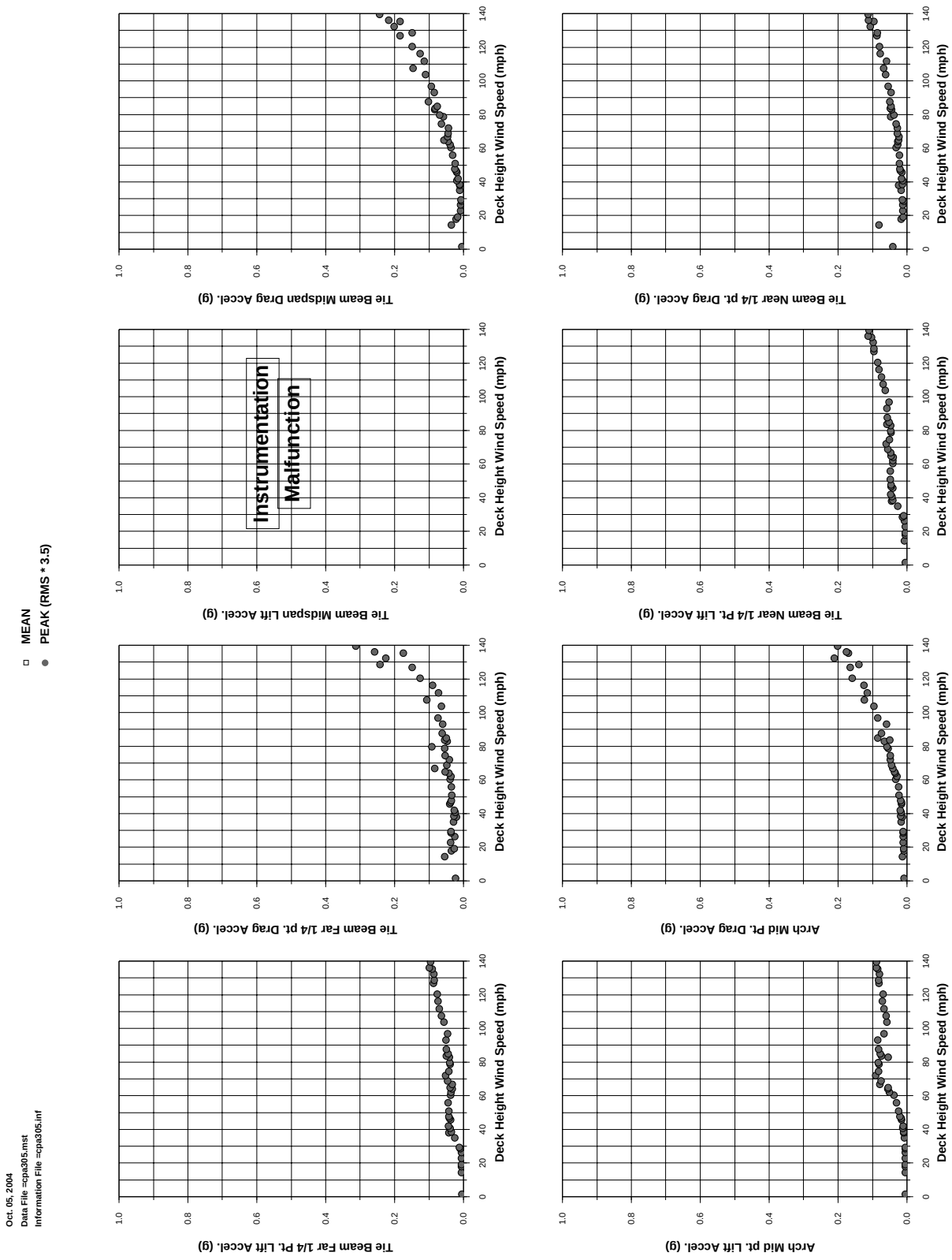

Indian River bridge, Cantilevered Tie Beam, open country profile, 90 degrees, with existing bridge

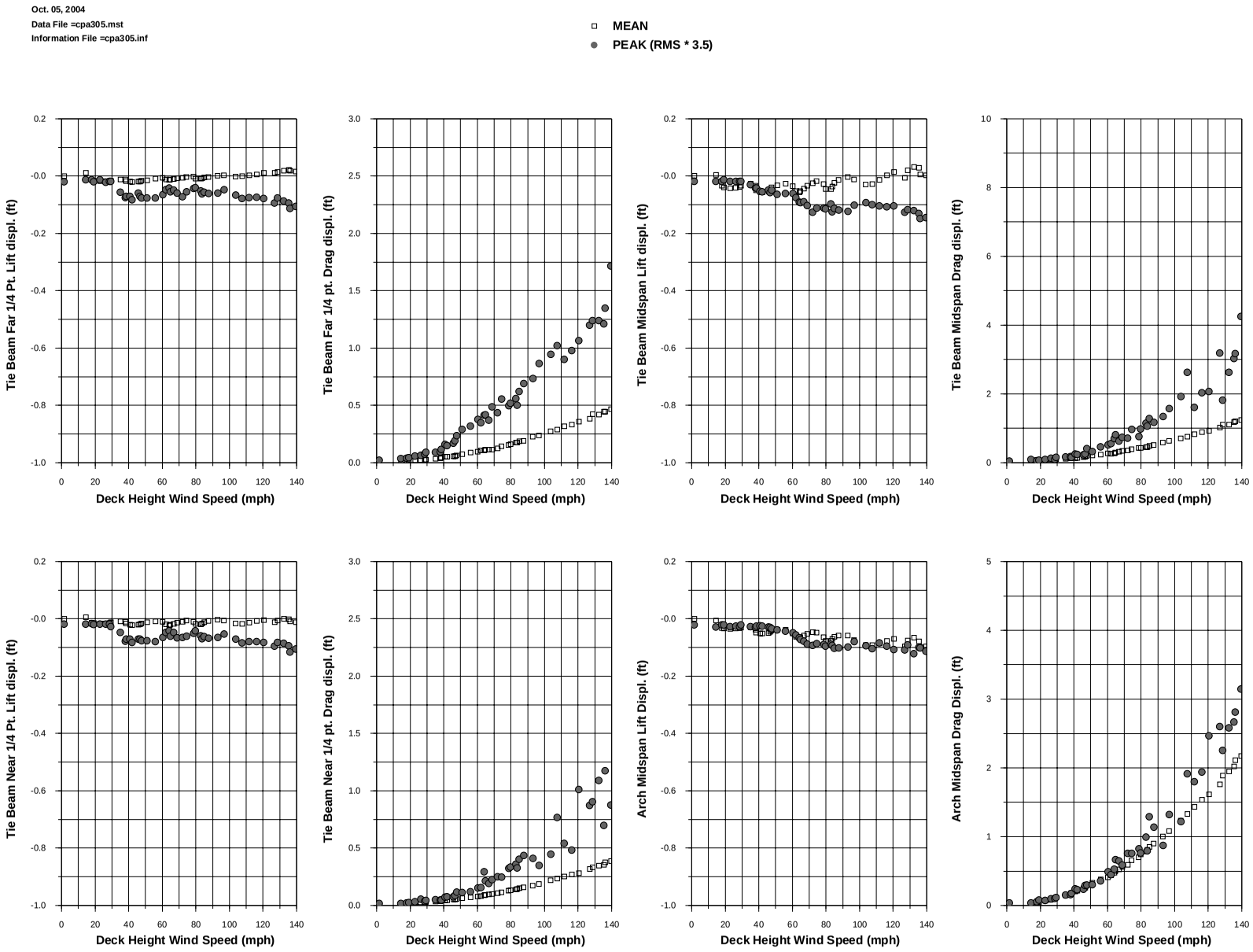

Indian River bridge, Cantilevered Tie Beam, open country profile, 90 degrees, with existing bridge

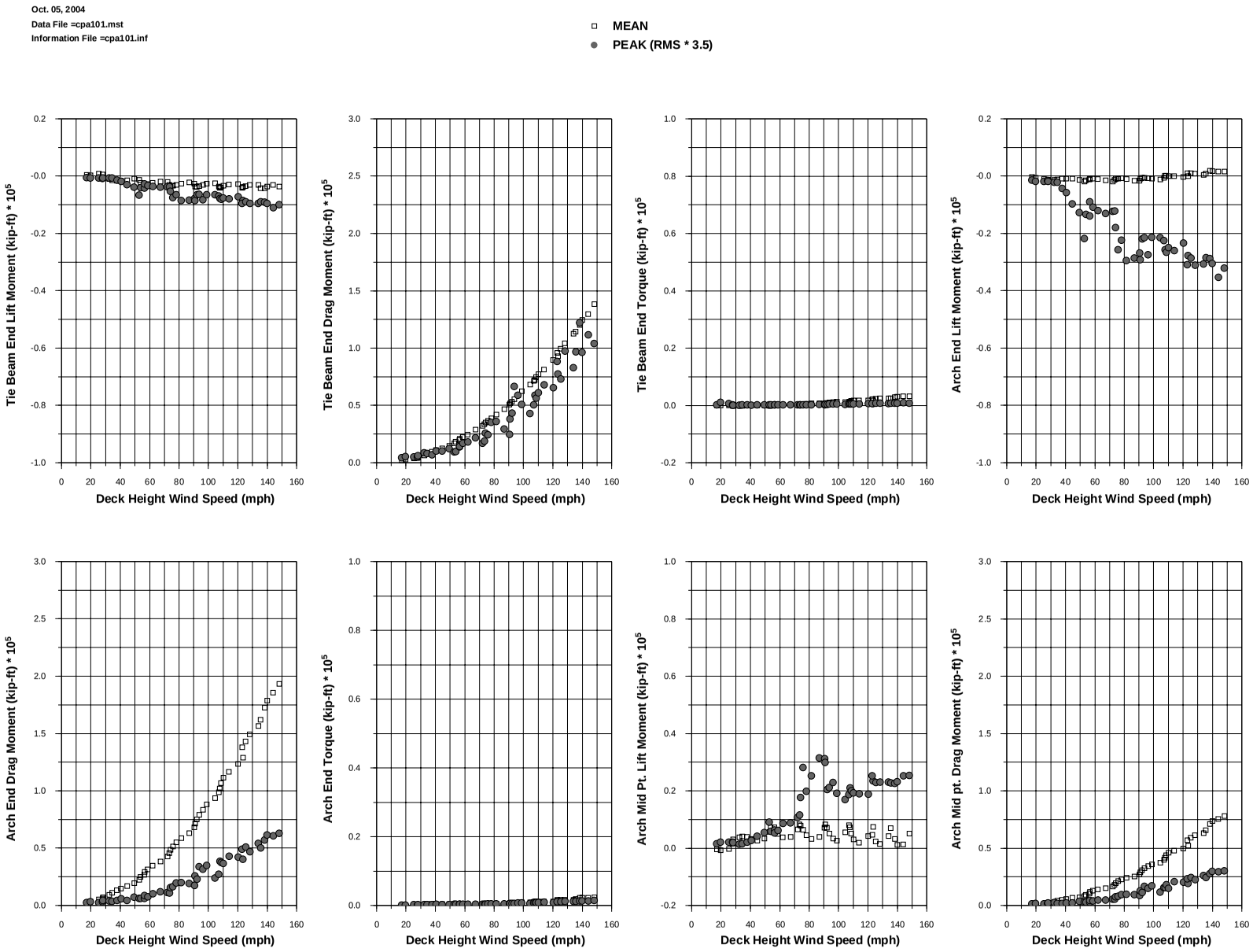

Indian River Bridge, Cantilevered Tie Beam, smooth flow, 90 degrees

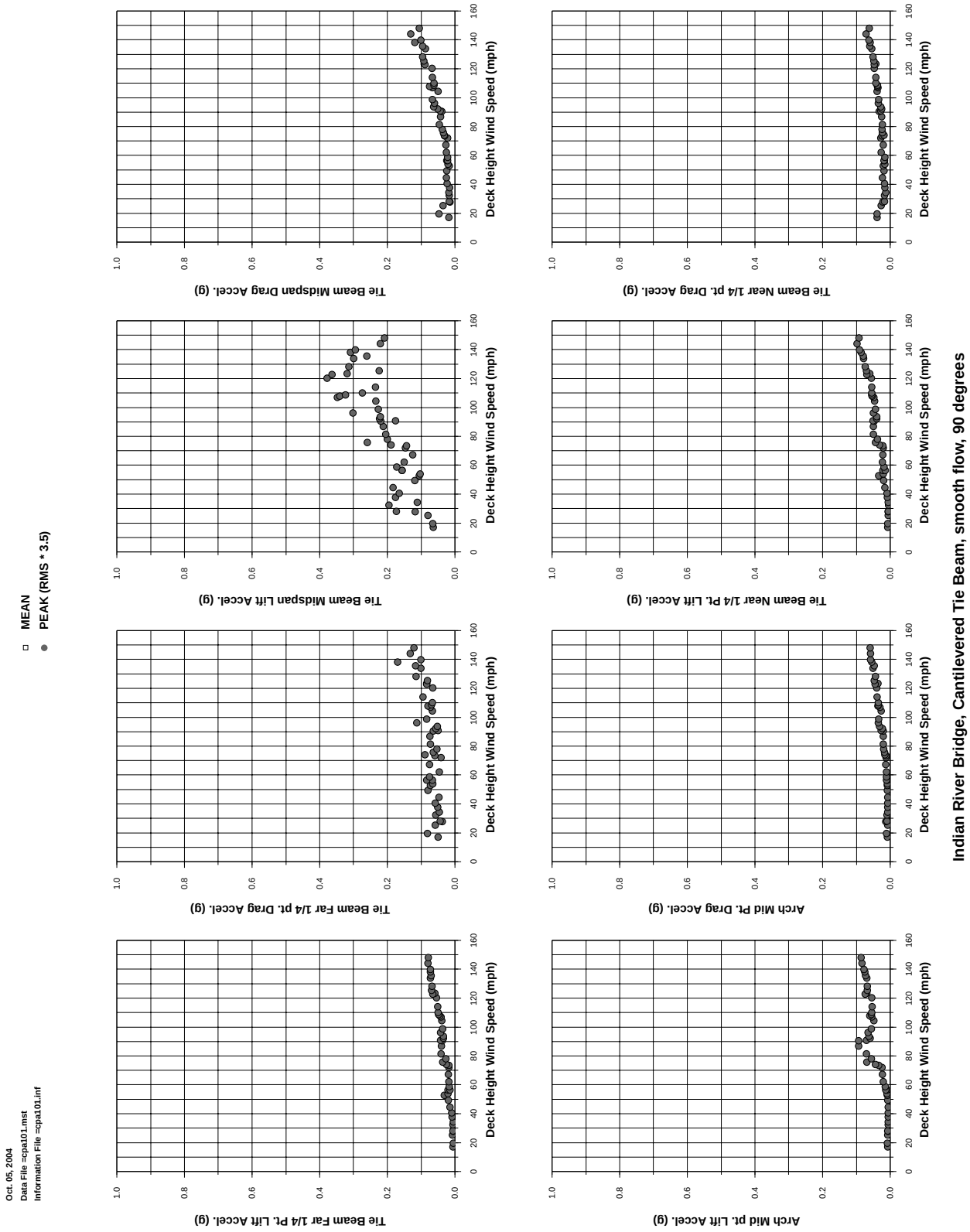

Indian River Bridge, Cantilevered Tie Beam, smooth flow, 90 degrees

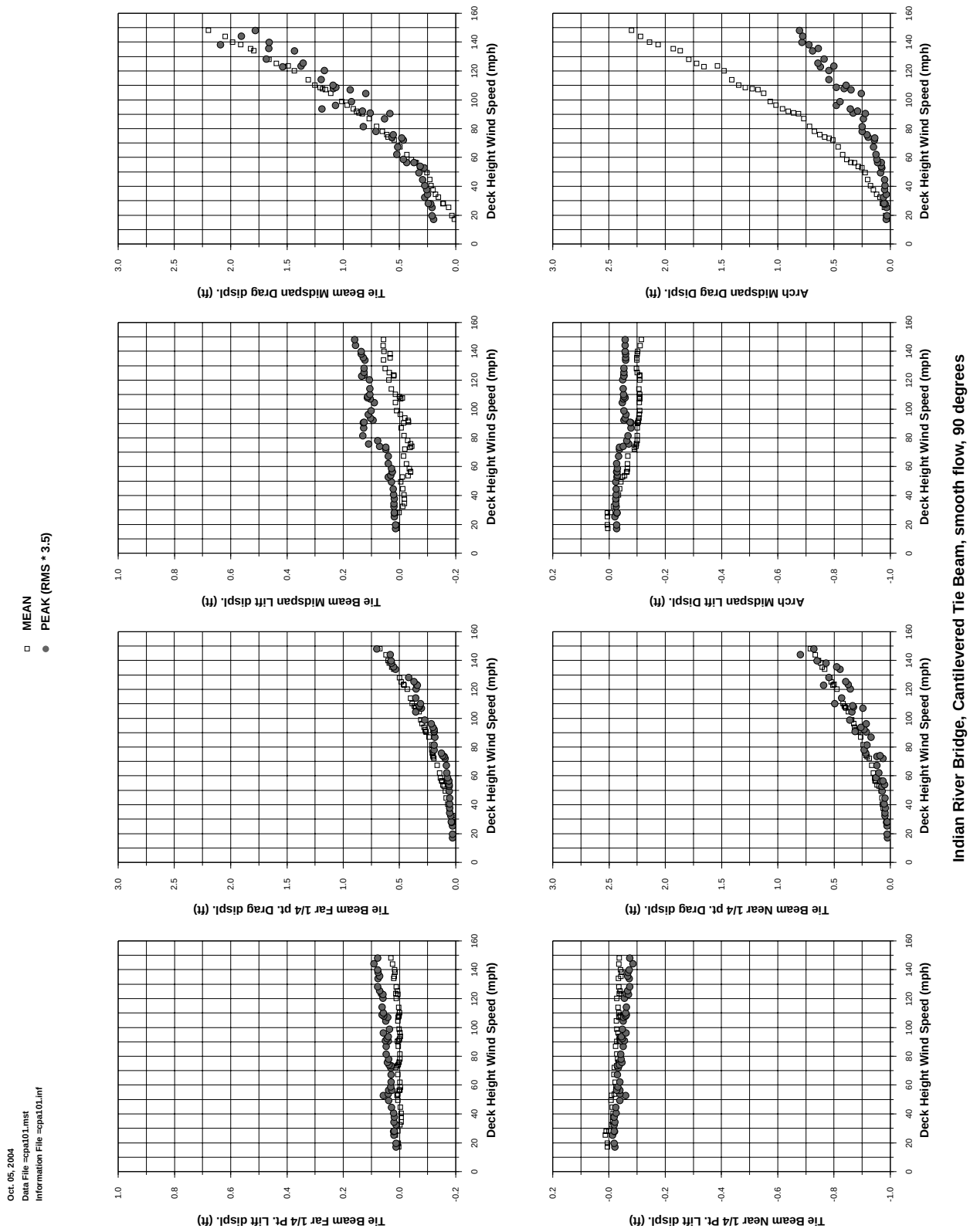

Indian River Bridge, Cantilevered Tie Beam, smooth flow, 90 degrees

APPENDIX J

RESULTS OF FULL BRIDGE AEROELASTIC TESTS, CONSTRUCTION STAGE – CANTILEVERED ARCH

Notes:

1. The bending moments given in the plots have the unit of kip-ft. The numbers read directly from the plots should be multiplied by 10^5 to obtain the actual bending moments in kip-ft. For example on page J6 of the Arch End Drag Moment (the second figure from the left on the top row), the mean and peak drag moments at about 120mph are approximately 1.0×10^5 kip-ft (not 1.0 kip-ft) and 0.25×10^5 kip-ft (not 0.25 kip-ft).

2. The total response is equal to the mean, plus or minus the peak.

3. X is along the longitudinal direction, Y is the lateral direction (drag direction), and Z is the vertical direction (lift direction). Thus M_x is the torque, M_y is the lift moment (generated by the lift) and M_z is the drag moment (generated by the drag).

TABLE J1 INSTRUMENTATION LOCATIONS, CONSTRUCTION STAGE – CANTILEVERED ARCH

Instrumentation **x – longitudinal, y – lateral (Drag), z – vertical (Lift)**	**Instrumentation Locations** **(Refer to Figure J1)**
Strain Gages:	
M_x, M_y and M_z at **Arch** End	Lift and Drag Moments, as well as Torque at 42ft from Arch-Deck connection
M_y and M_z at **Arch** Crown	Lift and Drag Moments at 44ft from Arch Crown
Accelerometers:	
y and z accel. at **Arch** ¼ Point	Lift and Drag Accelerations at the ¼ point on the Arch (235ft from the arch crown in the deck longitudinal direction)
y and z accel. at **Arch** Crown	Lift and Drag Accelerations at 20ft from Arch Crown
Displacement Lasers:	
y and z displacements at **Arch** Crown	Lift and Drag Displacements at 20ft from Arch Crown
y displacement at **Arch** ¼ Point	Drag Displacement at the ¼ point on the Arch (240ft from the arch crown in the deck longitudinal direction)
y displacement at **Arch** other ¼ Point	Drag Displacement at the ¼ point on the Arch (245ft from the arch crown in the deck longitudinal direction)
Wind Speeds:	
Deck Level	Deck Height
Arch Level	Arch Crown Height

TABLE J2 SUMMARY OF TESTS, CONSTRUCTION STAGE – CANTILEVERED ARCH, INDIAN RIVER BRIDGE

Test File	Test No.	Flow condition	Existing bridge	Wind direction (Test angle)	V_{deck} (mph) Maximum wind speed at deck height	Vortex shedding peaks at wind speeds
CPB101	1	Smooth Flow	No	Perpendicular to bridge (90°)	153	30 and 80~90 mph
CPB201	2	Hurricane profile	No	Perpendicular to bridge (90°)	135	80 mph
CPB202	3	Hurricane profile	No	60° to the bridge	140	30~40 mph
CPB203	4	Hurricane profile	No	30° to the bridge	139	Not observed
CPB204	5	Hurricane profile	No	Along the bridge (0°)	142	Not observed
CPB205	6	Hurricane profile	Yes	Perpendicular to bridge (90°)	138	80 mph
CPB301	7	Open Country profile	Yes	Perpendicular to bridge (90°)	136	Not observed
CPB302	8	Open Country profile	No	Perpendicular to bridge (90°)	143	30 mph
CPB303	9	Open Country profile	No	60° to the bridge	142	30 mph
CPB304	10	Open Country profile	No	30° to the bridge	142	50 mph
CPB305	11	Open Country profile	No	Along the bridge (0°)	144	Not observed
CPB306 (without crane on arch)	12	Open Country profile	No	Perpendicular to bridge (90°)	143	30 and 80~90 mph

Note: for tests No. 1 to 11, a simulated construction crane is on side of the arch crown.

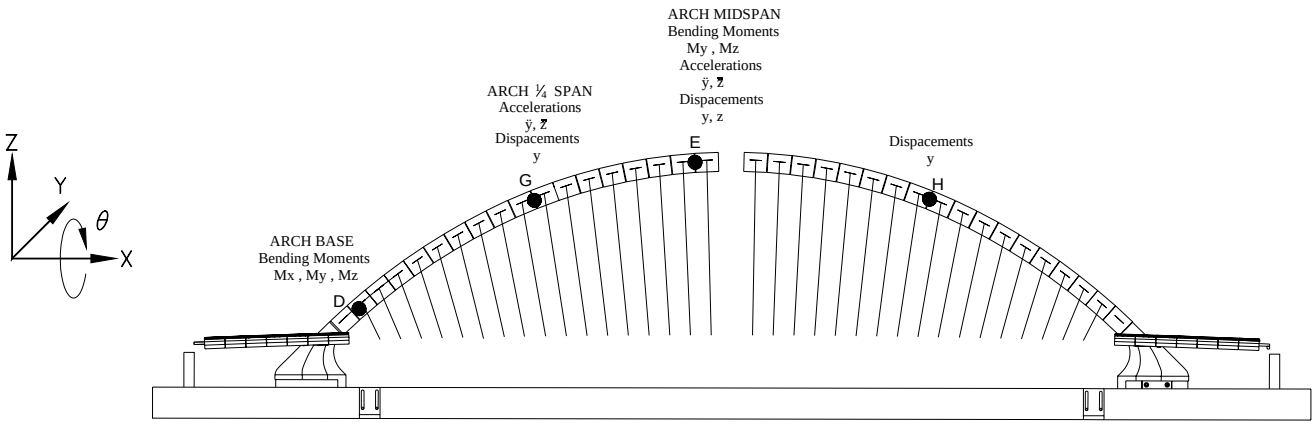

FIGURE J1 INSTRUMENTATION LOCATIONS, CONSTRUCTION STAGE – CANTILEVERED ARCH

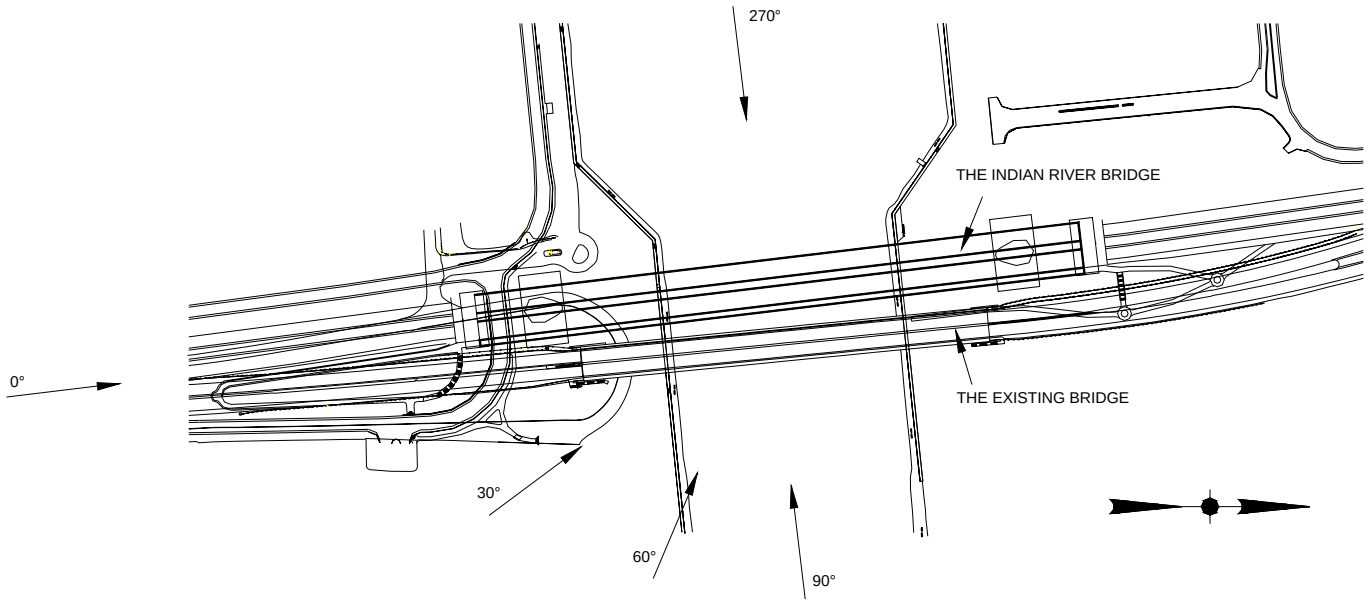

FIGURE J2 WIND ANGLES DEFINED IN WIND TUNNEL TESTS

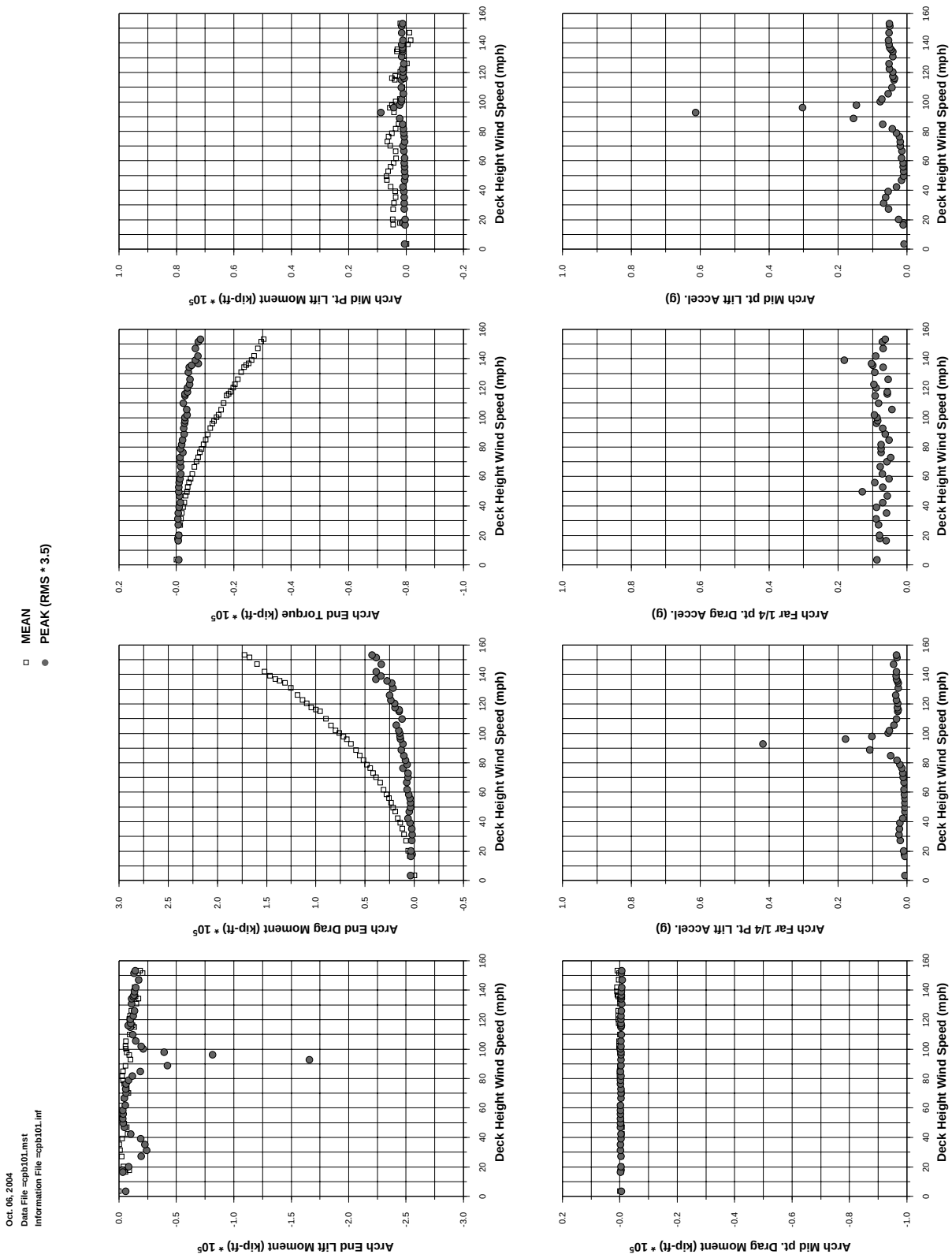

Indian River Bridge, Cantilevered Arch, smooth flow, 90 degrees

Oct. 06, 2004
Data File =cpb101.mst
Information File =cpb101.inf

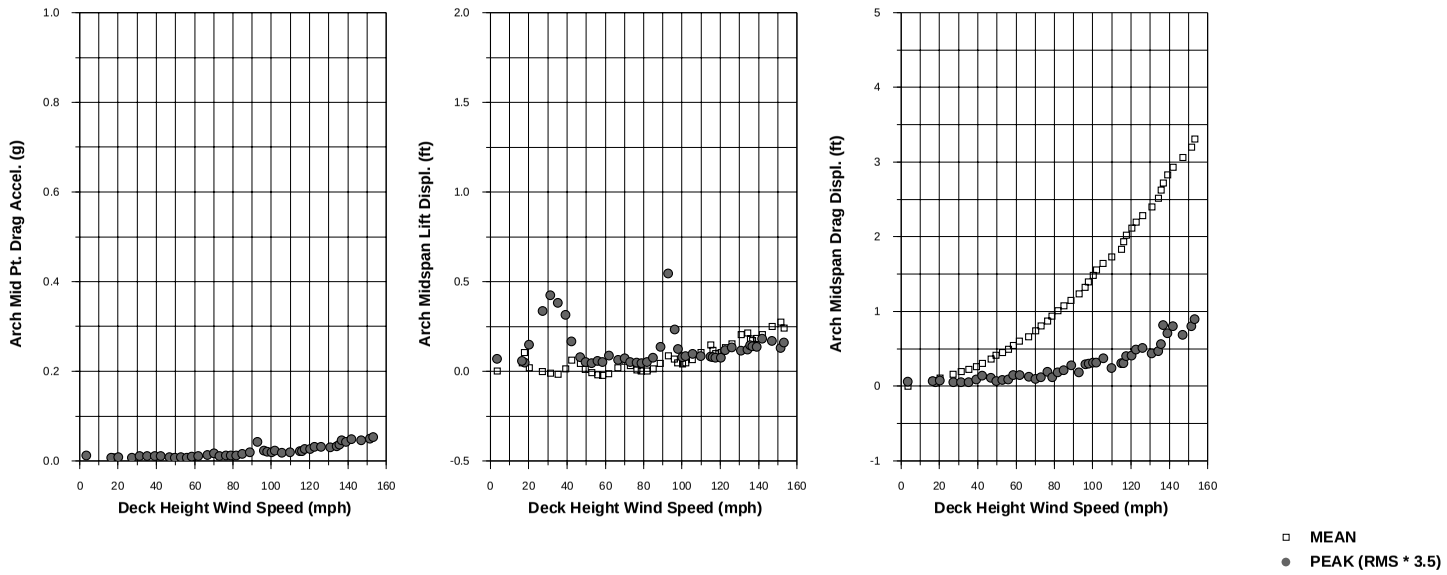

Indian River Bridge, Cantilevered Arch, smooth flow, 90 degrees

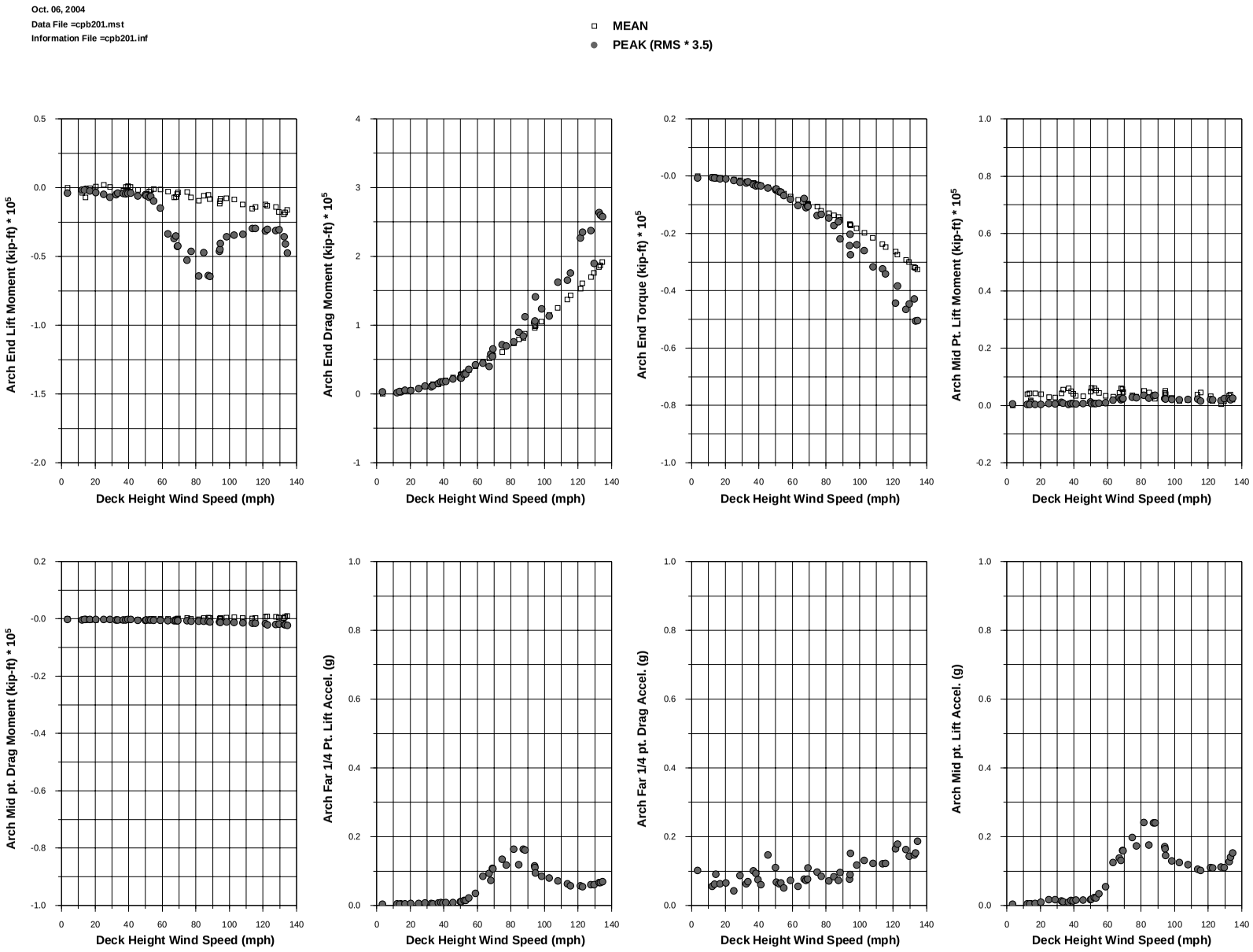

Indian River Bridge, Cantilevered Arch, hurricane profile, 90 degrees, without existing bridge

Oct. 06, 2004
Data File =cpb201.mst
Information File =cpb201.inf

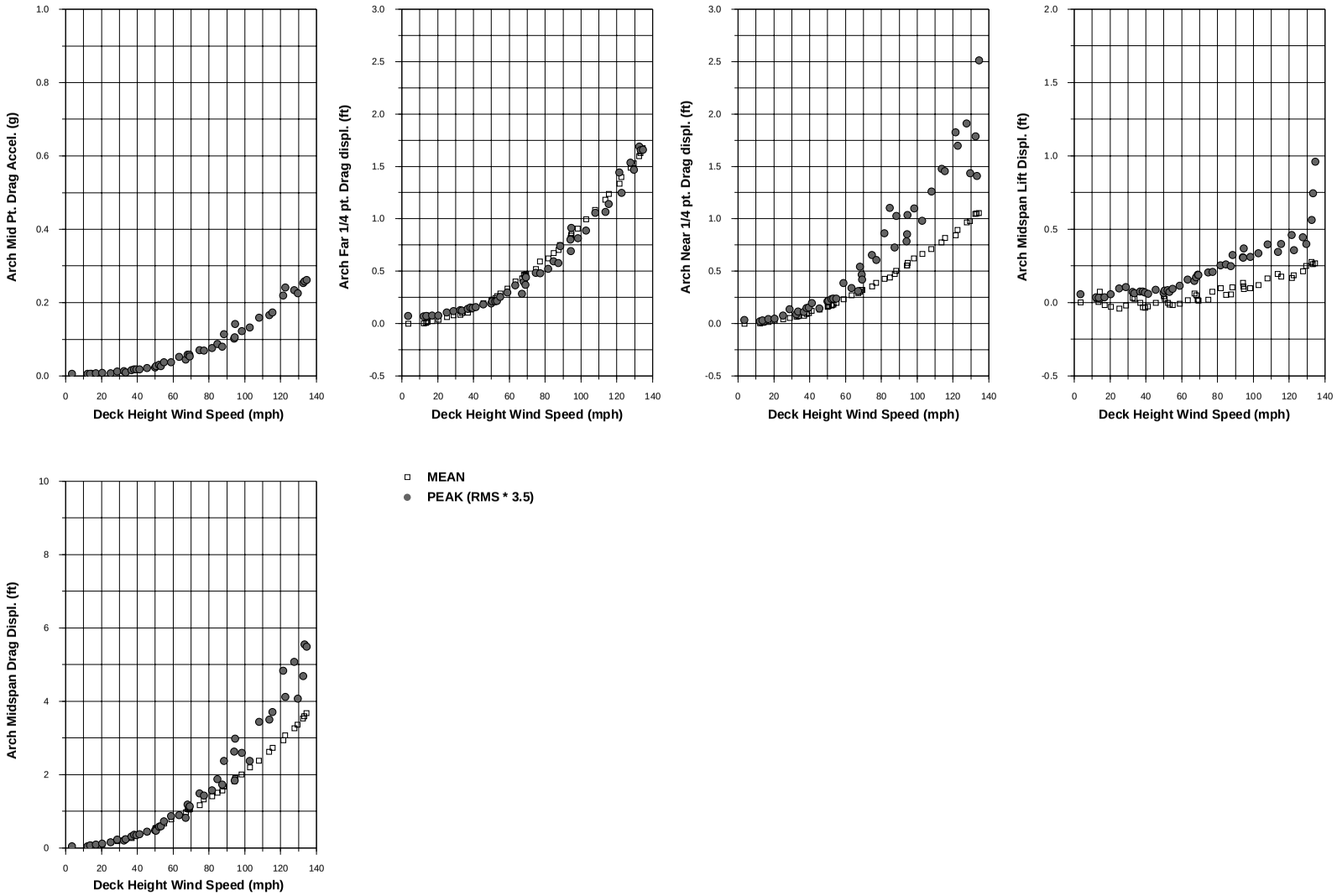

Indian River Bridge, Cantilevered Arch, hurricane profile, 90 degrees, without existing bridge

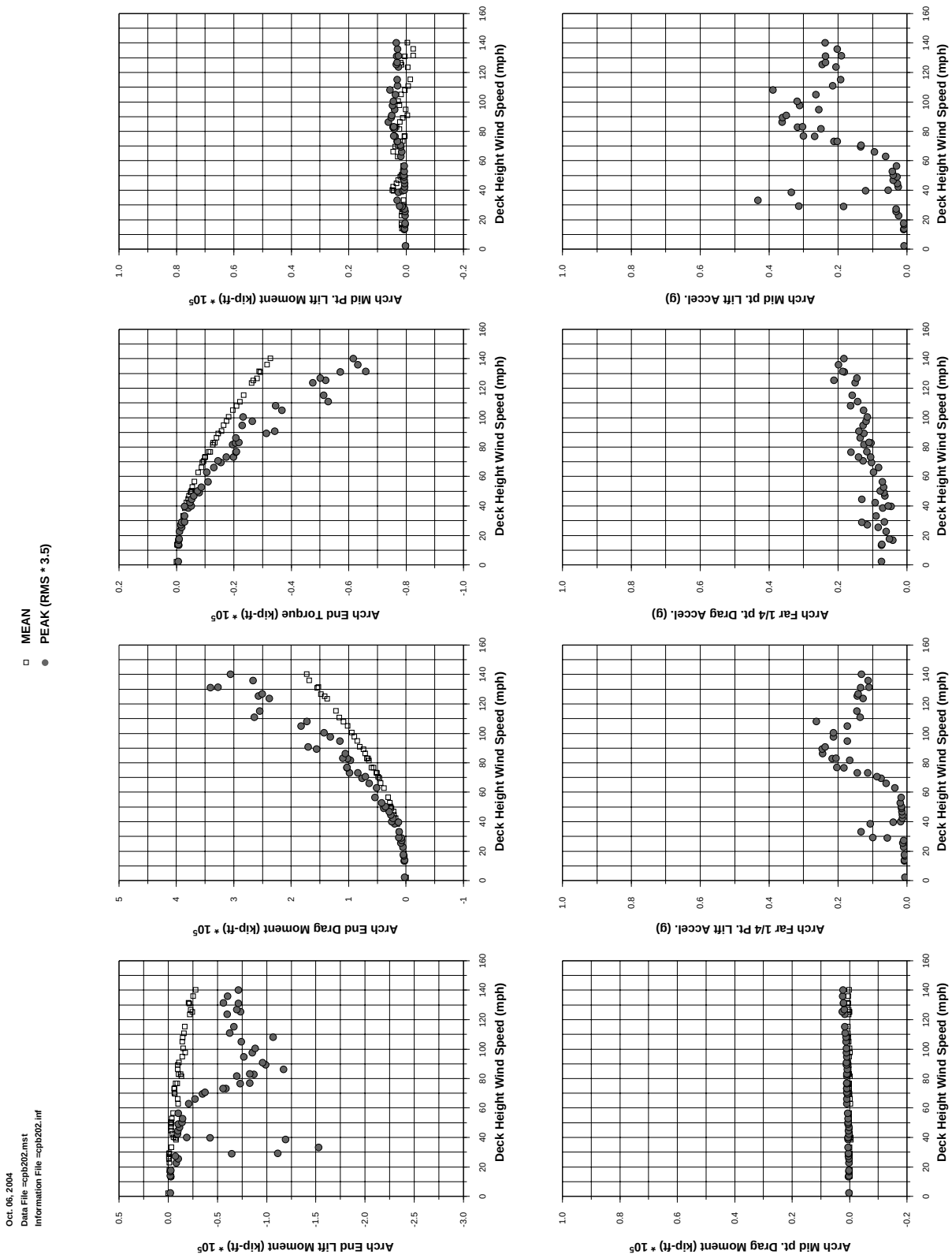

Indian River Bridge, Cantilevered Arch, hurricane profile, 60 degrees

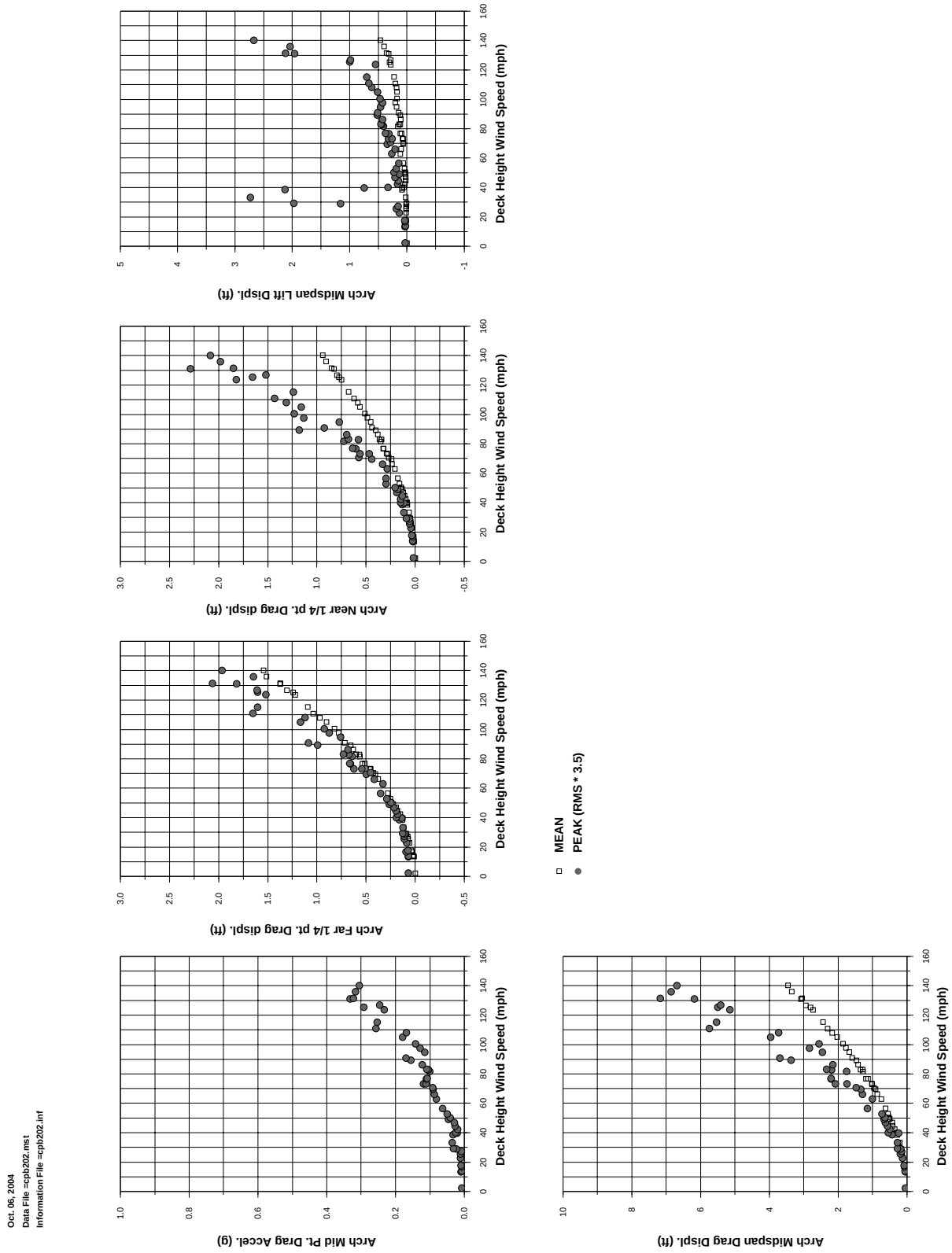

Indian River Bridge, Cantilevered Arch, hurricane profile, 60 degrees

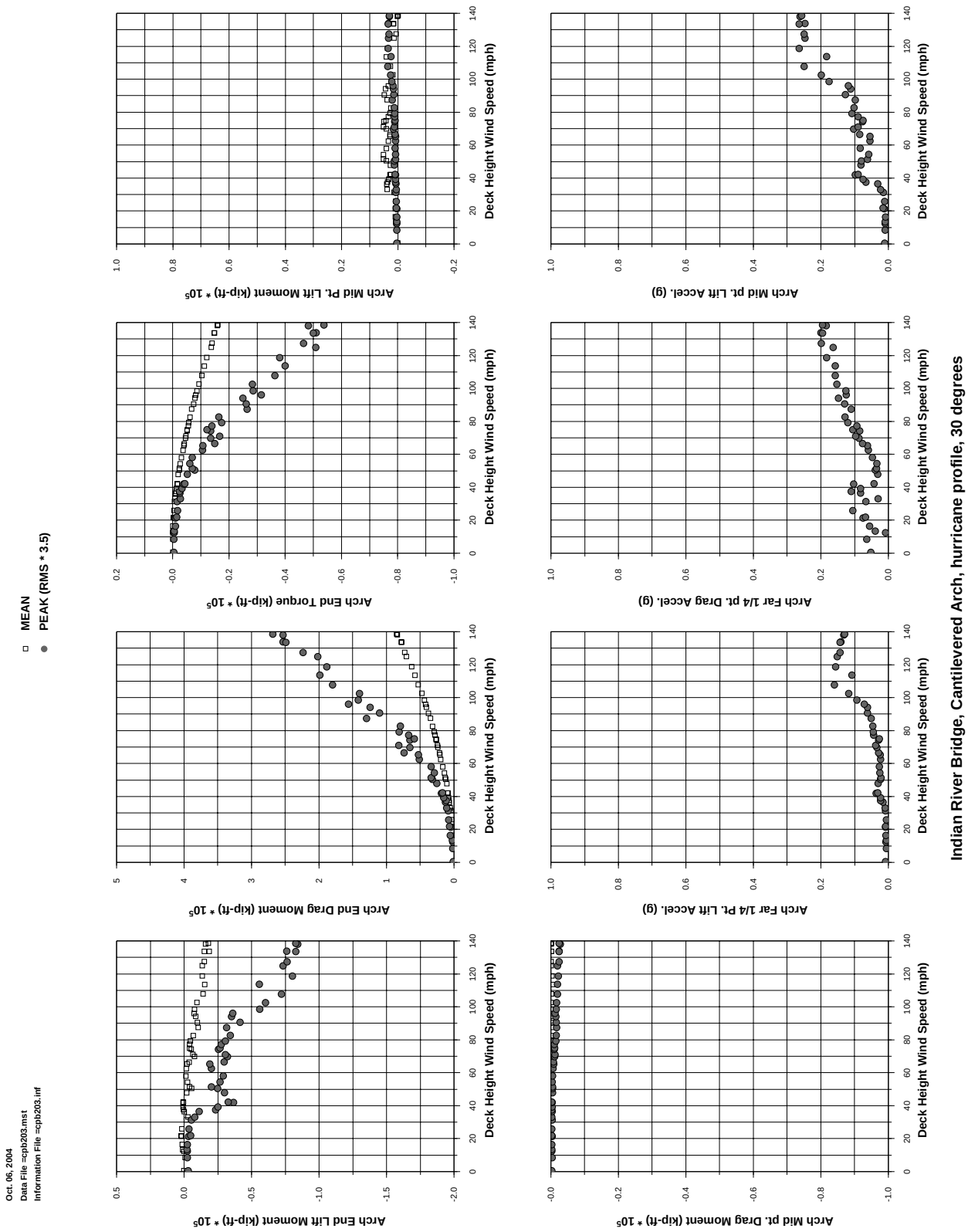

Indian River Bridge, Cantilevered Arch, hurricane profile, 30 degrees

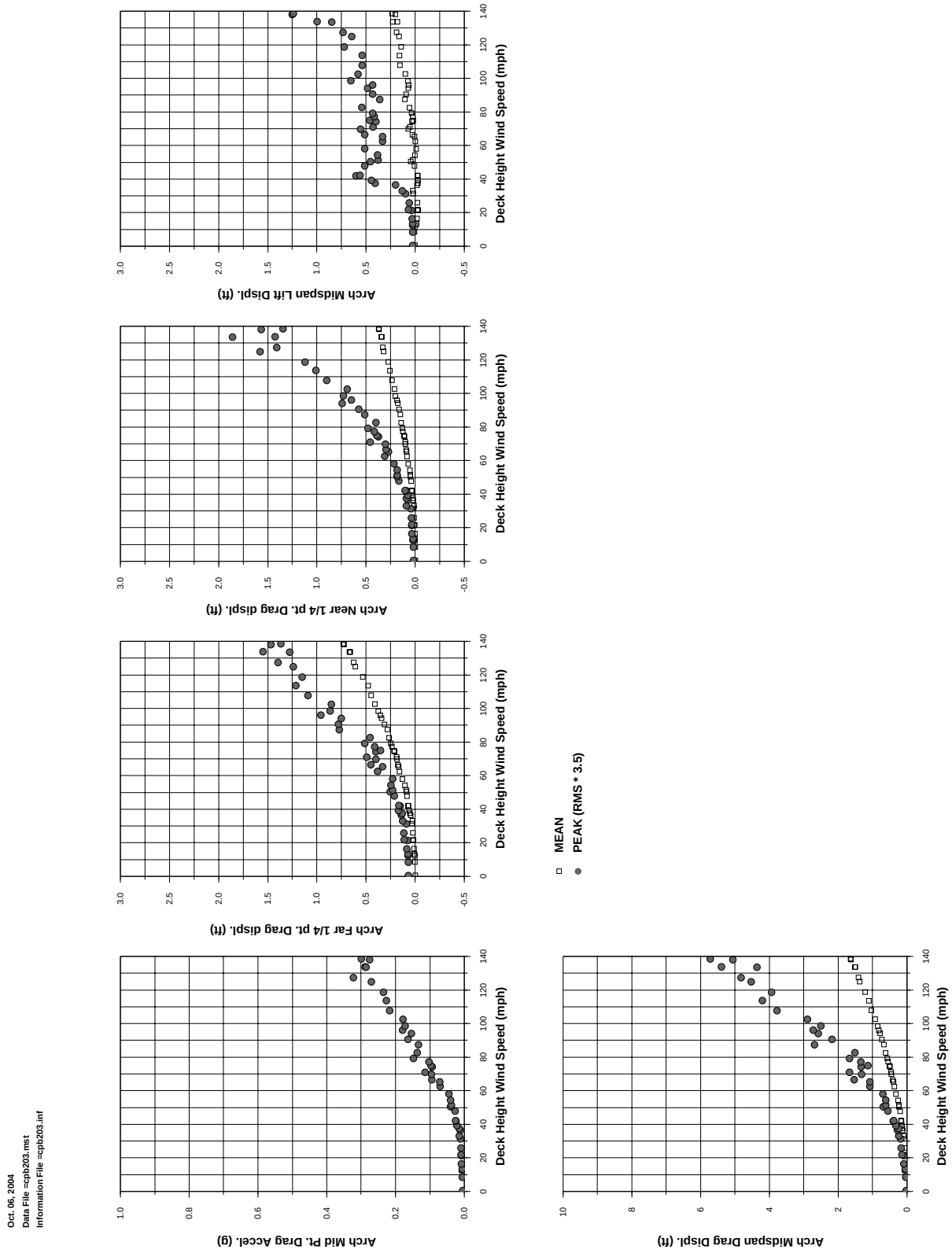

Indian River Bridge, Cantilevered Arch, hurricane profile, 30 degrees

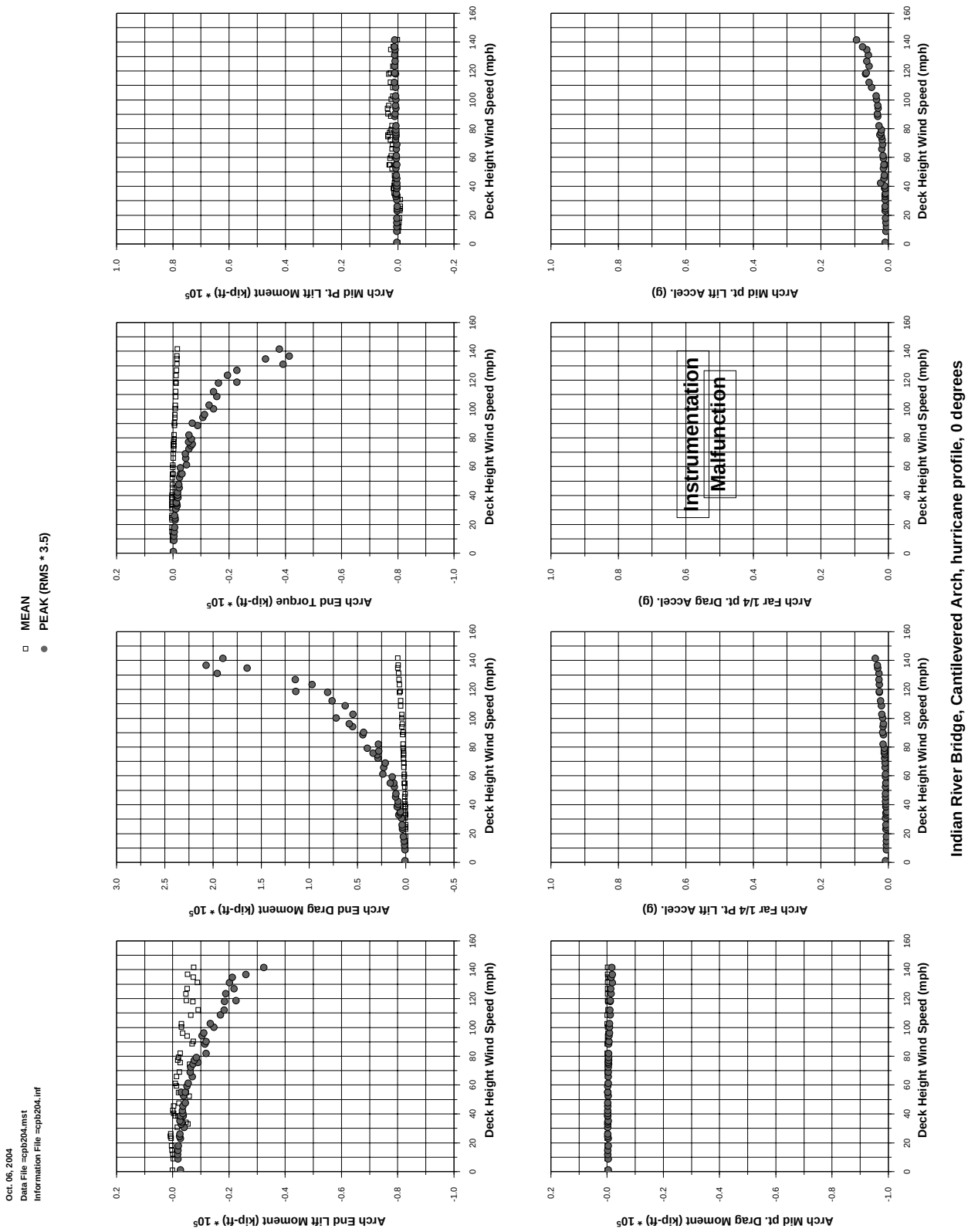

Indian River Bridge, Cantilevered Arch, hurricane profile, 0 degrees

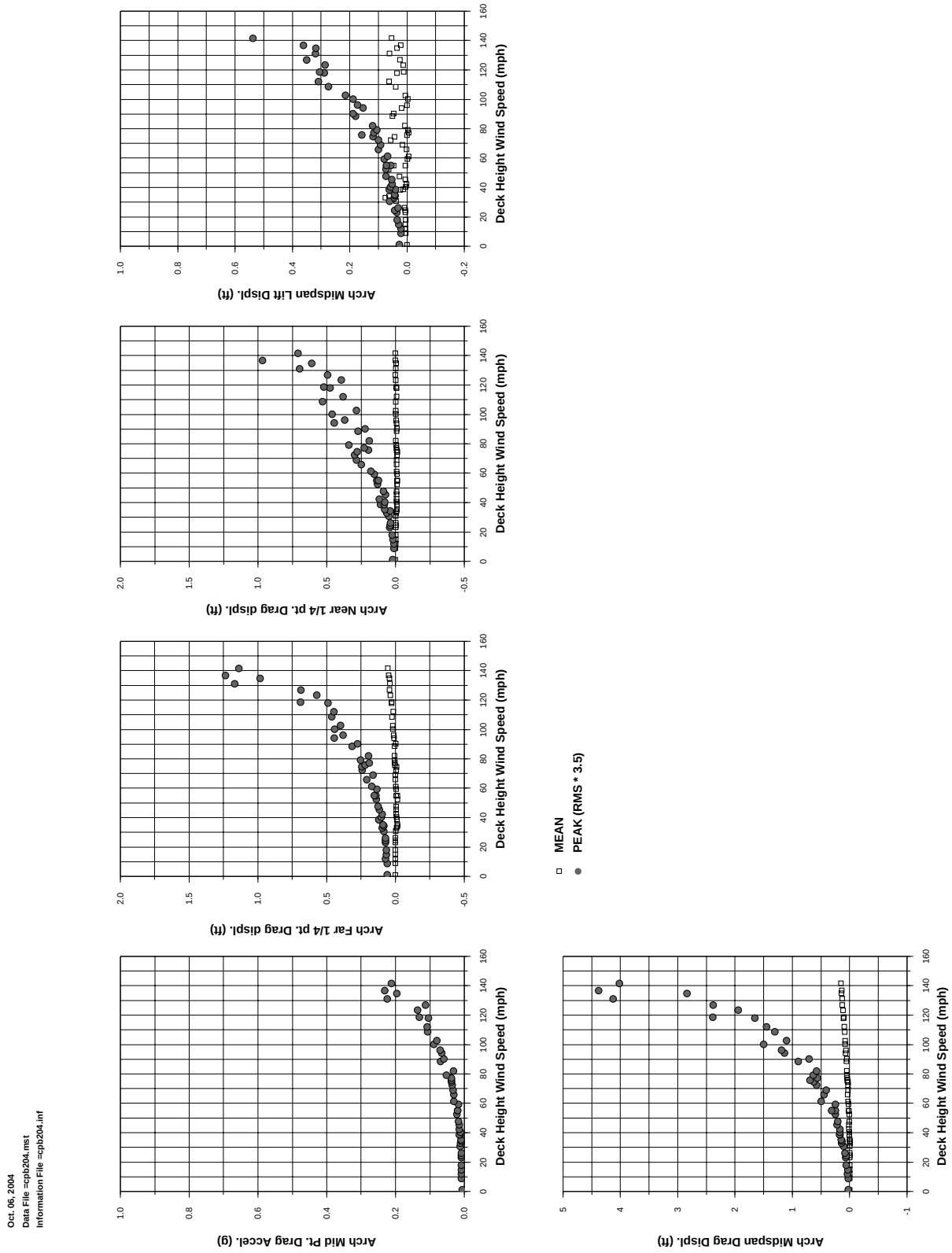

Indian River Bridge, Cantilevered Arch, hurricane profile, 0 degrees

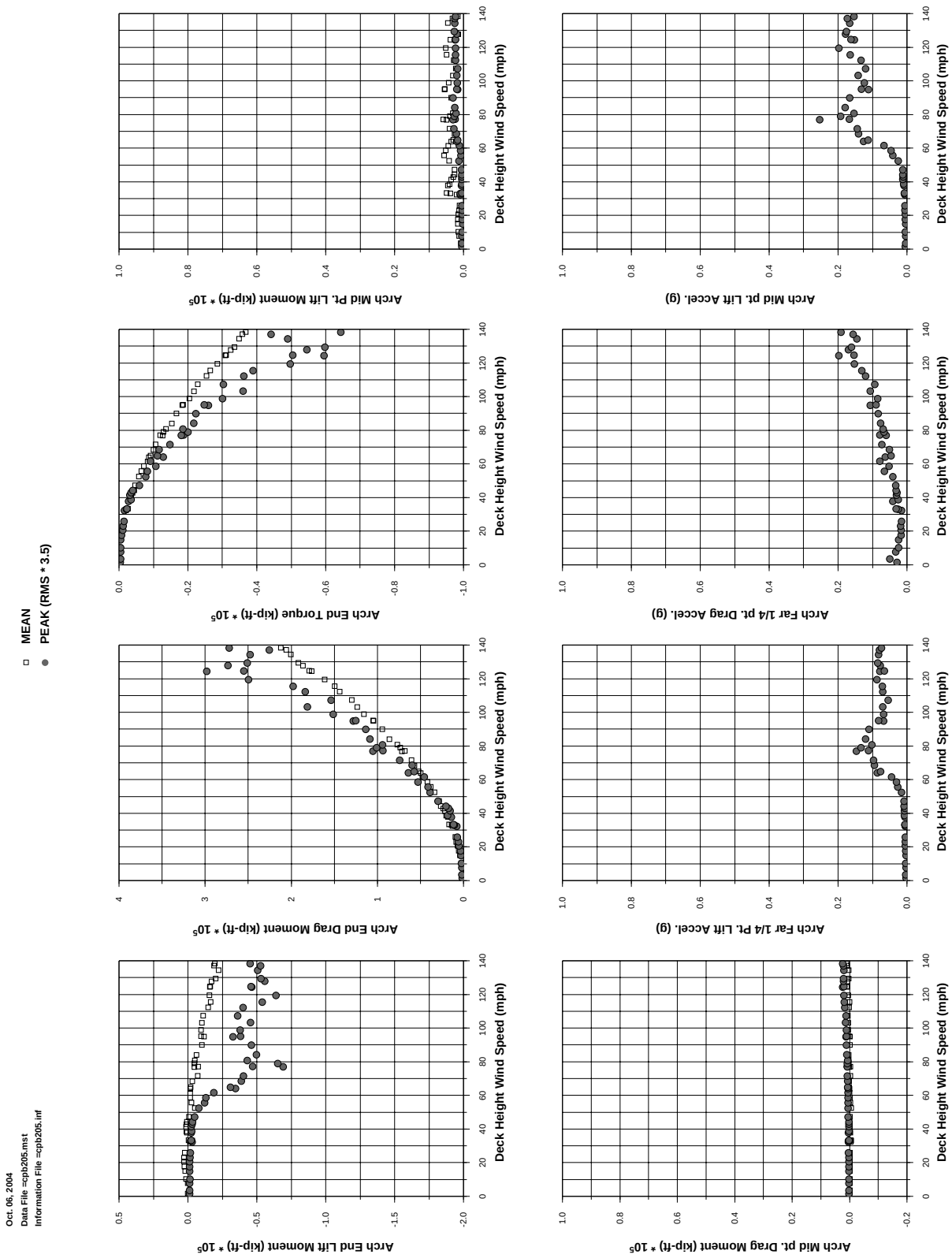

Indian River Bridge, Cantilevered Arch, hurricane profile, 90 degrees, with existing bridge

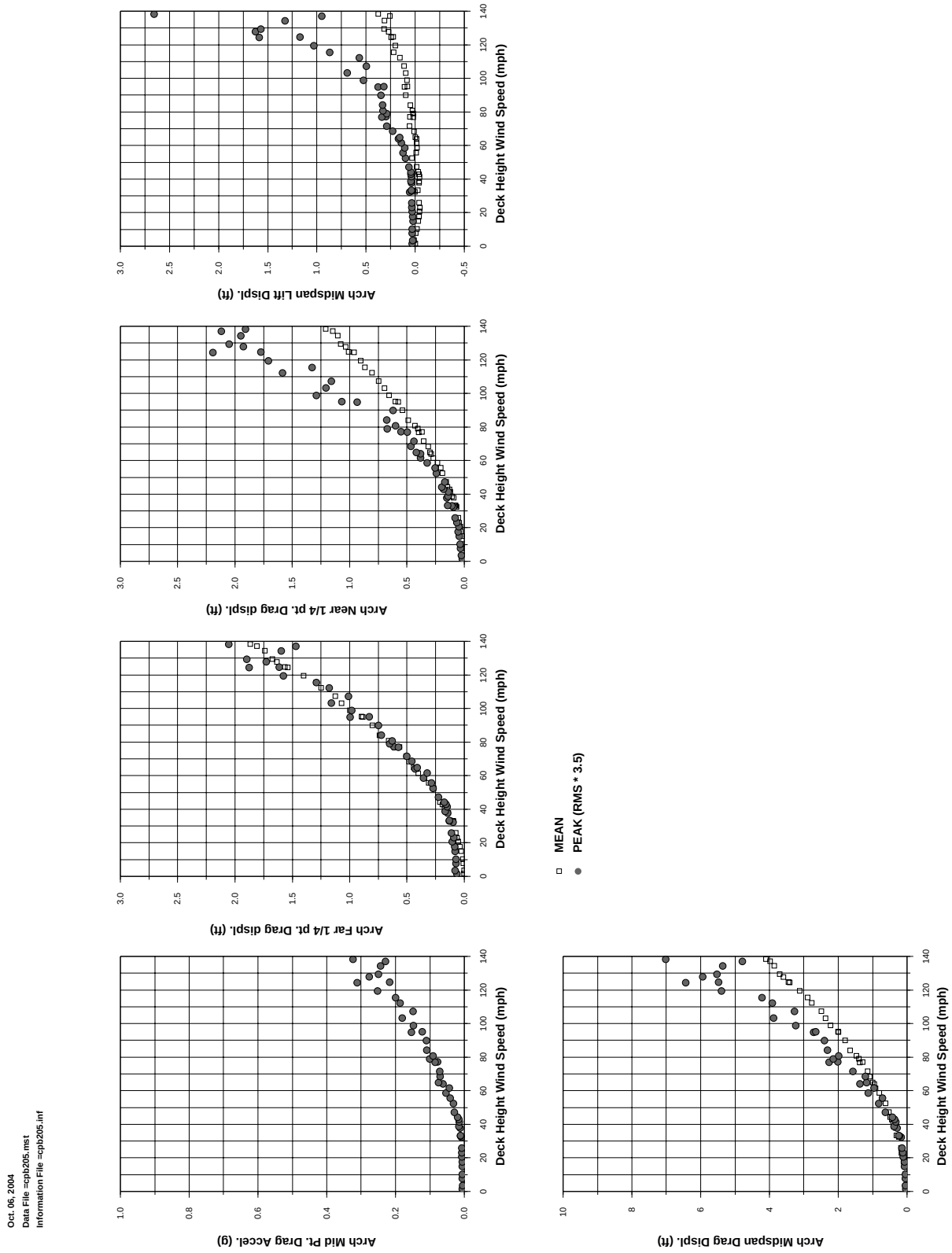

Indian River Bridge, Cantilevered Arch, hurricane profile, 90 degrees, with existing bridge

Oct. 06, 2004
Data File =cpb301.mst
Information File =cpb301.inf

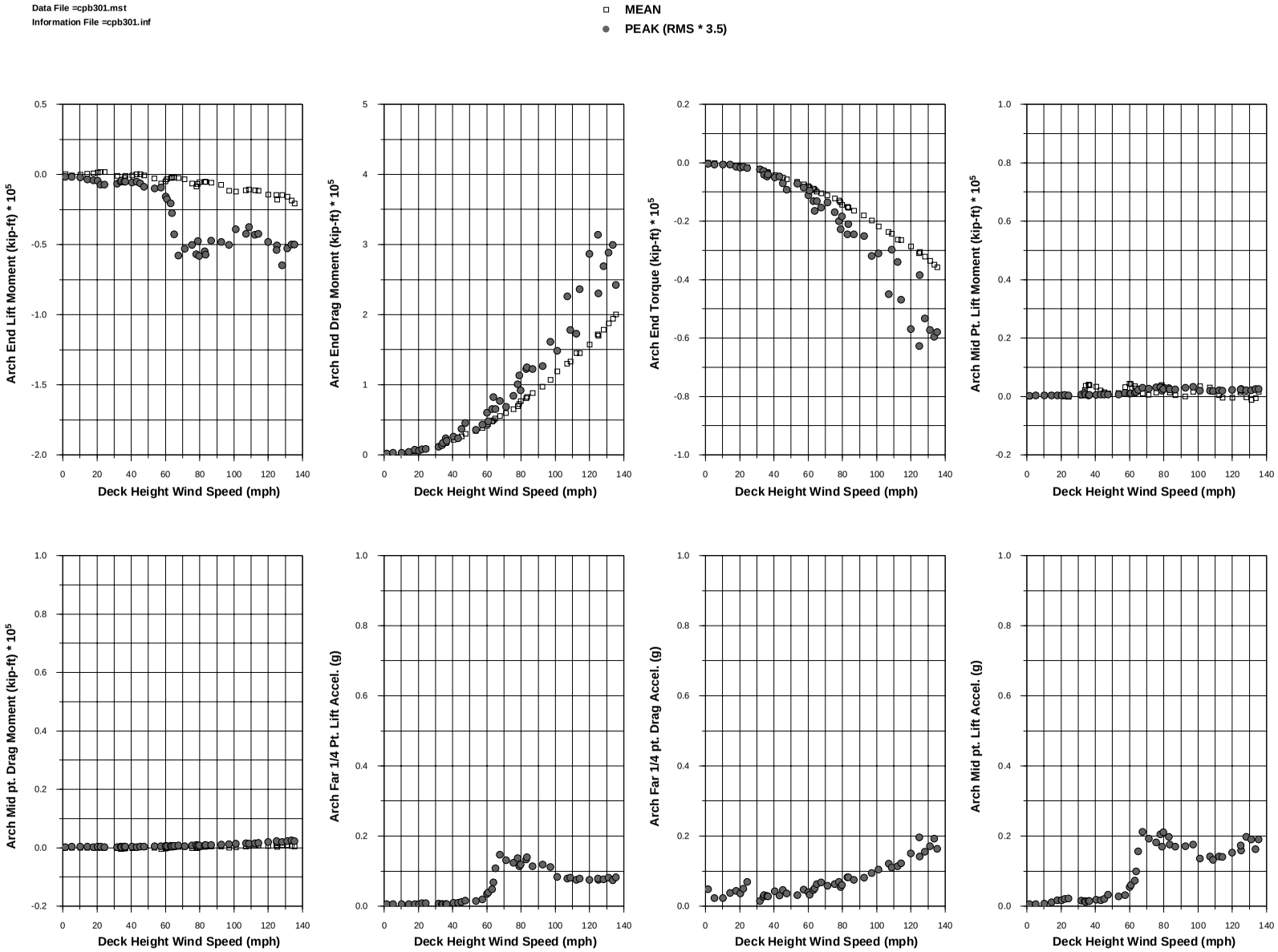

Indian River Bridge, Cantilevered Arch, open country profile, 90 degrees, with existing bridge

Oct. 06, 2004
Data File =cpb301.mst
Information File =cpb301.inf

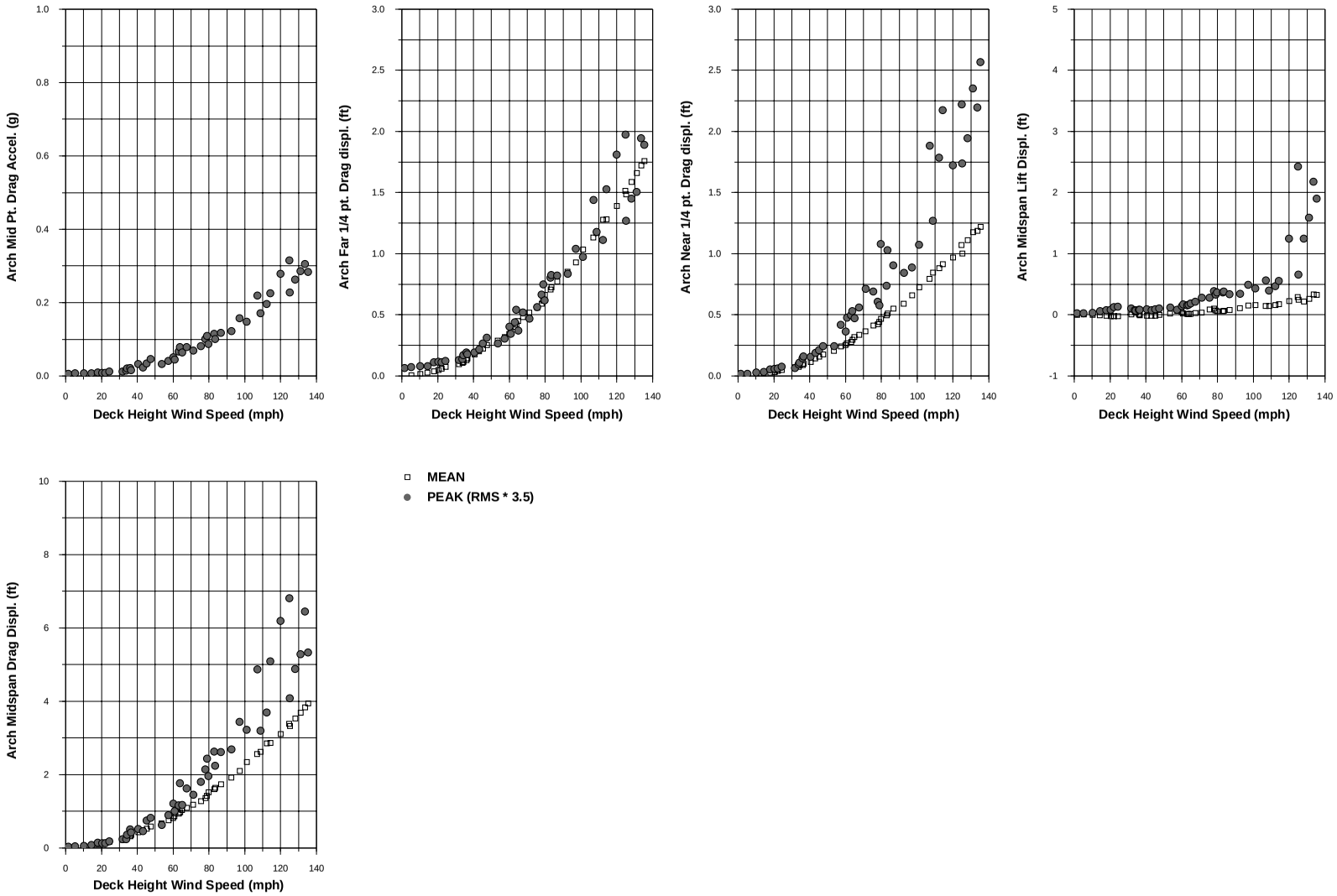

Indian River Bridge, Cantilevered Arch, open country profile, 90 degrees, with existing bridge

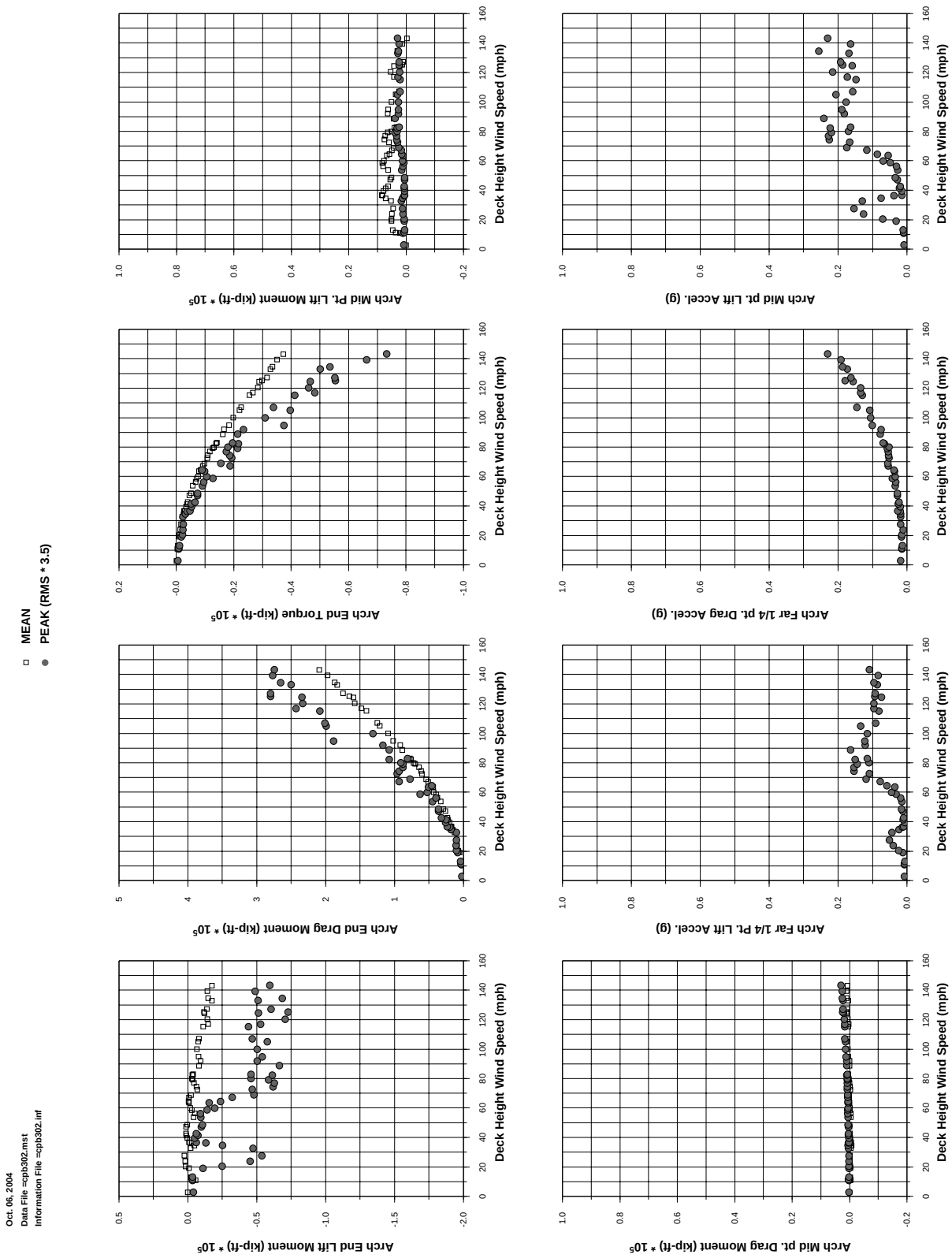

Indian River Bridge, Cantilevered Arch, open country profile, 90 degrees, without existing bridge

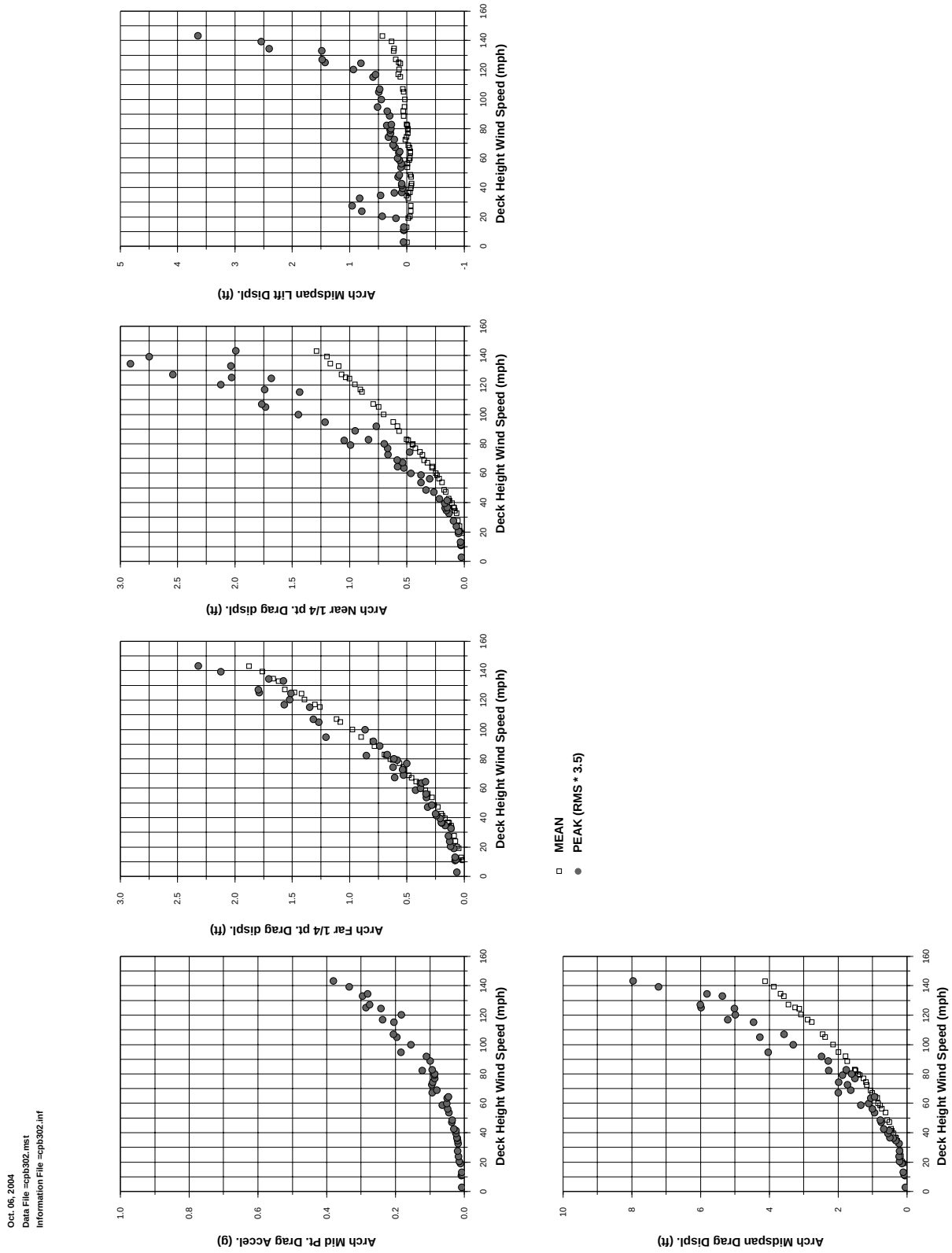

Indian River Bridge, Cantilevered Arch, open country profile, 90 degrees, without existing bridge

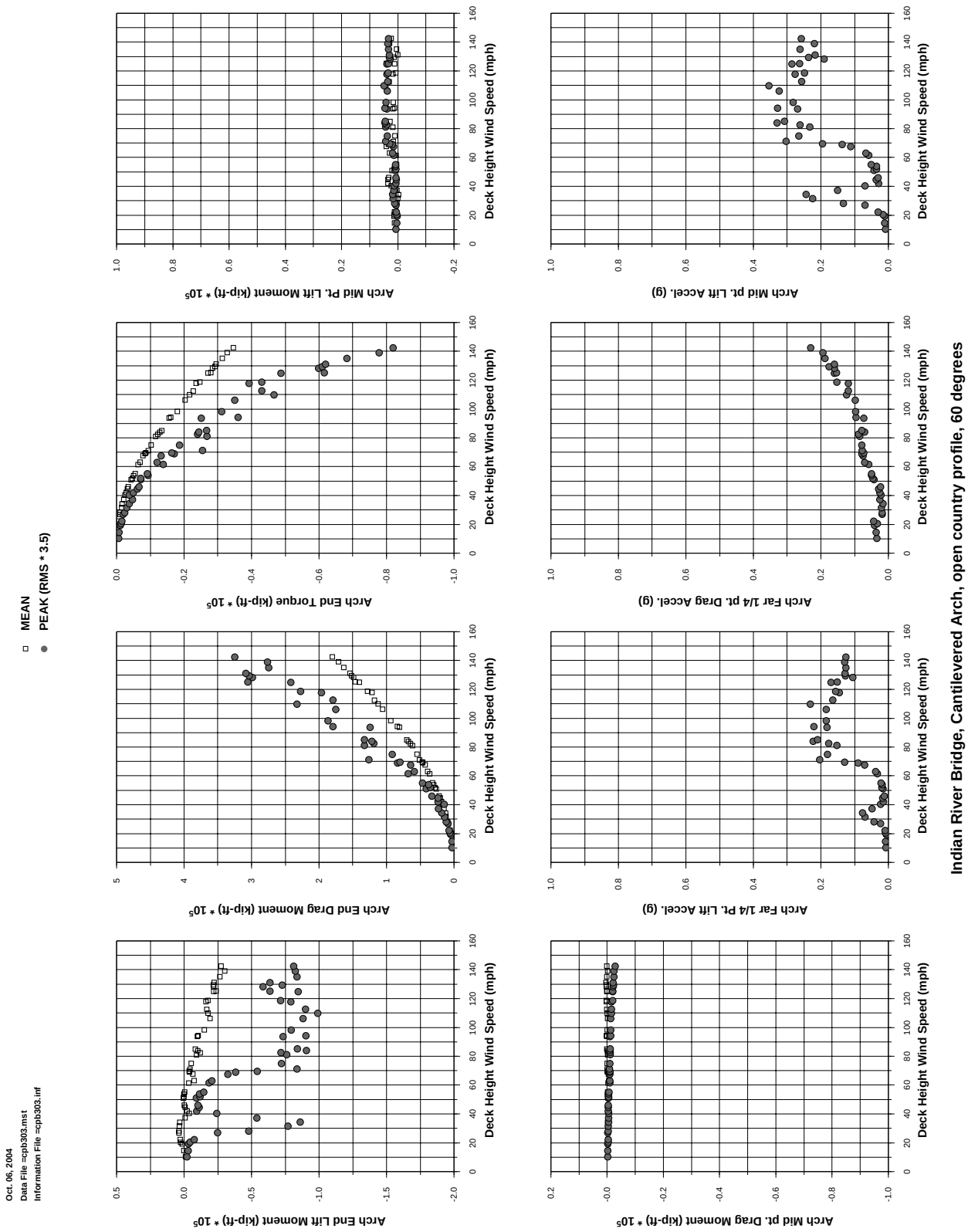

Indian River Bridge, Cantilevered Arch, open country profile, 60 degrees

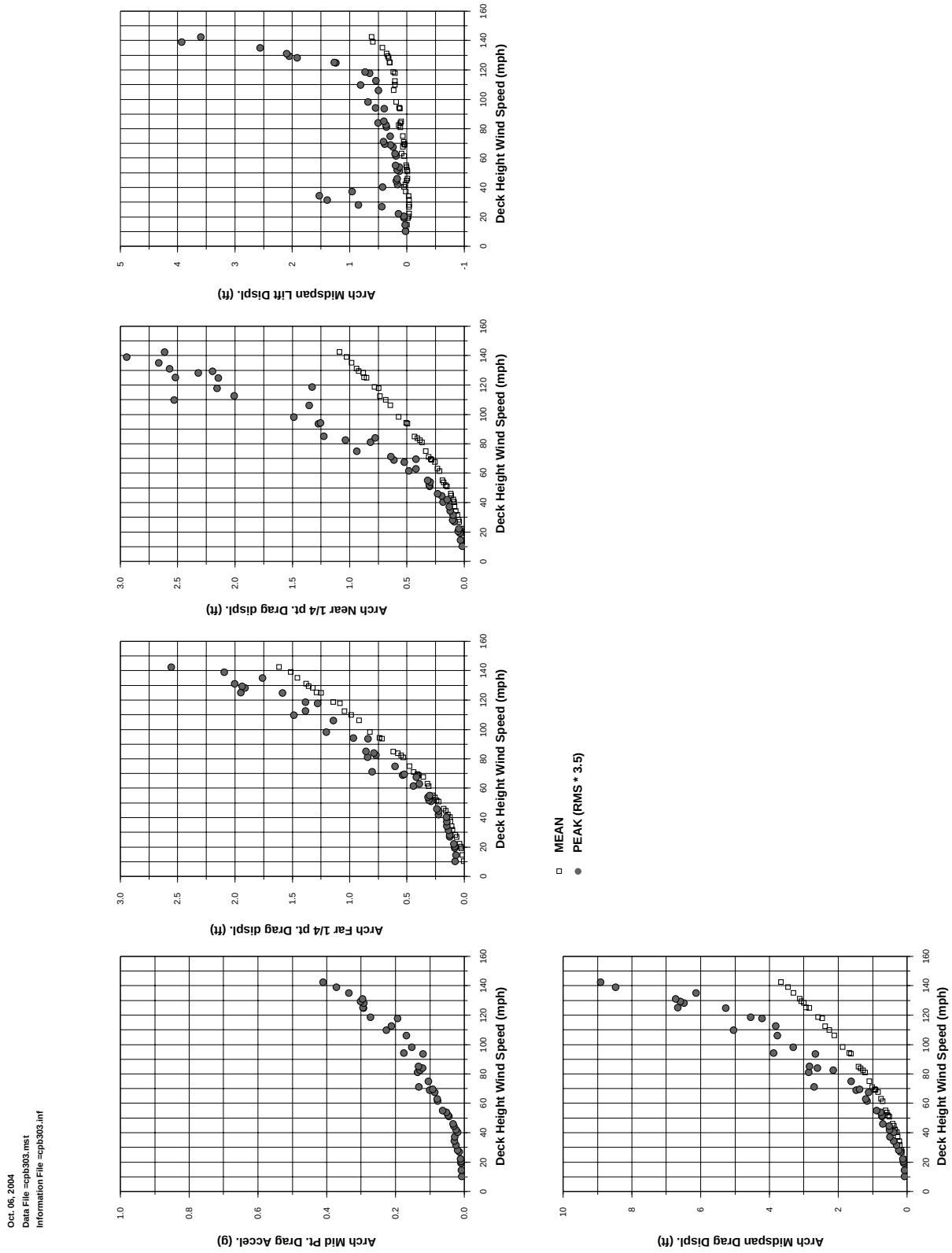

Indian River Bridge, Cantilevered Arch, open country profile, 60 degrees

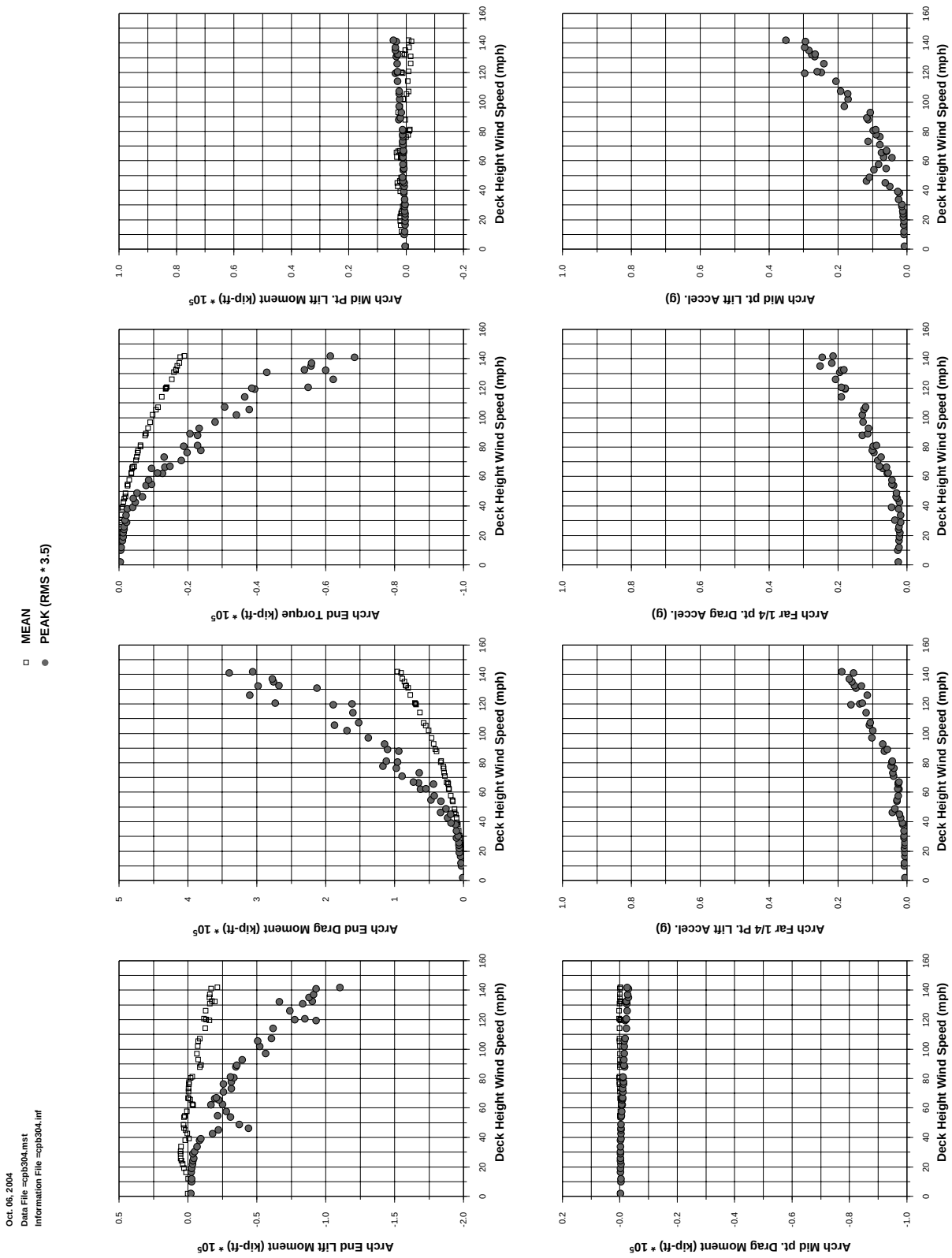

Indian River Bridge, Cantilevered Arch, open country profile, 30 degrees

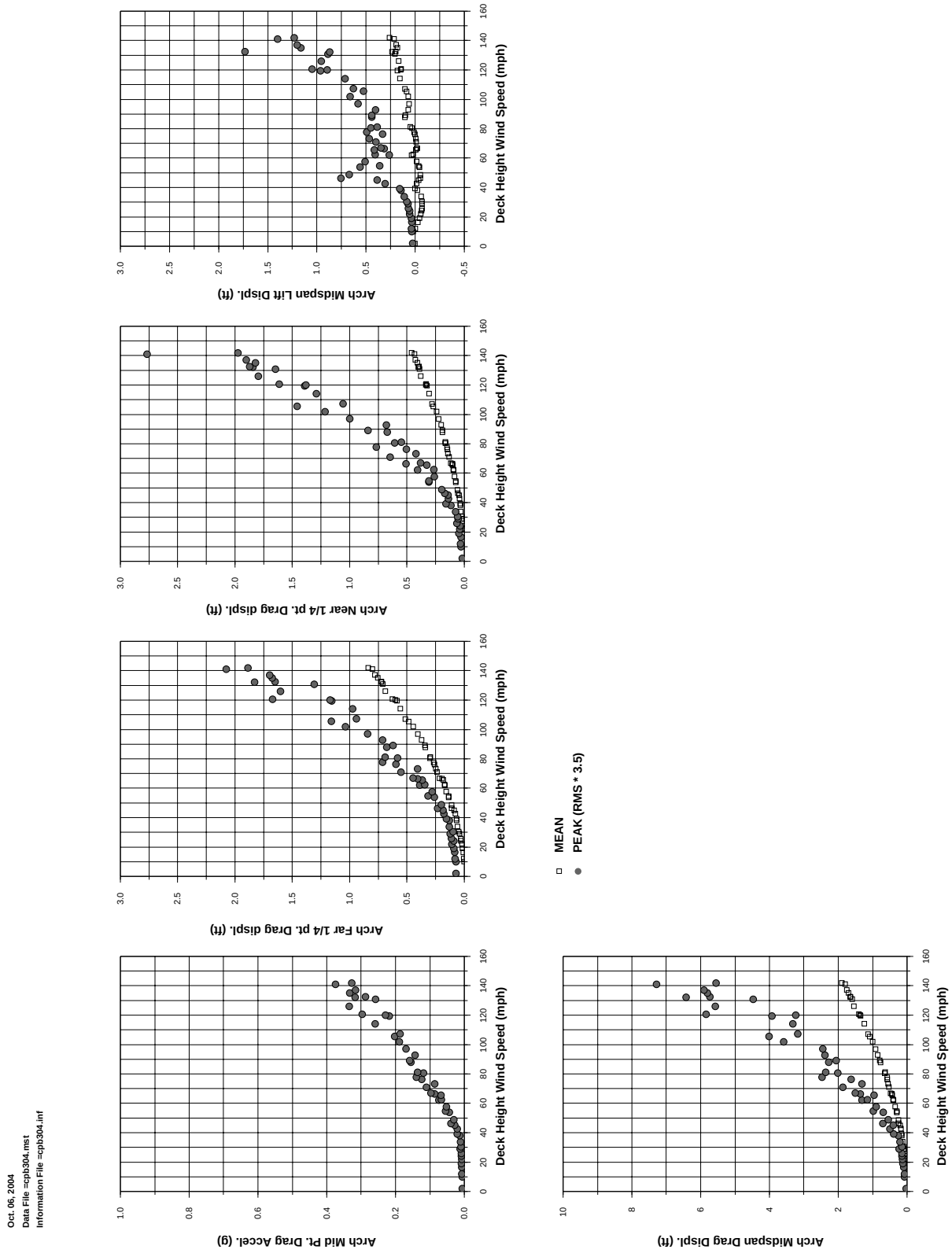

Indian River Bridge, Cantilevered Arch, open country profile, 30 degrees

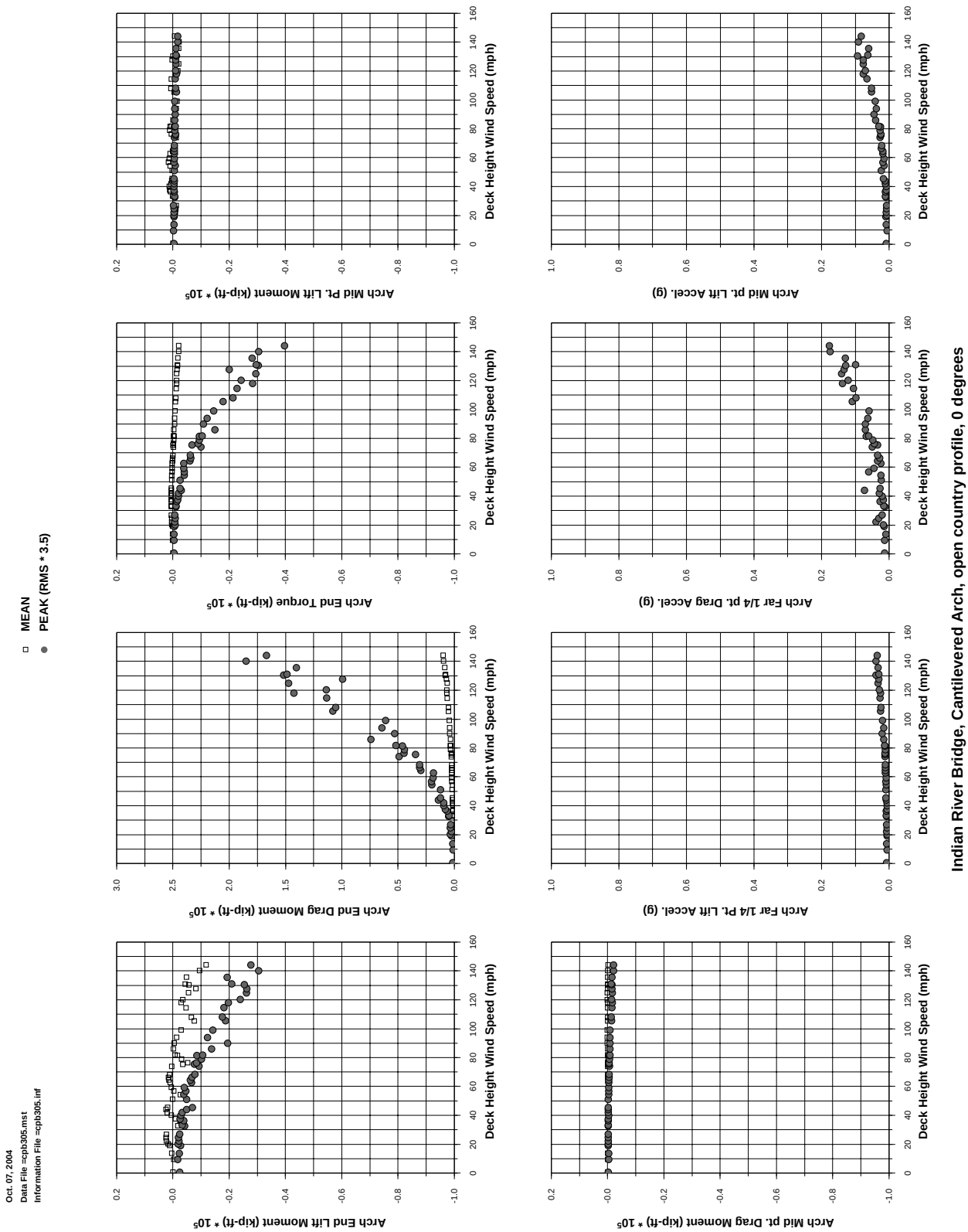

Indian River Bridge, Cantilevered Arch, open country profile, 0 degrees

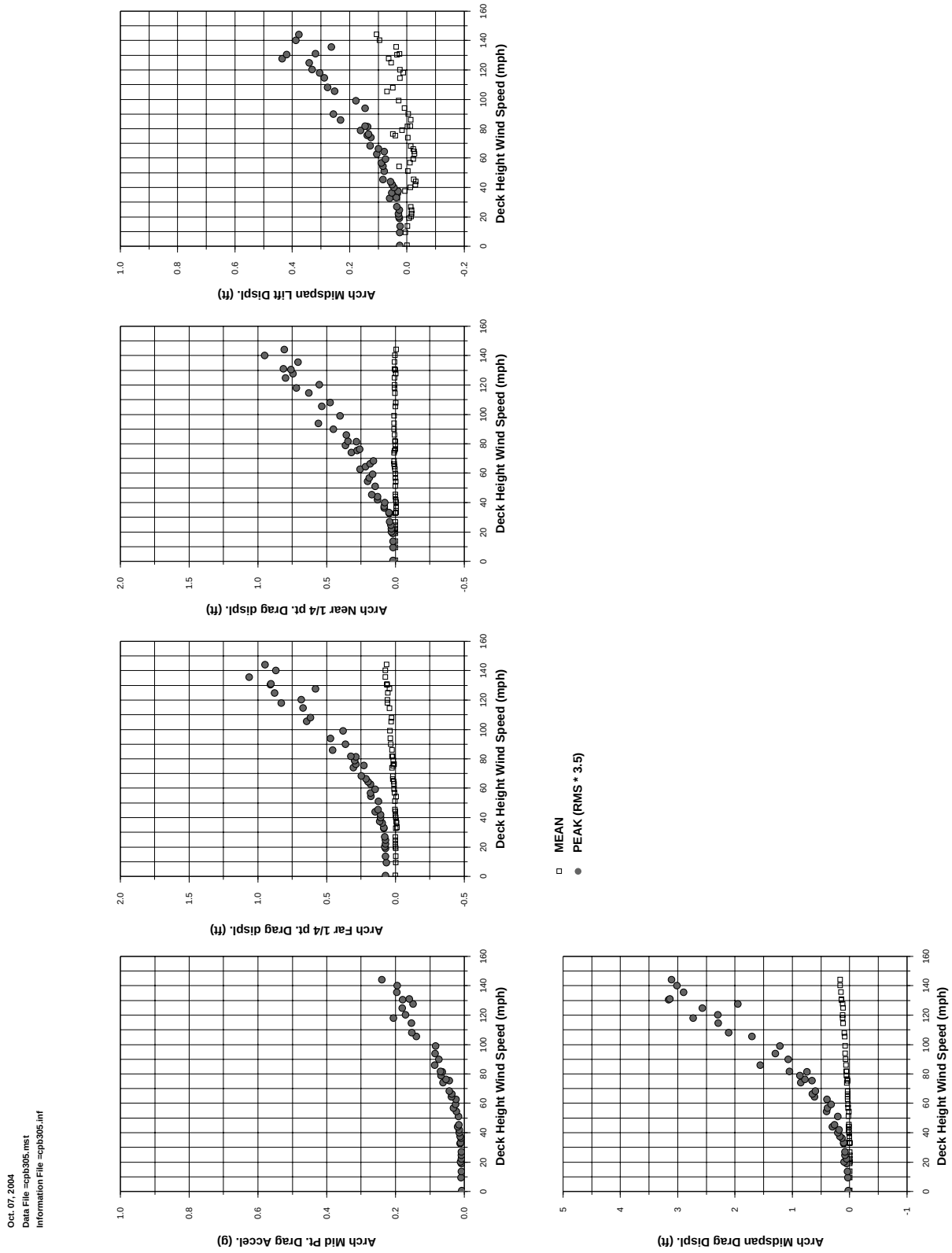

Indian River Bridge, Cantilevered Arch, open country profile, 0 degrees

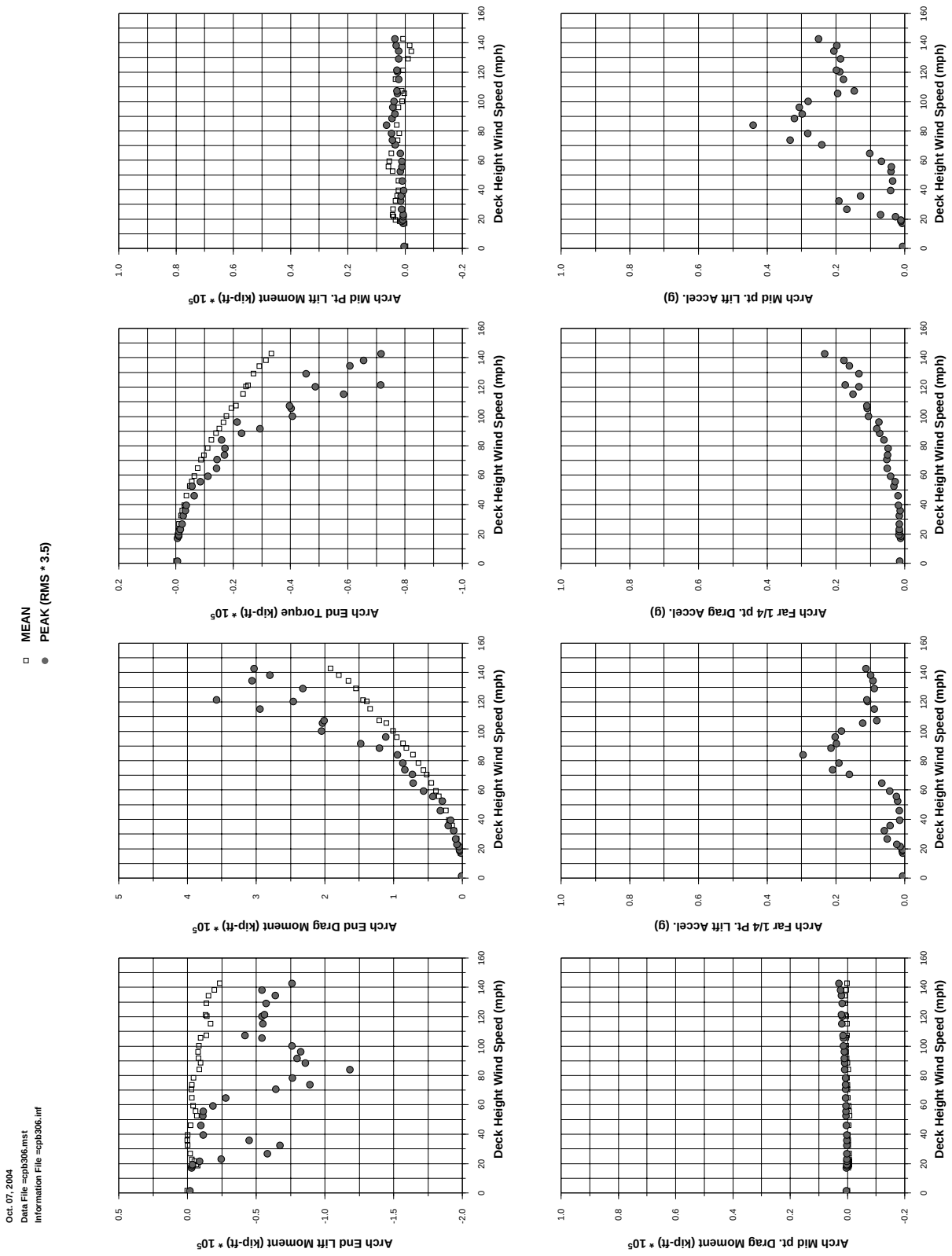

Indian River Bridge, Cantilevered Arch, open country profile, 90 degrees, without existing bridge, no crane on arch

Oct. 07, 2004
Data File =cpb306.mst
Information File =cpb306.inf

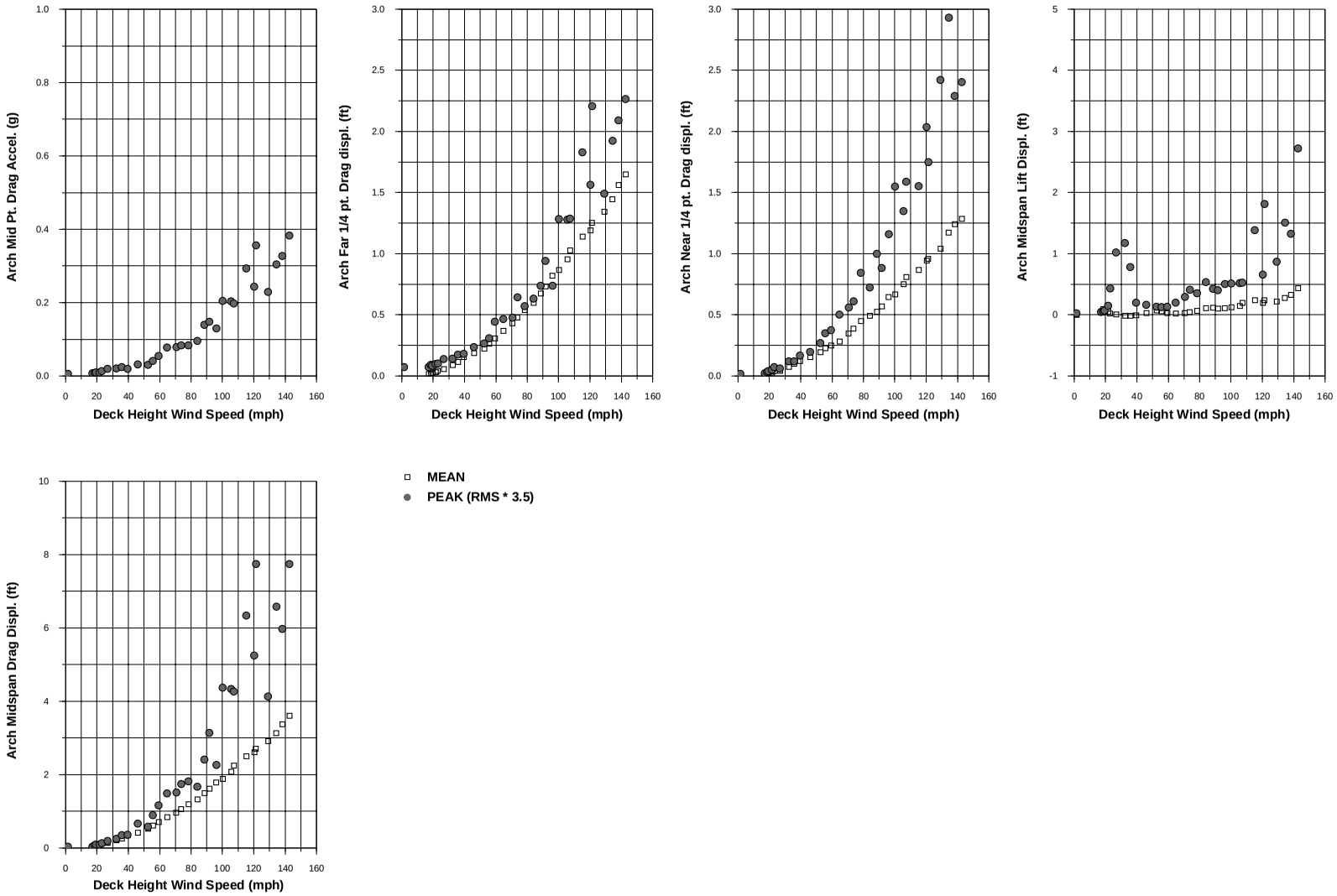

Indian River Bridge, Cantilevered Arch, open country profile, 90 degrees, without existing bridge, no crane on arch

APPENDIX K

RESULTS OF FULL BRIDGE AEROELASTIC TESTS, CONSTRUCTION STAGE – PRIOR TO DECK COMPLETION

Notes:

1. The bending moments given in the plots have the unit of kip-ft. The numbers read directly from the plots should be multiplied by 10^5 to obtain the actual bending moments in kip-ft. For example on page K6 of the Arch End Drag Moment (the lower right figure on that page), both the mean and peak drag moments at about 100mph are approximately 1.0×10^5 kip-ft (not 1.0 kip-ft).

2. The total response is equal to the mean, plus or minus the peak.

3. X is along the longitudinal direction, Y is the lateral direction (drag direction), and Z is the vertical direction (lift direction). Thus M_x is the torque, M_y is the lift moment (generated by the lift) and M_z is the drag moment (generated by the drag).

TABLE K1 INSTRUMENTATION LOCATIONS, CONSTRUCTION STAGE – PRIOR TO DECK COMPLETION

Instrumentation **x – longitudinal, y – lateral (Drag), z – vertical (Lift)**	**Instrumentation Locations** **(Refer to Figure K1)**
Strain Gages:	
M_x, M_y and M_z at **Deck** End (marked **A**)	Lift and Drag Moments, as well as Torque at 438ft from Midspan
M_x, M_y and M_z at **Deck** 1/4 Point (marked **B**)	Lift and Drag Moments, as well as Torque at 238ft from Midspan
M_x, M_y and M_z at **Arch** End (marked **D**)	Lift and Drag Moments, as well as Torque at 42ft from Arch-Deck connection
M_y and M_z at **Arch** Crown (marked **E**)	Lift and Drag Moments at 44ft from Arch Crown
Accelerometers:	
y, z and θ accel. at **Deck** Midspan (marked **C**)	Lift, Drag and Torsional Accelerations at Midspan
y, z and θ accel. at **Deck** 1/4 Point (marked **B**)	Lift, Drag and Torsional Accelerations at 225ft from Midspan
y and z accel. at **Arch** ¼ Point (marked **G**)	Lift and Drag Accelerations at about the ¼ point on the Arch (approximately 30ft closer to the arch crown than to the arch-deck connection)
y and z accel. at **Arch** Crown (marked **E**)	Lift and Drag Accelerations at 14ft from Arch Crown
Displacement Lasers:	
y, z and θ displacements at **Deck** Midspan (marked **C**)	Lift and Drag Displacements, as well as Deck Rotation at 12ft from Midspan
y, z and θ displacements at **Deck** 1/4 point (marked **B**)	Lift and Drag Displacements, as well as Deck Rotation at 225ft from Midspan
y, z and θ displacements at **Deck** other 1/4 point (marked **F**)	Lift and Drag Displacements, as well as Deck Rotation at 240ft from Midspan
y and z displacements at **Arch** Crown	Lift and Drag Displacements at 14ft from Arch Crown
Wind Speeds:	
Deck Level	Deck Height
Arch Level	Arch Crown Height

TABLE K2 SUMMARY OF TESTS, CONSTRUCTION STAGE – PRIOR TO DECK COMPLETION, INDIAN RIVER BRIDGE

Test File	Test No.	Flow condition	Existing bridge	Wind direction (Test angle)	V_{deck} (mph) Maximum wind speed at deck height	Vortex shedding peaks at wind speeds
CPD201	1	Hurricane profile	Yes	Perpendicular to bridge (90°)	139	50 mph
CPD202	2	Hurricane profile	No	Perpendicular to bridge (90°)	131	50 mph
CPD203	3	Hurricane profile	No	Along the Bridge (0°)	143	Not observed
CPD204	4	Hurricane profile	No	30° to the bridge	138	Not observed
CPD205	5	Hurricane profile	No	60° to the bridge	145	50 mph
CPD206	6	Hurricane profile	No	Perpendicular to bridge (270°)	139	Not observed
CPD301	7	Open Country profile	No	60° to the bridge	154	Not observed
CPD302	8	Open Country profile	No	30° to the bridge	154	Not observed
CPD303	9	Open Country profile	No	Along the Bridge (0°)	149	Not observed
CPD304	10	Open Country profile	No	Perpendicular to bridge (90°)	153	Not observed
CPD305	11	Open Country profile	Yes	Perpendicular to bridge (90°)	150	Not observed
CPD306	12	Open Country profile	No	Perpendicular to bridge (270°)	152	Not observed
CPD101	13	Smooth Flow	No	Perpendicular to bridge (90°)	185	50 mph

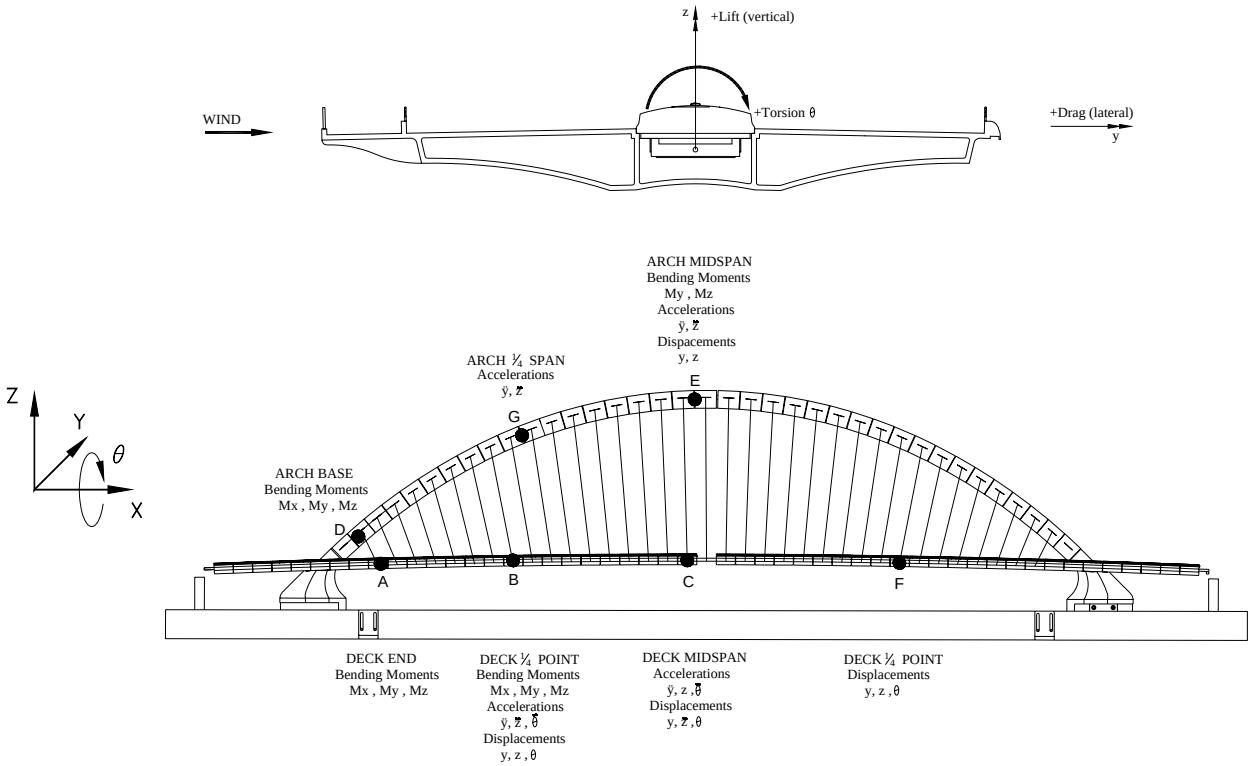

FIGURE K1 BRIDGE SIGN CONVENTION AND INSTRUMENTATION LOCATIONS, CONSTRUCTION STAGE – PRIOR TO DECK COMPLETION

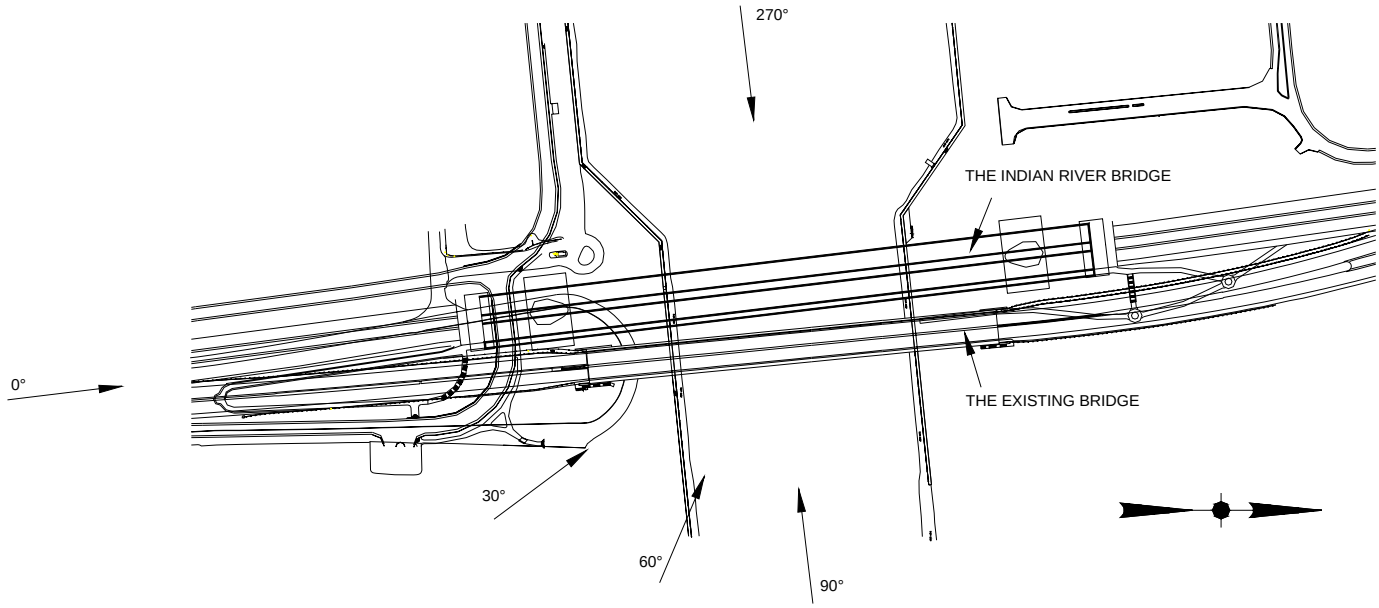

WIND DIRECTION DEFINITION

FIGURE K2 WIND ANGLES DEFINED IN WIND TUNNEL TESTS

Nov. 23, 2004
Data File =cpd201.mst
Information File =cpd201.inf

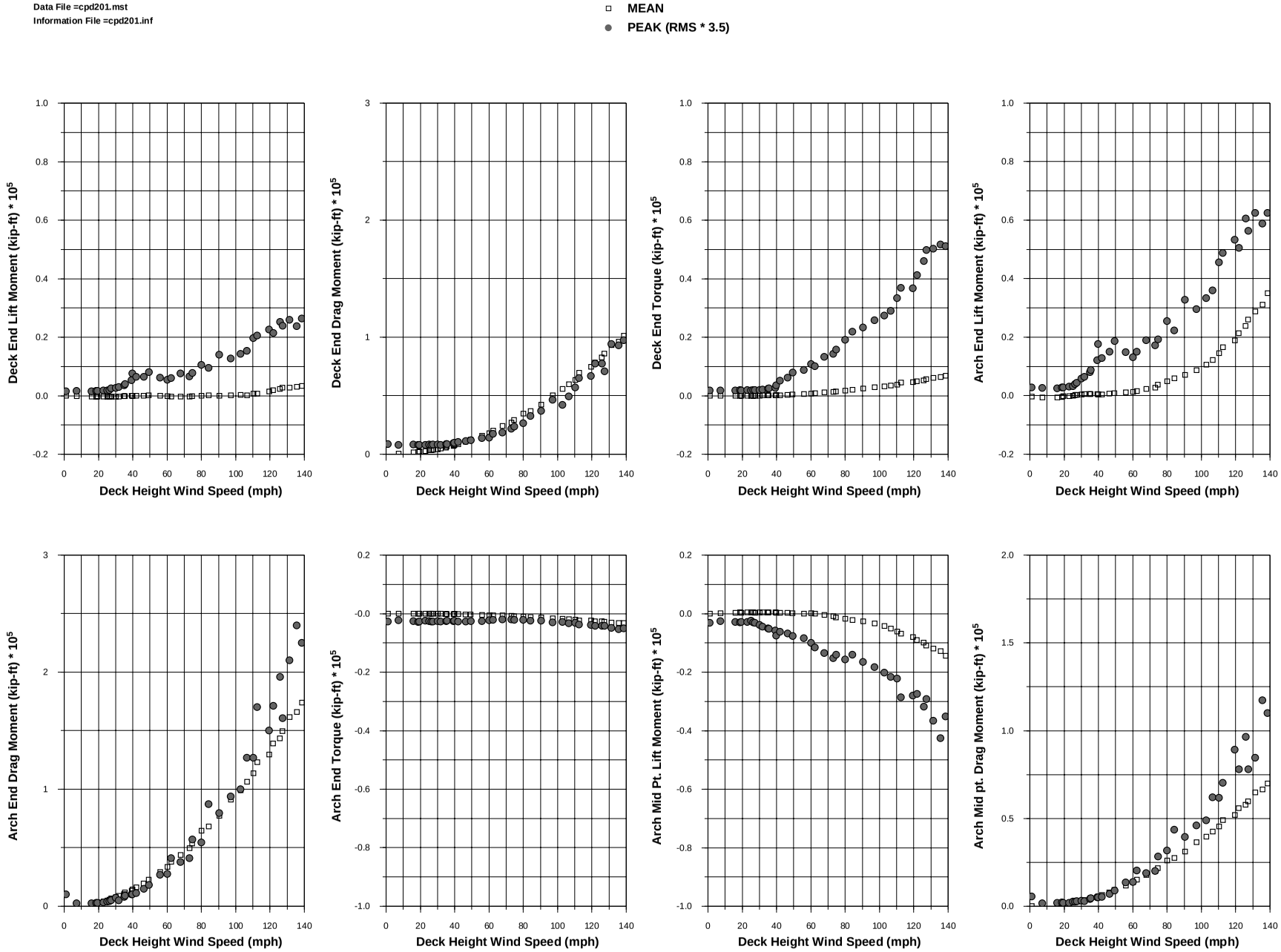

Indian River Bridge, Construction Stage Prior to deck completion, hurricane profile, 90 degrees, with existing bridge

Nov. 23, 2004
Data File =cpd201.mst
Information File =cpd201.inf

MEAN
PEAK (RMS * 3.5)

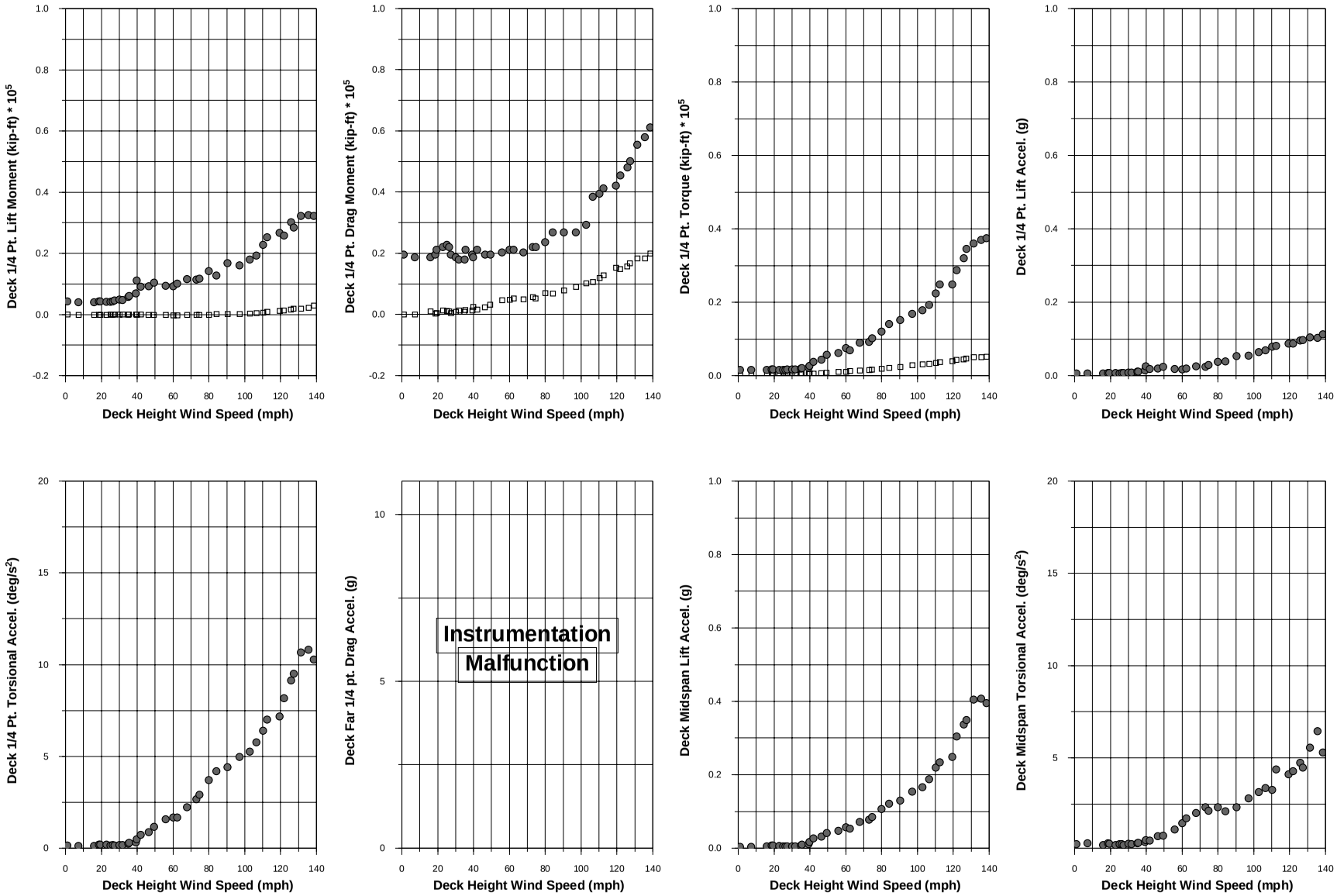

Indian River Bridge, Construction Stage Prior to deck completion, hurricane profile, 90 degrees, with existing bridge

Nov. 23, 2004
Data File =cpd201.mst
Information File =cpd201.inf

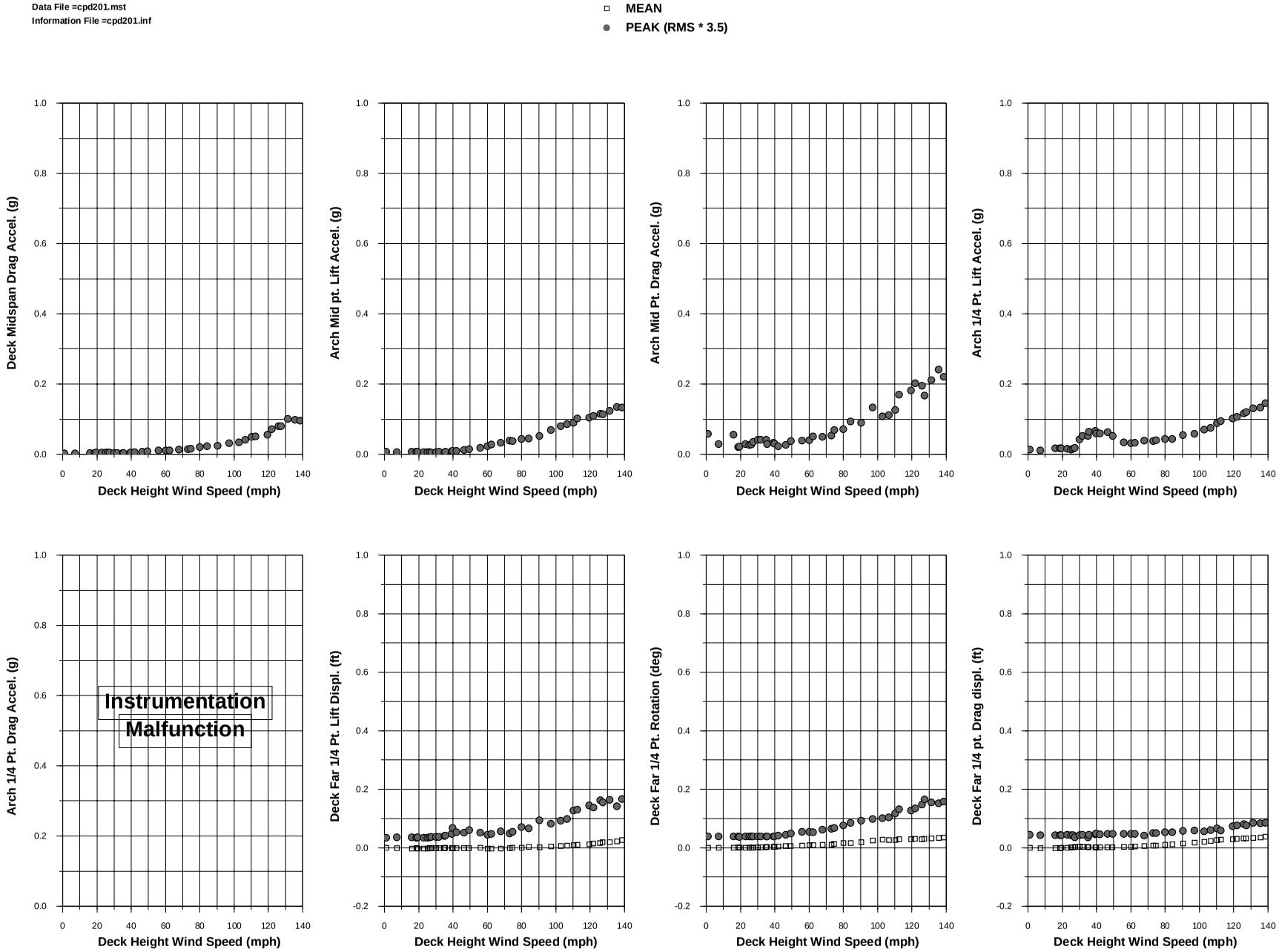

Indian River Bridge, Construction Stage Prior to deck completion, hurricane profile, 90 degrees, with existing bridge

Nov. 23, 2004
Data File =cpd201.mst
Information File =cpd201.inf

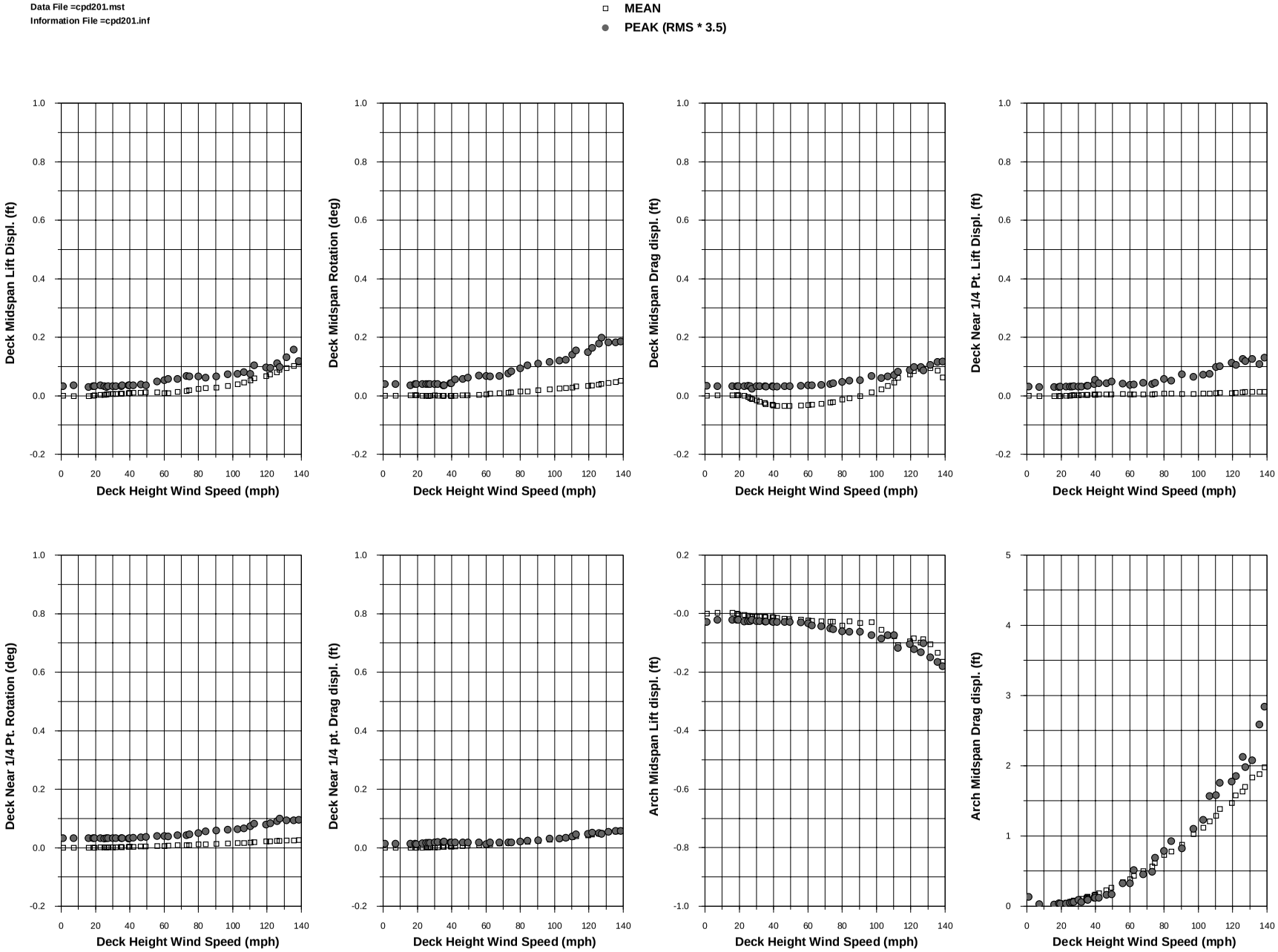

Indian River Bridge, Construction Stage Prior to deck completion, hurricane profile, 90 degrees, with existing bridge

Nov. 23, 2004
Data File =cpd202.mst
Information File =cpd202.inf

MEAN
PEAK (RMS * 3.5)

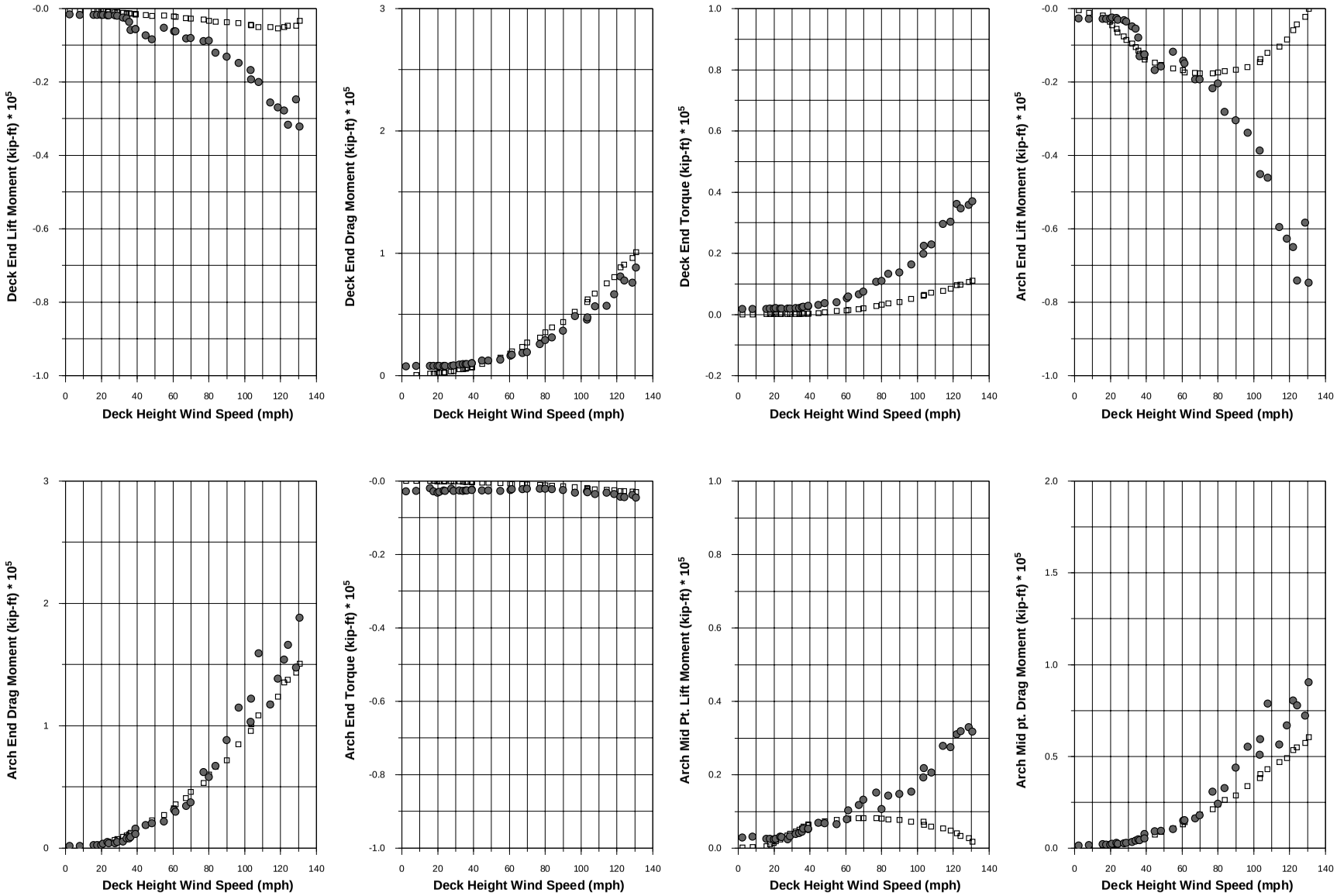

Indian River Bridge, construction stage prior to deck completion, hurricane profile, 90 degrees, without existing bridge

Nov. 23, 2004
Data File =cpd202.mst
Information File =cpd202.inf

MEAN
PEAK (RMS * 3.5)

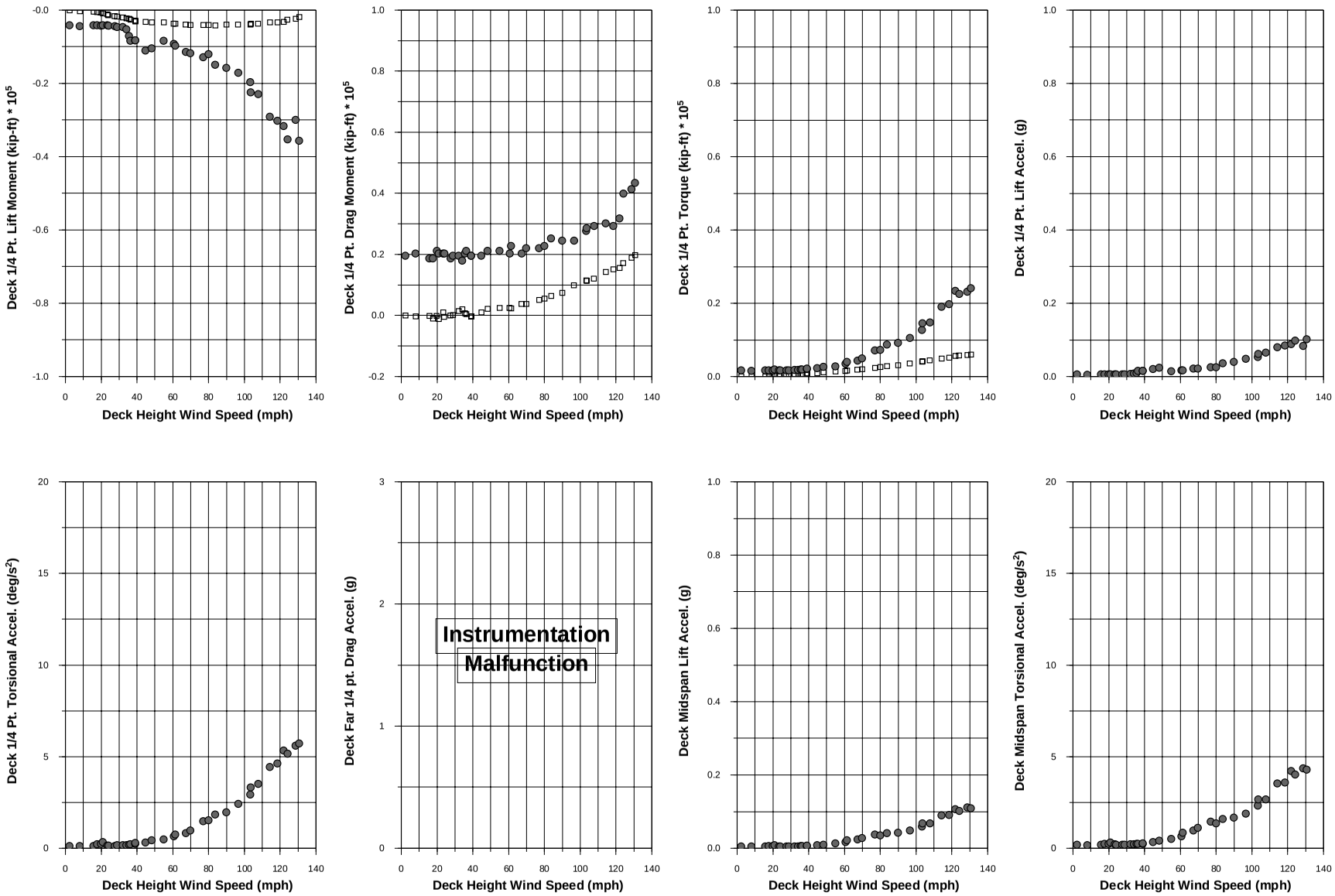

Indian River Bridge, construction stage prior to deck completion, hurricane profile, 90 degrees, without existing bridge

Nov. 23, 2004
Data File =cpd202.mst
Information File =cpd202.inf

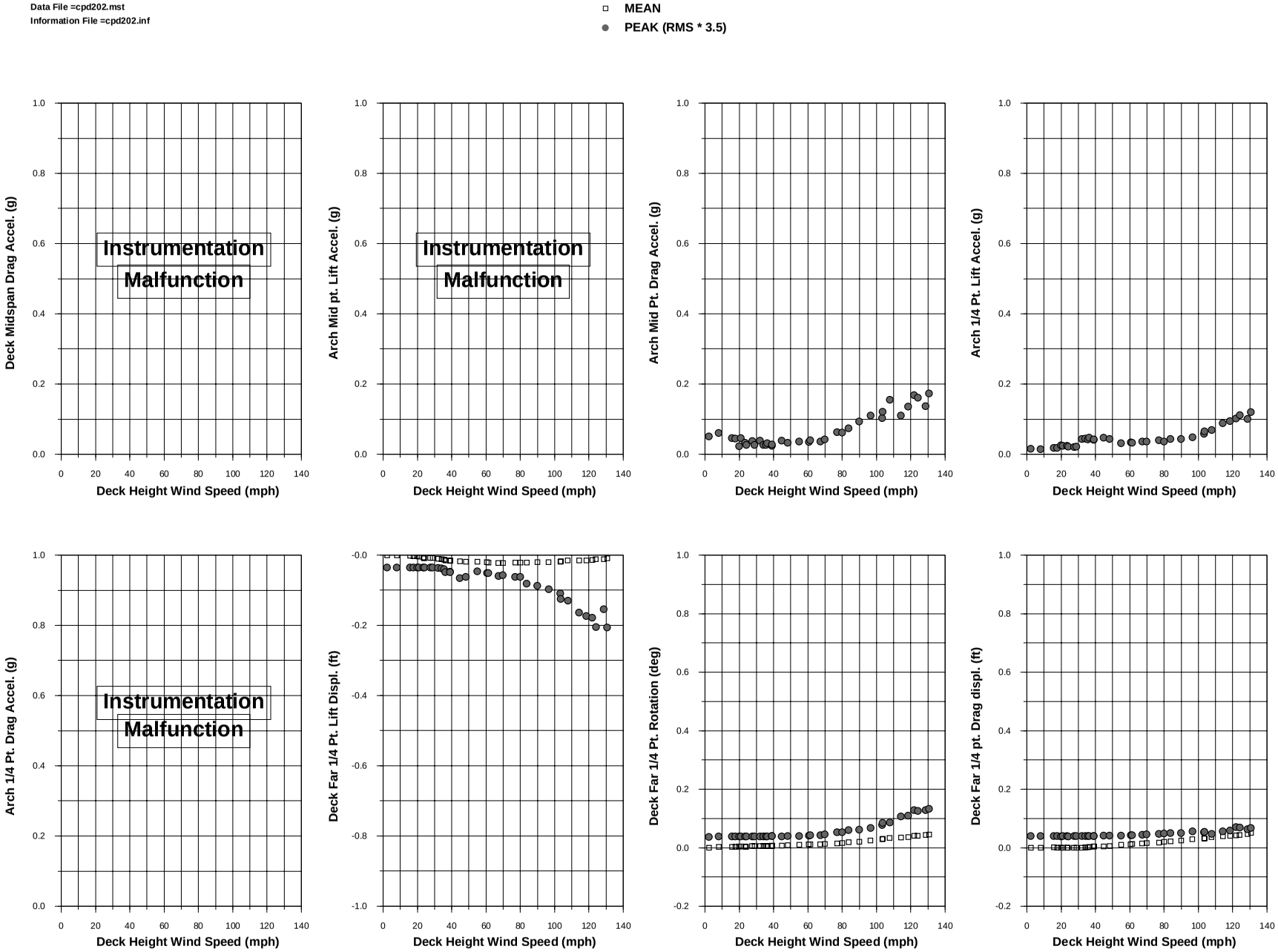

Indian River Bridge, construction stage prior to deck completion, hurricane profile, 90 degrees, without existing bridge

Nov. 23, 2004
Data File =cpd202.mst
Information File =cpd202.inf

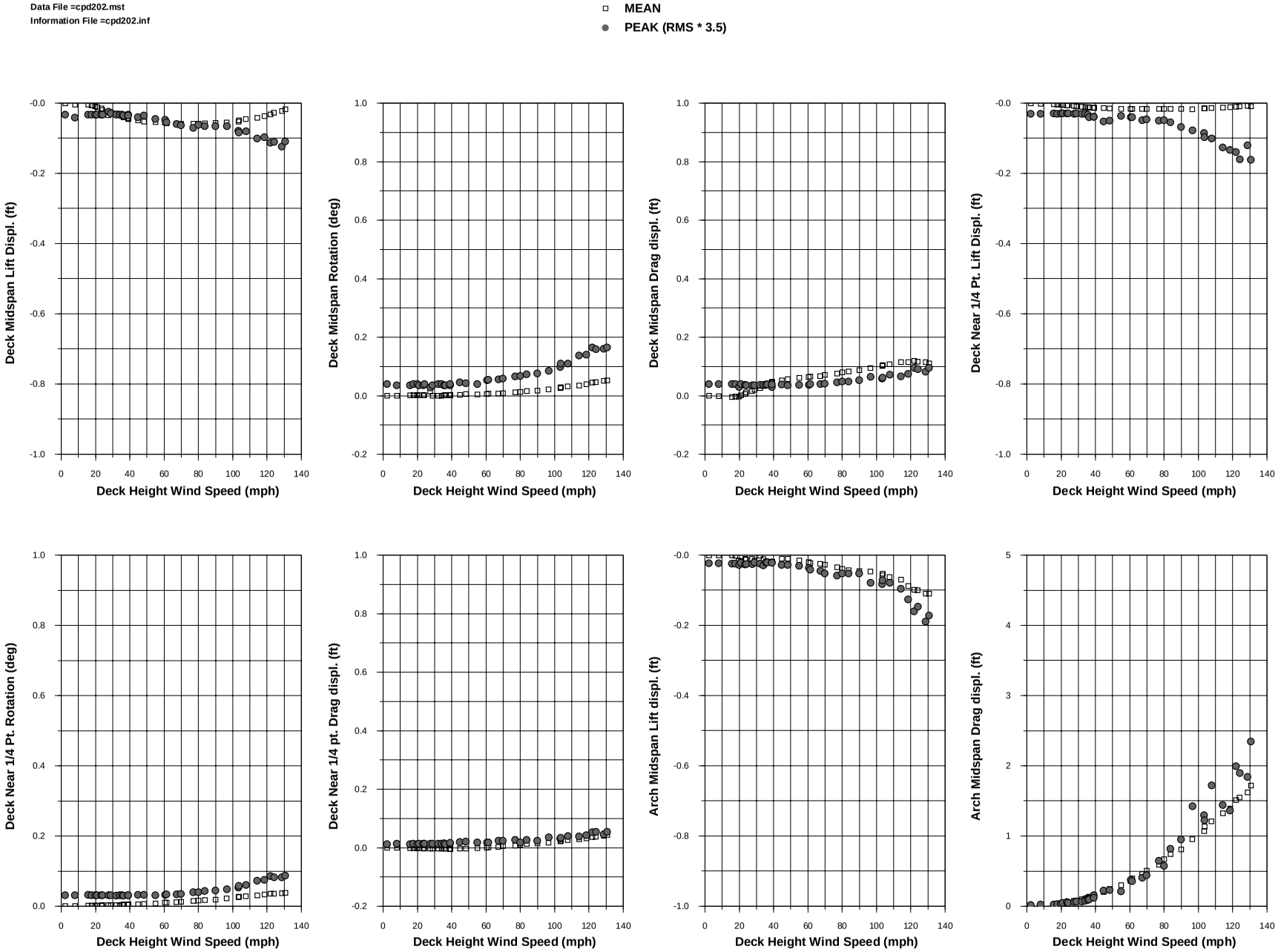

Indian River Bridge, construction stage prior to deck completion, hurricane profile, 90 degrees, without existing bridge

Nov. 23, 2004
Data File =cpd203.mst
Information File =cpd203.inf

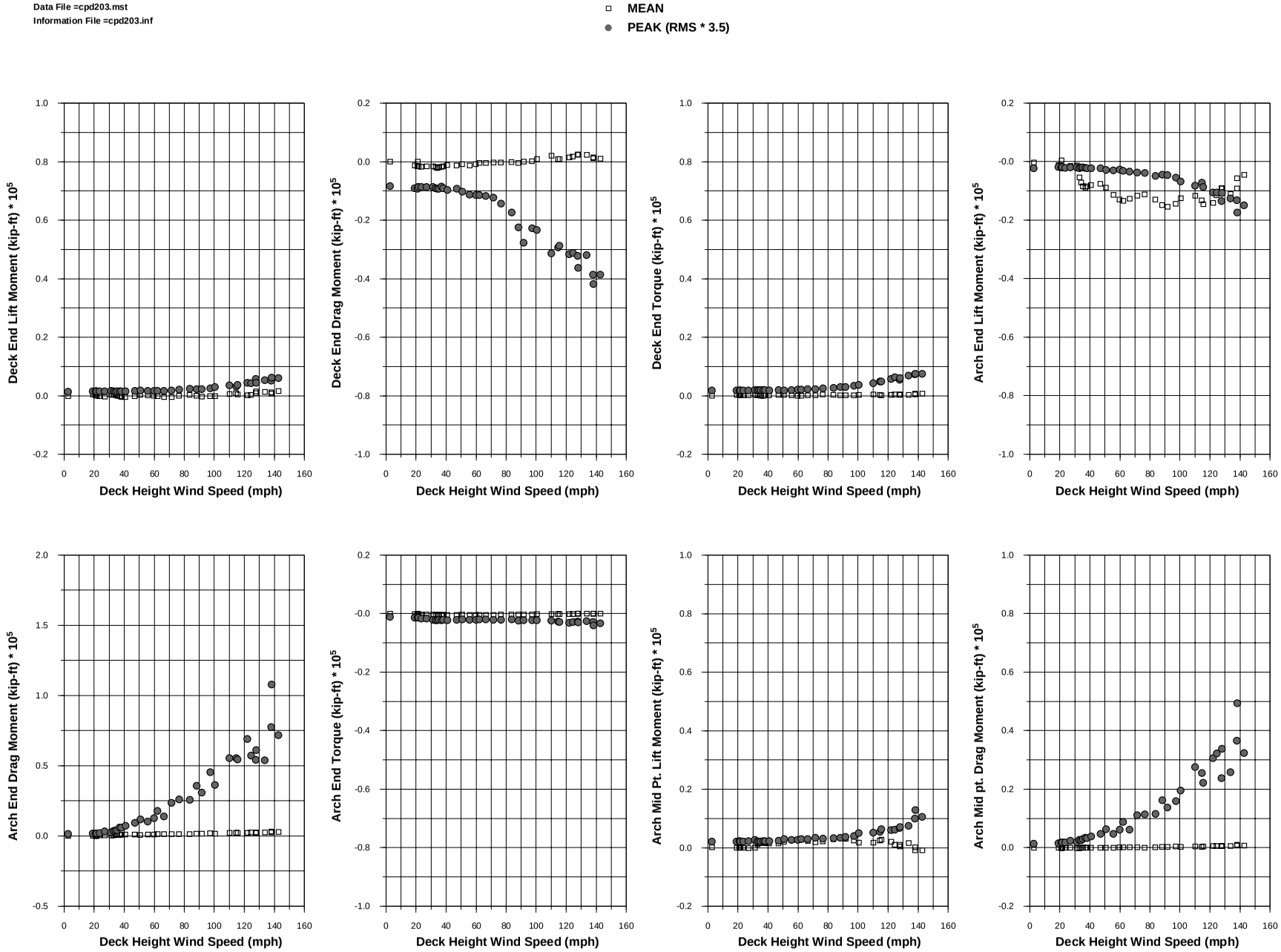

Indian River Bridge, construction stage prior to deck completion, hurricane profile, 0 degrees (along bridge)

Nov. 23, 2004
Data File =cpd203.mst
Information File =cpd203.inf

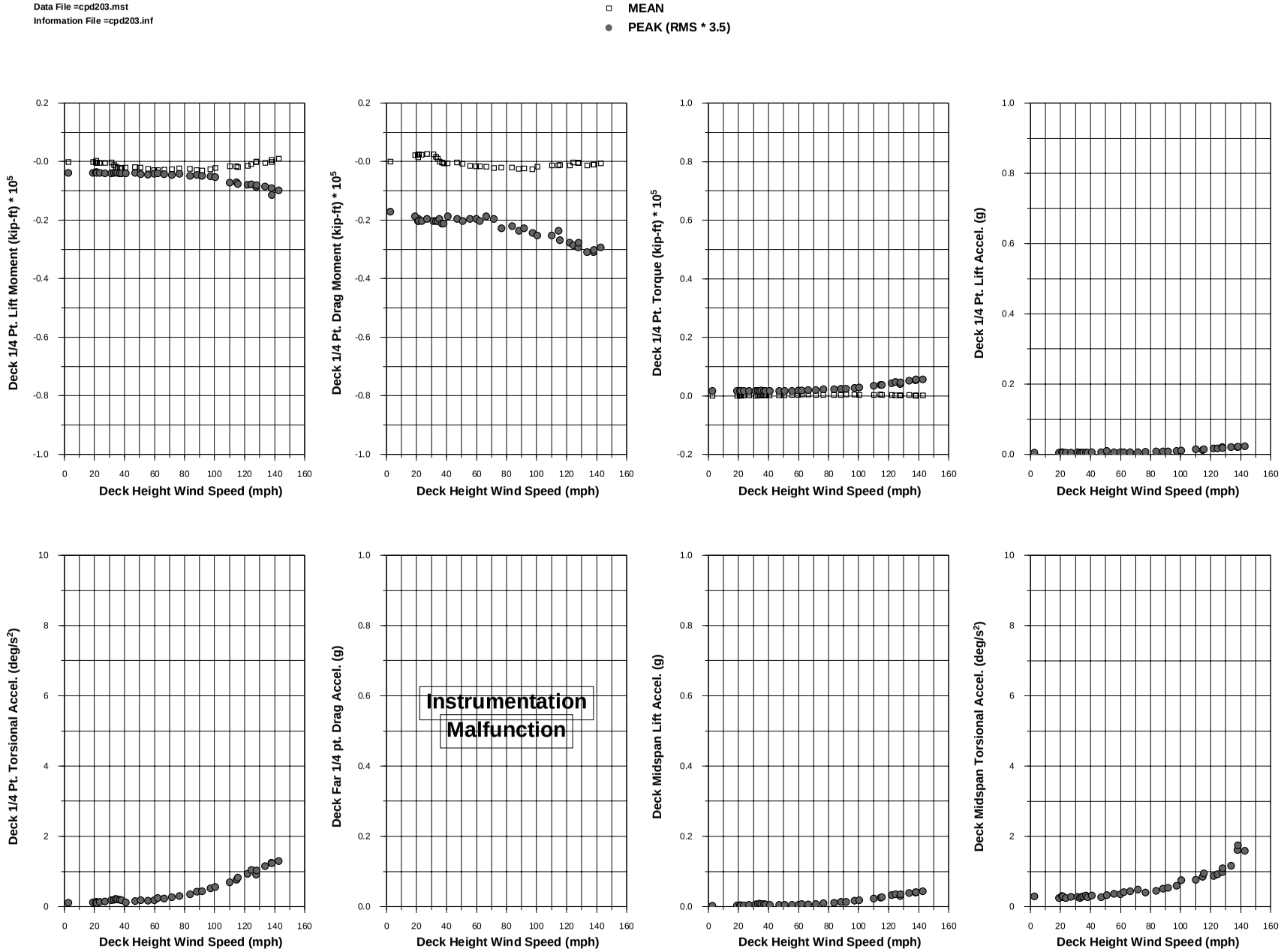

Indian River Bridge, construction stage prior to deck completion, hurricane profile, 0 degrees (along bridge)

Nov. 23, 2004
Data File =cpd203.mst
Information File =cpd203.inf

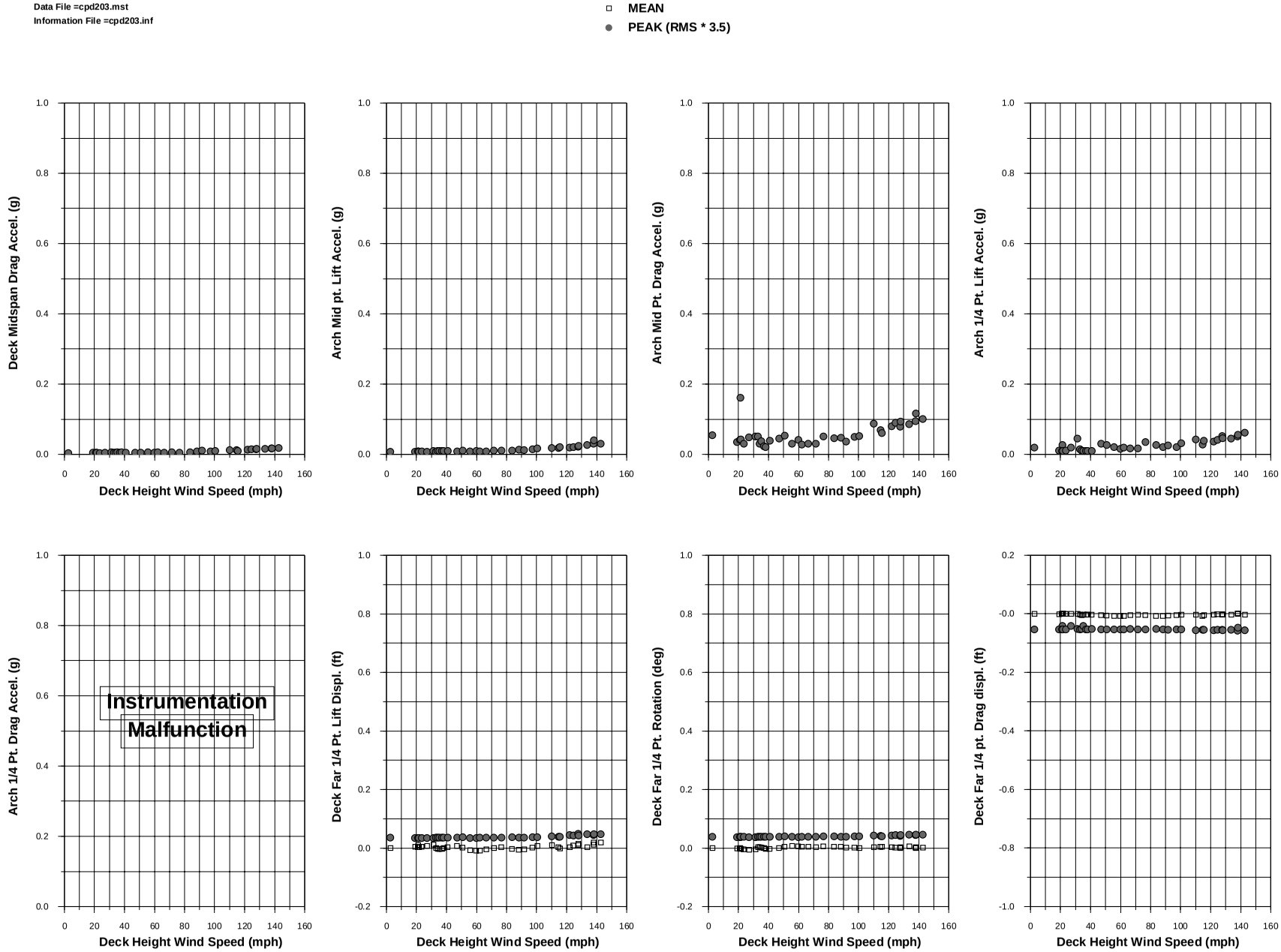

Indian River Bridge, construction stage prior to deck completion, hurricane profile, 0 degrees (along bridge)

Nov. 23, 2004
Data File =cpd203.mst
Information File =cpd203.inf

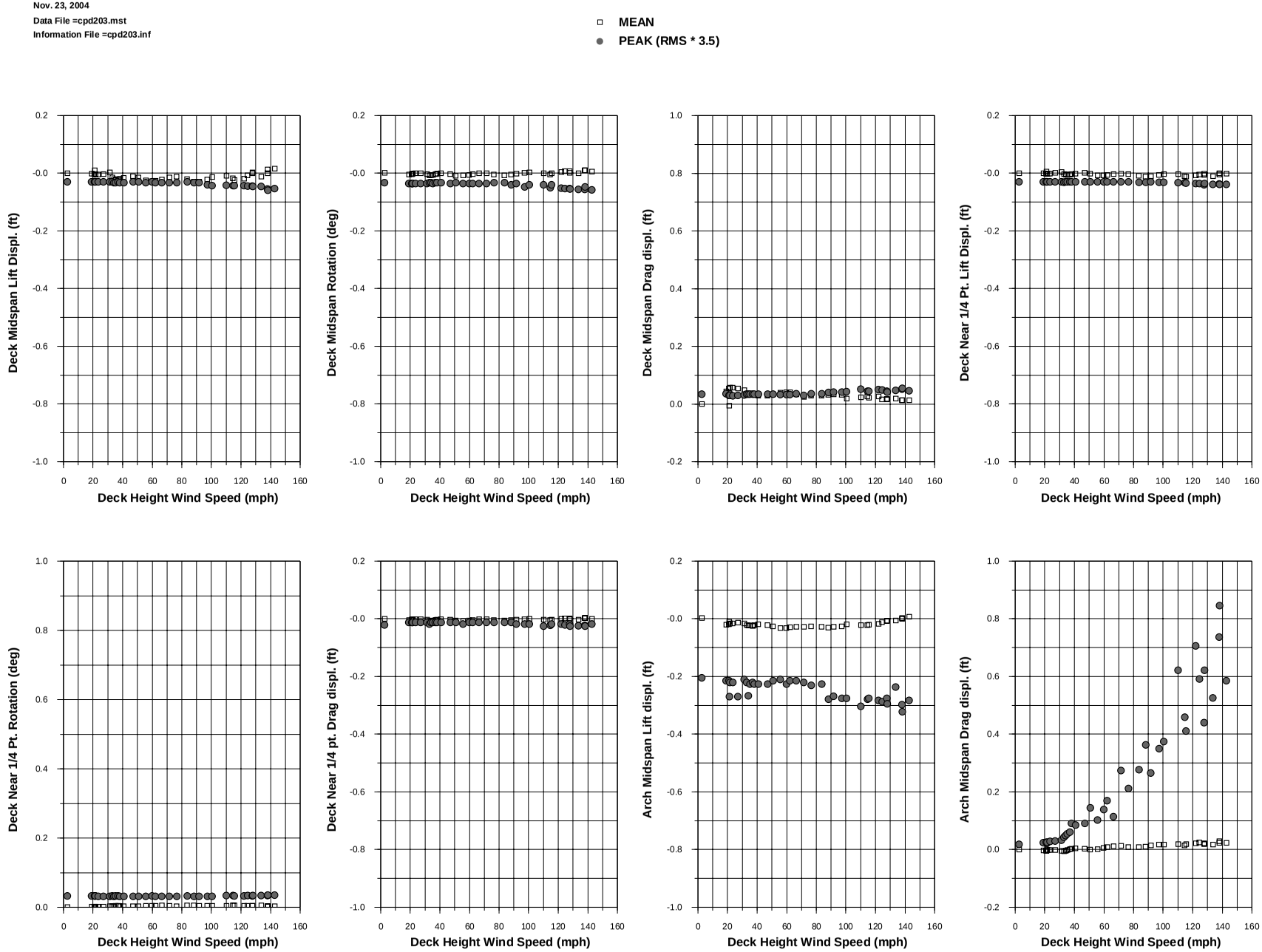

Indian River Bridge, construction stage prior to deck completion, hurricane profile, 0 degrees (along bridge)

Nov. 24, 2004
Data File =cpd204.mst
Information File =cpd204.inf

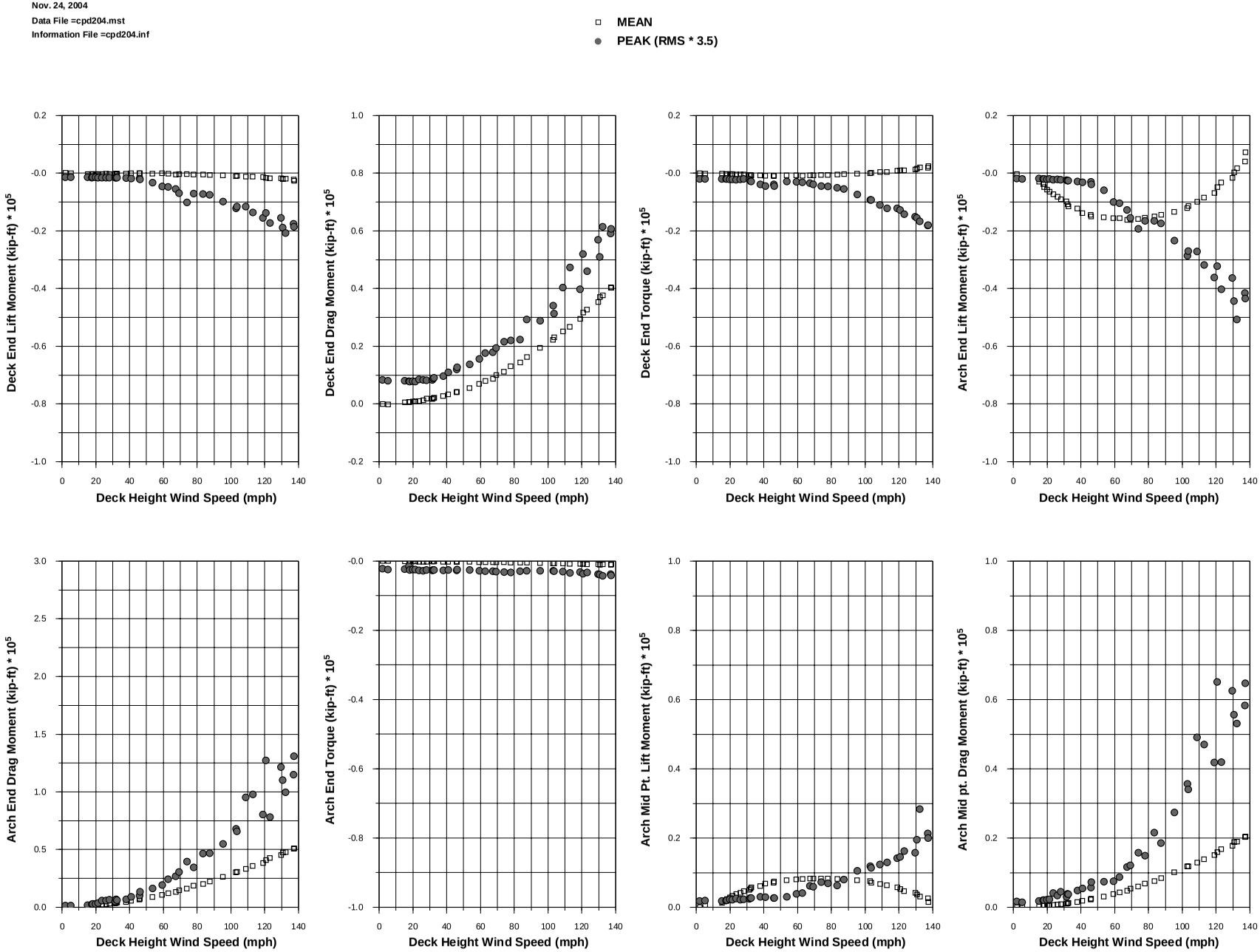

Indian River Bridge, construction stage prior to deck completion, hurricane profile, 30 degrees

Nov. 24, 2004
Data File =cpd204.mst
Information File =cpd204.inf

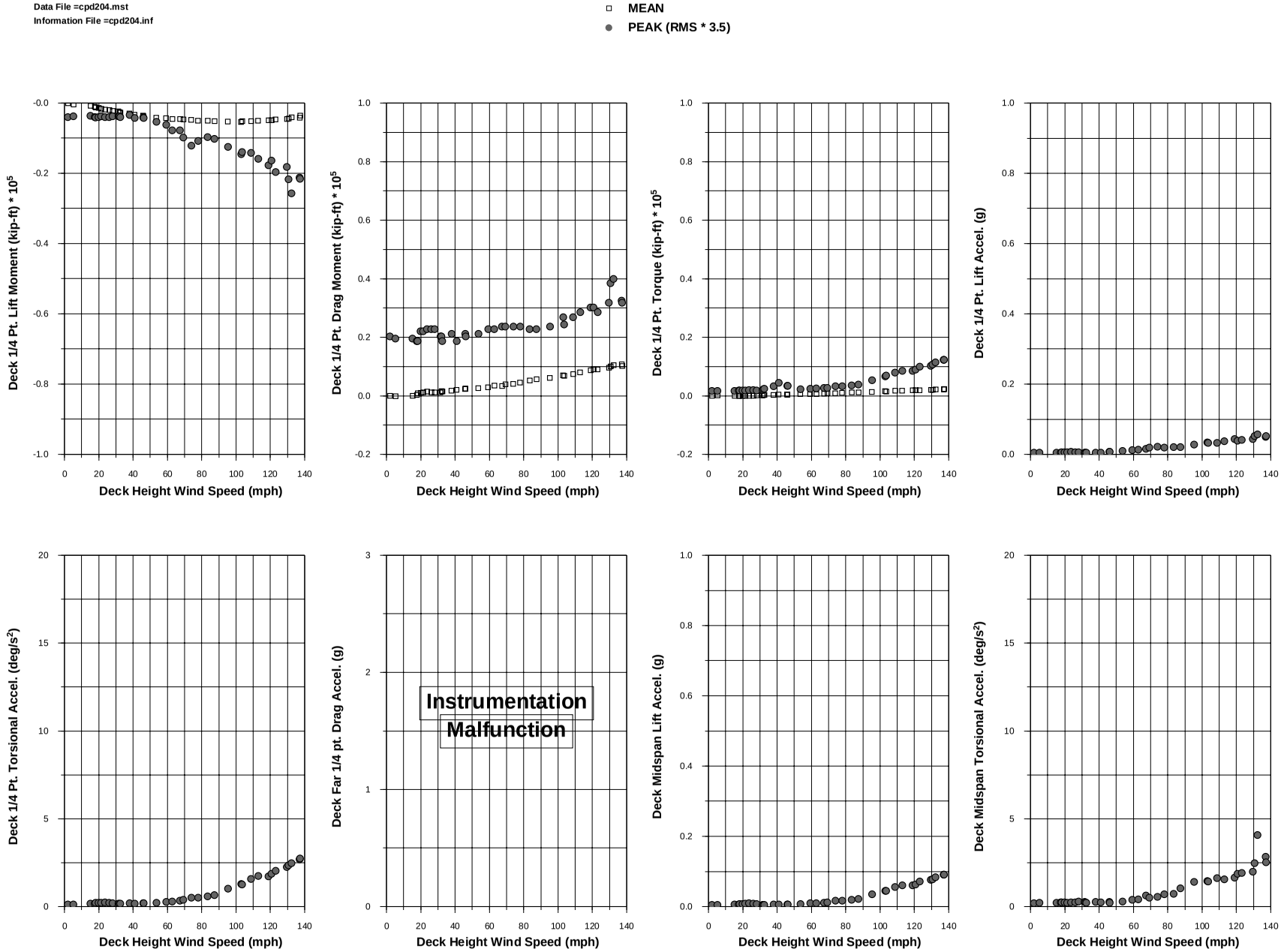

Indian River Bridge, construction stage prior to deck completion, hurricane profile, 30 degrees

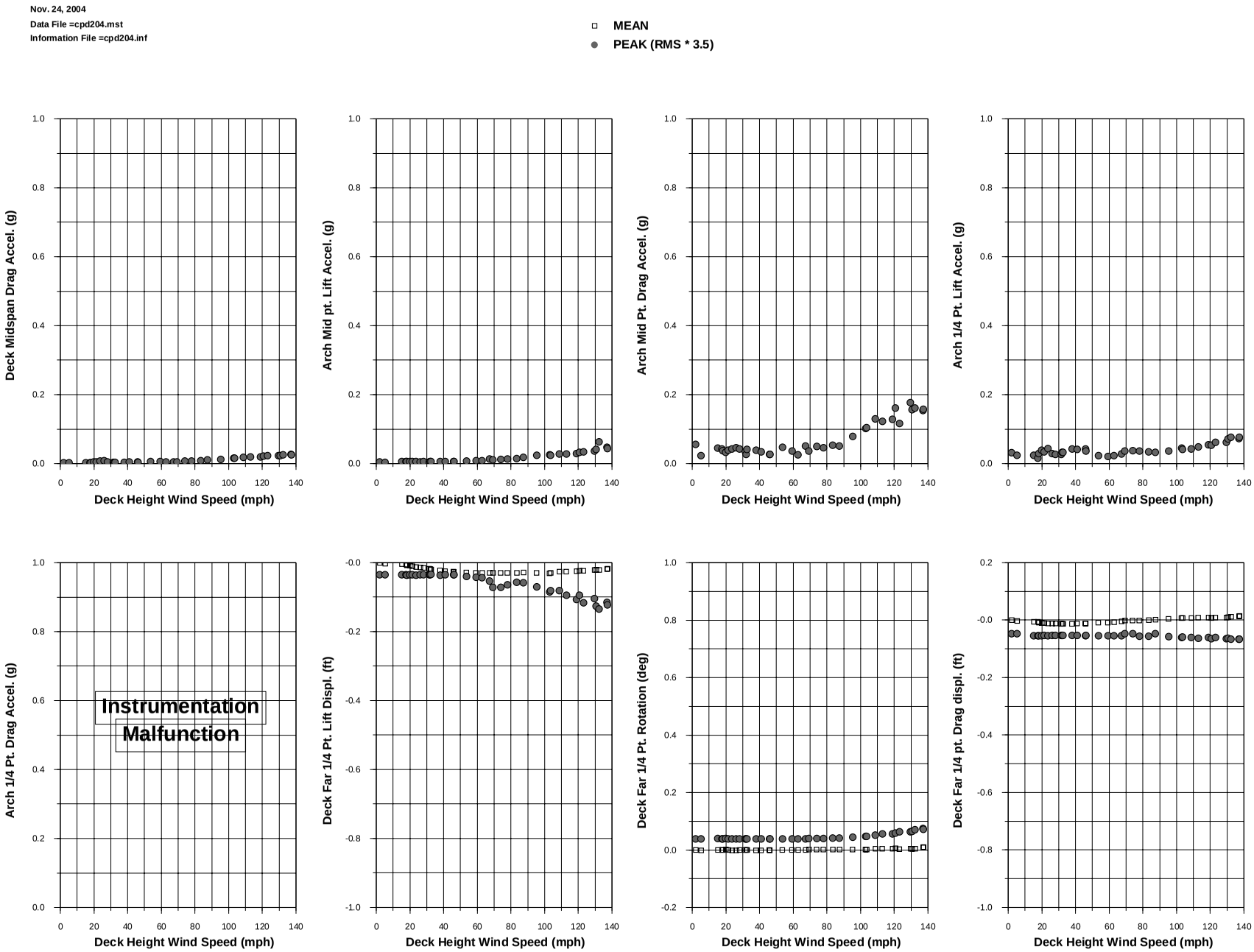

Indian River Bridge, construction stage prior to deck completion, hurricane profile, 30 degrees

Nov. 24, 2004
Data File =cpd204.mst
Information File =cpd204.inf

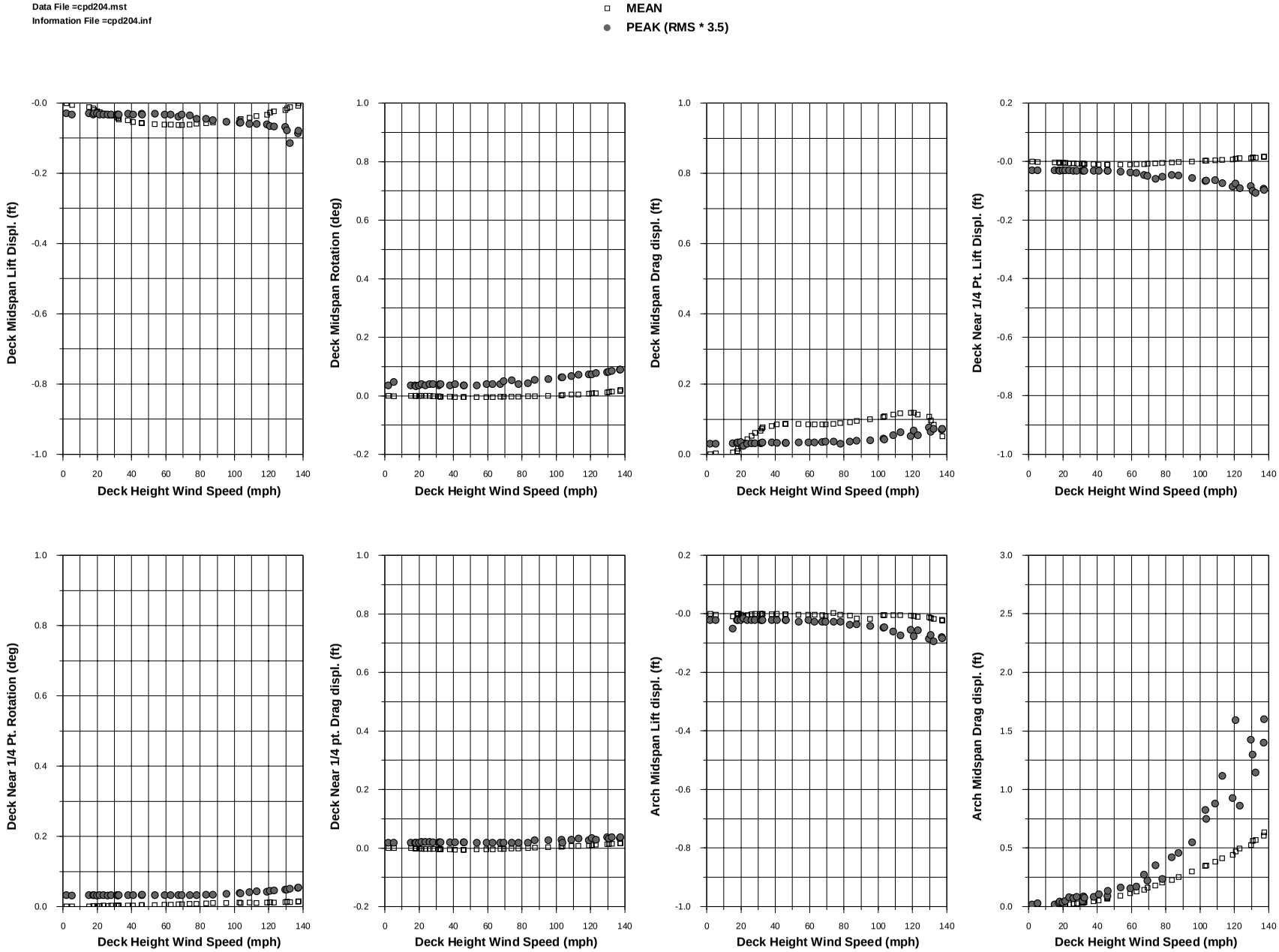

Indian River Bridge, construction stage prior to deck completion, hurricane profile, 30 degrees

Nov. 24, 2004
Data File =cpd205.mst
Information File =cpd205.inf

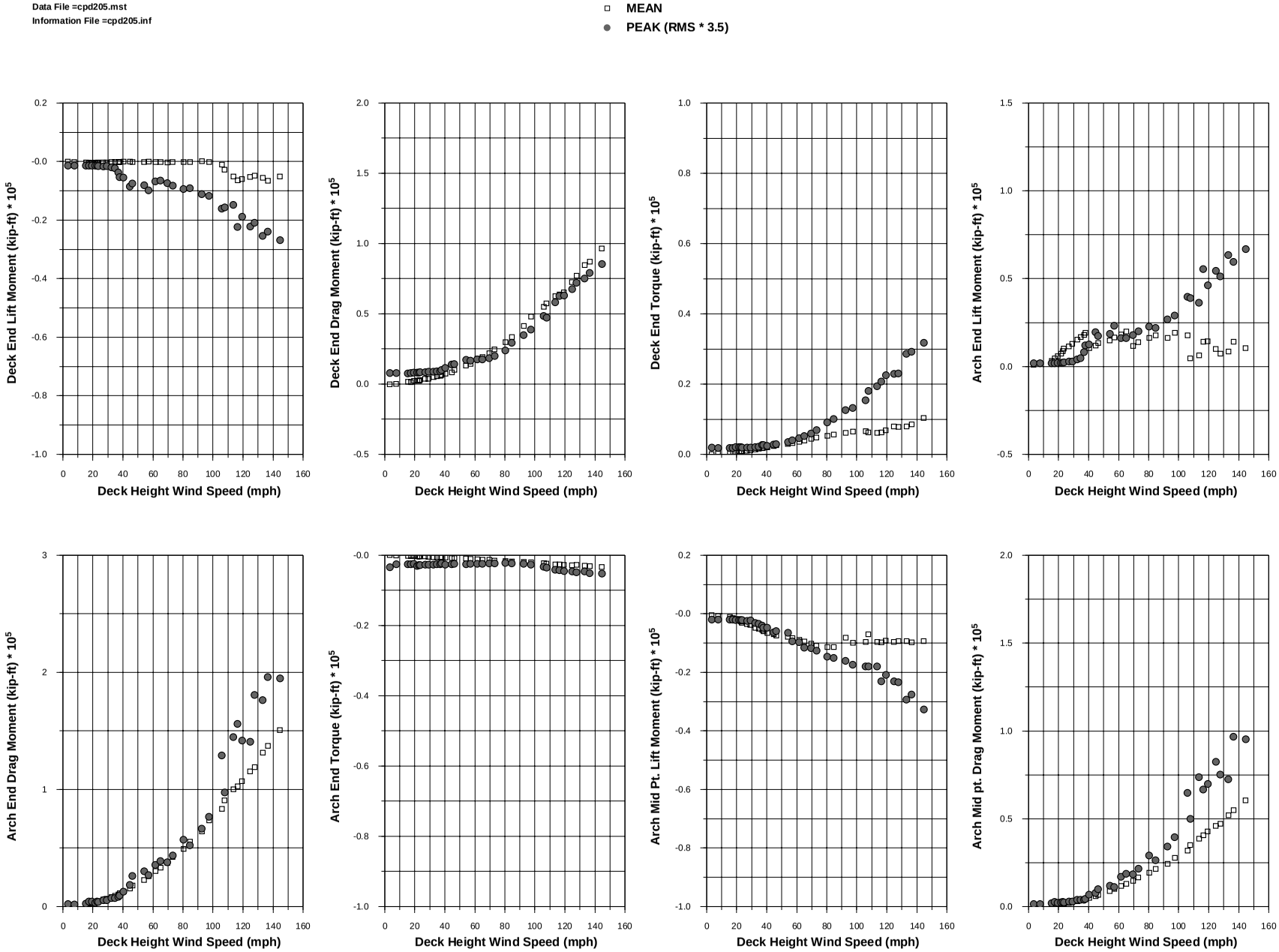

Indian River Bridge, construction stage prior to deck completion, hurricane profile, 60 degrees

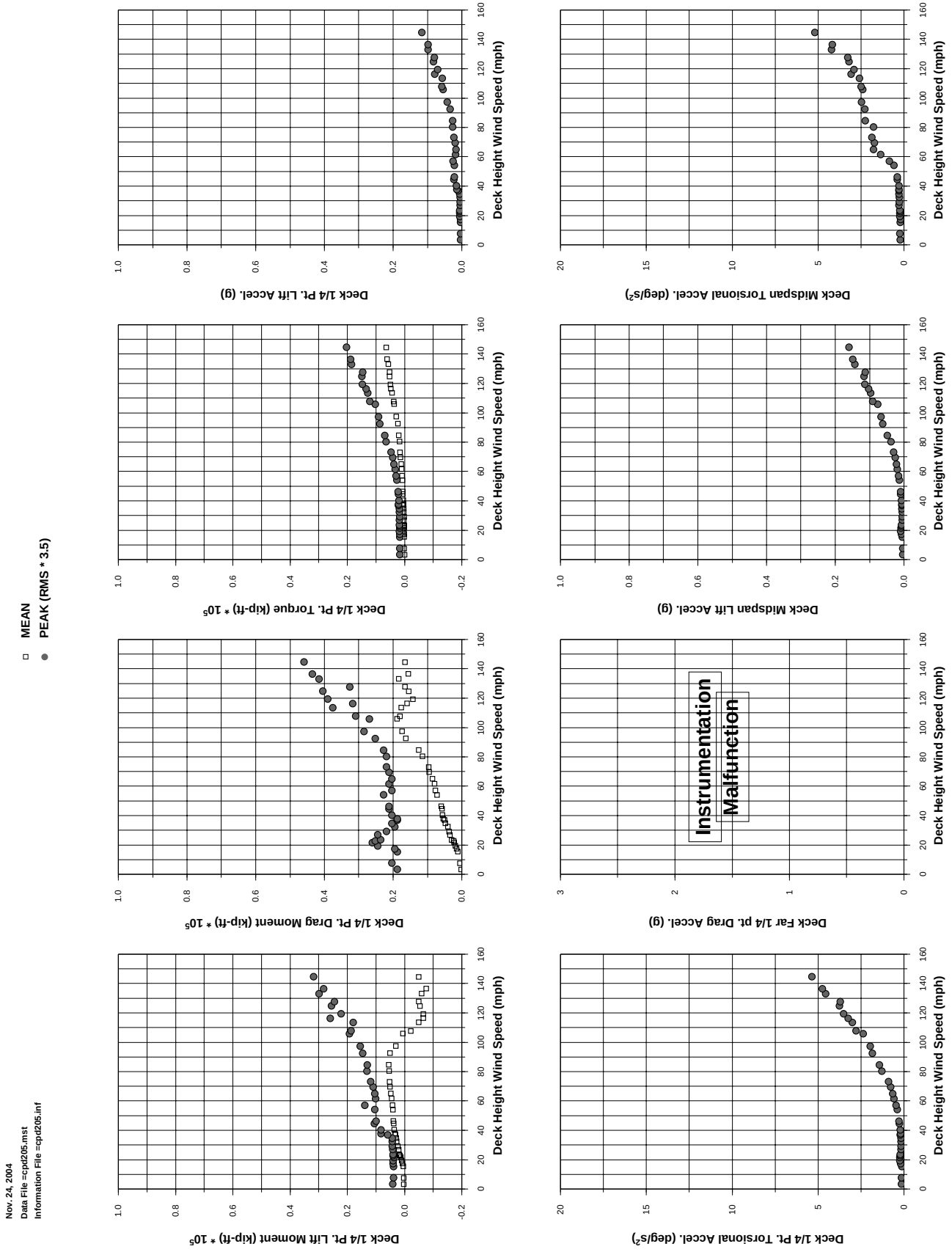

Indian River Bridge, construction stage prior to deck completion, hurricane profile, 60 degrees

Nov. 24, 2004
Data File =cpd205.mst
Information File =cpd205.inf

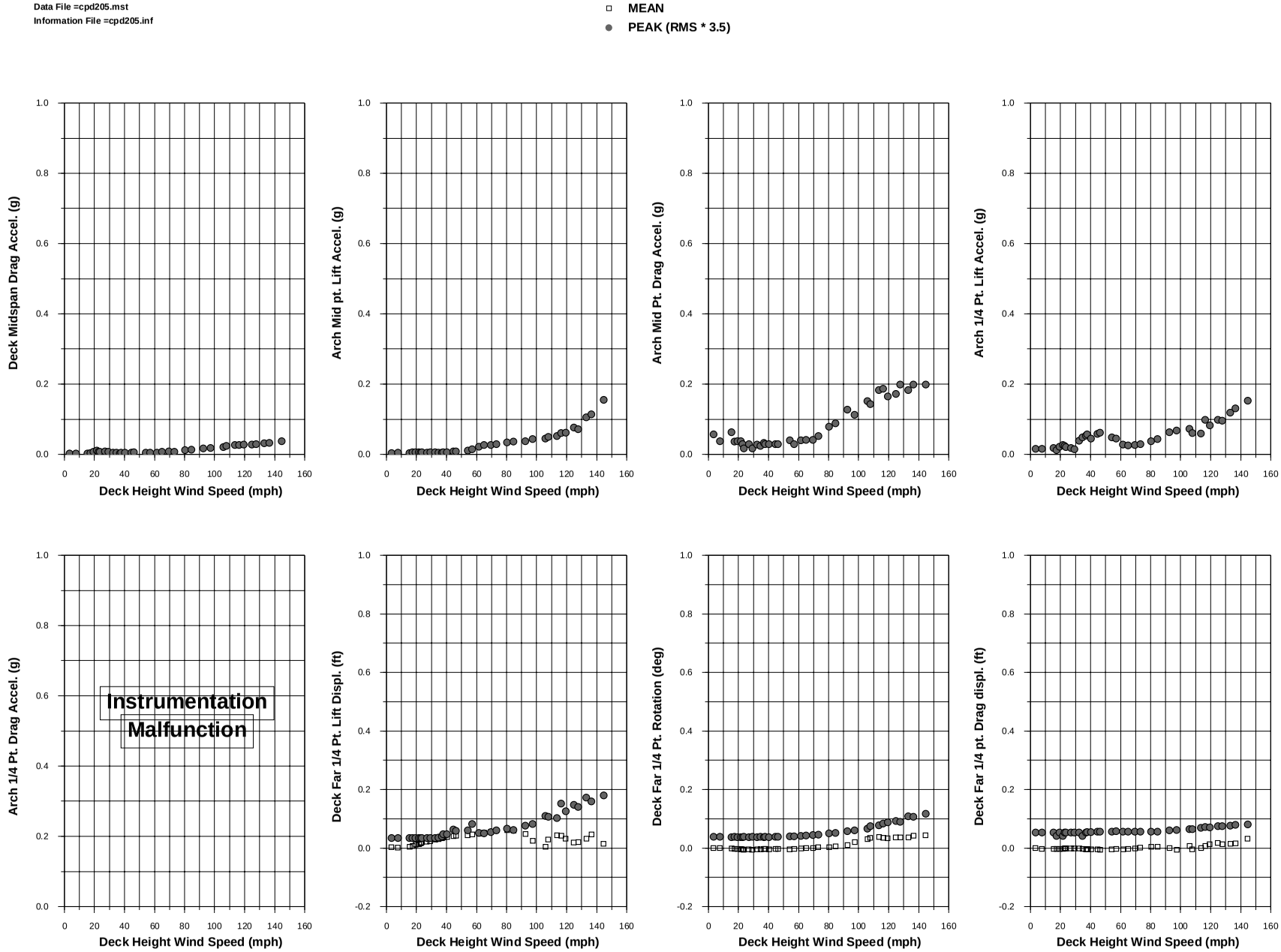

Indian River Bridge, construction stage prior to deck completion, hurricane profile, 60 degrees

Nov. 24, 2004
Data File =cpd205.mst
Information File =cpd205.inf

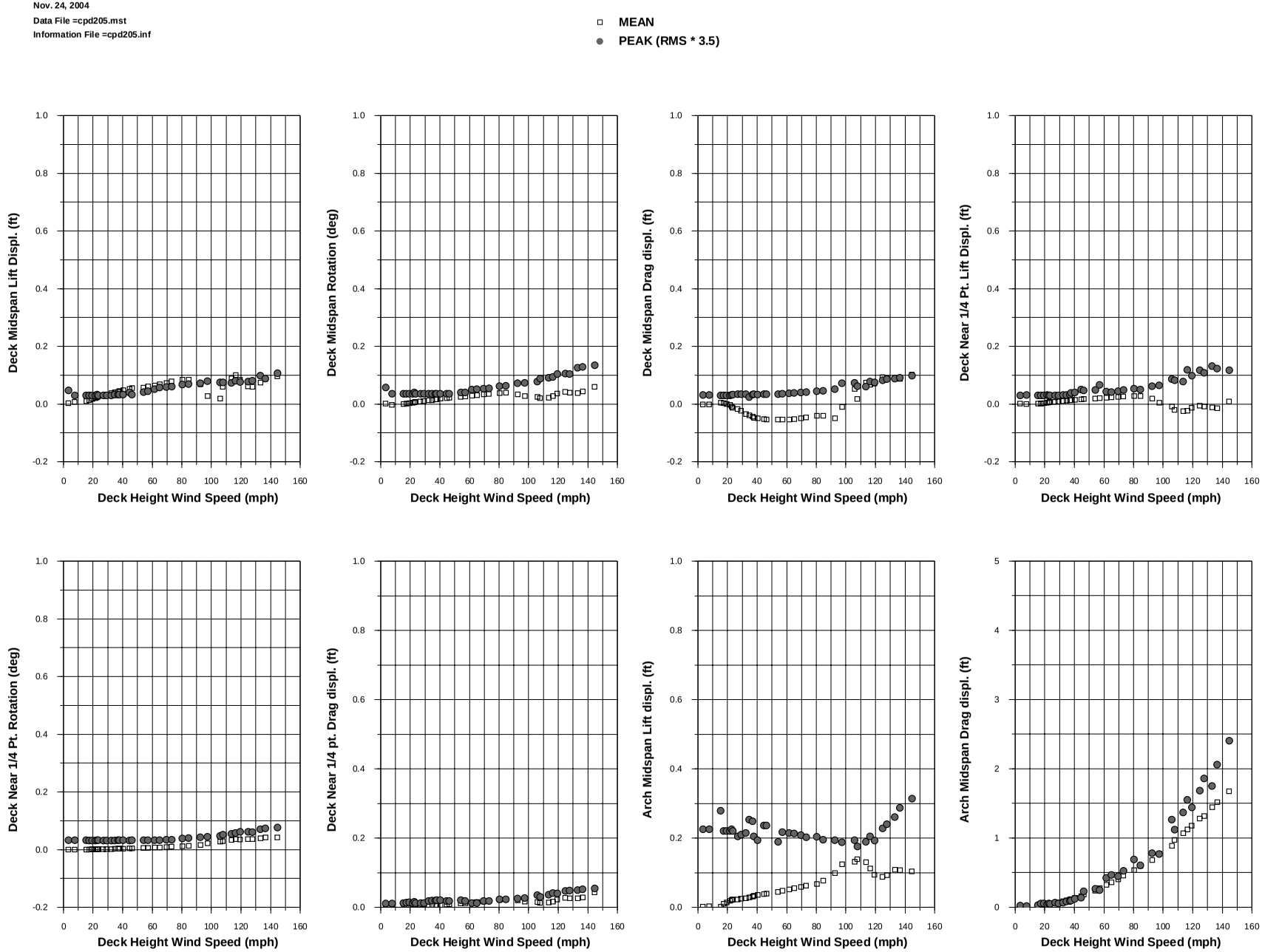

Indian River Bridge, construction stage prior to deck completion, hurricane profile, 60 degrees

Nov. 24, 2004
Data File =cpd206.mst
Information File =cpd206.inf

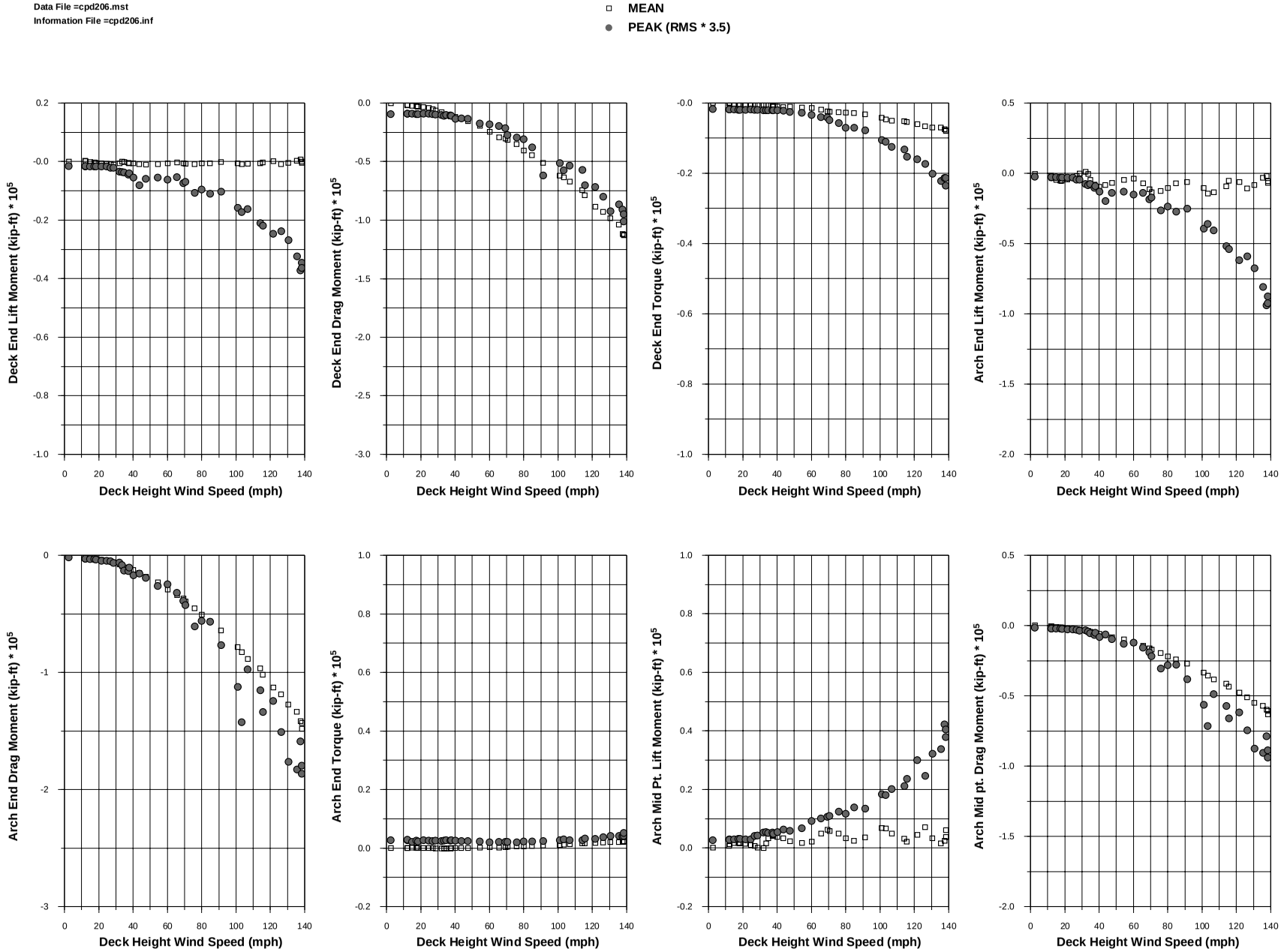

Indian River Bridge, construction stage prior to deck completion, hurricane profile, 270 degrees

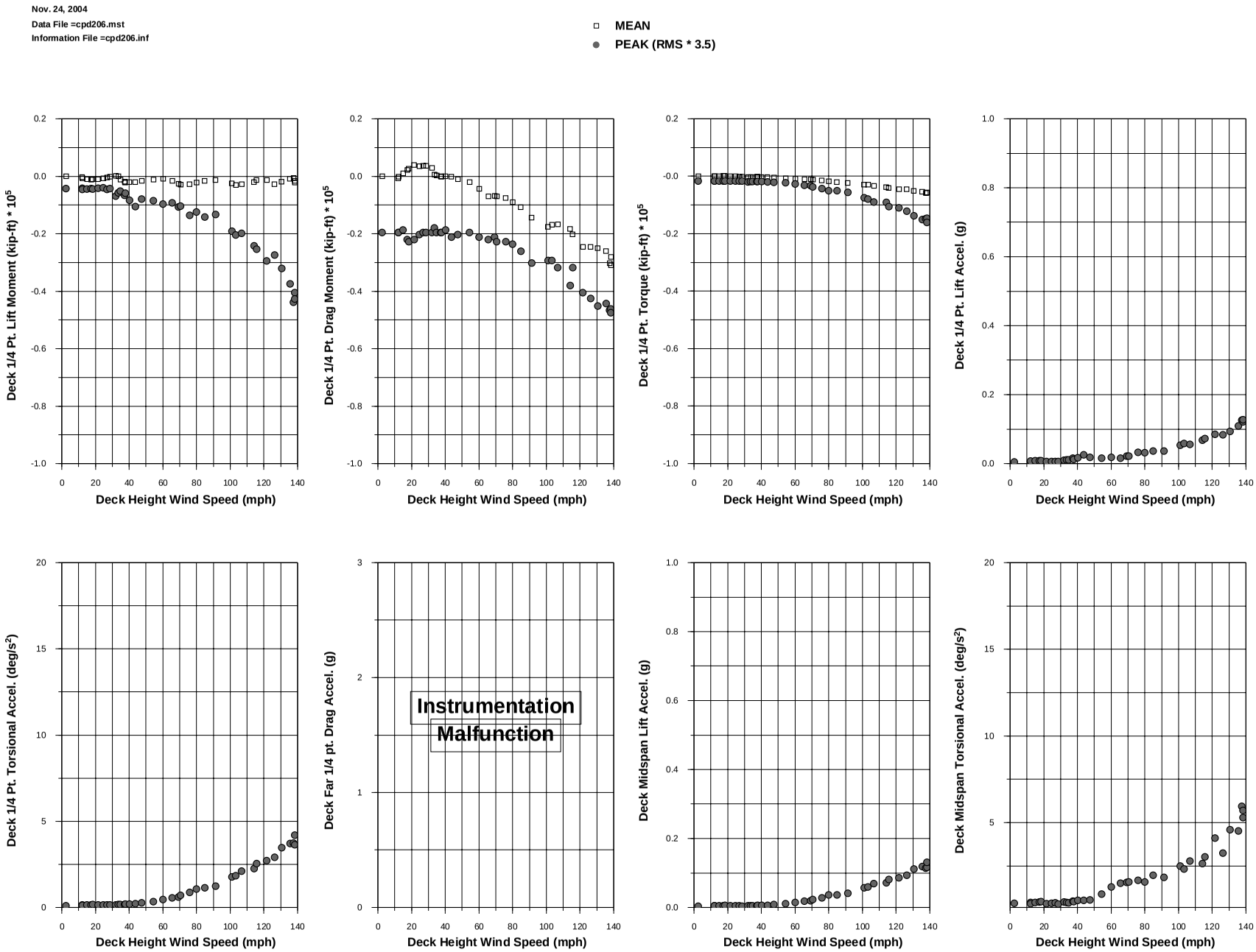

Indian River Bridge, construction stage prior to deck completion, hurricane profile, 270 degrees

Nov. 24, 2004
Data File =cpd206.mst
Information File =cpd206.inf

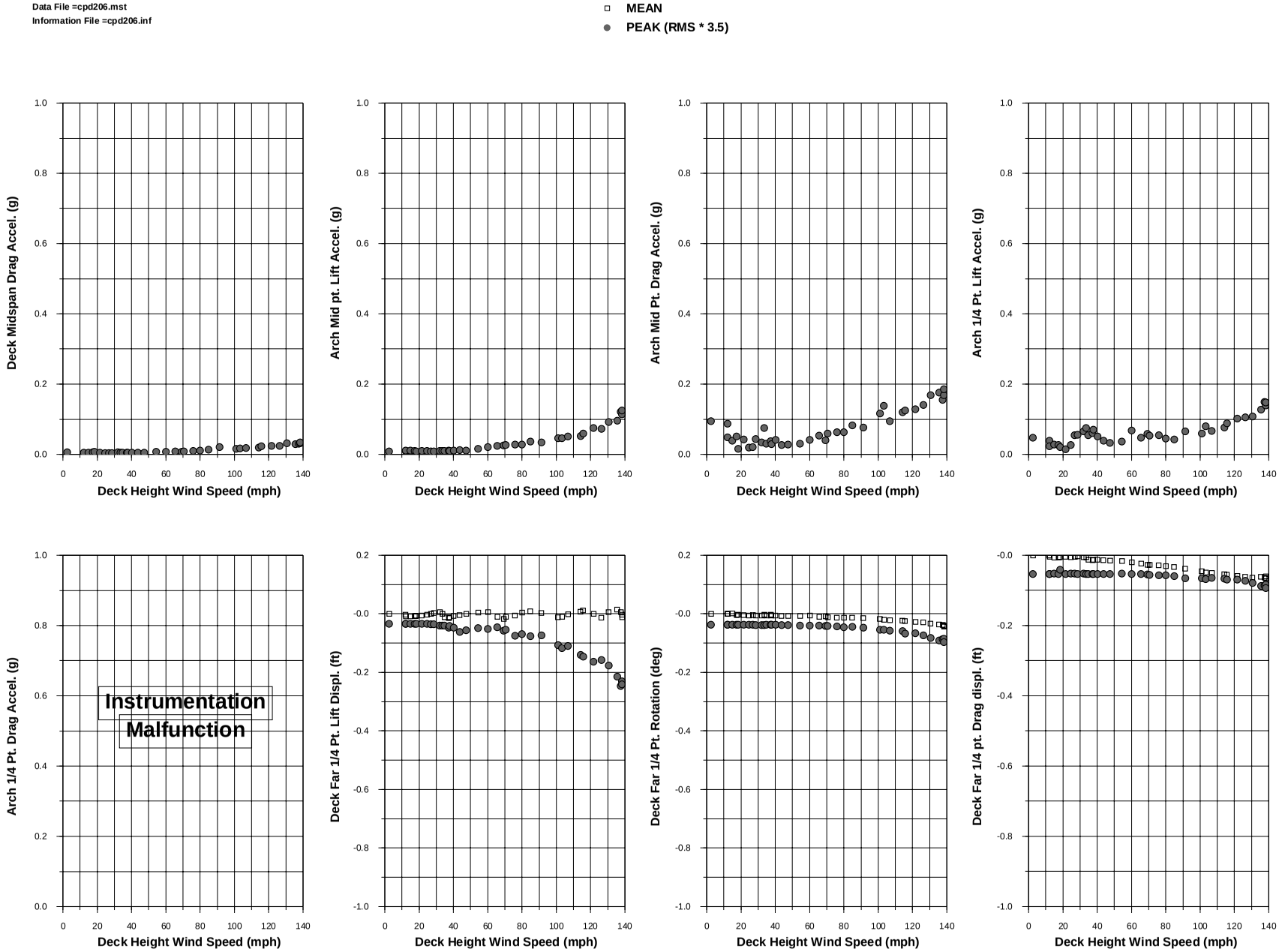

Indian River Bridge, construction stage prior to deck completion, hurricane profile, 270 degrees

Nov. 24, 2004
Data File =cpd206.mst
Information File =cpd206.inf

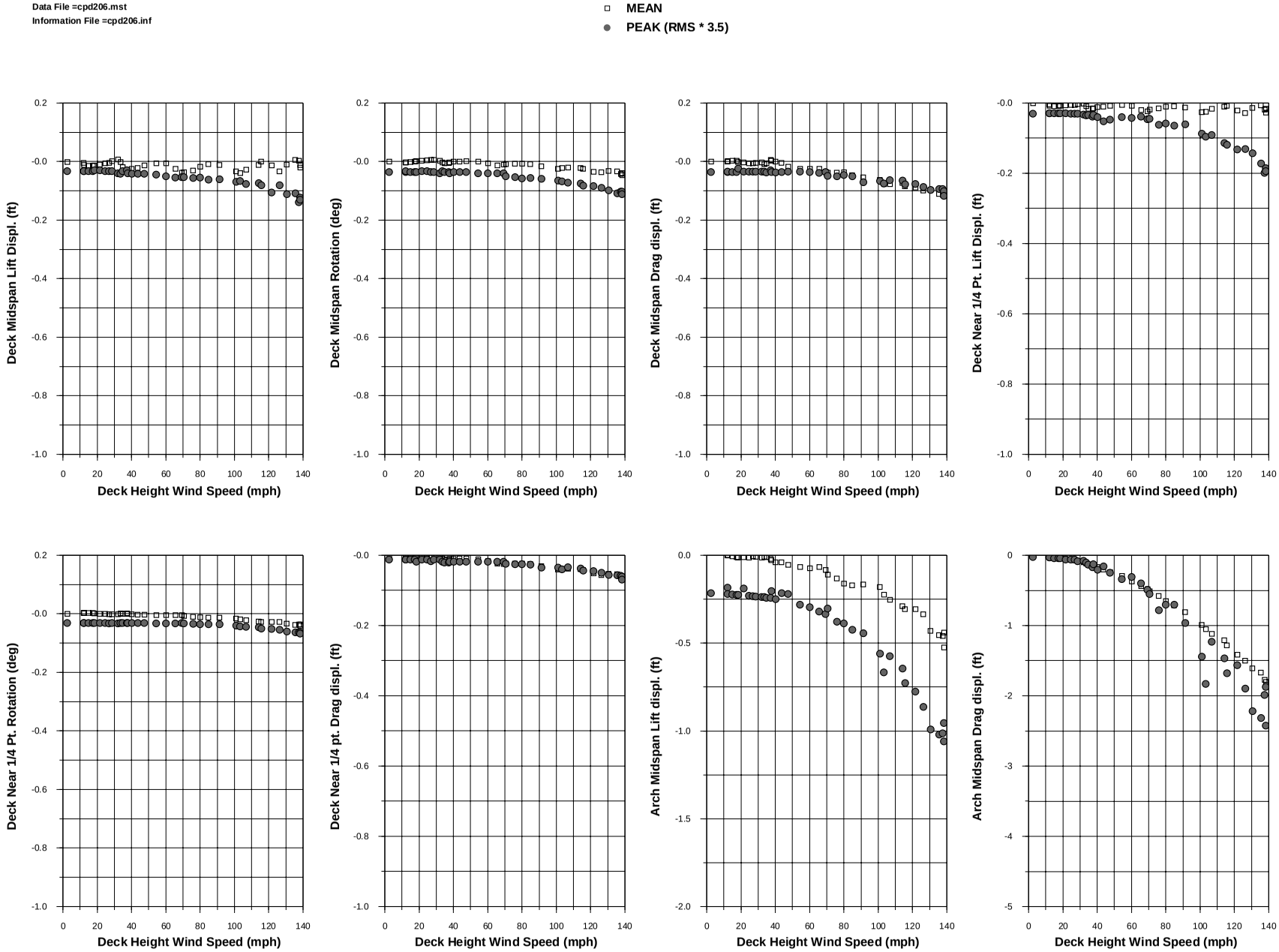

Indian River Bridge, construction stage prior to deck completion, hurricane profile, 270 degrees

Nov. 24, 2004
Data File =cpd301.mst
Information File =cpd301.inf

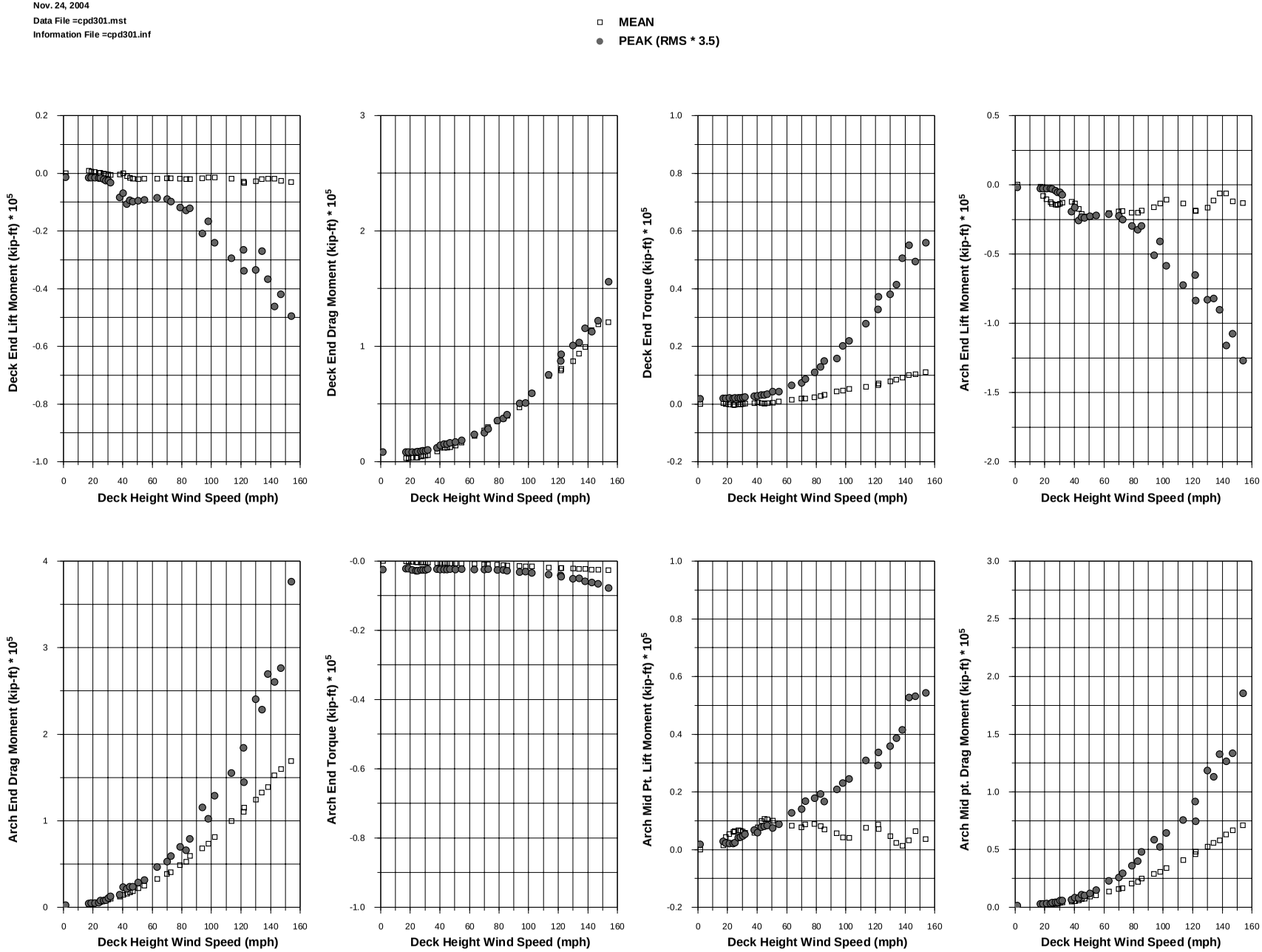

Indian River Bridge, construction stage prior to deck completion, open country profile, 60 degrees

Nov. 24, 2004
Data File =cpd301.mst
Information File =cpd301.inf

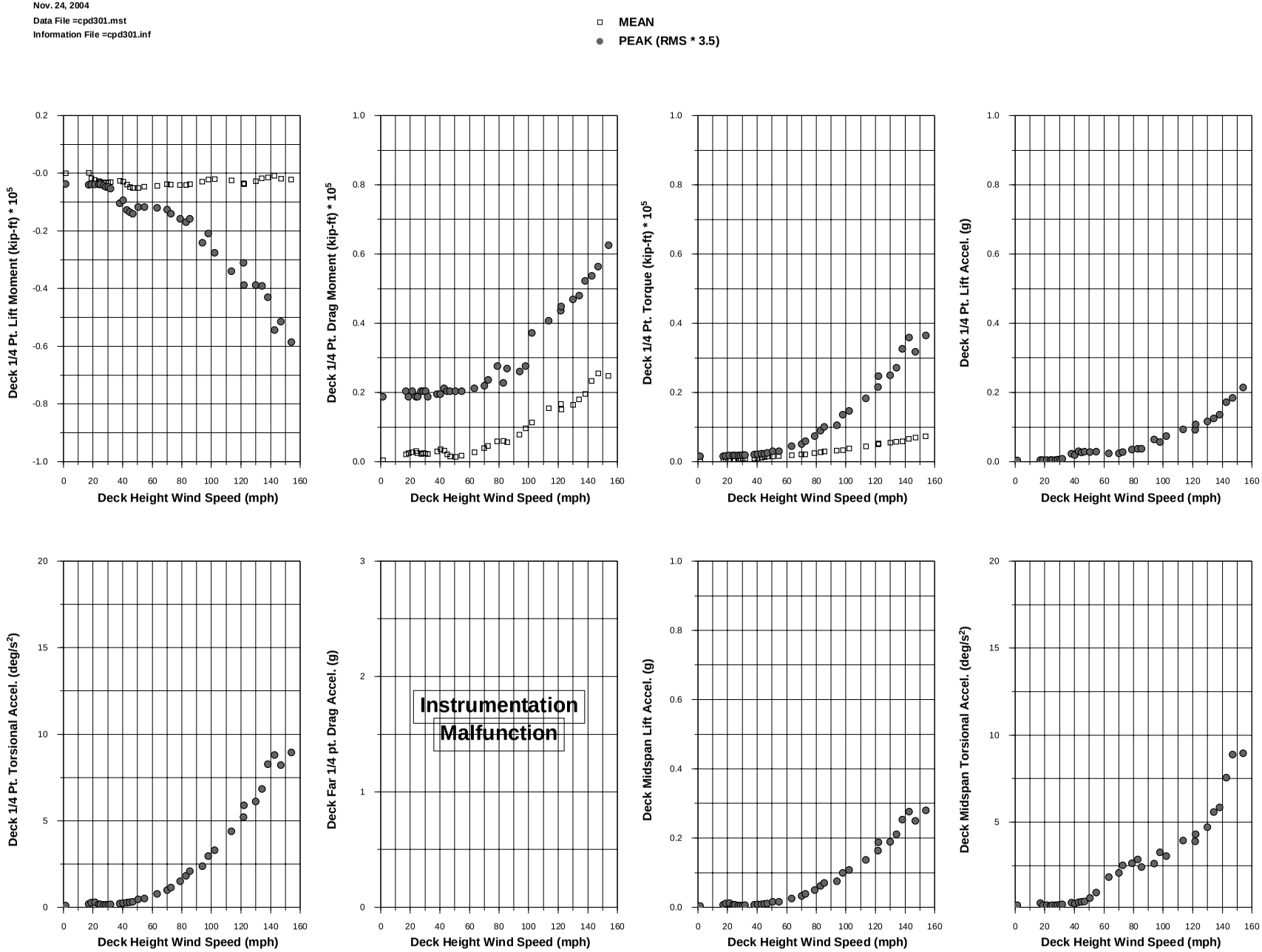

Indian River Bridge, construction stage prior to deck completion, open country profile, 60 degrees

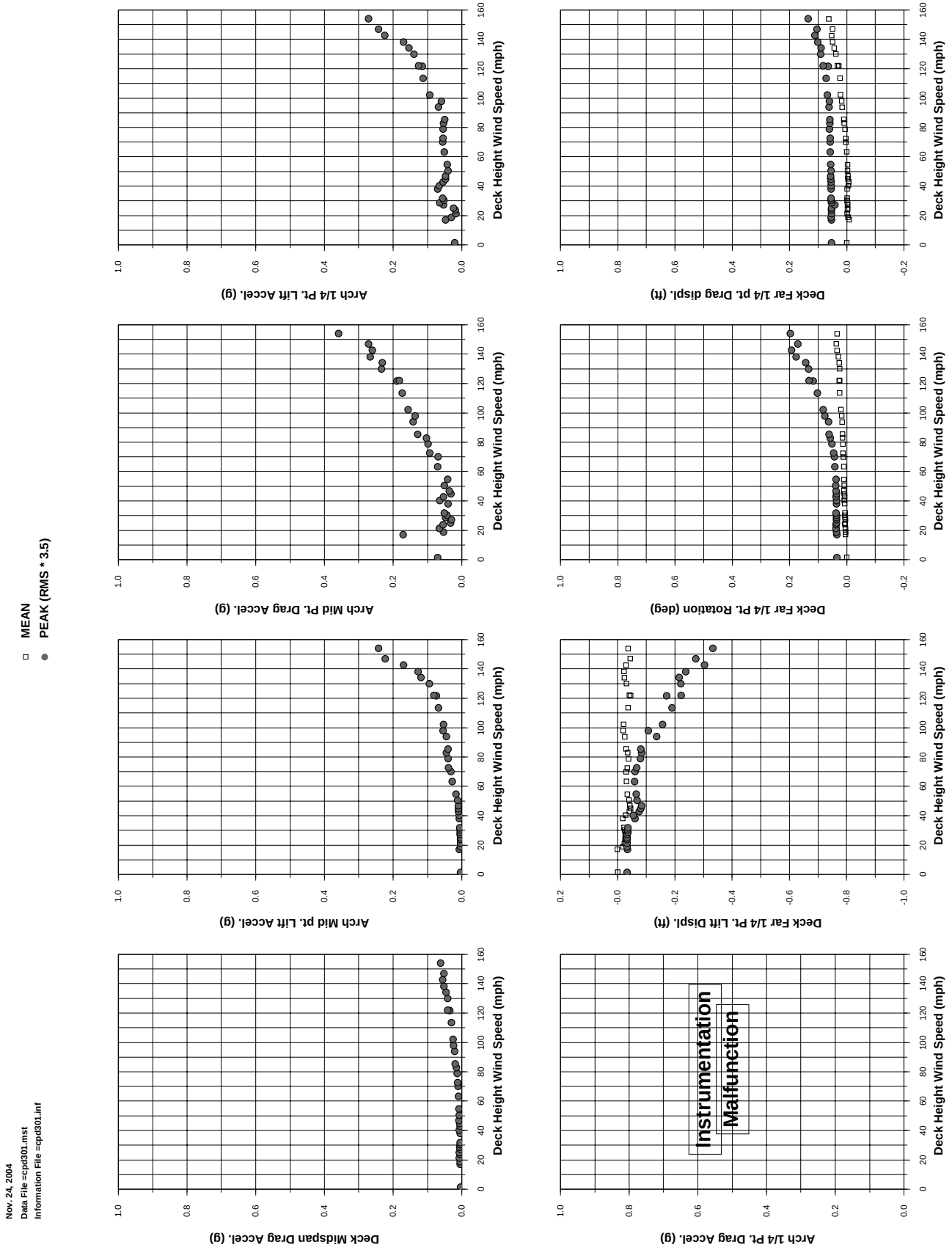

Indian River Bridge, construction stage prior to deck completion, open country profile, 60 degrees

Nov. 24, 2004
Data File =cpd301.mst
Information File =cpd301.inf

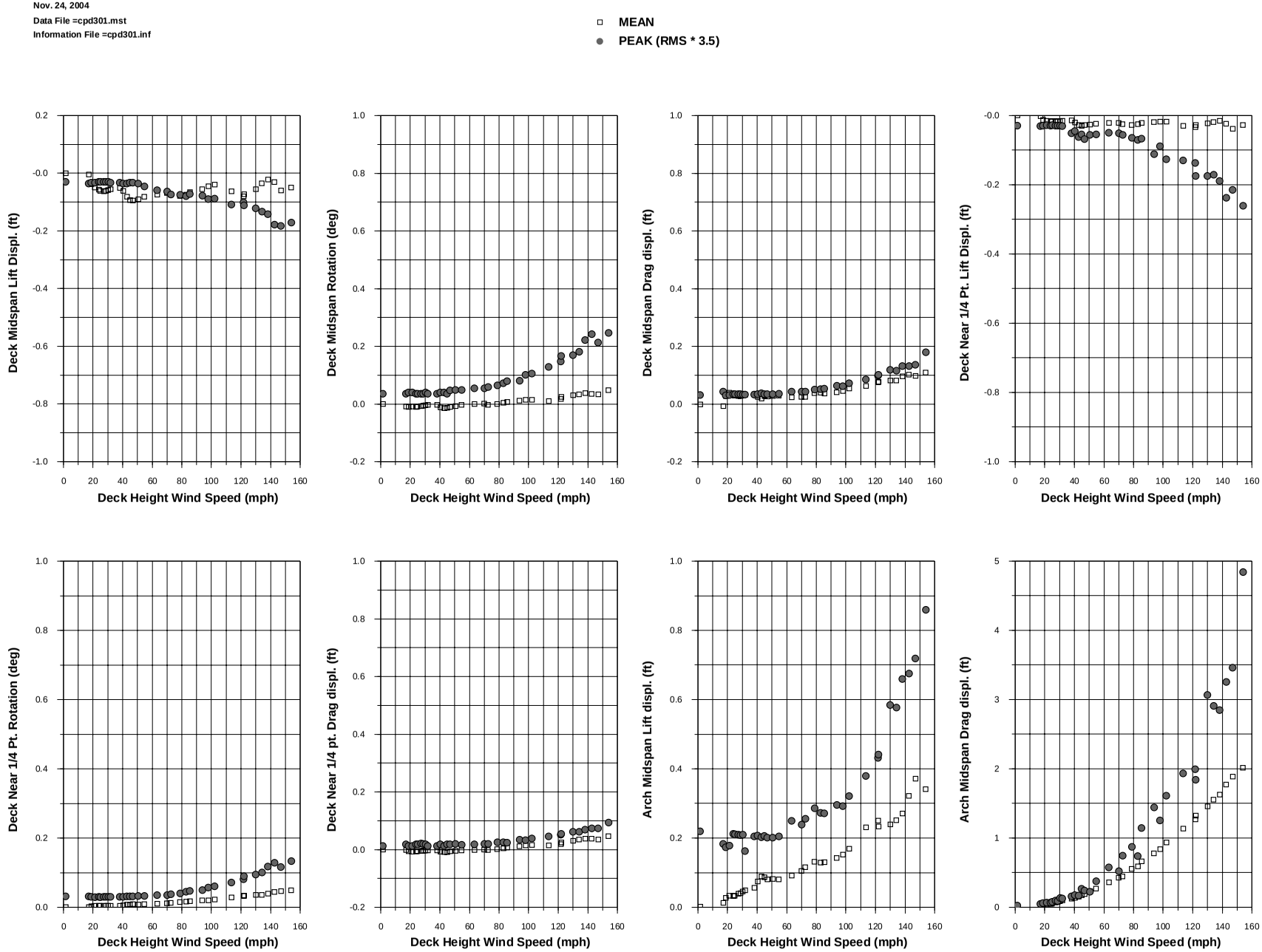

Indian River Bridge, construction stage prior to deck completion, open country profile, 60 degrees

Nov. 24, 2004
Data File =cpd302.mst
Information File =cpd302.inf

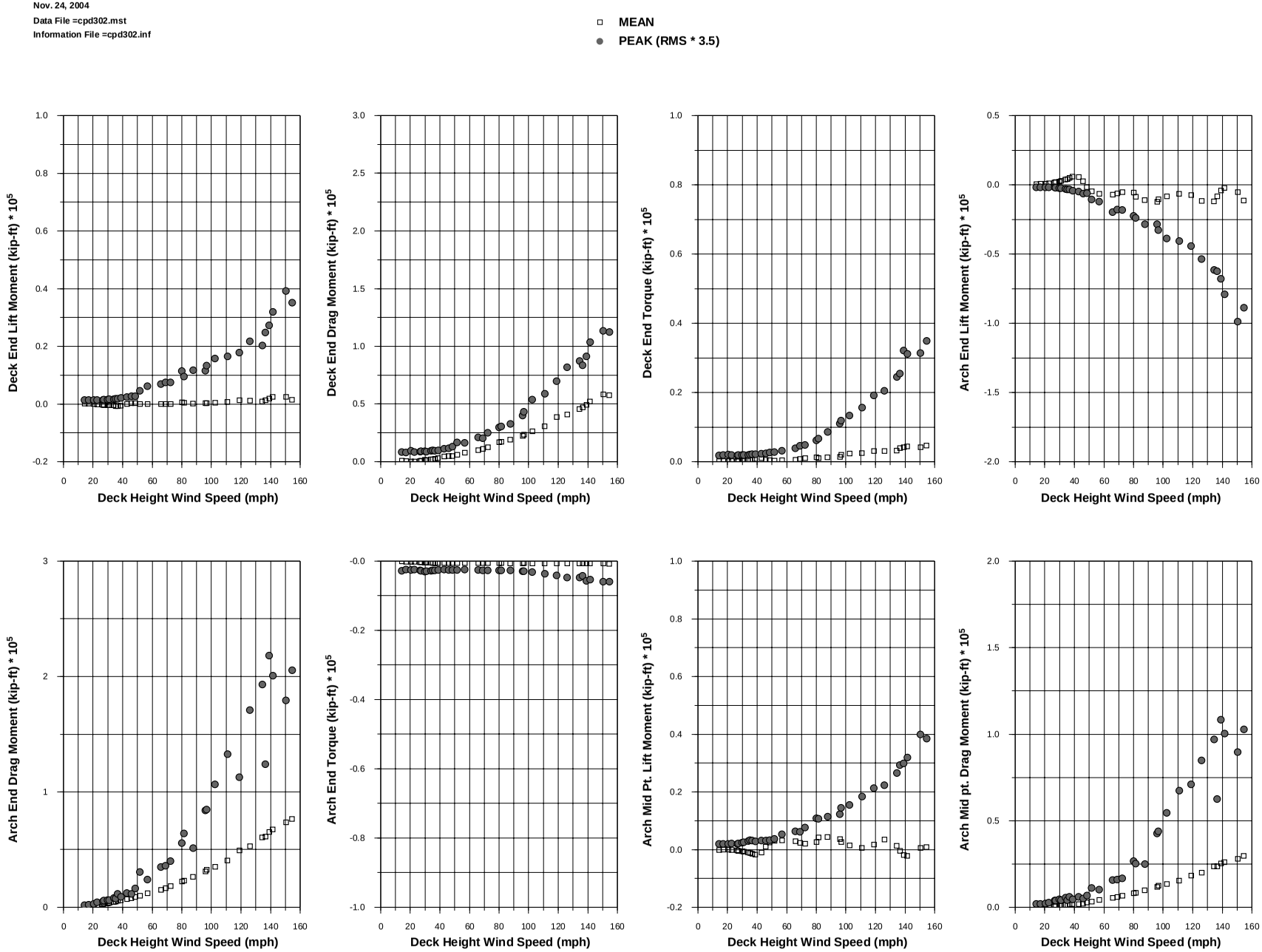

Indian River Bridge, construction stage prior to deck completion, open country profile, 30 degrees

Nov. 24, 2004
Data File =cpd302.mst
Information File =cpd302.inf

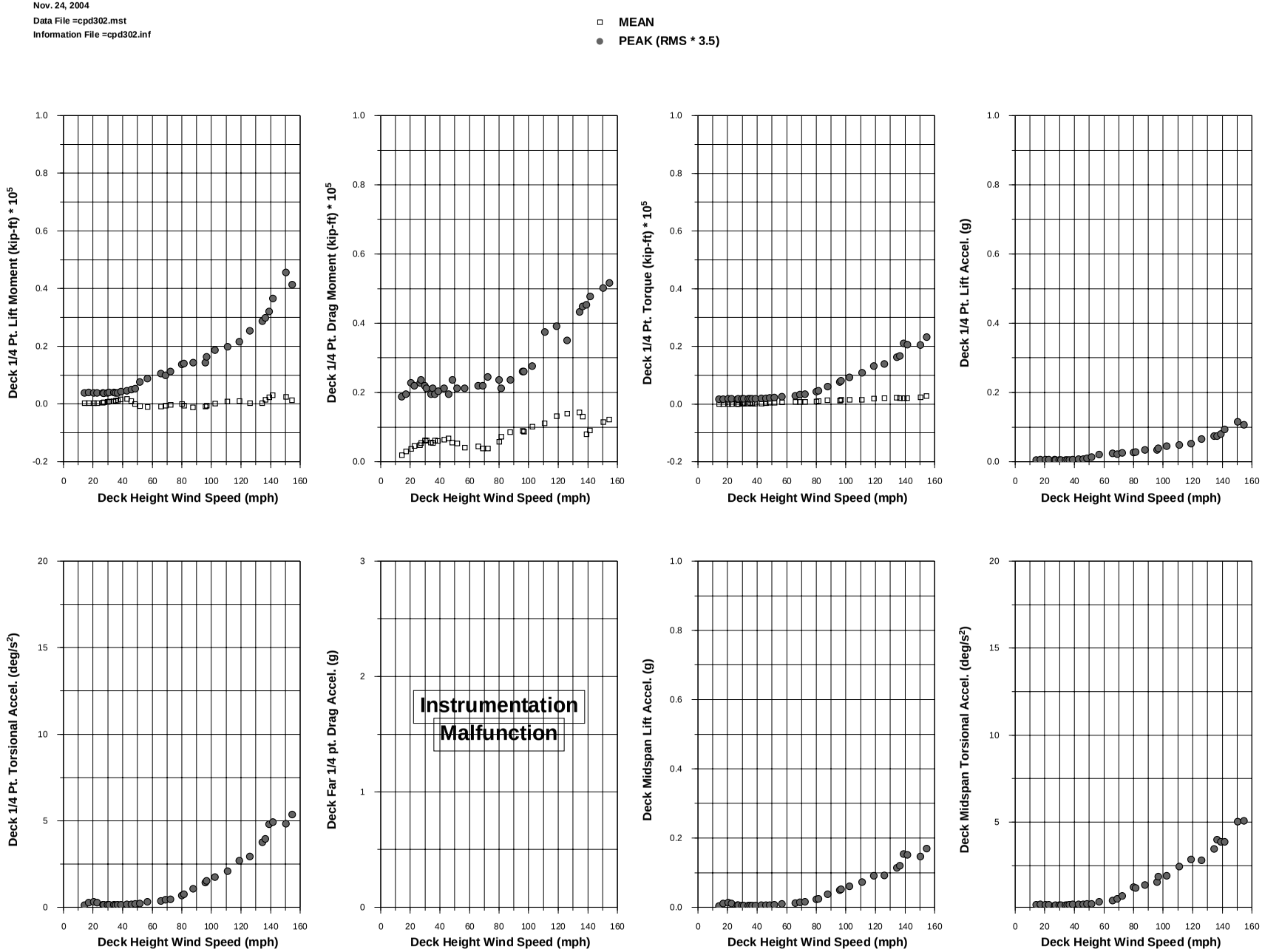

Indian River Bridge, construction stage prior to deck completion, open country profile, 30 degrees

Nov. 24, 2004
Data File =cpd302.mst
Information File =cpd302.inf

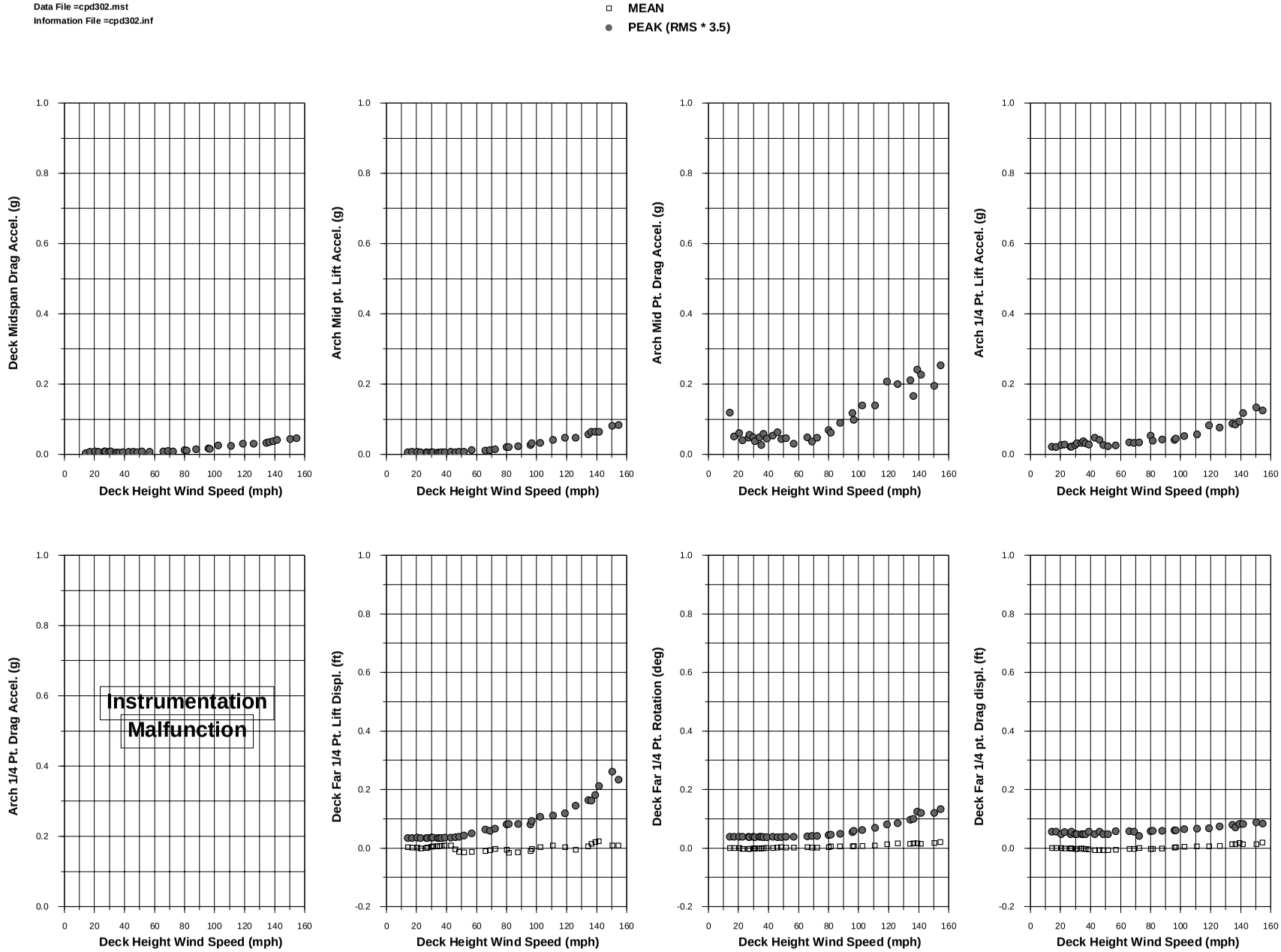

Indian River Bridge, construction stage prior to deck completion, open country profile, 30 degrees

Nov. 24, 2004
Data File =cpd302.mst
Information File =cpd302.inf

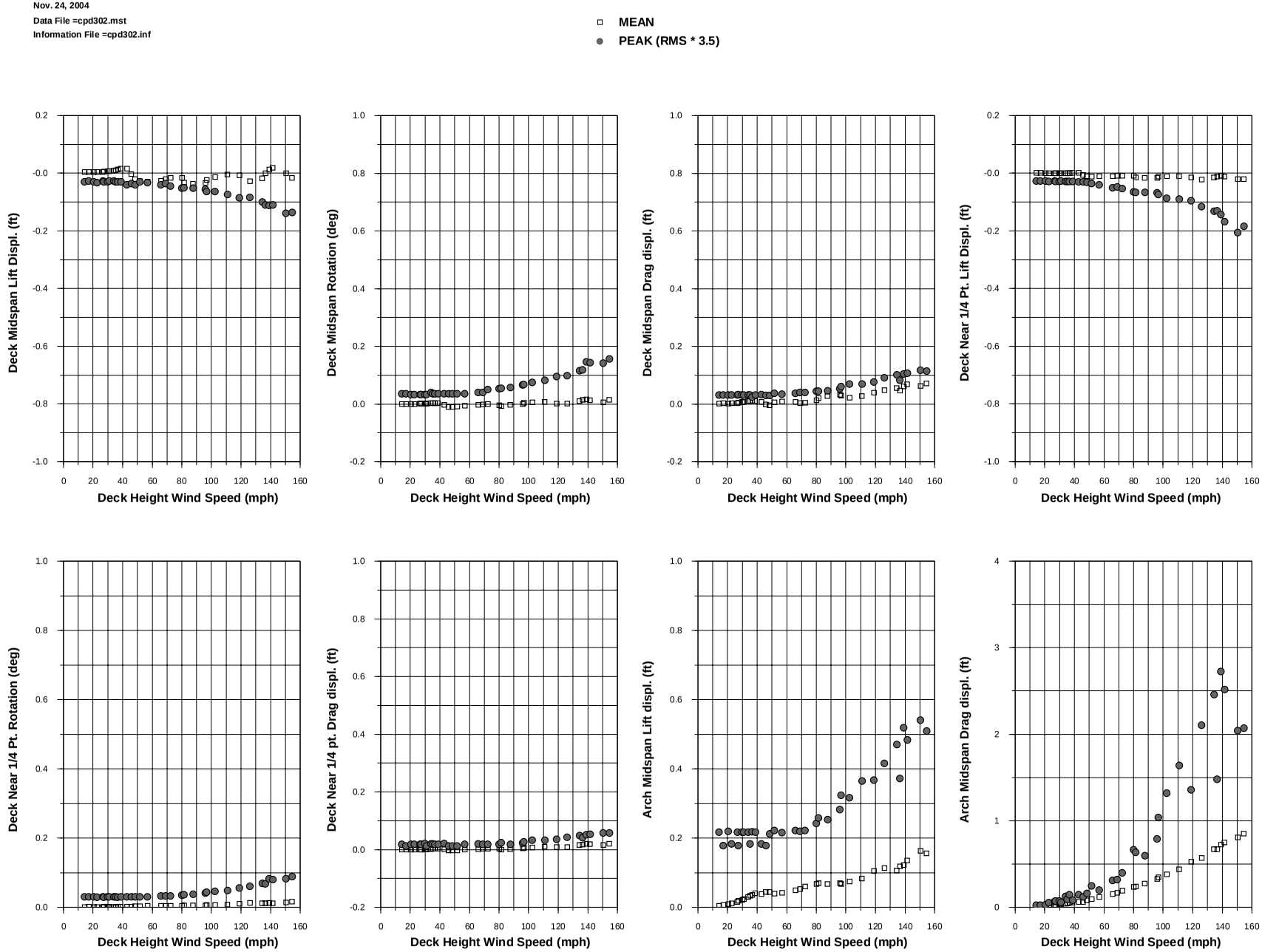

Indian River Bridge, construction stage prior to deck completion, open country profile, 30 degrees

Nov. 24, 2004
Data File =cpd303.mst
Information File =cpd303.inf

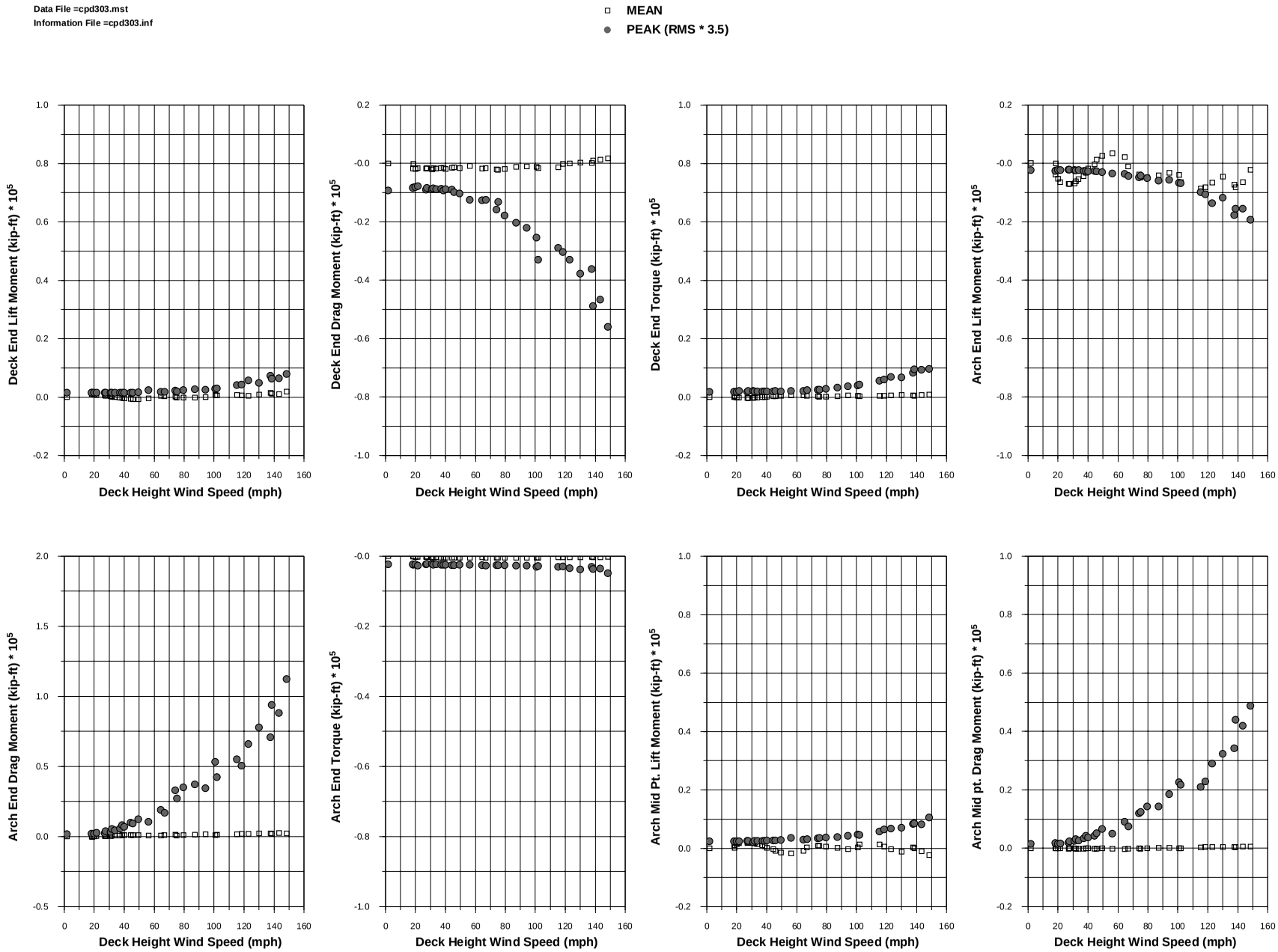

Indian River Bridge, Construction stage prior to deck completion, open country profile, 0 degrees (along bridge)

Nov. 24, 2004
Data File =cpd303.mst
Information File =cpd303.inf

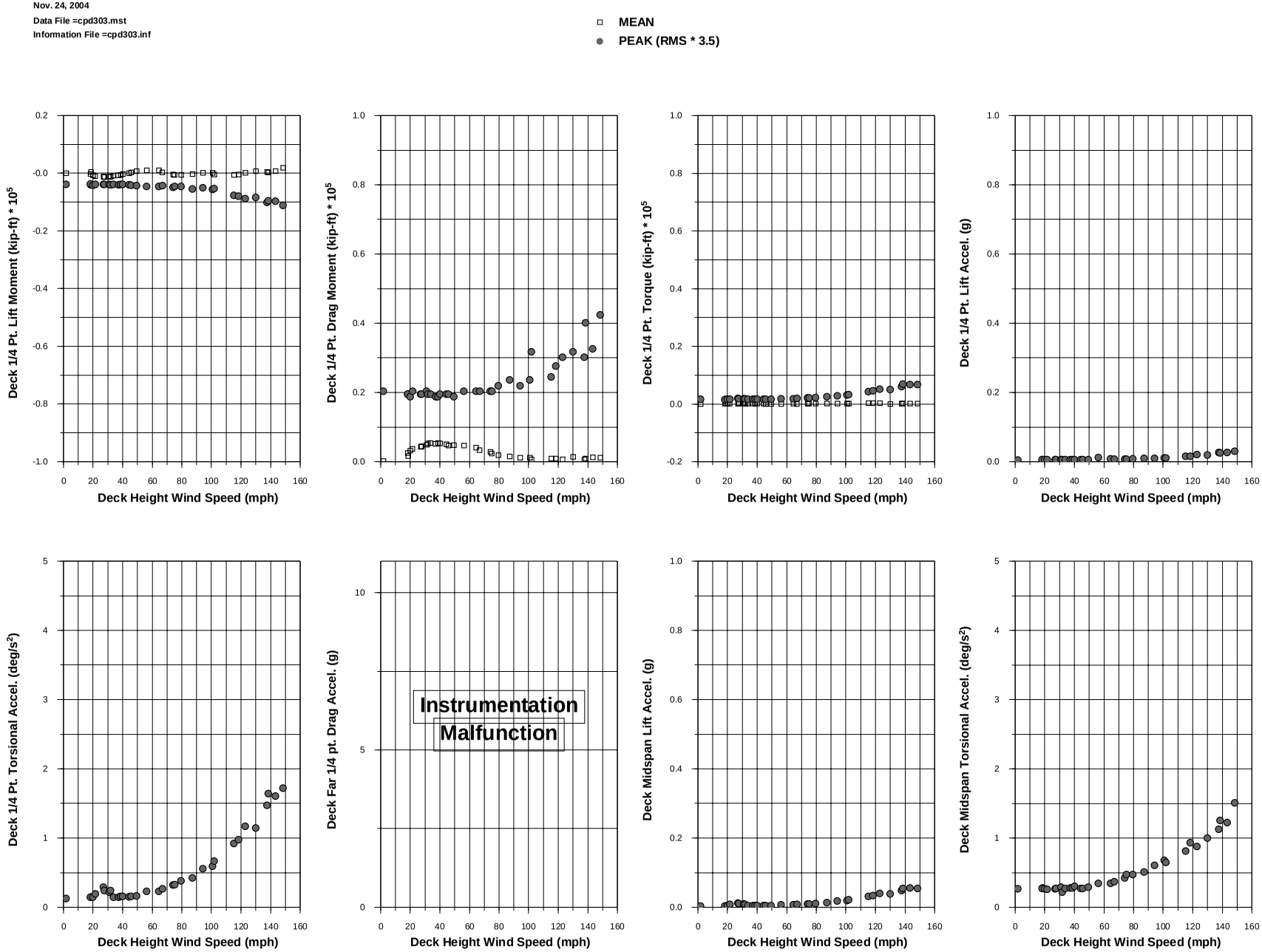

Indian River Bridge, Construction stage prior to deck completion, open country profile, 0 degrees (along bridge)

Nov. 24, 2004
Data File =cpd303.mst
Information File =cpd303.inf

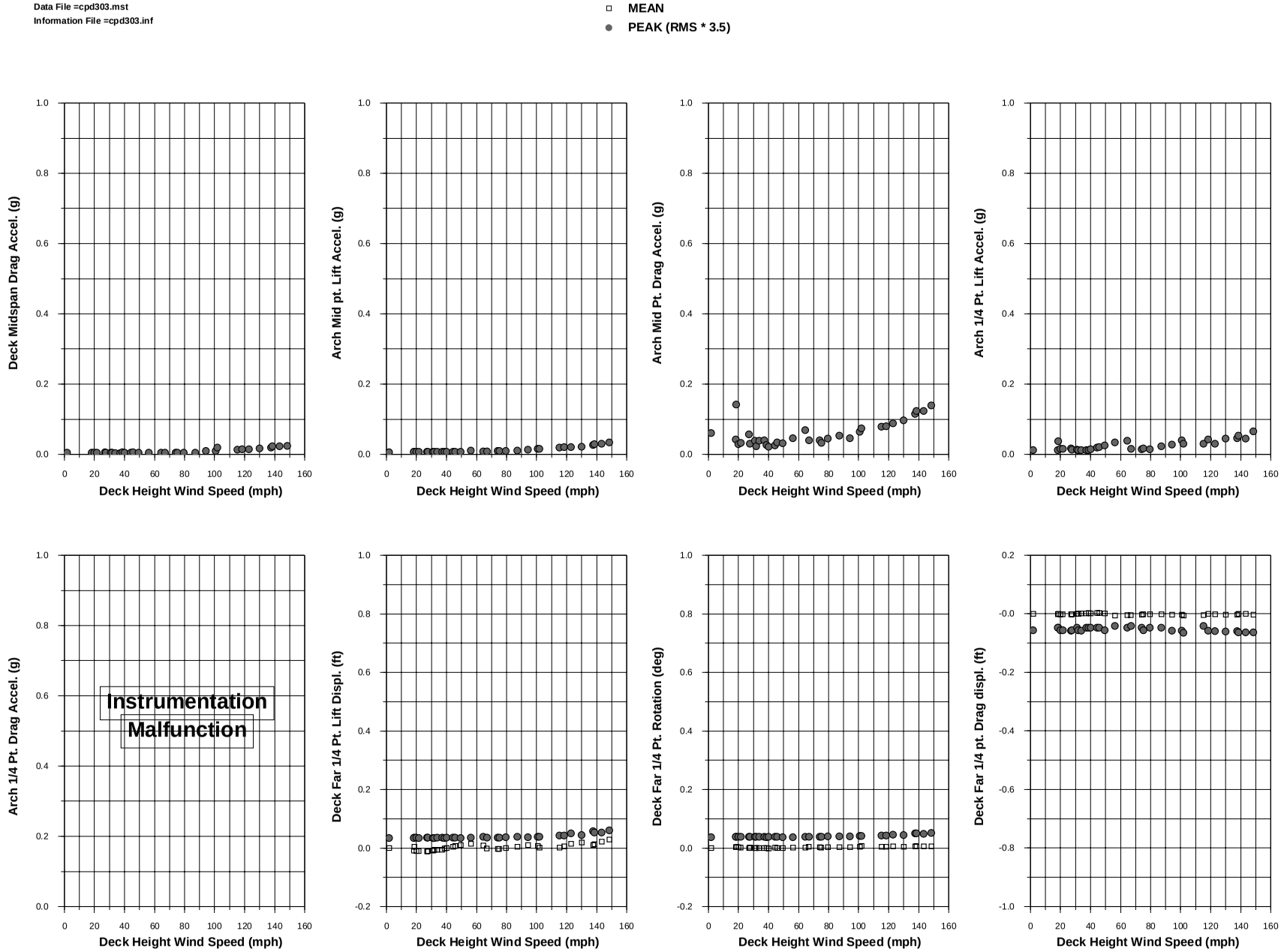

Indian River Bridge, Construction stage prior to deck completion, open country profile, 0 degrees (along bridge)

Nov. 24, 2004
Data File =cpd303.mst
Information File =cpd303.inf

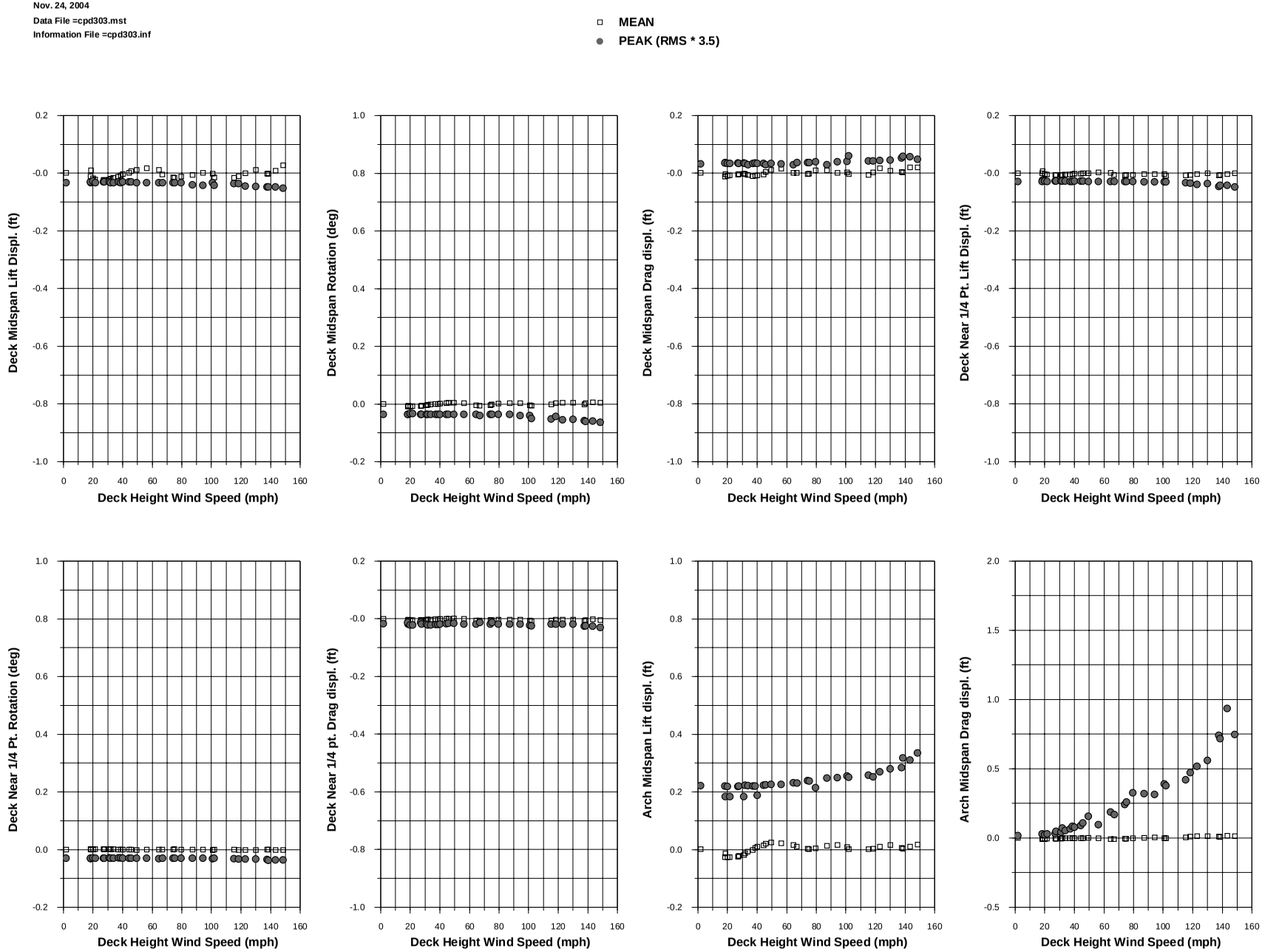

Indian River Bridge, Construction stage prior to deck completion, open country profile, 0 degrees (along bridge)

Nov. 24, 2004
Data File =cpd304.mst
Information File =cpd304.inf

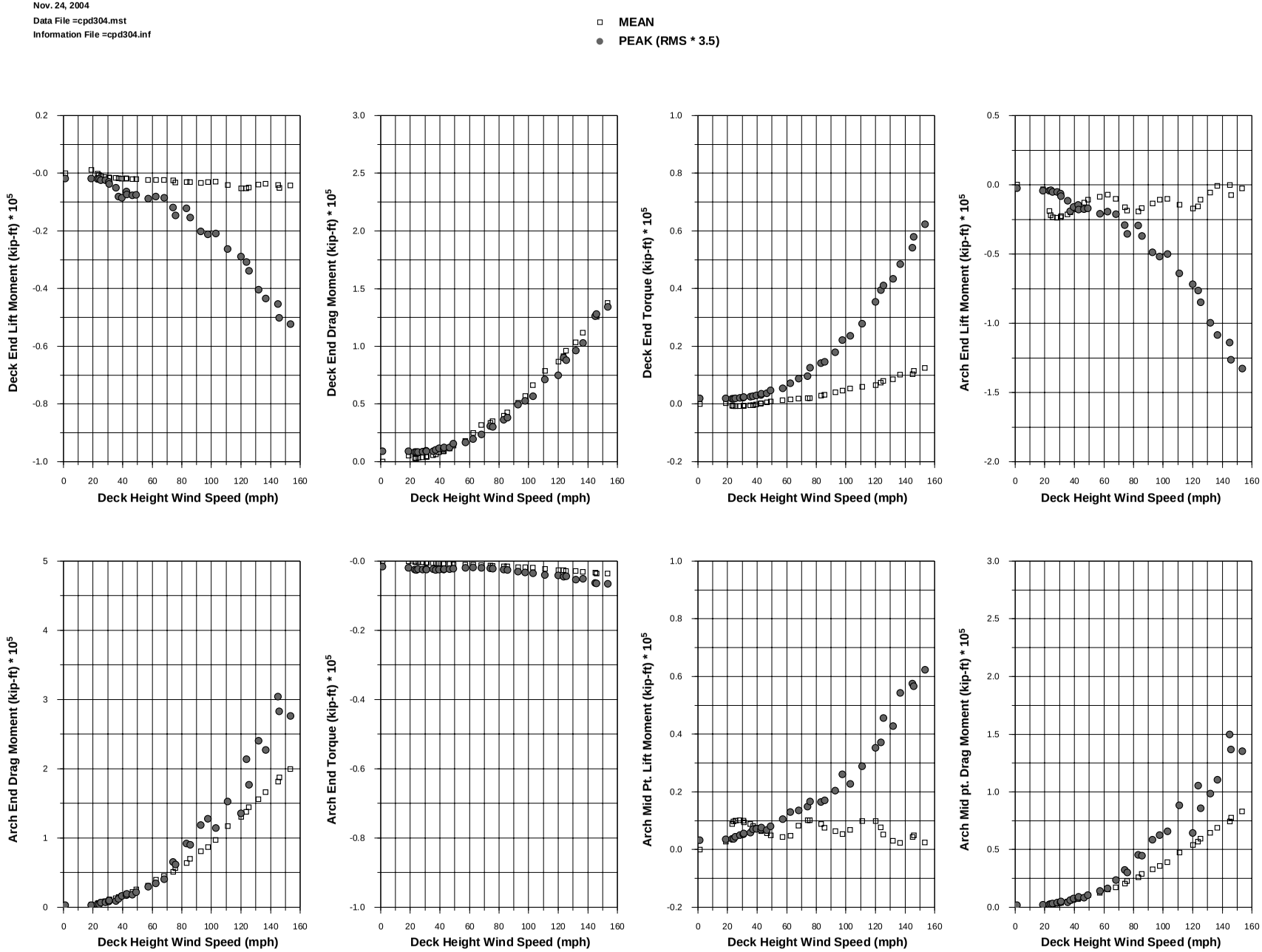

Indian River Bridge, construction stage prior to deck completion, open country profile, 90 degrees, without existing bridge

Nov. 24, 2004
Data File =cpd304.mst
Information File =cpd304.inf

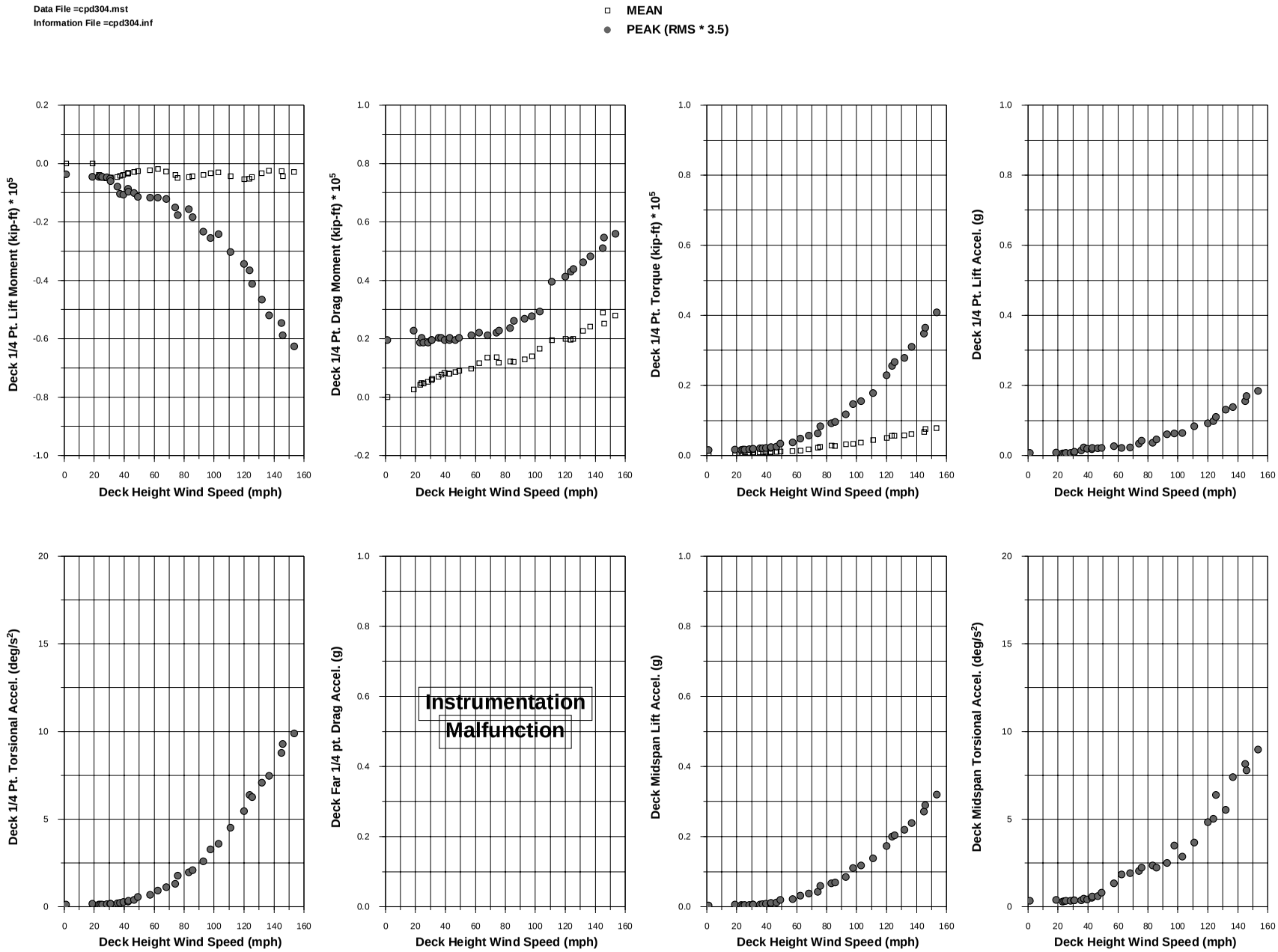

Indian River Bridge, construction stage prior to deck completion, open country profile, 90 degrees, without existing bridge

Nov. 24, 2004
Data File =cpd304.mst
Information File =cpd304.inf

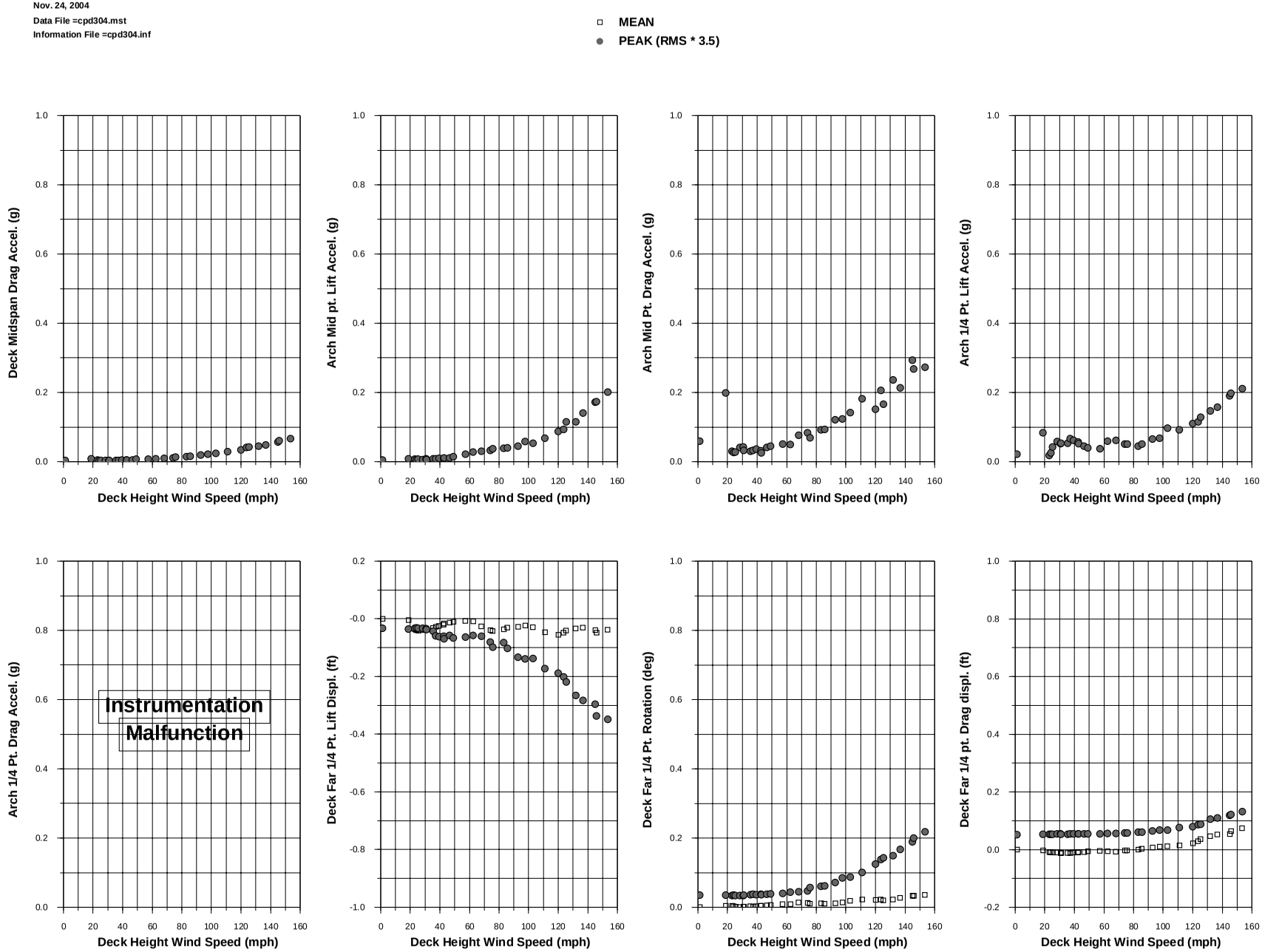

Indian River Bridge, construction stage prior to deck completion, open country profile, 90 degrees, without existing bridge

Nov. 24, 2004
Data File =cpd304.mst
Information File =cpd304.inf

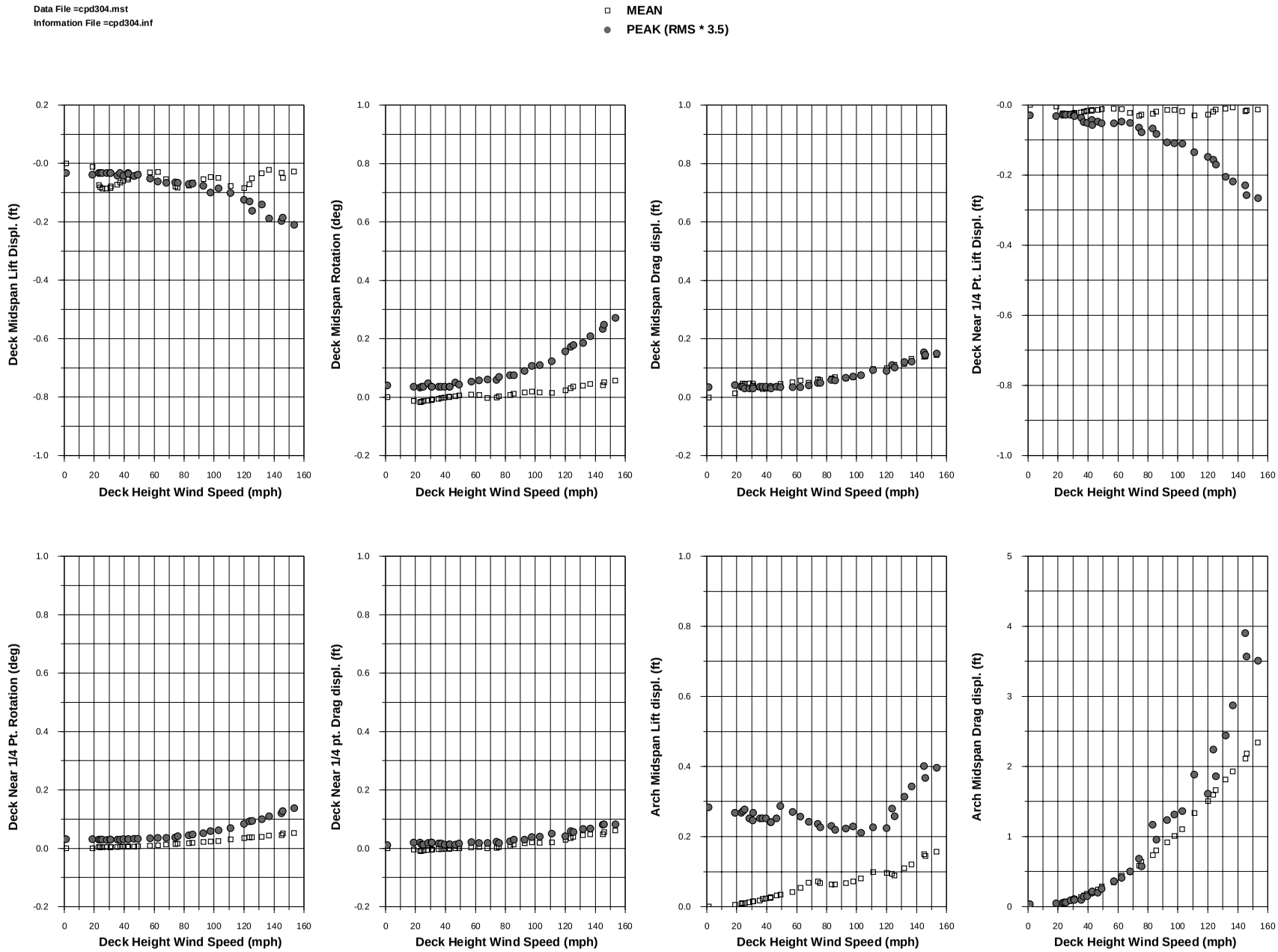

Indian River Bridge, construction stage prior to deck completion, open country profile, 90 degrees, without existing bridge

Nov. 24, 2004
Data File =cpd305.mst
Information File =cpd305.inf

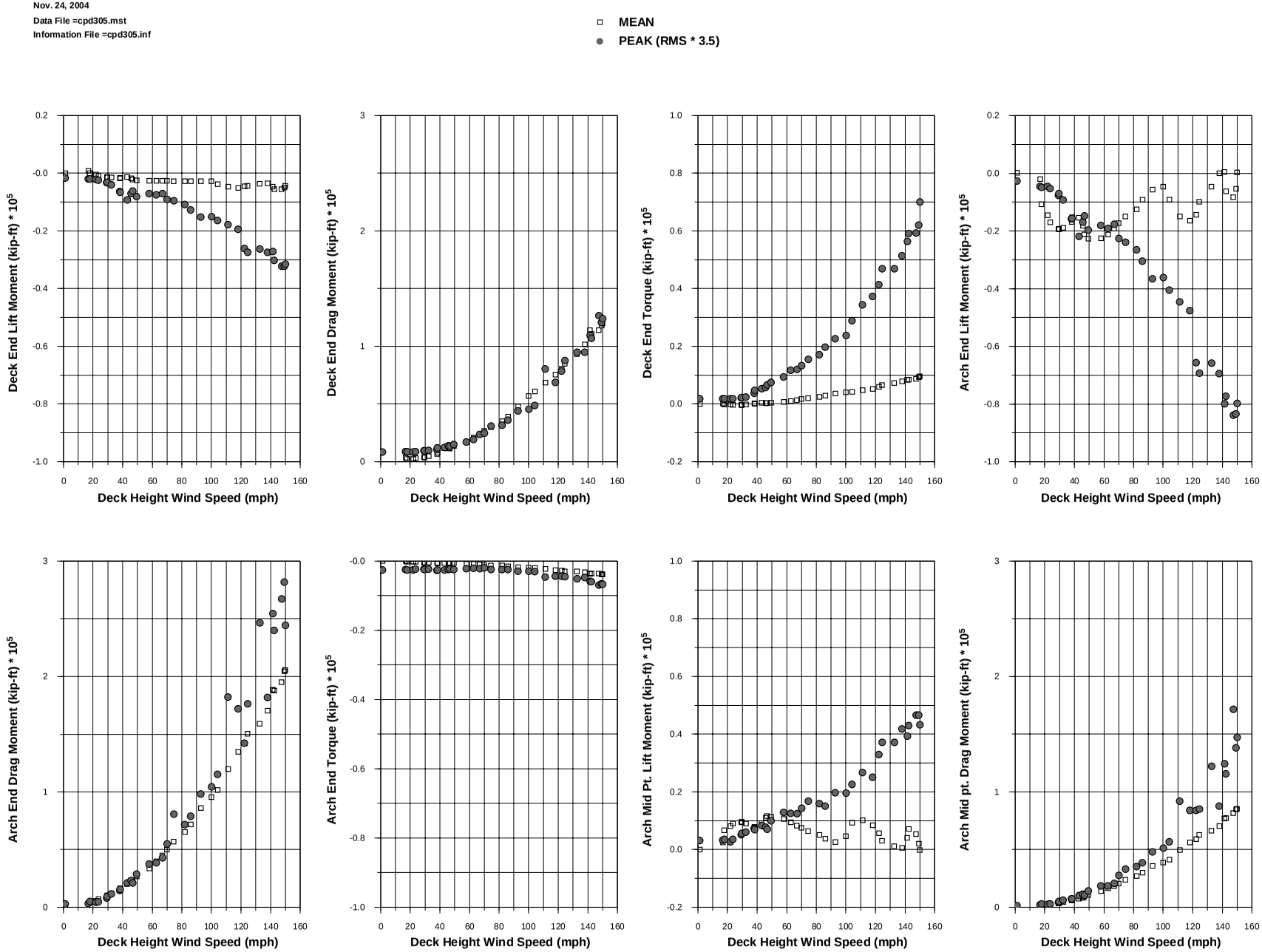

Indian River Bridge, construction stage prior to deck completion, open country profile, 90 degrees, with existing bridge

Nov. 24, 2004
Data File =cpd305.mst
Information File =cpd305.inf

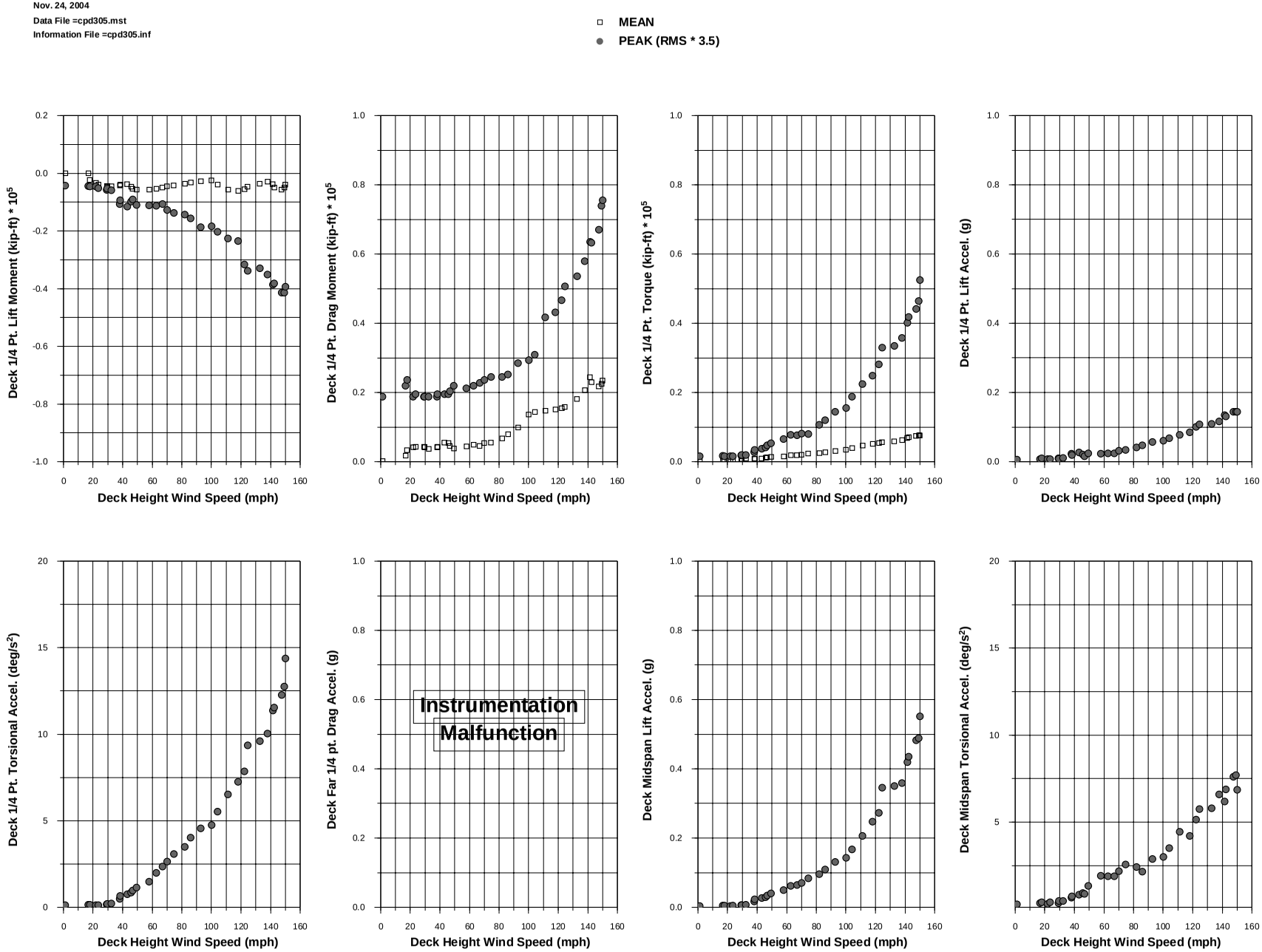

Indian River Bridge, construction stage prior to deck completion, open country profile, 90 degrees, with existing bridge

Nov. 24, 2004
Data File =cpd305.mst
Information File =cpd305.inf

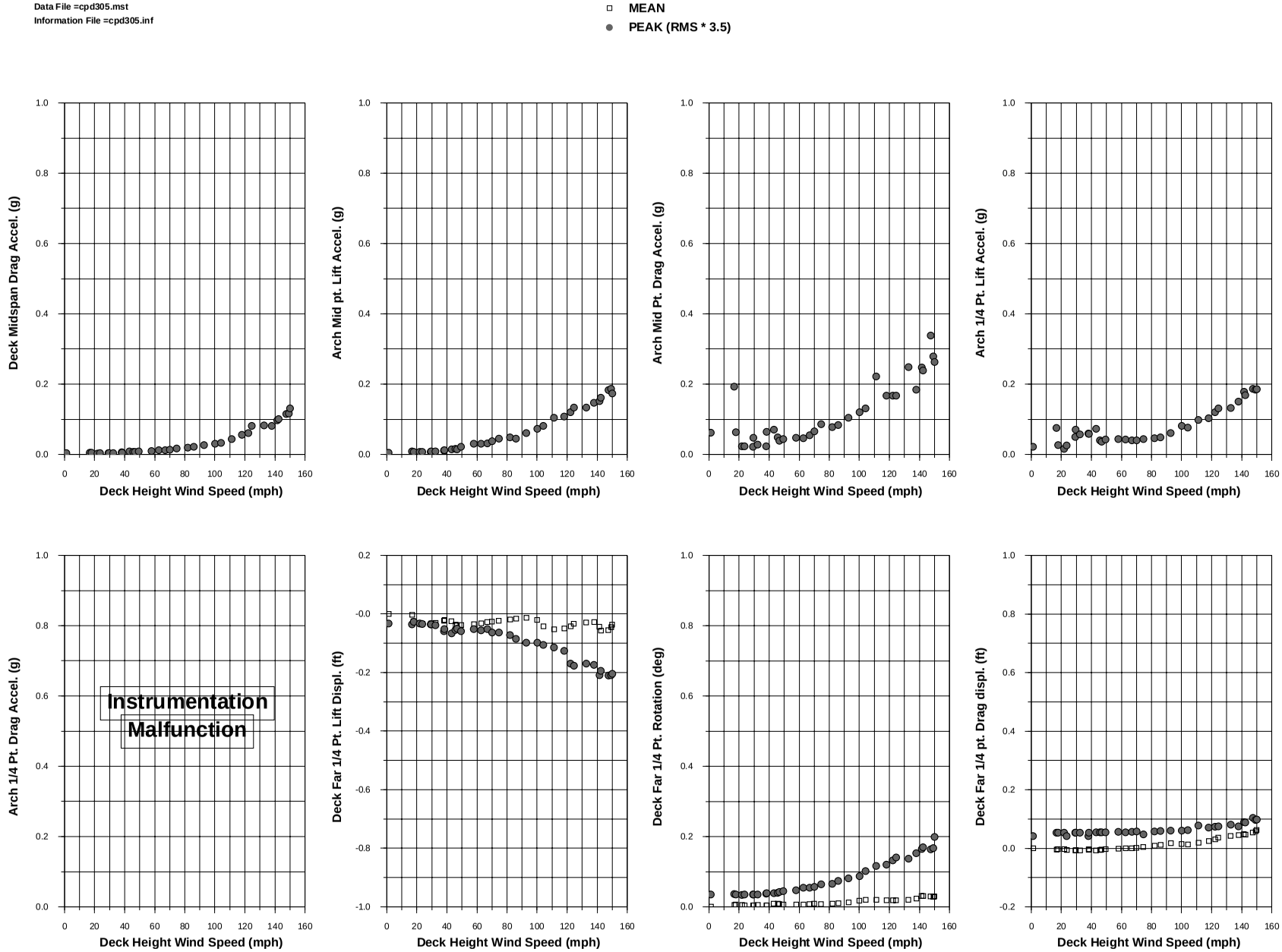

Indian River Bridge, construction stage prior to deck completion, open country profile, 90 degrees, with existing bridge

Nov. 24, 2004
Data File =cpd305.mst
Information File =cpd305.inf

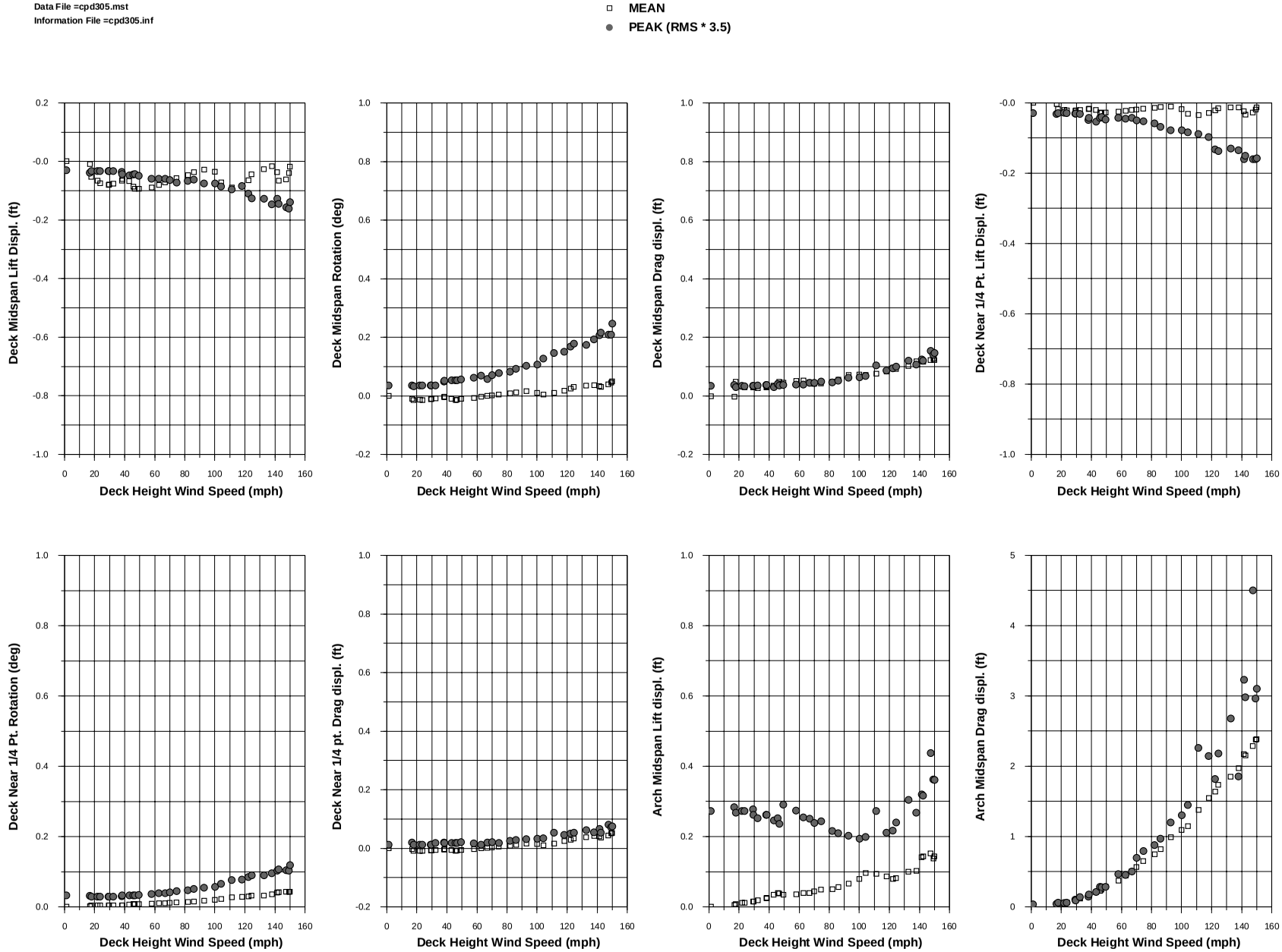

Indian River Bridge, construction stage prior to deck completion, open country profile, 90 degrees, with existing bridge

Nov. 24, 2004
Data File =cpd306.mst
Information File =cpd306.inf

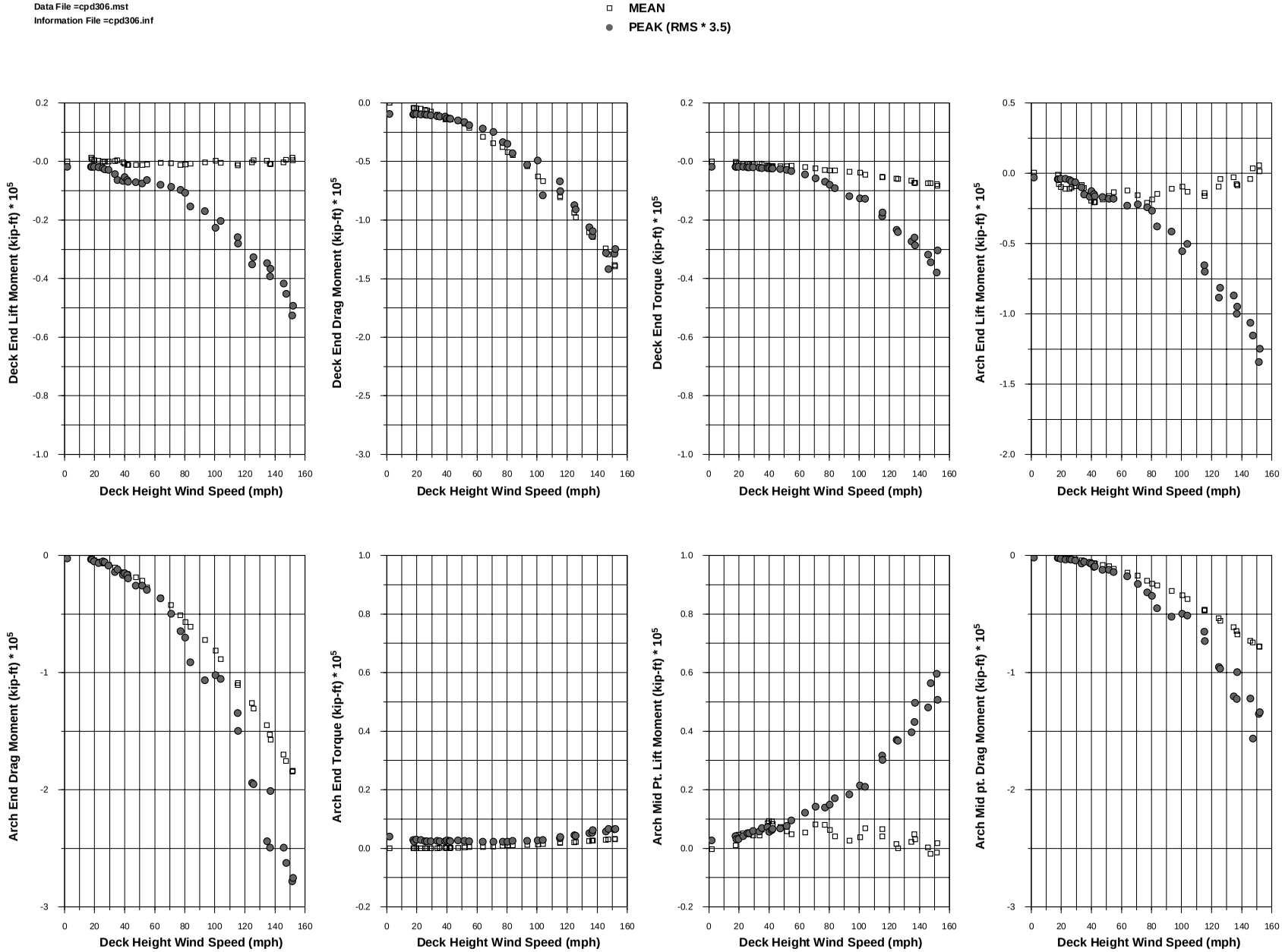

Indian River Bridge, construction stage prior to deck completion, open country profile, 270 degrees

Nov. 24, 2004
Data File =cpd306.mst
Information File =cpd306.inf

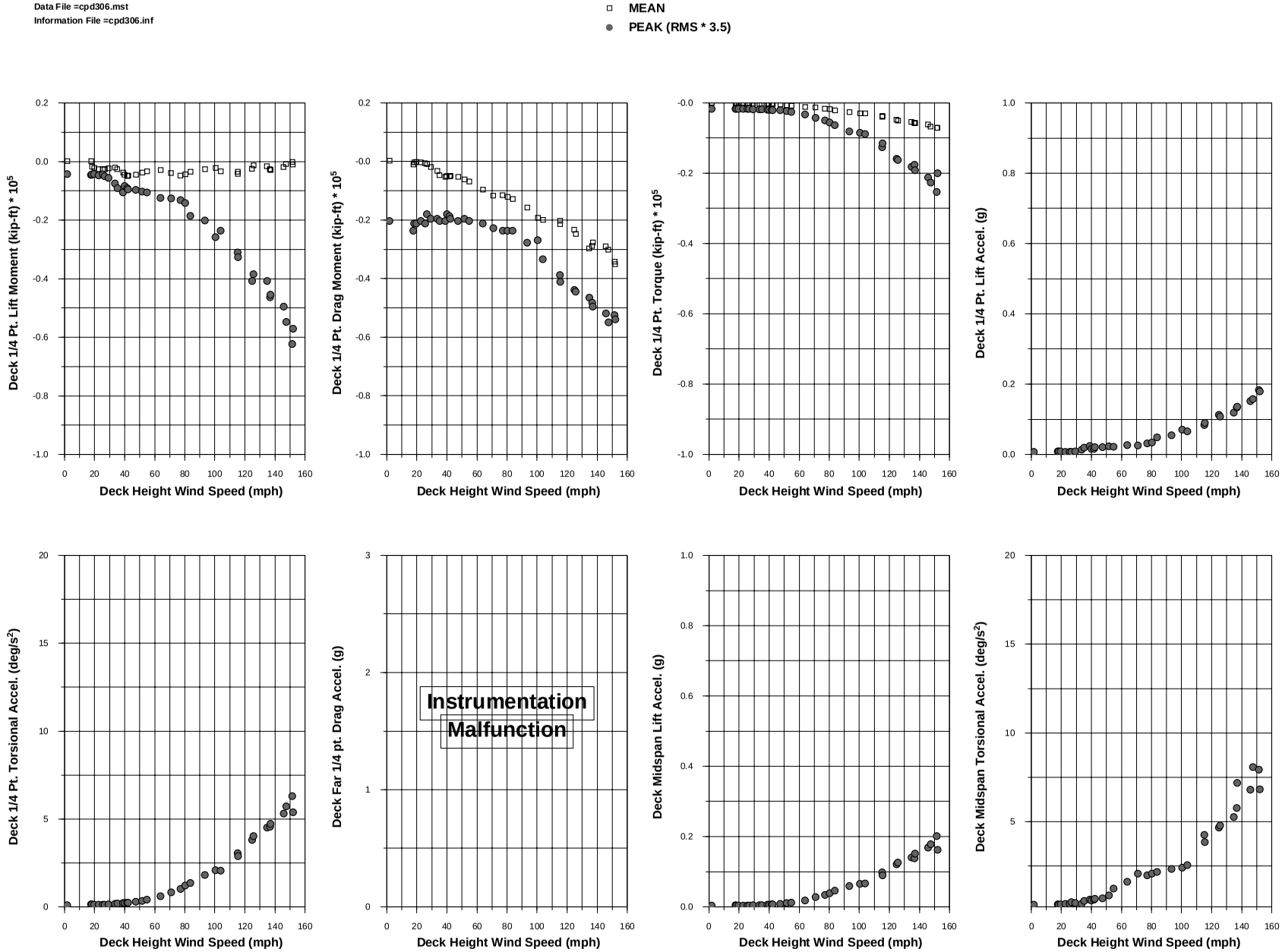

Indian River Bridge, construction stage prior to deck completion, open country profile, 270 degrees

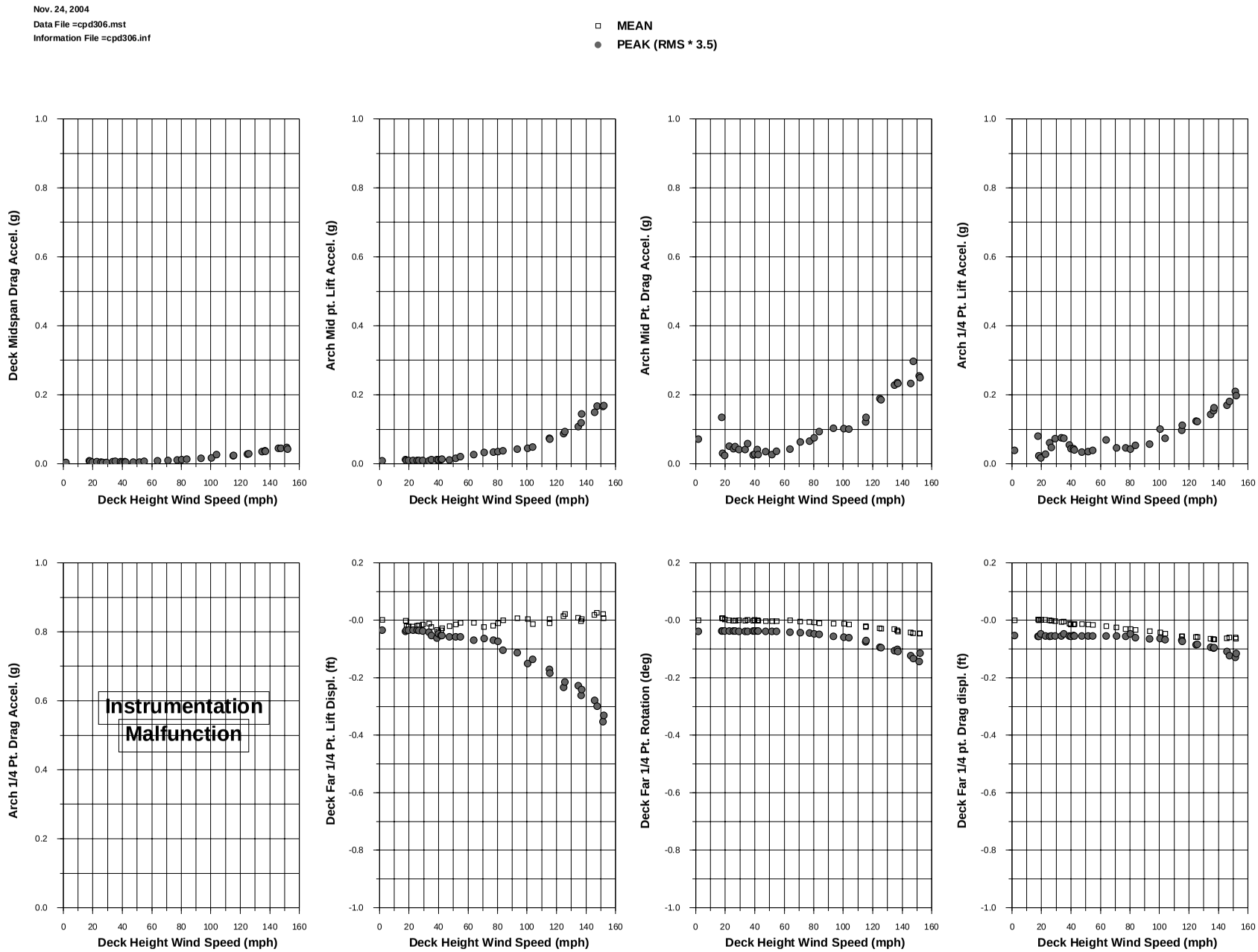

Indian River Bridge, construction stage prior to deck completion, open country profile, 270 degrees

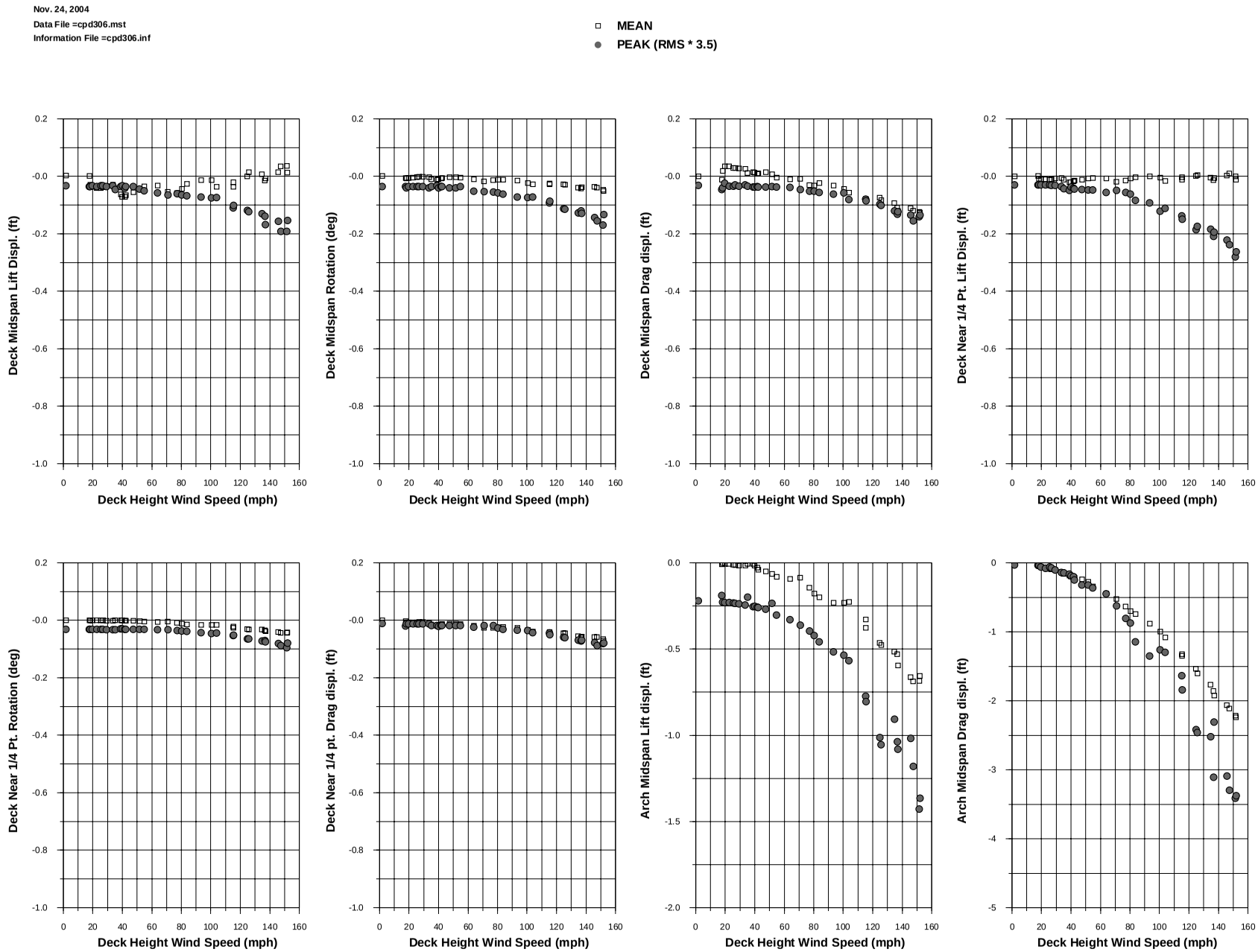

Indian River Bridge, construction stage prior to deck completion, open country profile, 270 degrees

Nov. 24, 2004
Data File =cpd101.mst
Information File =cpd101.inf

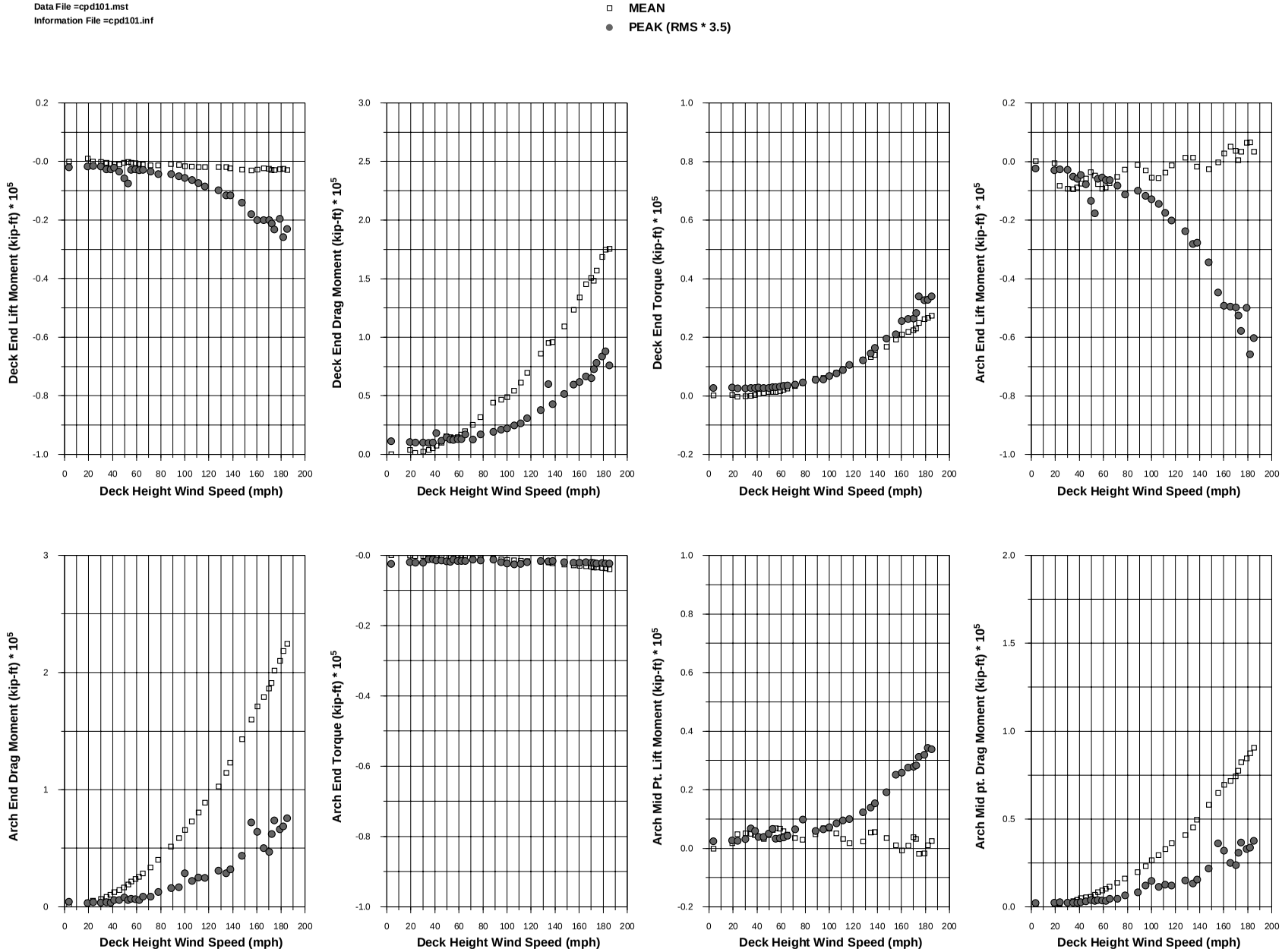

Indian River Bridge, construction stage prior to deck completion, smooth flow, 90 degrees

Nov. 24, 2004
Data File =cpd101.mst
Information File =cpd101.inf

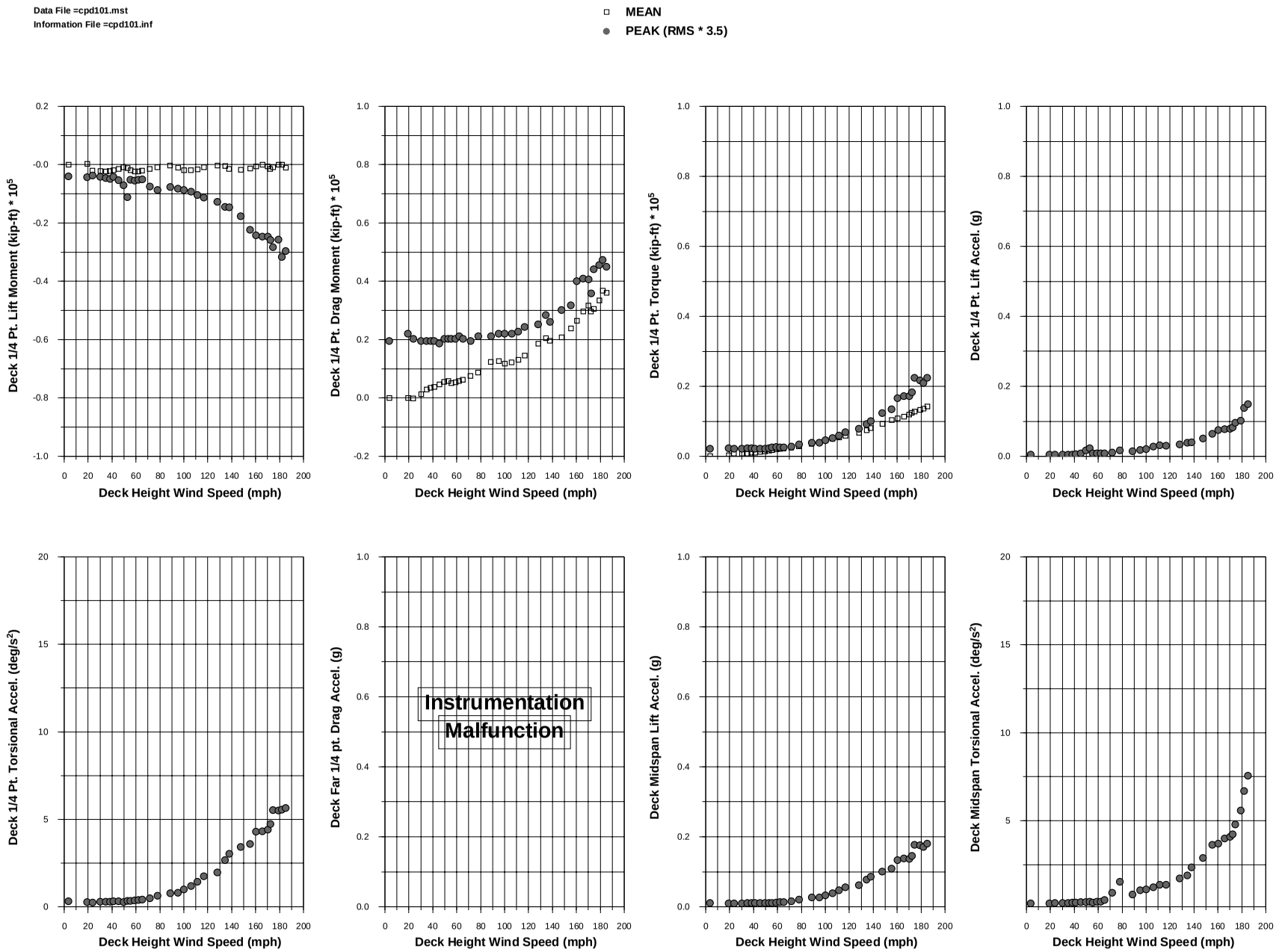

Indian River Bridge, construction stage prior to deck completion, smooth flow, 90 degrees

Nov. 24, 2004
Data File =cpd101.mst
Information File =cpd101.inf

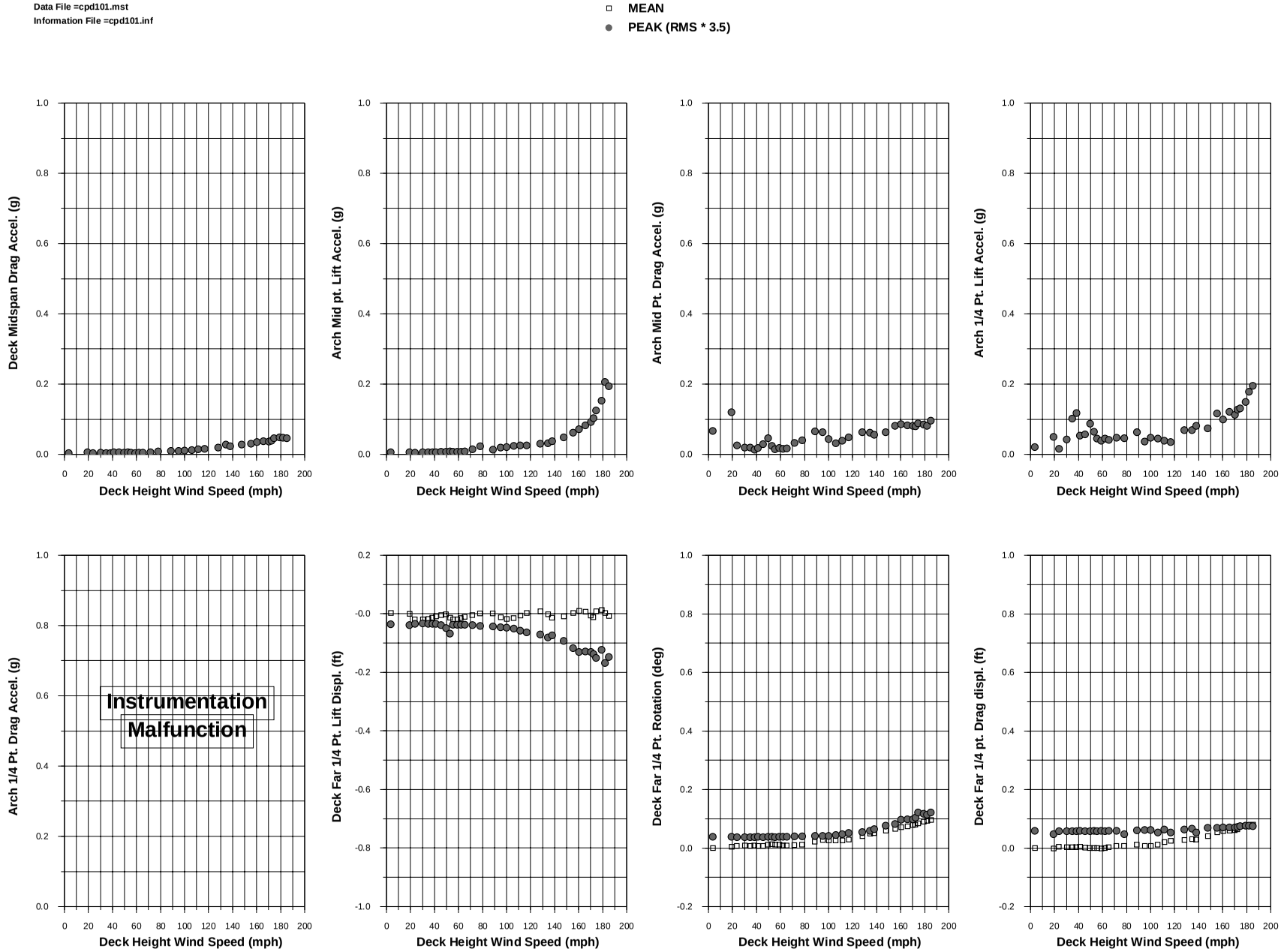

Indian River Bridge, construction stage prior to deck completion, smooth flow, 90 degrees

Nov. 24, 2004
Data File =cpd101.mst
Information File =cpd101.inf

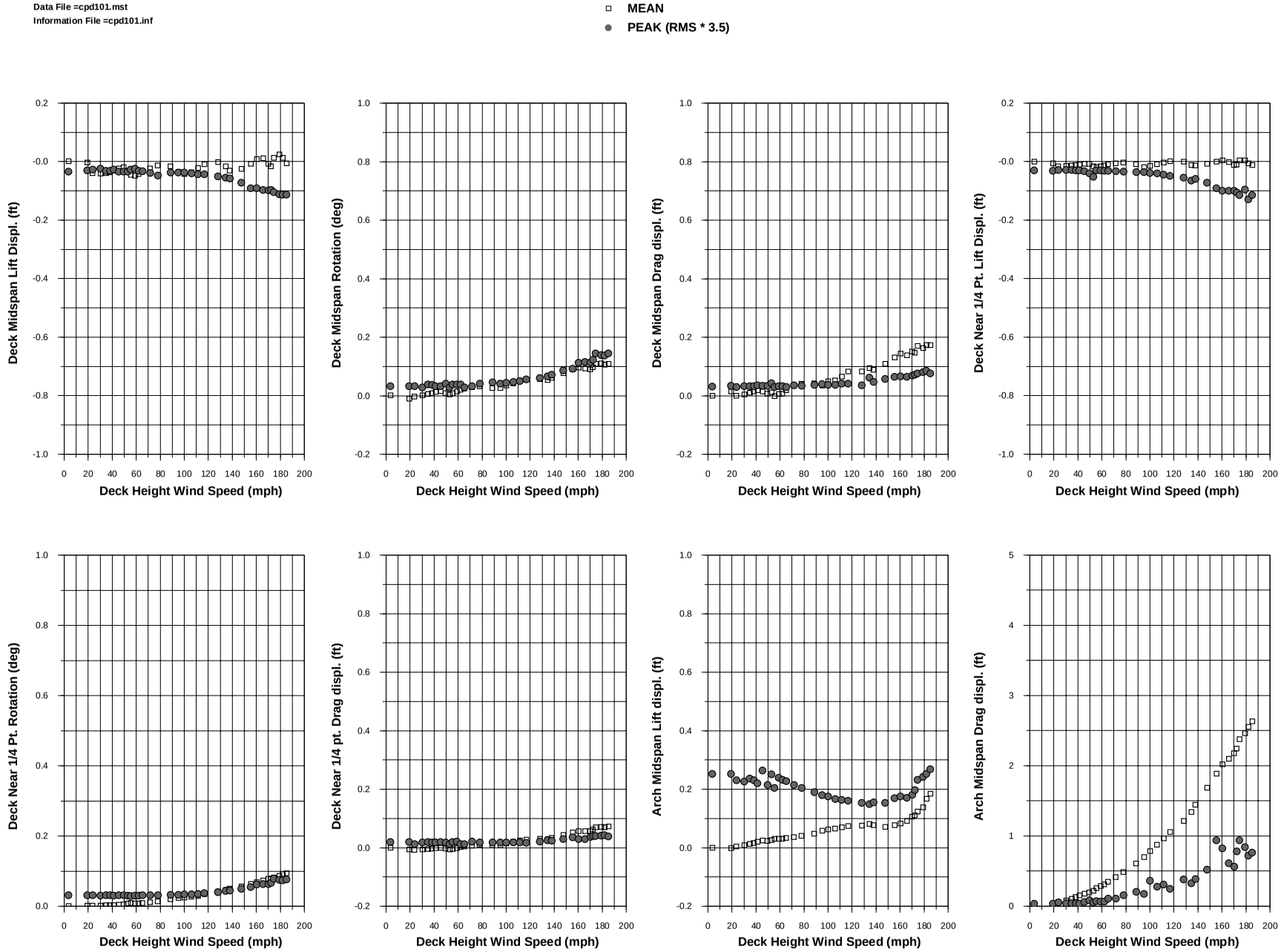

Indian River Bridge, construction stage prior to deck completion, smooth flow, 90 degrees